

ORGANIC-INORGANIC HYBRID MATERIALS: NEW FUNCTIONALISED POLYOXOTUNGSTATES

by

LAURA MARY PERKINS

A thesis submitted to
The University of Birmingham
for the degree of
DOCTOR OF PHILOSOPHY

School of Chemistry
University of Birmingham
November 2009

UNIVERSITY OF
BIRMINGHAM

University of Birmingham Research Archive

e-theses repository

This unpublished thesis/dissertation is copyright of the author and/or third parties. The intellectual property rights of the author or third parties in respect of this work are as defined by The Copyright Designs and Patents Act 1988 or as modified by any successor legislation.

Any use made of information contained in this thesis/dissertation must be in accordance with that legislation and must be properly acknowledged. Further distribution or reproduction in any format is prohibited without the permission of the copyright holder.

ACKNOWLEDGEMENTS

I would like to thank my supervisor Ian Shannon for the opportunity to undertake this research and for all his advice and support.

The members of the IJS group, Marco, Ying and James, along with everyone on level 4, who have made the time during my PhD so enjoyable.

Benson Kariuki and Louise Male for the time spent helping with the X-ray crystallography and Sarah Horswell for her help with the electrochemistry.

The members of the technical staff in the School of Chemistry for their help; Neil Spencer for the NMR spectroscopy, Peter Ashton, Nick May and Lianne Hill for the mass spectrometry and elemental analysis.

Financial support received from the University of Birmingham and the EPSRC.

A big thank you to my family, Mum, Dad, Stephen and Claire who have always encouraged and supported me and to my husband, Stuart for everything he has done to help and support me.

ABSTRACT

Polyoxometalates are the polyoxoanions of the early transition metals, especially tungsten, molybdenum and vanadium. Although they were first described in the 19th century, their development was slow until modern experimental techniques enabled a greater understanding of their structures and properties. In the last 40 years a large variety of shapes, sizes and compositions have been investigated; functionalisation via covalent grafting of organic groups onto the polyoxometalate clusters is less investigated and provides a method of fine tuning the properties of these materials towards desired applications.

Polyoxotungstates (polyoxometalates with tungsten as the metal) are investigated here, those with the Keggin structure being of interest due to the relatively easy formation of lacunary anions which have a highly nucleophilic surface and can react with electrophilic groups to add functionality to the cluster. Organophosphonyl and organosilyl derivatives are prepared with formulae $(\text{NR}^1_4)_3\text{H}_n[\text{XW}_{10}\text{O}_{36}(\text{R}^2\text{PO})_2]$, $(\text{NBu}_4)_3[\text{XW}_9\text{O}_{34}(\text{R}^3\text{SiO})_3(\text{R}^3\text{Si})]$, $(\text{NBu}_4)_3\text{H}_n[\text{XW}_9\text{O}_{34}(\text{tBuSiOH})_3]$, $(\text{NBu}_4)_3\text{H}_n[\text{XW}_9\text{O}_{34}(\text{tBuSiO})_3(\text{SiR}^4)]$, $(\text{NBu}_4)_3\text{H}_n[\text{XW}_9\text{O}_{34}(\text{R}^2\text{PO})_2]$ or $(\text{NBu}_4)_3\text{Na}[\text{SiW}_9\text{O}_{34}(\text{R}^2\text{PO})_3]$ ($\text{X} = \text{Si}$ or P ; $\text{R}^1 = \text{Bu}$ or Et ; $\text{R}^2 = \text{Et}$, $\text{H}_2\text{C}=\text{CH}$, $\text{H}_2\text{C}=\text{CHCH}_2$, $\text{H}_2\text{C}=\text{CHC}_6\text{H}_4$, $\text{HOOC}(\text{CH}_2)_m$ ($m = 1$ or 2) or $\text{H}_3\text{CCOC}_6\text{H}_4$; $\text{R}^3 = \text{H}_2\text{C}=\text{CH}$ or $\text{H}_2\text{C}=\text{CHCH}_2$; $\text{R}^4 = \text{R}^3$ or $(\text{CH}_2)_3\text{Br}$; $n=0$ or 1). The structures are confirmed and investigated using multinuclear NMR (^1H , ^{31}P and ^{29}Si), IR, MS, EA, single crystal X-ray diffraction and Cyclic Voltammography.

The derivatised polyoxotungstate clusters have the potential to take part in further reactions using the organic functionalities to create inorganic-organic hybrid materials which retain the electrochemical properties of the polyoxotungstate units. Examples include the

polymerisation of carbon double bonds and condensation reactions of carboxylic acids and amines; both are investigated here. Radical polymerisation is successful in creating polymeric materials, either through single reaction of the polyoxotungstate cluster or a co-polymerisation reaction with a second co-monomer. Reaction with amines did not proceed as expected, instead one of the RPO groups was removed from the cluster, producing a new set of singly derivatised clusters, $[\text{SiW}_{10}\text{O}_{36}(\text{R}^2\text{PO})]^{6-}$ from $[\text{SiW}_{10}\text{O}_{36}(\text{R}^2\text{PO})_2]^{4-}$. These create potential for a product with asymmetrically functionised polyoxotungstates containing a mixture of R groups $[\text{SiW}_{10}\text{O}_{36}(\text{R}^2\text{PO})(\text{R}^{2b}\text{PO})]^{4-}$, thus providing greater control over the organic functionality on the cluster and increasing the number of potential derivatives available.

ABBREVIATIONS

1,2-dce	1,2-dichloroethane
AIBN	2,2'-azobis(2-methylpropionitrile)
Bu	Butyl
CHN	Carbon, Hydrogen and Nitrogen
CV	Cyclic Voltammetry
d	doublet
DMF	Dimethylformamide
DMSO	Dimethyl Sulfoxide
EA	Elemental Analysis
Et	Ethyl
HCl	Hydrochloric Acid
Hz	Hertz
IR	Infrared
J	coupling constant
M	Metal
m	multiplet
m/z	Mass-to-charge ratio
Maldi-TOF	Matrix-assisted laser desorption/ionisation - Time of Flight
Me	Methyl
MeCN	Acetonitrile
MS	Mass Spectrometry
NBu ₄	Tetrabutylammonium
NEt ₄	Tetraethylammonium
NMR	Nuclear Magnetic Resonance
Ph	Phenyl
POM	Polyoxometalate
ppm	Parts per million

R	Organic group
s	singlet
SCE	Saturated Calomel Electrode
t	triplet
THF	Tetrahydrofuran
UV	Ultraviolet
vis	visible
<i>vs.</i>	Verses
XRD	X-ray Diffraction
δ	chemical shift
ϵ	molar absorptivity, $\text{Lmol}^{-1}\text{cm}^{-1}$
λ	Wavelength, nm
ν	frequency

CONTENTS

1.	INTRODUCTION	1
1.1	History	1
1.2	Structures	2
1.2.1	Keggin Structure	3
1.3	Derivatised polyoxometalates	6
1.3.1	Derivatization with organosilanes	7
1.3.2	Derivatization with Phosphonic acids	10
1.3.3	Derivatization with organotin/organogermanium	13
1.3.4	Other Derivatives	15
1.4	Reactions of the R groups	16
1.5	On Surfaces	18
1.6	Immobilisation of POMs	19
1.6.1	Polymeric Species	20
1.6.2	Crystalline Networks	23
1.6.3	Other Methods of Immobilisation	25
1.7	Techniques	25
1.7.1	Infrared Spectroscopy	26
1.7.2	NMR	26
1.7.3	Mass Spectroscopy	28
1.7.4	X-ray Diffraction	29
1.7.5	Electrochemistry	30

1.7.5.1	Loss of Octahedra	34
1.7.5.2	Derivatized Compounds	36
1.7.5.3	Polymers	37
1.8	Applications	38
1.8.1	Catalysis	38
1.8.2	Medicine	40
1.9	Project Aims	41
1.10	References	43
2.	DERIVATIZATION OF $[\text{XW}_{10}\text{O}_{36}]^{n-}$	49
2.1.	Phosphonic Acid Synthesis	49
2.1.1.	Allylphosphonic Acid Synthesis	49
2.1.1.1.	Diethyl allylphosphonate	49
2.1.1.2.	Allylphosphonic acid	50
2.1.2.	Diethyl Styrylphosphonate	51
2.1.3.	Diethyl 4-acetylphenylphosphonate	55
2.1.4.	Phosphonic acids	56
2.2.	Polyoxotungstate Synthesis	58
2.2.1.	γ -Decatungstosilicate synthesis	58
2.3.	Derivatization of polyoxotungstates	60
2.3.1.	Derivatization of $[\text{SiW}_{10}\text{O}_{36}]^{8-}$	61
2.3.1.1.	$[\text{SiW}_{10}\text{O}_{36}(\text{C}_2\text{H}_5\text{PO})_2]^{4-}$	61
2.3.1.2.	$[\text{SiW}_{10}\text{O}_{36}(\text{C}_2\text{H}_3\text{PO})_2]^{4-}$	69
2.3.1.3.	$[\text{SiW}_{10}\text{O}_{36}(\text{H}_2\text{C}=\text{CHCH}_2\text{PO})_2]^{4-}$	72

2.3.1.4.	$[\text{SiW}_{10}\text{O}_{36}(\text{H}_2\text{C}=\text{CHC}_6\text{H}_4\text{PO})_2]^{4-}$	81
2.3.1.5.	$[\text{SiW}_{10}\text{O}_{36}(\text{HOOCCH}_2\text{PO})_2]^{4-}$	86
2.3.1.6.	$[\text{SiW}_{10}\text{O}_{36}(\text{HOOCCH}_2\text{CH}_2\text{PO})_2]^{4-}$	90
2.3.1.7.	$[\text{SiW}_{10}\text{O}_{36}(\text{H}_3\text{CCOC}_6\text{H}_4\text{PO})_2]^{4-}$	96
2.3.1.8.	Summary of $[\text{SiW}_{10}\text{O}_{36}(\text{RPO})_2]^{4-}$	100
2.4.	Synthesis of $[\text{PW}_{10}\text{O}_{36}]^{7-}$	102
2.4.1.	Derivatization of $[\text{PW}_{10}\text{O}_{36}]^{7-}$	103
2.5.	References	105
3.	DERIVATISATION OF $[\text{XW}_9\text{O}_{34}]^{n-}$	108
3.1.	Synthesis of $[\text{XW}_9\text{O}_{34}]^{n-}$ (X = Si or P, n = 10 or 9)	108
3.1.1.	α -Nonatungstosilicate synthesis	109
3.1.2.	α -Nonatungstophosphate synthesis	109
3.2.	Derivatization of $[\text{XW}_9\text{O}_{34}]^{n-}$	109
3.2.1.	Derivatization with trichlorosilanes	110
3.2.1.1.	$(\text{NBu}_4)_n[\text{XW}_9\text{O}_{34}(\text{RSiO})_3(\text{RSi})]$ (X = P, n = 3 or X = Si, n = 4; R = C_2H_3 or C_3H_5)	110
3.2.1.2.	$(\text{NBu}_4)_3\text{H}_n[\text{XW}_9\text{O}_{34}(t\text{-BuSiOH})_3]$ (X = P, n = 0 or X = Si, n = 1)	114
3.2.1.3.	$(\text{NBu}_4)_3\text{H}_n[\text{XW}_9\text{O}_{34}(t\text{-BuSiO})_3(\text{SiR})]$ (X = P, n = 0 or X = Si, n = 1; R = C_2H_3 , C_3H_5 or $(\text{CH}_2)_3\text{Br}$)	118
3.2.2.	Derivatization with triethoxysilanes	121
3.2.2.1.	$(\text{NBu}_4)_3\text{H}_n[\text{XW}_9\text{O}_{34}(t\text{-BuSiO})_3(\text{HS}(\text{CH}_2)_3\text{Si})]$	121
3.2.3.	Phosphonic acids	124
3.2.3.1.	$[\text{PW}_9\text{O}_{34}]^{9-}$	124

3.2.3.2. $[\text{SiW}_9\text{O}_{34}]^{10-}$	126
3.2.3.3. Altering the Conditions	129
3.2.3.3.1. pH	130
3.2.3.3.2. Temperature	136
3.2.3.4. Other Derivatives	136
3.2.3.4.1. $(\text{NBu}_4)_3\text{Na}[\text{SiW}_9\text{O}_{34}(\text{H}_2\text{C}=\text{CHPO})_3]$	136
3.2.3.4.2. $(\text{NBu}_4)_3\text{Na}[\text{SiW}_9\text{O}_{34}(\text{H}_2\text{C}=\text{CHCH}_2\text{PO})_3]$	140
3.2.3.4.3. $(\text{NBu}_4)_3\text{Na}[\text{SiW}_9\text{O}_{34}(\text{H}_2\text{C}=\text{CHC}_6\text{H}_4\text{PO})_3]$	144
3.2.3.4.4. $(\text{NBu}_4)_3\text{Na}[\text{SiW}_9\text{O}_{34}(\text{HOOCCH}_2\text{PO})_3]$	147
3.2.3.4.5. $(\text{NBu}_4)_3\text{Na}[\text{SiW}_9\text{O}_{34}(\text{HOOCCH}_2\text{CH}_2\text{PO})_3]$	150
3.2.3.4.6. $(\text{NBu}_4)_3\text{Na}[\text{SiW}_9\text{O}_{34}(\text{H}_3\text{CCOC}_6\text{H}_4\text{PO})_3]$	154
3.2.4. Reaction with EtPCl_2	162
3.2.4.1. Cation exchange	162
3.2.4.2. All in one pot $(\text{NBu}_4)_3[\text{PW}_9\text{O}_{34}(\text{EtPO})_3]$ preparation from EtPCl_2	163
3.2.4.3. $(\text{NBu}_4)_3\text{H}[\text{SiW}_9\text{O}_{34}(\text{EtPO})_3]$ preparation from EtPCl_2	168
3.3. Conclusion.....	169
3.4. References.....	170
4. POLYMERISATION REACTIONS	172
4.1. $[\text{SiW}_{10}\text{O}_{36}(\text{RPO})_2]^{4-}$	172
4.1.1. Solvent	173
4.1.2. Initiator	176
4.1.3. Temperature	177
4.1.4. Time	177

4.1.5.	Co-polymerisation of $[\text{SiW}_{10}\text{O}_{36}(\text{H}_2\text{C}=\text{CHC}_6\text{H}_4\text{PO})_2]^{4-}$	186
4.2.	$[\text{SiW}_9\text{O}_{34}(\text{RPO})_3]^{4-}$	199
4.2.1.	Co-polymers	205
4.3.	$[\text{XW}_9\text{O}_{34}(\text{R}^1\text{SiO})_3(\text{R}^2\text{Si})]^{4-}$	210
4.3.1.	$\text{R}^1, \text{R}^2 = \text{Vinyl or Allyl}$	210
4.3.2.	$\text{R}^1 = t\text{-Bu}$	211
4.4.	Conclusion	212
4.5.	References	213
5.	REACTION WITH AMINES	215
5.1	$[\text{SiW}_{10}\text{O}_{36}(\text{RPO})_2]^{4-}$	215
5.1.1	Condensation Reactions, $\text{R} = \text{HOOC}(\text{CH}_2)_n$	215
5.1.2	Imine Formation, $\text{R} = \text{H}_3\text{CCCOC}_6\text{H}_4$	219
5.1.3	Loss of R group	224
5.1.3.1	Reaction of product	228
5.1.3.2	Polymerisation	235
5.1.3.3	Co-polymerization	240
5.2	$[\text{SiW}_9\text{O}_{34}(\text{RPO})_3]^{4-}$	244
5.2.1	Reaction of product	247
5.3	$[\text{XW}_9\text{O}_{34}(t\text{-BuSiO})_3(\text{Si}(\text{CH}_2)_3\text{Br})]^{4-}$	251
5.4	Conclusion	254
5.5	References	255
6.	CONCLUSION	256

7.	EXPERIMENTAL	262
7.1.	Phosphonic acids	263
7.1.1.	Synthesis of Diethyl allylphosphonate (Compound A)	263
7.1.2.	Synthesis of Allylphosphonic acid (Compound B)	263
7.1.3.	Synthesis of Diethyl styrenephosphonate (Compound 1)	264
7.1.4.	Styrenephosphonic acid (Compound 2)	265
7.1.5.	Diethyl 4-acetylphenylphosphonate (Compound C)	265
7.1.6.	4-Acetylphenylphosphonic acid (Compound 3)	266
7.2.	Synthesis of $K_8[\beta_2\text{-SiW}_{11}\text{O}_{39}]\cdot 14\text{H}_2\text{O}$ (Compound D)	267
7.3.	Synthesis of $K_8[\gamma\text{-SiW}_{10}\text{O}_{36}]\cdot 12\text{H}_2\text{O}$ (Compound E)	267
7.4.	Derivatization of $[\text{SiW}_{10}\text{O}_{36}]^{8-}$	268
7.4.1.	Synthesis of $(\text{NBu}_4)_3\text{H}[\gamma\text{-SiW}_{10}\text{O}_{36}(\text{EtPO})_2]$ (Compound F)	268
7.4.2.	Synthesis of $(\text{NEt}_4)_3\text{H}[\gamma\text{-SiW}_{10}\text{O}_{36}(\text{EtPO})_2]$ (Compound G)	268
7.4.2.1.	Crystallisation of $(\text{NBu}_4)_2(\text{NEt}_4)\text{H}[\text{SiW}_{10}\text{O}_{36}(\text{EtPO})_2]$ (Structure 1).....	269
7.4.3.	Synthesis of $(\text{NBu}_4)_3\text{H}[\gamma\text{-SiW}_{10}\text{O}_{36}(\text{H}_2\text{C}=\text{CHPO})_2]$ (Compound H)	269
7.4.4.	Synthesis of $(\text{NEt}_4)_3\text{H}[\gamma\text{-SiW}_{10}\text{O}_{36}(\text{H}_2\text{C}=\text{CHPO})_2]$ (Compound I)	270
7.4.5.	Synthesis of $(\text{NBu}_4)_3\text{H}[\gamma\text{-SiW}_{10}\text{O}_{36}(\text{H}_2\text{C}=\text{CHCH}_2\text{PO})_2]$ (Compound J)	270
7.4.6.	Synthesis of $(\text{NEt}_4)_3\text{H}[\gamma\text{-SiW}_{10}\text{O}_{36}(\text{H}_2\text{C}=\text{CHCH}_2\text{PO})_2]$ (Compound K)	271
7.4.6.1.	Crystallisation of $(\text{NBu}_4)_2(\text{NEt}_4)\text{H}[\text{SiW}_{10}\text{O}_{36}(\text{H}_2\text{C}=\text{CHCH}_2\text{PO})_2]$ (Structure 2)	271
7.4.7.	Synthesis of $(\text{NBu}_4)_3\text{H}[\gamma\text{-SiW}_{10}\text{O}_{36}(\text{H}_2\text{C}=\text{CHC}_6\text{H}_4\text{PO})_2]$ (Compound 4).....	272
7.4.8.	Synthesis of $(\text{NEt}_4)_3\text{H}[\gamma\text{-SiW}_{10}\text{O}_{36}(\text{H}_2\text{C}=\text{CHC}_6\text{H}_4\text{PO})_2]$ (Compound 5).....	273
7.4.9.	Synthesis of $(\text{NBu}_4)_3\text{H}[\gamma\text{-SiW}_{10}\text{O}_{36}(\text{HOOCCH}_2\text{PO})_2]$ (Compound 6).....	273

7.4.10. Synthesis of $(\text{NEt}_4)_3\text{H}[\gamma\text{-SiW}_{10}\text{O}_{36}(\text{HOOCCH}_2\text{PO})_2]$ (Compound 7).....	274
7.4.11. Synthesis of $(\text{NBu}_4)_3\text{H}[\gamma\text{-SiW}_{10}\text{O}_{36}(\text{HOOC}(\text{CH}_2)_2\text{PO})_2]$ (Compound L)	274
7.4.12. Synthesis of $(\text{NEt}_4)_3\text{H}[\gamma\text{-SiW}_{10}\text{O}_{36}(\text{HOOC}(\text{CH}_2)_2\text{PO})_2]$ (Compound M)	275
7.4.13. Synthesis of $(\text{NBu}_4)_3\text{H}[\gamma\text{-SiW}_{10}\text{O}_{36}(\text{H}_3\text{CCOC}_6\text{H}_4\text{PO})_2]$ (Compound 8).....	276
7.4.14. Synthesis of $(\text{NEt}_4)_3\text{H}[\gamma\text{-SiW}_{10}\text{O}_{36}(\text{H}_3\text{CCOC}_6\text{H}_4\text{PO})_2]$ (Compound 9).....	276
7.5. Synthesis of $\text{Cs}_6[\text{P}_2\text{W}_5\text{O}_{23}]$ (Compound N)	277
7.6. Synthesis of $\text{Cs}_7[\text{PW}_{10}\text{O}_{36}]$ (Compound O)	278
7.6.1. Synthesis of $(\text{NBu}_4)_3[\gamma\text{-PW}_{10}\text{O}_{36}(\text{EtPO})_2]$ (Compound 10)	278
7.6.2. Synthesis of $(\text{NBu}_4)_3[\gamma\text{-PW}_{10}\text{O}_{36}(\text{H}_2\text{C}=\text{CHPO})_2]$ (Compound 11)	278
7.6.3. Synthesis of $(\text{NBu}_4)_3[\gamma\text{-PW}_{10}\text{O}_{36}(\text{H}_2\text{C}=\text{CHCH}_2\text{PO})_2]$ (Compound 12).....	279
7.6.4. Synthesis of $(\text{NBu}_4)_3[\gamma\text{-PW}_{10}\text{O}_{36}(\text{HOOCCH}_2\text{PO})_2]$ (Compound 13)	280
7.6.5. Synthesis of $(\text{NBu}_4)_3[\gamma\text{-PW}_{10}\text{O}_{36}(\text{HOOC}(\text{CH}_2)_2\text{PO})_2]$ (Compound 14).....	280
7.6.6. Synthesis of $(\text{NBu}_4)_3[\gamma\text{-PW}_{10}\text{O}_{36}(\text{H}_2\text{C}=\text{CHC}_6\text{H}_4\text{PO})_2]$ (Compound 15).....	281
7.7. Synthesis of $\alpha\text{-A-K}_{7-x}\text{Na}_x[\text{PW}_{11}\text{O}_{39}]\cdot 14\text{H}_2\text{O}$ (Compound P)	281
7.8. Synthesis of $\alpha\text{-A-K}_9[\text{PW}_9\text{O}_{34}]\cdot 16\text{H}_2\text{O}$ (Compound Q)	281
7.9. Synthesis of $\text{Na}_{10}[\alpha\text{-SiW}_9\text{O}_{34}]\cdot \text{solvent}$ (Compound R)	282
7.9.1. Reaction with trichlorosilane	282
7.9.1.1. Synthesis of $(\text{NBu}_4)_3[\text{PW}_9\text{O}_{34}(\text{C}_2\text{H}_3\text{SiO})_3(\text{C}_2\text{H}_3\text{Si})]$ (Compound S)	282
7.9.1.2. Synthesis of $(\text{NBu}_4)_3[\text{PW}_9\text{O}_{34}(\text{C}_3\text{H}_5\text{SiO})_3(\text{C}_3\text{H}_5\text{Si})]$ (Compound T)	283
7.9.1.3. Synthesis of $(\text{NBu}_4)_3\text{H}[\text{SiW}_9\text{O}_{34}(\text{C}_2\text{H}_3\text{SiO})_3(\text{C}_2\text{H}_3\text{Si})]$ (Compound 16)	284
7.9.1.4. Synthesis of $(\text{NBu}_4)_3\text{H}[\text{SiW}_9\text{O}_{34}(\text{C}_3\text{H}_5\text{SiO})_3(\text{C}_3\text{H}_5\text{Si})]$ (Compound 17)	284
7.9.1.5. Synthesis of $(\text{NBu}_4)_3[\text{PW}_9\text{O}_{34}(t\text{-BuSiOH})_3]$ (Compound U)	285
7.9.1.6. Synthesis of $(\text{NBu}_4)_3\text{H}[\text{SiW}_9\text{O}_{34}(t\text{-BuSiOH})_3]$ (Compound 18)	286

7.9.1.7. Synthesis of $(\text{NBu}_4)_3[\text{PW}_9\text{O}_{34}(t\text{-BuSiO})_3(\text{H}_2\text{C}=\text{CHSi})]$ (Compound V)	286
7.9.1.8. Synthesis of $(\text{NBu}_4)_3[\text{PW}_9\text{O}_{34}(t\text{-BuSiO})_3(\text{H}_2\text{C}=\text{CHCH}_2\text{Si})]$ (Compound W)	287
7.9.1.9. Synthesis of $(\text{NBu}_4)_3[\text{PW}_9\text{O}_{34}(t\text{-BuSiO})_3(\text{Br}(\text{CH}_2)_3\text{Si})]$ (Compound 19).....	288
7.9.1.10. Synthesis of $(\text{NBu}_4)_3\text{H}[\text{SiW}_9\text{O}_{34}(t\text{-BuSiO})_3(\text{H}_2\text{C}=\text{CHSi})]$ (Compound 20)	288
7.9.1.11. Synthesis of $(\text{NBu}_4)_3\text{H}[\text{SiW}_9\text{O}_{34}(t\text{-BuSiO})_3(\text{H}_2\text{C}=\text{CHCH}_2\text{Si})]$ (Compound 21)	289
7.9.1.12. Synthesis of $(\text{NBu}_4)_3\text{H}[\text{SiW}_9\text{O}_{34}(t\text{-BuSiO})_3(\text{Br}(\text{CH}_2)_3\text{Si})]$ (Compound 22)	290
7.9.2. Reaction with triethoxysilane	290
7.9.2.1. Synthesis of $(\text{NBu}_4)_3\text{H}[\text{SiW}_9\text{O}_{34}(t\text{-BuSiO})_3(\text{Si}(\text{CH}_2)_3\text{SH})]$ (Compound 23).....	290
7.9.2.2. Synthesis of $(\text{NBu}_4)_3[\text{PW}_9\text{O}_{34}(t\text{-BuSiO})_3(\text{Si}(\text{CH}_2)_3\text{SH})]$ (Compound 24)....	291
7.9.3. Reaction with phosphonic acid	291
7.9.3.1. Synthesis of $(\text{NBu}_4)_3\text{Na}/\text{H}_2[\text{PW}_9\text{O}_{34}(\text{EtPO})_2]$ (Compound X)	291
7.9.3.2. Synthesis of $(\text{NBu}_4)_3\text{H}_2[\text{PW}_9\text{O}_{34}(\text{C}_2\text{H}_3\text{PO})_2]$ (Compound 25)	292
7.9.3.3. Synthesis of $(\text{NBu}_4)_3\text{H}_2[\text{PW}_9\text{O}_{34}(\text{C}_3\text{H}_5\text{PO})_2]$ (Compound Y)	293
7.9.3.4. $(\text{NBu}_4)_3\text{H}_3[\text{SiW}_9\text{O}_{34}(\text{EtPO})_2]$ (Compound 26)	293
7.9.3.5. $(\text{NBu}_4)_3\text{H}_3[\text{SiW}_9\text{O}_{34}(\text{H}_2\text{C}=\text{CHPO})_2]$ (Compound 27)	294
7.9.3.6. $(\text{NBu}_4)_3\text{H}_3[\text{SiW}_9\text{O}_{34}(\text{H}_2\text{C}=\text{CHCH}_2\text{PO})_2]$ (Compound 28)	294
7.9.3.7. $(\text{NBu}_4)_3\text{Na}[\text{SiW}_9\text{O}_{34}(\text{EtPO})_3]$ (Compound 29)	295
7.9.3.8. $(\text{NBu}_4)_3\text{Na}[\text{SiW}_9\text{O}_{34}(\text{H}_2\text{C}=\text{CHPO})_3]$ (Compound 30)	296
7.9.3.9. $(\text{NBu}_4)_3\text{Na}[\text{SiW}_9\text{O}_{34}(\text{H}_2\text{C}=\text{CHCH}_2\text{PO})_3]$ (Compound 31)	296

7.9.3.10. (NBu ₄) ₃ Na[SiW ₉ O ₃₄ (HOOCCH ₂ PO) ₃] (Compound 32)297
7.9.3.11. (NBu ₄) ₃ Na[SiW ₉ O ₃₄ (HOOCCH ₂ CH ₂ PO) ₃] (Compound 33)298
7.9.3.12. (NBu ₄) ₃ Na[SiW ₉ O ₃₄ (H ₃ CCOC ₆ H ₄ PO) ₃] (Compound 34)299
7.9.3.13. (NBu ₄) ₃ Na[SiW ₉ O ₃₄ (H ₂ C=CHC ₆ H ₄ PO) ₃] (Compound 35)300
7.9.4. Cation exchange301
7.9.4.1. [PW ₉ O ₃₄] ⁹⁻301
7.9.4.1.1. (NBu ₄) ₃ [PW ₁₁ O ₃₉ (EtPO) ₂] (Compound Z)301
7.9.4.2. [SiW ₉ O ₃₄] ¹⁰⁻301
7.9.4.3. [SiW ₉ O ₃₄] ¹⁰⁻302
7.9.5. Reaction with EtPCl ₂302
7.9.5.1. (NBu ₄) ₃ H ₂ [PW ₉ O ₃₄ (EtPO) ₂] ‘all in one’ method (Compound 36)302
7.9.5.2. (NBu ₄) ₃ Na[SiW ₉ O ₃₄ (EtPO) ₃] ‘all in one’ method (Compound 37)303
7.10. Polymerization of (NBu ₄) ₃ H[SiW ₁₀ O ₃₆ (RPO) ₂]303
7.11. Co-polymerization of (NBu ₄) ₃ H[SiW ₁₀ O ₃₆ (H ₂ C=CHC ₆ H ₄ PO) ₂]304
7.12. Polymerization of (NBu ₄) ₃ Na[SiW ₉ O ₃₄ (RPO) ₃]305
7.13. Co-polymerisation of (NBu ₄) ₃ Na[SiW ₉ O ₃₄ (H ₂ C=CHC ₆ H ₄ PO) ₃]305
7.14. Reaction with amines306
7.14.1. Reaction of (NBu ₄) ₃ H[SiW ₁₀ O ₃₆ (HOOCCH ₂ PO) ₂] with benzylamine (Compound 38)306
7.14.2. Reaction of (NBu ₄) ₃ H[SiW ₁₀ O ₃₆ (HOOC(CH ₂) ₂ PO) ₂] with benzylamine (Compound 39)306
7.14.2.1. Crystals of (NBu ₄) ₄ (C ₆ H ₅ CH ₂ NH ₃) ₇ Mg[SiW ₁₀ O ₃₆ (HOOC(CH ₂) ₂ PO) ₂]	

(Structure 21)	307
7.14.3. Reaction of $(\text{NBu}_4)_3\text{H}[\text{SiW}_{10}\text{O}_{36}(\text{H}_3\text{CCOC}_6\text{H}_4\text{PO})_2]$ with amines (Compound 40)	308
7.14.4. Reaction of $(\text{NEt}_4)_3\text{H}[\text{SiW}_{10}\text{O}_{36}(\text{H}_3\text{CCOC}_6\text{H}_4\text{PO})_2]$ with benzylamine (Compound 41)	308
7.14.5. Reaction of $(\text{NBu}_4)_3\text{H}[\text{SiW}_{10}\text{O}_{36}(\text{EtPO})_2]$ with benzylamine (Compound 42)....	309
7.14.6. Reaction of $(\text{NEt}_4)_3\text{H}[\text{SiW}_{10}\text{O}_{36}(\text{H}_2\text{C}=\text{CHPO})_2]$ with benzylamine (Compound 43)	310
7.14.7. Reaction of $(\text{NEt}_4)_3\text{H}[\text{SiW}_{10}\text{O}_{36}(\text{H}_2\text{C}=\text{CHCH}_2\text{PO})_2]$ with benzylamine (Compound 44)	310
7.14.8. Reaction of $(\text{NEt}_4)_3\text{H}[\text{SiW}_{10}\text{O}_{36}(\text{H}_2\text{C}=\text{CHCH}_2\text{PO})_2]$ with butylamine (Compound 45)	311
7.14.9. Examples of reactions to give $(\text{NEt}_4)_3\text{H}[\text{SiW}_{10}\text{O}_{36}(\text{R}^1\text{PO})(\text{R}^2\text{PO})]$	312
7.14.9.1. $(\text{NEt}_4)_3\text{H}[\text{SiW}_{10}\text{O}_{36}(\text{H}_3\text{CCOC}_6\text{H}_4\text{PO})(\text{EtPO})]$ (Compound 46).....	312
7.14.9.2. $(\text{NBu}_4)_3\text{H}[\text{SiW}_{10}\text{O}_{36}(\text{EtPO})(\text{H}_2\text{C}=\text{CHC}_6\text{H}_4\text{PO})]$ (Compound 47)	312
7.14.9.3. $(\text{NEt}_4)_3\text{H}[\text{SiW}_{10}\text{O}_{36}(\text{H}_2\text{C}=\text{CHPO})(\text{H}_2\text{C}=\text{CHCH}_2\text{PO})]$ (Compound 48)....	313
7.14.9.4. $(\text{NEt}_4)_3\text{H}[\text{SiW}_{10}\text{O}_{36}(\text{H}_2\text{C}=\text{CHCH}_2\text{PO})(\text{HOOCCH}_2\text{CH}_2\text{PO})]$ (Compound 49)	314
7.14.10. Polymerisation of $(\text{NBu}_4)_3\text{H}[\text{SiW}_{10}\text{O}_{36}(\text{EtPO})(\text{H}_2\text{C}=\text{CHC}_6\text{H}_4\text{PO})]$	315
7.14.11. Co-polymerisation of $(\text{NBu}_4)_3\text{H}[\text{SiW}_{10}\text{O}_{36}(\text{EtPO})(\text{H}_2\text{C}=\text{CHC}_6\text{H}_4\text{PO})]$	315
7.14.12. Reaction of $(\text{NBu}_4)_3\text{H}[\text{SiW}_9\text{O}_{34}(\text{H}_2\text{C}=\text{CHCH}_2\text{PO})_3]$ with benzylamine (Compound 50)	315
7.14.13. $(\text{NBu}_4)_3\text{H}[\text{SiW}_9\text{O}_{34}(\text{H}_2\text{C}=\text{CHCH}_2\text{PO})_2(\text{C}_6\text{H}_5\text{PO})]$ (Compound 51)	316

7.14.14. $(\text{NBu}_4)_3\text{H}[\text{SiW}_9\text{O}_{34}(\text{H}_2\text{C}=\text{CHCH}_2\text{PO})_2(\text{HOOCCH}_2\text{PO})]$ (Compound 52)	317
7.15. Reaction of $(\text{NBu}_4)_3[\text{XW}_9\text{O}_{34}(t\text{-BuSiO})_3(\text{Si}(\text{CH}_2)_3\text{Br})]$ with amines	317
7.15.1. Reaction of $(\text{NBu}_4)_3[\text{PW}_9\text{O}_{34}(t\text{-BuSiO})_3(\text{Si}(\text{CH}_2)_3\text{Br})]$ with glycine (Compound 53)	317
7.15.2. Reaction of $(\text{NBu}_4)_3[\text{PW}_9\text{O}_{34}(t\text{-BuSiO})_3(\text{Si}(\text{CH}_2)_3\text{Br})]$ with sarcosine (Compound 54)	318
7.15.3. Reaction of $(\text{NBu}_4)_3\text{H}[\text{SiW}_9\text{O}_{34}(t\text{-BuSiO})_3(\text{Si}(\text{CH}_2)_3\text{Br})]$ with glycine (Compound 55)	319
7.15.4. Reaction of $(\text{NBu}_4)_3\text{H}[\text{SiW}_9\text{O}_{34}(t\text{-BuSiO})_3(\text{Si}(\text{CH}_2)_3\text{Br})]$ with sarcosine (Compound 56)	319
7.15.5. Reaction of $(\text{NBu}_4)_3[\text{PW}_9\text{O}_{34}(t\text{-BuSiO})_3(\text{Si}(\text{CH}_2)_3\text{Br})]$ with benzylamine (Compound 57)	320
7.15.6. Reaction of $(\text{NBu}_4)_3\text{H}[\text{SiW}_9\text{O}_{34}(t\text{-BuSiO})_3(\text{Si}(\text{CH}_2)_3\text{Br})]$ with benzylamine (Compound 58)	321
7.15.7. Reaction of $(\text{NBu}_4)_3[\text{PW}_9\text{O}_{34}(t\text{-BuSiO})_3(\text{Si}(\text{CH}_2)_3\text{Br})]$ with p-xylylenediamine (Compound 59)	321
7.15.8. Reaction of $(\text{NBu}_4)_3\text{H}[\text{SiW}_9\text{O}_{34}(t\text{-BuSiO})_3(\text{Si}(\text{CH}_2)_3\text{Br})]$ with p-xylylenediamine (Compound 60)	322
7.16. Electrochemistry	322
7.17. References	323
8. APPENDIX	324

1. INTRODUCTION

Polyoxometalates are discrete cluster anions formed from early transition metals ($M = V, Nb, Ta, Mo$ or W) in their highest oxidation state and oxygen atoms. They have a wide range of molecular structural diversity, existing in a variety of shapes, sizes and compositions.

1.1 History

The first example of a polyoxometalate material was in 1826 when Berzelius described the yellow precipitate produced when ammonium molybdate is added to phosphoric acid,^{1,2} this is now known as ammonium 12-phosphomolybdate, $(NH_4)_3[PMo_{12}O_{40}] \cdot aq$. The composition of such materials was not precisely determined until the discovery and characterisation of the first heteropolytungstates by Marignac in 1862,^{2,3} but for many years the structures of heteropolyanions were largely unknown. Rosenheim separated them into two classes, those containing 12 metal ions and those containing 6 metal ions. The 12 metal class was described by Miolati-Rosenheim (MR) theory to be based on a central $[XO_4]^{n-}$ group ($X = H_2, n = 10$; $X = B, n = 9$; $X = Si, n = 8$ or $X = P, n = 7$) with the oxygen atoms replaced by $M_2O_7^{2-}$ groups.^{2,4} 12-tungstosilicic acid ($H_4[SiW_{12}O_{40}]$) was described by MR theory as $H_8[Si(W_2O_7)_6]$ (note the different basicity). However MR theory offered no explanation for the characteristic properties of the polyoxometalates.

In 1909, Werner suggested that the metal atoms were connected through several oxygen atoms thus anticipating edge and face-sharing polyhedra.^{5,6} In 1929, Pauling proposed a different structure based on the crystal radii of the metal ions Mo^{6+} and W^{6+} being appropriate for octahedral coordination. The resulting MO_6 octahedra combine by corner sharing with the 36

remaining oxygen ions each taking up a hydrogen ion to stabilize the negative charge. The resultant structure has a central tetrahedral group (XO_4) ($\text{X} = \text{H}_2, \text{B}, \text{Si}, \text{P}$ or As etc), with 12-tungstosilicic acid being written as $[\text{SiO}_4\text{W}_{12}\text{O}_{18}(\text{OH})_{36}]$.⁴ This structure (Figure 1.1) is closer to reality than that suggested by MR theory.

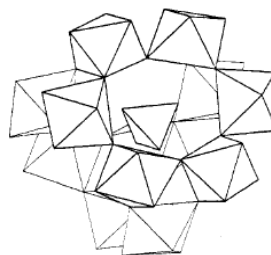


Figure 1.1. The structure of the 12-tungstosilicate anion proposed by Pauling in 1929.⁴

The correct structure of $\text{H}_3[\text{PW}_{12}\text{O}_{40}]\cdot 5\text{H}_2\text{O}$ was solved using X-ray diffraction in 1933, by Keggin, who showed that the structure consisted of MO_6 octahedra units as proposed by Pauling but these units were linked by both corner and edge sharing interactions. This structure became known as the Keggin structure.⁷

Further progress was slow (only ~25 X-ray diffraction investigations by 1971⁶) until developments in X-ray crystallography allowed for easier structural determination. Now the number of heteropoly-molybdate and -tungstate anions is vast with large ranges of heteroelements, stoichiometries and structures; compounds range from the small and relatively simple $[\text{Mo}_6\text{O}_{19}]^{2-}$,⁸ to large nanosized polyoxomolybdates such as $[\text{H}_x\text{Mo}_{368}\text{O}_{1032}(\text{H}_2\text{O})_{240}(\text{SO}_4)_{48}]^{48-}$.⁹

1.2 Structures

Polyoxometalates are based on MO_p and XO_q polyhedra, some basic structures include the Lindquist (a), Keggin (b), Wells-Dawson (c) and Anderson (d) structures (See Figure 1.2).

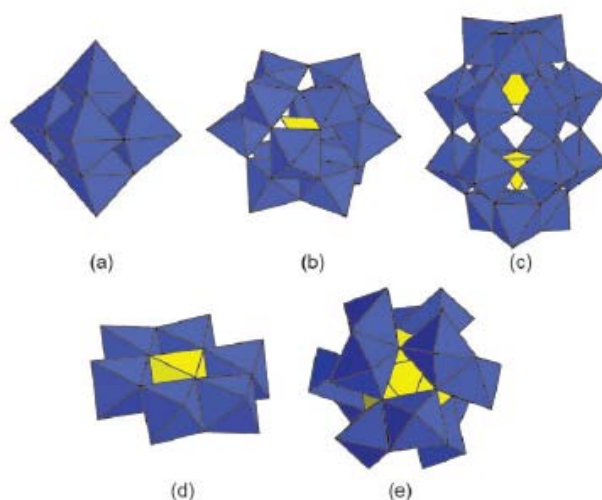


Figure 1.2. Basic POM structures, (a) $[M_6O_{19}]^{n-}$, (b) $[\alpha-XM_{12}O_{40}]^{n-}$, (c) $[\alpha-X_2M_{18}O_{62}]^{n-}$, (d) $[H_xXMo_6O_{24}]^{n-}$ and (e) $[XM_{12}O_{42}]^{8-}$.¹⁰

Structure (e) (Figure 1.2) is an inverted-Keggin structure with a central icosahedron, which is only known for a small number of heteropolymolybdates.^{10,11}

1.2.1 Keggin Structure

The Keggin structure is the most widely studied structure for tungsten POMs, having α , β , γ and ϵ isomers based on $[XM_{12}O_{40}]^{n-}$ where $M = W, Mo$ and X can be an elemental cation (eg. Si, P, Ge or As) or even a molecular species. The central X atom forms a tetrahedron (XO_4) surrounded by twelve octahedrally coordinated metal atoms (MO_6)¹² (Figure 1.3).

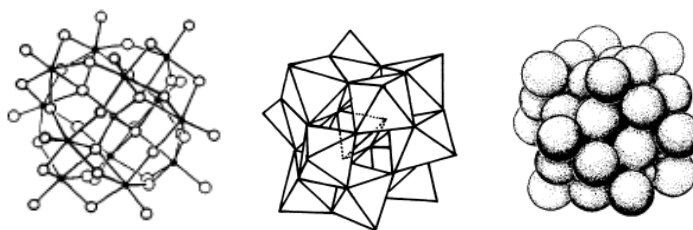
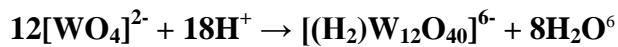


Figure 1.3. Diagram showing the Keggin structure.^{6,13}

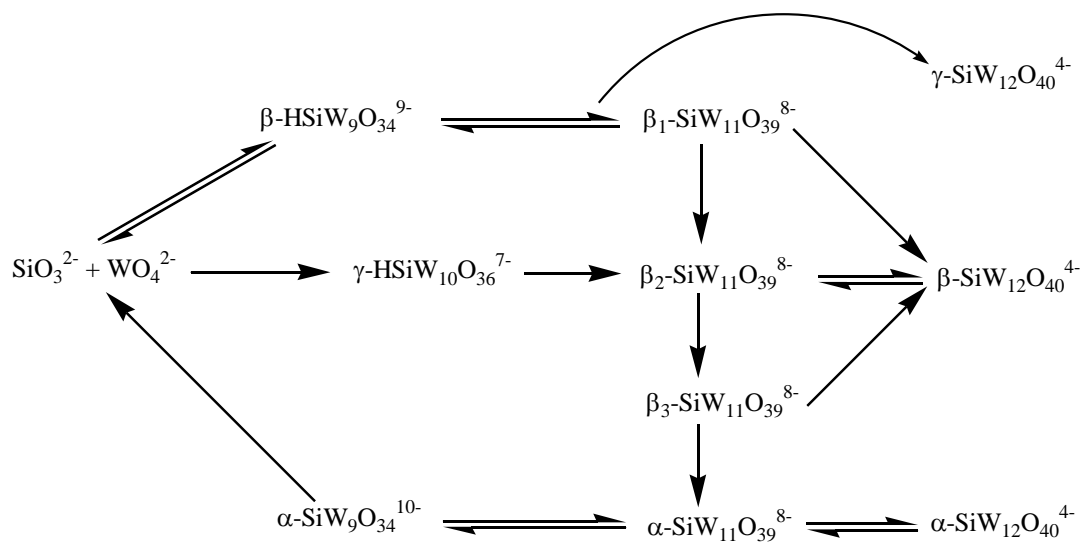
The structure is formed by a self-assembly approach, the basic arrangement of MO_6 octahedra forming even when no central tetrahedral nucleus is present.



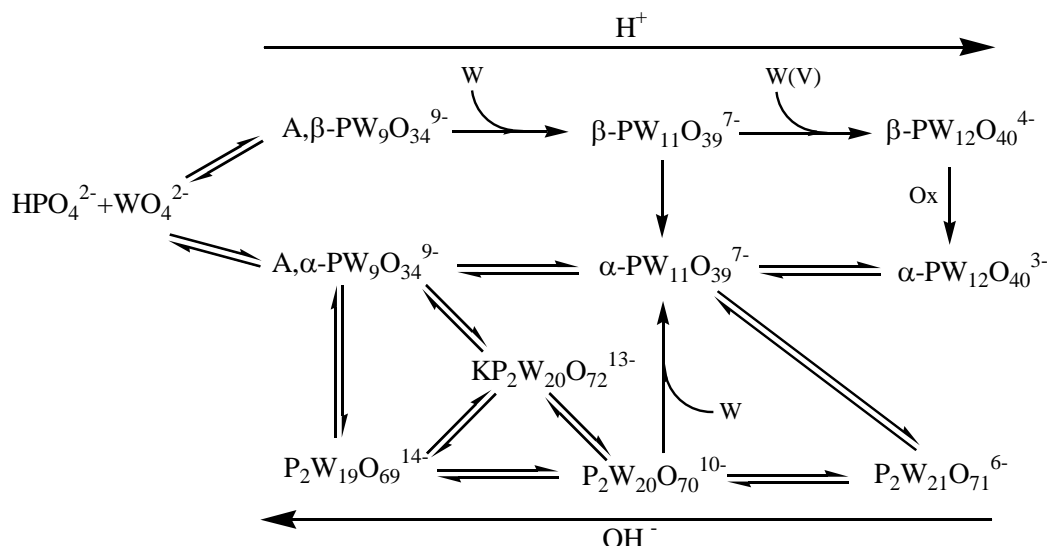
Scheme 1.1

The most common structure is the α -isomer containing four groups of edge shared M_3O_{13} octahedra. The β -isomer is obtained by rotation of one M_3O_{13} group by 60° , while γ -isomer is formed by rotation of two groups² and the ε -isomer by rotation of all four groups.⁶

The most stable structures are the tungstosilicates obtained with Si^{IV} as the heteroelement, the dodecatungstosilicates (12-tungsten) being stable in acid solution. Increasing the pH causes hydrolytic cleavage of W-O bonds¹⁴ converting it to the undecatungstosilicate (11-tungsten atoms) at pH 6-8 of which four structural isomers can be obtained, due to rotation of one or more octahedra.¹⁵ Raising the pH to 9 causes further W-O bond cleavage, either losing one or two more WO_6 octahedra and giving either $\gamma\text{-HSiW}_{10}\text{O}_{36}$, $\beta\text{-SiW}_9\text{O}_{34}$ or $\alpha\text{-SiW}_9\text{O}_{34}$ depending on the starting $\text{SiW}_{11}\text{O}_{39}$ isomer (Scheme 1.2). Three dodecatungstosilicates (12-tungsten), four undecatungstosilicates (11-tungsten), one decatungstosilicate (10-tungsten) and two nonatungstosilicates (9-tungsten) are known.

Scheme 1.2. Showing the routes for synthesis of tungstosilicates.¹⁴

Tungsten polyoxometalates with P^V as the heteroelement are structurally similar to the tungstosilicates, but not as thermodynamically stable with equilibria between the different possible isomers producing isomeric mixtures. Again their formation is pH dependent in solution, the cleavage of W-O bonds resulting in loss of W octahedra at high pH (Scheme 1.3).^{16,17}



Scheme 1.3. Showing routes of synthesis for tungstophosphates.¹⁶

Unlike the tungstosilicates, a decatungstophosphate cluster of the form $[\gamma\text{-PW}_{10}\text{O}_{36}]^{7-}$ structurally analogous to $[\gamma\text{-SiW}_{10}\text{O}_{36}]^{8-}$ is not formed during these equilibria, however this species can be prepared separately via $\text{Cs}_6[\text{P}_2\text{W}_5\text{O}_{23}]$.^{18, 19}

The stability of polyanions in aqueous solution depends on the isomer present, the central heteroatom²⁰ and the nature of the counterion, with different cations stabilizing different polyanions. The importance of counterions can be seen by the effect of replacing cesium hydroxide by potassium hydroxide in the synthesis of $\text{Cs}_6[\text{P}_2\text{W}_5\text{O}_{23}]$, giving $\text{K}_9[\text{PW}_9\text{O}_{34}]$ rather than $\text{K}_6[\text{P}_2\text{W}_5\text{O}_{23}]$.¹⁸

1.3 Derivatised polyoxometalates

There is great potential for derivatisation of polyoxometalates and any element from groups 14, 15, 16 or 17 can be introduced,²¹ either as a single atom or as part of an organic or organometallic fragment. The substitution can tune the properties of the framework altering solubility and other physical properties which can increase utility as catalysts, in materials applications or change activity and toxicity in medicine. The most developed class of materials involves the polyoxometalate coordinating with metal ions.^{6,22}

A second class of materials involving polyoxometalates covalently linked to an organic moiety is less developed. This approach has potential advantages, such as the structures produced being more stable, the possibility of an interaction between the inorganic and organic components of the structure or with other organic groups having the potential to be used to direct the long range order of the materials.

Complete polyoxometalates are usually only weakly basic and nucleophilic, but when these parent species are altered from their original $[\text{XW}_{12}\text{O}_{40}]^{n-}$ structure by the loss of tungsten octahedral, this creates vacancies and the surface oxygen atoms remaining around these sites have a higher charge density associated with them than the other terminal oxygen atoms, therefore they are more reactive. For example, the decatungstate $[\gamma\text{-XW}_{10}\text{O}_{36}]^{n-}$ has lost two octahedra leaving four nucleophilic surface oxygen atoms and the nonatungstate $[\text{XW}_9\text{O}_{34}]^{n-}$ has lost three octahedra leaving six nucleophilic surface oxygen atoms (Figure 1.4).

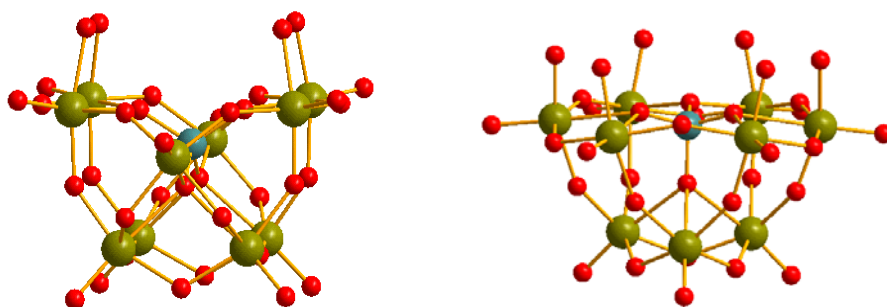


Figure 1.4. The structures of $[\gamma\text{-XW}_{10}\text{O}_{36}]^n$ and $[\text{XW}_9\text{O}_{34}]^n$ showing the nucleophilic surface oxygen atoms on the top of the structures in the vacancies left from lost of tungsten octahedra.

In 1976 the first example of a polyoxometalate covalently bound to an organometallic group ($[(\text{CpTi})\text{PW}_{11}\text{O}_{39}]^{4-}$) was prepared by Klemperer,²³ since then a relatively large number of organometallic-substituted polyoxometalates have been prepared²¹ by reactions with either organosilanes RSiCl_3 and R_2SiCl_2 , organophosphonic acids $\text{RPO}(\text{OH})_2$ and organotin species RSnCl_3 and Me_2SnCl_2 .

1.3.1 Derivatization with organosilanes

Organosilyl derivatives of polyoxometalates are obtained by reaction with trichlorosilanes under phase-transfer conditions.

Early examples of organic-inorganic hybrid materials obtained from polyoxotungstates were derived from the undecatungstate (11-tungsten) anions, these being the most stable lacunary anions. $[\text{SiW}_{11}\text{O}_{39}(\text{SiR})_2\text{O}]^{4-}$ was obtained by reaction with chlorosilicates²⁴ and consists of a $[\text{SiW}_{11}\text{O}_{39}]^{8-}$ unit with two SiR groups filling the gap left by the removal of a tungsten octahedra from the parent anion ($[\text{SiW}_{12}\text{O}_{40}]^{4-}$). A number of compounds made from polyvacant compounds have been obtained. In 1991, Thouvenot *et al.* found that the trivacant $[\text{SiW}_9\text{O}_{34}]^{10-}$ anion can easily react with alkyl trichlorosilanes RSiCl_3 under phase transfer conditions (NBu_4Br) to give the fully saturated $[\text{SiW}_9\text{O}_{34}(\equiv\text{SiR})_3(\text{O}_3\text{SiR})]^{4-}$ ($\text{R} = \text{H}, \text{Et}, \text{n-butyl}, \text{vinyl}, \text{phenyl}, \text{p-tolyl}$) anion,

the compounds being characterized by IR and multinuclear NMR (^{29}Si , ^{183}W) spectroscopy.²⁵ These spectroscopic methods indicated that the structure consisted of an $[\alpha\text{-SiW}_9\text{O}_{34}]^{10-}$ unit with three SiR groups each attached to two oxygen atoms from the vacant site, the structure being completed by a O_3SiR capping group. This structure has since been confirmed by single crystal XRD for the related $[\text{PW}_9\text{O}_{34}(\text{C}_2\text{H}_5\text{SiO})_3(\text{C}_2\text{H}_5\text{Si})]^{3-}$ unit (Figure 1.5).²⁶

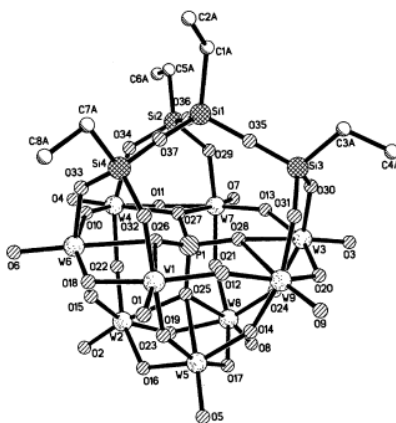
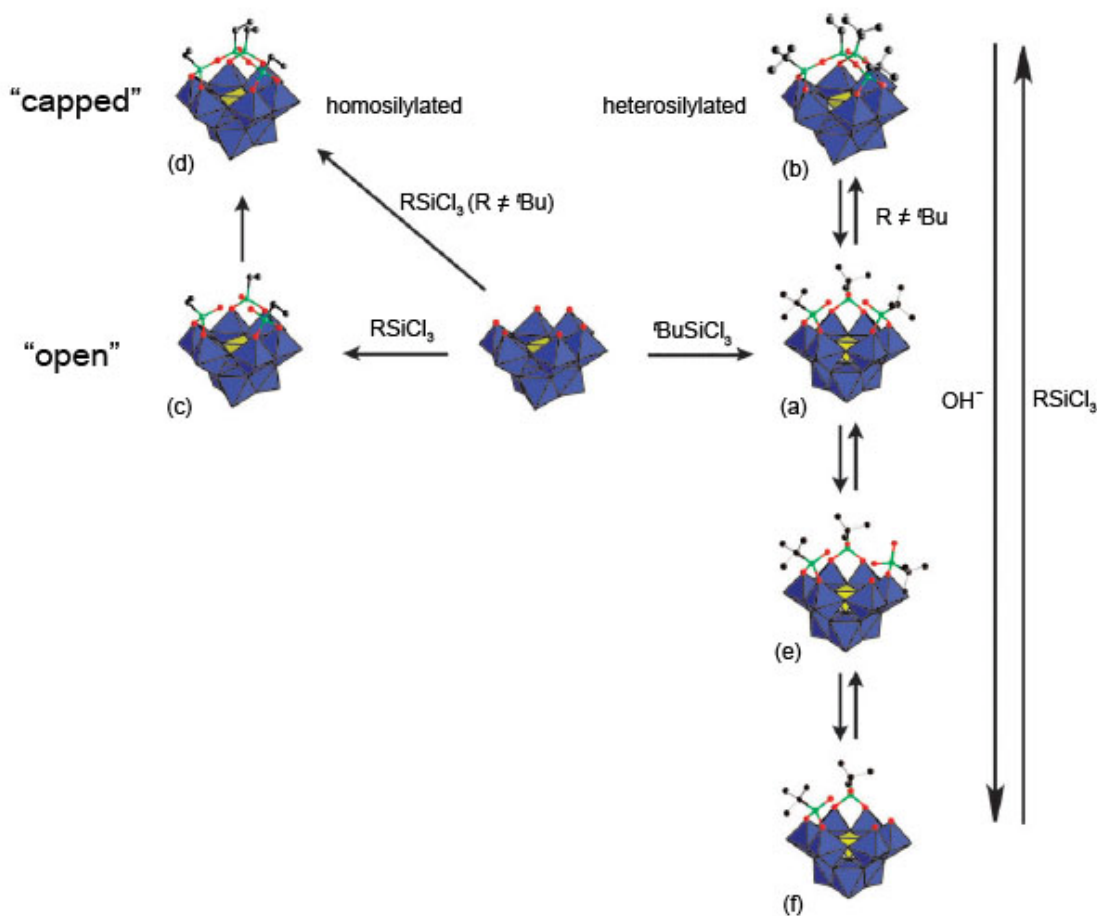


Figure 1.5. Structure of $[\text{PW}_9\text{O}_{34}(\text{ethylSiO})_3(\text{ethylSi})]^{3-}$.²⁶

This closed cage like structure is formed by reaction with many different alkyl trichlorosilanes, however it is not obtained by reaction with $t\text{BuSiCl}_3$, only the triply derivatized $[\alpha\text{-PW}_9\text{O}_{34}(t\text{BuSiOH})_3]^{3-}$ being formed presumably due to steric crowding.²⁷ This ‘open’ structure gives the possibility for mixed organosilyl derivatives $[\text{XW}_9\text{O}_{34}(t\text{BuSiO})_3(\text{RSi})]^{3-}$ ($\text{X} = \text{P}$ or Si , $\text{R} = \text{H}$, Me , Et , $\text{CH}=\text{CH}_2$ or $\text{CH}_2\text{-CH}_2\text{-CH}_2\text{-Cl}$) to be formed by further reaction with RSiCl_3 (the smaller R groups being more reactive), the closed structure being characterized by multi-nuclear NMR spectroscopy.

The structure can also be degraded in a controlled manner (when $\text{X} = \text{P}$) using $^n\text{Bu}_4\text{NOH}$ to successively break Si-O-W bonds giving structures such as $[\alpha\text{-PW}_9\text{O}_{34}(t\text{BuSiOH})_2(t\text{BuSi}(\text{OH})_2)]^{4-}$ and $[\alpha\text{-PW}_9\text{O}_{34}(t\text{BuSiOH})_2]^{5-}$ (Scheme 1.4).¹⁰



Scheme 1.4. Organosilyl derivatives obtained from $[\text{PW}_9\text{O}_{34}]^{7-}$: (a) $[\alpha\text{-PW}_9\text{O}_{34}(t\text{BuSiOH})_3]^{3-}$, (b) $[\alpha\text{-PW}_9\text{O}_{34}(t\text{BuSiO})_3(\text{SiEt})]^{3-}$, (c) $[\alpha\text{-PW}_9\text{O}_{34}(\text{EtSiOH})_3]^{3-}$, (d) $[\alpha\text{-PW}_9\text{O}_{34}(\text{EtSiOH})_3(\text{SiEt})]^{3-}$, (e) $[\alpha\text{-PW}_9\text{O}_{34}(t\text{BuSiOH})_2(t\text{BuSiOH}_2)]^{4-}$, (f) $[\alpha\text{-PW}_9\text{O}_{34}(t\text{BuSiOH})_2]^{5-}$.¹⁰

The synthesis of organosilane derivatives from divacant $[\text{XW}_{10}\text{O}_{36}]^{n-}$ structures has been reported; the anion $[\gamma\text{-SiW}_{10}\text{O}_{36}]^{8-}$ reacting with either trimethoxy- or triethoxysilanes $\text{RSi}(\text{OR}')_3$ in the presence of hydrochloric acid to give $[\gamma\text{-SiW}_{10}\text{O}_{36}(\text{RSi})_2\text{O}]^{4-}$ and $[\gamma\text{-SiW}_{10}\text{O}_{36}(\text{RSiO})_4]^{4-}$ with the stoichiometry of the reactants determining which product is formed.²⁸ Although the anion $[\gamma\text{-PW}_{10}\text{O}_{36}]^{7-}$ is unstable in aqueous solution, one study found that $[\text{PW}_{10}\text{O}_{36}(t\text{BuSiOH})_2]^{3-}$ was easily prepared from the reaction of $[\gamma\text{-PW}_{10}\text{O}_{36}]^{7-}$ with $t\text{BuSiCl}_3$ under phase-transfer conditions, the structure being confirmed by NMR and single crystal XRD crystallography. Like

the other ‘open structures’ this anion can undergo a further reaction with smaller organochlorosilanes to obtain the capped structure, $[\text{PW}_{10}\text{O}_{36}(\text{tBuSiO})_2(\text{SiMe}_2)]^{3-}$ (Figure 1.6).²⁹

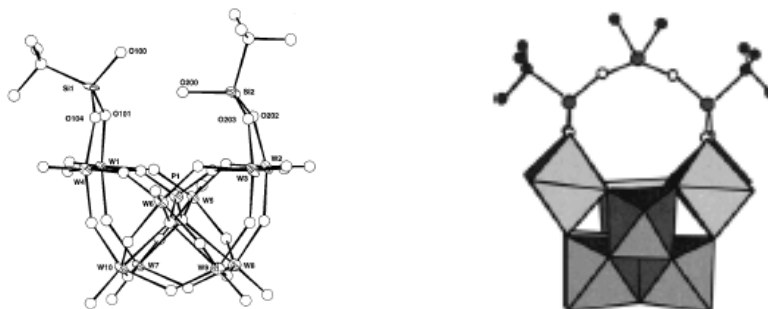


Figure 1.6. (a) Structure of $[\gamma\text{-PW}_{10}\text{O}_{34}(\text{tBuSiOH})_2]^{3-}$ and (b) postulated structure of $[\gamma\text{-PW}_{10}\text{O}_{34}(\text{tBuSiO})_2(\text{SiMe}_2)]^{3-}$.

1.3.2 Derivatization with Phosphonic acids

Hill *et al.* reported the formation of phenylphosphoryl derivatives of undecatungstophosphate and undecatungstosilicate (11-tungsten) from the reaction of the lacunary complexes $[\alpha\text{-XW}_{11}\text{O}_{39}]^{(12-n)-}$ ($\text{X} = \text{Si}$ or P) with “ $\text{PhP}(\text{O})^{2+}$ ” prepared either from phenylphosphonoyl dichloride ($\text{PhP}(\text{O})\text{Cl}_2$) or dichlorophenylphosphine (PhPCl_2) and AgNO_3 . The product $[\text{XW}_{11}\text{O}_{39}(\text{PhPO})_2]^{n-}$ ($\text{X} = \text{P}$, $n = 3$; $\text{X} = \text{Si}$, $n = 4$) was confirmed by multinuclear (^1H , ^{31}P , ^{183}W) NMR spectroscopy and X-ray crystallography, this being the first example of a X-ray structure obtained for an organically modified lacunary Keggin polyoxometalate that does not show severe disorder. The structure consists of the $[\text{PW}_{11}\text{O}_{39}]^{7-}$ anion with two PhPO^{2+} groups each attached via two W-O-P bonds to two oxygen atoms in the vacant site. The reaction with the electrophilic phosphonic acid $\text{PhP}(\text{O})(\text{OH})_2$ did not give any organic derivatization indicating that a highly electrophilic $\text{PhP}(\text{O})^{2+}$ moiety is needed.³⁰

The first investigation into the direct reaction of lacunary polyoxotungstates with organophosphonic acids was reported by Mayer and Thouvenot in 1998.³¹ The triply vacant anion $[\text{PW}_9\text{O}_{34}]^{9-}$ was suspended in a acidified acetonitrile solution containing organophosphonic

acid ($\text{RPO}(\text{OH})_2$) and tetra-butylammonium bromide (NBu_4Br) and this led to the hybrid organic-inorganic species $[\text{PW}_9\text{O}_{34}(\text{RPO})_2]^{5-}$ being obtained as the product. Although the starting anion $[\text{PW}_9\text{O}_{34}]^{9-}$ is trivacant, only a doubly derivatized product was obtained. This was confirmed by multinuclear NMR (^{31}P , ^{183}W) spectroscopy, as the coupling suggested that the structure consists of an $[\alpha\text{-PW}_9\text{O}_{34}]^{9-}$ unit with two RPO^{2+} groups grafted onto it, each through two P-O-W bridges with the two intact terminal oxygen being adjacent (Figure 1.7). Crystals suitable for XRD analysis could not be obtained.

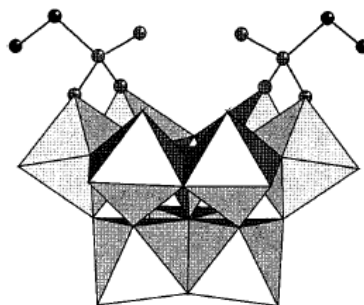


Figure 1.7. Representation of $[\text{PW}_9\text{O}_{34}(\text{RPO})_2]^{5-}$.³¹

Similar compounds of the formula $[\text{PW}_9\text{O}_{34}(\text{R})_2]^{5-}$ ($\text{R} = \text{C}_6\text{H}_5\text{P}(\text{S})$, $\text{C}_6\text{H}_{11}\text{P}(\text{O})$) were synthesized in 1999 by Liu *et al.* these being prepared by reaction of the lacunary polyoxometalate with phosphonyl dichlorides ($\text{C}_6\text{H}_5\text{P}(\text{S})\text{Cl}_2$ or $\text{C}_6\text{H}_{11}\text{P}(\text{O})\text{Cl}_2$). These are more electrophilic than the phosphonic acids, but still only give doubly derivatized products.³²

Also in 1999, Thouvenot *et al.* reported the first fully saturated polyoxometalate species derivatised with phosphonic acids. This was obtained from the divacant anion $[\gamma\text{-HSiW}_{10}\text{O}_{36}]^{8-}$ again using an acidified acetonitrile solution containing the appropriate phosphonic acid and tetra-butylammonium bromide, producing the fully saturated hybrid $[\gamma\text{-SiW}_{10}\text{O}_{36}(\text{RPO})_2]^{4-}$ ($\text{R} = \text{H}$, Et, *n*-Bu, *t*-Bu, $(\text{CH}_2)_2\text{COOH}$ or Ph).³³ These hybrids were characterised by multinuclear NMR and although most crystals obtained were poorly diffracting and/or twinned so could not be

used for X-ray structural determination, a suitable crystal was obtained for the phenyl derivative using a mixture of $\text{NBu}_4^+/\text{NEt}_4^+$ cations in a 2:1 ratio. The structure shows the anion to be built from $[\gamma\text{-SiW}_{10}\text{O}_{36}]^{8-}$ with two phenylphosphoryl groups (PhPO^{2+}) each linked to the two oxygen atoms on the two edge shared WO_6 octahedra (Figure 1.8).

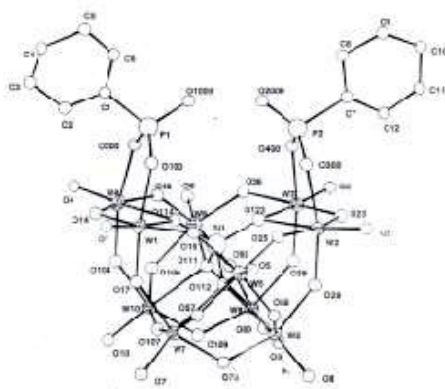


Figure 1.8. The structure of $[\gamma\text{-SiW}_{10}\text{O}_{36}(\text{phenylPO})_2]^{4-}$.³³

Derivatization of the lacunary anion $[\text{SiW}_{11}\text{O}_{39}]^{8-}$ using phosphonic acids was reported in 2003, showing that the method previously used to produce both $[\text{PW}_9\text{O}_{34}(\text{RPO})_2]^{5-}$ and $[\gamma\text{-SiW}_{10}\text{O}_{36}(\text{RPO})_2]^{4-}$ could be used to produce $[\text{SiW}_{11}\text{O}_{39}(\text{RPO})_2]^{4-}$ (R= C_6H_{11} , PhCH_2 , PhCH_2CH_2 or $\text{H}_2\text{NCH}(n\text{-Pr})$).³⁴

More recently in 2007, methyl/ethyl phosphonic acids have been used to synthesize molybdophosphates with an inverted-Keggin structure (Figure 1.9).¹¹

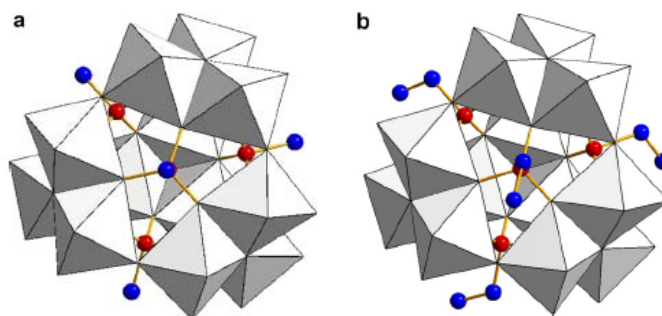
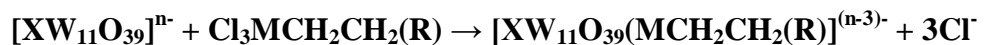


Figure 1.9. Representation of $[(\text{RPO}_3)_4\text{Mo}_{12}\text{O}_{34}]^{4-}$, (a) $\text{R} = \text{Me}$, (b) $\text{R} = \text{Et}$, these anions have an inverted kegglin structure.¹¹

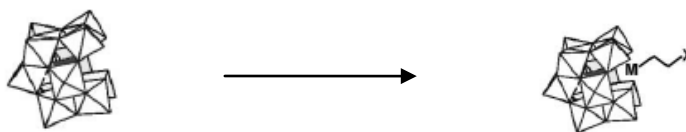
1.3.3 Derivatization with organotin/organogermanium

Other examples of heteroatoms being used as linkers for attachment of organic moieties to a polyoxotungstate unit include tin and germanium. This is easily achieved by reaction of RMCl_3 ($\text{M} = \text{Sn}$ or Ge) in a similar way to trichlorosilanes and results in anions in which missing WO_6 octahedra have been replaced by MR groups.³⁵

The anion $[\text{XW}_{11}\text{O}_{39}]^{n-}$ reacts with one RMCl_3 to give a product which has one MR group grafted on to the structure replacing the missing WO_6 octahedra (Scheme 1.5.).



($\text{X} = \text{Si}, \text{Ge}$ or Ga ; $\text{M} = \text{Si}$ or Ge ; $\text{R} = \text{COOH}, \text{COOCH}_3, \text{CONH}_3$ or CN)



Scheme 1.5.

The structures have been confirmed by multinuclear NMR spectroscopy (^1H , ^{13}C , ^{119}Sn and ^{183}W) although a mixture of isomers is present. The formation of a complex was achieved using this method to attach four polyoxometalates to the oligomer pentaerythritol tetraacrylate $(\text{Cl}_3\text{GeCH}_2\text{CH}_2\text{COOCH}_2)_4\text{C}$ (Figure 1.10).³⁵

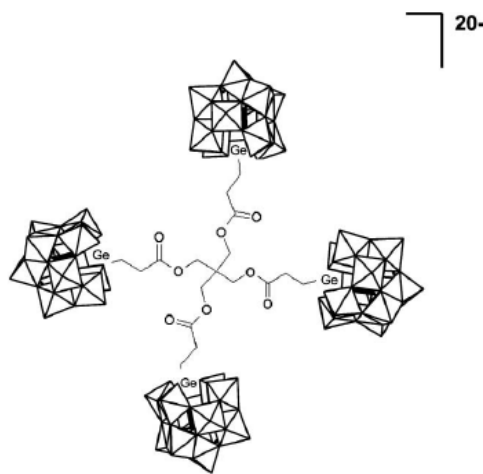


Figure 1.10. Representation of $[\text{SiW}_{11}\text{O}_{39}(\text{GeCH}_2\text{CH}_2\text{COOCH}_2)_4]^{20-}$.³⁵

The reaction of the divacant $[\text{SiW}_{10}\text{O}_{36}]^{8-}$ with PhSnCl_3 does not yield the expected $[\text{SiW}_{10}\text{O}_{36}(\text{SnR})_2]^{8-}$ anion, instead two tin atoms are sandwiched between two $[\text{SiW}_{10}\text{O}_{36}]^{8-}$ groups, each tin atom being bound by two oxygen atoms from each $[\text{SiW}_{10}\text{O}_{36}]^{8-}$ group. The phenyl groups point away from the structure with water molecules also acting as ligands to the tin atoms resulting in an octahedral coordination (Figure 1.11).³⁶

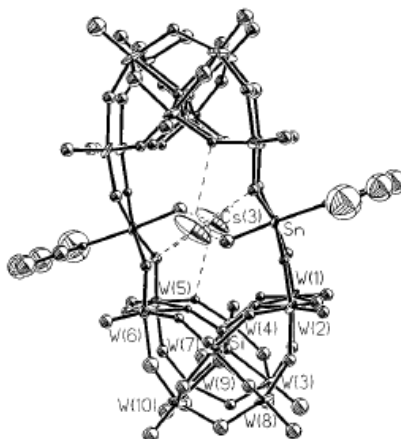


Figure 1.11. Structure of $[(\gamma\text{-SiW}_{10}\text{O}_{36})_2(\text{PhSnOH}_2)_2] \cdot 36$.

A similar sandwich-type structure was obtained by reaction of organotin chloride (RSnCl_3) with trivacant $[\text{PW}_9\text{O}_{34}]^{9-}$ to give $[(\text{RSn})_3(\text{PW}_9\text{O}_{34})_2]^{12-}$.³⁷ However, Wang *et al.* investigated the reaction with the analogous $[\text{SiW}_9\text{O}_{34}]^{10-}$ anion and found that both $[(\text{RSnO})_3(\text{SiW}_9\text{O}_{34})]^{4-}$ and a sandwich complex $[(\text{RSn})_3(\text{SiW}_9\text{O}_{34})_2]^{14-}$ could be obtained depending on the initial ratio of RSnCl_3 and $[\text{SiW}_9\text{O}_{34}]^{10-}$.³⁸ Recently in 2008, $\text{C}_6\text{H}_5\text{SnCl}_3$ has been reacted with the trivacant 9-tungstogermanate $[\alpha\text{-GeW}_9\text{O}_{34}]^{10-}$ to form the single hybrid polyanion $[\{(\text{C}_6\text{H}_5)\text{Sn}(\text{OH})\}_3(\alpha\text{-GeW}_9\text{O}_{34})]^{4-}$ regardless of the ratio of the reactants;³⁹ the different products show how a small modification can alter the reactivity of the precursor.

A different technique for the synthesis of organotin polyoxometalate hybrids has been proposed recently by Neumann *et al.* involving two steps; firstly the vacant site in the lacunary

polyoxometalate is filled by a Sn-Cl moiety, which then reacts with excess amine to give an organopolyoxometalate hybrid.⁴⁰

Large structures based on twelve $[XW_9O_{34}]^{n-}$ anions linked via organotin groups using the precursor $(CH_3)_2SnCl_2$ have also been obtained (Figure 1.12).^{41,42}

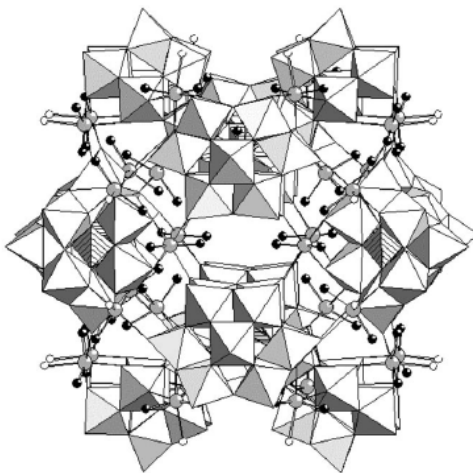


Figure 1.12. Representation of $[\{Sn(CH_3)_2(H_2O)\}_{24}\{Sn(CH_3)_2\}_{12}-(A-XW_9O_{34})_{12}]^{36-}$ ($X = P$ or As).⁴²

1.3.4 Other Derivatives

Various other examples of heteroatoms being used as a linker for the addition of organic groups on to a polyoxometalate structure exist, one such example is the use of chromium (III) in groups on to a polyoxometalate structure exist, one such example is the use of chromium (III) in $[\gamma-SiW_{10}O_{36}(OH)Cr_2(OOCCH_3)_2(OH_2)_2]^{5-}$, this is prepared by the reaction of the lacunary anion $[SiW_{10}O_{36}]^{8-}$ with $[Cr(OH_2)_6]^{3+}$ in buffer solutions and introduces magnetic behaviour to the anion. The structure of this anion consists of two CrO_6 octahedra each attached to two surface oxygen atoms of the $[SiW_{10}O_{36}]$ unit, the CrO_6 octahedra are further linked by two bridging acetate groups. Attempts to link the $[\gamma-SiW_{10}O_{36}]$ Keggin anions together by the addition of dicarboxylic acids which could coordinate with the chromium(III) were unsuccessful (Figure 1.13).⁴³

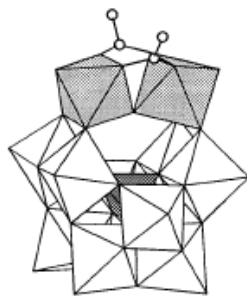
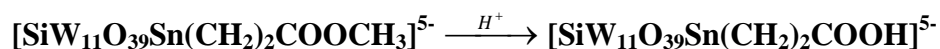


Figure 1.13. Structure of $[\gamma\text{-SiW}_{10}\text{O}_{36}(\text{OH})\text{Cr}_2(\text{OOCCH}_3)_2(\text{OH}_2)_2]^{5-}$, the CrO_6 octahedra are shown in grey.⁴³

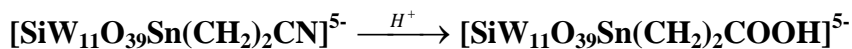
1.4 Reactions of the R groups

The addition of an organic ‘R’ group to the POM can introduce the possibility for further reaction, thus increasing the range of derivatives available. Reactions on the ‘R’ groups on polyoxotungstates functionalized using tin linkers, show the main unit to be unaffected by the conditions used. Hydrolysis of $-\text{COOCH}_3$ to $-\text{COOH}$ has been observed by refluxing the ester in a pH 1.6 solution for 40 minutes (Scheme 1.6).



Scheme 1.6.

Hydrolysis of $-\text{CN}$ to $-\text{COOH}$ has also been observed, however this required more severe conditions (pH 0.8) and even after refluxing for 11 hours only a 50 % conversion was seen (Scheme 1.7).⁴⁴



Scheme 1.7.

The polyoxometalate unit remains unchanged under these conditions showing its stability in acidic conditions, in fact they were found to be stable (monitored by Sn-NMR) in solutions upto pH 6.7, but irreversibility changed at pH 7.⁴⁴

Esterification and amidation of carboxylate derivatives has been achieved by coupling reactions. A large number of amines have been reacted with the functionalized Wells-Dawson polyoxotungstate $[\alpha\text{-P}_2\text{W}_{17}\text{O}_{61}(\text{Sn}(\text{CH}_2)_2\text{COOH})]^{7-}$ the ease of the reaction depending on the complexity of the amine, with most showing conversion of > 50 %, although degradation of the products or isomersion was observed in some cases (Table 1.1).^{45,46}

Table 1.1. Coupling of amines to α_2 -Wells Dawson polyoxotungstates functionalised with a carboxylic acid group.⁴⁵

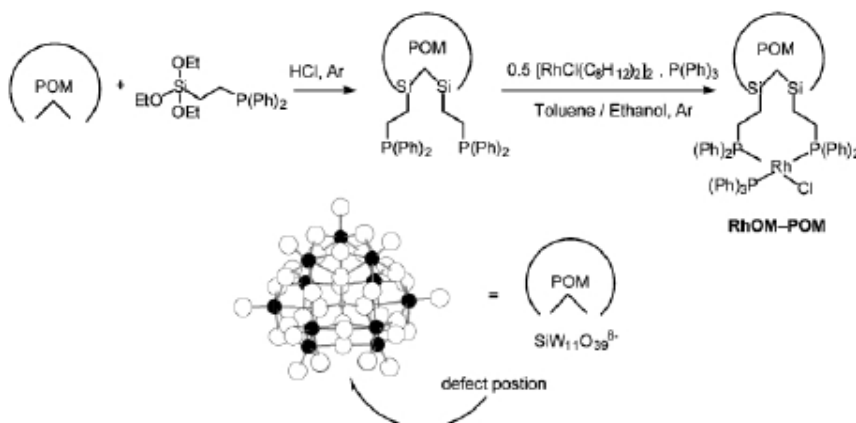
Reaction scheme: $\alpha_2\text{-P}_2\text{W}_{17}\text{O}_{61}\text{Sn}(\text{CH}_2)_2\text{COOH}^{7-}$ (3) + XH (n equiv) $\xrightarrow{\text{EEDQ, MeCN, } \Delta}$ $\alpha_2\text{-P}_2\text{W}_{17}\text{O}_{61}\text{Sn}(\text{CH}_2)_2\text{COX}^{7-}$ (6a-h)

Entry	XH	n	t [h]	Product, yield [%]
1	BnNH ₂	3	4	6a , 86
2	Bn ₂ NH	2	8	6b , 90
3	<i>i</i> Pr ₂ NH	3	12	6c , 80
4	$(\text{H}_2\text{N}-\text{CH}_2-\text{CH}_2-\text{O}-\text{CH}_2)_2\text{O}$	6	140	6d , 70
5	$\text{H}_2\text{N}-\text{C}_6\text{H}_4-\text{NH}_2$	6	120	6e , 66
6	$\text{H}_2\text{N}-\text{CH}_2-\text{CH}_2-\text{NH}_2$	7	120	[a]
7	$\text{H}_2\text{N}-\text{CH}_2-\text{CH}_2-\text{CH}_2-\text{CH}_2-\text{CO}_2\text{H}$	3	36	6f , 50
8		3	36	6g , 90
9	BnOH	2	12	6h , 86

[a] Maximum conversion was 80 %. Rapid degradation followed. EEDQ = 2-ethoxy-1-ethoxycarbonyl-1,2-dihydroquinoline.

In 2003, Neumann *et al.* used the organosilane $(\text{OEt})_3\text{SiCH}_2\text{CH}_2\text{PPh}_2$ to synthesize $[\text{SiW}_{11}\text{O}_{39}(\text{O}(\text{SiCH}_2\text{CH}_2\text{PPh}_2)_2)]^{4-}$. The functionality on this anion was reacted with a rhodium complex in the presence of $\text{P}(\text{Ph})_3$ and gave the Wilkinson's type-polyoxometalate hybrid compound $[\text{SiW}_{11}\text{O}_{39}(\text{O}(\text{SiCH}_2\text{CH}_2\text{PPh}_2)_2)\text{PPh}_3\text{Rh}(\text{I})\text{Cl}]^{4-}$ (Scheme 1.8). The catalytic efficiency of the rhodium site was enhanced compared to the classic $(\text{Ph}_3\text{P})_3\text{Rh}(\text{I})\text{Cl}$ Wilkinson's catalyst

probably due to the improved stability of the intermediate Rh(III) species provided by the alkyl chains, the hybrid species having advantages due to their potential for dual applications and by providing a means of separation such as nanofiltration or phase separation.⁴⁷



Scheme 1.8. Synthetic scheme for the preparation of a rhodium based metal-organic-polyoxotungstate hybrid.⁴⁷

1.5 On Surfaces

POM materials of the formula $[\gamma\text{-SiW}_{10}\text{O}_{36}(\text{HS}(\text{CH}_2)_3\text{Si})_2\text{O}]^{4-}$ have been synthesized and covalently linked to gold particles by use of the thiol group. The nano hybrid systems are stable in solution and have been characterized by powder XRD, transmission electron microscopy (TEM) and UV/vis spectroscopy along with IR and NMR spectroscopy confirming the presence of the $[\text{POM}(\text{SH})_2]^{4-}$ moiety.⁴⁸

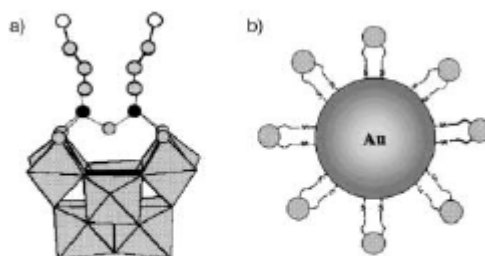
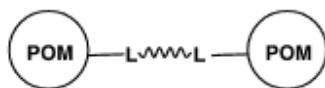


Figure 1.14. (a) The difunctionalised $[\text{SiW}_{10}\text{O}_{36}(\text{RSi})_2\text{O}]^{4-}$ ($\text{R} = \text{HS}(\text{CH}_2)_3$) and (b) an picture of it linked through S-Au bridges to an Au nanoparticle.⁴⁸

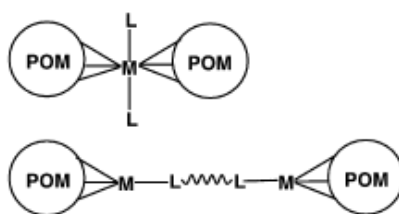
1.6 Immobilisation of POMs

Linking POMs to build solid state materials is of great interest from a structural point of view for developing their properties for applications. The main approaches for these linkages are;



Scheme 1.9.

1. Through an organic ligand, normally involving a coupling reaction of the organic derivatives on the POM anions (Scheme 1.9.).



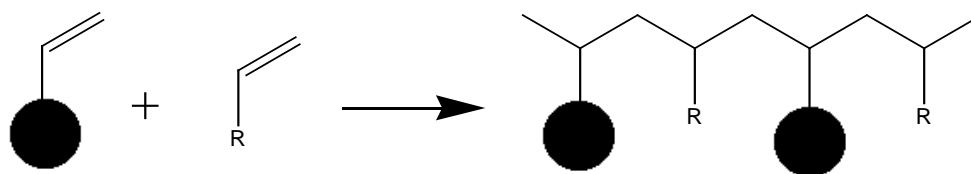
Scheme 1.10.⁴⁹

2. Through coordination by use of a self assembly approach, often involving metal ions acting as linker atoms. This can be either by direct coupling to the metal ion or through use of an intermediate bidentate organic ligand (Scheme 1.10).
3. A third approach is to treat a polyoxometalate containing two nucleophilic sites with a bis(electrophilic) group. This has been done using the divacant $[\gamma\text{-SiW}_{10}\text{O}_{36}]^{8-}$ anion and bis(phosphonate) $\text{H}_2\text{O}_3\text{PCH}_2(\text{C}_6\text{H}_4)_n\text{CH}_2\text{PO}_3\text{H}_2$ ($n=1,2$) in acidic solution to produce the corresponding polymer with monomer unit $[\gamma\text{-SiW}_{10}\text{O}_{36}(\text{O}=\text{PCH}_2(\text{C}_6\text{H}_4)_n\text{CH}_2\text{P}=\text{O})]^{8-}$.⁵⁰

1.6.1 Polymeric Species

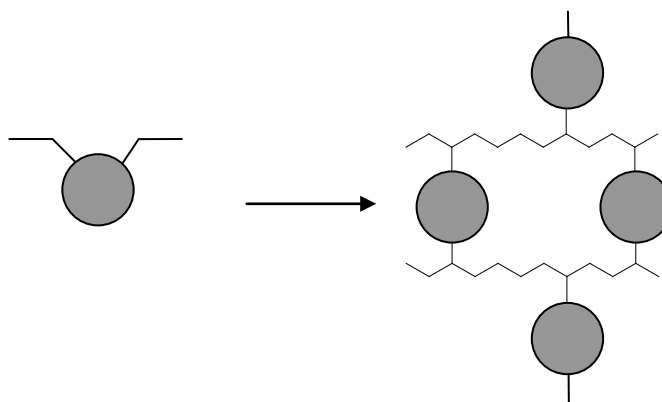
Modified polyoxometalates with functional groups containing double bonds can be used as precursors to produce polymeric materials through free-radical polymerisation.

The way the cluster is functionalised will influence the material produced.



Scheme 1.11.

1. Monofunctionalized polyoxometalates give a polymer backbone with the polyoxometalate units as pendent's to the main chain (Scheme 1.11). An example being the styrylimido-hexamolybdate $[\text{Mo}_6\text{O}_{18}(\text{NC}_6\text{H}_5\text{CH}=\text{CH}_2)]^{2-}$ anion which was co-polymerized with 4-methyl-styrene using the radical initiator AIBN to give a polymethylstyrene backbone with the polyoxometalate as a pendent.⁵¹



Scheme 1.12.

2. Bifunctionalized polyoxometalates with two functional organic groups can react at both ends and act as cross-linkers between polymer chains, producing disordered polymeric materials with the polyoxometalate units incorporated into the main-structure (Scheme 1.12). The first inorganic-organic polymers based on polyoxometalate units reported by Judeinstein in 1992⁵² were synthesized in this way using organically modified Keggin polyoxometalates $[\text{SiW}_{11}\text{O}_{39}(\text{RSi})_2\text{O}]^{4-}$ each with two bifunctional organosilane groups (R = vinyl, allyl, methacryl or styryl). Polymerization occurred via polyoxometalate radicals which are formed using radical initiators, the radicals form polymers with the

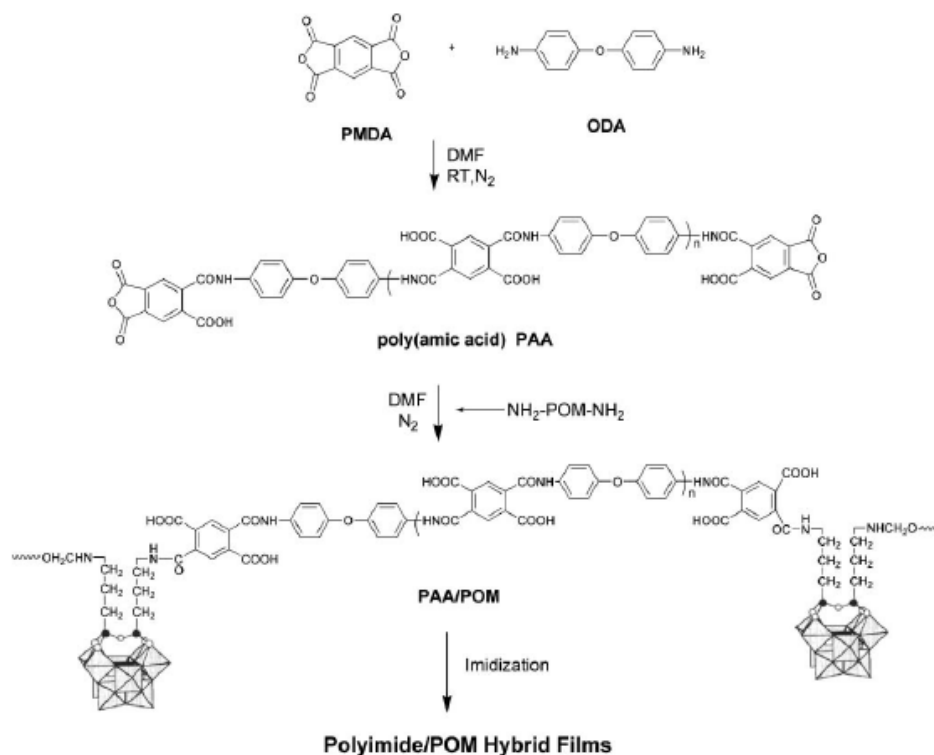
polyoxometalate units connected through their functional groups in various different spatial repetitions. The nature of the solvent and type and ratio of initiator influences the polymerization yield as does the functional group, with reactivity increasing in the order $R = \text{vinyl (polymerization yield 5\% in DMF)} \ll \text{allyl (20\%)} < \text{methacryl (65-70\%)} < \text{styryl (100\%)}$. The materials produced have been shown to have properties characteristic of the POM structure with two successive one-electron processes being observed in the cyclic voltamogram and UV irradiation turning the solutions blue.

In 2000, Mayer and Thouvenot produced a NBu_4^+ salt of the hybrid $[\gamma\text{-SiW}_{10}\text{O}_{36}(\text{H}_2\text{C}=\text{C}(\text{CH}_3)\text{C}(\text{O})\text{OPrSi})_2\text{O}]^{4-}$ and found that free radical polymerization of this product with ethyl methacrylate in acetonitrile produced a cross-linked polymeric network where the POM anion acts as a cross-linker between poly(ethyl methacrylate) chains.⁵¹ The polymeric materials were not soluble, but swelled in certain solvents to give gels where the quantity of solvent absorbed into the materials was found to be dependent on the cross-linking density of the materials, set by the initial POM to ethyl methacrylate ratio and reached a maximum of 58.4 g/g (grams of solvent per gram of dry gel). The sodium salt of this POM was produced later in the same year and being water soluble allowed hydrogels to be produced upon polymerization with acrylamide, the POM unit again acting as a cross-linker. The degree of swelling was found to depend on the initial ratio of monomers present, reaching the range for super-absorbent materials (up to 268 g/g).⁵³ Preparation of these hydrogels in the presence of maghemite nanoparticles ($\gamma\text{-Fe}_2\text{O}_3$) gives super-absorbent materials with magnetic properties increasing the properties and potential applications for the materials.⁵⁴

Polymers of this type have also been produced using other types of bifunctionalised POM clusters. The Lindqvist organoimido-polyoxomolybdate $[\text{Mo}_6\text{O}_{18}(\text{NAr})_2]^{2-}$ was used to produce a conjugated polymer with the POM unit in the main-chain. A different method of synthesis involving a Pd-catalyzed coupling reaction was used giving a conjugated oligomer with about 18 repeating units.^{55,56}

Recently the organosilyl-modified dawson POM $[\alpha_2\text{-P}_2\text{W}_{17}\text{O}_{61}(\text{H}_2\text{C}=\text{C}(\text{CH}_3)\text{COO}(\text{CH}_2)_3\text{Si})_2\text{O}]^{6-}$ has been polymerized with methyl methacrylate, employing a free-radical polymerization approach using AIBN in acetonitrile. Different ratio's of POM to methyl methacrylate were used giving co-polymers with varying cross-linking densities and therefore varying mechanical properties. Exchange of the cations for H^+ (using a cation-exchange resin column) before polymerization resulted in a free-acid polymer where the acidity of the monomer unit is retained upon polymerization.⁵⁷

3. Another approach to co-polymerization was used by Yang *et al.* in 2007, where a POM functionalised with two amine groups $[\text{SiW}_{10}\text{O}_{36}(\text{H}_2\text{N}(\text{CH}_2)_3\text{Si})_2\text{O}]^{8-}$ was covalently incorporated into polyimide chains by reaction with poly(amic acid) to give a hybrid film (Scheme 1.13).⁵⁸



Scheme 1.13. Preparation of polyimide/POM hybrid films.⁵⁸

1.6.2 Crystalline Networks

Linking POM anions to build materials with long range order can be done by coordination using a self assembly approach, often by using metal ions. Examples based on a link to the external oxygen atoms of POMs giving chain structures have been observed, examples being $[\text{UMo}_{12}\text{O}_{42}]^{8-}$ with Th^{4+} ions,⁵⁹ $[\text{Mo}_8\text{O}_{27}]^{6-}$ with Eu^{3+} ions,⁶⁰ and $[\text{P}_2\text{W}_{18}\text{O}_{62}]^{6-}$ with Gd^{3+} ions.⁶⁰

The first characterized compound containing a chain of Keggin polyoxoanions was $(\text{ET})_8[\text{PMnW}_{11}\text{O}_{39}] \cdot 2\text{H}_2\text{O}$ (ET = bis(ethylenedithio)tetrathiafulvalene), this was reported by Coronado *et al.* in 1995.⁶¹ It was made up of undecatungstate anions with the vacant site being filled by a Mn-O group, this group connecting to a tungsten atom on an adjacent anion through a Mn-O-W bridge and these interactions extending through the structure forming ordered chains. This effect only happens for the Mn derivatives, with ET salts made from other derivatives

forming a sub lattice containing discrete Keggin units.⁶² A similar chain was observed for the NEt_4^+ salt of $[\text{PCoW}_{11}\text{O}_{39}]^{5-}$.⁶³ The sodium salt of the lacunary Keggin tungstate $[\text{XW}_{11}\text{O}_{39}]^{8-}$ has Na^+ ions coordinating to the oxygen atoms in the vacant site, the Na^+ completing its octahedra coordination through a linkage to an oxygen atom on an adjacent $[\text{XW}_{11}\text{O}_{39}]^{8-}$ anion, thus forming a chain running through the structure (Figure 1.15).^{64,65}

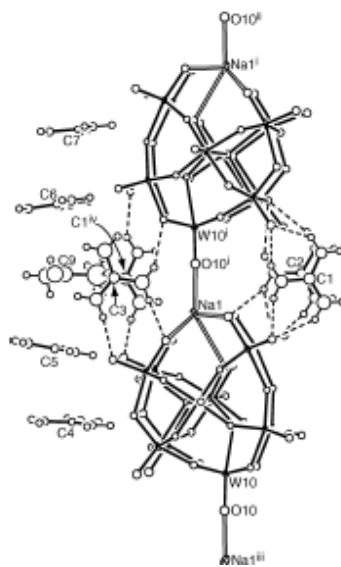


Figure 1.15. The chain structure of $[\text{SiW}_{11}\text{O}_{39}]^{8-}$ linked by Na^+ , stabilised by coordination to cation and solvent molecules.⁶⁵

POMs have been linked by the coordination of bidentate organic ligands to a transition metal or lanthanide group attached to the POM unit. This approach has been used to obtain 1D frameworks such as those given by $[\epsilon\text{-PMo}_{12}\text{O}_{37}(\text{OH})_3\{\text{La}(\text{H}_2\text{O})_4(\text{C}_5\text{H}_6\text{O}_4)_{0.5}\}_4]\cdot 2\text{H}_2\text{O}$ with glutarate ($\text{C}_5\text{H}_6\text{O}_4^{2-}$) linkers and by $[\epsilon\text{-PMo}_{12}\text{O}_{37}(\text{OH})\{\text{La}(\text{H}_2\text{O})_6\}_2\{\text{La}(\text{H}_2\text{O})_5(\text{C}_4\text{O}_4)_{0.5}\}_2]\cdot 17\text{H}_2\text{O}$ with squarate ($\text{C}_4\text{O}_4^{2-}$) linkers.⁴⁹

Networks containing POMs can also be obtained using ionic interactions, examples including the assemblies formed from calix[4]arene- Na^+ complexes and Keggin POMs. The Na^+ ions bind with the organic moiety by a host-guest interaction; generating a three-dimensional grid

like structure in the solid state, which acts as a surrounding for the $[\alpha\text{-PW}_{12}\text{O}_{40}]^{3-}$ anions, binding to them through weak intermolecular interactions or Na-O coordinative bonds.⁶⁶

Cationic frameworks have also been obtained using the copper complex $[\text{Cu}(\text{bipy})_2(\text{H}_2\text{O})_2]^+$ (bipy = 2,2'-bipyridine) with POM clusters being trapped in channels created by the coordination polymer network^{67,68,69} or weakly interacting with the framework through Cu-O interactions.⁶⁸

Co-crystallization of POMs with polyammonium cations can give differing results depending on the structure and charge of the polycation. A comparison by Vasylyev *et al.* found that a tri-ammonium cation with short and flexible 'arms' gave an insoluble two-dimensional microporous or channelled structure, whereas a tetra-ammonium cation with an extended and rigid structure gave a lamellar structure.⁷⁰

1.6.3 Other Methods of Immobilisation

Other methods of immobilization have been reported, including using inert supports such as chemically modified silica,^{71,72} mesoporous MCM-41,⁷³ cationic nanoparticles⁷⁴ or cationic polymers⁷⁵ which interact with the polyoxometalate through electrostatic or coordination interactions.

1.7 Techniques

Polyoxometalates are complex systems, methods to analyse these structures include IR, multinuclear NMR, Mass spectrometry, XRD and electrochemistry.

1.7.1 Infrared Spectroscopy

Infrared (IR) spectroscopy is extensively used in polyoxometalate chemistry, the fingerprint region $1000\text{--}400\text{ cm}^{-1}$ has absorptions due to the metal-oxygen stretching vibrations; the positions, shapes and relative intensities of these bands indicates the structure of the material.

1.7.2 NMR

Polyoxometalates can potentially contain a number of NMR active atoms, for example ^1H , ^{13}C , ^{28}Si , ^{31}P , ^{95}Mo and ^{183}W ; studying the NMR spectra for these atoms is useful in determining the structure.

When the central heteroatom is NMR active, information on the structure can be obtained from its NMR spectroscopy. For example, in ^{31}P NMR the signal for a central phosphorus atom appears as a singlet, the chemical shift of which is determined by the shielding of this phosphorus atom which depends on the environment of the oxygen atoms in the central PO_4 tetrahedron. In the fully saturated $[\text{PW}_{12}\text{O}_{40}]^{3-}$ anion the chemical shift for phosphorus is -14.6 or -13.7 ppm dependent on the isomer of the structure,¹⁷ but as tungsten-oxygen octahedra are removed the chemical shift becomes less negative (Table 1.2).

Table 1.2. ^{31}P peak positions for various polyoxotungstates.¹⁷

Tungstophosphates	Chemical Shift (ppm)
A-PW ₁₂	-14.6
B-PW ₁₂	-13.7
A-PW ₁₁	-10.2
B-PW ₁₁	-8.6
A- α -PW ₉	-5.1
A- β -PW ₉	-3.2

This change is due to a change in the environment of the oxygen atoms in the vacant site, this change results in a change to the P-O bond strengths in the central PO_4 and therefore changes the electron density around the phosphorus.⁷⁶ It was observed that filling this vacant site will result in the chemical shift for the phosphorus reverting back to that for the saturated starting material when a metal atom covalently bonds to the site, but not when a cation is ionically bonded to the site.⁷⁶ The relationship between the chemical shift and the saturation of the POM structure can be used to determine the extent of saturation of a complex; for example, the formation of $[\text{PW}_9\text{O}_{34}(\text{RPO})_2]^{6-}$ was inferred by its ^{31}P NMR chemical shift being an intermediate value ($\delta \sim -11$ ppm) between the starting anion $[\text{PW}_9\text{O}_{34}]^{9-}$ ($\delta -5$ ppm) and the fully saturated anion $[\text{PW}_9\text{O}_{34}(\text{tBuSiOH})_3]^{3-}$ ($\delta -15.9$ ppm).³¹

Polyoxotungstates can also be studied using ^{183}W NMR spectroscopy, although observation of tungsten signals can be difficult due to tungsten having a low resonance frequency and a natural abundance of 14.3 % giving a low receptivity. ^{183}W NMR was first introduced into the study of POMs by Baker and co-workers in the late 1970s^{77,78} who showed the Keggin anion $[\text{XW}_{12}\text{O}_{40}]^{(8-n)-}$ to have one very sharp resonance (except for when $\text{X} = \text{P}$ where the signal is split by coupling between the W and P) due to all the tungsten atoms being equivalent. Other isomers of the Keggin structure show a larger number of signals the tungsten atoms no longer being equivalent, the number of signals increasing as the symmetry decreases ($\alpha \rightarrow \beta \rightarrow \gamma$).⁷⁷ Removal of W-O octahedral from the saturated structure produces lacunary anions which have lower symmetry and therefore give more tungsten signals than the parent structure. Occupation of the vacant sites by other atoms does not change the symmetry so the number of signals remains the same, although their positions can be affected.⁷⁶

When the POMs are functionalised with organometallic groups and/or have cations containing an organic species the presence of these groups can be confirmed by ^1H , ^{13}C and where appropriate ^{31}P or ^{28}Si NMR spectroscopy. Extra information on the connections between atoms can be obtained from the coupling between atoms. When phosphorus is the linker atom, coupling between the tungsten atoms and the phosphorus can be observed, the number and integration of these peaks showing the number of connections the phosphorus has to tungsten atoms.⁷⁹ An example of this is the anion $[\text{P}_4\text{W}_{14}\text{O}_{58}]^{12-}$ in which the phosphorus atoms are bonded to four tungsten atoms through P-O-W bonds and the ^{31}P NMR spectrum shows the main peak to be flanked by four satellite peaks, agreeing with the theoretical pattern predicted for a phosphorus bound to four tungsten atoms⁸⁰ using the equation:

$$f_i = \frac{\sigma}{\sigma_i} a^w b^x c^y \dots$$

(Where: σ = symmetry number of the parent molecule, σ_i = symmetry number of particular isomer, a = natural abundance of a isotope, w = times a occurs, b = natural abundance of another isotope, x = times b occurs etc).

In cases where further characterization is not possible multinuclear NMR investigations can be used for structural determination. Organophosphoryl derivatives of formula $[\alpha\text{-PW}_9\text{O}_{34}(\text{RPO})_2]^{5-}$ were characterized using ^{31}P and ^{183}W NMR by detailed study of the spectra and comparison to the theoretical spectra for the possible structures.³¹

1.7.3 Mass Spectroscopy

Mass Spectrometry of POMs can be studied using different techniques, the most common being Matrix-Assisted Laser Desorption/Ionization Time-of-Flight (MALDI-TOF) and Electrospray Ionization mass spectrometry. MALDI-TOF mass spectrometry gives mostly singly-charged species making assignment relatively simple and being useful in determining if dimers or

polymers are present (although non-covalent aggregates can sometimes be formed during the desorption process).⁵⁰ The Maldi-TOF spectra of POMs have certain characteristics, all the signals observed being relatively broad due to partially resolved isotopic patterns from different isotopes of tungsten,²⁸ with resolution depending on both the conditions and the sensitivity of the equipment. Often several signals are observed corresponding to species with different numbers of cations, the charge of the anion being balanced by protons.⁸¹

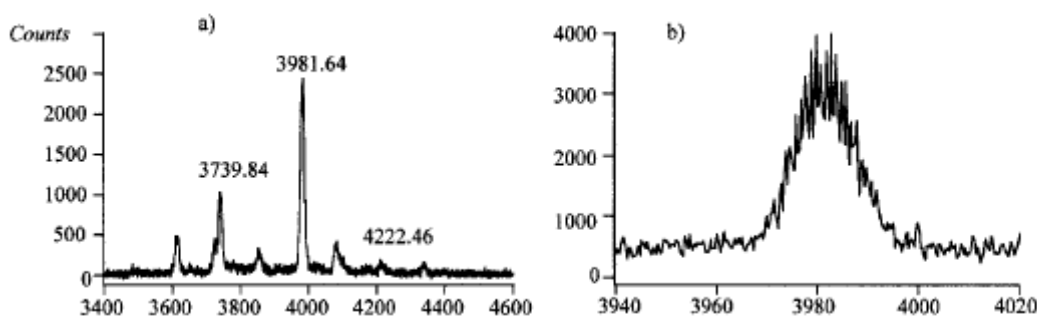


Figure 1.16. Maldi-TOF mass spectra of $(\text{NBu}_4)_3\text{H}[\text{SiW}_{10}\text{O}_{36}(\text{C}_3\text{H}_6\text{OC}(\text{O})\text{C}(\text{CH}_3)=\text{CH}_2)_2]$: a) full spectrum, b) expansion of signal at m/z 3982.²⁸

1.7.4 X-ray Diffraction

Single Crystal X-ray Diffraction (XRD) is a useful technique for determining the structure of crystalline materials, especially for materials which appear similar using other methods of analysis. The first polyoxometalate structure to be solved was $\text{H}_3[\text{PW}_{12}\text{O}_{40}]\cdot 5\text{H}_2\text{O}$ in 1933.⁷ Although further progress was initially slow (only ~25 X-ray diffraction investigations by 1971),⁶ developments in X-ray crystallography now allows for easier structural determination and the number of heteropoly-molybdate and -tungstate structures is vast with a number of structures being discussed previously (Section 1.6.2). The structure is determined by studying the scattering of the X-ray beam after it has gone through a crystal; this gives information on the density of electrons within the crystal and is used to predict the position of atoms within the structure. The

metal ions (W or Mo) within the structure are very large, having a large electron density, and so these tend to dominate the scattering often making identification and location of the other atoms difficult.

1.7.5 Electrochemistry

Polyoxometalates have interesting electrochemical properties, the redox behaviour of the anions giving them potential in various applications including catalysis. Electrochemical techniques give information on the ease of reduction and stability of the reduced species formed.

Polyoxometalates of the Keggin structure can accept a limited number of electrons without decomposition, in general a maximum charge of 8- is possible.^{82,83} The number of reductions observed do not necessarily all correspond to reductions in the charge of the cluster, as in acidic conditions protonation of the anion can be associated with a reduction (this is deduced from the pH dependence of some reductions).^{2,82,84}

The Cyclic Voltammograms are often complex and difficult to interpret due to complex clusters and a large numbers of variables. However in general the reduction potentials of Keggin polyoxometalates are controlled by the following factors;

1. The isomer of the structure; with the reducibility increasing in the order α -, β -, γ -.^{2,85}
2. The central metal atoms (X); mainly due to the difference in the charge of the cluster when different X atoms are present. Increasing the charge makes reduction of the cluster more difficult, electrostatic interactions making the addition of extra electrons more difficult (Figure 1.17).^{2,85}

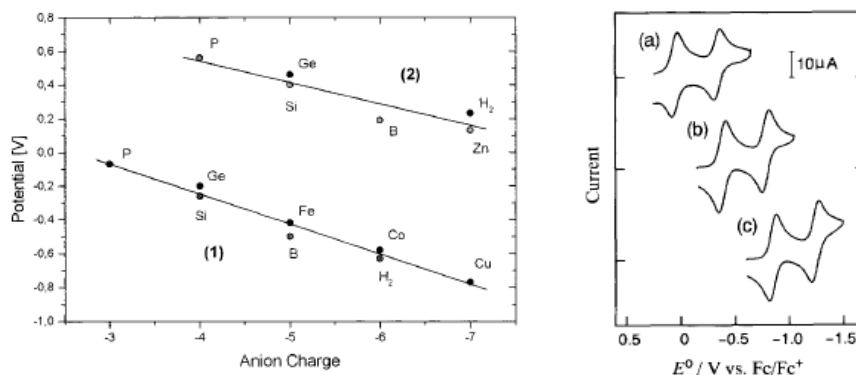


Figure 1.17. (a) The dependence of the first one-electron reduction potentials on negative charge (1) $[\text{XW}_{12}\text{O}_{40}]^{n-}$ and (2) $[\text{XW}_{11}\text{VO}_{40}]^{n-}$,⁸⁵ (b) Cyclic Voltammograms of (a) $[\text{SMo}_{12}\text{O}_{40}]^{2-}$, (b) $[\text{PMo}_{12}\text{O}_{40}]^{3-}$ and (c) $[\text{SiMo}_{12}\text{O}_{40}]^{4-}$.⁸⁶

3. The conditions used; although the combination of these factors is not fully understood, making direct comparisons between results obtained in different conditions difficult. Consideration needs to be taken into the solvent used, the pH of the solution and the reference electrode.

a. Solvent – Organic solvents shift the positions and separations of the reductions relative to one another,⁸⁶ the first one-electron reduction peak potential of the Keggin anion $[\alpha\text{-SiW}_{12}\text{O}_{40}]^{4-}$ in various organic solvents was found to relate to the acceptor number (which describes the lewis acid properties) of the solvent, with the reduced $[\alpha\text{-SiW}_{12}\text{O}_{40}]^{5-}$ being stabilized more easily by solvents with a higher acceptor number (Figure 1.18).⁸⁵

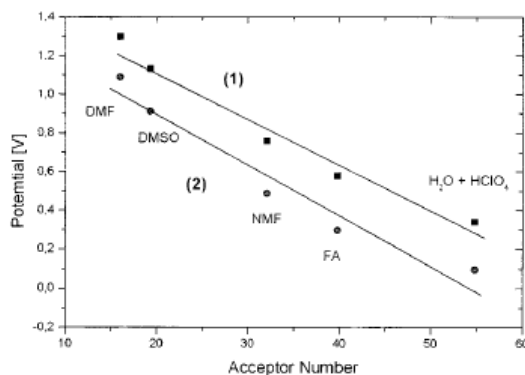


Figure 1.18. Relationship between the first one-electron reduction peak potential of (1) $[\text{SiW}_{12}\text{O}_{40}]^{4-}$ and (2) $[\text{P}_2\text{W}_{18}\text{O}_{62}]^{6-}$ vs. the reduction peak potential of ferrocene and the acceptor number of the solvent (H_2O (54.8) > formamide (39.8) > *N*-methylformamide (32.1) > DMSO (19.3) > DMF (16.0).) Conditions: glassy carbon working electrode, platinum counter electrode.⁸⁵

- b. In aqueous conditions the pH of the solution needs to be considered, as the H^+ protonates the anions and changes the reduction potential (Figure 1.19).

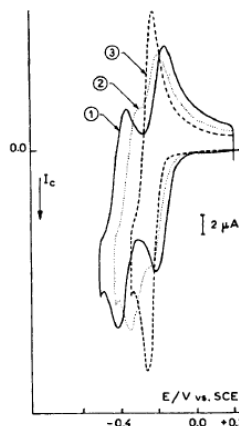


Figure 1.19. The CV of $[\text{SiW}_{12}\text{O}_{40}]^{4-}$ (1mM) with perchloric acid concentration in aqueous solution; (1) 1 M HClO_4 , (2) 4 M HClO_4 and (3) 7 M HClO_4 . Using a glassy carbon working electrode, platinum counter electrode, SCE reference electrode, 100 mV/s.⁸⁵

- c. The Reference electrode varies between reports in the literature, although this does not effect the reduction properties of the species studied it will affect the position at which the peaks appear.

Reversible reductions indicate that only minor structural changes occur during the reduction process; a reduction can be considered by looking at the MO_6 octahedra individually. In the fully saturated parent structure $[\text{XW}_{12}\text{O}_{40}]^{n-}$ the MO_6 octahedra each have one terminal oxygen atom, the molecular orbital diagram (Figure 1.20) shows that an electron added to the metal centre enters into a predominantly non-bonding orbital² and this is therefore easy to do.

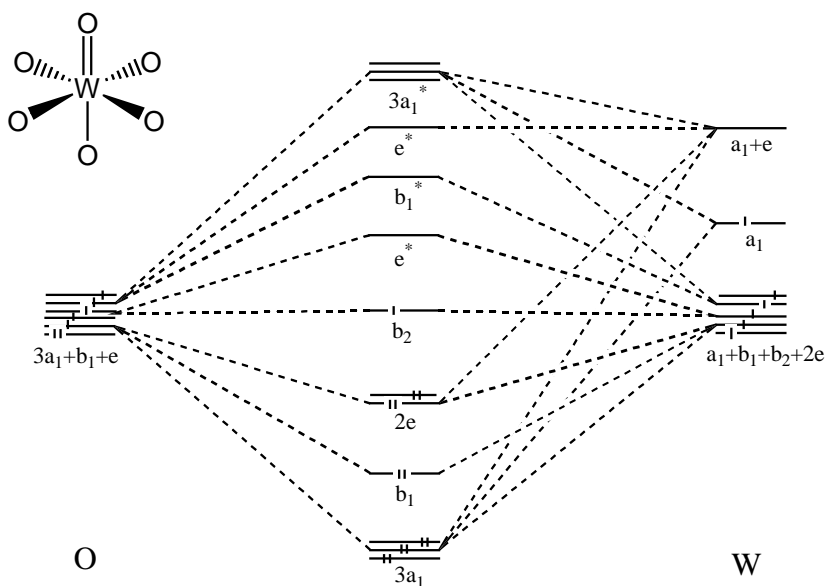
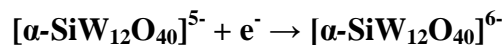
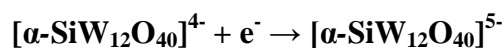


Figure 1.20. Molecular Orbital Diagram for MO_6 when it has one terminal oxygen ($\text{W}=\text{O}$).

The reduction of the Keggin-anion $[\text{SiW}_{12}\text{O}_{40}]^{4-}$ has been studied in aqueous solution and it was found that in acidic solution it has five reduction waves, although only the first three are reversible, the fourth and fifth waves being accompanied by chemical reactions of the complex (Figure 1.21). The first two waves are each due to the addition of one electron to the anion.



The third wave is a two electron wave and at pH 1-5 it is accompanied by protonation of the anion.⁸²



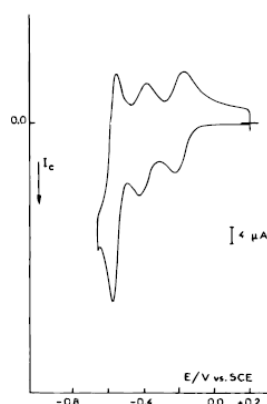


Figure 1.21. Cyclic Voltammogram of $[\text{SiW}_{12}\text{O}_{40}]^{4-}$ in 1 mM HClO_4 aqueous solution. Conditions: glassy carbon working electrode, platinum counter electrode, SCE reference electrode, scan rate 100 mV/s.⁸⁷

Studying the anion $[\text{SiW}_{12}\text{O}_{40}]^{4-}$ in DMF shows the same five reduction waves,^{85,87,88,89} the first two are diffusion controlled, one-electron waves and quasireversible, the third wave being larger and corresponding to about 1.4 electrons.

1.7.5.1 Loss of Octahedra

Cyclic voltammetry for the lacunary $[\text{XW}_{11}\text{O}_{39}]^{(n-4)-}$ anion in both aqueous and organic solvents shows two two-electron waves with the potentials being significantly more negative than those for the first two waves of $[\text{XW}_{12}\text{O}_{40}]^{n-}$ (Figure 1.22 and Table 1.3).

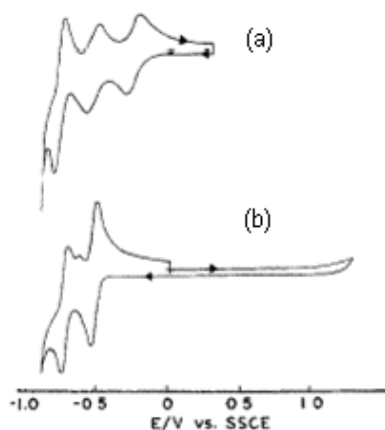


Figure 1.22. Cyclic voltammetry of (a) $[\text{SiW}_{12}\text{O}_{40}]^{4-}$ and (b) $[\text{SiW}_{11}\text{O}_{39}]^{8-}$, in aqueous solution (0.1 M NaClO_4 + 0.01 M HClO_4 , scan rate 50 mV/s.⁹⁰

Table 1.3. Cyclic Voltammetric data (Cathodic peak potentials and cathodic-to-anodic peak separation) in acetonitrile vs. Ag/Ag^+ ; working electrode: glassy carbon; $[\text{M}]$ concentration $1.0 \times 10^{-2} \text{ M}$; supporting electrolyte TBAClO_4 ; scan rate 100 mV/s .⁹¹

	$E^{\circ}_1 \text{ (mV)}$	$E^{\circ}_2 \text{ (mV)}$	$E^{\circ}_3 \text{ (mV)}$
SiW_{12}	-1078 (70)	-1593 (78)	-2289 (92)
SiW_{11}	-1119 (124)	-1626 (124)	-2284 (121)
PW_{12}	-629 (65)	-1170 (73)	-1875 (72)
PW_{11}	-1150 (91)	-1702 (128)	

The range of CV studies on the lacunary Keggin anions is limited, although polarogram studies have been carried out on a wider range of anions derived from the Keggin structure,¹⁴ the peak potentials being comparable to those seen for CV under aqueous conditions.

Table 1.4. The peak potentials seen in polarogram studies for lacunary Keggin anions in 1 M acetic acid – 1 M sodium acetate buffer, pH 4.7, reference electrode SCE (Saturated calomel electrode).¹⁴

	$E^{\circ}_1 \text{ (V)}$	E°_2	E°_3
$[\alpha\text{-SiW}_{12}\text{O}_{40}]^{4-}$	-0.24	-0.48	-0.95
$[\beta\text{-SiW}_{12}\text{O}_{40}]^{4-}$	-0.14	-0.42	-0.78
$[\alpha\text{-SiW}_{11}\text{O}_{39}]^{8-}$	-0.76	-0.93	
$[\beta_1\text{-SiW}_{11}\text{O}_{39}]^{8-}$	-0.63	-0.83	
$[\beta_2\text{-SiW}_{11}\text{O}_{39}]^{8-}$	-0.63	-0.77	
$[\beta_3\text{-SiW}_{11}\text{O}_{39}]^{8-}$	-0.69	-0.89	
$[\gamma\text{-SiW}_{10}\text{O}_{36}]^{8-}$	-0.75	-0.84	
$[\alpha\text{-SiW}_9\text{O}_{34}]^{10-}$	-0.80		
$[\beta\text{-SiW}_9\text{O}_{34}]^{10-}$	-0.82	-0.93	

It can be seen (Table 1.4) that as WO octahedra are lost from the parent $[\text{SiW}_{12}\text{O}_{40}]^{4-}$ anion, the first reduction generally shifts to more negative values, meaning reduction is more difficult. This is due to the increased charge of the cluster, electrostatic interactions making the

addition of electrons harder. Also there is a decrease in the number of WO_6 octahedra that are available to be reduced, considering the individual WO_6 octahedra; when they have one terminal oxygen atom an additional electron enters a predominantly non-bonding orbital, however when the WO_6 octahedra are adjacent to vacant sites they contain two terminal oxygen atoms and the first available orbital for an electron to enter will be an anti-bonding orbital, this will result in large structural changes and be unfavourable.² As the number of WO_6 octahedra lost increases, more of the WO_6 octahedra remaining have two terminal oxygen atoms, so fewer orbitals are available for electrons to enter and reduction is less likely.

1.7.5.2 Derivatized Compounds

Limited studies have been carried out into the electrochemistry of Keggin-type anions derivatised with organic moieties. Thouvenot *et al.* investigated the chromogenic properties of the hybrid polyoxometalate $[\text{PW}_{11}\text{O}_{39}(\text{SiR})_2\text{O}]^{3-}$ ($\text{R} = \text{Et}, (\text{CH}_2)_n\text{CH}=\text{CH}_2$ ($n = 0, 1$ or 4), $\text{CH}_2\text{CH}_2\text{SiEt}_3$ or $\text{CH}_2\text{CH}_2\text{SiMe}_2\text{Ph}$), cyclic voltammetry showing the compounds to have three or four one-electron reduction waves (Figure 1.23).⁹²

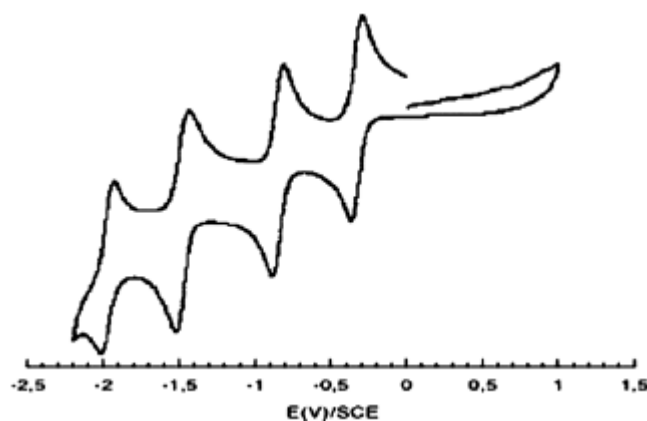


Figure 1.23. Cyclic Voltammogram of $(\text{NBu}_4)_3[\text{PW}_{11}\text{O}_{39}(\text{SiEt})_2\text{O}]$ in acetonitrile.⁹²

The first reduction (-0.32 to -0.40 V) is at a less negative value compared to $[\text{PW}_{11}\text{O}_{39}]^{7-}$ (-0.70 V) due to the lower charge of the complete structure, being at a similar position to the parent $[\text{PW}_{12}\text{O}_{40}]^{3-}$ anion (-0.34 V). The position of the redox potentials was found to be only slightly dependent on the nature of the organic group grafted on to the polyoxometalate unit.⁹²

The lacunary anion $[\alpha\text{-XW}_{11}\text{O}_{39}]^{n-}$ (X = P, B, Si or Ge) has been functionalised by coordination to a transition metal ion M^{m+} (M = Co, Ni, Fe, Cr, Mn or Ir). The electrochemistry of these anions^{91,93,94} shows that the M^{m+} ion has an affect, noticeable shifts with either no obvious correlation between the substituted metal atom and the reduction potentials of the tungsten atoms^{91,85,90,93,95} or small shifts which are influenced by the metal atoms in a more obvious way are reported.^{85,93}

1.7.5.3 Polymers

Electrochemistry has been carried out on a small number of polymeric compounds derived from polyoxometalates. In 1992 Judeinstein produced polymers of $[\text{SiW}_{11}\text{O}_{39}(\text{RSi})_2\text{O}]^{4-}$ (R = vinyl, allyl or methacrylate), and the CV of one polymer in DMF/ NBu_4BF_4 electrolyte showed the characteristic reductions of the polyoxometalate structure to be retained.⁵² A more detailed study on polymers produced from $[\text{Mo}_6\text{O}_{18}(\text{NC}_6\text{H}_2(\text{C}(\text{CH}_3))_2(\text{I}))_2]$ or $[\text{Mo}_6\text{O}_{18}(\text{NC}_6\text{H}_2(\text{C}(\text{CH}_3))_2(\text{C}\equiv\text{CH}))_2]$ also shows the polymers to have similar reduction potentials to their monomer species.⁵²

1.8 Applications

Polyoxometalates have a large number of possible applications including in catalysis, medicine, recording materials (e.g. photography), dyes or pigments and in fire resistance coatings.²⁶ Their use in catalysis is of interest here and will be discussed.

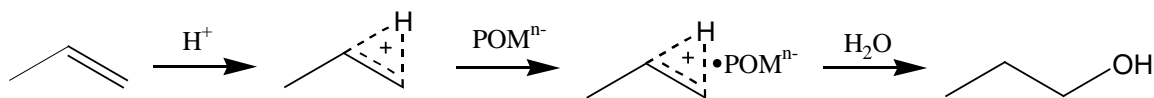
1.8.1 Catalysis

A significant property of polyoxometalates is the ability to accept and release electrons reversibly with little structural rearrangement; this introduces the potential for application as acid and oxidation catalysts. POMs have the advantages of their large versatility in composition, the tunability of their properties, relatively easy preparation and compatibility with environmentally friendly conditions (eg. O₂ and H₂O₂).⁹⁶ They can also possess multifunctionality, a property not found in many materials giving them potential in reactions where different types of synthetic steps are required.¹³ However the use of polyoxometalates in catalysis is limited by two main problems; firstly their weakness in directing the substrate towards the catalytically active centre when used as homogeneous catalysts in solution and secondly their catalytic activities in the solid state being limited due to a low specific surface area making use as heterogeneous catalysts more difficult. One way to overcome these problems is to immobilize polyoxometalates onto a support or entrap them into a matrix,¹⁰ a wide variety of ways in which this can be done having been discussed above. (Section 1.6)

Although, a wide variety of potential uses as catalysts are available,^{13,97} only a few examples will be discussed, focusing on POMs based on the Keggin structure $[XM_{12}O_{40}]^{n-}$ (X = heteroatom, M = W or Mo). Their potential as acid catalysts has been exploited in a number of reactions including alkene hydration, alkane oxidation and epoxidation reactions.⁹⁸ Most include

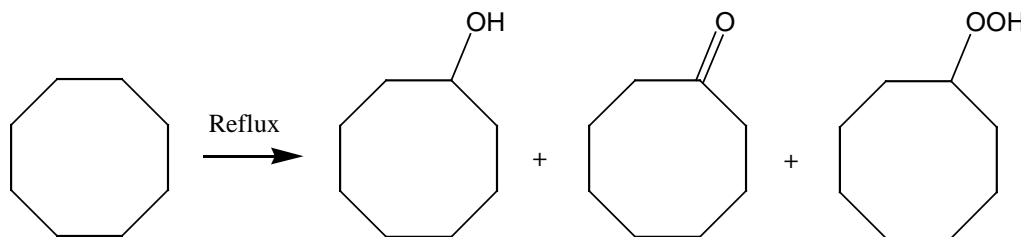
a second transition metal in the structure, although this is not necessary, with good results also being obtained for the lacunary or parent anions.^{99,100}

The first commercial application of a polyoxometalate as a catalyst was for the hydration of the alkene, propene in the manufacture of 2-propanol in 1972.⁹⁸ It has been proposed that the polyoxometalate acts to stabilise the protonated intermediate through coordination as well as speeding up the reaction by means of its acidity (Scheme 1.14).



Scheme 1.14. A proposed reaction pathway for the hydration of propene.

The oxygenation of alkanes using hydrogen peroxide has been studied, an example being the study on the oxidation of cyclooctane⁹⁹ to give a mixture of products (Scheme 1.15).




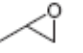

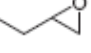
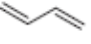
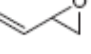





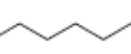
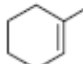
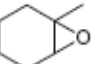




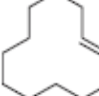
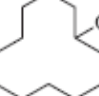
Scheme 1.15. The possible products for the oxidation of cyclooctane.⁹⁹

Good conversions are observed (up to 100 % conversion after 12 hours) with varying selectivity; cyclooctyl hydroperoxide is the major product (100 % selectivity for the SiW_{11} catalyst) with little cyclooctanol being detected in all cases.

Epoxidation of olefins has been performed using hydrogen peroxide and a catalytic POM, an example being $[\gamma\text{-SiW}_{10}\text{O}_{36}]^{8-}$ which has been protonated to give $[\gamma\text{-SiW}_{10}\text{O}_{34}(\text{H}_2\text{O})_2]^{4+}$. This acts as a catalyst for reaction of both cyclic olefins such as cyclohexene and terminal olefins such

as propylene and 1-butene with yields of > 88 % and selectivity of > 99 % to the desired epoxide (Table 1.5).¹⁰⁰

Table 1.5. Epoxidation of various olefins catalysed by $[\gamma\text{-SiW}_{10}\text{O}_{34}(\text{H}_2\text{O})_2]^{4-}$ ¹⁰⁰

Entry	Substrate	Product	Time (h)	Yield (%)
1[b]	 10a	 10b	8	90
2[b]	 11a	 11b	8	88
3[b]	 12a	 12b	9	91
4	 13a	 13b	10	90
5	 14a	 14b	3	>99 (only <i>cis</i>)
6	 15a	 15b	14	91 (only <i>trans</i>)
7	 16a	 16b	4	95
8	 17a	 17b	4	>99 (only <i>exo</i>)
9	 18a	 18b	2	99
10[c]	 19a	 19b	4	97

[a]Reaction conditions: substrate (5mmol), tetra-*n*-butylammonium salt of II (8 μmol), H₂O₂ (30% aqueous, 1 mmol), MeCN (6 mL), 305 K. Yields are based on H₂O₂.

[b]Propylene (6 atm), 1-butene (3 atm), 1,3-butadiene (2.5 atm).

[c]MeCN (9 mL).

1.8.2 Medicine

The correct organic derivative can produce polyoxometalates with antibacterial and antiviral activities which are of use in medicinal applications.

A large number of polyoxometalates have been investigated, although the exact mechanism is unknown it has been found that they interfere with the binding of various viruses

thereby inhibiting the cellular uptake of the virus. This stops the spread of viruses which reproduce in the macrophages of cells before being released to infect other cells.^{101,102} These viruses include human immunodeficiency virus (HIV), herpes simplex virus (HSV), influenza virus (fluV) and respiratory syncytial virus (RSV).

$[(\text{RSnO})_3\text{SiW}_9\text{O}_{34}]^{7-}$ and $[(\text{RSn})_3(\text{SiW}_9\text{O}_{34})_2]^{11-}$ possess antitumoral activity to two human cancer cells Hela and SSMC-7721 without degradation of the polyoxometalate materials. It has been proposed that the antitumoral effect of polyoxometalates is related to a single electron oxidation/reduction, the stronger the oxidation ability the higher the inhibitory effect on the tumor cells.³⁸ This was observed by the sandwich structures being both easier to reduce and having a larger inhibitory effect.

1.9 Project Aims

The properties of polyoxotungstates can be tailored for specific applications by the addition of organic groups which introduce functionality to the clusters. Here lacunary Keggin polyoxotungstates of general formula $[\text{XW}_{10}\text{O}_{36}]^{n-}$ or $[\text{XW}_9\text{O}_{34}]^{m-}$ ($\text{X} = \text{P}$ or Si ; $n = 7$ or 8 ; $m = 9$ or 10) will be investigated. The addition of organophosphonate groups (RPO) will be studied with the aim of adding new functionalities to the clusters, these functionalities having the ability to be used to control the long-range ordering of the materials either through further reaction or coordination of the organic groups. The aim is to synthesis new and interesting materials where the intrinsic properties of the single polyoxotungstate anions are retained and can be exploited, the effect of different organic functionalities will be investigated and the possibility of reacting the groups containing double bonds to produce polymers will be tested with the aim of producing materials which could have applications in heterogeneous catalysis.

Firstly chapter 2 considers the synthesis of organophosphonic acids including a new styryl phosphonic acid, these organic groups can then be grafted onto the clusters. The synthesis of the divacant $[\gamma\text{-XW}_{10}\text{O}_{36}]^{n-}$ will be studied followed by its derivatisation to produce some new polyoxotungstate derivatives. The products obtained being confirmed and investigated by multinuclear NMR (^1H and ^{31}P), IR, MS, EA, Single Crystal XRD and Cyclic Voltammography.

Chapter 3 investigates derivatisation of the trivacant $[\alpha\text{-XW}_9\text{O}_{34}]^{m-}$ anion, firstly the reaction with highly electrophilic organotrichlorosilanes will be tested before exploring the less reactive phosphonic acids, with the aim of obtaining new fully saturated $[\text{XW}_9\text{O}_{34}(\text{R})_3]^{(m-6)-}$ clusters.

Chapter 4 looks at radical polymerisation reactions involving the polyoxotungstate clusters which have had double bonds grafted on to them, investigating their reactivity under different conditions and the electrochemical properties of the products obtained to see if polymeric materials can be obtained which retain the properties of the single polyoxotungstate anions.

Finally, Chapter 5 explores the reactivity of polyoxotungstate clusters with either carboxylic acid or ketone functionalities grafted on to the structure towards amine molecules, thus looking at the possibility of creating condensation type polymers by reacting with diamine molecules. The work in this last chapter has also opened up an interesting synthetic route to new asymmetrically functionalised polyoxometalates.

1.10. References

1. J. Berzelius, *Poggendorff's Ann. Phys.*, **1826**, 6, 369.
2. M.T. Pope, *Heteropoly and Isopoly Oxometalates*, Springer-Verlay, Berlin, **1983**.
3. C. Marignac, *C. R. Acad. Sci.*, **1862**, 25, 362.
4. L. Pauling, *J. Am. Chem. Soc.*, **1929**, 51, 2868.
5. A. Werner, *Neuere Amschauungen auf dem Gebiete der Anorganischem Chemie*, **1909**.
6. M. T. Pope and A. Müller, *Angew. Chem. Int. Ed. Engl.*, **1991**, 30, 34.
7. J. F. Keggin, *Nature*, **1933**, 132, 351.
8. H. R. Allcock, E. C. Bissell and E. T. Shawl, *J. Am. Chem. Soc.*, **1972**, 94, 8603.
9. A. Müller, E Beckmann, H. Bogge, M. Schmidtman and A. Dress, *Angew. Chem. Int. Ed.*, **2002**, 41, 1162.
10. A. Proust, R. Thouvenot and P. Gouzerh, *Chem. Commun.*, **2008**, 16, 1837.
11. T. Ueda, T. Yonemura, M. Shiro, M. Fukudome and M. Hojo, *Inorg. Chem. Comm.*, **2007**, 10, 1301.
12. M.T. Pope and A. Müller, *Polyoxometalate Chemistry From Topolgy via Self-Assembly to Applications*, Kluwer, **2001**.
13. F. Cavani, *Catal. Today*, **1998**, 41, 73.
14. A. Tézé and G. Hervé, *Inorg. Synth.*, **1990**, 27, 85.
15. J. Canney, A. Tézé, R. Thouvenot and G. Hervé, *Inorg. Chem.*, **1986**, 25, 2114.
16. R. Contant, *Can. J. Chem.*, **1987**, 65, 568.
17. S. Himeno, M. Takamoto and T. Ueda, *Bull. Chem. Soc. Jpn.*, **2005**, 78, 1463.
18. W.H. Knoth and R.L. Harlow, *J. Am. Chem. Soc.*, **1981**, 103, 1865.

19. P. J. Domaille, *Inorg. Synth.*, **1990**, 27, 96.
20. S-H. Wang and S. A. Jansen, *Chem. Mater.*, **1994**, 6, 2130.
21. P. Gouzerh and A. Proust, *Chem. Rev.*, **1998**, 98, 77.
22. X-Y Zhang, C. J. O'Connor, G. B. Jameson and M. T. Pope, *Inorg. Chem.*, **1996**, 35, 30.
23. R. K. C. Ho and W. G. Klemperer, *J. Am. Chem. Soc.*, **1976**, 100, 21, 6772.
24. W. H. Knoth, *J. Am. Chem. Soc.*, **1979**, 101, 759.
25. N. Ammari, G. Hervè and R. Thouvenot, *New J. Chem.*, **1991**, 15, 607.
26. J. Niu, J. Zhao, J. Wang and M. Li, *J. Molec. Struct.*, **2003**, 655, 243.
27. A. Mazeaud, N. Ammari, F. Robert and R. Thouvenot, *Angew. Chem. Int. Ed. Engl.*, **1996**, 35, 17, 1961.
28. C. R. Mayer, I. Fournier and R. Thouvenot, *Chem. Eur. J.*, **2000**, 6, 1, 105.
29. A. Mazeaud, Y. Dromzee and R. Thouvenot, *Inorg. Chem.*, **2000**, 39, 4735.
30. G. S. Kim, K. S. Hagen and C.L. Hill, *Inorg. Chem.*, **1992**, 31, 5316.
31. C. R. Mayer and R. Thouvenot, *J. Chem. Soc., Dalton Trans.*, **1998**, 7.
32. Z. G. Sun, J. X. Li, Q. Liu and J. F. Liu, *Chinese Chem. Lett.*, **1999**, 10,11, 971.
33. C.R. Mayer, P. Herson and R. Thouvenot, *Inorg. Chem.*, **1999**, 38, 6152.
34. Z. G. Sun, W. S. You, J. Li and J. F. Liu, *Inorg. Chem. Commun.*, **2003**, 6, 238.
35. G. Sazani and M. T. Pope, *Dalton Trans.*, **2004**, 13, 1989.
36. F. B. Xin and M. T. Pope, *Inorg. Chem.*, **1996**, 35, 5693.
37. F. B. Xin and M. T. Pope, *Organometallics*, **1994**, 13, 4881.
38. X. H. Wang, H. C. Dai and J. F. Liu, *Polyhedron*, **1999**, 18, 2293.
39. S. Reinoso, M. H. Dickman, A. Pretorius, L. F. Piedra-Garza and U. Kortz, *Inorg. Chem.*, **2008**, 47, 19, 8798.

40. I. Bar-Nahum, J. Ettedgui, L. Konstantinovski, V. Kogan and R. Neumann, *Inorg. Chem.*, **2007**, 46, 5798.
41. U. Kortz, F. Hussain and M. Reicke, *Angew. Chem. Int. Ed.*, **2005**, 44, 24, 3773.
42. B. Keita, P. de Oliveira, L. Nadjio and U. Kortz, *Chem. Eur. J.*, **2007**, 13, 5480.
43. K. Wassermann, H. J. Lunk, R. Palm, J. Fuchs, N. Steinfeldt, R. Stosser and M. T. Pope, *Inorg. Chem.*, **1996**, 35, 3273.
44. G. Sazani and M. T. Pope, *Dalton Trans.*, **2004**, 1989.
45. S. Bareyt, S. Piligkos, B. Hasenknopf, P. Gouzerh, E. Lacôte, S. Thorimbert and M. Malacria, *Angew. Chem. Int. Ed.*, **2003**, 42, 3404.
46. S. Bareyt, S. Piligkos, B. Hasenknopf, P. Gouzerh, E. Lacôte, S. Thorimbert and M. Malacria, *J. Am. Chem. Soc.*, **2005**, 127, 18, 6788.
47. I. Bar-Nahum and R. Neumann, *Chem. Commun.*, **2003**, 2690.
48. C. R. Mayer, S. Neveu and V. Cabuil, *Angew. Chem. Int. Ed.*, **2002**, 41, 3, 501.
49. A. Dolbecq, P. Mialane, L. Lisnard, J. Marrot and F. Sécheresse, *Chem. Eur. J.*, **2003**, 9, 2914.
50. C.R. Mayer, M. Hervé, H. Lavanant, J.-C. Blais and F. Secheresse, *Eur. J. Inorg. Chem.*, **2004**, 973.
51. C.R. Mayer and R. Thouvenot. *Chem. Mater.*, **2000**, 12, 257.
52. P. Judeinstein, *Chem. Mater.*, **1992**, 4, 4.
53. C. R. Mayer and R. Thouvenot, *Macromolecules*, **2000**, 33, 12, 4433.
54. C. R. Mayer, V. Cabuil, T. Lalot and R. Thouvenot, *Angew. Chem. Int. Ed.*, **1999**, 38, 24, 3672.

55. L. Xu, M. Lu, B. Xu, Y. Wei, Z. Peng and D.R. Powell, *Angew. Chem. Int. Ed.*, **2002**, 41, 4129.
56. Z. Peng, *Angew. Chem. Int. Ed.*, **2004**, 43, 930.
57. T. Hasegawa, H. Murakami, K. Shimizu, Y. Kasahara, S. Yosida, T. Kurashina, H. Seki and K. Nomiya, *Inorganica Chim. Acta*, **2008**, 361, 1385.
58. H. Chen, L. Xie, H. Lu and Y. Yang, *J. Mater. Chem.*, **2007**, 17, 1258.
59. V. N. Molchanov, I. C. Tatjanina, E. A. Torchenkova and L. P. Kazansky, *J. Chem. Soc. Chem. Commun.*, **1981**, 3, 93.
60. T. Yamase and H. Naruke, *J. Chem. Soc. Dalton Trans.*, **1991**, 285.
61. J. R. Galán-Mascarós, C. Giménez-Saiz, S. Triki, C. J. Gómez-García, E. Coronado and L. Ouahab, *Angew. Chem. Int. Ed.*, **1995**, 34, 13-14, 1460.
62. E. Coronado, J. R. Galán-Mascarós, C. Giménez-Saiz, C. J. Gómez-García and S. Triki, *J. Am. Chem. Soc.*, **1998**, 120, 4671.
63. H. T. Evans, T. J. R. Weakley and G. B. Jameson, *J. Chem. Soc. Dalton Trans.*, **1996**, 2537.
64. N. Honma, K. Kusaka and T. Ozeki, *Chem. Commun.*, **2002**, 23, 2896.
65. H. Chiba, A. Wada and T. Ozeki, *J. Chem. Soc. Dalton Trans.*, **2006**, 1213.
66. Y. Ishii, Y. Takenaka and K. Konishi, *Angew. Chem. Int. Ed.*, **2004**, 43, 2702.
67. F-X. Meng, Y. G. Chen, H. B. Liu, H. J. Pang, D. M. Shi and Y. Sun, *J. Molec. Struct.*, **2007**, 837, 224.
68. Y. Wang, D. R. Xiao, L. F. Fan, E. B. Wang and J. Liu, *J. Molec. Struct.*, **2007**, 843, 87.
69. Y. Lu, E. B. Wang, Y. Q. Guo, X. X. Xu and L. Xu, *J. Molec. Struct.*, **2005**, 737, 183.
70. M. Vasylyev, R. Popovitz-Biro, L. J. W. Shimon and R. Neumann, *J. Molec. Struct.*, **2003**, 656, 27.

71. M. Cohen, R. Neumann, *J. Mol. Catal. A: Chem.*, **1999**, 146, 291.
72. T. Sakamoto, C. Pac, *Tetrahedron Lett.*, **2000**, 41, 10009.
73. A. M. Khenkin, R. Neumann, A. B. Sorokin, A. Tuel, *Catal. Lett.*, **1999**, 63, 189.
74. N. M. Okun, T. M. Anderson, C. L. Hill, *J. Am. Chem. Soc.*, **2003**, 125, 3194.
75. K. Nomiya, H. Murasaki, M. Miwa, *Polyhedron*, **1986**, 5, 1031.
76. R. Massart, R. Contant, J. M. Fruchart, J. P. Ciabrini and M. Fournier, *Inorg. Chem.*, **1977**, 16, 11, 2916.
77. Y. G. Chen, J. Gong and L. Y. Qu, *Coordination Chem. Rev.*, **2004**, 248, 245.
78. R. Acerete, C. F. Hammer and L. C. W. Baker, *J. Am. Chem. Soc.*, **1979**, 101, 267.
79. D. M. McDaniel, *Inorg. Chem.*, **1976**, 15, 3187.
80. R. Thouvenot, A. Tézé, R. Constant and G. Hervé, *Inorg. Chem.*, **1988**, 27, 3, 524.
81. C. R. Mayer, C. Roch-Marchal, H. Lavanant, R. Thouvenot, N. Sellier, J-C. Blais and F. Sécheresse, *Chem. Eur. J.*, **2004**, 10, 5517.
82. M. T. Pope and G. M. Varga, *Inorg. Chem.*, **1966**, 5, 7, 1249.
83. J. J. Altenau, M. T. Pope, R. A. Prados and H. So, *Inorg. Chem.*, **1975**, 2, 417.
84. S. Himeno and M. Takamoto, *J. Electroanal. Chem.*, **2002**, 528, 170.
85. M. Sadakane and E. Steckhan, *Chem. Rev.*, **1998**, 98, 219.
86. K. Maeda, H. Katano, T. Osakai, S. Himeno and A. Saito, *J. Electroanal. Chem.*, **1995**, 389, 167.
87. B. Keita and L. Nadjjo, *J. Electroanal. Chem.*, **1985**, 191, 441.
88. B. Keita and L. Nadjjo, *J. Electroanal. Chem.*, **1987**, 217, 287.
89. B. Keita and L. Nadjjo, *J. Electroanal. Chem.*, **1987**, 219, 355.
90. J. E. Toth and F. C. Anson, *J. Electroanal. Chem.*, **1988**, 256, 361.

91. M. S. Balula, J. A. Gamelas, H. M. Carapuça, A. M. V. Cavaleiro and W. Schlindwein, *Eur. J. Inorg. Chem.*, **2004**, 619.
92. D. Agustin, J. Dallery, C. Coelho, A. Proust and R. Thouvenot, *J. Organomet. Chem.*, **2007**, 692, 746.
93. F. A. R. S. Couto, A. M. V. Cavaleiro, J. D. Pedrosa de Jesus and J. E. J. Simão, *Inorg. Chim. Acta*, **1998**, 281, 225.
94. W. Sun, H. Liu, J. Kong, G. Xie and J. Deng, *J. Electroanal. Chem.*, **1997**, 437, 67.
95. B. Keita, Y. W. Lu, L. Nadjo and R. Constant, *Eur. J. Inorg. Chem.*, **2000**, 2463.
96. C. L. Hill and C. M. Prosser-McCartha, *Coordination Chemistry Rev.*, **1995**, 143, 407.
97. N. Mizuno and M. Misono, *Chem. Rev.*, **1998**, 98, 199.
98. T. Okuhara, *Chem. Rev.*, **2002**, 102, 3641.
99. A. M. V. Cavaleiro, *J. Molec. Catalysis A:Chemical*, **2004**, 222, 159.
100. N. Mizuno and K. Yamaguchi, *The Chemical Record*, **2006**, 12.
101. L. Ni, P. Greenspan, R. Gutman, C. Kelloes, M. A. Farmer and F. D. Boudinot, *Antivir. Res.*, **1996**, 32, 141.
102. S. Shigeta, S. Mori, E. Kodama, J. Kodama, K. Takahashi and T. Yamase, *Antivir. Res.*, **2003**, 58, 265.
103. T. Yamase, *Mol. Eng.*, **1993**, 3, 241.

2. DERIVATIZATION OF $[XW_{10}O_{36}]^{n-}$

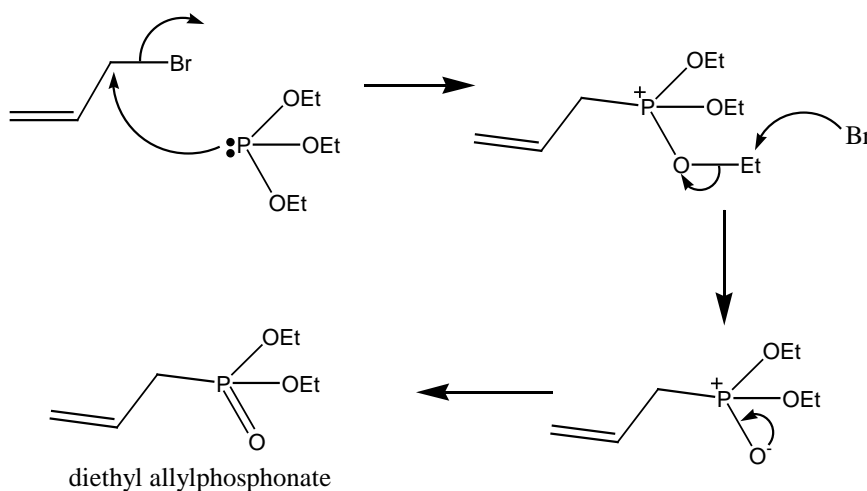
2.1. Phosphonic Acid Synthesis

2.1.1. Allylphosphonic Acid Synthesis

Allylphosphonic acid was synthesized in order to produce the allyl derivatized polyoxometalates, via diethyl allylphosphonate according to the Michaelis-Arbuzov Reaction¹ which is one of the most versatile pathways for the formation of carbon-phosphorus bonds.

2.1.1.1. Diethyl allylphosphonate

Diethyl allylphosphonate (Compound A) is synthesized from triethylphosphite and allylbromide. The lone pair of electrons on the phosphite attacks the organic group and forms an addition compound which then loses an ethyl group to form a P=O bond, this bond formation being the driving force for the rearrangement (Scheme 2.1).¹

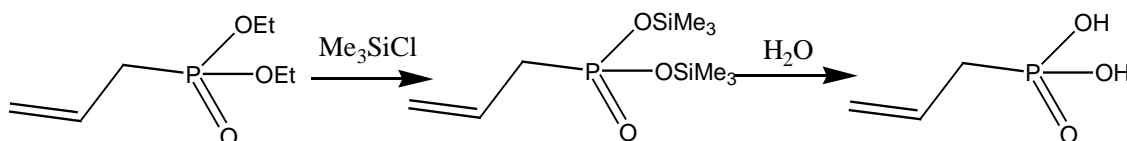


Scheme 2.1. Mechanism for the production of diethyl allylphosphonate.

^1H NMR. The production of diethyl allylphosphonate is confirmed by five signals in the ^1H NMR spectra. The first is a 6H triplet at 1.25 corresponding to the CH_3 on the ester split by the neighbouring CH_2 , the second at 2.55 is a 2H double doublet due to the CH_2 next to the phosphorus split by the CH ($^3J_{\text{HH}} = 7.4$) and the phosphorus (^{31}P has a spin $I = 1/2$) ($^2J_{\text{PH}} = 21.8$ Hz). A peak at 4.00 is a 4H double quartet due to the CH_2 in the ester, the quartet arising from coupling to the CH_3 group, with the peak then split further by coupling to phosphorus. The two multiplets at 5.10-5.20 and 5.60-5.85 ppm are due to the hydrogen atoms on the double bond, the first due to the terminal CH_2 and the other the CH.

2.1.1.2. Allylphosphonic acid

Allylphosphonic acid (Compound B) is prepared from diethyl allylphosphate, first by exchanging the ester groups with trimethylsilyl groups by reaction with trimethylchlorosilane, then these groups react with water to give O-H groups (Scheme 2.2).



Scheme 2.2. The production of the allylphosphonic acid from its diethyl phosphonate.

^1H NMR. The production of the desired product is confirmed by loss of the signals corresponding to the ester with the other three signals remaining.

^{31}P NMR. The spectrum has one peak at 27.7 ppm, in the H-coupled spectrum this peak is similar to a triplet of quartets (Figure 2.1).

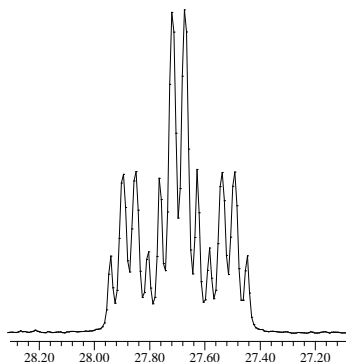


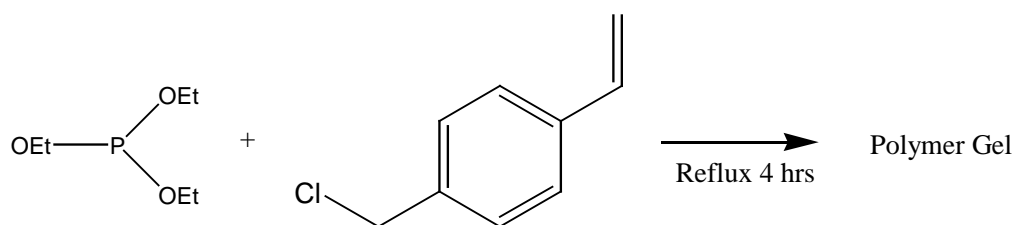
Figure 2.1. The H-coupled ^{31}P NMR spectrum for allylphosphonic acid.

The coupling constant for the triplet is $^2J_{\text{PH}} = 21.3$ Hz which corresponds to the splitting seen in the ^1H NMR. The further coupling has $J \sim 5.6$ Hz, which arises due to the coupling to both the CH ($J \sim 7$ Hz on ^1H spectrum) and to the terminal CH_2 . The coupling to the terminal CH_2 is 4-bond coupling, but in ^{31}P NMR the coupling constants vary widely depending more on the dihedral angle between the bonds than on the number of bonds, therefore a 4-bond coupling could easily equal or be greater than a 3-bond coupling.^{2,3,4}

^{13}C NMR. The spectrum shows three carbon signals. The CH_2 next to the phosphorus is at 32.8 ppm, this peak is split by the phosphorus to give a doublet ($^1J_{\text{PC}} = 133.6$ Hz), the two carbon atoms in the double bond give peak at 120.8 and 128.4 ppm (CH_2 and CH respectively) both coupling to the phosphorus atom ($^2J_{\text{PC}} = 10.9$ and $^3J_{\text{PC}} = 14.0$ Hz).

2.1.2. Diethyl Styrylphosphonate

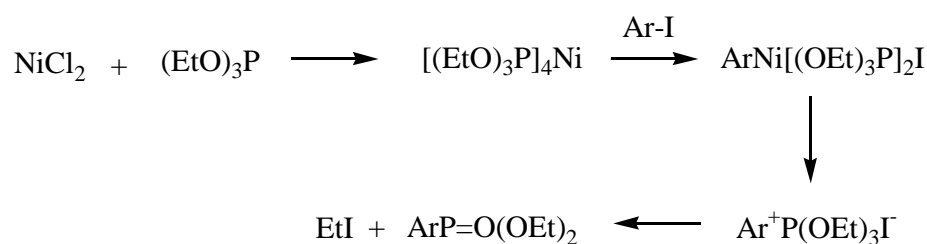
The coupling of phosphites with alkylhalides via the Michaelis-Arbuzov reaction is a successful method for synthesizing alkyl phosphonates with a CH_2 attached to the phosphorus atom. However a phosphonate containing a styrene group could not be prepared using this method (Scheme 2.3), as a gel-like polymer is formed due to the triethylphosphite reacting with the vinyl group as well as the halide.



Scheme 2.3. Attempted synthesis of a styryl phosphonate via the Michaelis-Arbuzov Reaction.

A less vigorous method was needed for the preparation of the styrene derivative.

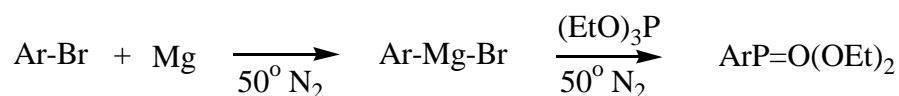
Synthesis using a Nickel-catalysed Arbuzov reaction has successfully produced diethyl phenylphosphonates⁵ so a similar procedure was attempted and is shown in Scheme 2.4.



Scheme 2.4. Procedure for synthesizing the phosphonate using a Nickel-catalysed reaction.

The reaction involves making a nickel containing intermediate tetrakis(triethylphosphite)nickel(0) $[(\text{EtO})_3\text{P}]_4\text{Ni}$.⁵ This complex was reacted with 4-vinylbenzylchloride and triethylphosphite, but again a polymer was formed as the conditions were still too harsh.

A magnesium grinyard reagent was tried, as this method is used to make diethyl alkylphosphonates,⁶ with alkylphosphonates formed as a by-product of this reaction. If this procedure (Scheme 2.5) appeared to be successful then the method might be able to be altered to increase the yield of the desired phosphonate.

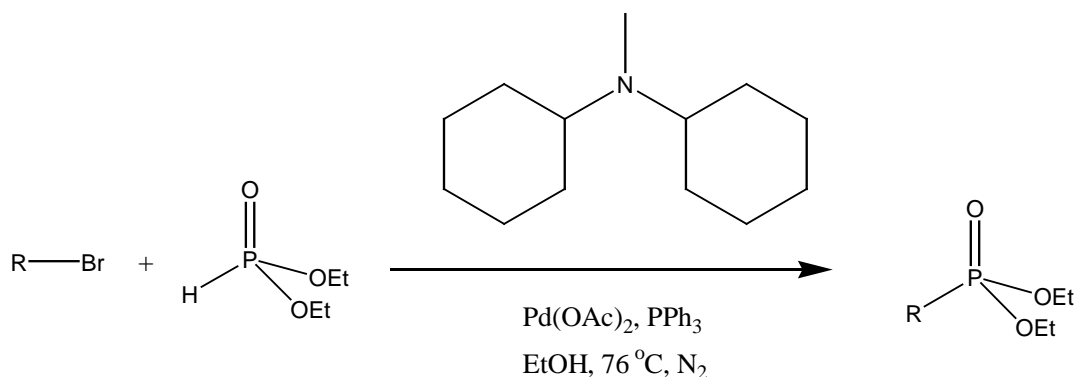


Scheme 2.5. Proposed synthesis via a Magnesium grinyard reagent.

However, this also gave a gel-like product which dissolved when extra solvent (THF) was added. This suggested that not all the product was polymerized, however the product could not be isolated as under gentle heating to distil the products decomposition occurred giving a brown solid.

Various methods for synthesizing arylphosphonates or arylphosphonic acids have been proposed in the literature, the traditional method being by a Friedel-Crafts reaction of an arene with a phosphonic acid derivative,⁷ however this method involves harsh conditions so would also be incompatible with more sensitive functionalities.

The use of palladium as a catalyst for the reaction of dialkyl phosphite with aryl halides has been disclosed,^{8,9} the procedure being refined for the preparation of functionalised aryl phosphonates by Gooßen and Dezfuli¹⁰ and found to be broadly applicable. The best conditions used $Pd(OAc)_2$ as the pre-catalyst, with triphenylphosphine, dicyclohexylmethylamine as the base and ethanol as the solvent (Scheme 2.6).



Scheme 2.6. Synthesis of diethyl styrylphosphonate using a Palladium catalyst.

Using these conditions 4-bromostyrene was reacted with diethyl phosphite to give the styrenephosphonate $H_2C=CHC_6H_4PO(OEt)_2$ (Compound 1) in a reasonable yield and production of the product was confirmed by means of NMR (1H , ^{13}C and ^{31}P), IR and Mass Spectrometry.

^1H NMR. The spectrum (Figure 2.2) shows the environments from the styryl group as two 2H multiplets at 7.45-7.50 and 7.73-7.80 due to the four hydrogen atoms on the ring and 1H signals at 5.37 (doublet), 5.85 (doublet) and 6.73 ppm (double doublet) from the three hydrogen atoms on the double bond with both *cis* and *trans* coupling ($J_{\text{HH,cis}} = 11.1$, $J_{\text{HH,trans}} = 17.7$ Hz) due to the lack of rotation of this bond. Signals due to the ethyl groups are present at 1.31 and 3.99-4.18 ppm with intensities of 6H and 4H respectively. The position and intensity of the signals confirm the desired diethyl styrylphosphonate.

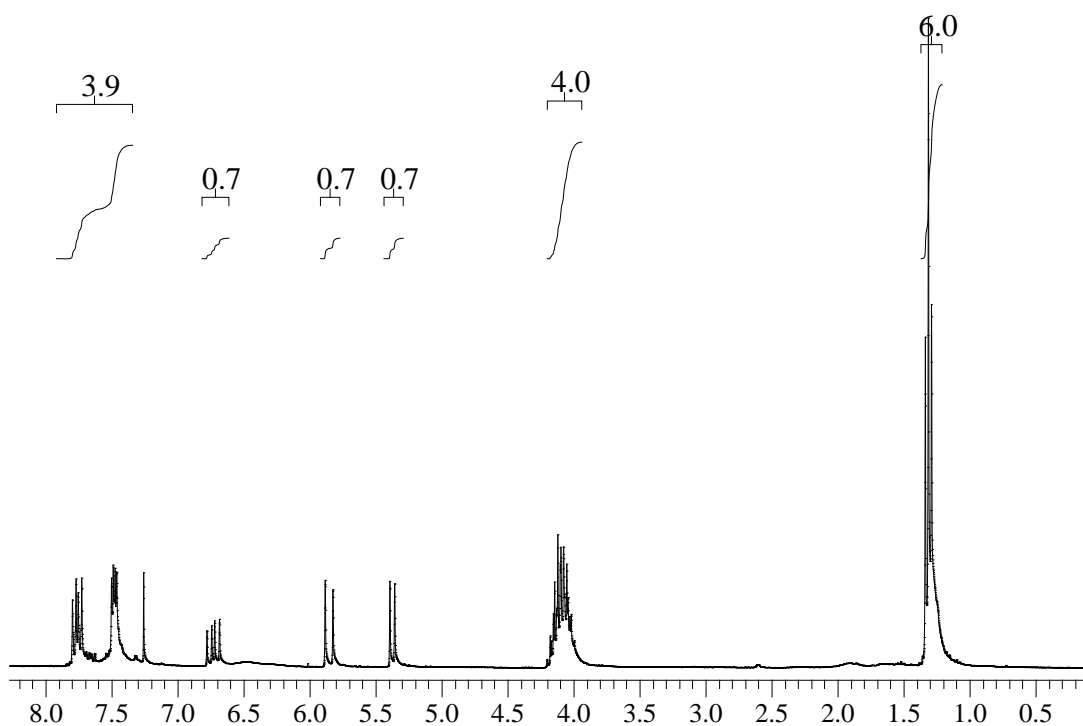


Figure 2.2. ^1H NMR Spectrum for the diethyl styrylphosphate synthesized using a Palladium catalyst, solvent Chloroform (7.26 ppm).

^{31}P NMR. The spectrum has one peak showing that only one type of product containing a phosphorus atom is present.

^{13}C NMR. The spectrum shows the correct number and position of peaks to indicate formation of the product.

Mass Spectrometry. The electrospray mass spectrum of the product has two main signals, although these are both at higher masses than expected (240), they have been assigned to $[M+Na]^+$ (263) and $[M+Na+MeOH]^+$ (295), so indicate that the correct product is obtained.

All the spectral information indicates that the formation of the desired product, diethyl styrylphosphonate has been successfully achieved. The reaction was relatively clean; however a small quantity of quinoline remained in the product, which was subsequently removed by altering the procedure. The ethanol was removed in *vacuo* before diluting the oil with ethyl acetate and during the separation the organic layer was washed twice with a stronger (2 M) HCl acid solution. These changes from the published procedure¹⁰ helped to protonate the dicyclohexylmethanamine so allowing for an easier separation.

This is the first example of a styrene group being directly coupled to a phosphorus atom giving the diethyl styrenephosphonate and shows that the double bond is unaffected by the reaction conditions.

2.1.3. Diethyl 4-acetylphenylphosphonate

The same procedure was used to obtain diethyl 4-acetylphenylphosphonate (Compound C),¹⁰ this proving a useful method of introducing a ketone functionality which would also be susceptible to side reactions under Arbuzov conditions. The formation of product was confirmed by multinuclear NMR (1H , ^{13}C and ^{31}P), IR and MS.

1H NMR. The spectrum shows environments with the correct chemical shifts and intensities for the desired product; the $H_3CCOC_6H_4$ group appears as two 2H double doublets (7.90 and 8.00 ppm) for the ring and a 3H singlet (2.60 ppm) for the CH_3 group.

^{13}C NMR. The spectrum shows the desired number and position of peaks.

³¹P NMR. One peak is seen indicating one phosphorus containing product.

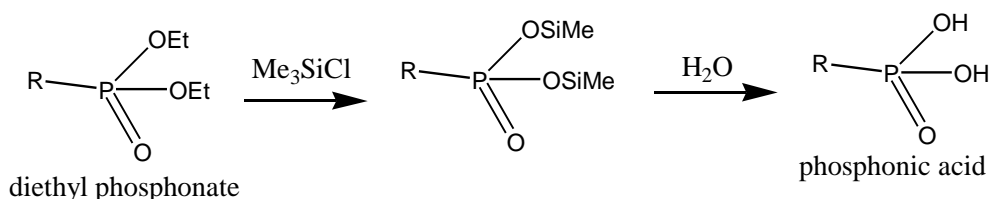
IR Spectroscopy. The main feature of the IR spectrum is a band due to the C=O at 1690.6 cm^{-1} , although bands due to the other groups are also seen.

Mass Spectrometry. Electrospray MS shows the main peak to be at 279, this is assigned to $[M+Na]^+$.

All the spectral evidence points towards formation of the desired product, the yield is good (80 %), but not quite as good as that quoted in the literature (87 %).¹⁰

2.1.4. Phosphonic acids

The diethyl phosphonates are converted into their corresponding phosphonic acids (Compounds 2 and 3) using the same method as previously used for making the allylphosphonic acid, the conditions being relatively mild and known to not alter double bond functionalities.



Scheme 2.7. Synthesis of phosphonic acid from diethyl phosphonate.

^1H NMR. Formation of the appropriate phosphonic acid from its diethyl phosphonate can be confirmed by the loss of signals associated with the ethyl groups in both the ^1H (Figure 2.3 vs. Figure 2.2) and ^{13}C NMR spectra. The other signals are shifted slightly due to the change in environment caused by replacing O-Et with O-H.

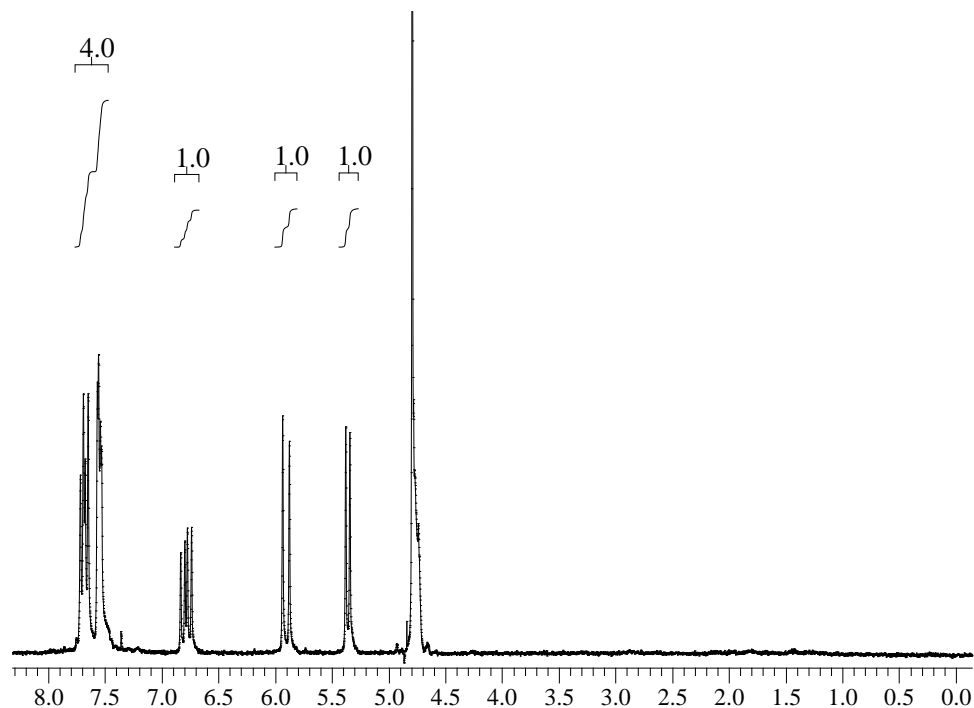


Figure 2.3. ^1H NMR spectrum for styrylphosphonic acid, solvent D_2O (4.79 ppm).

^{31}P NMR. The chemical shift of the phosphorus peak has moved by 2-3 ppm. H-coupling shows the peak to be similar to a triple triplet for both the styryl and 4-acetylphenylphosphonic acids (Figure 2.4), showing that the phosphorus is not affected by the functional group only coupling with the hydrogen atoms on the ring.

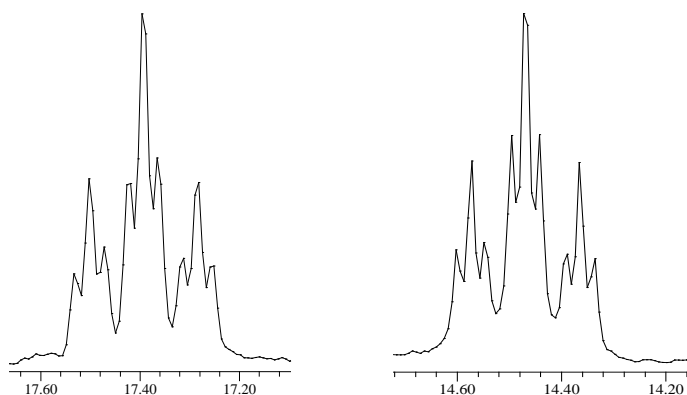


Figure 2.4. The H-coupled ^{31}P NMR spectra for (a) styrenephosphonic acid and (b) 4-acetylphenylphosphonic acid, showing the coupling to be the same in both cases, solvent MeCN-d_3 .

Mass Spectrometry. The mass spectra show signals for $[M]^+$ confirming the production of the phosphonic acids for both R groups.

UV/vis. The phosphonic acids both contain aromatic rings which absorb light in the UV region. A styrene group normally exhibits three peaks these being an intense peak at 248 (14000) and two small peaks at 282 (750) and 291 nm (500 $\text{Lmol}^{-1}\text{cm}^{-1}$). For the styrylphosphonic acid, peaks were observed (255 (17000), 283 (1800) and 293 (1200 $\text{Lmol}^{-1}\text{cm}^{-1}$)) with only a small shift due to the phosphonate group.

An aromatic ring with a ketone group attached to it will normally have a peak in the UV/vis spectrum at 245.5 nm (9800 $\text{Lmol}^{-1}\text{cm}^{-1}$), this peak was seen for 4-acetylphenylphosphonic acid (250 nm (25600 $\text{Lmol}^{-1}\text{cm}^{-1}$)) again showing a small shift due to the phosphonate.

2.2. Polyoxotungstate Synthesis

2.2.1. γ -Decatungstosilicate synthesis

The γ -Decatungstosilicate $[\gamma\text{-SiW}_{10}\text{O}_{36}]^{8-}$ (Compound E) was synthesized using a method described in the literature¹¹ via the intermediate β_2 -undecatungstosilicate $[\beta_2\text{-SiW}_{11}\text{O}_{39}]^{8-}$ (Compound D).

The α -isomer of the Keggin structure $[\alpha\text{-SiW}_{12}\text{O}_{40}]^{4-}$ can be thought of as a central SiO_4 tetrahedron surrounded by four W_3O_{13} groups, each group made from three edge-shared WO_6 octahedra. The β -isomer can be derived from the α -isomer by the rotation of one W_3O_{13} group by 60° (overall C_{3v} symmetry); three different β -isomers of undecatungstosilicate can be obtained

(Figure 2.5), each by removal of different tungsten-oxygen octahedra from the parent structure using a slightly different procedure.

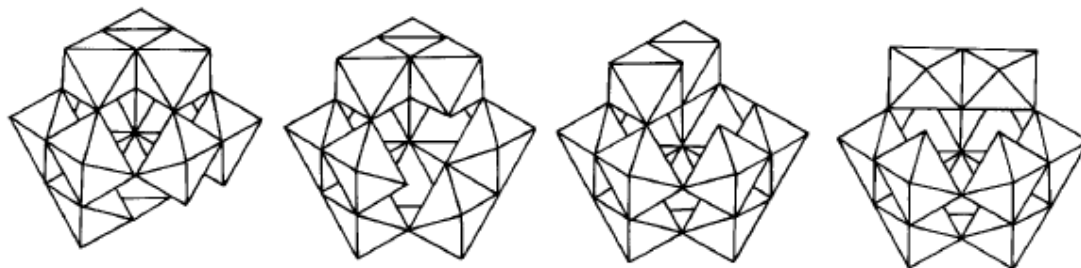
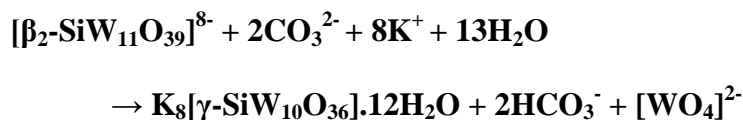


Figure 2.5. The four different isomers of $[XW_{11}O_{39}]^{n-}$, (a) β_1 , (b) β_2 , (c) β_3 and (d) α .¹²

The $[\beta_2\text{-SiW}_{11}\text{O}_{39}]^{8-}$ structure is prepared from sodium tungstate ($\text{Na}_2\text{WO}_4 \cdot 2\text{H}_2\text{O}$) and sodium metasilicate ($\text{Na}_2\text{SiO}_3 \cdot 5\text{H}_2\text{O}$) using a self assembly approach. As with the preparation of all Keggin polyoxotungstates, pH control determines which structure is obtained and the pH is maintained at 5-6 by the addition of HCl for the synthesis of $[\beta_2\text{-SiW}_{11}\text{O}_{39}]^{8-}$. $[\beta_2\text{-SiW}_{11}\text{O}_{39}]^{8-}$ is a white, water soluble solid, but is not thermodynamically stable so spontaneously isomerizes into the β_3 and then the α -isomer,¹³ thus specificity of the reaction is due to kinetic control. This lacunary polyoxotungstate is characterised by IR spectroscopy, the position of the signals confirming formation of the correct product by comparison to the literature.¹¹

Potassium γ - decatungstosilicate $[\gamma\text{-SiW}_{10}\text{O}_{36}]^{8-}$ is synthesized from $[\beta_2\text{-SiW}_{11}\text{O}_{39}]^{8-}$ by accurate control of the pH using K_2CO_3 to adjust the pH to 9.1.



The γ -structure is derived from a Keggin structure with two W_3O_{13} groups rotated by 60° . In $[\gamma\text{-SiW}_{10}\text{O}_{36}]^{8-}$ the two octahedra that have become edge shared are removed (overall C_{2v}

symmetry), this stabilizes the otherwise unstable structure as the edge sharing results in electrostatic repulsions. At pH 9.1, $[\beta_2\text{-SiW}_{11}\text{O}_{39}]^{8-}$ rearranges to this structure instead of β -10-tungstosilicate, because it has a lower negative charge, even though it is a complex reaction involving the loss of a tungsten-oxygen octahedra and the rotation of a bitungstic group simultaneously.¹³ $[\gamma\text{-SiW}_{10}\text{O}_{36}]^{8-}$ is soluble in water and stable below pH 8, being stabilized by forming complexes with alkali-metal cations such as potassium, rubidium and cesium.¹³ The product is characterized by IR spectroscopy, the signals agreeing with the literature values¹ so indicating formation of the correct product.

2.3. Derivatization of polyoxotungstates

The loss of tungsten-oxygen octahedra from the saturated Keggin framework $[\gamma\text{-XW}_{12}\text{O}_{40}]^{n-}$ leads to an increase and localization of the anionic charge in the vacancies left behind. The resulting lacunary anion $[\gamma\text{-SiW}_{10}\text{O}_{36}]^{8-}$ is highly nucleophilic and reactive towards electrophilic groups. The successful reaction of decatungstosilicates $[\gamma\text{-SiW}_{10}\text{O}_{36}]^{8-}$ with organophosphonic acids $\text{RPO}(\text{OH})_2$ ($\text{R} = \text{Et}, \text{Bu}, \text{C}_3\text{H}_5, (\text{CH}_2)_2\text{COOH}$ or Ph) has been studied by Thouvenot *et al.*,¹⁴ under phase-transfer conditions (NBu_4^+) with a catalytic amount of HCl , with derivatised polyoxotungstates of formula $(\text{NBu}_4)_3\text{H}[\text{SiW}_{10}\text{O}_{36}(\text{RPO})_2]$ being obtained.



The same procedure was used here to obtain derivatives of the $[\gamma\text{-SiW}_{10}\text{O}_{36}]^{8-}$ anion with various phosphonic acids $\text{RPO}(\text{OH})_2$. Firstly the synthesis and structure of the ethyl ($\text{R} = \text{Et}$) derivative was studied, followed by phosphonic acids which contain double bonds ($\text{R} = \text{H}_2\text{C}=\text{CH}$, $\text{H}_2\text{C}=\text{CHCH}_2$, $\text{H}_2\text{C}=\text{CHC}_6\text{H}_4$) to obtain products with the potential for making polymeric

materials and finally other derivatives ($R = \text{HOOCCH}_2$, $\text{HOOC}(\text{CH}_2)_2$ or $\text{H}_3\text{CCOC}_6\text{H}_4$) which could provide other methods for controlling the ordering within the materials (H-bonding and the potential for condensation polymers).

2.3.1. Derivatization of $[\text{SiW}_{10}\text{O}_{36}]^{8-}$

2.3.1.1. $[\text{SiW}_{10}\text{O}_{36}(\text{C}_2\text{H}_5\text{PO})_2]^{4-}$

The ethyl derivative (Compounds F and G) is obtained from the reaction of $[\text{SiW}_{10}\text{O}_{36}]^{8-}$ with ethyl phosphonic acid ($\text{EtPO}(\text{OH})_2$). The $\text{NBu}_4^+/\text{H}^+$ salt has been synthesized previously by Thouvenot *et al.*¹⁴ and was synthesized again here along with the $\text{NEt}_4^+/\text{H}^+$ salt, the production of the desired product being confirmed by multinuclear NMR (^1H and ^{31}P), IR, MS, EA and Single Crystal XRD.

^1H NMR. The spectra for both the NBu_4^+ and NEt_4^+ salts are dominated by the cation signals, these having much greater intensities than the EtPO. The $(\text{NBu}_4)_3\text{H}[\text{SiW}_{10}\text{O}_{36}(\text{EtPO})_2]$ spectrum shows the four environments for the cations, a 36H triplet at 0.98 from the CH_3 , a 24H sextet at 1.36 from the neighbouring CH_2 , a 24H quintet at 1.61 from the next CH_2 and a 24H multiplet at 3.06-3.13 ppm from the CH_2 next to the nitrogen. The splittings are all consistent with the rule that equal coupling to n neighbouring hydrogen atoms will give a signal with $n+1$ lines. The CH_2 next to the nitrogen appears as a multiplet because of ^4J interactions with other CH_2 groups attached to the nitrogen. The $(\text{NEt}_4)_3\text{K}[\text{SiW}_{10}\text{O}_{36}(\text{EtPO})_2]$ spectrum shows the NEt_4^+ environments as a 36H multiplet at 1.15-1.27 ppm due to the CH_3 (shifted compared to the NBu_4^+ CH_3 because it is closer to the nitrogen) and a 24H multiplet at 3.04-3.12 ppm due to the CH_2 . The EtPO group gives two signals; these are seen as multiplets at 1.27-1.40 (CH_2) and 1.55-1.70 ppm (CH_3) in both spectra, although they are masked by the cation signals.

^{31}P NMR. Under proton decoupling both the ^{31}P NMR spectra have one signal at 29 ppm; indicating that the molecular structure of the anion in solution is symmetrical with both the phosphorus atoms in the structure being equivalent. This signal has tungsten satellite peaks ($^2J_{\text{PW}} = 10.1$ Hz) associated with it; integration of these satellite peaks with respect to the central line shows that the phosphorus atom is connected to two tungsten atoms of the polyoxotungstate framework through P-O-W bonds (Figure 2.6).^{15,16}

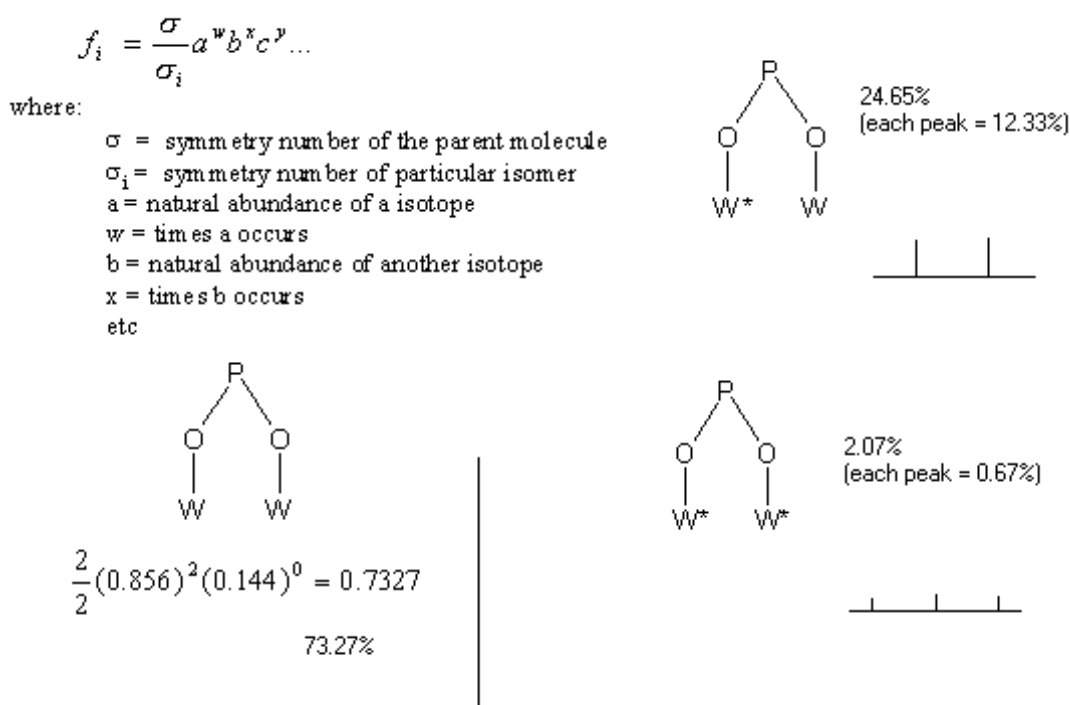


Figure 2.6. Theoretical pattern of the ^{31}P resonance for a $\text{P}(\text{OW})_2$ fragment of $[\gamma\text{-SiW}_{10}\text{O}_{36}(\text{RPO})_2]$ according to the relative abundances of the isotopes. [Equation from Ref. 16]

The H-coupled ^{31}P NMR spectrum shows further splitting of the phosphorus peak (Figure 2.7); the phosphorus is expected to couple to the neighbouring CH_2 group to give a triplet and also to the CH_3 group to give a quartet, making a signal similar to a triplet of quartets. The observed signal appears to have six main peaks each equal distance apart with intensities similar

to that of a sextet, this could be explained by the coupling to all five hydrogen atoms being equal, as phosphorus-hydrogen coupling does not depend on distance alone, but also on the dihedral angle between the atoms.^{2,3,4}

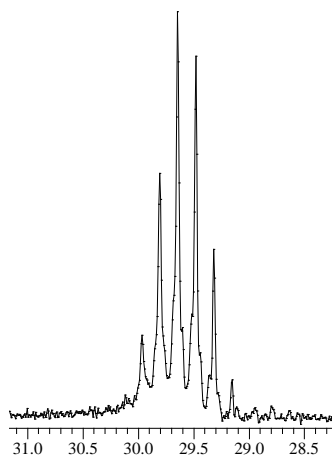


Figure 2.7. ^{31}P - ^1H coupling showing the spectrum for $[\text{SiW}_{10}\text{O}_{36}(\text{EtPO})_2]^{4-}$.

IR Spectroscopy. There are various changes in the IR spectrum compared to that for $\text{K}_8[\text{SiW}_{10}\text{O}_{36}]$. Firstly bands have appeared at around 2965 cm^{-1} due to C-H stretches both in the ethylphosphonate and the tetra-alkyl ammonium cations, also a band has appeared at 1173 cm^{-1} due to the P-C asymmetric stretch and there are various stretches between $1100\text{--}1000\text{ cm}^{-1}$ from the P=O, P-O and Si-O bonds. There are also more bands in the fingerprint region than for the lacunary $[\text{SiW}_{10}\text{O}_{36}]^{8-}$ anion, due to a lowering of the symmetry for the derivatised structure.

Mass Spectrometry. Maldi-TOF MS of the product shows a number of signals and so is hard to interpret, however signals have been assigned to the anion $[\text{SiW}_{10}\text{O}_{36}(\text{EtPO})_2]^{4-}$ having varying numbers of cations associated with it, the anion still giving a positively charged species due to reduction of the tungsten atoms. Signals are also assigned to the anion losing all or part of an EtPO group. Overall the mass spectra indicate that the correct product has been formed.

Elemental Analysis. EA for polyoxometalates is in general not very reliable¹ so can not be used to determine structural purity. In this case the percentage of carbon found does not match that calculated although the percentages of nitrogen and hydrogen match relatively well.

Single Crystal X-ray Diffraction. Crystals suitable for XRD could not be obtained for either the NBu_4^+/H^+ or NEt_4^+/H^+ salts, however crystals of a good enough quality were obtained by evaporation of a solution containing a 2:1 mixture of the salts in a similar way to the PhPO derivative in the literature.¹⁴

Table 2.1. Crystallographic Data for $(NBu_4)_2(NEt_4)H[SiW_{10}O_{36}(EtPO)_2]$.

Orthorhombic	Spacegroup			P n 2 ₁ a
Cell axes (Å)	a = 21.9890(9)	b = 25.4008(21)	c = 13.8974(6)	
Cell angles (deg)	α = 90.00	β = 90.00	γ = 90.00	
Cell Volume (Å ³)	7762.23(5)			

[Full details in appendix (Structure 1)]

The crystal structure was solved and refined using SHELXL97¹⁷ present in the WinGx¹⁸ suite of programmes. Final refinements were carried out with anisotropic thermal parameters for all non-hydrogen atoms. An asymmetric unit consists of one $[SiW_{10}O_{36}(EtPO)_2]^{4-}$ unit, two NBu_4^+ cations and one NEt_4^+ cation (matching the solution), along with a H^+ to balance the charge.

The anion (Figure 2.8) consists of a $[\gamma-SiW_{10}O_{36}]^{8-}$ unit on to which two phosphonate groups ($EtPO^{2+}$) are attached, each through two W-O-P bonds between the terminal oxygen atoms that were created by loss of WO octahedra when forming the lacunary anion. This anion is symmetrical with both EtPO groups being identical, the P=O bonds point towards one another with a relatively short distance ($d_{O-O}=2.38$ Å) between them, this is similar to the O-O distance in $[SiW_{10}O_{36}(PhPO)_2]^{4-}$ at 2.4 Å⁴ and $[PW_{11}O_{39}(PhPO)_2]^{3-}$ at 2.43 Å¹⁹; a H^+ is thought to form a strong hydrogen bond between these two terminal oxygen atoms, although it can not be seen as

SC XRD does not allow for determination of hydrogen atoms. The anion structure is related to the phenyl derivative $[\text{SiW}_{10}\text{O}_{36}(\text{PhPO})_2]^{4-}$ which is formed using the same method.¹⁴

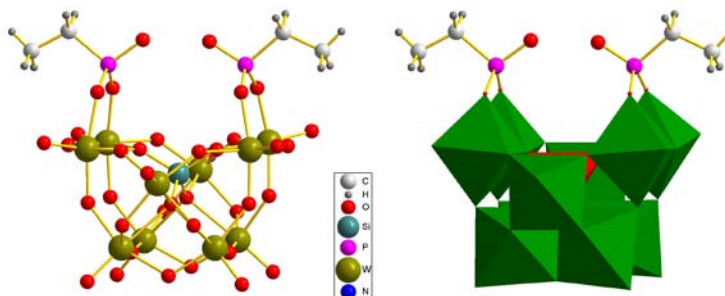


Figure 2.8. The structure of $[\text{SiW}_{10}\text{O}_{36}(\text{EtPO})_2]^{4-}$, shown as (a) ball and stick and (b) polyhedra representations.

In the structure, the anion clusters form layers along planes in the direction of the a - c axes. These layers can be viewed by looking down the c -axis (Figure 2.9), which shows that all the anions within a layer point in the same direction, with anions in alternate layers pointing in the opposite direction, the organic groups on the top of one cluster pointing towards the bottom of the next cluster, minimising the interactions of the negative charge. The layers are held together by layers of NBu_4^+ cations between them.

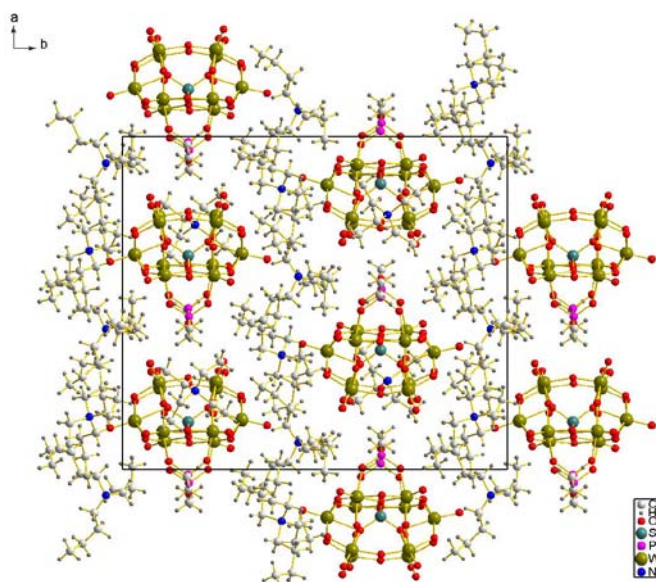


Figure 2.9. The crystal structure of $(\text{NBu}_4)_2(\text{NEt}_4)\text{H}[\text{SiW}_{10}\text{O}_{36}(\text{EtPO})_2]$ viewed down the c -axis.

The packing of the anions within one layer (Figure 2.10) can be described as rows of anions all pointing in the same direction, the anions in adjacent rows sit above or below the gaps in the first row, the rows repeating in an *a-b-a-b* fashion, with the gaps in the layers being filled by the smaller NEt_4^+ cations.

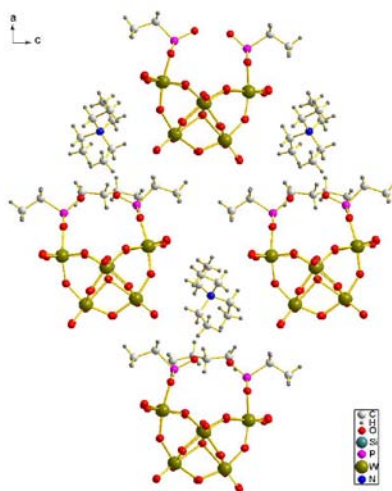


Figure 2.10. The crystal structure of $(NBu_4)_2(NEt_4)H[SiW_{10}O_{36}(EtPO)_2]$ viewed down the *b*-axis.

Electrochemical Analysis. Cyclic Voltammograms in acetonitrile were carried out using NBu_4BF_4 as the electrolyte, a glassy carbon working electrode and a platinum counter electrode; in the range of potentials studied (0.7 to -2.0 V *vs.* SCE) three waves corresponding to the reduction of the tungsten atoms²⁰ were observed. The positions of the waves are shifted towards less negative values than those reported for the parent anion in acetonitrile.²¹ This is the opposite effect to when removing WO_6 octahedra from $[SiW_{12}O_{40}]^{4-}$ to form lacunary species, where for example the first wave for $[SiW_{11}O_{39}]^{8-}$ (-1.12 V *vs.* Ag/Ag^+ ,²¹ which would convert to ~ -0.80 V *vs.* SCE) is found to be at a more negative potential than for $[SiW_{12}O_{40}]^{4-}$ (-1.08 V *vs.* Ag/Ag^+ ,²¹ which would convert to ~ -0.75 V *vs.* SCE) and shows that in $[SiW_{10}O_{36}(RPO)_2]^{4-}$ the polyoxometalate structure can be considered to be fully saturated (the reduction of the anion $[SiW_{10}O_{36}]^{8-}$ has not been reported and could not be performed under similar conditions due to

limitations in its solubility). The addition of the EtPO groups has made the cluster easier to reduce, in part due to the derivatised cluster effectively having a less negative charge (3- rather than 4-) on account of the H^+ strongly coordinating to the P=O groups still being present in solution; this lower charge will make the addition of further electrons easier. The position of the first wave is similar to for $[PW_{11}O_{39}(SiEt)_2O]^{3-}$ (-0.32 V)²² which has a charge of 3- (due to the central atom being a phosphorus). The normal effect of a more negative X atom causing the waves to shift to a more negative position^{23,24} is not seen, because the H^+ ion balances the extra positive charge of the silicon. When using a molecular orbital approach to explain the observations, the W-O octahedra can all be considered as having only one terminal oxygen atom, so an additional electron will go into a non-bonding orbital, this is easier than in the lacunary anions where some of the non-bonding orbitals are already full.

The first wave (-0.21 V) is an one-electron process with a peak separation of 70 mV, it has been observed using both a stationary electrode (Figure 2.11) and a rotating disc electrode (Figure 2.12) so as to obtain an accurate position for its potential.

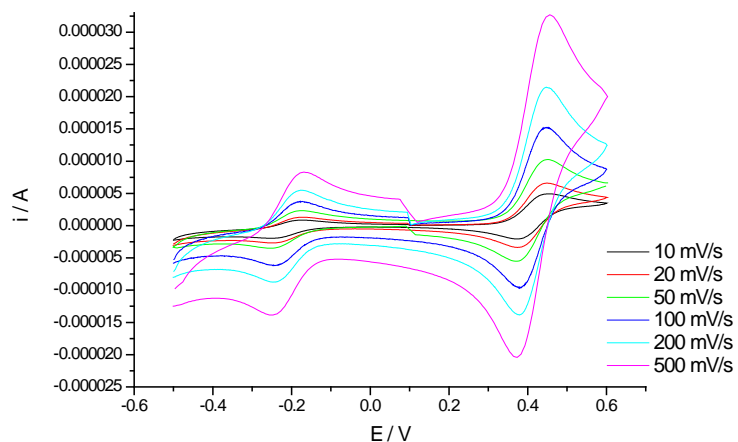


Figure 2.11. Cyclic Voltammogram showing the first reduction wave for $(NBu_4)_3H[SiW_{10}O_{36}(EtPO)_2]$ and the wave for ferrocene (used as the internal reference) vs SCE, the reaction was carried out in acetonitrile using NBu_4BF_4 as the electrolyte, a glassy carbon working electrode and a platinum counter electrode.

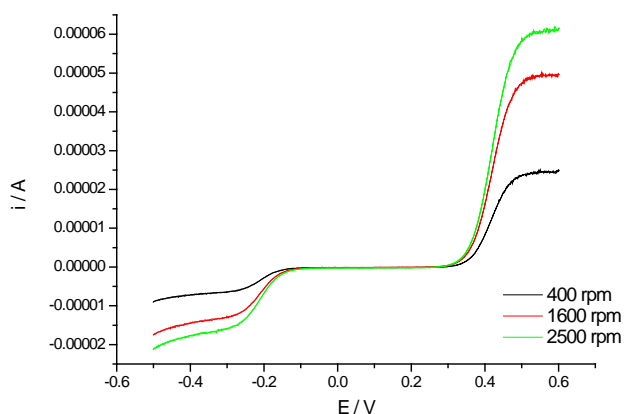


Figure 2.12. Rotating Disc Electrode experiment for $(NBu_4)_3H[SiW_{10}O_{36}(EtPO)_2]$ and ferrocene vs. SCE.

In Cyclic Voltammetry the peak height i_p can be used to predicted the diffusion coefficient of the compound under consideration by use of the Randles-Sevcík equation:

$$\frac{i_p}{A} = 2.69 \times 10^5 n^{3/2} D^{1/2} C v^{1/2}$$

Where the peak height i_p depends on the number of electrons taking part in the process n , the diffusion coefficient, D and concentration, C of the analyte, the sweep rate $v^{1/2}$ (the rate at which the potential changes) and the area of the electrode, A . The Randles-Sevcík equation shows the peak height, i_p to be proportional to the square root of the sweep rate and so plotting i_p against $v^{1/2}$ should give a straight line, the gradient of which can be used to determine the diffusion coefficient of the compound under consideration.

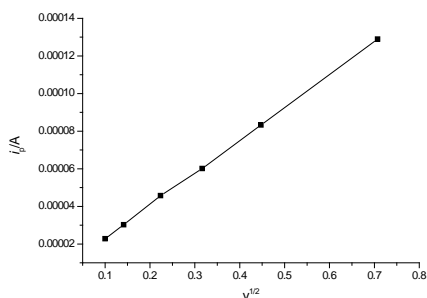


Figure 2.13. A plot of peak height i_p vs. $(\text{sweep rate})^{1/2}$ for $(NBu_4)_3H[SiW_{10}O_{36}(EtPO)_2]$.

By using the Randles-Sevcik equation the diffusion coefficient for $(NBu_4)_3H[SiW_{10}O_{36}(EtPO)_2]$ is calculated as being $1.66 \times 10^{-6} \text{ cm}^2 \text{ s}^{-1}$. This value is relatively low compared to ferrocene ($2.3 \times 10^{-5} \text{ cm}^2 \text{ s}^{-1}$) due to the larger size and charge of the anion which restricts the rate at which it can move towards the electrode.

Further reductions could only be observed using the stationary electrode (Figure 2.14), the general downward slope of the graph (due to oxygen) making the beginning and end of the waves unclear in rotating disc experiments. The second and third waves are at -0.77 and -1.73 V, these are again less negative than the corresponding waves for the parent anion $[SiW_{12}O_{40}]^{4-}$ for the reasons discussed above.

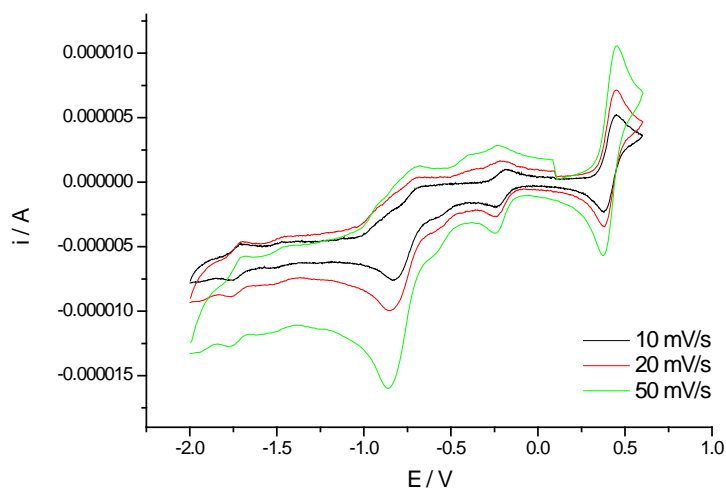


Figure 2.14. Cyclic Voltammogram for $(NBu_4)_3H[SiW_{10}O_{36}(EtPO)_2]$ and ferrocene (used as the internal reference) vs. SCE.

2.3.1.2. $[SiW_{10}O_{36}(C_2H_3PO)_2]^{4-}$

Reaction of $[\gamma-SiW_{10}O_{36}]^{8-}$ with the commercially available vinylphosphonic acid ($H_2C=CHPO(OH)_2$) demonstrates a way of introducing double bond functionality to the cluster (Compounds H and I). Production of the desired product is confirmed by multinuclear NMR (1H

and ^{31}P), IR, MS and EA. Crystals suitable for single crystal XRD could not be obtained for this derivative despite attempts using different solvents (acetonitrile and DMF) and techniques.

^1H NMR. The spectra (Figure 2.15) are dominated by the cation signals. The vinyl functionality is easily seen as a multiplet at 5.95-6.34 ppm, the intensity of these being approximately correct to show that two vinyl groups are present for three NBu_4^+ cations.

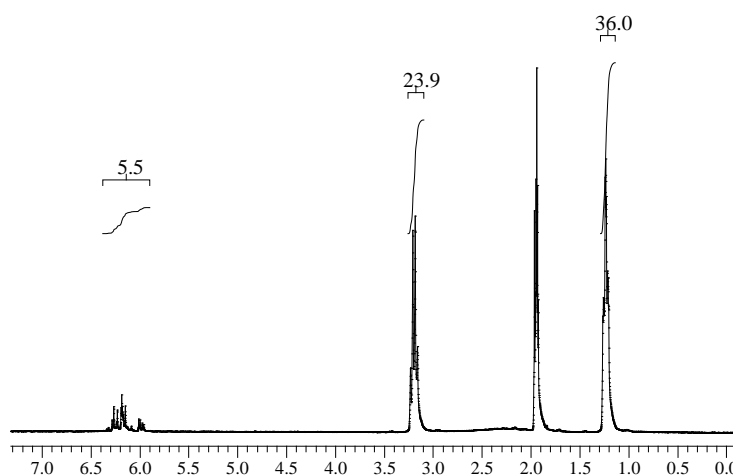


Figure 2.15. ^1H NMR Spectrum for $(\text{NEt}_4)_3\text{H}[\text{SiW}_{10}\text{O}_{36}(\text{H}_2\text{C}=\text{CHPO})_2]$ showing the vinyl multiplet at 5.95-6.34 ppm, the NEt_4^+ cation signals at 1.12-1.32 and 3.18 ppm and the solvent (MeCN) at 1.94 ppm.

^{31}P NMR. Under proton decoupling each ^{31}P NMR spectrum has one signal at 14.8 ppm; this peak has shifted in comparison with the ethyl derivative (29 ppm) due to conjugation with the double bond. The signal has tungsten satellite peaks associated with it; the satellite peaks being of the correct intensity in comparison to the middle peak to indicate that each phosphorus is attached to two tungsten atoms through P-O-W bonds (See section 2.3.1.1). The proton coupled spectra (Figure 2.16) shows the signal to be split by the three hydrogen atoms in the vinyl group, the signal is split into five peaks with intensities of 1:2:2:2:1, this is assigned as an overlapping double triplet where the middle peak is a combination of two peaks, one from each triplet.

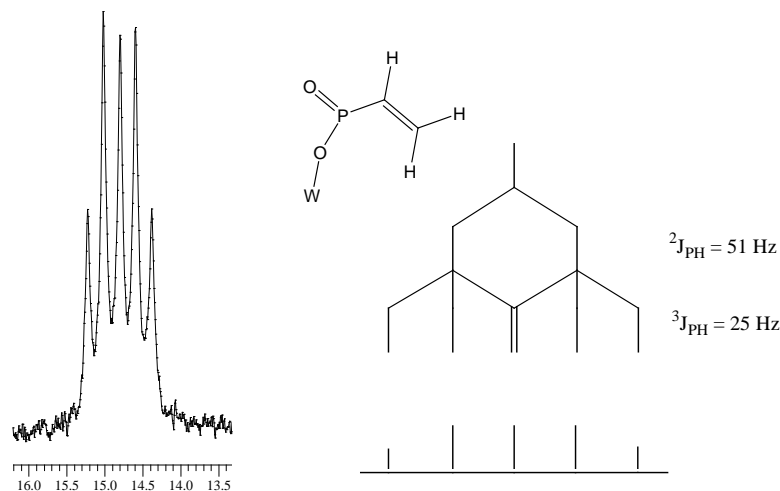


Figure 2.16. The hydrogen coupled ^{31}P NMR for $(\text{NBu}_4)_3\text{H}[\text{SiW}_{10}\text{O}_{36}(\text{H}_2\text{C}=\text{CHPO})_2]$ (a) observed spectrum, (b) predicted spectrum.

IR Spectroscopy. The IR spectrum can be used to indicate formation of the product as the fingerprint region shows characteristic polyoxometalate bands, the exact position of which can help in determining the structure of the anion present. A larger number of bands are present in the fingerprint region in comparison with the lacunary $[\text{SiW}_{10}\text{O}_{36}]^{8-}$ anion, this shows that the symmetry of the structure has been lowered, which is consistent with the addition of two phosphonate groups. Comparison of the position of these peaks with those reported¹⁴ for similar compounds shows a good correlation so indicates that the products have similar structures. The presence of the organic group is confirmed by bands due to C-H, C=C and P-C.

Mass Spectrometry. Electrospray Ionisation (ES) MS shows the major m/z to be for $(\text{NBu}_4)_2[\text{SiW}_{10}\text{O}_{36}(\text{EtPO})_2]^+$, proving that the predicted anion has been formed.

Electrochemical Analysis. Cyclic Voltammetry was carried out using the same conditions as for the ethyl derivative. $[\text{SiW}_{10}\text{O}_{36}(\text{H}_2\text{C}=\text{CHPO})_2]^{4-}$ was seen to exhibit three cathodic/anodic waves in a similar manner to the parent anion $[\text{SiW}_{12}\text{O}_{40}]^{4-}$,²⁵ but with the position of the waves shifted towards less negative values (Figure 2.17). This is similar to when $\text{R}=\text{Et}$, the spectra obtained for both derivatives showing the first three reduction waves to occur

in approximately the same positions, this shows the addition of a double bond within the R group to have little effect on the electrochemical properties of the polyoxotungstate framework.

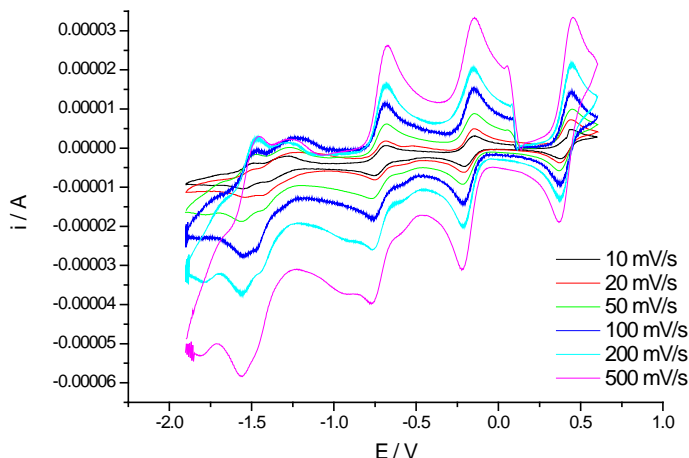


Figure 2.17. Cyclic Voltammogram for $(NBu_4)_3H[SiW_{10}O_{36}(H_2C=CHPO)_2]$ and ferrocene, vs. SCE.

2.3.1.3. $[SiW_{10}O_{36}(H_2C=CHCH_2PO)_2]^{4-}$

Derivatization of the $[\gamma-SiW_{10}O_{36}]^{8-}$ with allylphosphonic acid results in $[\gamma-SiW_{10}O_{36}(H_2C=CHCH_2PO)_2]^{4-}$ as a pale green salt with either NBu_4^+ or NEt_4^+ cations (Compounds J and K). The desired product is confirmed by multinuclear NMR (1H , ^{13}C and ^{31}P), IR, MS, EA and Single Crystal XRD.

1H NMR. In addition to signals for the appropriate cations (NBu_4^+ or NEt_4^+) there are peaks due to the $H_2C=CHCH_2PO$. A double doublet at 2.60 ppm is assigned to the CH_2 nearest the PO group which couples to both the neighbouring CH ($^3J_{HH}=7.2$ Hz) and the phosphorus atom ($^2J_{PH} = 23.2$ Hz). A multiplet due to the terminal CH_2 group is at 5.14-5.27 and a multiplet due to the middle CH group at 5.79-5.96 ppm, the middle CH group couples to the four neighbouring hydrogen atoms so appearing similar to a quintet, but has extra coupling to the phosphorus atom. These allyl signals have similar shifts and couplings to in allylphosphonic acid.

^{31}P NMR. The spectrum shows one signal at 24.5 ppm, which has associated with it tungsten satellite peaks ($^2J_{\text{PW}} = 11.3$ Hz); again integration of these satellite peaks with respect to the central line shows that the phosphorus atom is connected to two tungsten atoms of the polyoxotungstate framework.^{15,16} The H-coupled ^{31}P NMR spectrum shows further splitting of this peak, to give a similar pattern to for allylphosphonic acid ($^2J_{\text{PH}} = 23.3$, $^3J_{\text{PH}}/^4J_{\text{PH}} \sim 6$ Hz giving a pattern that looks like a triplet of quartets), but with extra coupling to the tungsten atoms.

IR Spectroscopy. The IR spectrum of this compound confirms the polyoxotungstate unit to be present with vibrations from W-O-W and W=O_{ter} (942-745 cm^{-1}), a larger number of bands are seen compared to $[\text{SiW}_{10}\text{O}_{36}]^{8-}$ due to a lowering of the symmetry and they are generally shifted to slightly higher frequency due to saturation of the moiety. Bands at around 2960 cm^{-1} have appeared due to the C-H stretches of both the allyl group and the tetra-alkylammonium cations. Also bands have appeared due to P-C and P-O (1200-1000 cm^{-1}) and a weak band is seen at around 1600 cm^{-1} due to the C=C bond.

Mass Spectrometry. The mass spectrum indicates the correct product was formed. Electrospray ionization (ESI) MS on the NBu_4^+ salt shows signals due to the anion with less than three NBu_4^+ cations, (the most intense is at 3104 and is assigned to $(\text{NBu}_4)_2[\text{SiW}_{10}\text{O}_{36}(\text{H}_2\text{C}=\text{CHCH}_2\text{PO})_2]^-$). Maldi-TOF MS on the NEt_4^+ salt shows signals due to the anion with 3 or more NEt_4^+ cations, (the most intense being at 3138 m/z and assigned to $(\text{NEt}_4)_4[\text{SiW}_{10}\text{O}_{36}(\text{H}_2\text{C}=\text{CHCH}_2\text{PO})_2]^+$). Both spectra show the more intense peaks to be due to the anion product with varying numbers of cations, but the signals are weaker due to the product having lost fragments of the allyl group which was grafted onto the structure are also seen.

Elemental Analysis. The results for the NEt_4^+ salt agree well with the predicted values, whereas the values for the NBu_4^+ salt do not agree so well; both sets of values are close enough to

indicate that there are three tetra-alkylammonium cations per anion, the 4- charge of the anion being balanced by a H^+ , which is thought to hydrogen bond to the $P=O$ groups on top of the derivatised unit.

UV/vis Spectroscopy. In the region available for UV/vis spectroscopy only part of a peak due to the polyoxotungstate cluster is seen, this peak is caused by absorption of the W-O bonds.

Single Crystal X-ray Diffraction. Two different crystal structures have been obtained for the $[SiW_{10}O_{36}(H_2C=CHCH_2PO)_2]^{4-}$ anion. Previous work²⁶ led to crystals obtained from a mixture of $NBu_4^+/NEt_4^+/H^+$ cations, the structure of which is studied in more detail here using data obtained from Station 9.8 at the synchrotron source at Daresbury. A second crystal structure was obtained containing NEt_4^+/H^+ cations. These two crystal structures show some interesting differences in both the individual anion structure and the long range ordering of the anions.

Firstly considering the mixed tetra-alkyl ammonium cation structure, this was obtained by dissolving a (2:1 ($NBu_4^+:NEt_4^+$)) mixture of the crude salts in acetonitrile. Slow evaporation of this solution did not yield crystals, so diethyl ether was allowed to diffuse into a fresh solution over several days and gave a low yield of small crystals.

Table 2.2. Crystallographic Data for $(NBu_4)_2(NEt_4)H[SiW_{10}O_{36}(H_2C=CHCH_2PO)_2]$.

Monoclinic	Spacegroup		C c
Cell axes (Å)	a = 18.7759(16)	b = 24.6394(21)	c = 17.1317(15)
Cell angles (deg)	$\alpha = 90.00$	$\beta = 106.406(1)$	$\gamma = 90.00$
Cell Volume (Å ³)	7602.89(26)		

[Full details in appendix (Structure 2)]

The anion (Figure 2.18) is made up of the lacunary $[SiW_{10}O_{36}]^{8-}$ cluster onto which two allyl phosphonate groups have been grafted each bonding to two oxygen atoms on the surface of the vacant site.

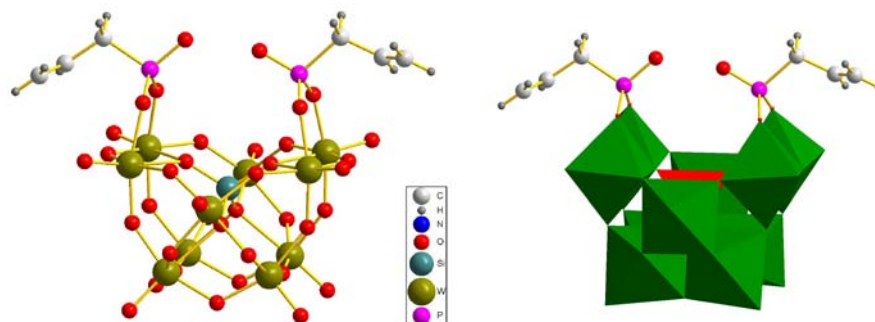


Figure 2.18. The structure of $[SiW_{10}O_{36}(H_2C=CHCH_2PO)_2]^{4-}$ obtained from the crystal structure, shown as (a) ball and stick and (b) polyhedra representations.

Although the symmetry of the $[SiW_{10}O_{36}]^{8-}$ framework is retained the overall structure has a lower symmetry due to differences in the two phosphonate groups, the two P=O bonds being at different angles and having different bond lengths, so making the phosphonate groups nonequivalent. This difference can be interpreted by considering the P-O bond lengths and the O-O distance (2.36 Å), (Figure 2.19) the relatively short distance between the two oxygen atoms indicates the presence of a hydrogen bond formed with the H^+ present in the structure. The differences in the P-O bond lengths show that the H^+ is more closely associated with one of the oxygen atoms, lengthening that P-O bond and giving it more O-H bond character ($d_{P-O}=1.54$ Å), the second P-O bond retains more double bond characteristics ($d_{P-O}=1.46$ Å) and acts as a hydrogen bond acceptor to the hydrogen atom on the first oxygen. A similar effect has been observed for $[\gamma-PW_{10}O_{36}(tBuSiOH)_2]^{3-}$,²⁷ where the observed asymmetry is also assigned to hydrogen bonding between a Si-O-H and Si-O, although as the hydrogen atoms can not be seen by single crystal XRD in either case this can not be confirmed.

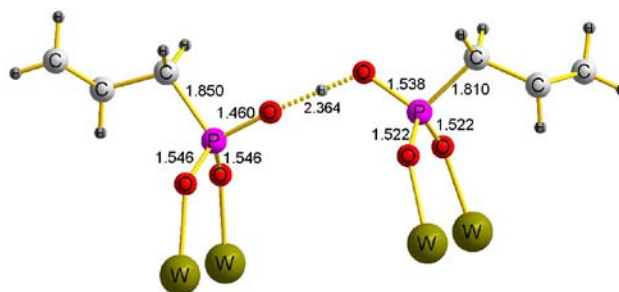


Figure 2.19. The local environment of the phosphorus atoms in $(NBu_4)_2(NEt_4)H[SiW_{10}O_{36}(H_2C=CHCH_2PO)_2]$.

Studying the long range order within the crystal structure it can be seen that the anion clusters are arranged in columns which all face in the same direction (Figure 2.20).

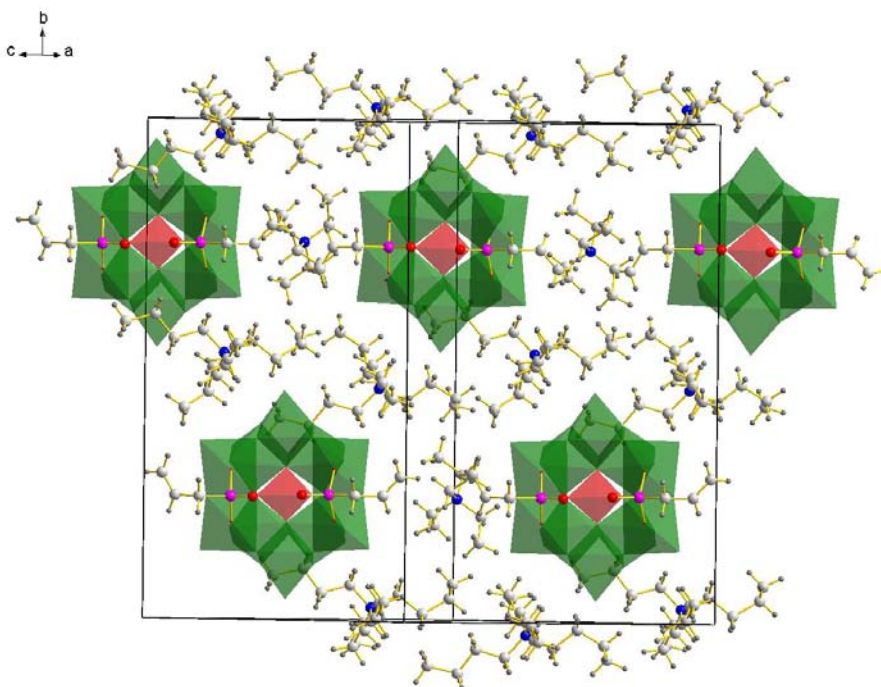


Figure 2.20. The Crystal Structure of $(NBu_4)_2(NEt_4)H[SiW_{10}O_{36}(H_2C=CHCH_2PO)_2]$ showing the columns of anions running through the structure.

Within a column the clusters are arranged with the top of one ~ 3.5 Å below the bottom of the one above it, with the allyl groups from one cluster pointing towards the allyl groups on clusters in neighbouring columns, thus forming layers (Figure 2.21). The gaps within these layers

are occupied by NEt_4^+ cations and the gaps between layers are filled with NBu_4^+ cations, in a similar manner to in the structure of the ethyl derivative.

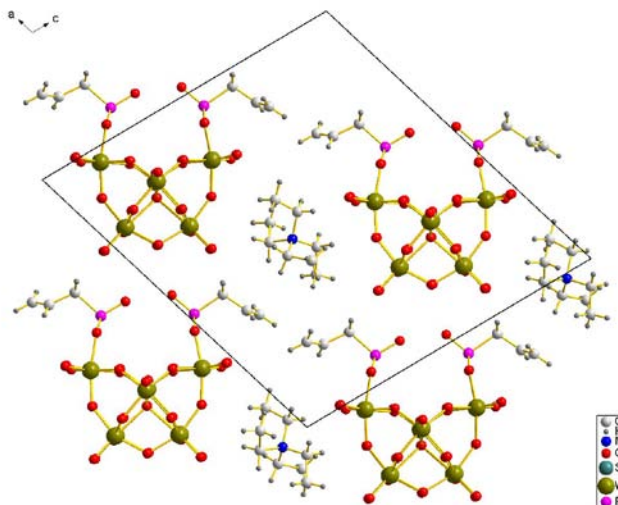


Figure 2.21. The Crystal Structure of $(NBu_4)_2(NEt_4)H[SiW_{10}O_{36}(H_2C=CHCH_2PO)_2]$ viewed down the b -axis.

$(NEt_4)_3H[SiW_{10}O_{36}(H_2C=CHCH_2PO)_2]$ crystals were obtained from an acetonitrile solution into which diethyl ether was slowly diffused over several days.

Table 2.3. Crystallographic Data for $(NEt_4)_3H[SiW_{10}O_{36}(H_2C=CHCH_2PO)_2] \cdot (H_3CCN)_2$.

Monoclinic		Spacegroup		C 2/c
Cell axes (\AA)	$a = 24.4789(54)$	$b = 10.8285(20)$	$c = 27.3078(51)$	
Cell angles (deg)	$\alpha = 90.00$	$\beta = 94.509(23)$	$\gamma = 90.00$	
Cell Volume (\AA^3)	$7216.07(134)$			

[Full details in appendix (Structure 3)]

The anion (Figure 2.22) is made from the lacunary $[SiW_{10}O_{36}]^{8-}$ cluster with two allyl phosphonate groups, each bonding to two oxygen atoms from edge sharing octahedra in the vacant site.

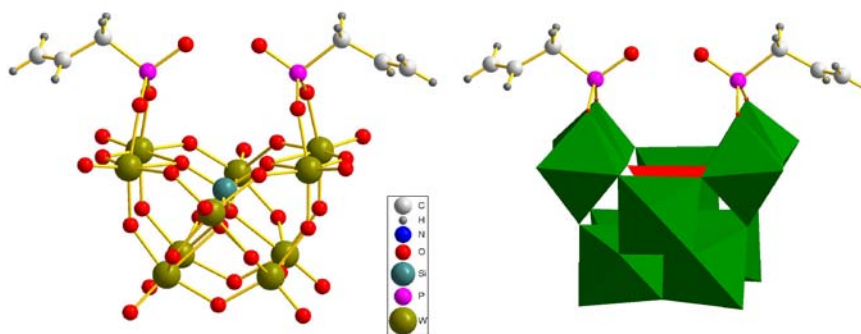


Figure 2.22. The structure of $[\text{SiW}_{10}\text{O}_{36}(\text{H}_2\text{C}=\text{CHCH}_2\text{PO})_2]^{4-}$ obtained from the crystal structure for the NEt_4^+ salt, shown as (a) ball and stick and (b) polyhedra representations.

The anions are of a higher symmetry than for the mixed $\text{NBu}_4^+/\text{NEt}_4^+$ structure with a plane of symmetry running through the centre of the cluster so that the two phosphonate groups are mirror images of one another and are equivalent. The $\text{P}=\text{O}$ bonds are of an equal length (1.51 Å), this length being intermediate between the two seen for the $\text{P}-\text{O}$ bonds in the previous structure. The distance between the two oxygen atoms (2.37 Å) is of a length to indicate a hydrogen bond meaning that the two $\text{P}=\text{O}$'s must bind equally to the H^+ in the same way as that seen in $(\text{NBu}_4)_2(\text{NEt}_4)\text{H}[\text{SiW}_{10}\text{O}_{36}(\text{EtPO})_2]$ (Section 2.3.1.1). Comparison of the IR spectra (Figure 2.23) for the two sets of crystals shows the region containing signals due the $\text{P}-\text{O}$ and $\text{P}=\text{O}$ bonds to be simpler for the symmetrical anions in $(\text{NEt}_4)_3\text{H}[\text{SiW}_{10}\text{O}_{36}(\text{H}_2\text{C}=\text{CHCH}_2\text{PO})_2]$ compared to the unsymmetrical anions in $(\text{NBu}_4)_2(\text{NEt}_4)\text{H}[\text{SiW}_{10}\text{O}_{36}(\text{H}_2\text{C}=\text{CHCH}_2\text{PO})_2]$ which has a larger number of signals between $1100\text{--}1000\text{ cm}^{-1}$ caused by the lower symmetry.

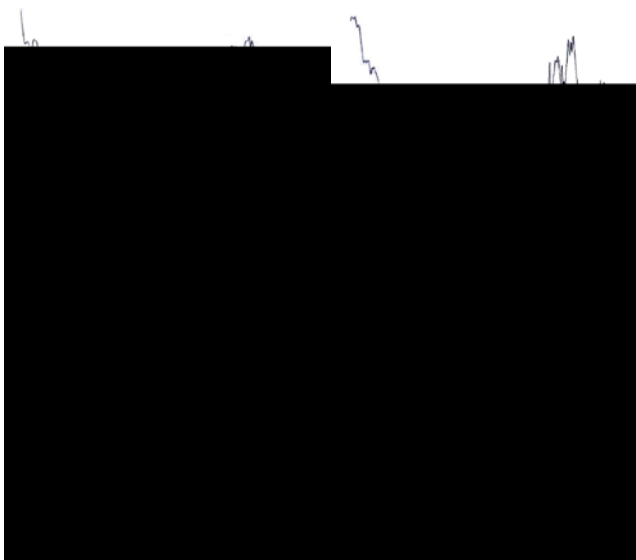


Figure 2.23. The IR spectra for the crystals of $(NEt_4)_3H[SiW_{10}O_{36}(H_2C=CHCH_2PO)_2]$ (left) and $(NBu_4)_2(NEt_4)H[SiW_{10}O_{36}(H_2C=CHCH_2PO)_2]$ (right).

Considering the long range order of the anion clusters, columns of anions running parallel to the b -axis are formed (Figure 2.24), within a column all the anions point in the same direction with gaps of $\sim 3.5 \text{ \AA}$ between them.

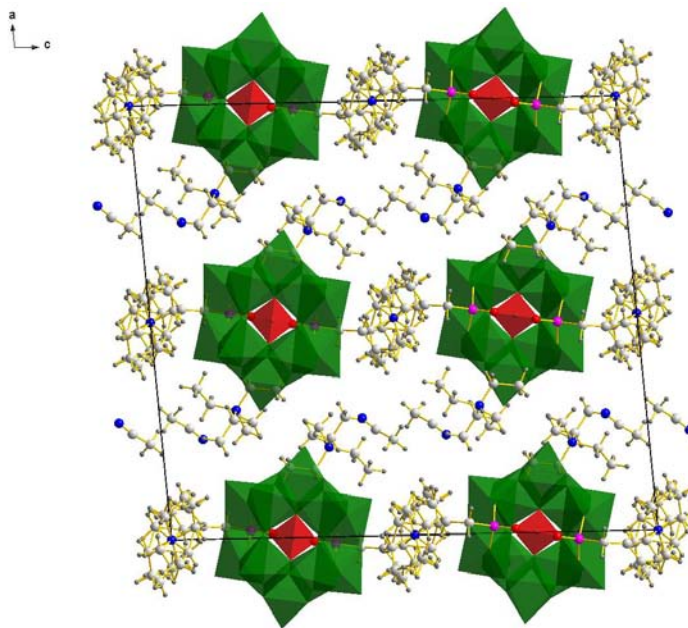


Figure 2.24. Crystal Structure of $(NEt_4)_3H[SiW_{10}O_{36}(H_2C=CHCH_2PO)_2]$ viewed down the b -axis.

The allylphosphonate groups within a column point towards the phosphonate groups on the anions in neighbouring columns, thus forming layers running through the structure. The anions in adjacent columns within a layer point in opposite directions (Figure 2.25), with the gaps in these layers filled by disordered NEt_4^+ cations and the rest of the NEt_4^+ cations located between the layers.

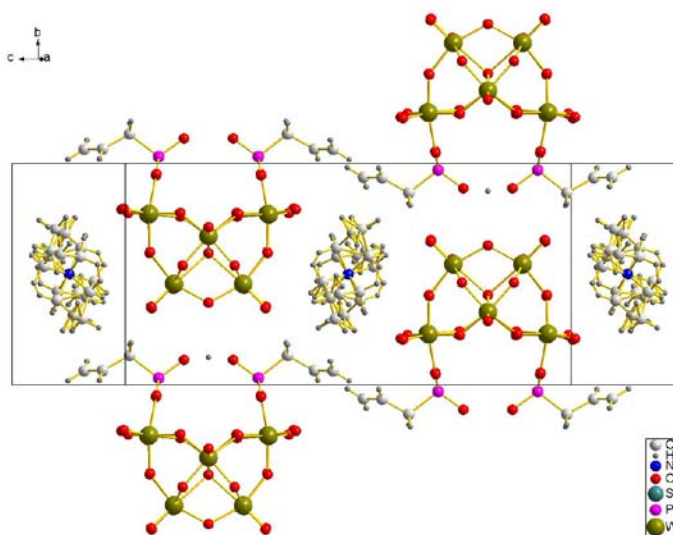


Figure 2.25. Crystal Structure of $(NEt_4)_3H[SiW_{10}O_{36}(H_2C=CHCH_2PO)_2]$ showing a layer of anions which is formed.

Overall the two crystal structures obtained containing $[SiW_{10}O_{36}(H_2C=CHCH_2PO)_2]^{4-}$ are quite different. Although the size and packing of the different cations will contribute to this and would explain the long range ordering the reasons for the symmetrical and unsymmetrical anion structures remain unclear as both take part in hydrogen-bonding with an H^+ ion.

Electrochemical Analysis. Cyclic voltammetry was performed, using similar conditions to for the ethyl derivative, but with an Ag/Ag^+ reference electrode.

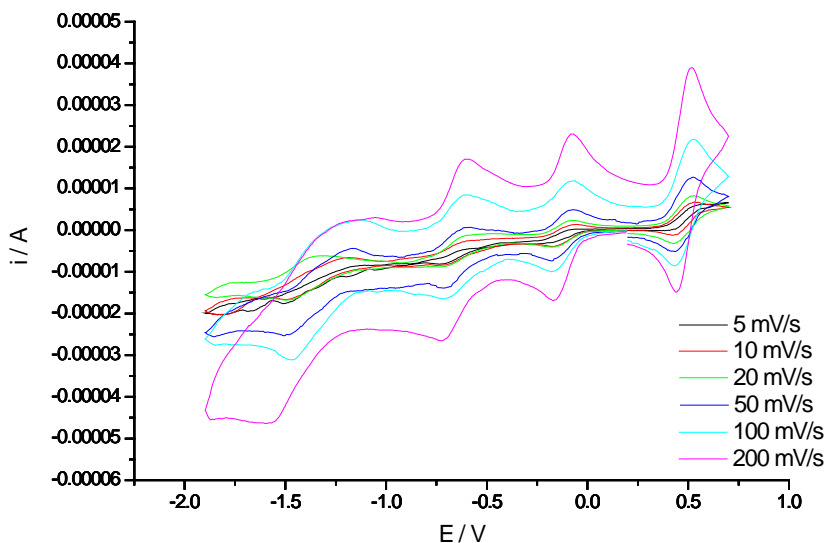


Figure 2.26. The cyclic voltammogram of $[\text{SiW}_{10}\text{O}_{36}(\text{H}_2\text{C}=\text{CHCH}_2\text{PO})_2]^{4-}$ and Ferrocene.

The anion has three cathodic/anodic waves (Figure 2.26), similar to when R = Ethyl or Vinyl. Using ferrocene as an internal reference and setting its peak potential to be at zero, the position of the first two waves are in approximately the same position as for the vinyl derivative, although a slight shift to a more negative value is seen, the extra CH_2 group making the R group slightly less electron withdrawing and more like the ethyl group (Table 2.4).

Table 2.4. The First two reduction potentials for $(\text{NBu}_4)_3\text{H}[\text{SiW}_{10}\text{O}_{36}(\text{RPO})_2]$, 1.0 mM solutions, E° quoted relative to ferrocene.

R	$E(1) / (\text{mV})$	$E(2) / (\text{mV})$
Ethyl	-0.62	-1.19
Vinyl	-0.59	-1.12
Allyl	-0.60	-1.14

2.3.1.4. $[\text{SiW}_{10}\text{O}_{36}(\text{H}_2\text{C}=\text{CHC}_6\text{H}_4\text{PO})_2]^{4-}$

Derivatization of the $[\text{SiW}_{10}\text{O}_{36}]^{8-}$ anion using styrylphosphonic acid $\text{H}_2\text{C}=\text{CHC}_6\text{H}_4\text{PO}(\text{OH})_2$ leads to an anion with two styryl groups grafted on to the framework (Compounds 4 and 5). This adds double bond functionality to the structure like the vinyl and allyl

derivatives, but has the additional benefit of the double bond conjugating to an aromatic ring which should aid in the polymerization of the clusters. The synthesis was carried out by the method used previously; although the styrylphosphonic acid had limited solubility in acetonitrile the reaction still went to completion, giving $[\text{SiW}_{10}\text{O}_{36}(\text{H}_2\text{C}=\text{CHC}_6\text{H}_4\text{PO})_2]^{4-}$ as a salt with tetra-alkylammonium cations (NBu_4^+ or NEt_4^+).

^1H NMR. The spectra for both salts are again dominated by the cation environments (Figure 2.27). The peaks due to the styryl functionality being easily distinguishable, in approximately the same position as for the styrylphosphonic acid, with the aromatic ring multiplet between 7.55-7.96 ppm and three signals at 5.35, 5.95 and 6.74-6.88 ppm due to the three hydrogen atoms on the double bond. The intensities indicate that two styryl groups are present for every three tetra-alkylammonium cations.

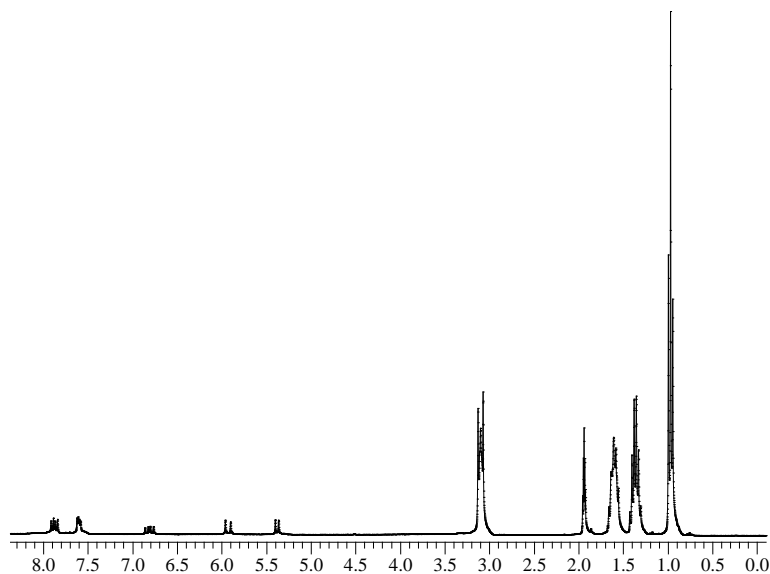


Figure 2.27. The ^1H NMR spectrum for $(\text{NBu}_4)_3\text{H}[\text{SiW}_{10}\text{O}_{36}(\text{H}_2\text{C}=\text{CHC}_6\text{H}_4\text{PO})_2]$ in MeCN-d_3 (1.94 ppm).

^{31}P NMR. The ^{31}P NMR spectra have one peak (15.4 ppm), indicating that the two phosphorus atoms in the structure are equivalent. This peak has tungsten satellite peaks associated with it confirming that the phosphorus is attached to two tungsten atoms in the same

way as that seen previously. The hydrogen coupled spectra show that the coupling seen for the styrylphosphonic acid is retained with the addition of the extra coupling to the tungsten atoms; confirming that the phosphorus atom remains attached to the styryl group and so acts as a linker between it and the polyoxotungstate framework.

IR Spectroscopy. The IR spectra for both salts of the $[\text{SiW}_{10}\text{O}_{36}(\text{H}_2\text{C}=\text{CHC}_6\text{H}_4\text{PO})_2]^{4-}$ cluster show bands in the fingerprint region due to the polyoxotungstate framework, these are the same as for the other derivatives, confirming that the structures are related. Bands due to the styryl group can also be seen, most importantly the C=C double bond peak at 1600 cm^{-1} and those due to the C-H, P-C and the aromatic ring ($\sim 1650\text{ cm}^{-1}$).

Mass Spectrometry. The Maldi-TOF mass spectra indicates that the correct product was formed; for the NEt_4^+ salt, signals are seen for the complete anion with varying numbers of cations associated with it and in some cases also a sodium cation (Na^+) which is introduced during the mass spectrum preparation. The spectrum for the NBu_4^+ salt shows the anion to lose either all or part of a styryl group upon ionisation; enough of the groups being present to indicate that two groups were originally attached to the anion.

Elemental Analysis. The elemental analysis results for the NBu_4^+ salt are close to that predicted, however results for the NEt_4^+ salt show a large difference in the amount of carbon (calc C 15.3, found C 12.1).

UV/vis Spectroscopy. Although UV/vis spectroscopy in the region available shows only the edge of a peak due to the polyoxotungstate it can be used to confirm the presence of the aromatic groups. The spectra for $[\text{SiW}_{10}\text{O}_{36}(\text{H}_2\text{C}=\text{CHC}_6\text{H}_4\text{PO})_2]^{4-}$ (Figure 2.28) shows peaks due to the styryl similar to those for the styrylphosphonic acid, the most intense peak having shifted

(257.8 nm), with the other two peaks shifting less. The intensity of the peaks has increased, the peaks being on the edge of the signal from the polyoxotungstate cluster.

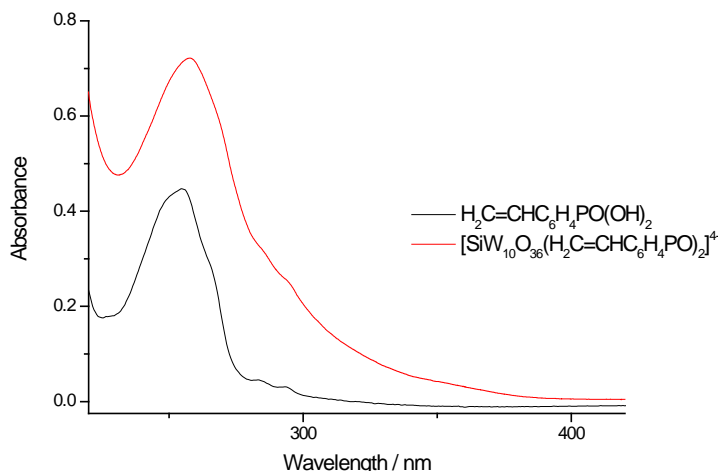


Figure 2.28. The UV/vis spectra for (a) styrylphosphonic acid and (b) $[\text{SiW}_{10}\text{O}_{36}(\text{H}_2\text{C}=\text{CHC}_6\text{H}_4\text{PO})_2]^{4-}$.

Single Crystal X-ray Diffraction. Small crystals were obtained by diffusion of diethyl ether into an acetonitrile solution of $(\text{NBu}_4)_3\text{H}[\text{SiW}_{10}\text{O}_{36}(\text{H}_2\text{C}=\text{CHC}_6\text{H}_4\text{PO})_2]$. Single Crystal XRD on the Bruker Smart 6000 diffractometer in Birmingham found the crystals to be poor quality and the unit cell to be very large (b -axis=60-70 Å), therefore synchrotron data was obtained for the sample on Station 16.2 at the SRS facility at the CCLRC Daresbury Laboratory.

Table 2.5. Crystallographic Data for $(\text{NBu}_4)_3\text{H}[\text{SiW}_{10}\text{O}_{36}(\text{H}_2\text{C}=\text{CHC}_6\text{H}_4\text{PO})_2]$.

Monoclinic	Spacegroup		
	P 2 ₁		
Cell axes (Å)	a = 14.3007(16)	b = 63.2438(71)	c = 28.0285(32)
Cell angles (deg)	α = 90.00	β = 91.120(1)	γ = 90.00
Cell Volume (Å ³)	25344.99(50)		

[Full details in appendix (Structure 4)]

The difference in the b -axis is thought to be due to the poor quality data collected at Birmingham meaning that the unit cell parameters were inaccurate. Although better quality data

was obtained at Daresbury, the crystal structure could still not be solved completely due to a very large asymmetric unit containing five anion clusters and 15 NBu_4^+ cations and the data quality. However the $[SiW_{10}O_{36}]^{8-}$ framework could be seen to be retained with the styrylphosphonate groups attached, although these groups could not be fully determined and the NBu_4^+ cations were only partly located (Figure 2.29).

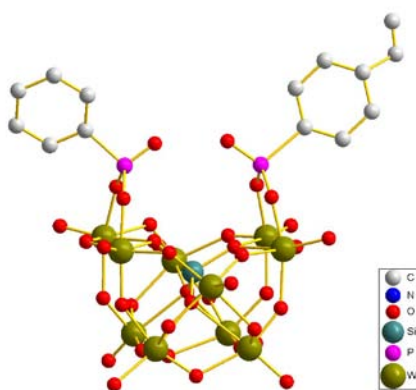


Figure 2.29. One of the anion structures obtained from the Single Crystal XRD of $(NBu_4)_3H[SiW_{10}O_{36}(H_2C=CHC_6H_4PO)_2]$, the $H_2C=CH$ group on one of the styrene's is missing due to the quality of the data and the complexity of the structure making it impossible to completely solve the structure.

Electrochemical Analysis. Cyclic Voltammetry was performed on the $(NBu_4)_3H[SiW_{10}O_{36}(H_2C=CHC_6H_4PO)_2]$ using a SCE reference electrode (Figure 2.30).

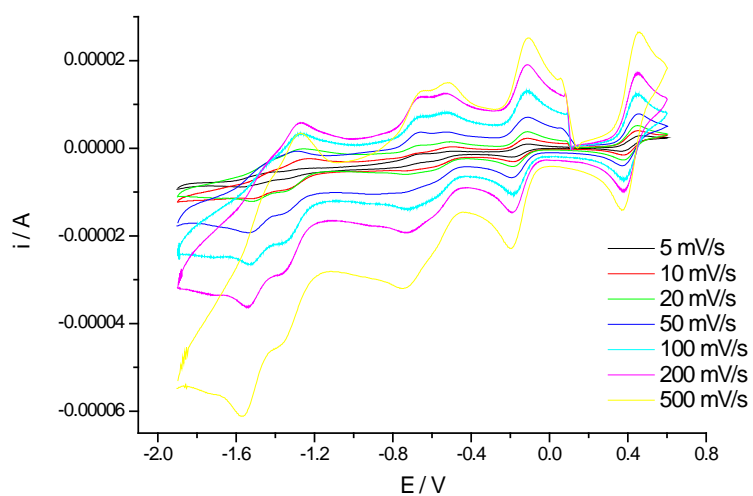


Figure 2.30. The cyclic voltammogram for $[SiW_{10}O_{36}(H_2C=CHC_6H_4PO)_2]^{4-}$ at varying scan rates.

As for the other $[SiW_{10}O_{36}]^{8-}$ derivatives the cyclic voltammogram exhibits three sets of cathodic/anodic waves. The first two waves are both due to one-electron processes and appear at slightly less negative positions than those for the other derivatives, this shift is attributed to the greater electron withdrawing properties of the styrene group. There are indications of other peaks around the second wave, which is most probably due to the product of a reaction of the reduced species similar to the $\alpha\beta$ isomerisation observed for other Keggin anions,^{28,29} this reaction appearing to be dependent on the R group. The third reduction wave (~ -1869 mV) is due to a two-electron process, in this case the two processes are split.

2.3.1.5. $[SiW_{10}O_{36}(HOOCCH_2PO)_2]^{4-}$

Derivatization of the $[SiW_{10}O_{36}]^{8-}$ anion using phosphonoacetic acid $HOOCCH_2PO(OH)_2$ results in a polyoxotungstate cluster derivatised with two carboxylic acid functionalities $[SiW_{10}O_{36}(HOOCCH_2PO)_2]^{4-}$ (Compounds 6 and 7). This functionality has the potential to be used to control the long range ordering of the clusters either through coordination or reaction of the carboxylic acid group. The functionalisation of a polymolybdate anion with phosphonoacetic acid has been reported in the literature giving $[(O_2CCH_2PO_3)_2Mo_5O_{15}]^{6-}$ in which the two carboxylic acid groups are on opposite sides of the ring shaped polyoxoanion, but carboxyderivatised structures have not been reported for Keggin type anions.

1H NMR. The 1H NMR spectra shows peaks due to the appropriate cations (NBu_4^+ or NEt_4^+) and one extra signal due to the CH_2 present in the functional group. This peak is at 2.90 ppm and couples to the phosphorus atom giving a doublet with $^2J_{PH} = 23.1$ Hz.

^{31}P NMR. The ^{31}P NMR spectra show one signal at 18.5 ppm, which has tungsten satellite peaks associated with it ($^2J_{\text{PW}} = 10$ Hz); integration of these peaks showing the phosphorus atom to be connected to two tungsten atoms of the polyoxotungstate framework.^{15,16}

IR Spectroscopy. The fingerprint region confirms the polyoxotungstate unit to be present, having a structure related to those for the other derivatives. The presence of the carboxylic acid group is confirmed by a C=O stretch at 1718 cm^{-1} and a O-H stretch at $\sim 3420\text{ cm}^{-1}$, along with C-H stretches from both the CH_2 group and the NR_4^+ cations and bands due to P-C and P-O.

Mass Spectrometry. Maldi-TOF mass spectrometry confirms production of the desired product in a relatively clean reaction, peaks due to the anion cluster with varying numbers of cations are present, along with a few peaks where the anion has lost part of the functional group (HOOCCH_2PO) during the ionisation process.

Elemental Analysis. Results for both the $\text{NBu}_4^+/\text{H}^+$ and $\text{NEt}_4^+/\text{H}^+$ salts show the percentages of carbon, nitrogen and hydrogen to be correct, indicating that the anion has three cations associated with it, the charge of the anion (4-) being balanced by a H^+ .

Single Crystal X-ray Diffraction. Crystals suitable for single crystal XRD were obtained by diffusion of diethyl ether into a DMF solution of $(\text{NEt}_4)_3\text{H}[\text{SiW}_{10}\text{O}_{36}(\text{HOOCCH}_2\text{PO})_2]$. Diffraction data was collected at Station 9.8 of the synchrotron source at Daresbury, to give a good quality dataset from which the structure could be solved.

Table 2.6. Crystallographic Data for $(\text{NEt}_4)_3\text{H}[\text{SiW}_{10}\text{O}_{36}(\text{HOOCCH}_2\text{PO})_2]$.

Monoclinic	Spacegroup		C c
Cell axes (\AA)	$a = 24.1700(2)$	$b = 10.7640(1)$	$c = 27.0430(5)$
Cell angles (deg)	$\alpha = 90.00$	$\beta = 98.113(1)$	$\gamma = 90.00$
Cell Volume (\AA^3)	$6965.25(0)$		

[Full details in appendix (Structure 5)]

The structure consists of a $[\text{SiW}_{10}\text{O}_{36}]^{8-}$ cluster onto which two phosphonate groups have been grafted via P-O-W bonds in the same way as previous structures.

The arrangement of clusters within the crystal structure is similar to for $(\text{NEt}_4)_3\text{H}[\text{SiW}_{10}\text{O}_{36}(\text{H}_2\text{C}=\text{CHCH}_2\text{PO})_2]$, with the clusters in columns, those within a column pointing in the same direction and those in alternate columns pointing in opposite directions (Figure 2.31).

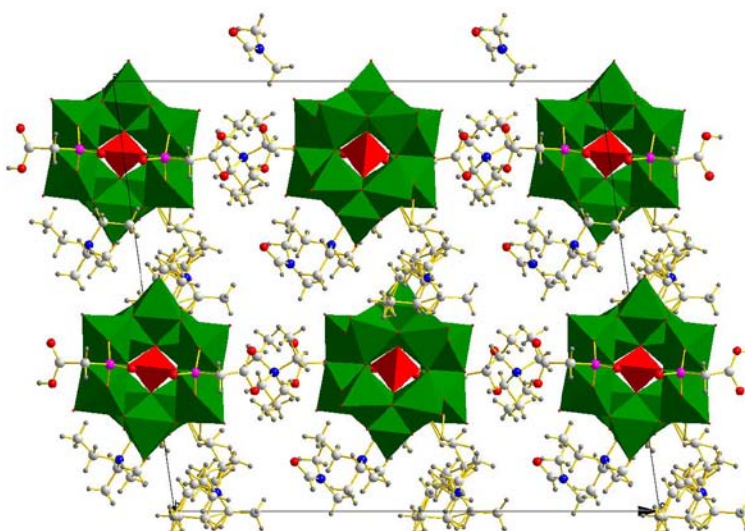


Figure 2.31. The structure of $(\text{NEt}_4)_3\text{H}[\text{SiW}_{10}\text{O}_{36}(\text{HOOCCH}_2\text{PO})_2]$ viewed along the b -axis.

The organic functional groups point towards one another to form layers (Figure 2.32), the carboxylic acid groups interacting via hydrogen bonds ($d_{\text{O}\cdots\text{O}} \sim 2.5 \text{ \AA}$) to form chains which run through the structure.

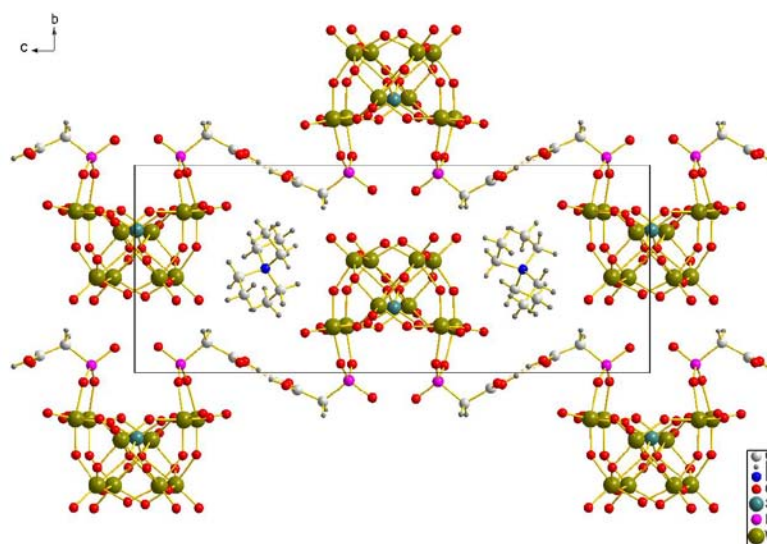


Figure 2.32. The structure of $(NEt_4)_3H[SiW_{10}O_{36}(HOOCCH_2PO)_2]$ viewed along the a -axis.

Electrochemical Analysis. Cyclic Voltammetry was performed on the product using a SCE reference electrode (Figure 2.33).

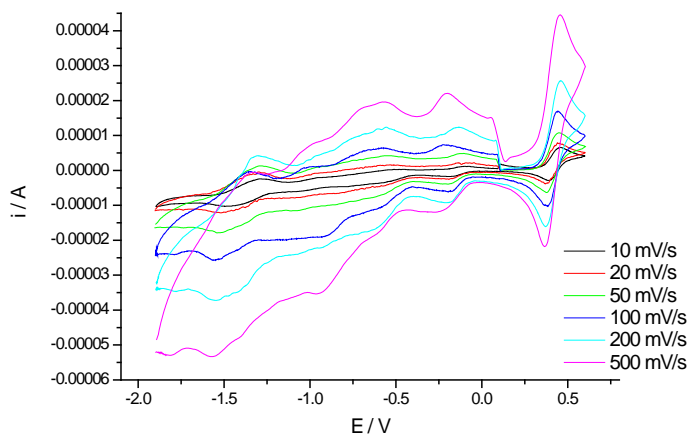


Figure 2.33. The cyclic voltammogram for $[SiW_{10}O_{36}(HOOCCH_2PO)_2]^{4-}$ at varying scan rates.

The cyclic voltammogram exhibits three sets of cathodic/anodic waves due to reductions of the tungsten atoms. The first two reduction waves are both due to one-electron processes and the third is due to a two-electron process. The waves are at similar positions to for the other derivatives, although they are at slightly more negative values than for the styrene derivative, but less negative than the others, showing that the carboxylic acid group has electron withdrawing

properties between those of styrene and the other functionalities. There are indications of other peaks around the second wave and again this is assigned to the reduction of a product formed from the reduced species similar to an $\alpha \rightarrow \beta$ isomerisation.^{28,29}

2.3.1.6. $[\text{SiW}_{10}\text{O}_{36}(\text{HOOCCH}_2\text{CH}_2\text{PO})_2]^{4-}$

Derivatization of the $[\text{SiW}_{10}\text{O}_{36}]^{8-}$ anion using $\text{HOOCCH}_2\text{CH}_2\text{PO}(\text{OH})_2$ results in the polyoxotungstate cluster $[\text{SiW}_{10}\text{O}_{36}(\text{HOOCCH}_2\text{CH}_2\text{PO})_2]^{4-}$ (Compounds L and M). Again the cluster is functionalised with two carboxylic acid groups, an extra CH_2 making the group more flexible and the carboxylic acid group further from the polyoxometalate framework.

^1H NMR. The ^1H NMR spectra show the cation environments (NBu_4^+ or NEt_4^+) and peaks due to the two CH_2 's within the functional group. These peaks appear as multiplets at 1.98-2.12 and 2.57-2.68 ppm with intensities to indicate that there are two $\text{HOOCCH}_2\text{CH}_2$ groups for every three cations.

^{31}P NMR. The ^{31}P NMR spectra show a peak at 26.9 ppm, with tungsten satellite peaks ($^2J_{\text{PW}} = 11.1$ Hz); these show the phosphorus atom to be connected to the polyoxotungstate framework in the same way as for the other derivatives. The hydrogen coupled spectrum shows the phosphorus signal to be split (Figure 2.34) giving a signal based on a triple triplet where the phosphorus is coupling to the hydrogen atoms in both the CH_2 groups, but with some of the peaks overlapping so only seven major peaks are seen, the tungsten coupling to each peak being clearly visible.

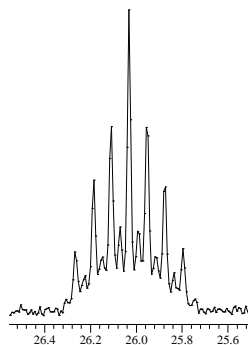


Figure 2.34. ^{31}P NMR hydrogen coupled spectrum for $(\text{NBu}_4)_3\text{H}[\text{SiW}_{10}\text{O}_{36}(\text{HOOCCH}_2\text{CH}_2\text{PO})_2]$.

IR Spectroscopy. The product shows bands characteristic of the polyoxotungstate framework in the fingerprint region. The presence of the carboxylic acid group is confirmed by a C=O stretch at 1734.2, the O-H at $\sim 3420\text{ cm}^{-1}$ and signals due to the C-H, P-C and P-O bonds.

Mass Spectrometry. The Maldi-TOF mass spectrum for the NBu_4^+ salt shows peaks due to the anion $[\text{SiW}_{10}\text{O}_{36}(\text{HOOCCH}_2\text{CH}_2\text{PO})_2]^{n-}$ with either four or five cations, along with peaks where the anion has lost all or part of a R group.

Elemental Analysis. The percentages of carbon, nitrogen and hydrogen found for both salts are relatively close to that predicted (within 1.5 %) so confirming that three cations are present per anion; however the results are not ideal.

Single Crystal X-ray Diffraction. Crystals of $(\text{NEt}_4)_3\text{H}[\text{SiW}_{10}\text{O}_{36}(\text{HOOCCH}_2\text{CH}_2\text{PO})_2]$ were obtained by dissolving the crude product in acetonitrile and slowly diffusing diethyl ether into the solution.

Table 2.7. Crystallographic Data for $(\text{NEt}_4)_3\text{H}[\text{SiW}_{10}\text{O}_{36}(\text{HOOCCH}_2\text{CH}_2\text{PO})_2] \cdot (\text{H}_3\text{CCN})_6$.

Monoclinic	Spacegroup		P 2/c
Cell axes (\AA)	$a = 24.6162(11)$	$b = 10.7582(5)$	$c = 32.6472(15)$
Cell angles (deg)	$\alpha = 90.00$	$\beta = 108.419(2)$	$\gamma = 90.00$
Cell Volume (\AA^3)	$8202.91(58)$		

[Full details in appendix (Structure 6)]

The structure of the anion is related to that seen for other derivatives, with the $[\text{SiW}_{10}\text{O}_{36}]^{8-}$ framework having two phosphonate groups grafted onto the oxygen atoms in the vacant sites through two P-O-W bonds. The anion is symmetrical with the two P=O bonds being of the same length and so both bonding equally to a H^+ to form a hydrogen bond. The $\text{CH}_2\text{CH}_2\text{COOH}$ chains point away from the central anion structure, the groups being related through rotational symmetry.

The unit cell parameters are similar to those for $(\text{NEt}_4)_3\text{H}[\text{SiW}_{10}\text{O}_{36}(\text{H}_2\text{C}=\text{CHCH}_2\text{PO})_2]$ and $(\text{NEt}_4)_3\text{H}[\text{SiW}_{10}\text{O}_{36}(\text{HOOCCH}_2\text{PO})_2]$, all having monoclinic structures with the a and b -axes being the same length. However, in this structure the c -axis is longer, this being the direction in which the R groups point, and so showing a relationship to the length of the group grafted onto the cluster. The β angle also increases in the order $\text{H}_2\text{C}=\text{CHCH}_2 < \text{HOOCCH}_2 < \text{HOOCCH}_2\text{CH}_2$, making the anions within one layer more off-set from the anions in adjacent layers. The arrangement of anions is the same for all three structures; columns of anions all pointing in the same direction run in the direction of the b -axis (Figure 2.35), with the R groups from one column all pointing towards those in adjacent columns, the anions in these columns aligning in the opposite direction to those in the first column (Figure 2.36).

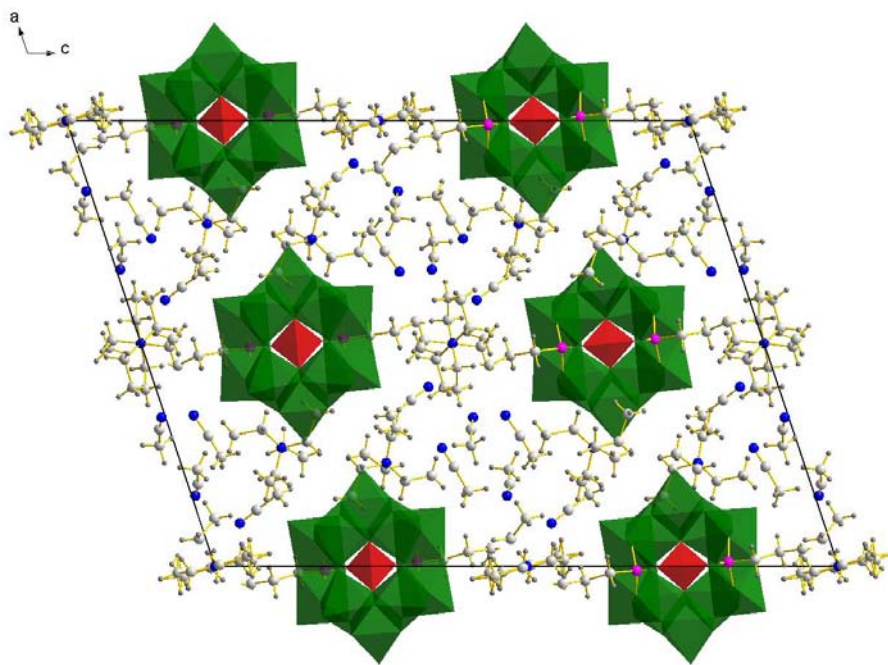


Figure 2.35. The structure of $(NEt_4)_3H[SiW_{10}O_{36}(HOOCCH_2CH_2PO)_2]$ viewed down the b -axis.

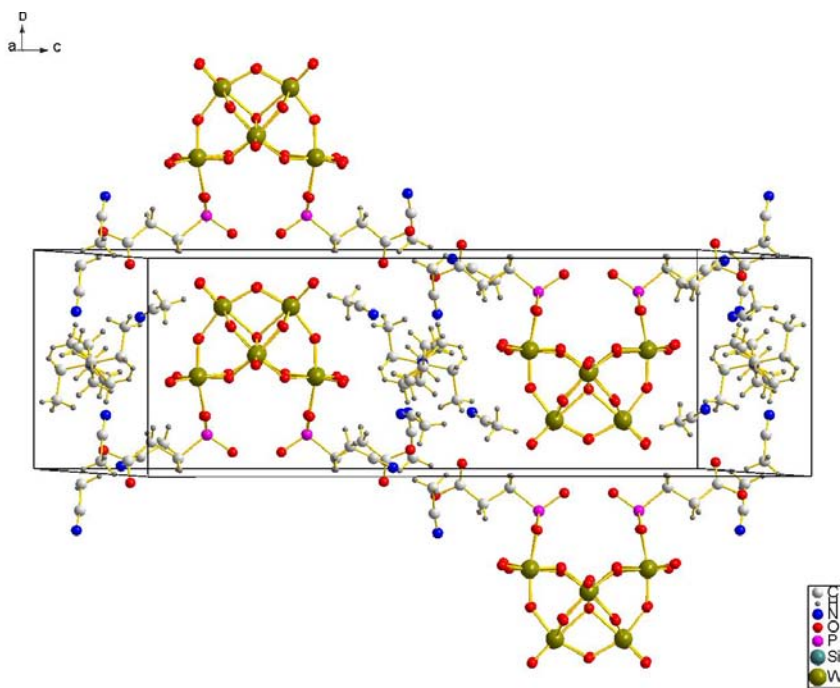


Figure 2.36. The structure of $(NEt_4)_3H[SiW_{10}O_{36}(HOOCCH_2CH_2PO)_2]$ showing the layers in the structure.

In the structure of $(NEt_4)_3H[SiW_{10}O_{36}(HOOCCH_2PO)_2]$ the carboxylic acid groups interacted via hydrogen-bonds to form chains, a similar effect would be expected for $(NEt_4)_3H[SiW_{10}O_{36}(HOOCCH_2CH_2PO)_2]$, however a large number of acetonitrile solvent molecules are present in the structure and these also take part in hydrogen-bonding, altering the interaction between the two carboxylic acid groups (Figure 2.37). The distances between the oxygen atoms on the carboxylic acid groups and the nitrogen atoms in the solvent molecules are between 2.74–3.42 Å, these distances and that between the two carboxylic acid groups (3.30 Å), are such to indicate weak hydrogen-bonds, the two hydrogen atoms from the two carboxylic acids being disordered over these sites.

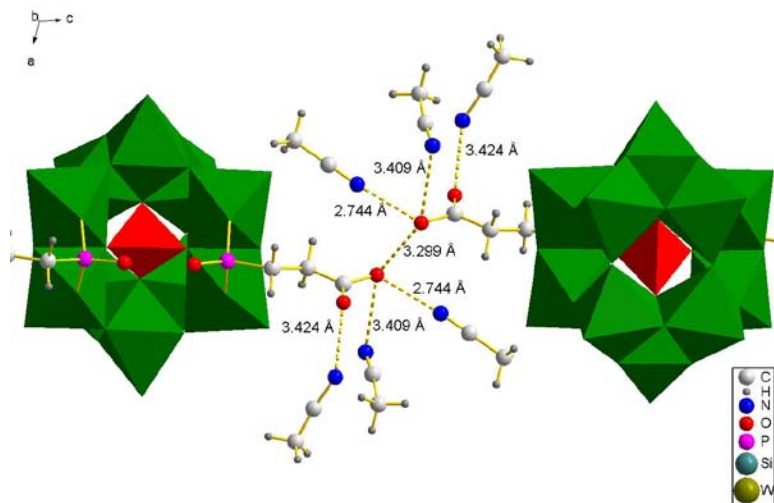


Figure 2.37. The structure of $(NEt_4)_3H[SiW_{10}O_{36}(HOOCCH_2CH_2PO)_2]$ showing the hydrogen-bond interactions.

Electrochemical Analysis. Cyclic Voltammetry on $(NBu_4)_3H[SiW_{10}O_{36}(HOOCCH_2CH_2PO)_2]$ was performed in a similar way to for the other derivatives, but using a non-aqueous Ag/Ag^+ reference electrode (Figure 2.38).

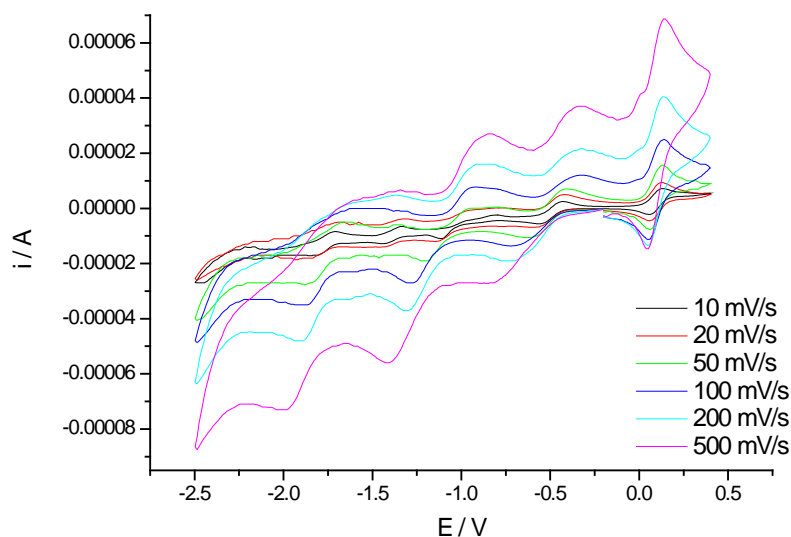


Figure 2.38. The cyclic voltammogram for $[\text{SiW}_{10}\text{O}_{36}(\text{HOOCCH}_2\text{CH}_2\text{PO})_2]^{4-}$ at various scan rates.

The Ag/Ag^+ reference electrode shifts the position of the peaks to more negative values, therefore the range which the cyclic voltammogram is taken over was changed to (-2.5-0.4 V). In this range $[\text{SiW}_{10}\text{O}_{36}(\text{HOOCCH}_2\text{CH}_2\text{PO})_2]^{4-}$ exhibits three sets of cathodic/anodic waves due to reductions of the tungsten atoms. The first two waves are both one-electron processes and the third wave a two-electron process. Although the reference electrode changes the positions of the waves they can be considered relative to the internal reference ferrocene and this shows the positions to be comparable to those seen for the other derivatives (Table 2.8). The first two waves are in the same position as the ethyl derivative, showing that the carboxylic acid group has much less effect on the observed potential when two methylene groups separate it from the phosphonate linker than when the carbon chain was shorter.

Table 2.8. The First two reduction potentials for $(\text{NBu}_4)_3\text{H}[\text{SiW}_{10}\text{O}_{36}(\text{RPO})_2]$, E° quoted relative to ferrocene.

R	E°_1 / mV	E°_2 / mV
Ethyl	-0.62	-1.19
HOOCCH_2	-0.57	-1.02
$\text{HOOCCH}_2\text{CH}_2$	-0.61	-1.14

2.3.1.7. $[\text{SiW}_{10}\text{O}_{36}(\text{H}_3\text{CCOC}_6\text{H}_4\text{PO})_2]^{4-}$

Derivatization of the $[\text{SiW}_{10}\text{O}_{36}]^{8-}$ anion using 4-acetylphenylphosphonic acid $\text{H}_3\text{CCOC}_6\text{H}_4\text{PO}(\text{OH})_2$ leads to an anion onto which two ketone functionalities have been grafted (Compounds 8 and 9). These functional groups have the potential to take part in further reactions, introducing additional functionality to the polyoxotungstate cluster.

^1H NMR. The spectra are dominated by the appropriate cations (NBu_4^+ or NEt_4^+), peaks due to the acetylphenyl functional group being seen in approximately the same positions as for the phosphonic acid. The aromatic ring multiplet appears between 7.96-8.14 ppm with the singlet due to the CH_3 group at 2.60 ppm. The intensities indicate that two groups are present for every three tetra-alkylammonium cations.

^{31}P NMR. The spectra shows a tungsten coupled peak at 14.0 ppm, little change in the position of this signal relative to the phosphonic acid (14.5 ppm) being seen.

The hydrogen-coupled spectra (Figure 2.39) shows that the coupling has changed from that for the phosphonic acid; although it can still be attributed to being based on a triple triplet the ^4J coupling constant is larger making the peaks overlap more and changing the shape.

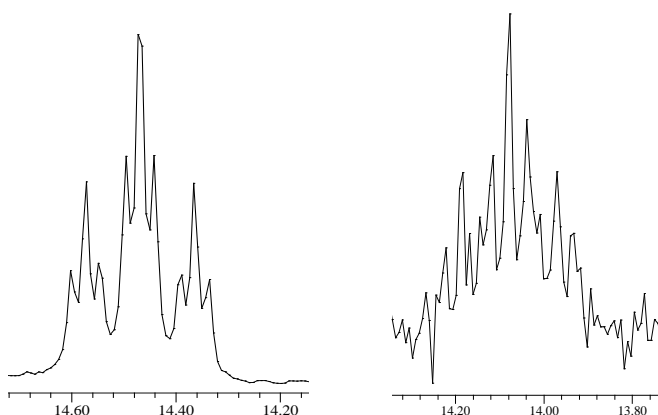


Figure 2.39. The hydrogen-coupled ^{31}P NMR spectra for (a) $\text{H}_3\text{CCOC}_6\text{H}_4\text{PO}(\text{OH})_2$ and (b) $[\text{SiW}_{10}\text{O}_{36}(\text{H}_3\text{CCOC}_6\text{H}_4\text{PO})_2]^{4-}$.

IR Spectroscopy. The bands due to the polyoxotungstate framework indicate formation of a structure similar to that for the other derivatives. The most significant signal from the R group is the C=O stretch at 1685 cm^{-1} , being at a higher wavelength than for the phosphonic acid (1654.5 cm^{-1}), there are also signals due to the aromatic ring, C-H, P-C and P-O bonds.

Mass Spectrometry. Maldi-TOF mass spectrometry shows signals due to $[\text{SiW}_{10}\text{O}_{36}(\text{RPO})_2]^{n-}$ plus varying numbers of cations, the largest peaks are all due to the complete anion so confirming that it is produced with little impurities.

Elemental Analysis. Results for the NEt_4^+ salt shows the percentage of carbon, nitrogen and hydrogen to be similar to the calculated value, however elemental analysis for the NBu_4^+ salt shows the percentages to be larger than expected (e.g. calc C 21.9; found C 24.0). This could be due to the product containing some solvent or extra cations, although elemental analysis of polyoxometalates is often inaccurate.¹¹

UV/vis spectroscopy Analysis. The aromatic ring with a ketone attached to it is observed at 247 nm ($47000\text{ Lmol}^{-1}\text{cm}^{-1}$), this is a similar position to for the 4-acetylphenylphosphonic acid (250 nm), but more intense due to the underlying polyoxotungstate signal (Figure 2.40).

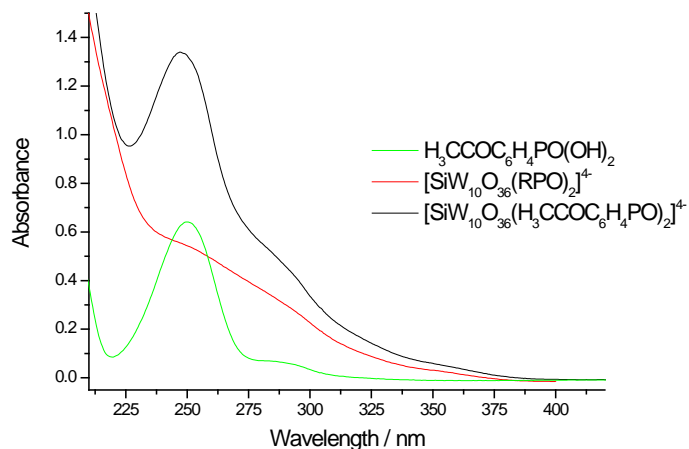


Figure 2.40. The UV/vis spectrum showing the anion derivatised with the acetophenone phosphonic acid, $[\text{SiW}_{10}\text{O}_{36}(\text{RPO})_2]^{4-}$ where R does not show up on the UV/vis spectrum and the phosphonic acid.

Single Crystal X-ray Diffraction. Diffusion of diethyl ether into an acetonitrile solution of $(NEt_4)_3H[SiW_{10}O_{36}(H_3CCOC_6H_4PO)_2]$ gave clear plate shaped crystals. XRD data was collected on Station 9.8 at Daresbury synchrotron source.

Table 2.9. Crystallographic Data for $(NEt_4)_3H[SiW_{10}O_{36}(H_3CCOC_6H_4PO)_2] \cdot (H_3CCN)_{2.35}((H_3CCH_2)_2O)_{0.65}$.

Triclinic	Spacegroup		P -1
Cell axes (Å)	a = 13.9167(11)	b = 15.4099(12)	c = 19.5468(15)
Cell angles (deg)	$\alpha = 98.548(1)$	$\beta = 110.271(1)$	$\gamma = 91.899(1)$
Cell Volume (Å ³)	3872.38(19)		

[Full details in appendix (Structure 7)]

The anion is made of a central $[SiW_{10}O_{36}]^{8-}$ framework onto which two phosphonate groups have been grafted each through two P-O-W bonds. The distance between the oxygen atoms in the P=O groups is 2.43 Å, indicative of a hydrogen bond involving a H^+ which also balances the charge. The two phosphonate groups are unsymmetrical, the P-O bonds being of different lengths, due to the two oxygen atoms bonding to the H^+ differently, one having more O-H bond character ($d_{PO} = 1.522(7)$ Å) than the other ($d_{PO} = 1.499(7)$ Å).

The long-range order within the structure is governed by the interaction of the aromatic rings. Each cluster interacts through π - π bonding of the aromatic rings on both its functional groups to both the aromatic rings on the functional groups on another cluster which is above and behind the first (Figure 2.41(a)), and also interacts through part of the ring and a ketone group to a group on a further cluster (Figure 2.41(b)).

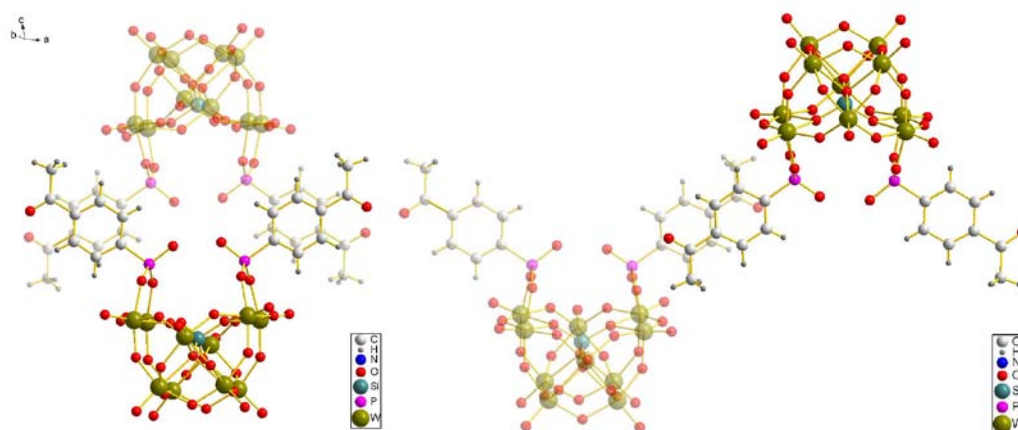


Figure 2.41. The two types of π -bonding in the crystal structure of $(NEt_4)_3H[SiW_{10}O_{36}(H_3CCOC_6H_4PO)_2]$ showing only the anions.

The π - π interactions hold the clusters together to form chains when viewed from above (Figure 2.42). These chains run through the structure and are surrounded by the NEt_4^+ cations.

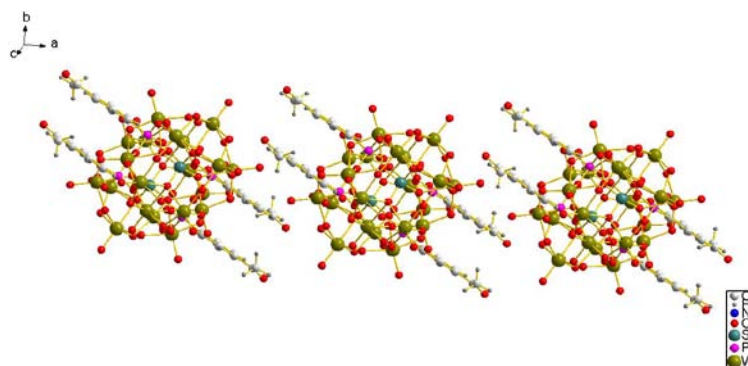


Figure 2.42. The structure of $(NEt_4)_3H[SiW_{10}O_{36}(H_3CCOC_6H_4PO)_2]$ showing only the anions, viewed to show the chains formed by the clusters.

Electrochemical Analysis. Cyclic Voltammetry was carried out on $(NBu_4)_3H[SiW_{10}O_{36}(H_3CCOC_6H_4PO)_2]$ using the same method as for the other derivatives using a SCE as the reference electrode.

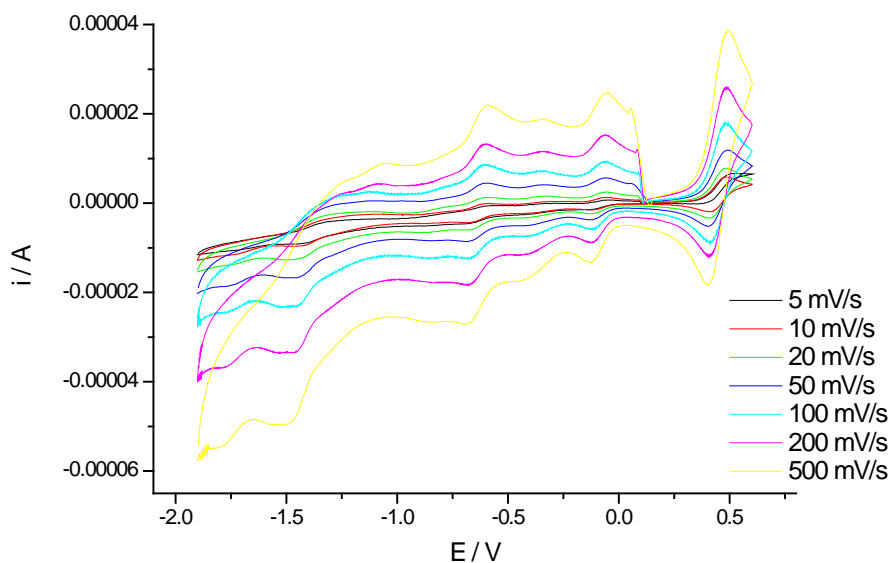


Figure 2.43. The Cyclic Voltammogram of $(NBu_4)_3H[SiW_{10}O_{36}(H_3CCOC_6H_4PO)_2]$ in acetonitrile, using NBu_4BF_4 as the electrolyte, a glassy carbon working electrode and a platinum counter electrode.

The cyclic voltammogram (Figure 2.43) shows three main anionic/cathodic reduction waves (between -2.0–0.7 V), although there is evidence of other waves around these main signals (due to the product of a reaction of the reduced species). The position of the waves is similar to for other derivatives, although the first and second waves are at less negative potentials due to the electron withdrawing properties of the functional group.

2.3.1.8. Summary of $[SiW_{10}O_{36}(RPO)_2]^{4-}$

The polyoxotungstate anion $[SiW_{10}O_{36}]^{8-}$ can be derivatised with phosphonic acids to give the appropriate functionalised anion cluster $[SiW_{10}O_{36}(RPO)_2]^{4-}$, the structures being confirmed and investigated by multinuclear NMR (1H and ^{31}P), IR, MS, EA, Single Crystal XRD and Cyclic Voltammography.

The structures obtained from Single Crystal X-ray Diffraction studies differ depending on both the cations in the structure and the organic ‘R’ groups which are attached to the structure (Table 2.10).

Table 2.10. Table of the unit cell parameters for the crystals obtained from $[SiW_{10}O_{36}]^{8-}$ derivatives.

	Structure	Spacegroup	a (Å)	b (Å)	c (Å)	α	β	γ	V /Å ³
(NBu ₄) ₃ (NEt ₄)H[SiW ₁₀ O ₃₆ (EtPO) ₂]	1	P n 21a	21.99	25.40	13.90	90.0	90.0	90.0	7762
(NBu ₄) ₂ (NEt ₄)H[SiW ₁₀ O ₃₆ (CH ₂ CHCH ₂ PO) ₂]	2	C c	18.79	24.65	17.12	90.0	106.4	90.0	7604
(NEt ₄) ₃ H[SiW ₁₀ O ₃₆ (CH ₂ CHCH ₂ PO) ₂]	3	C 2/c	24.48	10.83	27.31	90.0	94.5	90.0	7216
(NBu ₄) ₃ [SiW ₁₀ O ₃₆ (H ₂ C=CHC ₆ H ₄ PO) ₂]	4	P 21	14.34	63.43	28.13	90.0	91.2	90.0	25576
(NEt ₄) ₃ H[SiW ₁₀ O ₃₆ (HOOCCH ₂ PO) ₂]	5	C c	24.16	10.73	27.05	90.0	97.7	90.0	6951
(NEt ₄) ₃ H[SiW ₁₀ O ₃₆ (HOOCCH ₂ CH ₂ PO) ₂]	6	P2/c	24.62	10.76	32.65	90.0	108.4	90.0	8203
(NEt ₄) ₃ H[SiW ₁₀ O ₃₆ (H ₃ CCOC ₆ H ₄ PO) ₂]	7	P -1	13.93	15.41	19.50	98.7	110.0	91.8	3872

[Full details of the crystal structures in appendix]

Although there is no direct relationship between some of the structures, the ones obtained when R = H₂C=CHCH₂, HOOCCH₂ and HOOCCH₂CH₂ are all related, the *a* and *b*-axes remaining constant with the *c*-axis lengthening and the β -angle increasing as the length of the R group increases.

The electrochemistry of the anions was studied by cyclic voltammetry and although different reference electrodes were used (as we refined our technique) the results can be compared by considering the peak potential relative to ferrocene (Table 2.11).

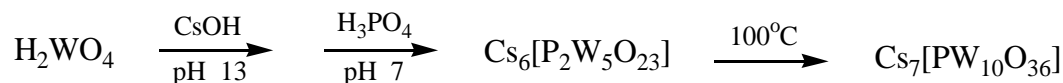
Table 2.11. The reduction potentials for $(NBu_4)_3H[SiW_{10}O_{36}(RPO)_2]$, 1.0 mM solutions, E° relative to ferrocene.

R	E°_3 / mV	E°_2 / mV	E°_1 / mV	E (ferrocene)
Et	-2140	-1190	-620	0.00
$H_2C=CH$	-1750	-1120	-590	0.00
$H_2C=CHCH_2$	-1840	-1140	-600	0.00
$H_2C=CHC_6H_4$	-1870	-1120	-560	0.00
$HOOCCH_2$	-1840	-1020	-570	0.00
$HOOCCH_2CH_2$	-1870	-1140	-610	0.00
$H_3CCOC_6H_4$	-1840	-1090	-540	0.00

The first two reduction potentials are all at approximately the same potential, with some minor variation due to the electron withdrawing properties of the group grafted on to the polyoxotungstate framework. The third potential waves vary more, the position estimated for these being less reliable, as they are made up from two reduction waves which are sometimes separate.

2.4. Synthesis of $[PW_{10}O_{36}]^{7-}$

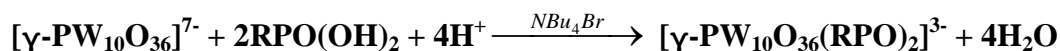
The γ - decatungstophosphate $[\gamma-PW_{10}O_{36}]^{7-}$ is structurally analogous to $[\gamma-SiW_{10}O_{36}]^{8-}$, however it is more difficult to prepare as several polyanions are present in solution. It is prepared via the intermediate $Cs_6[P_2W_5O_{23}]$ (Compound N) which is formed in solution at pH 7 and is stable if not heated above 60°C. Above this temperature it converts into the relatively insoluble $Cs_7[PW_{10}O_{36}]$ (Compound O) which can be collected by filtration.



Both products were characterized by IR spectroscopy and agree with the literature.^{30,31}

2.4.1. Derivatization of $[PW_{10}O_{36}]^{7-}$

Like $[\gamma-SiW_{10}O_{36}]^{8-}$ decatungstophosphate $[\gamma-PW_{10}O_{36}]^{7-}$ is based on the saturated Keggin framework $[\gamma-XW_{12}O_{40}]^{n-}$ with two tungsten-oxygen octahedra having been removed from the structure, leading to an increased and localized anionic charge in the vacancies left behind. This lacunary anion is highly nucleophilic and reactive towards electrophilic groups, although it is less reactive than the decatungstosilicate due to its lower charge. Reaction of $[\gamma-PW_{10}O_{36}]^{7-}$ with organophosphonic acids $RPO(OH)_2$ ($R = Et, H_2C=CH, C_2H=CHCH_2, (CH_2)_2COOH$ or $H_2C=CHC_6H_4$) (Compounds 10-15) was studied, using the same procedure used to obtain $[SiW_{10}O_{36}(RPO)_2]^{4-}$.



The reaction proceeds under phase transfer conditions using NBu_4Br with a catalytic amount of HCl . The products were analysed by multinuclear NMR (1H and ^{31}P), IR, MS and EA.

1H NMR. Like for $(NBu_4)_3H[SiW_{10}O_{36}(RPO)_2]$ the spectra are dominated by signals due to the tetra-alkylammonium cations (NBu_4^+ or NEt_4^+). Peaks due to the appropriate R group appear in approximately the correct positions with ratio's to show that there are two R groups and three cations in the structure.

^{31}P NMR. The spectra are expected to exhibit two signals; one due to the organophosphonate groups grafted onto the structure and one from the phosphorus atom in the middle of the polyoxotungstate framework. However, in all cases a number of signals were observed even after purification of the product (Figure 2.44), these signals being around the positions for the two predicted phosphorus environments. The messy spectrum indicates a

number of different phosphorus environments, due to different isomers of the $[PW_{10}O_{36}]^{7-}$ framework being produced (α or β) during the reaction as isomerisation occurs easily.³⁰

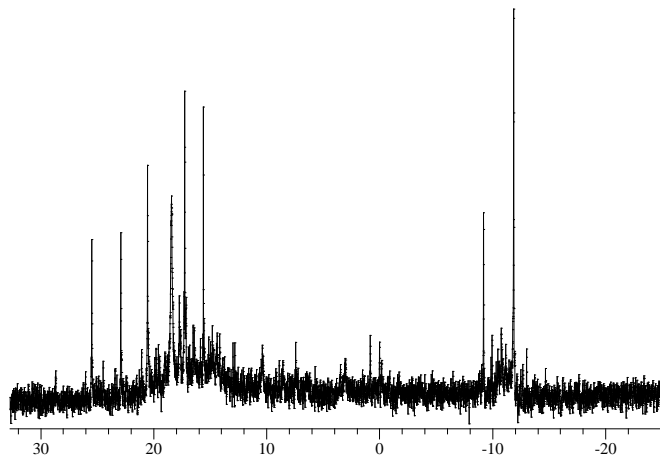


Figure 2.44. The ^{31}P NMR Spectrum for $(\text{NBu}_4)_3[\text{PW}_{10}\text{O}_{36}(\text{H}_2\text{C}=\text{CHPO})_2]$.

IR Spectroscopy. In the fingerprint region the different derivatives all appear very similar, the signals due to the $\text{W}=\text{O}$ and $\text{W}-\text{O}-\text{W}$ asymmetric stretches have shifted from those for the lacunary anion $[\text{PW}_{10}\text{O}_{36}]^{7-}$. In general the bands move to higher frequencies showing saturation of the framework through the fixation of the organophosphonate groups, the bands are broader than for the lacunary anions due to overlap of stretching bands from different (but similar) isomers. The $\text{P}-\text{O}$ stretches due to both the central XO_4 tetrahedron and the RPO groups are between $1200\text{--}1000\text{ cm}^{-1}$. The bands due to the R groups vary depending on the functionality present, for example in $\text{HOOCCH}_2\text{CH}_2$ the carboxylate group is at 1734 cm^{-1} this is the same position as for $[\text{SiW}_{10}\text{O}_{36}(\text{HOOCCH}_2\text{CH}_2\text{PO})_2]^{4-}$.

Mass Spectrometry. MALDI-TOF mass spectrometry shows peaks with the correct mass for $[\text{PW}_{10}\text{O}_{36}(\text{RPO})_2]^{3-}$ with varying numbers of cations. There are also signals due to the anions with the RPO group partly or completely lost in a similar way to those seen for the tungstosilicate derivatives. However, other peaks are also present which can not be easily assigned, these are

thought to be due to other derivatives of tungstophosphates, such as $[PW_{10}O_{36}]^{7-}$, $[PW_{11}O_{39}(RPO)_2]^{4-}$ or $[PW_9O_{34}(RPO)]^{5-}$.

Elemental Analysis. As often seen for polyoxometalates, there is a difference between the observed and predicted values, therefore they can not be used to differentiate between different isomers and do not indicate the purity of the product. However, the results tend to suggest that three cations are present per anion.

Conclusion. Considering all the evidence it appears that the decatungstophosphate $[\gamma-PW_{10}O_{36}]^{7-}$ can be derivatised with phosphonic acids adding functionality to the cluster. However the ^{31}P NMR spectra indicates that the product is not very pure and this is confirmed by the IR and MS results. Isomerisation of the $[\gamma-PW_{10}O_{36}]^{7-}$ cluster is thought to occur during the reaction, meaning that a number of different derivatised isomers are produced. The isomerisation is a lot more evident for the $[PW_{10}O_{36}]^{7-}$ anion than for $[SiW_{10}O_{36}]^{8-}$ as the cluster is less stable with a phosphorus atom at the centre.¹³ Due to problems obtaining single phase samples only a limited time was spent studying tungstophosphates, the decision being made to concentrate on the more productive area of the tungstosilicates.

2.5. References

1. A. K. Bhattacharya and G. Thyagarajan, *Chem. Rev.*, **1981**, 81, 415.
2. D.G. Gorenstein, *Phosphorus-31 NMR, principles and applications*, Academic, **1984**.
3. L.C. Thomas, *The Identification of functional groups in organophosphorus compounds*, London Academic Press, **1974**.
4. R.H. Contrevas and J.E. Peralta, *Progress Nuc. Mag. Reson. Spec.*, **2000**, 37, 321.
5. T. M. Balthazor and R. C. Grabiak, *J.Org.Chem.*, **1980**, 45, 5425.

6. I. Petneházy, Z. M. Jászay, A. Szabó and K. Everaert, *Synth. Commun.*, **2003**, 33, 10, 1665.
7. G. M. Kosolapoff, *J. Am. Chem. Soc.*, **1952**, 74, 4119.
8. T. Hirao, T. Masunga, Y. Ohshiro and T. Agawa, *Synthesis*, **1981**, 56.
9. T. Hirao, T. Masunga, N. Yamada, Y. Ohshiro and T. Agawa, *Bull. Chem. Soc. Jpn.*, **1982**, 55, 909.
10. L. J. Gooßen and M. K. Dezfuli, *Synlett*, **2005**, 3, 445.
11. A. Tézé and G. Hervé, *Inorg. Synth.*, **1990**, 27, 85.
12. A. Tézé and G. Hervé, *J. Inorg. Nucl. Chem.*, **1977**, 39, 2151.
13. J. Canney, A. Tézé, R. Thouvenot and G. Hervé, *Inorg. Chem.*, **1986**, 25, 2114.
14. C. R. Mayer, P. Herson and R. Thouvenot, *Inorg. Chem.*, **1999**, 38, 6152.
15. R. Thouvenot, A. Tézé, R. Contant, G. Hervé. *Inorg. Chem.*, **1988**, 27, 524.
16. D.M. McDaniel, *Inorg. Chem.*, **1976**, 15, 3187.
17. G.M. Sheldrick, SHELX97 (release 97-2), Program for Crystal Structure Analysis, Universität Göttingen, Germany, **1998**.
18. L.J. Farrugia, *J. Appl. Cryst.*, **1999**, 32, 837.
19. G-S Kim, K. S. Hagen and C. L. Hill, *Inorg. Chem.*, **1992**, 31, 5316.
20. M.T. Pope, *Heteropoly and Isopoly Oxometalates*, Springer-Verlag, Berlin, **1983**.
21. M. S. Balula, J. A. Gamelas, H. M. Carapuça, A. M. V. Cavaleiro and W. Schlindwein, *Eur. J. Inorg. Chem.*, **2004**, 619.
22. D. Agustin, J. Dallery, C. Coelho, A. Proust and R. Thouvenot, *J. Organomet. Chem.*, **2007**, 692, 746.
23. J. J. Altenau, M. T. Pope, R. A. Prados and H. So, *Inorg. Chem.*, **1975**, 2, 417.

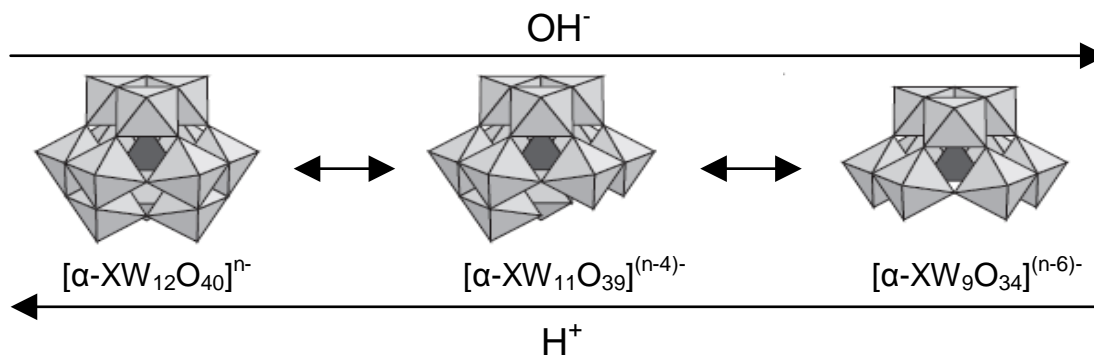
24. K. Maeda, H. Katano, T. Osakai, S. Himeno and A. Saito, *J. Electroanal. Chem.*, **1995**, 389, 167.
25. M. S. Balula, J. A. Gamelas, H. M. Carapuça, A. M. V. Cavaleiro and W. Schlindwein, *Eur. J. Inorg. Chem.*, **2004**, 619.
26. L. Churchill, *From Polyoxometalates to Functional Polymers, Masters Project*, University of Birmingham, **2005**.
27. A. Mazeaud, Y. Dromzee and R. Thouvenot, *Inorg. Chem.*, **2000**, 39, 4735.
28. F. A. R. S. Couto, A. M. V. Cavaleiro, J. D. Pedrosa de Jesus and J. E. J. Simão, *Inorg. Chim. Acta*, **1998**, 281, 225.
29. J. Toth and F. Anson, *J. Electroanal. Chem.*, **1988**, 256, 361.
30. W.H. Knoth and R.L. Harlow, *J. Am. Chem. Soc.*, **1981**, 103, 1865.
31. P.J. Domaille, *Inorg. Synth.*, **1990**, 27, 96.

3. DERIVATISATION OF $[XW_9O_{34}]^{n-}$

Triply derivatised polyoxotungstates have the potential to be prepared from trivacant nonatungstates $[XW_9O_{34}]^{n-}$ by the reaction with an electrophilic group, such reactions will be investigated here.

3.1. Synthesis of $[XW_9O_{34}]^{n-}$ (X = Si or P, n = 10 or 9)

The structure of $[\alpha-XW_9O_{34}]^{n-}$ (X = P, n = 9 or X = Si, n = 10) is based on the parent Keggin anion $[\alpha-XW_{12}O_{40}]^{n-}$ with three WO_6 octahedra having been removed, without any rotation of the remaining groups (Scheme 3.1).^{1,2,3} The structure consists of a central XO_4 tetrahedra, with nine WO_6 octahedra, three of these forming an edge-shared W_3O_{13} group which shares an oxygen with the XO_4 group. The other tungsten-oxygen octahedra exist in pairs which are edge-sharing; one of the oxygen atoms in this edge also being part of the central XO_4 group and an oxygen atom from each octahedra corner sharing with the W_3O_{13} group. The central XO_4 is covered on three faces by these octahedra. The three vacant sites created by the removal of three adjacent tungsten-oxygen octahedra creates a surface containing six reactive terminal oxygen atoms.



Scheme 3.1. General route for the synthesis of nonatungstates.³

3.1.1. α -Nonatungstosilicate synthesis

Sodium α -nonatungstosilicate $Na_{10}[SiW_9O_{34}].H_2O$ (Compound R) is prepared directly from sodium tungstate and sodium metasilicate. The product is obtained as a white solid which is slightly soluble in water giving a stable solution at all pHs which isomerises only very slowly.² It is characterised by infrared spectroscopy which confirms the product to be the same as that reported in the literature.

3.1.2. α -Nonatungstophosphate synthesis

The procedure devised by Contant⁴ was followed, in order to obtain $K_9[\alpha-PW_9O_{34}].16H_2O$ (Compound Q) via the intermediate $K_{7-x}Na_x[\alpha-PW_{11}O_{39}].14H_2O$ (Compound P). The parent structure $[PW_{12}O_{40}]^{3-}$ is only kinetically stable at $pH < 2$, above this pH the lacunary anion $[\alpha-PW_{11}O_{39}]^{7-}$ is formed, which converts to the $[\alpha-PW_9O_{34}]^{9-}$ anion at $pH > 7$, the pH being controlled by addition of potassium carbonate.

Both products were characterised by infrared spectroscopy which show that the stretches agree well with the literature⁴ indicating formation of the correct product.

3.2. Derivatization of $[XW_9O_{34}]^{n-}$

The $[\alpha-XW_9O_{34}]^{n-}$ unit is trivacant containing six nucleophilic surface oxygen atoms created by removal of three tungsten-oxygen octahedra (WO_6) from the parent structure. Electrophilic groups can be grafted onto these oxygen atoms, each group bridging between two surface oxygen atoms via W-O-X bonds. When the group grafted onto the structure contains an organic functionality an organic-inorganic hybrid species is created. In the literature trivacant tungstate anions $[XW_9O_{34}]^{n-}$ ($X = Si$, $n = 10$; $X = P$ or As , $n = 9$) have been reacted with

trichloroalkylsilanes, $RSiCl_3$ ($R = t\text{-Bu, H, Me, Et, CH=CH}_2$ or $CH_2\text{-CH}_2\text{-CH}_2\text{-Cl}$) to give organosilicon derivatives such as $[XW_9O_{34}(t\text{-BuSiOH})_3]^{(n-6)-}$, $[XW_9O_{34}(t\text{-BuSiO})_3(RSi)]^{(n-6)-}$ and $[XW_9O_{34}(RSiO)_3(RSi)]^{(n-6)-}$ (where $R \neq t\text{-Bu}$)^{5,6,7,8}. All these hybrid anions have saturated structures where six Si-O-W bridges are formed connecting three groups to the polyoxometalate surface. When $R \neq t\text{-Bu}$ the reaction proceeds further and a fourth SiR group caps the structure producing a closed structure. However, attempts to obtain similar complexes using organophosphonic acids have proved to be more difficult, yielding only the doubly derivatised partially saturated hybrid anion, $[PW_9O_{34}(RPO)_2]^{5-}$ even though the starting polyoxotungstate unit is trivacant, the presence of only two RPO groups grafted onto the $[PW_9O_{34}]^{9-}$ being deduced spectroscopically.⁹ Fully saturated species with phosphonate groups only being obtained with mono- or di-vacant polyoxotungstates, such as $[XW_{11}O_{39}]^{n-}$ ($X = \text{Si or P, } n = 8 \text{ or } 7$) or $[\gamma\text{-SiW}_{10}O_{36}]^{8-}$, respectively.^{10,11} Here organosilane or organophosphonate groups will be added to the $[XW_9O_{34}]^{n-}$ ($X = \text{Si or P, } n = 10 \text{ or } 9$) framework and the reactions studied.

3.2.1. Derivatization with trichlorosilanes

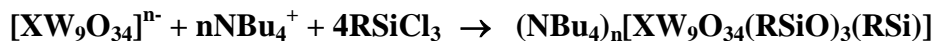
Trichlorosilanes ($RSiCl_3$) are strong electrophiles and react readily with polyoxometalates to yield a saturated structure. Various $[XW_9O_{34}]^{n-}$ anions have been derivatised using trichlorosilanes, giving structures with three organic groups grafted on to the framework,^{5,6,7,8} some reactions will be repeated here and related reactions also studied.

3.2.1.1. $(NBu_4)_n[XW_9O_{34}(RSiO)_3(RSi)]$ ($X = \text{P, } n = 3$ or $X = \text{Si, } n = 4$; $R = \text{C}_2\text{H}_5$ or C_3H_5)

Reactions have been studied in the literature, to form $[XW_9O_{34}(RSiO)_3(RSi)]^{n-}$ mainly with alkyl 'R' groups ($\text{H, Me, Et or } n\text{Bu}$)^{5,6} although vinyl and aryl silyl groups have been used in

one example,⁷ here two simple alkene groups ($H_2C=CH$ and $H_2C=CHCH_2$) will be introduced to the structure giving products with the potential to form polymers (Compounds S, T, 16 and 17).

Reacting the polyoxotungstate directly with trichlorosilanes where $R = H_2C=CH$ or $H_2C=CHCH_2$ gives a capped structure with four RSi groups on the structure (Scheme 3.2).



Scheme 3.2.

The reaction proceeds under phase-transfer conditions (NBu_4^+) at 0 °C, the strongly electrophilic trichlorosilane reacting relatively easily with the polyoxotungstate.

¹H NMR. The spectra show four environments due to the cations (NBu_4^+). The R group signals are present in approximately the correct ratio, both the vinyl ($H_2C=CH$) and allyl ($H_2C=CHCH_2$) groups give one multiplet for most examples corresponding to all the hydrogen atoms in the group, the vinyl group being similar to that for a phosphonate derivative, but the allyl group having changed, proximity to the silicon atom shifting some peaks to lower values.

³¹P NMR. ³¹P NMR was used only when $X = P$, the spectra showing this phosphorus atom as a single peak at -16.4 (or -16.8) ppm, which represents a shift from the lacunary anion (δ -5 ppm in the solid state,¹³ δ +3.2 ppm in solution⁴), indicating formation of a fully saturated structure capped by a fourth RSi group.

IR Spectroscopy. The IR vibrations show retention of the polyoxotungstate framework, the peaks having shifted to higher wavenumbers due to saturation of the structure, the position of the bands corresponding to those seen in the literature.^{5,6} Extra bands indicate the presence of the R group (1405, 1481 and $\sim 2900\text{ cm}^{-1}$); bands due to the double bond are hard to see as there is a

broad band at $\sim 1660\text{ cm}^{-1}$, although a weak band can be seen at $\sim 1600\text{ cm}^{-1}$ which may be assigned to the double bond.

Mass Spectrometry. The spectra show signals due to the appropriate anion with four RSi groups attached to the structure, there are also signals due to the anion having lost part or all of a RSiO group and for $[\text{SiW}_9\text{O}_{34}(\text{H}_2\text{C}=\text{CHSiO})_3(\text{H}_2\text{C}=\text{CHSi})]^{4-}$ having lost all four R groups.

Elemental Analysis. Elemental analysis of the products show the percentages of carbon found to be larger than predicted, however they are in the range to indicate that three cations are present when $X = \text{P}$ and four when $X = \text{Si}$; these balance the anion charges ($[\text{PW}_9\text{O}_{34}(\text{RSiO})_3(\text{RSi})]^{3-}$ and $[\text{SiW}_9\text{O}_{34}(\text{RSiO})_3(\text{RSi})]^{4-}$).

UV/vis Spectroscopy. Only one peak was visible in the range studied (200-700 nm) (Figure 3.1), λ_{max} being at 265 nm when $X = \text{P}$ and 263.5 nm when $X = \text{Si}$. This peak is characteristic of 12-heteropoly tungstophosphates assigned to the charge transfer absorption band of $\text{O} \rightarrow \text{W}$ where O is shared by two W atoms⁶. The start of a second peak which has a λ_{max} below 200 nm also being seen. The molar absorptivities are all approximately the same, so showing that the X atom has little effect on the absorption and only a slight effect on λ_{max} .

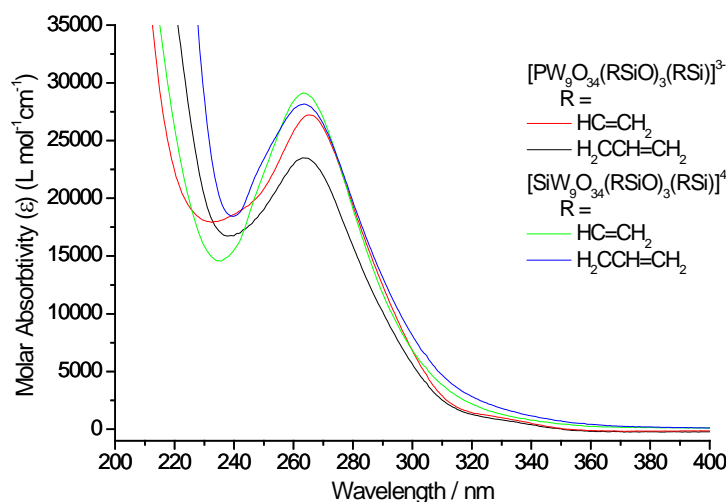


Figure 3.1. The UV/vis spectra for $[\text{XW}_9\text{O}_{34}(\text{RSiO})_3(\text{RSi})]^{n-}$ where $\text{R} = \text{HC}=\text{CH}_2$ or $\text{H}_2\text{CCH}=\text{CH}_2$.

Single Crystal X-ray Diffraction. Crystals suitable for single crystal XRD were obtained for $(NBu_4)_3[PW_9O_{34}(H_2C=CHSiO)_3(H_2C=CHSi)]$ by diffusion of diethyl ether into an acetonitrile solution (Table 3.1).

Table 3.1. Crystallographic Data for $(NBu_4)_3[PW_9O_{34}(H_2C=CHSiO)_3(H_2C=CHSi)]$.

Orthorhombic		Spacegroup	P c a 2 ₁
Cell axes (Å)	$a = 26.5084(72)$	$b = 14.4338(39)$	$c = 24.4262(66)$
Cell angles (deg)	$\alpha = 90.00$	$\beta = 90.00$	$\gamma = 90.00$
Cell Volume (Å ³)	9345.88(44)		

[Full details in appendix (Structure 8)]

The structure shows that the $[PW_9O_{34}]^{9-}$ cluster retains its α -symmetry, but has three $H_2C=CHSiO$ groups grafted on to it, each through two W-O-Si bridges to oxygen atoms on two edge-sharing octahedra. A fourth $H_2C=CHSi$ group caps the structure, the silicon bonding to the oxygen atoms on the three $H_2C=CHSiO$ groups through Si-O-Si bridges (Figure 3.2). The anion formed has a closed cage-like structure, similar to $[PW_9O_{34}(EtSiO)_3(EtSi)]^{3-}$.⁶

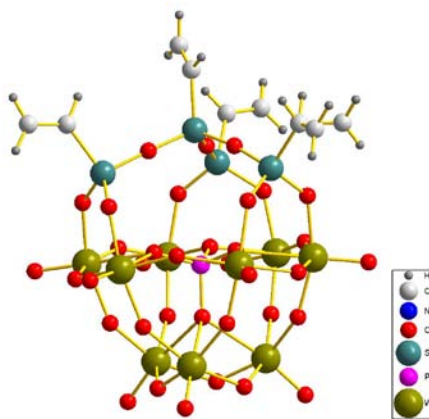


Figure 3.2. The anion cluster $[PW_9O_{34}(H_2C=CHSiO)_3(H_2C=CHSi)]^{3-}$ from the crystal structure.

The long range ordering of the anions is not the same as that for the closely related $[PW_9O_{34}(EtSiO)_3(EtSi)]^{3-}$ in the literature.⁶ The anion clusters form layers made up of rows of

equivalent clusters; within a row all the anions face in the same direction, with those in alternating rows facing in opposite directions. The second row is off-set from the first so that the clusters line up with the gaps in the first row, the gaps in the structure being filled by the NBu_4^+ cations (Figure 3.3).

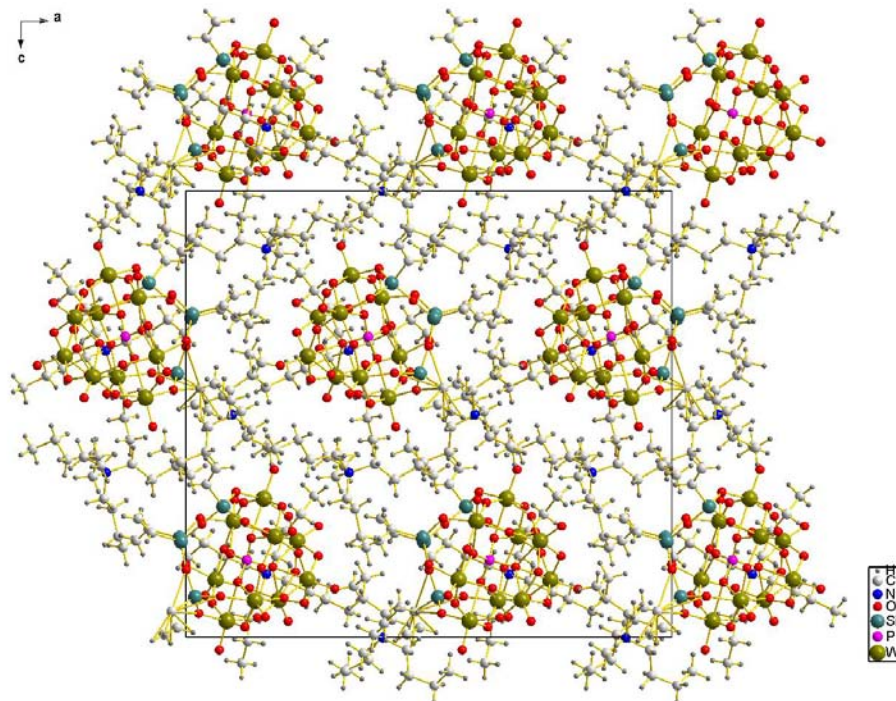
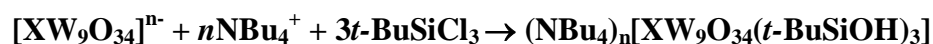


Figure 3.3. The structure of $(NBu_4)_3[PW_9O_{34}(H_2C=CHSiO)_3(H_2C=CHSi)]$ viewed along the b -axis.

3.2.1.2. $(NBu_4)_3H_n[XW_9O_{34}(t-BuSiOH)_3]$ ($X = P$, $n = 0$ or $X = Si$, $n = 1$)

The reaction with $t-BuSiCl_3$ gives an uncapped structure with three $t-BuSiOH$ groups on the polyoxotungstate (Scheme 3.3) (Compounds U and 18), it is unable to react further and produce a capped structure presumably due to steric crowding (this anion was previously obtained for $X = P^5$).



Scheme 3.3.

^1H NMR. The spectra shows the NBu_4^+ signals, in addition to these there is a singlet at 1.00 ppm overlapping with the CH_3 triplet; this singlet is due to the *t*-butyl group and there is also a weak OH signal at 4.94 ppm.

^{31}P NMR. The spectra for $[\text{PW}_9\text{O}_{34}(\text{t-BuSiOH})_3]^{3-}$ shows one clear peak at -15.7 ppm, which is in accordance with a structure containing three *t*-BuSiOH groups,⁵ but not as negative as for the capped $[\text{PW}_9\text{O}_{34}(\text{RSiO})_3(\text{RSi})]^{3-}$ ($\text{R} = \text{H}_3\text{C}_2$ or H_5C_3) structure.

IR Spectroscopy. The IR spectrum indicates formation of the desired product by the appearance of bands at $\sim 2900\text{ cm}^{-1}$ (C-H) from both the *t*-butyl groups and tetra-alkylammonium cations, along with a band at $\sim 1400\text{ cm}^{-1}$ due to the Si-C bond. There are extra bands in the fingerprint region due to a lowering of the symmetry of the anion, the bands being generally shifted to higher wavenumbers due to saturation of the framework.

Mass Spectrometry. The spectra show peaks due to the correct product. The complete $[\text{XW}_9\text{O}_{34}(\text{t-BuSiOH})_3]^{n-}$ anion is seen with three or four cations when $\text{X} = \text{P}$ and four or five cations when $\text{X} = \text{Si}$, the charge on the anion being more negative when $\text{X} = \text{Si}$. There are also peaks due to the anion having lost part or all of the organic groups.

Elemental Analysis. Analysis indicates that there are three cations per cluster for both anions ($\text{X} = \text{P}$ or Si). When $\text{X} = \text{Si}$ the product is expected to have a 4- charge instead of 3-, the charge being balanced by an H^+ , although the carbon percentage is quite high so a mixture might be formed with some having four NBu_4^+ cations.

UV/vis Spectroscopy. The spectra for the products shows a signal with $\lambda_{\text{max}} = 265\text{ nm}$ when $\text{X} = \text{P}$ and 261 nm when $\text{X} = \text{Si}$, the position of these signals indicate that the products are saturated (Figure 3.4), with similar spectra obtained from other saturated products (Section 3.2.1.1), the UV/vis not indicating whether a fourth group caps the structure.

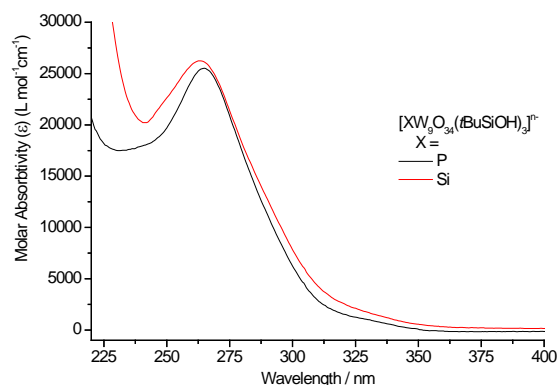


Figure 3.4. The UV/vis spectra for $[XW_9O_{34}(t\text{-BuSiOH})_3]^{n-}$.

Single Crystal X-ray Diffraction. Crystals suitable for analysis were easily produced for both anions ($X = P$ or Si) and gave similar structures which are also related to the one in the literature (Table 3.2 and Table 3.3).⁵

Table 3.2. Crystallographic Data for $(NBu_4)_3[PW_9O_{34}(t\text{-BuSiOH})_3]$.

Trigonal	Spacegroup			R 3 c
Cell axes (Å)	$a = 22.3113(5)$	$b = 22.3113(5)$	$c = 37.8917(12)$	
Cell angles (deg)	$\alpha = 90.00$	$\beta = 90.00$	$\gamma = 120.00$	
Cell Volume (Å ³)	16335(10)			

[Full details in appendix (Structure 9)]

Table 3.3. Crystallographic Data for $(NBu_4)_3H[SiW_9O_{34}(t\text{-BuSiOH})_3]$.

Trigonal	Spacegroup			R 3 c
Cell axes (Å)	$a = 22.5166(12)$	$b = 22.5166(12)$	$c = 35.9924(14)$	
Cell angles (deg)	$\alpha = 90.00$	$\beta = 90.00$	$\gamma = 120.00$	
Cell Volume (Å ³)	15803.27(13)			

[Full details in appendix (Structure 10)]

The structures all have the same spacegroup (R 3 c) and the unit cell parameters are all similar except for the c -axis which varies. The polyoxotungstate part of the cluster has α -

symmetry onto which three *t*-BuSiOH groups have been grafted via reaction of the terminal oxygen atoms which remain on the surface of the anion after removal of tungsten-oxygen octahedra from the parent $[\alpha-XW_{12}O_{40}]^{n-}$ structure. The OH groups all point towards a vacant site at the top of the anion, all being equivalent and giving the anion 3-fold symmetry. An acetonitrile molecule sits above the structure, this solvent molecule occupies one position when $X = P$, but is disordered when $X = Si$.

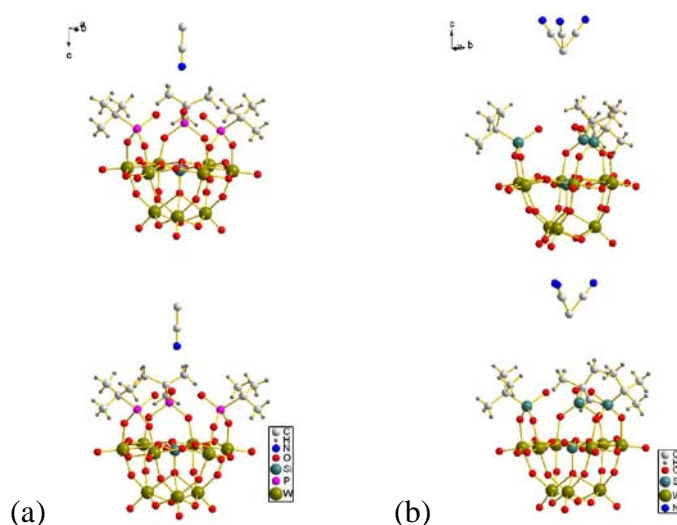


Figure 3.5. The columns of clusters in $(NBu_4)_3H_n[XW_9O_{34}(t-BuSiOH)_3]$, (a) $X = P$ and (b) $X = Si$, shown without any cations present.

The anions are arranged in columns (Figure 3.5) along the direction of the *c*-axis with a slight rotation between anions and the distance between the centre of one anion and the centre of the second (18-19 Å) being half the length of the *c*-axis. The difference in the *c*-axis is therefore explained by the difference in the arrangement of the solvent molecules in these columns.

The NBu_4^+ cations are positioned with their ‘arms’ between the *t*-Bu groups and filling the gaps between columns (Figure 3.6). When $X = Si$ a H^+ will also be present to balance the charge, the position of this ion can not be determined as hydrogen atoms can not be seen in the crystal structure.

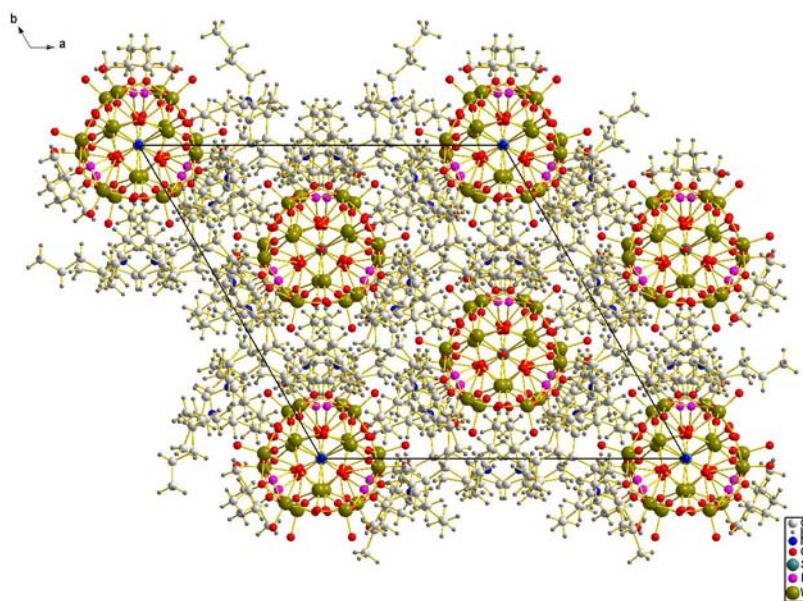


Figure 3.6. The structure of $(NBu_4)_3[PW_9O_{34}(t-BuSiOH)_3]$ viewed along the c -axis.

3.2.1.3. $(NBu_4)_3H_n[XW_9O_{34}(t-BuSiO)_3(SiR)]$ ($X = P$, $n = 0$ or $X = Si$, $n = 1$; $R = C_2H_5$, C_3H_5 or $(CH_2)_3Br$)

The $[XW_9O_{34}(t-BuSiOH)_3]^{n-}$ anion has an open structure so can react with less sterically hindered trichlorosilanes $RSiCl_3$, to cap the structure (Scheme 3.4) (Compounds V, W, 19-22).⁵



Scheme 3.4.

1H NMR. The spectra show the NBu_4^+ signals and t -butyl singlet. In addition to these, signals due the appropriate R group have appeared. When $R = H_2C=CH$ the peaks due to this group are seen as a multiplet, when $R = H_2C=CHCH_2$ or $(CH_2)_3Br$ three small multiplets are seen for the three hydrogen environments.

^{31}P NMR. ^{31}P NMR was used when $X = P$. The spectra do not appear as clean as for $(NBu_4)_3[PW_9O_{34}(t-BuSiOH)_3]$, with major peaks at -15.7 and -16.5 ppm, the first is due to

unreacted $(NBu_4)_3[PW_9O_{34}(t\text{-BuSiOH})_3]$ and the second due to product. This small shift agrees with that seen for derivatives made by Thouvenot et al.⁵

IR Spectroscopy. The spectra do not show any significant changes in the fingerprint region meaning that the polyoxotungstate framework is retained, the transformation taking place far from this unit. The R groups can not be seen clearly; the C-Br band will be at $< 700\text{ cm}^{-1}$ so is hidden by bands in the fingerprint region and the C=C double bonds signals are weak.

Mass Spectrometry. The spectra show a number of peaks, which include ones corresponding to the mass for $[XW_9O_{34}(t\text{-BuSiO})_3(\text{SiR})]^{n-}$ with varying numbers of cations, as well as peaks for the anion having lost some or all of the SiR group, often accompanied by oxygen atoms from the $t\text{-BuSiOH}$ groups.

Elemental Analysis. Results shows that three cations are present for all structures, the extra charge being balanced by a H^+ when $X = \text{Si}$.

UV/vis Spectroscopy. The spectra all have one peak above 220 nm (Figure 3.7), λ_{max} and the molar absorptivity not having shifted significantly from the position for $[XW_9O_{34}(t\text{-BuSiOH})_3]^{n-}$, showing that capping the structure with a fourth R group does not affect the absorbance.

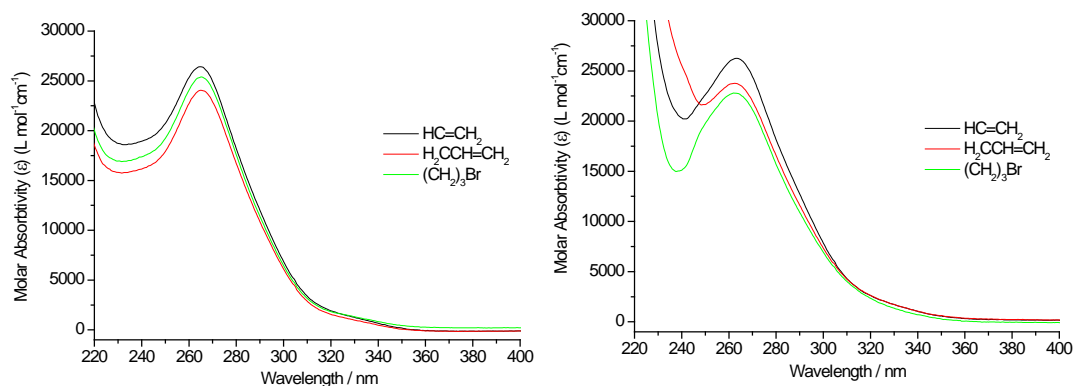


Figure 3.7. The UV/vis spectra for $[XW_9O_{34}(t\text{-BuSiO})_3(\text{SiR})]^{4-}$ ($X=\text{P}$ (left) and $X=\text{Si}$ (right)).

Single Crystal X-ray Diffraction. Crystals suitable for Single Crystal XRD were obtained when $X = P$ and $R = CH_2CH=CH_2$ or $(CH_2)_3Br$, by diffusion of diethyl ether into an acetonitrile solution over several days (Table 3.4 and Table 3.5).

Table 3.4. Crystallographic Data for $(NBu_4)_3[PW_9O_{34}(t-BuSiO)_3(SiCH_2CH=CH_2)]$.

Trigonal	Spacegroup			R 3 c
Cell axes (Å)	$a = 22.4981(4)$	$b = 22.4981(4)$	$c = 36.7371(11)$	
Cell angles (deg)	$\alpha = 90.00$	$\beta = 90.00$	$\gamma = 120.00$	
Cell Volume (Å ³)	16103.76(6)			

[Full details in appendix (Structure 11)]

Table 3.5. Crystallographic Data for $(NBu_4)_3[PW_9O_{34}(t-BuSiO)_3(Si(CH_2)_3Br)]$.

Trigonal	Spacegroup			R 3 c
Cell axes (Å)	$a = 22.4078(22)$	$b = 22.4078(22)$	$c = 36.5706(60)$	
Cell angles (deg)	$\alpha = 90.00$	$\beta = 90.00$	$\gamma = 120.00$	
Cell Volume (Å ³)	15902.34(34)			

[Full details in appendix (Structure 12)]

The structures obtained have the same space group and similar unit cell parameters to those found for $(NBu_4)_3H_n[XW_9O_{34}(t-BuSiOH)_3]$, the only significant variation being in the c -axis. The anion structure is similar to the $[XW_9O_{34}(t-BuSiOH)_3]^{n-}$ structure, the reaction with organotrichlorosilane $RSiCl_3$ causing the SiR group to be grafted onto the top of the structure bonding to the three oxygen atoms from the OH groups and capping the structure (Figure 3.8). The clusters have three-fold symmetry, with the ‘R’ group being disordered over three sites at the top of the cluster.

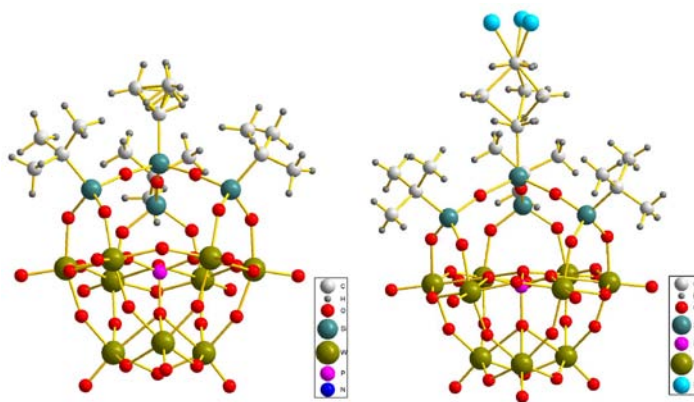


Figure 3.8. Crystal structures of $[PW_9O_{34}(t\text{-BuSiO})_3(\text{SiR})]^{3-}$ where R = (a) $\text{CH}_2\text{CH}=\text{CH}_2$ or (b) $(\text{CH}_2)_3\text{Br}$.

The long range order of the structure remains the same, the R group replacing the acetonitrile molecule that was above the structure in $[XW_9O_{34}(t\text{-BuSiOH})_3]^{n-}$. This group runs along the direction of the *c*-axis, however the length of the *c*-axis does not relate to the length of this group in the way that might be expected.

3.2.2. Derivatisation with triethoxysilanes

3.2.2.1. $(\text{NBu}_4)_3\text{H}_n[\text{XW}_9\text{O}_{34}(t\text{-BuSiO})_3(\text{HS}(\text{CH}_2)_3\text{Si})]$

The reaction of the open $[XW_9O_{34}(t\text{-BuSiOH})_3]^{n-}$ structure with organo-trichlorosilanes appears to be relatively easy. However, not all functional groups can be obtained as a trichlorosilane and so the related, less electrophilic triethoxysilanes $(\text{RSi}(\text{OEt})_3)$, with different functionalities provide a possible route to different derivatives. The reaction of a triethoxysilane $(\text{HS}(\text{CH}_2)_3\text{Si}(\text{OEt})_3)$ will be investigated. The reaction will be attempted with the triethoxysilane replacing trichlorosilane, but the other conditions remaining the same.

^1H NMR. The reaction yields a product which shows no evidence for the $(\text{CH}_2)_3\text{SH}$ group on the ^1H NMR spectrum indicating that a reaction has not occurred.

^{31}P NMR. One peak is seen in the ^{31}P NMR spectra (when $X = \text{P}$) at -15.7 ppm, this being the same position as for $[\text{PW}_9\text{O}_{34}(t\text{-BuSiOH})_3]^{3-}$.

The NMR spectra show that replacing the trichlorosilane with a triethoxysilane, but using the same conditions shows no evidence of the $\text{HS}(\text{CH}_2)_3\text{Si}$ group in the product. This shows that the triethoxysilane is not a strong enough electrophile to react directly with the polyoxotungstate anion, therefore HCl will be added to the reaction to promote the reaction and act as a catalyst (Compounds 23 and 24).

^1H NMR. When HCl is added to the reaction, three new environments appear in the ^1H NMR spectrum. These are multiplets at ~0.60-0.80, 1.62-1.78 (under a cation signal) and 2.50-2.60 ppm and these have the correct intensities and indicate that the $(\text{CH}_2)_3\text{SH}$ group is present.

^{31}P NMR. When $X = \text{P}$ ^{31}P NMR shows one peak for the product, the position of this peak (-15.7 ppm) is the same as for $[\text{PW}_9\text{O}_{34}(t\text{-BuSiOH})_3]^{3-}$ and due to a saturated structure.⁵ Unlike the products obtained in section 3.2.1.3 no shift in the ^{31}P peak is seen, this could be due to the acidic environment or indicate that the $\text{Si}(\text{CH}_2)_3\text{SH}$ group is not attached to the cluster.

IR Characterisation. The spectra show the same peaks in the fingerprint region as were seen for both $[\text{XW}_9\text{O}_{34}(t\text{-BuSiOH})_3]^{n-}$ and $[\text{XW}_9\text{O}_{34}(t\text{-BuSiO})_3(\text{SiR})]^{n-}$ (section 3.2.1), with little change being seen as the reaction site is not close to the polyoxotungstate anion. There is evidence for a weak band at around 2600 cm^{-1} in the spectra which could be due to the -SH which exhibits a weak stretch in this region.

Mass Spectrometry. The spectra for both anions ($X = \text{P}$ or Si) are messy, with evidence for the predicted product mass along with masses due to the product without the $\text{Si}(\text{CH}_2)_3\text{SH}$ group. Although this evidence suggests that a mixture of anions could be present a lot of the

peaks have also lost additional oxygen atoms which could show that this group was attached and has been lost instead of not reacting in the first place.

Elemental Analysis. The CHN analysis shows the percentages found to be relatively close to that predicted for the product, especially when $X = P$, although this can not be used to show if the $Si(CH_2)_3SH$ group is present as the difference in predicted values would be within the large errors often observed for elemental analysis.

X-ray Diffraction. Crystals suitable for single crystal XRD could not be obtained, although material suitable for powder XRD showed a crystalline product.

UV/vis Spectroscopy. The spectra appear the same as for the other $[XW_9O_{34}(t\text{-BuSiO})_3(SiR)]^{n-}$ clusters, which is what was expected because the $(CH_2)_3SH$ group does not have a peak in the UV/vis region (Figure 3.9).

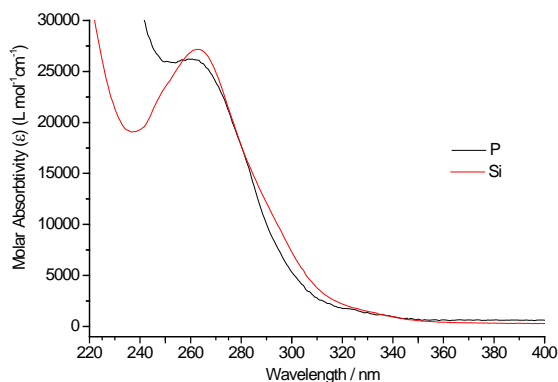
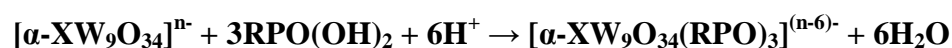


Figure 3.9. The UV/vis spectra for $(NBu_4)_3H_n[XW_9O_{34}(t\text{-BuSiO})_3(Si(CH_2)_3SH)]$.

The 1H NMR and MS suggest that the reaction has occurred, giving a capped structure, however the other evidence is not conclusive as little or no change is expected/observed. Overall the reaction shows that triethoxysilane is not as reactive as trichlorosilane, but its reaction can be promoted by the addition of HCl.

3.2.3. Phosphonic acids

In the literature the reaction of the trivacant $[PW_9O_{34}]^{9-}$ with phosphonic acid has been studied, however only the doubly derivatised anion has been obtained, this being confirmed spectroscopically.⁹ This reaction will be investigated along with the analogous reaction with $[SiW_9O_{34}]^{10-}$. The procedure used previously will be tested, being the same method used for the derivatization of the monovacant $[XW_{11}O_{39}]^{n-}$ ¹⁰ and divacant $[SiW_{10}O_{36}]^{8-}$,¹¹ involving a phase-transfer reaction using NBu_4^+ in refluxing acetonitrile, with a catalytic amount of HCl and an organophosphonic acid $RPO(OH)_2$ (Scheme 3.5).⁹



Scheme 3.5.

3.2.3.1. $[PW_9O_{34}]^{9-}$

Compounds will be synthesised using $RPO(OH)_2$ ($R = Et, C_2H_3$ or C_3H_5) (Compounds X, 25 and Y).

¹H NMR. The spectra show the cations to be present along with signals to show the appropriate R group. The intensities show that there are approximately two R groups per three cations, although the cation peaks are large in comparison with the R group peaks so the intensities of the smaller peaks are not accurate.

³¹P NMR. After crystallization to remove any impurities the spectra show two peaks which are in approximately a 2:1 ratio. The RPO peaks (intensity 2) are at similar chemical shifts to those for the groups in $[SiW_{10}O_{36}(RPO)_2]^{4-}$ (Section 2), showing a shift in position from the phosphonic acids. The $[PW_9O_{34}]$ peak (intensity 1) is at -12.5 ppm, the chemical shift being between that of the starting anion $[PW_9O_{34}]^{9-}$ (δ -5 ppm in the solid state,¹³ δ +3.2 ppm in

solution⁴) and of the fully saturated $[PW_9O_{34}(t\text{-BuSiOH})_3]^{3-}$ (δ -15.7 ppm) indicating that a partially saturated structure has been obtained and agreeing with the literature.⁹

IR Spectroscopy. The IR spectra show vibrations in the fingerprint region consistent with the polyoxotungstate unit, but with a shift to higher wavenumbers showing that the unit has become more saturated. The position of the vibrations corresponds to those observed in the literature,⁹ showing that the structure of the central polyoxotungstate cluster is the same. Bands due to the organic R group functionalities (P-C and C-H) indicate that they are present.

Mass Spectrometry. Maldi-TOF MS of the products shows the masses to correspond to anions of either $[PW_9O_{34}(RPO)_2]^{5-}$ or $[PW_9O_{34}(RPO)]^{7-}$ with varying numbers of cations or Na^+ ions. There is no evidence for any anions with three RPO groups.

Elemental Analysis. In the literature⁹ the elemental analysis results are consistent with the product having a general formula of $(NBu_4)_3Na_2[PW_9O_{34}(RPO)_2].xDMF$ ($x = 0, 0.5$ or 1). The results for my products also indicate that three NBu_4^+ cations are present, along with two Na^+ or H^+ ions to balance the charge and acetonitrile solvent molecules.

UV/vis Spectroscopy. The λ_{max} in the UV/vis spectra are at ~246 nm (Figure 3.10), a lower wavelength than for the fully saturated compounds,⁶ this agrees with the other data which indicates that the structure is only doubly functionalised. The molar absorptivity is similar to the values seen previously ($23300 \text{ Lmol}^{-1}\text{cm}^{-1}$) showing that it depends only on the structure of the polyoxotungstate and not on the number of R groups on the structure.

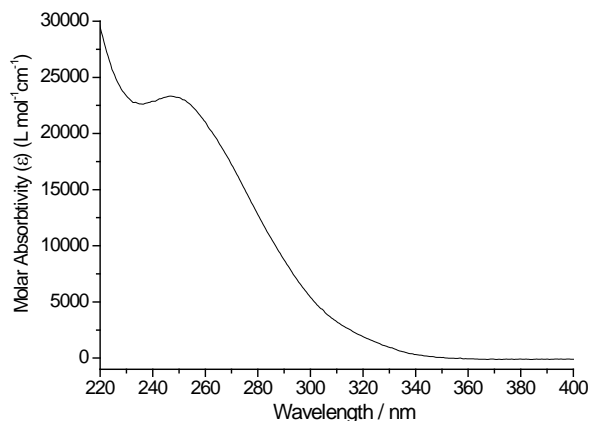


Figure 3.10. UV/vis spectrum for $(NBu_4)_3[PW_9O_{34}(EtPO)_2]$.

Single Crystal X-ray Diffraction. Attempts to make crystals suitable for XRD using various different methods were all unsuccessful; these were done using different solvents (Acetonitrile or DMF) and different methods of crystallization.

As in the literature^{9,12} only the doubly derivatised compound $[PW_9O_{34}(RPO)_2]^{5-}$ was obtained proving that phosphonic acids are not electrophilic enough to fully react with $[PW_9O_{34}]^{9-}$.

3.2.3.2. $[SiW_9O_{34}]^{10-}$

Although the α -nonatungstosilicate $[SiW_9O_{34}]^{10-}$ has previously been reacted with trichlorosilanes^{5,6,7,8} it has not been reacted with phosphonic acids and being analogous to $[PW_9O_{34}]^{9-}$ would be expected to react in a similar manner. The conditions of the reaction were kept the same so the effect of the central 'X' atom could be considered (Compounds 26-28).

1H NMR. The spectra are dominated by the cation signals (NBu_4^+), but also show signals due to the 'R' group which has been grafted on to the structure. The intensities point towards there being two R groups per three cations; although the intensity for the R group is slightly

larger than that expected, (normally the intensities of such groups being slightly lower than that expected) so this may indicate that on average there are more than two groups per anion.

^{31}P NMR. The ^{31}P NMR show peaks due to the RPO groups, shifted from the position of the original phosphonic acid environments with a number of peaks being seen. In most cases between two and four peaks are observed indicating that more than one phosphorus environment exists, most likely due to the polyoxotungstate anion either being derivatised by different numbers of RPO groups (1, 2 or 3) or in different ways. Three possible products are shown (Figure 3.11), all being symmetrical so the phosphorus atoms from each individual anion will appear in the same place, but those from different anions will have different chemical shifts.

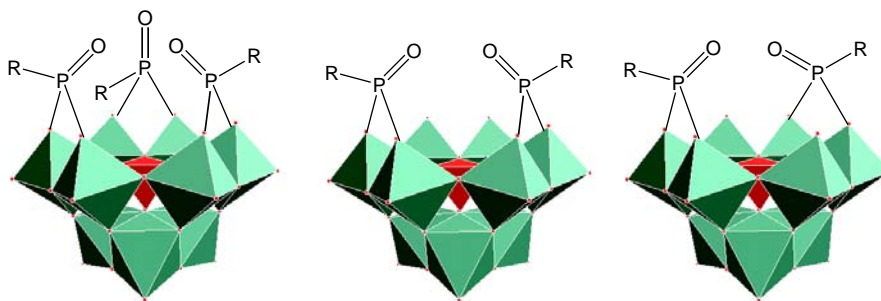


Figure 3.11. Possible products from the reaction of $[\text{SiW}_9\text{O}_{34}]^{10-}$ with organophosphonic acid. Showing it derivatised (a) three times, (b) twice with the vacant sites adjacent or (c) twice with vacant sites opposite.

^{29}Si NMR. ^{29}Si NMR for $[\text{SiW}_9\text{O}_{34}(\text{EtPO})_m]^{n-}$ shows two silicon environments (Figure 3.12). The first at -87.8 ppm (21.2 % intensity) is thought to be due to the fully saturated compound with three RPO groups on, as it has the same chemical shift as the fully saturated $[\text{SiW}_9\text{O}_{34}(\equiv\text{SiR})_3(\text{O}_3\text{SiR})]$.⁷ The other peak at -85.5 ppm (78.7 % intensity) is thought to be due to a less saturated anion with two RPO groups grafted on to the structure, showing that the majority of the product has two RPO groups and only a small quantity has reacted fully.

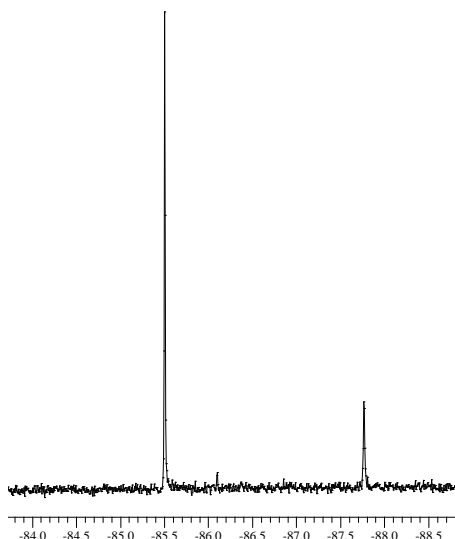


Figure 3.12. ^{29}Si NMR spectrum for $(\text{NBu}_4)_3\text{Na}[\text{SiW}_9\text{O}_{34}(\text{EtPO})_{2/3}]$.

IR Spectroscopy. The fingerprint region of the IR spectra shows retention of the polyoxotungstate unit, the shape of the peaks being similar to for the lacunary $[\text{SiW}_9\text{O}_{34}]^{10-}$ anion,² but with shifting of the bands to higher wavenumbers due to the species becoming more saturated.⁶ Other changes in the spectra are the appearance of bands due to P-O, P-C and C-H these are all indicative of the ‘R’ group.

Mass Spectrometry. The MS show a mixture of products. When $\text{R} = \text{Et}$ there are peaks corresponding to the anions $[\text{SiW}_9\text{O}_{34}(\text{EtPO})]^{8-}$ and $[\text{SiW}_9\text{O}_{34}(\text{EtPO})_2]^{6-}$ with varying numbers of cations. When $\text{R} = \text{H}_2\text{C}=\text{CH}$ or $\text{H}_2\text{C}=\text{CHCH}_2$ there are peaks due to $[\text{SiW}_9\text{O}_{34}(\text{RPO})_2]^{6-}$ and $[\text{SiW}_9\text{O}_{34}(\text{RPO})_3]^{4-}$ showing that both have been produced during the reaction.

Elemental Analysis. EA indicates that three cations are present, the anion charge must be balanced by H^+ or Na^+ ions giving either $(\text{NBu}_4)_3\text{H}/\text{Na}_3[\text{SiW}_9\text{O}_{34}(\text{RPO})_2]$ when it is derivatised twice or $(\text{NBu}_4)_3\text{H}/\text{Na}[\text{SiW}_9\text{O}_{34}(\text{RPO})_3]$ if it is derivatised three times.

UV/vis Spectroscopy. The derivatised $[\text{SiW}_9\text{O}_{34}]^{10-}$ cluster has a peak in the UV/vis spectrum, the position of this peak indicating the saturation of the structure. The products have a

peak at 257 nm (Figure 3.13), this position is between that for the doubly derivatised $[PW_9O_{34}(RPO)_2]^{3-}$ (246 nm) and the fully saturated products (Section 3.2.1) (262-266 nm),⁶ indicating that the anions are partly but not fully saturated.

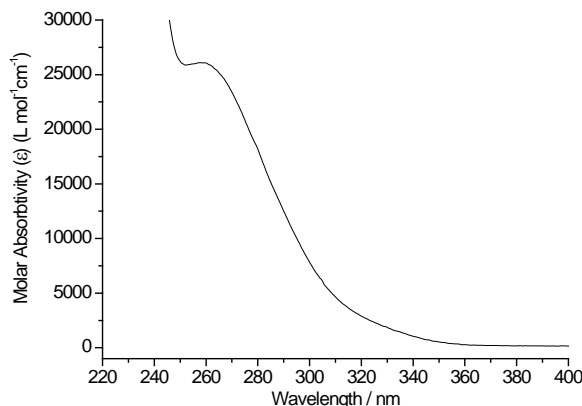


Figure 3.13. The UV/vis spectrum for $(NBu_4)_3H/Na[SiW_9O_{34}(EtPO)_2]^{3-}$

Overall the evidence indicates that it is possible to graft three RPO groups on to a $[SiW_9O_{34}]^{10-}$ unit, however the majority of the product only has two groups attached to the structure in the same way as for the $[PW_9O_{34}]^{9-}$ alternative.

3.2.3.3. Altering the Conditions

The original conditions used for reacting organophosphonic acids with polyoxotungstates^{9,10,11} do not give fully saturated structures with nonatungstates $[XW_9O_{34}]^{n-}$ ($X = P, n = 9$ or $X = Si, n = 10$), however when $X = Si$ there are indications that some fully saturated, triply functionalised product is formed. The conditions will be altered to see if the formation of this saturated product can be enhanced. While altering the conditions everything else will remain unchanged, the reaction being tested using ethylphosphonic acid as this has no other functionalities which could effect or be affected by the reaction.

3.2.3.3.1. pH

Firstly, the pH was changed in the hope that this would encourage the reaction to proceed further, an excess of both HCl and ethylphosphonic acid were used. Although polyoxotungstates are affected by the pH of the solution, the $[\text{SiW}_9\text{O}_{34}]^{10-}$ anion is metastable at most pH's.² Also as the reaction is a phase-transfer reaction the anion reacts relatively quickly once it is in solution, so the $[\alpha\text{-SiW}_9\text{O}_{34}]^{10-}$ anion structure was not affected by the pH.

The progress of the reaction was monitored by ^{31}P NMR (Figure 3.14), the intensities of the peaks from the product and the phosphonic acid being measured to give an estimate of how far the reaction has proceeded. The ratio of [polyoxotungstate]:phosphonic acid at the start of the reaction was 1:4. After 24 hours the product peak was slightly larger than that for the acid (1.2:1) giving approximately 2 RPO groups per anion. After 48 hours the size of the product peak had increased (1.5:1) remaining at this value after 72 hours, indicating that the rate of the reaction reduces with time due to the polyoxotungstate being consumed.

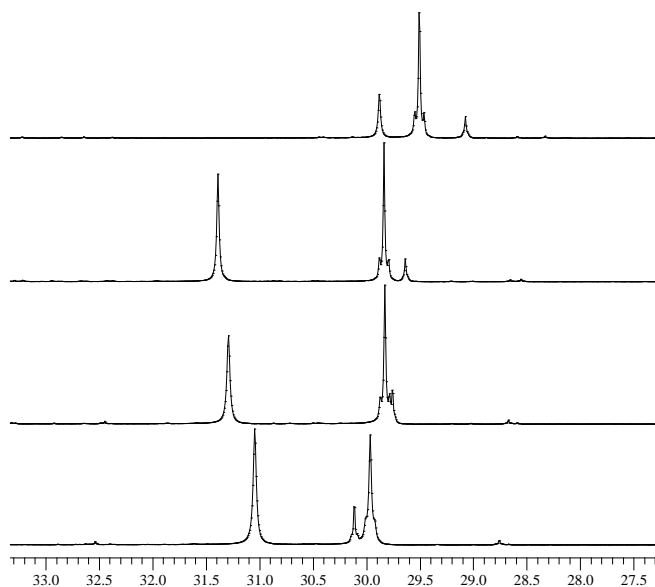


Figure 3.14. The ^{31}P NMR Spectra showing the formation of $(\text{NBu}_4)_3\text{Na}[\text{SiW}_9\text{O}_{34}(\text{EtPO}_3)_3]$ over time, showing (a) 24, (b) 48, (c) 72 and (d) 72 hours after washing with water.

After filtering and evaporating off the solvent, the product was washed with large quantities of water to remove the excess acids and any other water soluble impurities. The product was crystallised by diffusion of diethyl ether into an acetonitrile solution and analysed by multinuclear NMR (^1H and ^{31}P), IR, MS, EA, Single Crystal XRD and Cyclic Voltammetry.

3.2.3.3.1.1 $(\text{NBu}_4)_3\text{Na}[\text{SiW}_9\text{O}_{34}(\text{EtPO})_3]$

Reaction of the polyoxotungstate $[\text{SiW}_9\text{O}_{34}]^{10-}$ with ethylphosphonic acid over 72 hours gives a pale green product, which was analysed to see whether there are two or three EtPO groups per polyoxotungstate cluster (Compound 29).

^1H NMR. In addition to signals from the NBu_4^+ cations, the spectrum shows peaks characteristic of the ethyl group, their positions shifted downfield slightly from those for the ethylphosphonic acid. The relative intensities of these groups is hard to determine accurately as they overlap with the cation peaks, however they appear to be relatively large so indicating that more than two EtPO groups are present per polyoxotungstate unit.

^{31}P NMR. Under proton decoupling conditions the ^{31}P NMR spectrum contains one resonance, which has tungsten satellite peaks associated with it ($^2J_{\text{PW}} = 11.1 \text{ Hz}$); integration of these satellite peaks with respect to the central line shows the P atom to be connected to two tungsten atoms of the polyoxotungstate framework.^{14,15}

^{29}Si NMR. The ^{29}Si NMR spectrum contains one main peak, a singlet at -88.4 ppm; there is also a small peak (intensity 10 % of total) at -87.9 ppm; these are both in the expected chemical shift region for a fully saturated unit,⁷ indicating that three RPO groups are grafted on to the cluster. However, the presence of two peaks shows that the product is not pure, possibly due to a small amount of the β -isomer forming during the reaction.

IR Spectroscopy. Characteristic W-O vibrations confirm retention of the polyoxotungstate framework,² but are shifted to higher wavenumbers compared to the lacunary $[\text{SiW}_9\text{O}_{34}]^{10-}$ anion so indicating the framework to now be more saturated. The presence of the EtPO group is confirmed by P=O and C-H bands.

Mass Spectrometry. Maldi-TOF mass spectrometry of the product (Figure 3.15) shows two sets of signals, the main signals being due to the product $[\text{SiW}_9\text{O}_{34}(\text{EtPO})_3]^{4-}$ with either four or five cations, extra signals due to the addition of one or two Na^+ ions being associated with these signals. The signals are broad and split due to the different isotopes of the atoms that make up the structure.

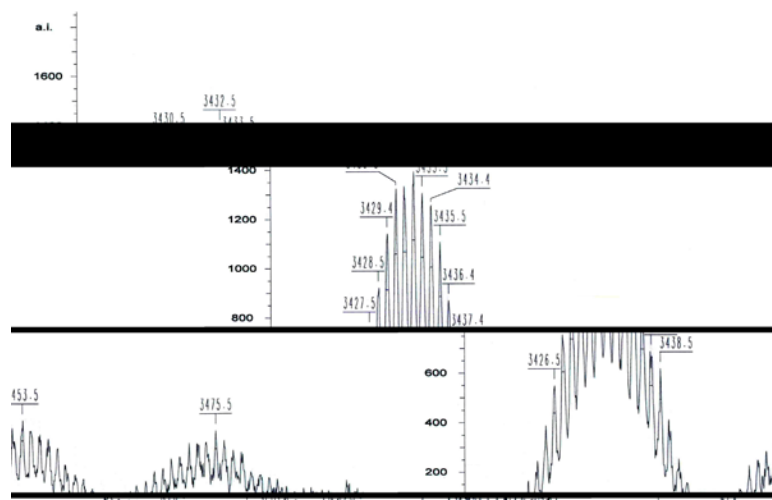


Figure 3.15. The mass spectrum for $(\text{NBu}_4)_3\text{Na}[\text{SiW}_9\text{O}_{34}(\text{EtPO})_3]$, showing signals with different isotopic patterns for $[M^+-\text{Na}]$, $[M^+]$ and $[M^++\text{Na}]$.

Elemental Analysis. The results show the polyoxotungstate anion to have three NBu_4^+ cations associated with it, although as with a lot of results for polyoxometalates the values found are not ideal.

UV/vis Spectroscopy. The spectrum has one absorption in the region studied, $\lambda_{\text{max}} = 266 \text{ nm}$ ($\epsilon = 25000 \text{ Lmol}^{-1}\text{cm}^{-1}$) (Figure 3.16). The position of this absorption correlates well

with the position of the fully saturated structures obtained using trichlorosilanes (Section 3.2.1), indicating that the anion has reacted fully producing a saturated structure, the signal has shifted in comparison to $[\text{SiW}_9\text{O}_{34}(\text{RPO})_2]^{6-}$ ($\lambda_{\text{max}} = 257 \text{ nm}$) (Section 3.2.3.2).

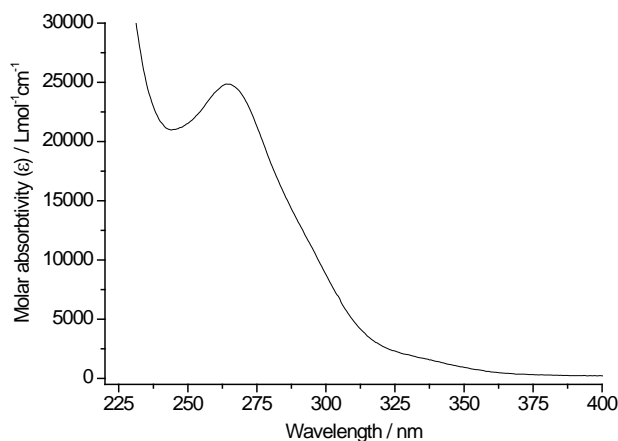


Figure 3.16. The UV/vis spectrum for $(\text{NBu}_4)_3\text{Na}[\text{SiW}_9\text{O}_{34}(\text{EtPO})_3]$.

Single Crystal X-ray Diffraction Studies. Crystals suitable for analysis were obtained by diffusion of diethyl ether into an acetonitrile solution. Diffraction data for these crystals were collected at the EPSRC crystallography service at Southampton (Table 3.6).

Table 3.6. Crystallographic Data for $(\text{NBu}_4)_3\text{H}[\text{SiW}_9\text{O}_{34}(\text{EtPO})_3]$.

Trigonal	Spacegroup			R 3 m
Cell axes (\AA)	$a = 20.7250(24)$	$b = 20.7250(22)$	$c = 22.4710(3)$	
Cell angles (deg)	$\alpha = 90.00$	$\beta = 90.00$	$\gamma = 120.00$	
Cell Volume (\AA^3)	$8358.77(281)$			

[Full details in appendix (Structure 13)]

The structure shows that the $[\text{SiW}_9\text{O}_{34}]^{10-}$ unit remains in the α -symmetry, onto it are grafted three RPO groups, each attached to two adjacent edge-shared WO_6 octahedra through two P-O-W bridges, creating a structure with three-fold symmetry (Figure 3.17). The structure contains a central SiO_4 tetrahedron, from which one oxygen is shared by three

tungsten atoms within a W_3O_{13} group, while the other three oxygen atoms on the silicon are each shared by two tungsten atoms. These W-O bonds are longer (2.28(2) or 2.18(1) Å) than the other bonds in the WO_6 octahedra (1.90(1) Å, except the terminal W=O (1.73(2) or 1.70(2) Å)). The three P=O groups are disordered between two positions both pointing towards a coordination site occupied by a H^+ ion, which balances the overall 4- charge on the derivatised polyoxometalate cluster along with three NBu_4^+ cations.

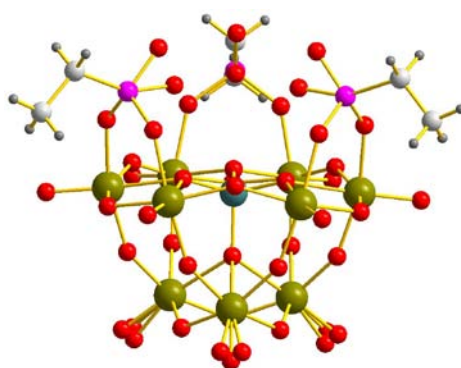


Figure 3.17. Structure of $[SiW_9O_{34}(EtPO)_3]^{4-}$ obtained from the crystal structure.

The long range order of the structure is related to that seen for the $(NBu_4)_3H_n[XW_9O_{34}(t-BuSiOH)_3]$ compounds (Section 3.2.1.2), the clusters arranged in columns running along the c -axis. The c -axis is 22.47 Å, this is shorter than for the other structures (~36-37 Å), the unit cell only containing half the number of clusters in this direction with 22.47 Å between the centres of two clusters.

Electrochemical Analysis. Cyclic Voltammetry in acetonitrile was performed on the product and shows four one-electron waves in the region studied (+0.7 V to -2.0 V vs. Ag/AgCl) (Figure 3.18) corresponding to the reduction of the tungsten atoms.¹⁶

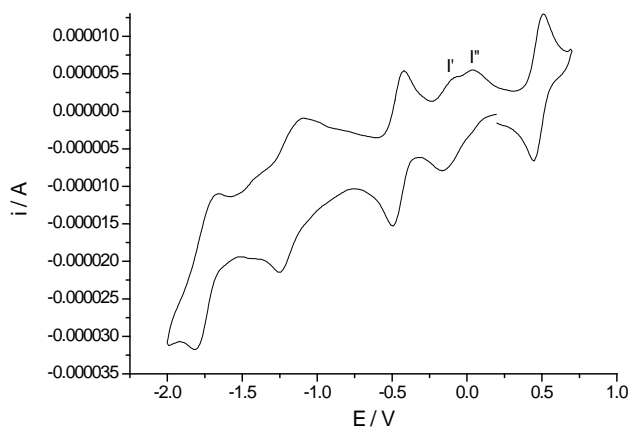


Figure 3.18. Cyclic Voltammetry of a 1.0 mM solution of $(NBu_4)_3Na[SiW_9O_{34}(EtPO)_3]$, at a glassy carbon electrode, with ferrocene as an internal reference and 0.1 M Bu_4NBF_4 as supporting electrolyte. Scan rate 50 mV/s.

At high scan rates the first reduction peak has two oxidation peaks associated with it (I' and I''), the relative sizes of these two peaks depending on the scan rate, with I' reducing as the scan rate is lowered (The same observation is seen when only scanning the first reduction peak (700 mV to -350 mV)). This behaviour suggests that the product of the first reduction (I') is unstable only being seen at the higher scan rates and quickly undergoes a chemical reaction to produce I''. An explanation of this reaction may be assigned to an $\alpha \rightarrow \beta$ isomerization of the reduced species,^{17,18} as it has been observed that the β -isomers of related Keggin structures are reduced at slightly more positive potentials than those for the α -isomers.¹⁶

Overall the evidence suggests that a triply derivatised anion is obtained from the reaction, the major product being $[\alpha-SiW_9O_{34}(EtPO)_3]^{4-}$. This is confirmed by single crystal XRD, however ^{29}Si NMR indicates that small quantities of a second fully saturated structure is formed, this being assigned as $[\beta-SiW_9O_{34}(EtPO)_3]^{4-}$, greater quantities of this species are formed during cyclic voltammetry experiments.

3.2.3.3.2. Temperature

A further alteration made to the reaction conditions in the hope of promoting the formation of the triply derivatised product was to change the temperature of the reaction. Normally the reaction takes place in refluxing acetonitrile (82 °C), to increase the temperature the solvent was changed to butyronitrile (bp 115-117 °C), and all other conditions remained the same as when excess acid was used. The reaction was monitored by ^{31}P NMR spectroscopy and after 24 hours the peaks due to the product and ethylphosphonic acid are in a 1:1 ratio. After 48 and 72 hours the peaks were in a 1.5:1 ratio showing that the reaction had proceeded further, but no further than when acetonitrile is the solvent, the increased temperature having no effect.

3.2.3.4. Other Derivatives

Reactions to obtain other derivatives will be attempted using the best conditions found above; a ratio of 1:4 ([polyoxotungstate]:phosphonic acid), an excess of HCl, a reaction time of three days and NBu_4Br as the phase-transfer agent in acetonitrile.

3.2.3.4.1. $(\text{NBu}_4)_3\text{Na}[\text{SiW}_9\text{O}_{34}(\text{H}_2\text{C}=\text{CHPO})_3]$

The reaction of vinylphosphonic acid with $[\text{SiW}_9\text{O}_{34}]^{10-}$ should proceed in the same way as for ethylphosphonic acid, but giving a product with three double bond functionalities attached to the framework (Compound 30).

^1H NMR. The spectrum is dominated by the NBu_4^+ cations, there is also a multiplet characteristic of the vinyl group (5.82-6.18 ppm), its position having shifted downfield compared to vinylphosphonic acid. The intensities indicate that three vinyl groups are present per three cations.

^{31}P NMR. The spectrum exhibits one peak due to the product; this is at 14.9 ppm and has tungsten satellite peaks associated with it which indicates that the phosphorus atoms are each connected to two tungsten atoms.^{14,15}

^{29}Si NMR. The spectrum shows one peak and therefore one silicon environment, this indicates that the entire product has the same structure with no isomerisation occurring, the position of the peak corresponds to a fully saturated structure.⁷

IR Spectroscopy. The spectrum shows the fingerprint region to have peaks in the same positions as those for $(\text{NBu}_4)_3\text{H}[\text{SiW}_9\text{O}_{34}(\text{EtPO})_3]$ so indicating that the structure is the same. Compared to the lacunary anion $[\text{SiW}_9\text{O}_{34}]^{10-}$ the IR has more peaks showing a lowering of the symmetry and the peaks are also at higher wavenumbers due to the anion being more saturated. The presence of the $\text{H}_2\text{C}=\text{CHPO}$ group is confirmed by C-H, P-O and C=C signals.

Mass Spectrometry. Maldi-TOF MS shows signals due to $[\text{SiW}_9\text{O}_{34}(\text{H}_2\text{C}=\text{CHPO})_3]^{n-}$ with either three, four, five or six NBu_4^+ cations and either none, one or two Na^+ ions, these peaks all have masses 14 units lower than calculated possibly due to a systemic error in the machine. The presence of these peaks with little indication of any singly or doubly derivatised clusters shows that the reaction has given a pure triply functionalised product.

Elemental Analysis. The results indicate the presence of three NBu_4^+ cations per polyoxotungstate anion, although again the results have more error in them than would be ideal, this can be partly explained by the presence of solvent which will increase the percentages of carbon and nitrogen present.

UV/vis Spectroscopy. The spectrum is similar to the ethyl derivative with λ_{max} and the molar absorptivity approximately the same (Figure 3.19), this shows the polyoxotungstate to have the same basic structure.

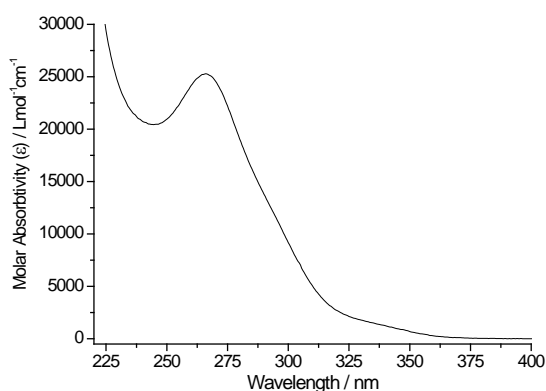


Figure 3.19. UV/vis spectrum for $(NBu_4)_3Na[SiW_9O_{34}(H_2C=CHPO)_3]$.

Single Crystal XRD. Crystals for single crystal XRD were grown by diffusion of diethyl ether into a DMF solution, the crystals were a suitable size and quality for data to be obtained by the lab Bruker Smart 6000 diffractometer in Birmingham (Table 3.7).

Table 3.7. Crystallographic Data for $(NBu_4)_3H[SiW_9O_{34}(H_2C=CHPO)_3]$.

Monoclinic	Spacegroup		P 2 ₁ / n
Cell axes (Å)	a = 18.7349(7)	b = 41.2914(18)	c = 28.3336(12)
Cell angles (deg)	α = 90.00	β = 115.473(3)	γ = 120.00
Cell Volume (Å ³)	19787.85(314)		

[Full details in appendix (Structure 14)]

The structure shows that the $[SiW_9O_{34}]^{10-}$ unit remains in the α -symmetry and has three $H_2C=CHPO$ groups grafted onto it, each attached to two adjacent edge-shared tungsten octahedra through two P-O-W bridges, creating a structure with three fold symmetry (Figure 3.20). The three P=O groups are all oriented to point towards a coordination site occupied by a Na^+ cation, this ion is derived from the starting sodium α -nonatungstosilicate salt and balances the overall 4- charge on the derivatised polyoxometalate cluster along with three NBu_4^+ cations. The Na^+ cation effectively caps the structure, in a similar manner to the proton found to reside

between the P=O groups in di-substituted decatungstosilicates¹¹ (the large electron density peak between these oxygen atoms precludes this site from being occupied by a proton here).

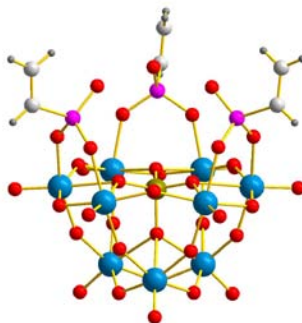


Figure 3.20. View of the $[\text{SiW}_9\text{O}_{34}(\text{C}_2\text{H}_3\text{PO})_3]^{4-}$ anion from the crystal structure.

The asymmetric unit consisting of two polyoxotungstate units and is repeated four times within a unit cell, these repeats are related by a two fold screw axis forming columns of clusters along the *b*-axis, the column being related to the next column by a centre of symmetry at $\frac{1}{2}, \frac{1}{2}, \frac{1}{2}$ forming a layer (Figure 3.21). The regions between the clusters are occupied by NBu_4^+ cations and solvent (DMF) molecules.

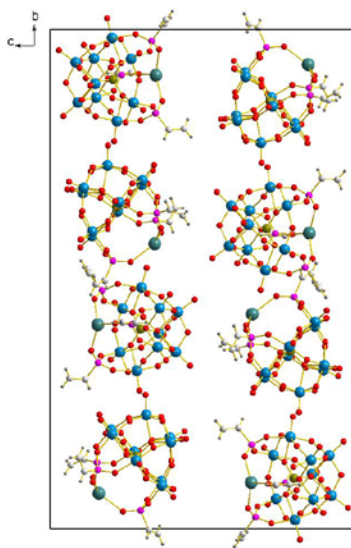


Figure 3.21. Structure of $(\text{NBu}_4)_3\text{Na}[\text{SiW}_9\text{O}_{34}(\text{C}_2\text{H}_3\text{PO})_3]$ viewed along the *a*-axis, showing only the polyoxotungstate units.

Electrochemistry. Cyclic Voltammetry was carried out and in the region 0.7 V to -2.0 V vs. Ag/AgCl and shows six electron waves corresponding to the reduction of the tungsten atoms (Figure 3.22); this is a larger number than for the ethyl derivative, probably due to the presence of a second isomer, although this was not seen in the other analysis.

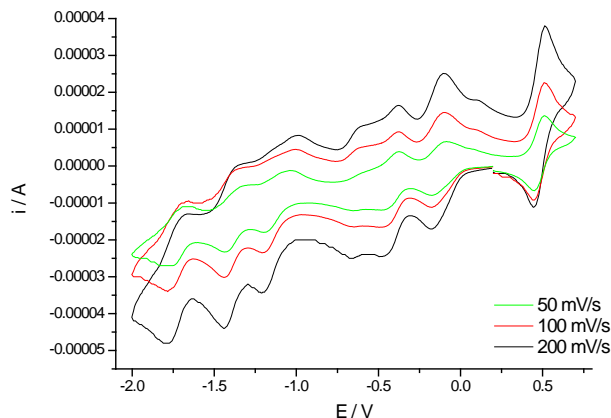


Figure 3.22. The Cyclic Voltammogram for $(NBu_4)_3Na[SiW_9O_{34}(H_2C=CHPO)_3]$ at varying scan rates.

3.2.3.4.2. $(NBu_4)_3Na[SiW_9O_{34}(H_2C=CHCH_2PO)_3]$

Derivatization of the α -nonatungstosilicate $[\alpha-SiW_9O_{34}]^{10-}$ with allylphosphonic acid gives a product with the potential for use in polymerisation reactions (Compound 31).

1H NMR. In addition to the signals for the cations $(NBu_4)^+$ there are three sets of peaks due to the allyl group $(H_2C=CHCH_2PO)$. These allyl peaks have similar shifts and couplings to that seen for $[SiW_{10}O_{36}(H_2C=CHCH_2PO)_2]^{4-}$.

^{31}P NMR. The spectrum exhibits one peak at 23.3 ppm, which has tungsten satellite peaks; these confirm that the phosphorus atoms are each connected to two tungsten atoms.

^{29}Si NMR. The spectrum has one silicon peak at -88.1 ppm, showing that the product is pure and has a fully saturated structure, indicating that $[SiW_9O_{34}(H_2C=CHCH_2PO)_3]^{4-}$ has been formed.

IR Spectroscopy. The fingerprint region is similar to those for the ethyl and vinyl derivatives, showing that the polyoxotungstate unit is the same, the position and shape of the bands indicating a saturated structure. The presence of P-O, P-C, C=C and C-H bands confirms that the $H_2C=CHCH_2PO$ groups are present.

Mass Spectrometry. The Maldi-TOF mass spectrum shows peaks due to the fully saturated anion $[SiW_9O_{34}(H_2C=CHCH_2PO)_3]^{4-}$ with either four or five cations, as well as peaks due to this anion having lost all or part of an C_3H_5PO group. As peaks due to $[SiW_9O_{34}(H_2C=CHCH_2PO)_2]^{4-}$ are present MS does not prove that all the clusters have reacted fully.

Elemental Analysis. The results indicate that three NBu_4^+ cations are present per polyoxotungstate anion, the analysis showing the values to be close to that predicted.

UV/vis Spectroscopy. The spectrum is the same as for both the ethyl and vinyl derivatives indicating that the triply derivatised product has been formed (Figure 3.23).

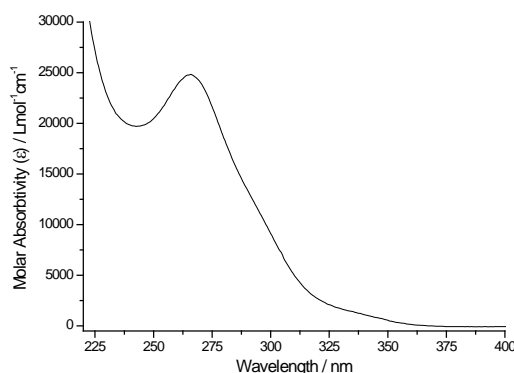


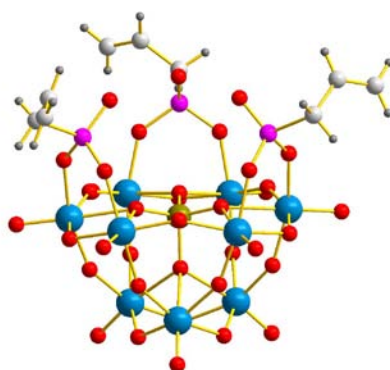
Figure 3.23. The UV/vis spectrum for $(NBu_4)_3Na[SiW_9O_{34}(H_2C=CHCH_2PO)_3]$.

Single Crystal X-ray Diffraction. Crystals suitable for single crystal XRD were grown by diffusion of diethyl ether vapour into an DMF solution. The crystals were weakly diffracting and so synchrotron data was obtained on Station 9.8 at the SRS facility at the CCLRC Daresbury Laboratory (Table 3.8).

Table 3.8. Crystallographic Data for $(NBu_4)_3H[SiW_9O_{34}(H_2C=CHCH_2PO)_3]$.

Trigonal	Spacegroup		R 3 c
Cell axes (Å)	$a = 22.2078(16)$	$b = 22.2078(16)$	$c = 34.9141(48)$
Cell angles (deg)	$\alpha = 90.00$	$\beta = 90.00$	$\gamma = 120.00$
Cell Volume (Å ³)	14912.23(26)		
[Full details in appendix (Structure 15)]			

The structure shows the $[SiW_9O_{34}]^{10-}$ unit to be retained and have three $H_2C=CHCH_2PO$ groups attached to it through P-O-W bonds (Figure 3.24), the cluster having three-fold symmetry with the asymmetric unit containing only a third of the cluster.

**Figure 3.24.** View of the $[SiW_9O_{34}(C_3H_5PO)_3]^{4-}$ anion from the crystal structure.

The three P=O groups all point towards a coordination site at the top of the structure, with a Na^+ ion filling this site and a water molecule coordinated to it giving the sodium ion a tetrahedral coordination.

The polyoxotungstate units are aligned in columns running along the c -axis, with all the units oriented in the same direction (Figure 3.25). The region between the units within a column is filled by the water molecule coordinating to the Na^+ atom and disordered solvent (MeCN) molecules, while the NBu_4^+ cations occupy the regions between columns. This structure is related to those for $(NBu_4)_3[XW_9O_{34}(t-BuSiOH)_3].CH_3CN$ and

$(NBu_4)_3[PW_9O_{34}(t-BuSiO)_3(SiR)]$ ($R=CH_2CH=CH_2$ or $(CH_2)_3Br$) having the same space group and approximate unit cell parameters, with the only significant variation being in the c -axis, this being due to differing distances between the clusters. Two sets of crystals were prepared; the first was analysed at Birmingham and found to have a c -axis of 37.34 Å (at 200 K), while the second was analysed at Daresbury and found to have a shorter c -axis (34.91 Å at 30 K and 35.02 Å at 200 K). This indicates that the length of the c -axis depends on the exact preparation conditions of the crystals, with the room temperature and therefore rate of diffusion of diethyl ether into the solution varying slightly.

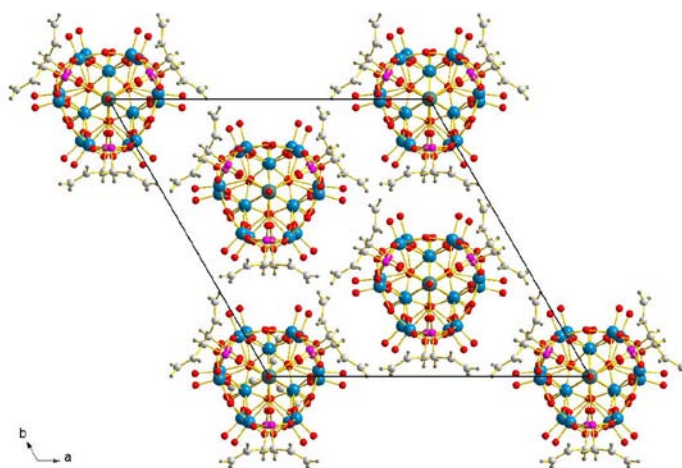


Figure 3.25. Structure of $(NBu_4)_3Na[SiW_9O_{34}(C_3H_5PO)_3]$, viewed along the c -axis, showing only the polyoxotungstate units.

Electrochemistry. Cyclic Voltammetry was carried out in the region +0.7 V to -2.0 V *vs.* Ag/AgCl. The data shows five electron waves corresponding to the reduction of the tungsten atoms (Figure 3.26), which is similar to that seen for the vinyl derivative and is due to a mixture of products.

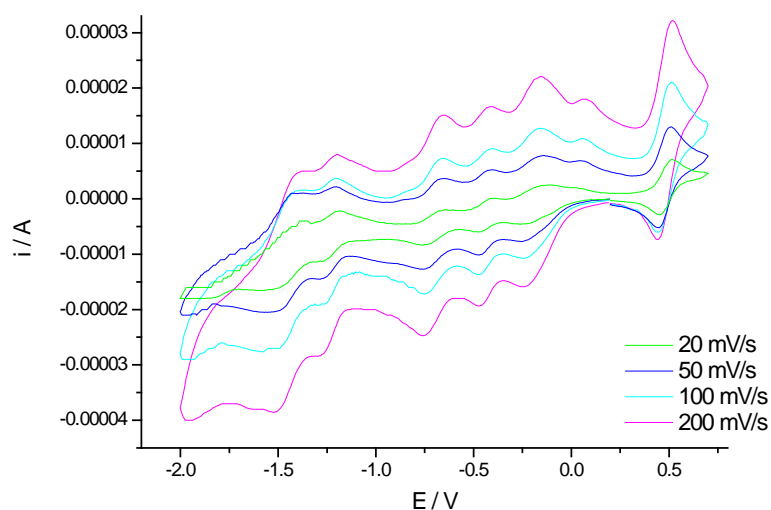


Figure 3.26. The Cyclic Voltammogram for $(NBu_4)_3Na[SiW_9O_{34}(H_2C=CHCH_2PO)_3]$ at varying scan rates.

3.2.3.4.3. $(NBu_4)_3Na[SiW_9O_{34}(H_2C=CHC_6H_4PO)_3]$

Reaction with the styrylphosphonic acid should produce a $[SiW_9O_{34}]^{10-}$ unit which has three styrene groups grafted onto the structure (Compound 35), with the potential for these groups to be reacted to produce polymeric materials which have polyoxotungstate units incorporated into the material.

1H NMR. The spectrum shows that the styrene groups are present with signals in the same position as for the styrylphosphonic acid. The cations (NBu_4^+) exhibit four signals in the same positions as seen for other examples.

^{31}P NMR. The spectrum has one peak at 13.5 ppm, this peak is relatively broad so the tungsten satellites can not be seen. The position of this peak is at a slightly lower value than the equivalent peak seen for $[SiW_{10}O_{36}(H_2C=CHC_6H_4PO)_2]^{4-}$ (15.4 ppm), but is within the region to show that a related product has been obtained.

IR Spectroscopy. The fingerprint region is characteristic of that previously seen for the triply derivatised $[\text{SiW}_9\text{O}_{34}]^{10-}$ polyoxotungstates. The presence of the styrene group is confirmed by the C=C stretch at 1600 cm^{-1} and C-H stretches.

Mass Spectrometry. The Maldi-TOF mass spectrum for the product is quite complicated although peaks are present which show the anion $[\text{SiW}_9\text{O}_{34}(\text{H}_2\text{C}=\text{CHC}_6\text{H}_4\text{PO})_3]^{4-}$ with either three, four or five cations and none, one or two Na^+ ions. These peaks confirm that the desired product was produced.

Elemental Analysis. The product has a higher percentage of carbon in it than the calculated value; this could show that some solvent is present.

UV/vis Spectroscopy. The spectrum observed for the product has a λ_{max} at 260.5 nm ($\epsilon = 74500\text{ L mol}^{-1}\text{ cm}^{-1}$); the peak is made up of the absorption due to the $[\text{SiW}_9\text{O}_{34}(\text{RPO})_3]^{4-}$ anion (normally $\lambda_{\text{max}} \sim 265$ (23500)) and the absorption of the styrene groups (styrylphosphonic acid $\lambda_{\text{max}}=254.5$ (17000)) (Figure 3.27). The position of λ_{max} is an intermediate between the two values and the molar absorptivity is a combination of the values for all the components ($23500 + 3 \times 17000 = 74500$).

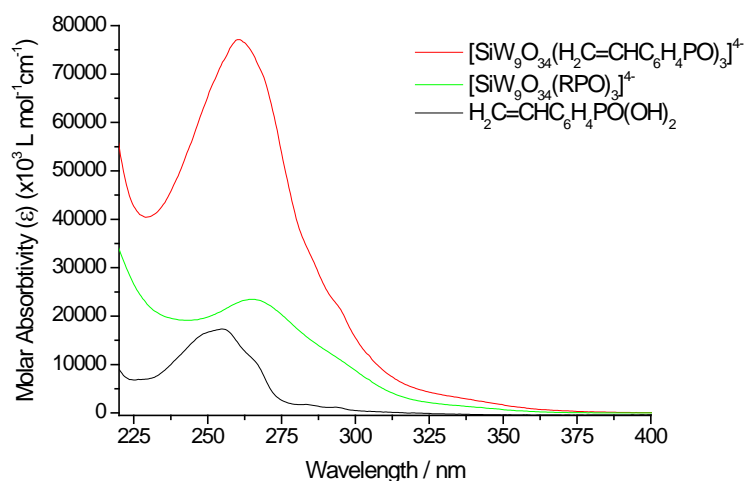


Figure 3.27. The UV/vis spectra for (a) $[\text{SiW}_9\text{O}_{34}(\text{H}_2\text{C}=\text{CHC}_6\text{H}_4\text{PO})_3]^{4-}$, (b) A general spectrum for $[\text{SiW}_9\text{O}_{34}(\text{RPO})_3]^{4-}$ and (c) $\text{H}_2\text{C}=\text{CHC}_6\text{H}_4\text{PO}(\text{OH})_2$.

Single Crystal X-ray Diffraction. Suitable crystals of the product could not be obtained, however the addition of cobalt(II) nitrate to a DMF solution containing the product yielded dark blue crystals after diffusion of diethyl ether into the solution. Diffraction data was collected on the diffractometer at Birmingham and was of a good quality (Table 3.9).

Table 3.9. Crystallographic Data for $(NBu_4)_3Co[SiW_9O_{34}(H_2C=CHC_6H_4PO)_3] \cdot (H_2O)(H_3C)_2NCO$.

Trigonal	Spacegroup			R 3 c
Cell axes (Å)	$a = 21.4049(45)$	$b = 21.4049(45)$	$c = 21.2166(92)$	
Cell angles (deg)	$\alpha = 90.00$	$\beta = 90.00$	$\gamma = 120.00$	
Cell Volume (Å ³)	8418.46(44)			

[Full details in appendix (Structure 16)]

The cluster has the same basic structure as seen for the other derivatives, with a $[\alpha-SiW_9O_{34}]^{10-}$ unit on to which three $H_2C=CHC_6H_4PO$ groups are grafted through P-O-W bonds, giving the anion three-fold symmetry (Figure 3.28). The three P=O groups all point towards a coordination site which is filled by a cobalt ion, the tetrahedral geometry of the cobalt being completed by coordination to a water molecule.

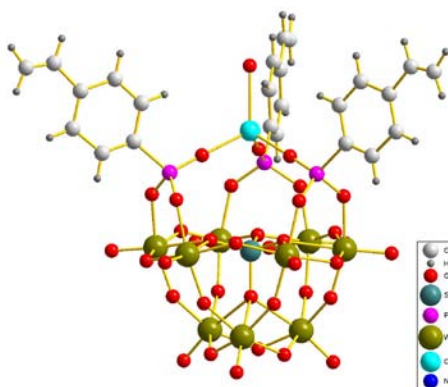


Figure 3.28. The structure of the $[SiW_9O_{34}(H_2C=CHC_6H_4PO)_3]Co(OH_2)^{2-}$ anion.

Within the crystal structure all the clusters are oriented in the same direction (parallel with the c -axis). The clusters are arranged so that the gaps between R groups point towards an adjacent cluster, with each cluster near to six other clusters giving a hexagonal type arrangement when viewed down the c -axis (Figure 3.29). The gaps in the structure are filled by the NBu_4^+ cations and disordered DMF molecules.

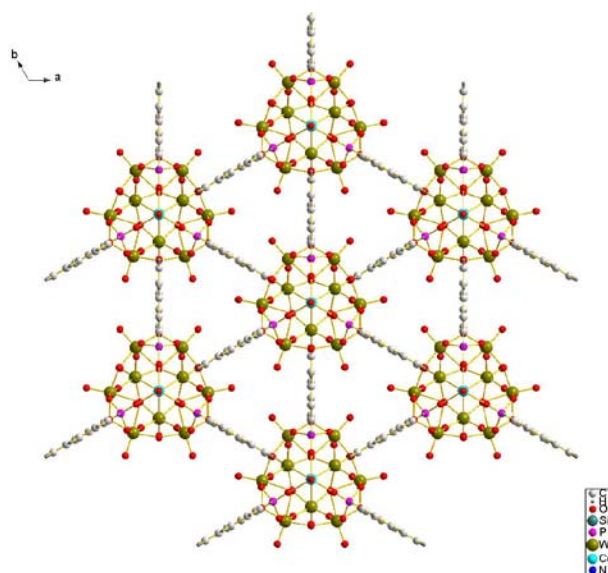


Figure 3.29. The structure of $(NBu_4)_3Co[SiW_9O_{34}(H_2C=CHC_6H_4PO)_3] \cdot (H_2O)(H_3C)_2NCO$.

3.2.3.4.4. $(NBu_4)_3Na[SiW_9O_{34}(HOOCCH_2PO)_3]$

Reaction of $[SiW_9O_{34}]^{10-}$ with $HOOCCH_2PO(OH)_2$ will create a polyoxotungstate which has carboxylic acid functionality (Compound 32). This functionality has the potential to be used to control the long range ordering of the clusters as well as taking part in reactions to add further functionality to the structure.

1H NMR. The presence of the $HOOCCH_2$ group is confirmed in the 1H NMR spectrum by a doublet at 2.70 ppm, the signal being split by coupling of the hydrogen atoms with the phosphorus. Signals from the NBu_4^+ cation are also seen.

^{31}P NMR. One broad signal can be seen in the spectrum; although some small peaks are seen around the main signal it would appear that the product obtained contains one phosphorus environment. The position of this signal (16.0 ppm) matches the signal in the doubly derivatised species $[\text{SiW}_{10}\text{O}_{36}(\text{HOOCCH}_2\text{PO})_2]^{4-}$ showing that the groups are in similar environments.

IR Spectroscopy. The fingerprint region has bands in the same positions as for other $[\text{SiW}_9\text{O}_{34}(\text{RPO})_3]^{4-}$ species, confirming that the polyoxotungstate unit has the same structure. The R group can be seen by the presence of P-O, P-C and C-H bands as well as the C=O stretch at 1718 cm^{-1} and the O-H stretch at 3421 cm^{-1} which confirm the retention of the carboxylic acid.

Mass Spectrometry. Signals are observed due to $[\text{SiW}_9\text{O}_{34}(\text{HOOCCH}_2\text{PO})_3]^{4-}$ with either four NBu_4^+ cations and a Na^+ ion, five or six NBu_4^+ cations or seven NBu_4^+ cations but having lost part of the R groups. These signals confirm that the product is triply functionalised and that the carboxylic acid groups are not altered during the reaction.

Elemental Analysis. The percentages of carbon, hydrogen and nitrogen in the product are close to the predicted values; although the product was dried well before analysis the difference can be explained by acetonitrile being present.

UV/vis Spectroscopy. λ_{max} is slightly lower (260.5 nm) than for other derivatives (Figure 3.30), perhaps indicating that the reaction has not gone to completion due to the lower solubility of the phosphonic acid.

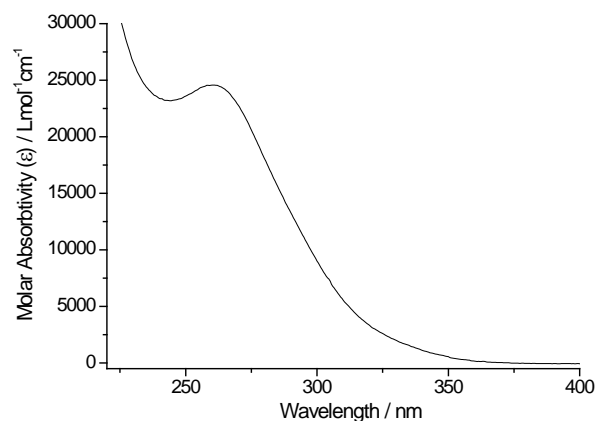


Figure 3.30. UV/vis spectrum for $(NBu_4)_3Na[SiW_9O_{34}(HOOCCH_2PO)_3]$.

Electrochemistry. The cyclic voltammogram for the product shows there to be three cathodic/anionic waves in the region studied (-2.2 to 0.35 V vs. Ag/Ag^+) (Figure 3.31), the first two are one-electron processes and the third one is a two-electron process, the positions of the waves corresponding to those given by $[SiW_9O_{34}(EtPO)_3]^{4-}$ with only slight shifts due to the electron withdrawing properties of the R group.

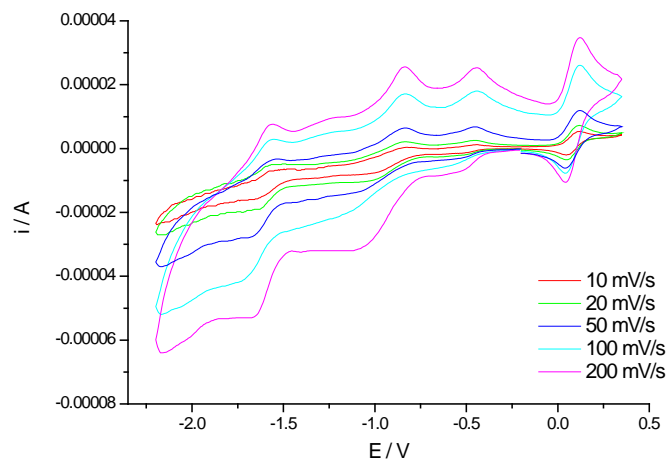


Figure 3.31. The Cyclic Voltammogram for $(NBu_4)_3Na[SiW_9O_{34}(HOOCCH_2PO)_3]$ and ferrocene using a Ag/Ag^+ reference electrode.

3.2.3.4.5. $(NBu_4)_3Na[SiW_9O_{34}(HOOCCH_2CH_2PO)_3]$

Reaction with $HOOCCH_2CH_2PO(OH)_2$ will functionalise the $[SiW_9O_{34}]^{10-}$ cluster with carboxylic acid groups (Compounds 33), but with the functionality further away from the polyoxotungstate than when using $HOOCCH_2PO(OH)_2$.

1H NMR. The spectrum shows four signals due to NBu_4^+ cations and two from the carbon chain in the R group. The intensities of these peaks illustrates that 2-3 R groups are present per three cations.

^{31}P NMR. One phosphorus environment can be observed; this is at 27.6 ppm and has tungsten satellite peaks associated with it.

IR Spectroscopy. The spectrum is similar to those for the other derivatives, showing the characteristic pattern of peaks in the fingerprint region and C=O and O-H stretches confirming the presence of the carboxylic acid functionality.

Mass Spectrometry. The main peaks in the Maldi-TOF mass spectrum prove that the triply derivatised polyoxotungstate has been produced. There is a large peak due to $(NBu_4)_4[SiW_9O_{34}(HOOCCH_2CH_2PO)_3]^+$ with smaller ones due to the anion with either three or five cations. There are also small peaks due to the doubly derivatised species, these could be a product of the ionisation or mean that the reaction did not produce a pure product.

Elemental Analysis. The results indicate that there are three NBu_4^+ cations per anion cluster, although the values are higher than expected, possibly due to some solvent being present.

UV/vis Spectroscopy. The spectrum has $\lambda_{max} = 265.5$ nm ($\epsilon = 23500$ Lmol $^{-1}$ cm $^{-1}$), this is the same position as for the other derivatives and shows the anion to be triply functionalised.

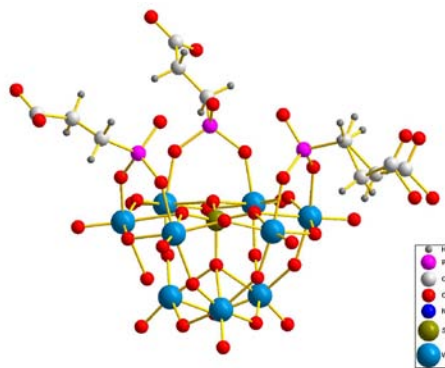
Single Crystal X-ray Diffraction. Suitable crystals were obtained by diffusion of diethyl ether into an acetonitrile solution (Table 3.10).

Table 3.10. Crystallographic Data for $(NBu_4)_3Na[SiW_9O_{34}(HOOCCH_2CH_2PO)_3]$.

Tetragonal	Spacegroup		P 4/n
Cell axes (Å)	a = 38.9645(14)	b = 38.9645(14)	c = 14.1781(7)
Cell angles (deg)	$\alpha = 90.00$	$\beta = 90.00$	$\gamma = 90.00$
Cell Volume (Å ³)	21525.65(15)		

[Full details in appendix (Structure 17)]

Each cluster is made up of an $[\alpha-SiW_9O_{34}]^{10-}$ anion with three $HOOCCH_2CH_2PO^{2+}$ groups grafted onto the surface, each through two W-O-P bonds (Figure 3.32). The three $HOOCCH_2CH_2PO$ groups point in different directions so the cluster no longer possesses three-fold symmetry.

**Figure 3.32.** $[SiW_9O_{34}(HOOCCH_2CH_2PO)_3]^{4-}$ structure.

Studying the long-range order, the clusters can be thought of as forming columns of identical clusters down the c -axis, with planes of clusters in the a - b plane. The clusters are related to one another through a four-fold rotation (Figure 3.33).

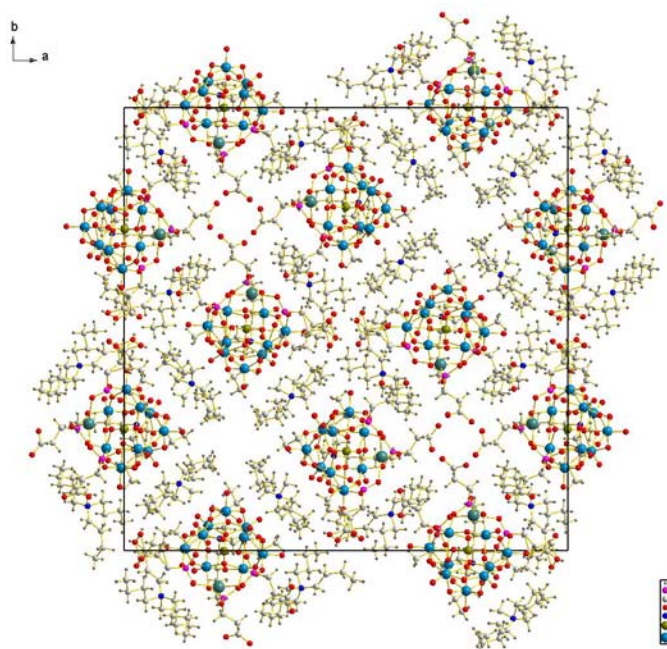


Figure 3.33. Crystal Structure of $(NBu_4)_3Na[SiW_9O_{34}(HOOCCH_2CH_2PO)_3]$ viewed along the c -axis.

The carboxylic acid groups on different polyoxotungstates interact with one another in three different ways; firstly four groups which are all equivalent interact via long and weak hydrogen-bonds ($d_{OO}=3.7\text{--}4.0\text{ \AA}$), the four hydrogen atoms from the OH groups being disordered between a large number of possible sites (Figure 3.34).

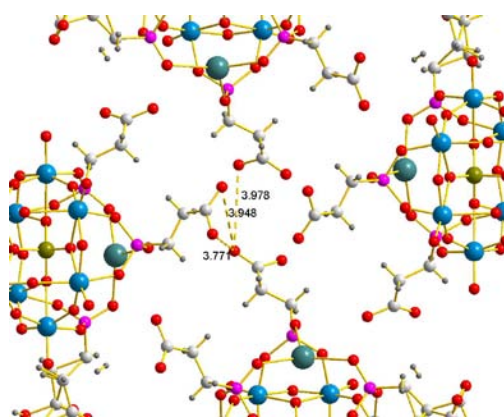


Figure 3.34. Crystal structure showing the hydrogen-bonding of the carboxylic acid groups.

The second set of hydrogen-bonding interactions involve the disordered $\text{HOOCCH}_2\text{CH}_2\text{PO}$ group, two equivalent groups hydrogen-bond via COOH-HOOC interactions ($d_{\text{OO}} = 2.69\text{--}3.00 \text{ \AA}$). A third carboxylic acid group forms hydrogen-bonds with the oxygen on the P=O group ($d_{\text{OO}} = 2.58 \text{ \AA}$), creating an unusual interaction (Figure 3.35).

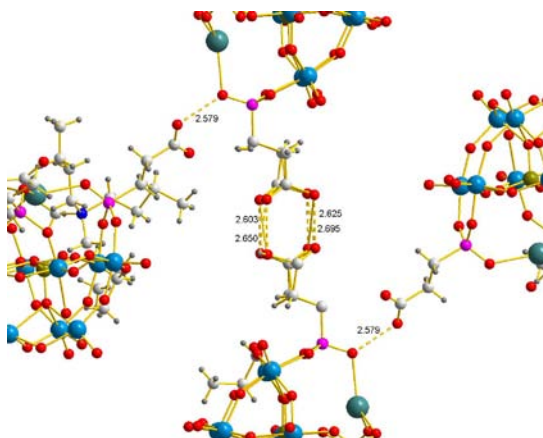


Figure 3.35. Crystal structure showing the hydrogen-bonding interactions.

All these hydrogen-bonding interactions hold the structure together with the NBu_4^+ cations filling the gaps in the structure and the Na^+ ions balancing the charge.

Electrochemistry. Cyclic voltammetry of the product shows three cathodic/anionic waves in the region studied (-2.2 to $0.35 \text{ V vs. Ag/Ag}^+$) (Figure 3.36), the first two being one-electron processes and the third a two-electron process. The third wave has a second small oxidation peak associated with it, which could show the oxidation of a product of a reaction of the reduced species.

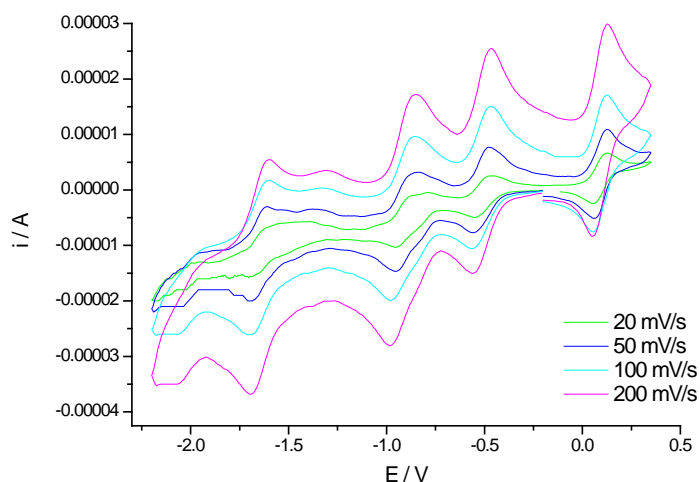


Figure 3.36. The Cyclic Voltammogram for $(NBu_4)_3Na[SiW_9O_{34}(HOOCCH_2CH_2PO)_3]$ vs. Ag/Ag^+ .

3.2.3.4.6. $(NBu_4)_3Na[SiW_9O_{34}(H_3CCOC_6H_4PO)_3]$

4-acetylphenylphosphonic acid was reacted with $[SiW_9O_{34}]^{10-}$ to give the triply derivatised product with three ketone group functionalities grafted on to the cluster (Compound 34).

1H NMR. The spectrum shows both the NBu_4^+ cations and acetylphenyl signals. The $H_3CCOC_6H_4$ group appears the same as for the phosphonic acid; a singlet due to the CH_3 at 2.60 ppm and a multiplet due to the ring at 7.88-8.08 ppm, the intensities of these signals predicting that 2-3 groups are present per three cations.

^{31}P NMR. A single peak is seen at 14.3 ppm, showing that a pure product is obtained. Tungsten satellite peaks are observed showing that the phosphorus is attached to two tungsten atoms from the polyoxotungstate cluster.

IR Spectroscopy. The fingerprint region shows the same bands due to the W-O stretches as seen for other derivatives proving that the same polyoxotungstate structure is present. There is also evidence of the $H_3CCOC_6H_4$ group, most noticeably the $C=O$ at 1684 cm^{-1} .

Mass Spectrometry. The Maldi-TOF mass spectrum has two main peaks, due to $(NBu_4)_4Na[SiW_9O_{34}(H_3CCOC_6H_4PO)_3]^+$ and $(NBu_4)_5Na[SiW_9O_{34}(H_3CCOC_6H_4PO)_3]^+$ proving that the triply substituted product was the main product of the reaction.

Elemental Analysis. The results show the percentages of carbon, nitrogen and hydrogen to be close to the predicted values, confirming that there are three cations per anion cluster.

UV/vis Analysis. The spectrum shows one intense peak at $\lambda_{max}=249.5$ nm ($\epsilon = 98000$ Lmol⁻¹cm⁻¹) which is a combination of the peak normally seen for $[SiW_9O_{34}(RPO)_3]^{4-}$ and the peak due to the acetylphenyl group (4-acetylphenylphosphonic acid $\lambda_{max}=251$ nm (25000)) (23500 + 3 x 25000 = 98500). The position of the peak is similar to that of the phosphonic acid as these peaks dominant the spectra (Figure 3.37).

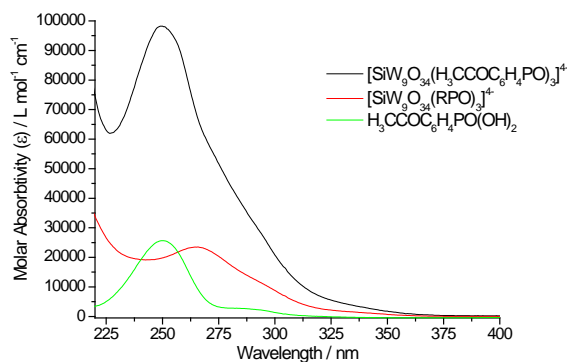


Figure 3.37. The UV/vis spectra for (a) $[SiW_9O_{34}(H_3CCOC_6H_4PO)_3]^{4-}$, (b) a general $[SiW_9O_{34}(RPO)_3]^{4-}$ and (c) $H_3CCOC_6H_4PO(OH)_2$.

Single Crystal X-ray Diffraction. Crystals suitable for X-ray Diffraction were obtained (Table 3.11).

Table 3.11. Crystallographic Data for $(NBu_4)_6Na[SiW_9O_{34}(H_3CCOC_6H_4PO)_3]_2 \cdot ((H_3C)_2NCO)_3$.

Triclinic	Spacegroup		P -1
Cell axes (Å)	$a = 18.5991(18)$	$b = 19.2421(16)$	$c = 20.8677(19)$
Cell angles (deg)	$\alpha = 94.186(6)$	$\beta = 116.047(5)$	$\gamma = 114.979(5)$
Cell Volume (Å ³)	5767.79(0)		

[Full details in appendix (Structure 18)]

The clusters are made up of a $[\alpha\text{-SiW}_9\text{O}_{34}]^{10-}$ anion with three $\text{H}_3\text{CCOC}_6\text{H}_4\text{PO}$ groups grafted onto the structure. The coordination site between the three $\text{P}=\text{O}$ groups at the top of the anion is occupied by a metal ion which is also coordinated to three $\text{P}=\text{O}$ groups on a second cluster, giving the ion an octahedral structure and holding two clusters together to form a dimer-type structure (Figure 3.38).

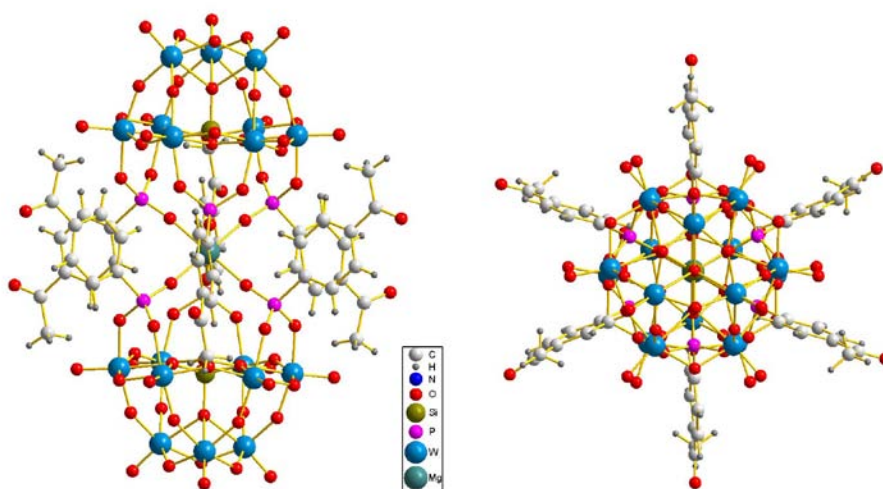


Figure 3.38. The structure of $[\text{SiW}_9\text{O}_{34}(\text{H}_3\text{CCOC}_6\text{H}_4\text{PO})_3]_2\text{M}$, viewed from (a) the side and (b) above.

The identity of this ion is unclear as the most likely metal ion to be present is sodium originating from the sodium α -nonatungstosilicate salt, however refinement of the structure does not like this assignment as the electron density does not agree. Also the octahedral geometry is unusual for a sodium ion and the charge in the structure would not be balanced by sodium, an extra H^+ also being needed. Another metal that has come into contact with the reactants is Mg^{2+} , through the use of MgSO_4 to dry the diethyl phosphonate, although it is unlikely for this to remain in the product. A third possible explanation being an impurity, but this is unlikely.

Looking at the extended structure the dimers are all aligned in the same direction, with the two sets of dimers within a unit cell surrounded by cations and DMF molecules (Figure 3.39).

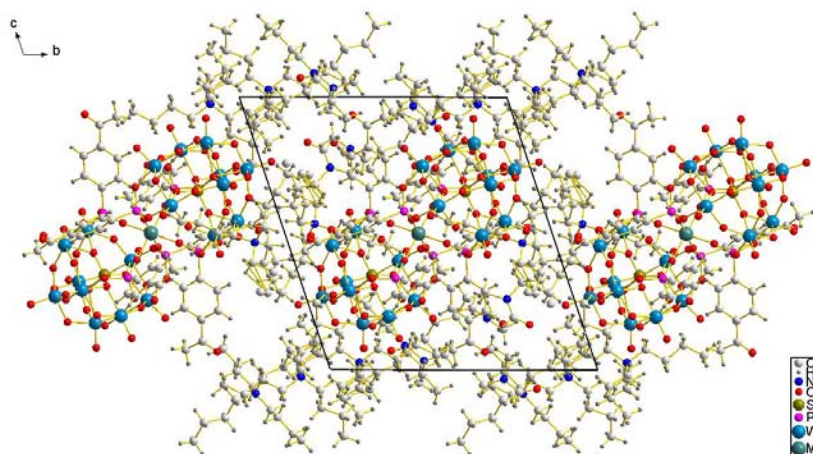


Figure 3.39. The crystal structure of $(NBu_4)_6M[SiW_9O_{34}(H_3CCOC_6H_4PO)_3]_2 \cdot ((H_3C)_2NCO)_3$.

Crystallization with Cobalt Salts. Crystals were also obtained from a mixture of the product and cobalt(II) nitrate, cobalt being used as it can occupy an octahedral coordination site. The mixture gave a blue solution, and brown crystals. The spectra were compared with those for the product without cobalt being present to see if any changes have occurred.

NMR Characterization. The 1H NMR spectrum is similar to that before the cobalt nitrate was added, however the CH_3 singlet is broader perhaps showing an interaction between the $C=O$ group and the cobalt ions. The ^{31}P NMR shows the phosphorus peak to have shifted from 14.3 to 5.5 ppm, due to the interaction of the $P=O$ groups with the cobalt ion. The peak also shows two sets of satellite peaks due to coupling with both the cobalt ion and tungsten atoms.

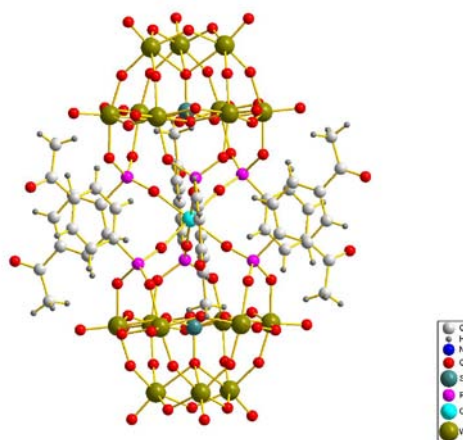
IR Spectroscopy. The spectrum shows little change on addition of cobalt nitrate except that the $C=O$ stretch has broadened and shifted slightly, indicating an interaction with the cobalt. There is little change in the $1100\text{--}1000\text{ cm}^{-1}$ region which shows the $P\text{--}O$ bonds.

Single Crystal X-ray Diffraction.**Table 3.12.** Crystallographic Data for $(NBu_4)_5Co[SiW_9O_{34}(H_3CCOC_6H_4PO)_3]_2 \cdot [Co((H_3C)_2NCO)_6] \cdot ((H_3C)_2NCO)_4$.

Monoclinic	Spacegroup		C 2/c
Cell axes (Å)	a = 22.0375(13)	b = 31.3129(19)	c = 33.7086(19)
Cell angles (deg)	$\alpha = 90.00$	$\beta = 91.085(3)$	$\gamma = 90.00$
Cell Volume (Å ³)	23256.72(27)		

[Full details in appendix (Structure 19)]

The local structure of the clusters was found to be the same as when no cobalt was present, with a metal ion in the coordination site created between the P=O groups, this metal has an octahedral coordination with the P=O groups on a second cluster (Figure 3.40). The metal ion is assigned as being Co(II), arising from the cobalt nitrate with which the product was crystallized, although it is possible it could be the same ion as was previously present. The fitting as cobalt gives a reasonable refinement.

**Figure 3.40.** The dimer structure of $[SiW_9O_{34}(H_3CCOC_6H_4PO)_3]_2$.

A second cobalt ion is also present in the structure, which coordinates to six DMF solvent molecules and is disordered over two sites which are 0.8 Å apart and related by a plane of symmetry. There are also five NBu_4^+ cations and four DMF molecules per dimer of clusters,

therefore to balance the charge of -8 (for 2 anion clusters) either the metal between the two anions will have a single charge (e.g. Na^+) or one of the clusters has been reduced.

Due to the presence of $Co(DMF)_6$ and a different number of cations, the overall structure is different from that obtained without $Co(NO_3)_2$. The dimers are arranged in rows within which they are angled alternatively at slightly different angles (Figure 3.41). The unit cell having planes of symmetry along both the $a-c$ and $a-b$ planes, the $Co(DMF)_6$, cations and solvent molecules filling the gaps in the structure.

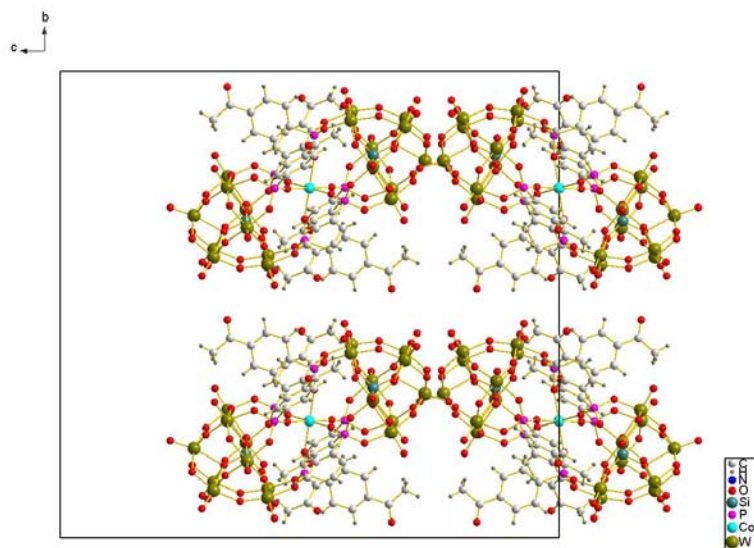


Figure 3.41. The crystal structure showing only the anion clusters, viewed down the a -axis.

Conclusion. Using the conditions derived above involving an excess of phosphonic acid, a catalytic amount of HCl and refluxing for three days gives a triply derivatised product for a variety of different phosphonic acid functionalities ($R=Et$, $H_2C=CH$, $H_2C=CHCH_2$, $H_2C=CHC_6H_4$, $HOOCCH_2$, $HOOCCH_2CH_2$ or $H_3CCOC_6H_4$) when the polyoxotungstate is $[SiW_9O_{34}]^{10-}$. The products are confirmed by multinuclear (1H , ^{31}P and ^{29}Si) NMR, IR, MS and UV/vis spectroscopy along with CHN analysis and Single Crystal XRD. Attempts to obtain a triply functionalised structure for the $[PW_9O_{34}]^{9-}$ anion using these conditions gave

only the doubly functionalised product with no indications of the anion becoming saturated.

The UV/vis spectra of the products indicates that the $[\text{SiW}_9\text{O}_{34}]^{10-}$ structures are saturated (Figure 3.42), with a shift in the position of λ_{max} to longer wavelengths compared with the doubly derivatised structures (Section 3.2.3 and those obtained from $[\text{PW}_9\text{O}_{34}]^{9-}$).

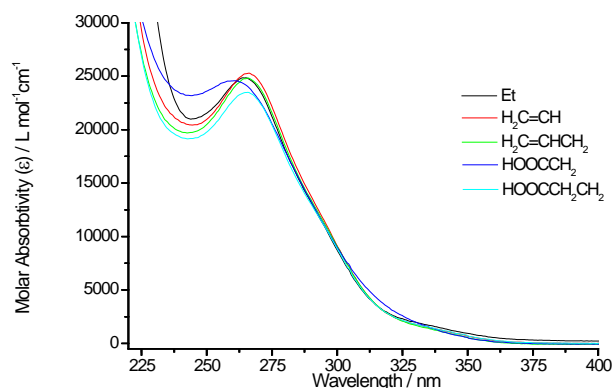


Figure 3.42. The UV/vis spectra for $[\text{SiW}_9\text{O}_{34}(\text{RPO})_3]^{4-}$.

The structures obtained by single crystal XRD (Table 3.13) all show the $[\text{SiW}_9\text{O}_{34}]^{10-}$ unit to be fully saturated, three P=O groups all point towards a coordination site at the top of the structure which is occupied by a Na^+ ion except when cobalt is introduced into the structure. The long range order of the units varies depending on the R group, with dimers of two polyoxometalate units being found when $\text{R} = \text{H}_3\text{CCOC}_6\text{H}_4$. When $\text{R} = \text{H}_2\text{C}=\text{CHCH}_2$ the unit cell parameters are similar to that for $(\text{NBu}_4)_3\text{H}[\text{SiW}_9\text{O}_{34}(t\text{-BuSiOH})_3]$ and when $\text{R} = \text{Et}$ or $\text{H}_2\text{C}=\text{CHC}_6\text{H}_4$ the structures are related, but with the length of the c -axis changing this being due to the gaps between the clusters varying.

Table 3.13. Table of the unit cell parameters for the crystals obtained from $[\text{SiW}_9\text{O}_{34}]^{9-}$ derivatives.

	Structure	Spacegroup	a (Å)	b (Å)	c (Å)	α	β	γ	V / Å ³
(NBu ₄) ₃ H[SiW ₉ O ₃₄ (<i>t</i> -BuSiOH) ₃]	10	R 3 c	22.52	22.52	35.99	90.0	90.0	120.0	15803
(NBu ₄) ₃ Na[SiW ₉ O ₃₄ (EtPO) ₃]	13	R 3 m	20.72	20.72	22.47	90.0	90.0	120.0	8358
(NBu ₄) ₃ H[SiW ₉ O ₃₄ (H ₂ C=CHPO) ₃]	14	P 21/c	18.73	41.29	28.33	90.0	115.5	90.0	19788
(NBu ₄) ₃ Na[SiW ₉ O ₃₄ (H ₂ C=CHCH ₂ PO) ₃]	15	R 3 c	22.21	22.21	34.91	90.0	90.0	120.0	14912
(NBu ₄) ₃ Co[SiW ₉ O ₃₄ (H ₂ C=CHC ₆ H ₄ PO) ₃]	16	R 3 m	21.40	21.40	21.22	90.0	90.0	120.0	8419
(NBu ₄) ₃ Na[SiW ₉ O ₃₄ (HOOCCH ₂ CH ₂ PO) ₃]	17	P 4/n	38.96	38.96	14.18	90.0	90.0	90.0	21526
(NBu ₄) ₆ M[SiW ₉ O ₃₄ (H ₃ CCOC ₆ H ₄ PO) ₃] ₂	18	P -1	18.60	19.24	20.87	94.2	116.0	115.0	5768
NBu ₄) ₅ Co[SiW ₉ O ₃₄ (H ₂ C=CHC ₆ H ₄ PO) ₃] ₂ · [Co((H ₃ C) ₂ NCO) ₆]	19	C 2/c	22.04	31.31	33.70	90.0	91.1	90.0	23257

The electrochemistry of the anions was studied by cyclic voltammetry and the results compared by considering the peak potential relative to ferrocene (Table 3.14).

Table 3.14. The reduction potentials for (NBu₄)₃H[SiW₉O₃₄(RPO)₃], 1.0 mM solutions, E° relative to ferrocene.

R	E° ₃ / mV		E° ₂ / mV		E° ₁ / mV		E (ferrocene)
Et	-2250		-1660		-940	-620	0.00
H ₂ C=CH	-2220	-1870	-1580	-1110	-894	-600	0.00
H ₂ C=CHCH ₂		-1940	-1710	-1190	-922	-664	0.00
H ₂ C=CHC ₆ H ₄	-2230	-1910		-1181		-644	0.00
HOOCCH ₂			-1695		-1030	-570	0.00
HOOCCH ₂ CH ₂			-1720		-1000	-600	0.00
H ₃ CCOC ₆ H ₄	-1875		-1090		-588		0.00

The number of reduction potentials varies as an isomerisation of one of the reduced species is observed in some cases. The first reduction potentials are all at approximately the same value, with some minor variation due to the electron withdrawing properties of the group grafted on to the polyoxotungstate framework.

3.2.4. Reaction with EtPCl_2

Although a triply derivatised product has been obtained by the reaction of phosphonic acids with $[\text{SiW}_9\text{O}_{34}]^{10-}$ only the doubly derivatised structure is obtained from the $[\text{PW}_9\text{O}_{34}]^{9-}$ analogue. To attempt to make a $[\text{PW}_9\text{O}_{34}]^{9-}$ compound which is triply functionalised with phosphonoyl groups a more highly electrophilic moiety is needed, 'EtPO²⁺' can be prepared by the reaction of EtPCl_2 with AgNO_3 in acetonitrile, with Ag^+ doubling as an agent to remove chloride and to oxidise the phosphorus atom.¹⁰ The 'EtPO²⁺' moiety is highly electrophilic and should allow the reaction to proceed further.

3.2.4.1. Cation exchange

Following the method used for the reaction of $[\text{XW}_{11}\text{O}_{39}]^{n-}$ in the literature¹⁰ the polyoxotungstate $[\text{PW}_9\text{O}_{34}]^{9-}$ was stirred with NBu_4Br in an aqueous solution to exchange the cations, however this proved to be unsuccessful with the polyoxotungstate unit isomerising, IR spectroscopy indicating that the anion present is $[\text{PW}_{11}\text{O}_{39}]^{9-}$, as the bands correspond to those for $(\text{NBu}_4)_4\text{H}_2\text{Na}[\text{PW}_{11}\text{O}_{39}]$.¹⁰ Reaction of this product with EtPO²⁺ produced from EtPCl_2 and AgNO_3 confirms that the polyoxotungstate anion was $[\text{PW}_{11}\text{O}_{39}]^{7-}$, the product obtained being $(\text{NBu}_4)_3[\text{PW}_{11}\text{O}_{39}(\text{EtPO})_2]$ (Compound Z). This was confirmed by IR, ³¹P NMR, MS and EA.

Cation exchange was also attempted on $\text{Na}_{10}[\text{SiW}_9\text{O}_{34}]$, by stirring the product with NBu_4Br and this gave a small quantity of an oily deposit which could not be isolated. Therefore the method for the synthesis of the $[\text{SiW}_9\text{O}_{34}]^{10-}$ anion was altered so that NBu_4Br was added in place of NaCO_3 during the precipitation step. Analysis of the IR spectrum for this product shows the fingerprint region to have similarities to that for both $[\text{SiW}_{12}\text{O}_{40}]^{4-}$ and $[\text{SiW}_{11}\text{O}_{39}]^{7-}$. To test which polyoxotungstate cluster had been obtained the product was reacted with EtPO²⁺, the

reaction gave a unchanged white powdery solid which showed no evidence for the attachment of any phosphonate groups when analysed by multinuclear NMR (^1H and ^{31}P) thus indicating that the product of the anion exchange was $(\text{NBu}_4)_4[\text{SiW}_{12}\text{O}_{40}]$.

Further attempts to exchange the cations were made using either 2M K_2CO_3 or 2M KOH to control the pH. The original reaction to form $[\text{PW}_9\text{O}_{34}]^{9-}$ uses K_2CO_3 which makes the pH rise to 9 before settling at ~ 8 , this being the pH where $[\text{PW}_9\text{O}_{34}]^{9-}$ is formed. The pH of either the NBu_4Br solution or $[\text{PW}_{11}\text{O}_{39}]^{9-}/[\text{PW}_9\text{O}_{34}]^{10-}$ solution is adjusted to pH 8, before addition of the second solution and readjustment of the pH to 8. However all attempts gave $[\text{PW}_{11}\text{O}_{39}]^{9-}$, an equilibrium existing in solution with the $[\text{PW}_9\text{O}_{34}]^{9-}$ anion being hard to isolate.



3.2.4.2. All in one pot $(\text{NBu}_4)_3[\text{PW}_9\text{O}_{34}(\text{EtPO})_3]$ preparation from EtPCl_2

As the method in the literature does not give the desired product the procedure was altered. An ‘all in one pot’ reaction was used so that the reaction with the EtPO^{2+} (which was prepared separately) and the cation exchange took place simultaneously. The reaction mixture was stirred for 1, 3 or 5 days (Compound 36).

^1H NMR. The spectrum shows the cation (NBu_4^+) signals and those due to the ethyl group. All are in the expected positions and the integration shows there to be approximately two EtPO groups per three cations, the ratio increasing over time, although the intensities of the ethyl groups are hard to determine due to overlap with the cation signals.

^{31}P NMR. The spectrum for the crystallized product exhibits two phosphorus environments. The first is due to the central phosphorus atom (PO_4) (-12.5) and the second due to

the EtPO group (32.0 ppm), the intensities of the two peaks being in an 1:4 ratio, showing there to be a larger quantity of phosphorus from the EtPO than expected. This is explained by the fact that the $[PW_9O_{34}]^{9-}$ unit could increase the relaxation time of the phosphorus atom in the centre and so making the peak size decrease, making comparison of the integrations meaning less. The position of the $[PW_9O_{34}]^{9-}$ peak does not indicate a fully saturated structure, it being in the same place as seen for the doubly derivatised product (Section 3.2.1).

IR Spectroscopy. Analysis of the product obtained after 24 hours shows the bands in the fingerprint region to be narrower than those for the sodium salt; a characteristic of NBu_4^+ salts. They are also shifted to higher wavelengths indicating increased saturation of the cluster, but differ from that of $(NBu_4)_3[PW_{11}O_{39}]$ proving that the polyoxotungstate cluster has not isomerized to the $[PW_{11}O_{39}]^{7-}$. After 3 and 5 days the position of the bands remain unchanged with the P-O bands becoming more pronounced indicating an increase in the ratio of phosphonate groups compared to the polyoxometalate cluster. The IR spectrum has bands in a similar position to the doubly derivatised cluster perhaps indicating that the product is also doubly functionalised, however only small shifts would be expected between this and the triply derivatised cluster.

Mass Spectroscopy. A Maldi-TOF MS was recorded on the product obtained after stirring for five days. It shows two peaks for the triply derivatised product $[PW_9O_{34}(EtPO)_3]^{3-}$ with either three or four NBu_4^+ cations, as well as two peaks which are 46 m/z units higher indicative of an extra two Na^+ ions being associated with the clusters.

Elemental Analysis. The results of CHN analysis for polyoxometalates are in general not very reliable so can not be used to determine structural purity. The differences in the expected percentages for the structure with either two or three EtPO groups is very small (C, 20.4 for $(NBu_4)_3[PW_9O_{34}(EtPO)_3]$ and C, 20.1 for $(NBu_4)_3H_2[PW_9O_{34}(EtPO)_2]$) and within the errors in

the results, therefore although the percentage found is closer to that for the doubly derivatised structure it can not be used to determine how many groups are on the cluster.

UV/vis Spectroscopy. The spectrum shows a peak with $\lambda_{\text{max}} = 258$ nm (Figure 3.43); this is a longer wavelength than seen for the related product obtained from reaction with ethylphosphonic acid (246 nm) and therefore indicates that the reaction has proceeded further and the cluster is more saturated. Although this indicates that the clusters are functionalised more than twice the wavelength does not correspond to the triply functionalised polyoxotungstate (265 nm) (Section 3.2.1), this points towards the product being a mixture of doubly and triply substituted clusters.

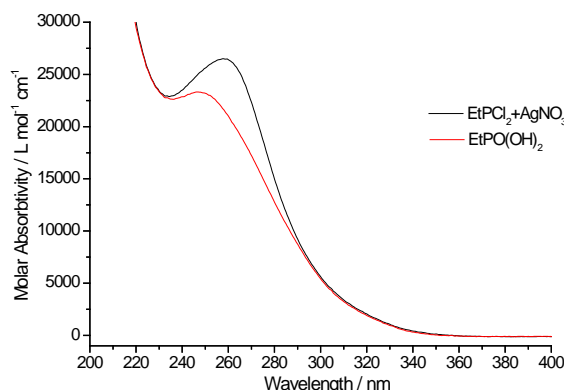


Figure 3.43. UV/vis spectra for $[PW_9O_{34}(EtPO)_{2/3}]^{n-}$.

Single Crystal X-ray Diffraction. Crystals were obtained by diffusion of diethyl ether into an acetonitrile solution, the crystals were poor quality and weakly diffracting so synchrotron data was obtained on Station 16.2 at the SRS facility at the CCLRC Daresbury Laboratory (Table 3.15). However the data was still of a poor quality so the structure solution is incomplete.

Table 3.15. Crystallographic Data for $(NBu_4)_3[PW_9O_{34}(EtPO)_3]$.

Monoclinic		Spacegroup		P a
Cell axes (Å)	$a = 19.1305(9)$	$b = 20.9327(10)$	$c = 23.4613(11)$	
Cell angles (deg)	$\alpha = 90.00$	$\beta = 100.853(4)$	$\gamma = 90.00$	
Cell Volume (Å ³)	9227.10(8)			
[Full details in appendix (Structure 20)]				

Crystals were obtained for the products after reaction for three or five days, the product obtained after three days was a mixture, some had similar unit cell parameters as above and all were not good quality. After five days the purity and quality of the crystals increases, with only one type of crystal being formed. However the quality is still not good and the structure refinement is incomplete so not all the clusters have the correct symmetry and it is hard to determine if there is disorder in some of the groups.

There are two clusters per asymmetric unit, these have α -symmetry, and consist of a central PO_4 tetrahedra surrounded by nine tungsten-oxygen octahedra (Figure 3.44). The six terminal oxygen atoms remaining in the vacant sites can all be seen along with evidence for phosphorus atoms bonding between two oxygen atoms which are part of edge-sharing octahedra. The first cluster has phosphorus atoms and evidence for the ethyl group in all three sites, refinement of the occupancy indicates that all these sites are fully occupied; the second cluster has two phosphorus atoms, with a vacant site still remaining. These two clusters indicate that some of the $[PW_9O_{34}]^{9-}$ anions have reacted three times and some twice, however due to the poor quality data the refinement of the occupancy can not be completely trusted. The two clusters are in close proximity, the surfaces to which EtPO groups are grafted facing one another and the groups on these surfaces being distorted by this proximity.

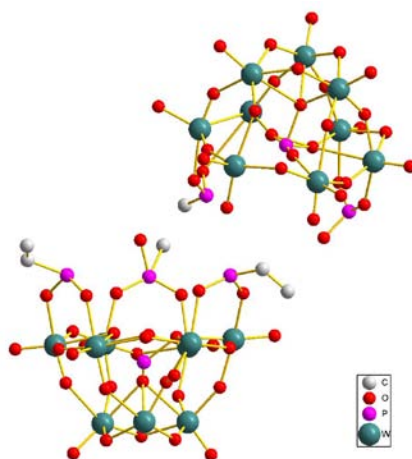


Figure 3.44. The two clusters within an asymmetric cell for the crystal structure of $[PW_9O_{34}(EtPO)_{2/3}]^{n-}$.

The anions are arranged in rows when viewed along the b -axis (Figure 3.45), with all the clusters within a row being the same and the adjacent row being of the other type of cluster.

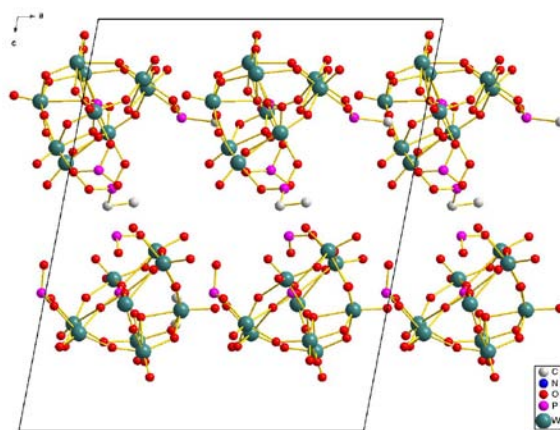


Figure 3.45. The structure of $(NBu_4)_3[PW_9O_{34}(EtPO)_{2/3}]$ showing only the anion clusters, viewed along the b -axis.

The results are not conclusive, the evidence suggesting that the $[PW_9O_{34}]^{9-}$ cluster can be triply derivatised using the electrophilic $EtPO^{2+}$ moiety created by the reaction of $EtPCl_2$ with $AgNO_3$. However this is difficult and a mixture of products is often formed.

3.2.4.3. $(NBu_4)_3H[SiW_9O_{34}(EtPO)_3]$ preparation from $EtPCl_2$

As the reaction for the $[PW_9O_{34}]^{9-}$ is not conclusive the same reaction will be attempted with the more reactive $[SiW_9O_{34}]^{10-}$ cluster (Compound 37) to confirm the greater reactivity of the $EtPO^{2+}$ group.

1H NMR. After stirring for 5 days the spectrum shows both the NBu_4^+ cation signals and those due to the $EtPO$ group, one of which is partially hidden by a cation signal. The integration of the ethyl peaks shows their intensities to be between that for two and three groups in a similar manner to the equivalent structure obtained from the reaction with ethylphosphonic acid.

^{31}P NMR. The spectrum shows two peaks due to the $EtPO$ group, the first at 29.9 ppm is in the same position as the peak for $[SiW_9O_{34}(EtPO)_3]^{4-}$ obtained from the ethylphosphonic acid. The second peak is at 34.4 ppm, this being similar to the peak seen for the $[PW_9O_{34}]^{9-}$ alternative. These two peaks have the same intensity and are both in a position that could show the $EtPO$ phosphorus. The ^{31}P NMR therefore indicates that two products are obtained, possibly different isomers (α or β) or clusters with different numbers of $EtPO$ groups grafted on to the structure.

IR Spectroscopy. The IR spectrum of the product shows the fingerprint region to differ from that for the product obtained by the reaction with ethylphosphonic acid with the peaks generally being broader, although the peak positions do not change much, suggesting that although the $[\alpha-SiW_9O_{34}(EtPO)_3]^{4-}$ is present it is not pure or crystalline.

Mass Spectrometry. The spectrum for the product shows the main peak to be due to $(NBu_4)_4[SiW_9O_{34}(EtPO)_3]^+$. There are also peaks indicating the presence of this anion with three or five cations, as well as small peaks due to the addition of Na^+ ions or the loss of an O_3PEt group (the extra oxygen atoms indicating that this is not due to a doubly derivatised anion).

Elemental Analysis. The CHN analysis is not accurate enough to determine the structure of the cluster. There is a large difference between the calculated and found percentages, so all that can be gathered is that there are approximately three NBu_4^+ cations per cluster.

UV/vis Spectroscopy. The spectrum obtained for the product shows λ_{\max} to be at 263.5 nm (Figure 3.46); although slightly lower than that for the ethylphosphonic acid product (266 nm) this position matches well with those for other fully saturated products (Section 3.2.1) and so confirms that the reaction has gone to completion.

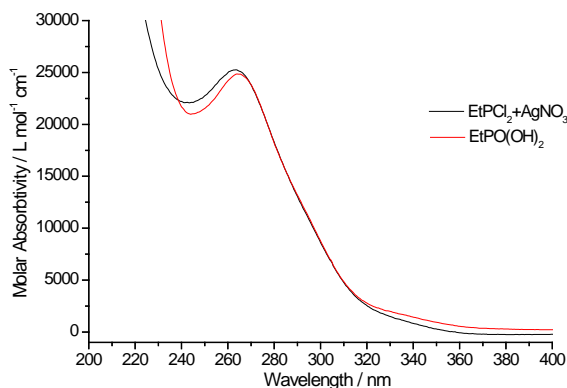


Figure 3.46. UV/vis spectra for $[SiW_9O_{34}(EtPO)_3]^{4-}$.

The results indicate that the reaction of the $EtPO^{2+}$ moiety with $[SiW_9O_{34}]^{10-}$ yields the triply functionalised $[SiW_9O_{34}(EtPO)_3]^{4-}$ anion. Although the ^{31}P NMR indicates that two different phosphorus environments are present, suggesting that the product may be a mixture of the α - and β -isomers. The reaction is not as clean as the alternative reaction with ethylphosphonic acid.

3.3. Conclusion

Triply substituted products have been obtained from the trivacant anions $[XW_9O_{34}]^{n-}$ ($X = Si$ or P). Reaction with the highly electrophilic organotrichlorosilanes gives products under mild

conditions at 0 °C. The less electrophilic organotriethoxysilane will react under these conditions with the addition of HCl which acts as a catalyst in the reaction. Reaction with organophosphonic acids is harder, the phosphonic acids not being as electrophilic, so the reaction requires promotion by the addition of catalytic HCl and heating in refluxing acetonitrile. This reaction only goes to completion when $X = \text{Si}$, with an excess of HCl and the reaction time being increased to 3 days. When $X = \text{P}$ the polyoxotungstate anion is less reactive and only gives a doubly functionalised product when reacting with the phosphonic acid. A more reactive 'EtPO²⁺' moiety was created by reaction of EtPCl₂ with AgNO₃, which allows the reaction to proceed further and although a triply derivatised product was obtained it was not pure.

Overall it is seen that when $X = \text{Si}$ the anion is more reactive due the higher charge of the anion in comparison to when $X = \text{P}$. The different reactivity of the group being added onto the cluster also makes a difference, with the reactivity in the order trichlorosilane > triethoxysilane > phosphonic acid. As the group becomes less electrophilic the reaction needs to be promoted by addition of HCl as a catalyst and increasing the temperature and time of the reaction.

3.4. References

1. G. Hervé and A. Tézé, *Inorg. Chem.*, **1977**, 16, 8, 2115.
2. A. Tézé and G. Hervé, *Inorg. Synth.*, **1990**, 27, 85.
3. S. Himeno, M. Takamoto and T. Ueda, *Bull. Chem. Soc. Jpn.*, **2005**, 78, 1463.
4. R. Contant, *Can. J. Chem.*, **1987**, 65, 568.
5. A. Mazeaud, N. Ammari, F. Robert and R. Thouvenot, *Angew. Chem. Int. Ed. Engl.*, **1996**, 35, 1961.
6. J. Niu, J. Zhao, J. Wang and M. Li, *J. Molec. Struct.*, **2003**, 655, 243.

7. N. Ammari, G. Hervé and R. Thouvenot, *New. J. Chem.*, **1991**, 15, 607.
8. A. Proust, R. Thouvenot and P. Gouzerh, *Chem. Commun.*, **2008**, 1837.
9. C. Mayer and R. Thouvenot, *J. Chem. Soc., Dalton Trans.*, **1998**, 7.
10. G. S. Kim, K. Hagen and C. Hill, *Inorg. Chem.*, **1992**, 31, 5316.
11. C. Mayer, P. Herson and R. Thouvenot, *Inorg. Chem.*, **1999**, 38, 6152.
12. Z. G. Sun, J. X. Li, Q. Liu and J. F. Liu, *Chinese Chem. Lett.*, **1999**, 10, 11, 971.
13. W.H. Knoth, P.J. Domaille, R.D. Farlee, *Organometallics*, **1985**, 4, 62.
14. R. Thouvenot, A. Tézé, R. Contant, G. Hervé. *Inorg. Chem.*, **1988**, 27, 524.
15. D.M. McDaniel, *Inorg. Chem.*, **1976**, 15, 3187.
16. M. T. Pope, *Heteropoly and Isopoly Oxometalates*, Springer-Verlag, Berlin, **1983**.
17. F. A. R. S. Couto, A. M. V. Cavaleiro, J. D. P. de Jesus and J. E. J. Simão, *Inorg. Chim. Acta*, **1998**, 281, 225.
18. J. E. Toth and F. C. Anson, *J. Electroanal. Chem.*, **1988**, 256, 361.

4. POLYMERISATION REACTIONS

Polyoxometalate materials have potential for use as acid and oxidation catalysts due to the high oxidation states of the metal atoms, the relative ease of reducing the clusters and the stability of the reduced species.^{1,2,3,4} The potential of kegglin polyoxometalates for use in catalysis can be further enhanced by immobilization to create heterogeneous systems with the practical advantage of the ease of separation of the catalyst from the reaction products. Various methods of immobilization have been reported, these include using inert supports such as chemically modified silica,^{5,6} mesoporous MCM-41,⁷ cationic nanoparticles⁸ or cationic polymers⁹ which interact with the polyoxometalate through electrostatic or coordination interactions.

Polyoxometalates functionalized with an organic group containing double bonds (C=C) have the potential for immobilization by covalently linking the clusters creating polymeric materials. Such materials have been studied in the literature, the first examples with polyoxometalates incorporated into the main chain of the polymer being produced by Judeinstein. The doubly functionalized polyoxometalate $[\text{SiW}_{11}\text{O}_{40}(\text{SiR})_2]$ (R = vinyl, allyl, methacryl or styryl) were reacted under free radical conditions to produce linear or branched and compact structures, the reactivity of the compounds increasing in the order R = vinyl (polymerisation yield 5 %) < allyl (20 %) < methacryl (65 %) < styryl (100 %).¹⁰

4.1. $[\text{SiW}_{10}\text{O}_{36}(\text{RPO})_2]^{4-}$

The polyoxotungstate units $[\text{SiW}_{10}\text{O}_{36}(\text{RPO})_2]^{4-}$ (R = $\text{H}_2\text{C}=\text{CH}$, $\text{H}_2\text{C}=\text{CHCH}_2$ or $\text{H}_2\text{C}=\text{CHC}_6\text{H}_4$) are doubly functionalised so they will react at both ends acting as cross-linkers between polymer chains and creating polymeric networks (Figure 4.1).¹¹

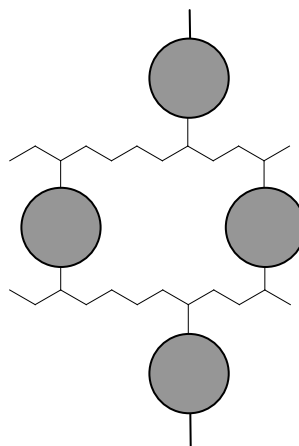


Figure 4.1. Representation of the cross-linking for the polymers obtained from clusters with two C=C groups.

Different solvents, initiators, temperatures and times will be investigated to find the optimum conditions for the reaction.

4.1.1. Solvent

The influence of solvent on the polymerisation was tested, the solubility of the polyoxotungstate clusters limiting the solvents available. Acetonitrile, 1,2-dichloroethane, DMF and DMSO were all used, all other conditions remaining constant during the reaction and using $(\text{NBu}_4)_3\text{K}[\gamma\text{-SiW}_{10}\text{O}_{36}(\text{C}_3\text{H}_5\text{PO})_2]$ to test the different solvents.

DMF/DMSO. The polyoxotungstate unit was heated in either DMF or DMSO with a radical initiator at temperatures between 50 and 110°C. Peaks appear in the ^{31}P NMR due to a phosphorus having lost its organic group, but still being attached to the polyoxotungstate unit (at 0 ppm with only tungsten-coupling) or having lost the double bond (at 20 ppm, only coupling to tungsten and the first CH_2 group in the H-coupled ^{31}P NMR). These show break up of the cluster, this being encouraged by increasing either the temperature or ratio of initiator.

Evidence for polymerisation was seen with DMF as the solvent; the product shows reduced intensities of the vinylic hydrogens in the ^1H NMR spectra and the appearance of peaks in the ^{31}P NMR with chemical shifts > 28 ppm (the same region as the ethylphosphonate group).

Blanks were run with no initiator (Figure 4.2), and showed a large number of peaks to be present; these peaks are attributed to solvent effects which causes the break down of the cluster. Solvent effects are also seen at a much slower rate when the sample is not heated.

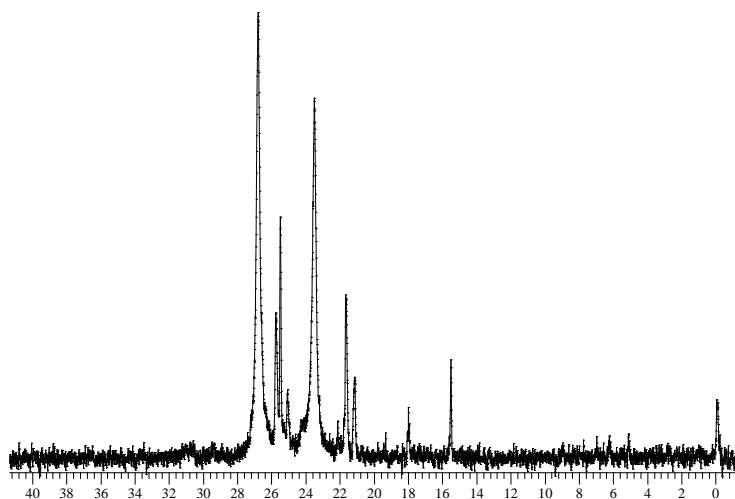


Figure 4.2. ^{31}P NMR Spectrum for $(\text{NBu}_4)_3\text{H}[\text{SiW}_{10}\text{O}_{36}(\text{H}_2\text{C}=\text{CHCH}_2\text{PO})_2]$ after heating at 70°C for 48 hours, in dry DMF (Blank).

In place of the main peak at 24.4 ppm two broad peaks are seen at 26.9 and 23.5 ppm, as well as other peaks between 15-28 ppm, showing a large number of different phosphorus environments. The broadening of the peaks indicates that the species is less mobile and the shifts show changes in the environment or bond order of the phosphorus bonds. Possible explanations are:

1. Gain or loss of H^+ ions H-bonding to the $\text{P}=\text{O}$'s affecting its bond strength;
2. H-bonding of oxygen in the cluster to water strengthening the $\text{P}-\text{C}$ bond;
3. Partial hydrolysis of one of the bridging organophosphoryl groups (Figure 4.3).¹²

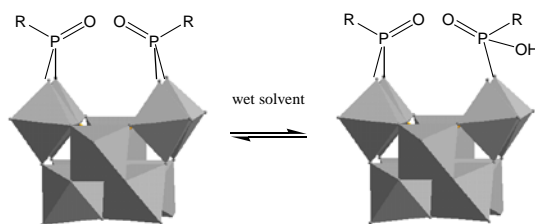


Figure 4.3. Representation of the hydrolysis of $[\gamma\text{-SiW}_{10}\text{O}_{36}(\text{C}_3\text{H}_5\text{PO})_2]^{4-}$ as might happen in wet solvent.

4. Coordination of polar solvent molecules making the anion larger and less mobile.

Acetonitrile/1,2-dichloroethane. The polyoxotungstate unit appears more stable when using these solvents, with no solvent effects being seen when heating without initiator, this means that any changes seen in the NMR after the reaction will be purely due to the products formed.

When $(\text{NBu}_4)_3\text{H}[\text{SiW}_{10}\text{O}_{36}(\text{H}_2\text{C}=\text{CHCH}_2\text{PO})_2]$ is heated in solvent with an initiator the maximum temperature used is 80 °C (boiling points: MeCN = 82 °C, 1,2-dce = 84 °C), at this temperature *t*BuPO has a very long half life (~20 days in benzene¹³) so no reaction occurs, the NMR spectra remaining unchanged. Using initiators with lower activation temperatures (AIBN (half life ~7 hours at 70 °C) and POB (half life ~9 hours at 78 °C¹³) produces a reaction. This is shown in the ¹H NMR spectra by reduction in the intensity of the allyl peaks in relation to those for the cations; any new peaks formed are not observed as they will be hidden under the cation peaks. The reduction of these peaks is relatively large (68 % for the reaction at 70 °C and 76 % at 80 °C using POB) although comparing the intensities with the cation signals is not very accurate.

The solubility of both the monomer and polymer is better in acetonitrile than 1,2-dce; although the monomer does dissolve reasonably well in 1,2-dce the polymer does not dissolve so easily. The monomer needs to be in solution to react, but a difference in the solubility between

the monomer and product could allow for a means of separation of the different species so potentially giving 1,2-dce an advantage, therefore 1,2-dce will be used as the solvent.

4.1.2. Initiator

The polymerisations are carried out using free radical reactions, this method being chosen because it uses mild conditions, is easy to perform and usually shows substantial reproducibility.¹⁴ Three different thermal initiators were tested, AIBN (2,2'-azobis(2-methylpropionitrile), POB (benzoyl peroxide) and *t*-BuPO (*tert*-butyl peroxide), the ¹H NMR spectra being used to estimate the extent of polymerisation by comparison of the heights of the allyl peaks with those due to the cations, assuming there to be three cations present per cluster.

The initiators were tested at a variety of temperatures and with the four solvents discussed previously (Section 4.1.1), the best results being compared (Table 4.1).

Table 4.1. The best results for polymerisation of $[\text{SiW}_{10}\text{O}_{36}(\text{H}_2\text{C}=\text{CHCH}_2\text{PO})_2]^{4-}$ using different initiators.

Initiator	Solvent	Temperature/°C	Polymerisation/%	Impurities/%
<i>t</i> BuPO	DMF	75	25	16
POB	DMF	90	28	24
AIBN	Acetonitrile / 1,2-dce	75	56	15

Impurities measured by ³¹P NMR.

The amount of polymerisation observed is greatest for the initiator AIBN (56 %) showing that this is the best initiator and this also produced the least impurities (estimated from the intensity of any extra peaks in the ³¹P NMR). The initiators *t*BuPO and POB give a smaller quantity of polymeric product, POB also giving a large quantity of impurities.

Varying the ratio of initiator to monomer used in the reaction had little effect as long as the ratio was at least 2× that of the monomer.

4.1.3. Temperature

The temperature will influence the rate of the reaction, proceeding quicker at higher temperatures as the half life of the initiator will be shorter, but the polyoxotungstate unit being more stable at lower temperatures. The temperature selected for the reaction is limited by the solvent, the boiling point of 1,2-dce being 84 °C, therefore the temperature selected was 80 °C.

4.1.4. Time

Keeping the conditions the same (1,2-dichloroethane, AIBN (2,2'-azobis(2-methylpropionitrile), 80 °C, under N₂) the effect of the time was investigated for each of the three different functionalised polyoxotungstate species (NBu₄)₃H[SiW₁₀O₃₆(RPO)₂] (R = H₂C=CH, H₂C=CHCH₂ or H₂C=CHC₆H₄).

¹H NMR. The extent of polymerisation can be estimated from analysis of the ¹H NMR spectra. Comparison of the integrals for the ¹H resonances due to the remaining vinylic protons with those for the NBu₄⁺ cations and where appropriate, any unreactive groups in the organic functionality (C₆H₄). For all three examples the vinylic hydrogen peaks initially reduce in intensity as the time increases, this reduction eventually leveling off when the maximum polymerisation possible for that compound is reached. Looking at the spectra for the polymerisation of the styryl-derivatised polyoxometalate [SiW₁₀O₃₆(H₂C=CHC₆H₄PO)₂]⁴⁻ (Figure 4.4) the extent of polymerisation increases quickly over the first 10 hours, before the rate of increase in polymerisation slows, this example being easier to see as the C₆H₄ ring peak intensities can be used as a reference.

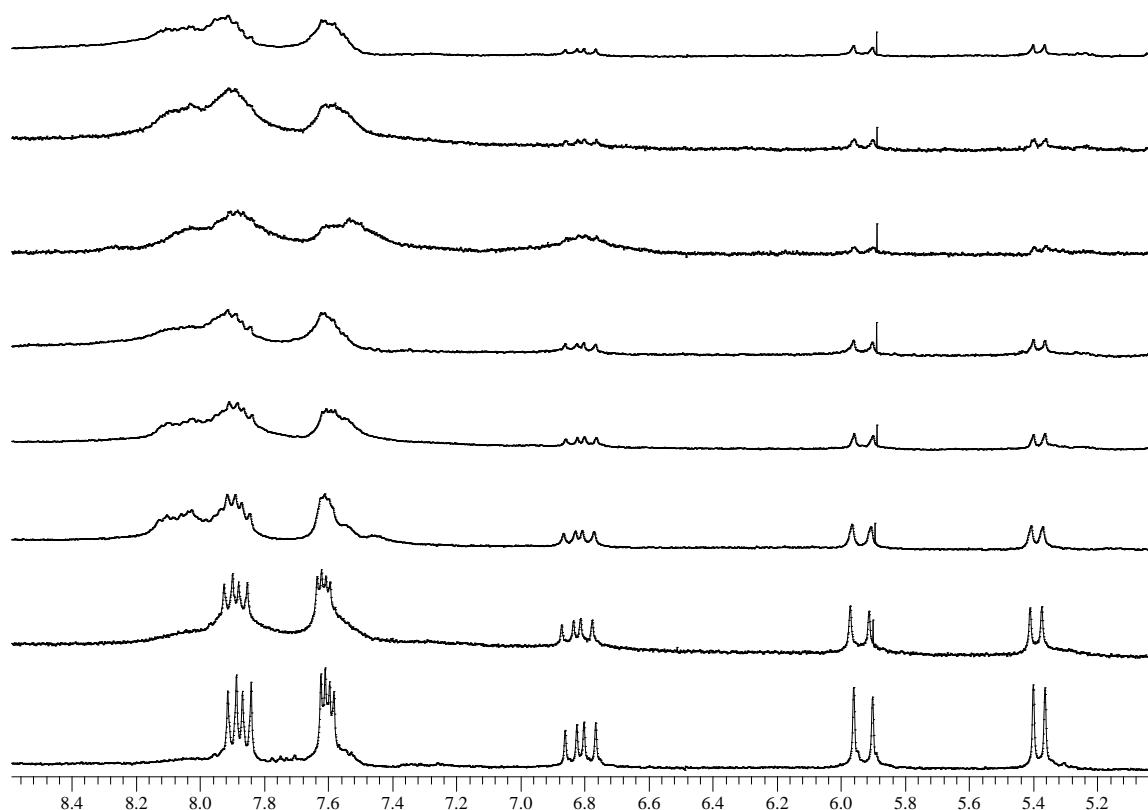


Figure 4.4. The ^1H NMR spectra showing the functional group peaks for $(\text{NBu}_4)_3\text{H}[\text{SiW}_{10}\text{O}_{36}(\text{H}_2\text{C}=\text{CHC}_6\text{H}_4\text{PO})_2]$ (5.35 ($\text{H}_2\text{C}=\text{CH}$), 5.95 ($\text{H}_2\text{C}=\text{CH}$), 6.74-6.88 ($\text{H}_2\text{C}=\text{CH}$), 7.55-7.96 (C_6H_4)); polymerisation time (from bottom to top) $t = 0, 2, 4, 6, 8, 24, 48$ and 72 hours.

The maximum degree of polymerisation achieved and the time to reach this goal is dependent on the functional group ($(\text{H}_2\text{C}=\text{CH})$ $t \sim 72$ hours; $(\text{H}_2\text{C}=\text{CHCH}_2)$ $t \sim 30$ hours; $(\text{H}_2\text{C}=\text{CHC}_6\text{H}_4)$ $t \sim 20$ hours) (Figure 4.5, Table 4.2). The exponential decay in reaction rate is due to the concentration of reactive double bonds ($\text{C}=\text{C}$) reducing over time, making a reaction less likely. Also, the polymers formed are of a larger size and so the mobility of the species in solution is reduced, making interaction between a propagation site and an unreacted monomer, and subsequent reaction, less likely.

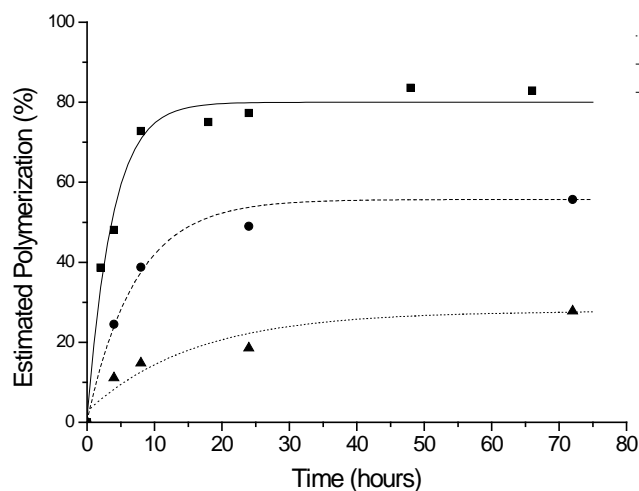


Figure 4.5. The extent of polymerisation over time for $(\text{NBu}_4)_3\text{H}[\text{SiW}_{10}\text{O}_{36}(\text{RPO})_2]$ ($\text{R} = \text{C}_2\text{H}_3$, C_3H_5 or $\text{C}_2\text{H}_3\text{C}_6\text{H}_4$) estimated from ^1H NMR.

Table 4.2. The maximum degree of polymerisation (%).

R group	Percentage Polymerisation / % ^(a)
Vinyl	28
Allyl	56
Styryl	80

(a) Estimated from the intensities of vinylic hydrogen resonances compared to the hydrogen intensities for unreactive groups on the ^1H NMR Spectra

The ^1H NMR spectra also show that as the polymerisation proceeds the resonances due to the protons in the aromatic ring broaden and all fine-structure is lost; this is due to the rings being constrained within the polymeric species and so becoming less mobile and moving slowly on the NMR timescale compared with the original monomer species.

Polymerisation increases in the order $\text{H}_2\text{C}=\text{CH} < \text{H}_2\text{C}=\text{CHCH}_2 < \text{H}_2\text{C}=\text{CHC}_6\text{H}_4$, due partly to the increased size of the organic functional group, which increases the distance between the polymerisable double bonds and the polyoxotungstate species, resulting in the steric factors

and repulsive interactions between the large, negatively charged polyoxotungstate units becoming less important because they do not need to come as close together to react. In addition to this, the styryl group contains an aromatic ring conjugated with the vinyl group which activates the double bond.

As the product contains some unreacted starting material purification is needed. The difference in solubility of the monomer and polymer can be used to purify the product, but a small quantity of double bonds are still present. These will be due to either units which have only reacted at one end or which have not reacted at either end, but have become trapped in the polymeric network. Further purification will be attempted, this will again use the solubility of the monomer species compared to the polymer. As monomer species is slightly soluble in methanol whereas the polymer is not, dissolving the product in acetonitrile and then adding a large quantity of methanol will precipitate out the polymer product while leaving the monomer in solution. ^1H NMR of the product after this procedure shows the peaks due to the vinylic hydrogen atoms to have reduced (from 0.4 to 0.1) and the C_6H_4 ring peaks to have changed shape (Figure 4.6), this shows that most of the unreacted groups were due to monomer species where the units had not reacted at either end. The small number of remaining vinylic hydrogen atoms are likely to be due to units where only one end has reacted, ~95 % of the phenyl rings are estimated as being part of the polymer in the purified product.

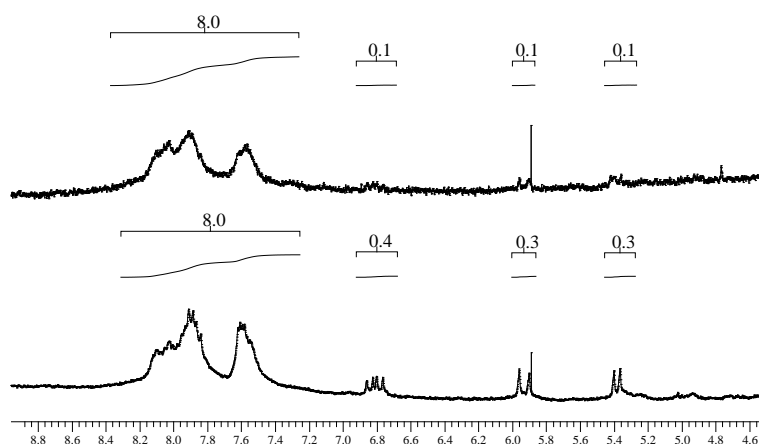


Figure 4.6. ^1H NMR Spectra for the product (bottom) and after stirring in methanol overnight (above).

^{31}P NMR. Upon polymerisation the peak in the ^{31}P NMR spectrum for the vinyl phosphonate would be expected to shift, as the functional group directly bound to the phosphorus becomes saturated. However no change is seen in the spectra, only one peak being seen and this peak remaining in the same position as for the unpolymerized monomer species, indicating that a reaction has not taken place. However, it should be noted that the maximum polymerisation observed by ^1H NMR was only 28 %, and any new peak in the ^{31}P NMR spectrum due to the polymer would be expected to be broad due to lack of free mobility and so may be difficult to see against the background if only small.

When $\text{R} = \text{H}_2\text{C}=\text{CHCH}_2$, the ^{31}P NMR of the polymerized product shows an intense peak at 24.5 ppm, which is due to the unreacted monomer species. The spectrum also shows a number of small peaks which have tungsten satellite peaks associated with them, indicating that some of the functional groups have reacted in different ways (exo- or endo- polymerisation across the double bond). The combined intensity of these peaks is *ca.* 25 % of the total phosphorus intensity giving a lower estimation of the degree of polymerisation to that given by the ^1H NMR. However, the main peak (24.5 ppm) is less symmetrical under hydrogen-coupled conditions so

could therefore be due to two signals; one from the unreacted monomer and one from a polymer, this would increase the estimated polymerisation.

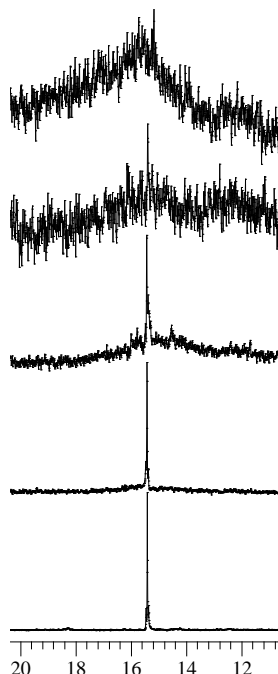


Figure 4.7. ^{31}P NMR Spectra for $[\text{SiW}_{10}\text{O}_{36}(\text{H}_2\text{C}=\text{CHC}_6\text{H}_4\text{PO})_2]^{4-}$ showing the broadening of the signal after polymerisation, (from bottom to top) $t = 0, 4, 8, 24$ and 48 hours.

When $\text{R} = \text{H}_2\text{C}=\text{CHC}_6\text{H}_4$, the position of the peak in the ^{31}P NMR spectrum does not shift (Figure 4.7), as the phosphorus is remote from the double bond so its local environment remains unchanged. However, this peak which was originally sharp with easily distinguished tungsten satellite peaks in the monomer species, becomes increasingly broader and loses any fine structure as the polymerisation proceeds (Figure 4.7). This change can be attributed to reduced mobility of the polymeric product which increases the relaxation time of the phosphorus atom¹⁰ compared to the NMR timescale like was also seen for the C_6H_4 signals in the ^1H NMR spectra.

IR Spectroscopy. The spectra show little change from those for the monomer species for all three R groups, the fingerprint region remaining unchanged indicating that the $[\gamma\text{-SiW}_{10}\text{O}_{36}]^{8-}$ subunit is intact, its structure not being altered by the polymerisation reaction. The weak peak at

$\sim 1600\text{ cm}^{-1}$ attributable to the C=C double bond has reduced, showing that polymerisation has occurred.

UV/vis Spectroscopy. The polymerisation of $[\text{SiW}_{10}\text{O}_{36}(\text{H}_2\text{C}=\text{CHC}_6\text{H}_4\text{PO})_2]^{4-}$ can also be followed by UV/vis spectroscopy. The conjugated styryl group gives rise to an absorption at $\lambda_{\text{max}} = 258\text{ nm}$, the intensity of which decreases as the reaction takes place on account of the reduced conjugation of the aromatic ring (Note that a peak due to the phenyl group occurs at a lower wavelength so cannot be seen due to the larger $\text{SiW}_{10}\text{O}_{36}$ peak and the range limits of the spectrometer) (Figure 4.8).

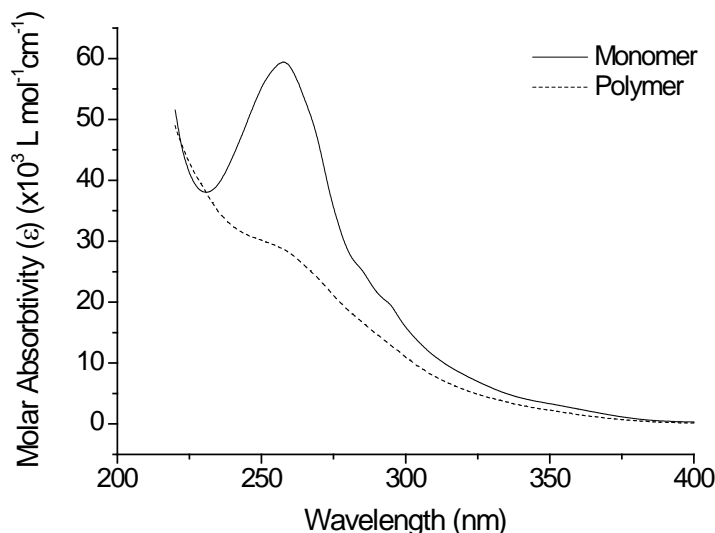


Figure 4.8. UV spectra for $[\text{SiW}_{10}\text{O}_{36}(\text{H}_2\text{C}=\text{CHC}_6\text{H}_4\text{PO})_2]^{4-}$ and the polymer formed from it after 24 hours.

Mass Spectrometry. The Maldi-TOF mass spectrum for the polymer after reaction for 24 hours is more complex than that obtained for the monomer species. Signals are seen due to one polyoxotungstate unit at 3300-5000 m/z and a much less intense (400 compared with 5200 a.i.) signal at 7000-8100 m/z due to two joined polyoxotungstate units. There are significant changes in the 3300-5000 m/z region when comparing it to the original monomer species $(\text{NBu}_4)_3\text{H}[\text{SiW}_{10}\text{O}_{36}(\text{H}_2\text{C}=\text{CHC}_6\text{H}_4\text{PO})_2]$. The mass spectrum for the original species had one

main signal (3687 m/z) and a few small signals, however the polymer has a large intense region with numerous signals. The assignments for the major signals in the region 3300-5000 m/z show the addition of cations to the species, as is often seen in the mass spectra of the polyoxotungstate compounds. The peaks also show either loss of a functional group (RPO, RO or R) or addition of a vinylic (H_2CCH) group, both these observations could indicate polymerisation as the functional groups on two polyoxotungstate units will be linked and it could be easier for the polymer to break at the polyoxotungstate when ionised for mass spectrometry.

Electrochemistry. Cyclic voltammetry was carried out on the product of the $[\text{SiW}_{10}\text{O}_{36}(\text{H}_2\text{C}=\text{CHC}_6\text{H}_4\text{PO})_2]^{4-}$ polymerisation (after reaction for 24 hours), using the same method as for the monomer, but with an Ag/AgCl reference electrode, ferrocene was used as an internal reference, the results being calibrated by setting the ferrocene peak potential to be 0 V (Figure 4.9). Reaction of the styryl group to give a polymeric species did not effect the position of the three reduction potentials in the cyclic voltammogram (Table 4.3) showing that the polyoxotungstate unit remains intact therefore retaining its electrochemical properties.

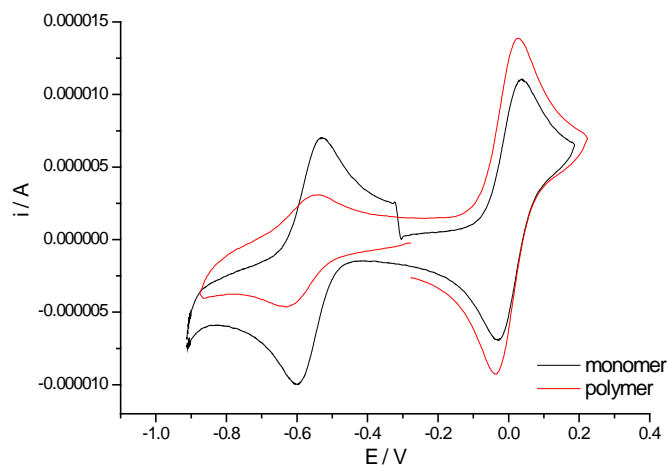


Figure 4.9. Cyclic Voltammograms of a 1.0 mM solution of $[\text{SiW}_{10}\text{O}_{36}(\text{H}_2\text{C}=\text{CHC}_6\text{H}_4\text{PO})_2]^{4-}$ and a 0.5 mM solution of its polymer formed after reaction for 24 hours, at a glassy carbon electrode, with ferrocene as an internal reference and 0.1 M Bu_4NBF_4 as supporting electrolyte. Scan rate 100 mV/s.

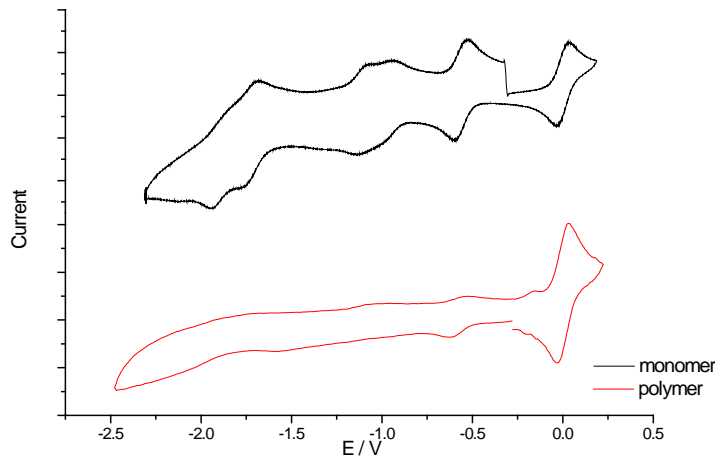


Figure 4.10. Cyclic Voltammograms of a 1.0 mM solution of $(\text{NBu}_4)_3\text{H}[\text{SiW}_{10}\text{O}_{36}(\text{H}_2\text{C}=\text{CHC}_6\text{H}_4\text{PO})_2]$ and a 0.5 mM solution of its polymer, at a glassy carbon electrode, with ferrocene as an internal reference and 0.1 M Bu_4NBF_4 as supporting electrolyte. Scan rate 100 mV/s.

Table 4.3. The reduction potentials for $(\text{NBu}_4)_3\text{H}[\text{SiW}_{10}\text{O}_{36}(\text{H}_2\text{C}=\text{CHC}_6\text{H}_4\text{PO})_2]$ and the polymer formed from it after reaction for 24 hrs (referenced to ferrocene).

	E(1) (mV)	E(2) (mV)	E(3) (mV)
Monomer	-560	-1119	-1869
Polymer	-575	-1097	-1920

Although the reduction potentials do not change on polymerisation, changes are observed due to the reduced solubility of the polymeric species caused by its increased size, these changes result in smaller, broader and less reversible peaks compared to those observed for the monomer, but are still characteristic of the polyoxotungstate structure (Figure 4.10).¹⁰

Cyclic Voltammetry was not carried out on the products obtained by polymerisation of $[\text{SiW}_{10}\text{O}_{36}(\text{RPO})_2]^{4-}$ ($\text{R} = \text{H}_2\text{C}=\text{CH}$ or $\text{H}_2\text{C}=\text{CHCH}_2$) as a large percentage of monomer remained present, this being hard to fully remove and therefore any peaks present could be due to the monomer species as well as the polymer.

4.1.5. Co-polymerisation of $[\text{SiW}_{10}\text{O}_{36}(\text{H}_2\text{C}=\text{CHC}_6\text{H}_4\text{PO})_2]^{4-}$

Using the styrylphosphonate functionalised polyoxometalate $[\text{SiW}_{10}\text{O}_{36}(\text{H}_2\text{C}=\text{CHC}_6\text{H}_4\text{PO})_2]^{4-}$, which was the easiest to polymerise along with a second monomer species (styrene, acrylic acid, acrylamide, ethyl acrylate or methyl methacrylate) allowed a co-polymerisation reaction to be carried out. Co-polymerisation should be easier than reaction of the single monomer species so hopefully giving a greater yield of polymer.

Co-polymers containing the polyoxotungstate $[\text{SiW}_{10}\text{O}_{36}]$ have been prepared previously in the literature from $[\text{SiW}_{10}\text{O}_{36}(\text{H}_2\text{C}=\text{CH}(\text{Me})\text{C}(\text{O})\text{OPrSi})_2\text{O}]^{4-}$ creating networks where the polyoxometalate units act as cross-linkers between ethyl methacrylate polymer chains.^{15,16}

Recently Dawson polyoxometalates derivatised with an organosilyl group to give $[\alpha_2\text{-P}_2\text{W}_{17}\text{O}_{61}\{\text{CH}_2=\text{C}(\text{CH}_3)\text{COO}(\text{CH}_2)_3\text{Si}\}_2\text{O}]^{6-}$ have been co-polymerized with methyl methacrylate to produce polymers that are cross-linked by the polyoxometalate species.¹⁷

The co-polymers produced would have differing properties (e.g. density, degree of cross-linking, solubility) both on account of the different distribution of polyoxotungstate units (controlled by the polyoxometalate:co-monomer ratio) and the properties of the individual co-monomer used. Such co-polymerisations represent a way to introducing further functionality to the system and fine-tuning of the properties towards desired applications.

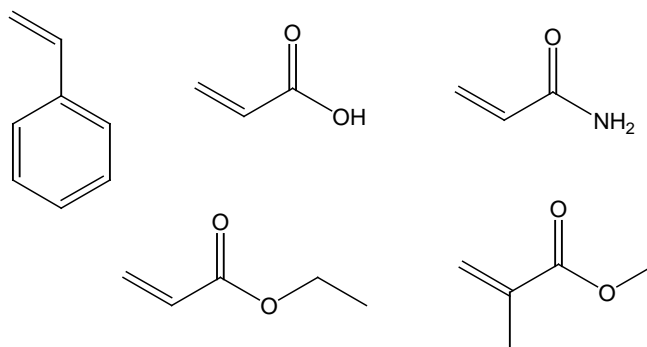


Figure 4.11. Co-monomers; styrene, acrylic acid, acrylamide, ethyl acrylate and methyl methacrylate.

The polymerisation conditions were kept the same as when using only $[\text{SiW}_{10}\text{O}_{36}(\text{H}_2\text{C}=\text{CHC}_6\text{H}_4\text{PO})_2]^{4-}$ (1,2-dichloroethane, AIBN, 80°C), but with the addition of a second monomer species (Figure 4.11) in varying ratios (where the ratio is expressed as moles of $[\text{SiW}_{10}\text{O}_{36}(\text{H}_2\text{C}=\text{CHC}_6\text{H}_4\text{PO})_2]^{4-}$:moles of co-monomer). The time for the reaction was fixed at 24 hours, selected as this was the time at which the polyoxotungstate monomer had reached the maximum polymerisation (Section 4.1).

^1H NMR. The ^1H NMR spectra were used to determine the polymerisation by comparison of the vinylic hydrogen signals with those due to the aromatic ring (Figure 4.12).

Co-polymerisation with styrene will produce polystyrene chains cross-linked with the polyoxotungstate units, using a small quantity of styrene gives only limited polymerisation, increasing the quantity increases the polymerisation (maximum of 60 % for ratio 1:6), however the solubility of the product decreases making analysis difficult when the ratio is >1:6. The peaks for both the functional groups on $[\text{SiW}_{10}\text{O}_{36}(\text{H}_2\text{C}=\text{CHC}_6\text{H}_4\text{PO})_2]^{4-}$ and the styrene co-monomer appear in similar positions making the analysis inaccurate.

When the co-monomer is either acrylic acid, acrylamide or ethyl acrylate the estimated percentage of polymerisation decreases when a small quantity (1:2) of co-monomer is present, in comparison to when none is present, although complete polymerisation of the smaller co-monomer is seen. As the quantity of co-monomer increases the polymerisation increases, until it is comparable with (or greater than) that of the polyoxotungstate species alone (the ratio when this is achieved is dependent on the co-monomer used). The initial reduction in polymerisation yield could be due to competition between the two monomer species, with the smaller co-monomer reacting more easily on steric grounds, however when the quantity of co-monomer increases there is a greater probability of the double bonds on the polyoxotungstate units coming

into contact and reacting with co-monomer radicals. Also the polyoxotungstate units do not need to be as close together as the degree of cross-linking will reduce, making any steric factors that might have hindered the reaction less important.

When methyl methacrylate is the co-polymer no decrease in polymerisation is seen when a small quantity of co-monomer is used, the polymerisation remaining similar to when no co-monomer was present. It then rises as the ratio of methyl methacrylate increases.

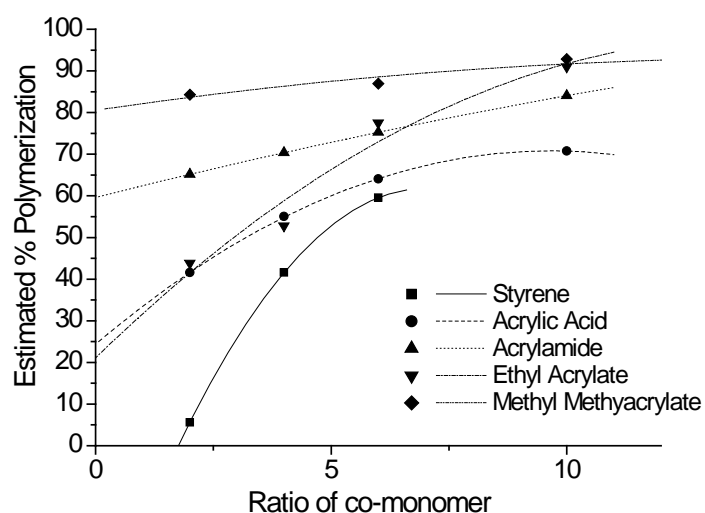


Figure 4.12. The extent of polymerisation estimated from ^1H NMR spectra for varying ratio's of co-monomer, where a higher ratio indicates a larger quantity of co-monomer in comparison to that of $[\text{SiW}_{10}\text{O}_{36}(\text{H}_2\text{C}=\text{CHC}_6\text{H}_4\text{PO})_2]^{4-}$.

The ^1H NMR spectra not only show reduction of the vinylic hydrogen peaks, but also broadening and loss of detail of the aromatic ring peaks, due to the reduced mobility of the groups once in the larger polymeric species (Figure 4.13).

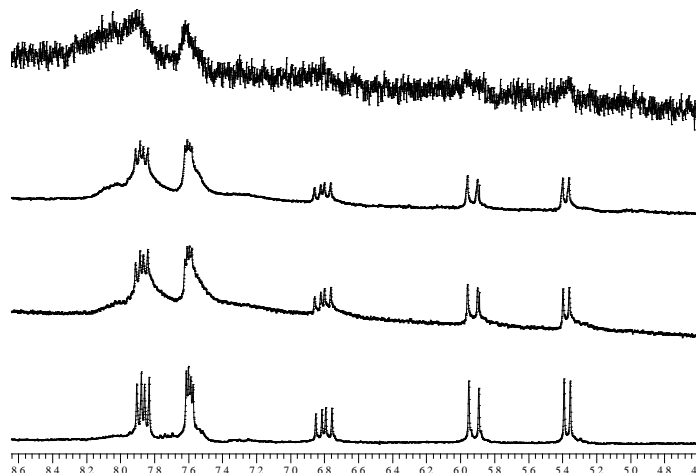


Figure 4.13. The ^1H NMR spectra showing the styryl functional group peaks for the co-polymerisation with ethyl acrylate. From bottom to top the spectra are for $[\text{SiW}_{10}\text{O}_{36}(\text{H}_2\text{C}=\text{CHC}_6\text{H}_4\text{PO}_2)_2]^{4-}$ and the polymers obtained after 24 hours with ethyl acrylate ratios of 1:2, 1:4 and 1:6.

The solubility of the polymeric product reduces as the quantity of co-monomer increases, because the chain lengths increase producing larger species which are more difficult to dissolve. The co-monomer also effects the solubility, acrylic acid, acrylamide, ethyl acrylate and methyl methacrylate all containing a carbonyl group and either an oxygen or nitrogen atom, which can interact with solvent molecules helping with the solubility of the products. The styrene co-polymers are less soluble as the polymer chains interact less strongly with the solvent molecules.

^{31}P NMR. Due to the reduced solubility of the products ^{31}P NMR could not be performed on most of the polymers. However, swelling was observed for some products (most significantly when the co-monomer was methyl methacrylate); this property allowed for ^{31}P NMR analysis to be carried out on the gels produced. The spectra show a broad signal due to the reduced mobility of the polyoxometalate species which is trapped in the polymeric gel and can not move freely (Figure 4.14).

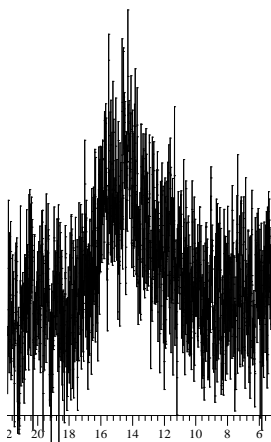


Figure 4.14. The ^{31}P NMR spectra for $(\text{NBu}_4)_3\text{H}[\text{SiW}_{10}\text{O}_{36}(\text{H}_2\text{C}=\text{CHC}_6\text{H}_4\text{PO})_2]$ co-polymerised with methyl methacrylate (1:10).

IR Spectroscopy. The spectra for all co-polymers show the fingerprint region to be unchanged, confirming that the polyoxotungstate unit is not affected by the reaction conditions and remains intact. The weak $\text{C}=\text{C}$ peak at $\sim 1601\text{ cm}^{-1}$, reduces in intensity as the amount of co-monomer present increases showing an increase in the polymerisation. The co-monomers acrylic acid, acrylamide, ethyl acrylate and methyl methacrylate all contain carbonyl groups, occurring at 1718 , 1670 , 1728 and 1734 cm^{-1} respectively, the intensity of these peaks increasing as the amount of the appropriate co-monomer increases.

UV/vis Spectroscopy. UV/vis spectroscopy can be used to monitor the reaction, the peak due to the styryl group (258 nm) reducing in intensity as the double bond reacts and the quantity of styryl present reduces. As the quantity of co-monomer increases the peak due to the styryl group reduces, this indicates a greater degree of polymerisation for these compounds, so showing that a larger quantity of co-monomer increases the extent of the reaction (Figure 4.15).

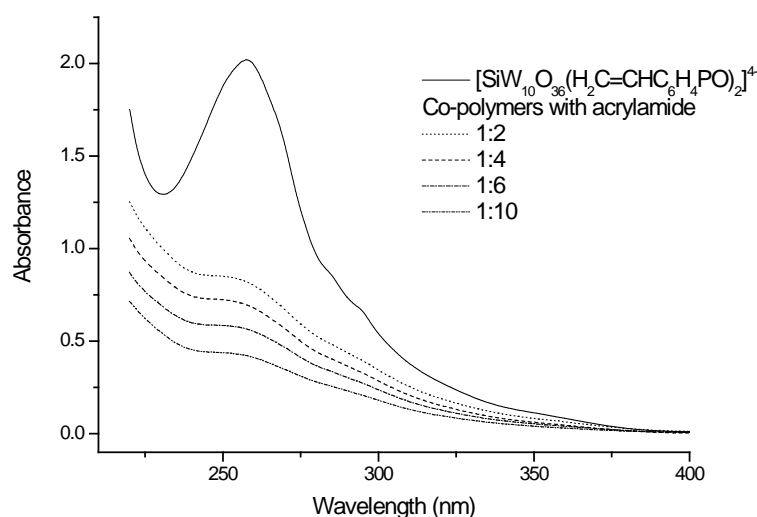


Figure 4.15. The UV spectra showing the peak due to the styryl group for $[\text{SiW}_{10}\text{O}_{36}(\text{H}_2\text{C}=\text{CHC}_6\text{H}_4\text{PO})_2]^{4-}$ before and after co-polymerisation with acrylamide (ratio's of $[\text{SiW}_{10}\text{O}_{36}(\text{H}_2\text{C}=\text{CHC}_6\text{H}_4\text{PO})_2]^{4-}$:acrylamide of (1:x)).

Mass Spectrometry. Maldi-TOF MS was carried out on some of the products, however problems with solubility and ionization meant that long chain polymers can not be seen. Mostly short fragments containing one polyoxotungstate unit with varying numbers of co-polymer groups attached are observed.

For example, the spectra for the styrene co-polymers show peaks in the regions 3400-5000 m/z and 6900-8000 m/z, with no significant signals observed at higher m/z values. Between 3400-5000 m/z the peaks are similar for all styrene ratio's, due to one polyoxotungstate unit with four or five cations. As the ratio increases other peaks become more significant, these peaks being assigned to the polyoxotungstate unit with extra styrene groups attached. In the region 6900-8000 m/z the peaks are much less intense and these peaks can be assigned to two joined polyoxotungstate units.

Elemental Analysis. The results give a guide to the ratio of polyoxotungstate:co-monomer in the product. As the ratio of co-monomer increases the percentages of carbon and hydrogen increase and the percentage of nitrogen decreases (except when using acrylamide)

(Table 4.4), this agrees with the trends expected however much smaller increases are seen than would be expected indicating smaller ratio's of co-monomer in the product to that initially put into the reaction.

Table 4.4. The observed and calculated elemental analysis results for co-polymers made with methyl methacrylate.

Initial	Observed (%)			Calculated	Calculated (%)		
Ratio	N	C	H	Ratio	N	C	H
1:0	1.5	21.9	3.7	1:0	1.2	22.1	3.5
1:2	1.3	23.9	3.8	1:1.75	1.15	23.9	3.8
1:6	1.2	24.4	3.7	1:2.25	1.1	24.4	3.9
1:10	0.95	25.8	3.9	1:3.70	1.1	25.8	4.1

Swelling Properties: Swelling of the products was observed for some materials on the addition of solvent. The amount of swelling being estimated by weight using a method similar to that used by Mayer and Thouvenot,¹⁵ the swelling index (I_{sw}) at the swelling equilibrium was calculated using the equation:

$$I_{sw} \text{ (g/g)} = (\text{wet weight} - \text{dry weight}) / \text{dry weight}$$

The wet weight is obtained by swelling the dry gel in an excess of solvent, removing the remaining solvent and weighing the product. The swelling index corresponds to the weight of solvent the dry material absorbs and is expressed in grams of solvent per grams of dry gel.

The amount of swelling was influenced by the composition of the material, with either the co-monomer species or ratio of polyoxometalate to co-monomer having an effect.

The affect of the different co-monomers (styrene, acrylic acid, acrylamide, ethyl acrylate or methyl methacrylate) was investigated; all the materials had an initial ratio of moles of

polyoxotungstate to moles of co-monomer of 1:10. The swelling index (I_{sw}) is dependent on the functional group in the co-monomer and the interaction of that group with the solvent molecules (Table 4.5).

Table 4.5. The Swelling Index calculated for co-polymers made from various different co-monomer units (initial ratio (1:10))

Co-Monomer	Swelling Index (I_{sw})(g/g)		
	Acetonitrile	1,2-dichloroethane	DMF
Styrene	2.47	1.87	3.87
Methyl Methacrylate	2.44	0.75	4.23
Ethyl Acrylate	1.03	0.76	1.06
Acrylic Acid	0.45	0.02	0.51
Acrylamide	0.76	0.47	0.78

The small quantity of swelling observed for the acrylic acid and acrylamide co-polymers shows that strong hydrogen-bonding interactions hold these polymer chains together. Although the initial ratio of polyoxotungstate to co-monomer (1:10) does not allow for a large amount of ordering and crystalline regions are unlikely to form, hydrogen-bonding interactions between polymer chains or between the polymer chains and the oxygen atoms on the polyoxotungstate unit could exist. These interactions are more favourable than interactions with the solvents and so only limited swelling is observed. The hydrogen-bond strength is greatest for O-H...O interactions and so the acrylic acid co-polymer having the smallest swelling index. Strong hydrogen-bonding interactions of this type are not possible for the other co-monomers as styrene

contains no heteroatoms and both methyl methacrylate and ethyl acrylate do not contain any hydrogen donor atoms (no OH or NH); any interactions involving these polymer chains will be weaker and more easily replaced by interactions with the solvent making swelling more likely.

The dry solids have properties related to the swelling properties of the materials, these properties also being governed by the strength of the interactions between polymer chains. When the co-monomer is acrylic acid or acrylamide a hard glassy orange/yellow solid is obtained, ethyl acrylate gives a semi-glassy pale orange solid and methyl methacrylate or styrene give a soft white solid.

All polymers show the greatest amount of swelling with DMF as the solvent and the least when 1,2-dichloroethane is used. DMF and acetonitrile have large dipole moments so interact favourably with the polyoxometalate units and cause the materials to swell and form gels to a larger extent than 1,2- dichloroethane.

The initial polyoxotungstate to co-monomer ratio affects the amount of cross linking and therefore the swelling properties of the product (Table 4.6), when the quantity of co-monomer used is low (1:2) the cross linking is high and the swelling index is small. As the amount of co-monomer increases the degree of cross linking decreases, making the materials less dense, with longer polymer chains between polyoxometalate units, holding them further apart and providing more space for solvent molecules and therefore increasing the swelling index. When the quantity of co-monomer is high (1:20), a significant amount of solvent can be absorbed into the material with a gel containing 3.3 g of acetonitrile or 4.9 g of DMF per 1.0 g of dry material. The swelling is less than that obtained by Mayer and Thouvenot¹⁵ for the polymeric material $(\text{NBu}_4)_3\text{H}[\text{SiW}_{10}\text{O}_{36}(\text{H}_2\text{C}=\text{C}(\text{CH}_3)\text{C}(\text{O})\text{OPrSi})_2\text{O}]:\text{H}_2\text{C}=\text{C}(\text{CH}_3)\text{COOC}_2\text{H}_5$ (ethyl methacrylate), using acetonitrile as the solvent, where a swelling index of 29.9 g/g was obtained. The difference

can be explained by the different organic functional groups (R); the styryl group used here being shorter, bulkier and more rigid than the methacrylate, therefore reducing the amount of space available for solvent molecules and reducing the swelling potential of the material.

Table 4.6. The Swelling Index obtained for co-polymers made with varying amounts of methyl methacrylate.

Ratio (1:x)	Swelling Index (I_{sw} /(g/g))				
	Acetonitrile	DMF	1,2-dichloroethane	Methanol	Diethyl Ether
2	0.45	0.44	0.59	0.13	0.02
4	1.53	4.35	0.89	0.19	0.03
6	2.42	4.58	1.06	0.11	0.08
10	2.44	4.23	0.75	0.27	0.06
20	3.32	4.87	2.58	0.78	0.24
50	0.94	0.93	0.71	0.39	0.12
100	0.65	0.62	0.27	0.30	0.005

At a polyoxotungstate:methyl methacrylate ratio of 1:20 the swelling index reaches a maximum, before beginning to fall. This reduction can be explained by the polymer chains between the cross linking polyoxotungstate units becoming longer and more flexible, meaning that although the spaces between the chains are larger the solvent molecules are not trapped in the material. Also the polymer chains will have more chance to interact with one another and form crystalline regions which will be less favourable to break.

Electrochemistry. Cyclic Voltammetry was carried out on some of the co-polymer products. The low solubility of the compounds meant that the method used previously for the single polyoxotungstate clusters can not be used. Instead the electrochemical properties of the gels containing acetonitrile were studied; the gel being pasted onto the working electrode and a 0.1 M K_2SO_4 solution used as the electrolyte.

When dealing with molecules on an electrode surface the cyclic voltammograms obtained will normally have the reduction and oxidation peaks at the same potential due to immobility of the species, however here the cyclic voltammograms appear similar to those for solution chemistry, indicating that the polyoxotungstate clusters have a degree of mobility in the gels instead of being fixed to the surface.

In the range studied (0.4 to -0.7 V vs. Ag/AgCl) two waves are seen (Figure 4.16), no ferrocene is present as an internal reference, due to possible reactions with the electrolyte so the peak potentials are relative to the Ag/AgCl reference electrode. The position of these peak potentials corresponds to the position of the first two peaks for the monomer $(\text{NBu}_4)_3\text{H}[\text{SiW}_{10}\text{O}_{36}(\text{H}_2\text{C}=\text{CHC}_6\text{H}_4\text{PO})_2]$. The aqueous conditions restrict the range of the experiment as a oxygen reduction peak appears at -1.0 V.

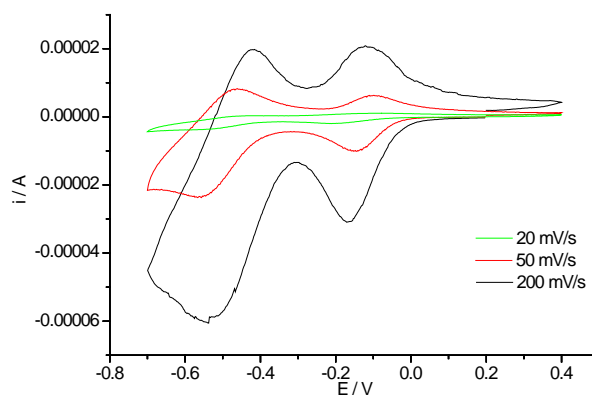


Figure 4.16. Cyclic Voltammetry for the acetonitrile gel of $(\text{NBu}_4)_3\text{H}[\text{SiW}_{10}\text{O}_{36}(\text{H}_2\text{C}=\text{CHC}_6\text{H}_4\text{PO})_2]$ polymerised with methyl methacrylate (1:10) on a glassy carbon electrode, 0.1 M K_2SO_4 .

Cyclic Voltammetry was only possible on the gels, the solvent gradually being lost and so only a small number of scans being possible before replacement of the gel or solvent is needed. The number of scans before the solvent is lost was dependent on the co-monomer present, where materials with the largest swelling index lost solvent more quickly. This can be explained by the interactions formed between the solvent molecules and the polymeric species. When acrylic acid ($\text{H}_2\text{C}=\text{CHCOOH}$) is used, both the $\text{C}=\text{O}$ and OH groups can interact with the acetonitrile solvent molecules and these interactions make the loss of solvent more difficult, as illustrated by the gradual reduction in the peak heights from the 2nd to 10th scan (the reduction is larger for the 1st scan as initially non-interacting solvent is also lost) (Figure 4.17).

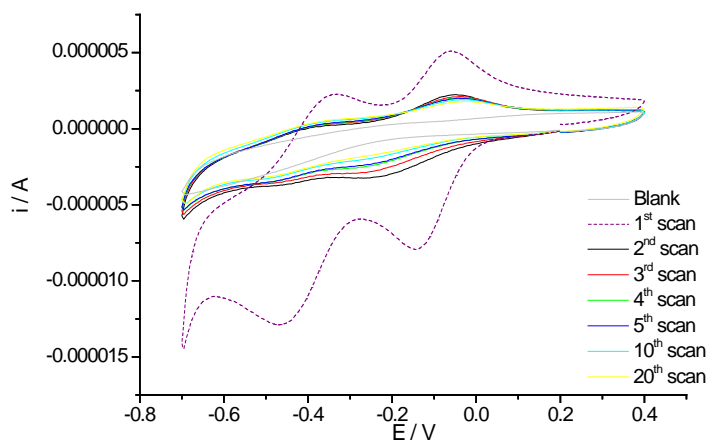


Figure 4.17. Cyclic Voltammograms for the polymer obtained from $(\text{NBu}_4)_3\text{H}[\text{SiW}_{10}\text{O}_{36}(\text{H}_2\text{C}=\text{CHC}_6\text{H}_4\text{PO})_2]$ and acrylic acid (1:10), on a glassy carbon electrode, 0.1 M K_2SO_4 , scan rate 50 mV/s.

When the co-monomer has less potential for interaction the swelling index was larger as solvent could easily be absorbed into the material, however there will be less holding the solvent into the system so solvent is lost just as easily. For example when the co-monomer is styrene ($\text{H}_2\text{C}=\text{CHC}_6\text{H}_5$), the peaks disappear after the 1st scan and a noticeable reduction is even seen in the peak height for the oxidation peak compared to the reduction peak due to the broadening of the peak as the polyoxotungstate mobility is reduced (Figure 4.18).

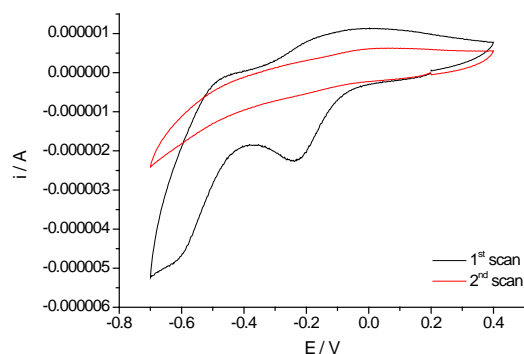


Figure 4.18. Cyclic Voltammogram of the acetonitrile gel formed from the $(\text{NBu}_4)_3\text{H}[\text{SiW}_{10}\text{O}_{36}(\text{H}_2\text{C}=\text{CHC}_6\text{H}_4\text{PO})_2]$ polymerised with styrene ($\text{H}_2\text{C}=\text{CHC}_6\text{H}_5$), 0.1 M K_2SO_4 , 50 mV/s

The rate of loss of solvent is in the order styrene > methyl methacrylate > ethyl acrylate > acrylamide > acrylic acid.

The effect of the amount of methyl methacrylate in the product was also looked at, all (ratio's 1:2, 1:10 and 1:20) products studied showing two reduction waves (Figure 4.19). Little difference was seen in the rate of loss of solvent from the gel with the solvent being lost quickly in all cases, although different swelling indexes had been observed.

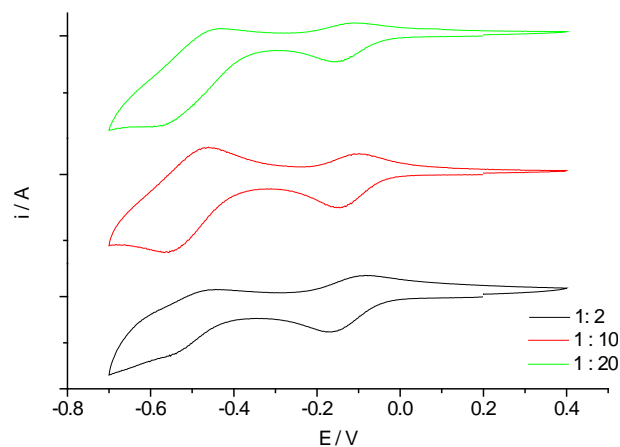


Figure 4.19. Stack plot of the cyclic voltammograms for $(\text{NBu}_4)_3\text{H}[\text{SiW}_{10}\text{O}_{36}(\text{H}_2\text{C}=\text{CHC}_6\text{H}_4\text{PO})_2]$ polymerised with methyl methacrylate (ratio's 1:2, 1:10, 1:20).

4.2. $[\text{SiW}_9\text{O}_{34}(\text{RPO})_3]^{4-}$

The best conditions used for the polymerisation of the doubly derivatised polyoxotungstates (Section 4.1) are used here to test the polymerisation potential of the triply derivatised $[\text{SiW}_9\text{O}_{34}(\text{RPO})_3]^{4-}$ ($\text{R} = \text{H}_2\text{C}=\text{CH}$, $\text{H}_2\text{C}=\text{CHCH}_2$ or $\text{H}_2\text{C}=\text{CHC}_6\text{H}_4$). Three polymerisable bonds on the clusters will produce products with a large degree of cross-linking and therefore the reaction is expected to be more difficult and give lower polymerisation yields. The extent of the reaction is estimated using NMR (^1H and ^{31}P) and UV/vis.

^1H NMR. Comparison of the signal intensities in the ^1H NMR spectra can be used to estimate the extent of the polymerisation. Signals due to the cations and C_6H_4 rings (when $\text{R} = \text{H}_2\text{C}=\text{CHC}_6\text{H}_4$) should be unchanged, however the vinylic hydrogen signals will have reduced in intensity being replaced by peaks which are hidden by the cation peaks.

When $\text{R} = \text{H}_2\text{C}=\text{CH}$ or $\text{H}_2\text{C}=\text{CHCH}_2$, the polymerisation is estimated by comparing the intensities for the vinylic hydrogen atoms with the cation peaks, assuming that there are still three NBu_4^+ cations per cluster (Figure 4.20, Table 4.7). The polymerisation increases over time, reaching a maximum after 24 (allyl) or 48 hours (vinyl), this time being shorter than that for the corresponding polymer obtained from the doubly derivatised product.

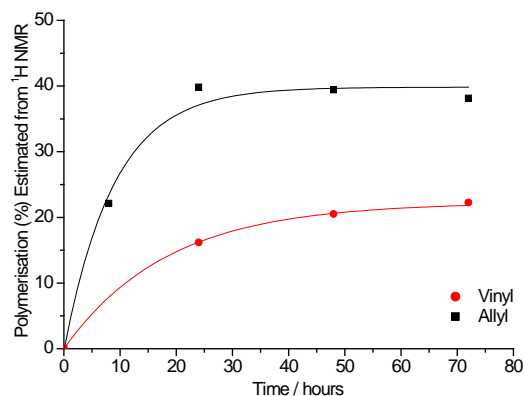


Figure 4.20. Polymerisation estimated from ^1H NMR for $[\text{SiW}_9\text{O}_{34}(\text{RPO})_3]^{4-}$ ($\text{R} = \text{H}_2\text{C}=\text{CH}$ or $\text{H}_2\text{C}=\text{CHCH}_2$).

Table 4.7. The maximum degree of polymerisation (%).

R group	Percentage Polymerisation / % ^(a)	
	$[\text{SiW}_{10}\text{O}_{36}(\text{RPO})_2]^{4-}$	$[\text{SiW}_9\text{O}_{34}(\text{RPO})_3]^{4-}$
Vinyl	28	22
Allyl	56	40

(a) Estimated from the intensities of vinylic hydrogen resonances compared to those for the cations in the ^1H NMR spectra.

The percentage of the polymerisable double bond groups which are estimated as having reacted is less for the triply substituted compounds than for the corresponding doubly substituted ones, agreeing with what was predicted. Sterics prevent the groups from reacting as easily and this becomes a bigger issue when one or two groups have already reacted.

When $\text{R} = \text{H}_2\text{C}=\text{CHC}_6\text{H}_4$, the polymerisation is estimated by comparing the intensities for the C_6H_4 hydrogen signals and the vinylic hydrogen peaks (Figure 4.21). The spectra show the intensity of the vinylic hydrogen atoms to have reduced, while the ring peaks have broadened due to the decreased mobility of the product. As time increases these effects are more pronounced, indicating a greater degree of polymerisation.

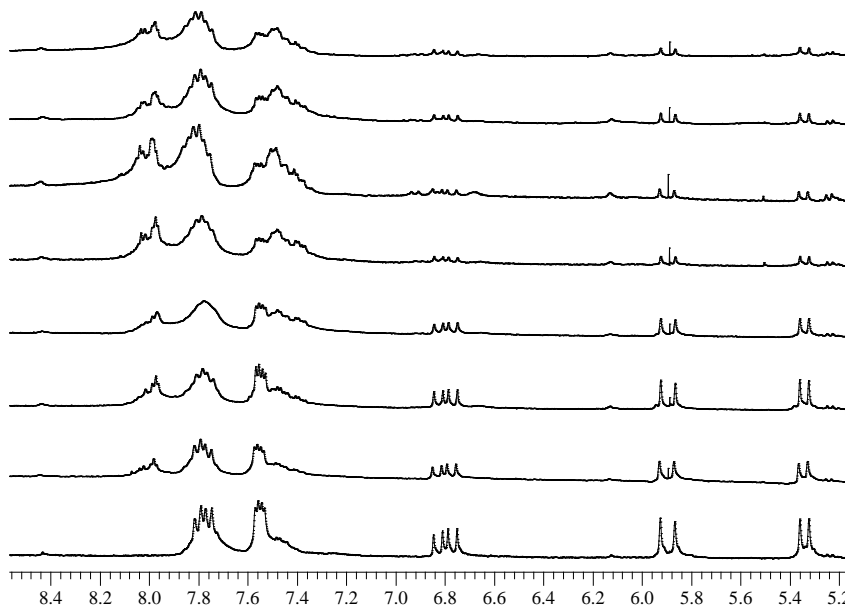


Figure 4.21. Polymerisation of $(\text{NBu}_4)_3\text{H}[\text{SiW}_9\text{O}_{34}(\text{H}_2\text{C}=\text{CHC}_6\text{H}_4\text{PO})_3]$ over time (0, 2, 4, 6, 8, 16, 24 and 32 hours) showing the region of the spectra between 5.2 and 8.4 ppm.

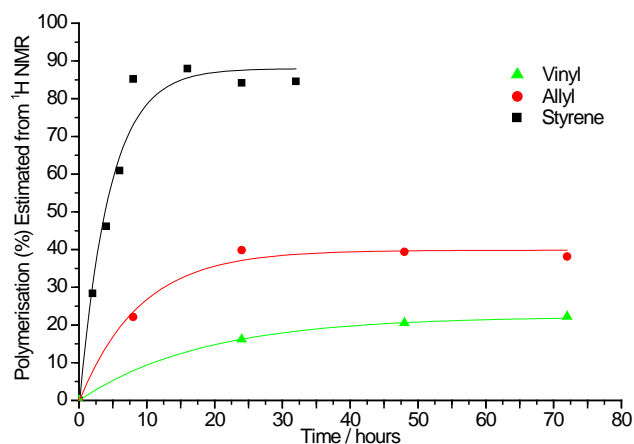


Figure 4.22. Polymerisation estimated from ^1H NMR for $(\text{NBu}_4)_3\text{H}[\text{SiW}_9\text{O}_{34}(\text{RPO})_3]$.

Table 4.8. The maximum degree of polymerisation (%).

	Percentage Polymerisation / % ^(a)	
	$[\text{SiW}_{10}\text{O}_{36}(\text{RPO})_2]^{4-}$	$[\text{SiW}_9\text{O}_{34}(\text{RPO})_3]^{4-}$
Styrene	80	88

(a) Estimated from the intensities of vinylic hydrogen resonances compared to the hydrogen intensities for unreactive groups on the ^1H NMR Spectra.

The polymerisation is greatest when $R = \text{styrene}$ (Figure 4.22) with 88 % of the double bonds having reacted for the triply substituted clusters, this being a higher percentage than for the doubly derivatised cluster (Table 4.8). The product obtained is noticeably more soluble than the one obtained from the doubly derivatised cluster, which could indicate that smaller aggregates are formed which dissolve more easily and also allow the reaction to proceed further.

^{31}P NMR. No shift in the phosphorus peak position is observed, although when $R = \text{H}_2\text{C}=\text{CH}$ or $\text{H}_2\text{C}=\text{CHCH}_2$ some small peaks surround the main peak. The main peak has broadened significantly for all R groups, showing the reduced mobility of the product due to the larger polymerisation species. When $R = \text{H}_2\text{C}=\text{CHC}_6\text{H}_4$ a second peak appears in the spectra at a slightly lower value than for the main peak (Figure 4.23), this is also broad so the phosphorus is also part of a polymeric product, but has a different phosphorus environment, possibly caused by break up of the product.

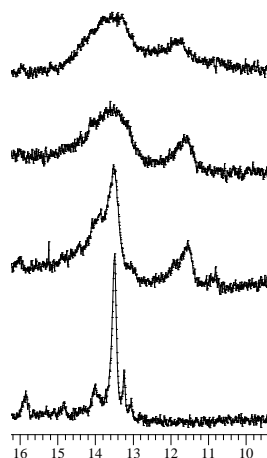


Figure 4.23. ^{31}P NMR Spectra for the polymerisation of $(\text{NBu}_4)_3\text{H}[\text{SiW}_9\text{O}_{34}(\text{H}_2\text{C}=\text{CHC}_6\text{H}_4\text{PO})_3]$ (0, 4, 8, 16 hours).

IR Spectroscopy. No significant changes are observed in the IR Spectra, indicating that the polyoxotungstate cluster is unchanged and has not been affected by the reaction. The $\text{C}=\text{C}$ band is weak and reduces in intensity as the reaction time increases.

Mass Spectrometry. The Maldi-TOF spectra for the $(\text{NBu}_4)_3[\text{SiW}_9\text{O}_{34}(\text{H}_2\text{C}=\text{CHC}_6\text{H}_4\text{PO})_3]$ polymer obtained after reaction for 16 hours shows a broad peak between 3500-4100 m/z , this is the mass for one polyoxotungstate cluster with 3-6 cations, a less intense peak between 6500-7600 m/z is also present, this being due to two clusters and 6-10 cations. The position for three clusters (10000-11000 m/z) is noisier than the surrounding background, possibly due to a small quantity of trimers being present. Overall the mass spectra is quite different to that for the monomer unit, however no peaks are seen at very large masses (>10000 m/z), due to a combination of the polymeric materials breaking up during the ionisation process and an exponential decay in peak intensities when going to high m/z values, alternatively it could show that only monomers and dimers are present.

UV/vis Spectroscopy. The spectrum for the monomer shows one intense peak at 260 nm arising from the absorption of both the $[\text{SiW}_9\text{O}_{34}]^{10-}$ unit and the styrene groups grafted onto the structure. Upon polymerisation the styrene peaks shift to a lower wavelength (which is off the scale for the instrument) and so the peak reduces in intensity until just the $[\text{SiW}_9\text{O}_{34}]^{10-}$ signal is present (Figure 4.24).

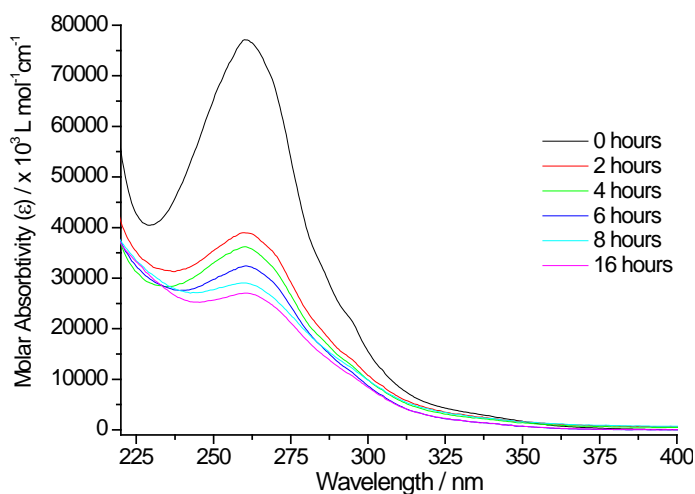


Figure 4.24. The UV spectra for $[\text{SiW}_9\text{O}_{34}(\text{H}_2\text{C}=\text{CHC}_6\text{H}_4\text{PO})_3]^{4-}$ after polymerisation for varying times.

Electrochemistry. Cyclic Voltammetry was performed on acetonitrile solutions of the polymeric product (Figure 4.25, Table 4.9), the first reduction peak is in the same position as for the monomer species, showing that polymerisation has not changed the ability of the polyoxotungstate cluster to accept an electron. The second peak has a more negative peak potential (135 mV less), indicating that a second electron is not accepted so easily; this could be explained by the proximity of the negatively charged clusters, addition of further electrons being unfavourable as the repulsion effects will increase. The separation of the reduction and oxidation peaks increases, due to the slower movement of the the larger polymeric product in comparison to the monomer species.

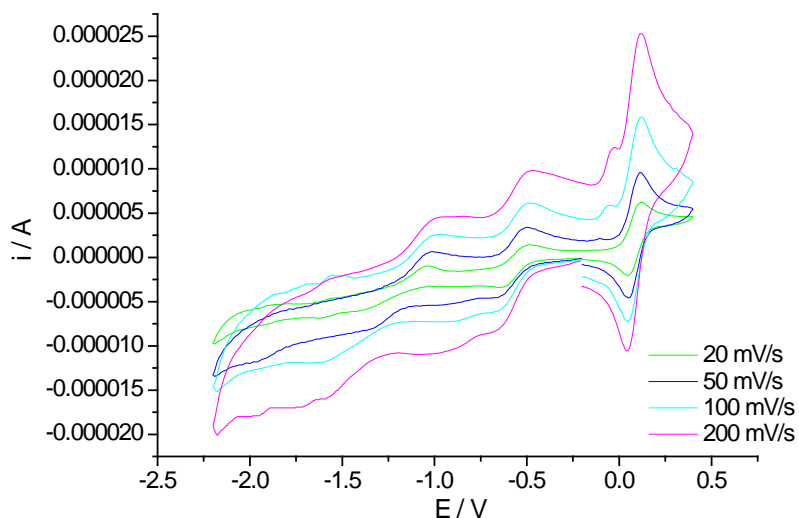


Figure 4.25. Cyclic Voltammograms for the $(\text{NBu}_4)_3\text{H}[\text{SiW}_9\text{O}_{34}(\text{H}_2\text{C}=\text{CHC}_6\text{H}_4\text{PO})_3]$ polymer at varying scan rates, using an Ag/Ag^+ reference electrode and Ferrocene as an internal reference. 0.5 mM solution.

Table 4.9. The reduction potentials for the monomer and polymer formed after reaction for 24 hrs.

	E(1) /mV	E(2) /mV	E(3) /mV
Monomer	-644	-1181	-1908
Polymer	-649	-1316	

At fast scan rates (200/100 mV/s) an oxidation peak is observed at -0.05 V, the origin of this peak is unclear, but as it only appears at fast scan rates it could indicate that it is due to an unstable product formed by a reaction of the reduced species, this product decaying quickly so it is not observed at slower scan rates.

4.2.1. Co-polymers

Co-polymers were prepared using $[\text{SiW}_9\text{O}_{34}(\text{H}_2\text{C}=\text{CHC}_6\text{H}_4\text{PO})_3]^{4-}$ and either ethyl acrylate or methyl methacrylate. The method used was similar to the one used previously.

^1H NMR. The ^1H NMR spectra is used to estimate the extent of the polymerisation; as the amount of co-monomer increases the intensity of the vinylic hydrogen peaks reduces and the C_6H_4 signals broaden and lose detail, these observations indicate an increased polymerisation (Figure 4.26, Figure 4.27).

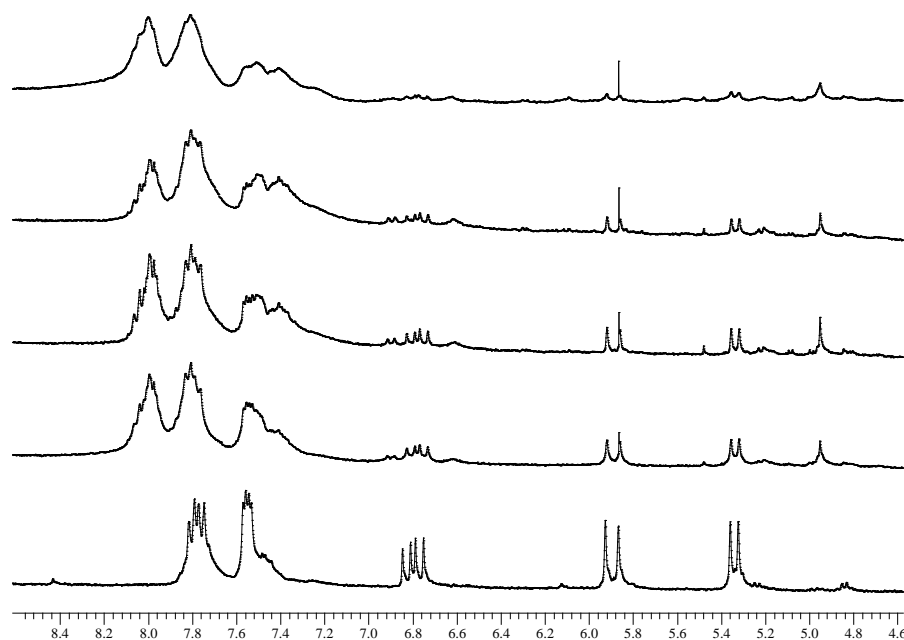


Figure 4.26. ^1H NMR Spectra for the co-polymerisation of $(\text{NBu}_4)_3\text{H}[\text{SiW}_9\text{O}_{34}(\text{H}_2\text{C}=\text{CHC}_6\text{H}_4\text{PO})_3]$ and ethyl acrylate, showing the monomer (bottom) and the products obtained from different ratio's of starting material (1:2, 1:4, 1:6 and 1:10).

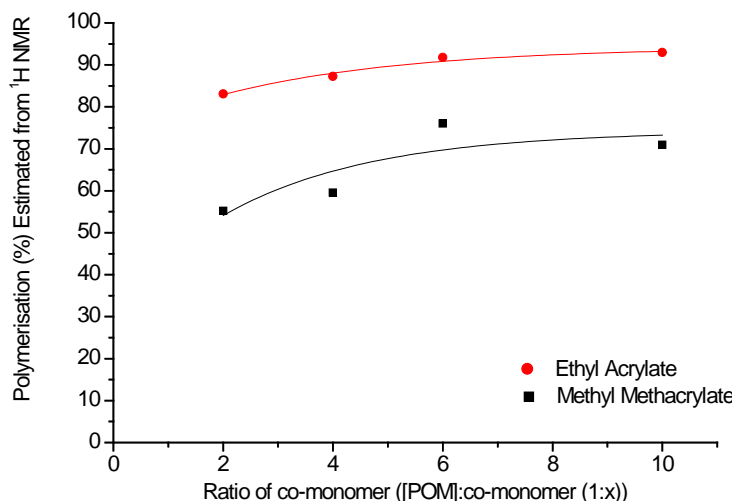


Figure 4.27. The estimated polymerisation for $(\text{NBu}_4)_3\text{H}[\text{SiW}_9\text{O}_{34}(\text{H}_2\text{C}=\text{CHC}_6\text{H}_4\text{PO})_3]$ co-polymers.

The amount of polymerisation observed decreases from that seen when no co-monomer was present before rising as the quantity of co-monomer present increases. This same observation was seen for $[\text{SiW}_{10}\text{O}_{36}(\text{H}_2\text{C}=\text{CHC}_6\text{H}_4\text{PO})_2]^{4-}$ and is assigned to the increased competition for the double bonds which is then balanced by the increased chance of coming into contact with a reactive group.

^{31}P NMR. One peak is seen on the ^{31}P NMR spectra at the same position as for the monomer species (15.9 ppm), this peak has broadened due to the limited mobility of the large polymeric product.

IR Spectroscopy. The fingerprint region indicates that the symmetry of the $[\text{SiW}_9\text{O}_{34}(\text{H}_2\text{C}=\text{CHC}_6\text{H}_4\text{PO})_3]^{4-}$ cluster is retained, the presence of the co-monomer being confirmed by C=O stretches, the intensity of which increases as the amount present increases.

Mass Spectrometry. The Maldi-TOF mass spectrum for the 1:2 ratio (polyoxometalate:ethyl acrylate) shows three sets of peaks, at 3500-5000, 7000-8000 and 10000-11500 m/z , the intensity decreasing as the m/z increases (Figure 4.28). These three sets of peaks

are attributed to polymer units containing either one, two or three clusters with additional ethyl acrylate units and/or cations. As the ratio of polyoxometalate to co-monomer increases the larger products are less soluble and less peaks are seen at higher m/z values.

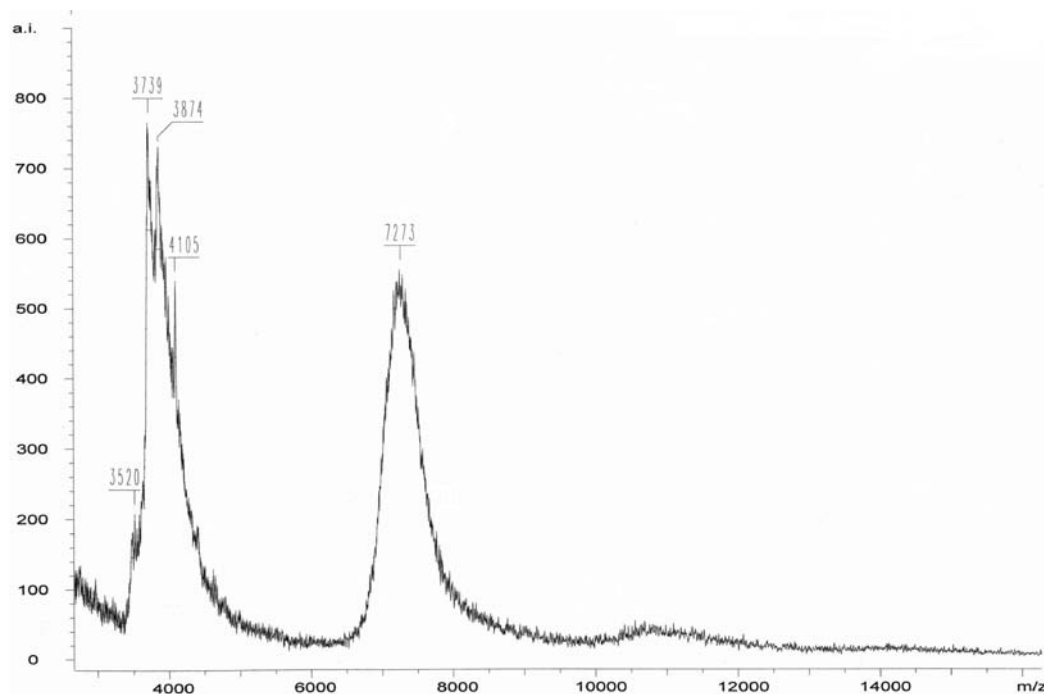


Figure 4.28. Maldi-TOF Mass Spectrum for $(\text{NBu}_4)_3\text{H}[\text{SiW}_9\text{O}_{34}(\text{H}_2\text{C}=\text{CHC}_6\text{H}_4\text{PO})_3]$ co-polymerised with ethyl acrylate (1:2).

UV/vis Spectroscopy. The UV/vis spectra for the co-polymers show a peak at 260 nm; the intensity of this peak has reduced significantly in comparison to the monomer species (Figure 4.29), due to reaction of the double bonds making the group less conjugated and its position shift to a lower wavelength.

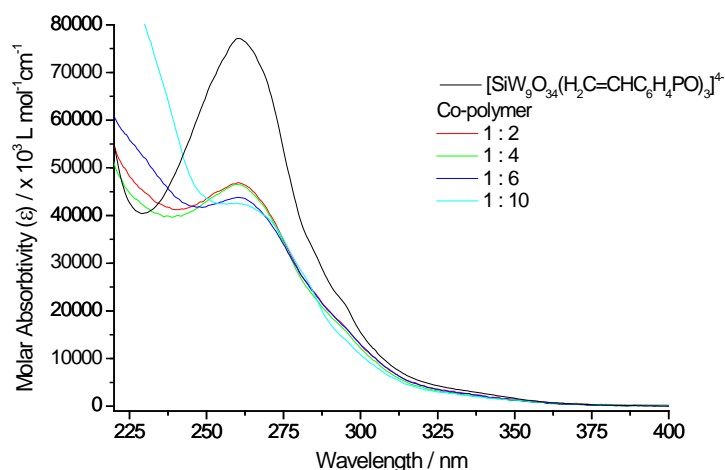


Figure 4.29. The UV spectra for the co-polymer obtained from $(\text{NBu}_4)_3\text{H}[\text{SiW}_9\text{O}_{34}(\text{H}_2\text{C}=\text{CHC}_6\text{H}_4\text{PO})_3]$ and ethyl acrylate at various ratios.

Elemental Analysis. The percentages of carbon, hydrogen and nitrogen present provides an indication of the ratio of polyoxotungstate to co-monomer in the product (Table 4.10).

Table 4.10. The Elemental Analysis results for the co-polymers made from $(\text{NBu}_4)_3\text{H}[\text{SiW}_9\text{O}_{34}(\text{H}_2\text{C}=\text{CHC}_6\text{H}_4\text{PO})_3]$ and ethyl acrylate.

Initial Ratio (1:x)	Amount found in the product (%)			Observed Ratio
	N	C	H	
2	1.4	26.75	4.2	1.5
4	1.4	28.0	4.7	3
6	1.5	29.05	4.55	4.25
10	1.2	30.0	4.9	5.5

The results suggest that the ratio of co-monomer present in the product is smaller than that put into the reaction, this shows that not all the co-monomer reacted, the unreacted units being removed when purifying the product.

Electrochemistry. The properties of the methyl methacrylate (1:10) co-polymer were investigated, a gel containing acetonitrile was pasted onto a glassy carbon electrode and cyclic

voltammetry performed in 0.1 M K_2SO_4 vs. Ag/AgCl. In the range studied (0.4 to -0.7 V) (Figure 4.30) one reduction/oxidation wave is observed, the second wave in the monomer (~ -710 mV) not completely seen. The first wave is at approximately the same position as for the monomer (if the reference electrode is taken into account) showing that gaining and removing one electron is relatively easy, thus indicating a potential for use of the material in catalysis.

The solvent is gradually lost from the acetonitrile gel, with each scan having a smaller peak height than the previous one; however the loss of solvent is slower for this co-polymer than for the polymers obtained from the doubly derivatised product, the slower loss of solvent being due to the higher cross-linking of the product.

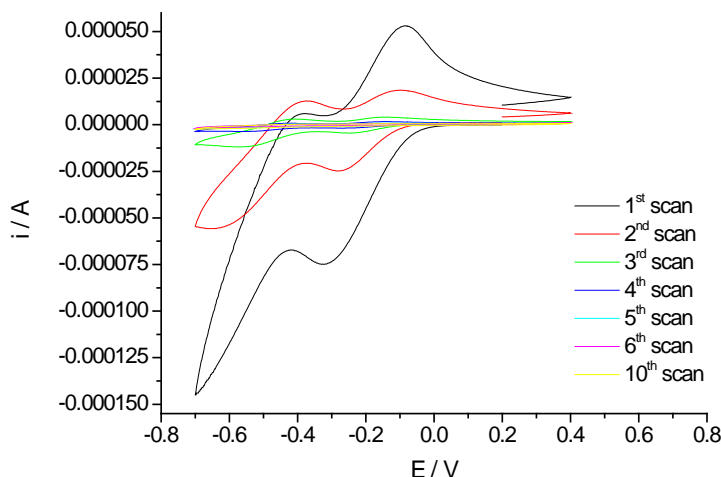


Figure 4.30. Cyclic Voltammograms for the gel of the polymer obtained from $(\text{NBu}_4)_3\text{H}[\text{SiW}_9\text{O}_{34}(\text{H}_2\text{C}=\text{CHC}_6\text{H}_4\text{PO})_3]^{4-}$ and methyl methacrylate (1:10), 0.1 M K_2SO_4 , 50 mV/s.

Conclusion. The co-polymerisations are successful for the triply functionalised $[\text{SiW}_9\text{O}_{34}(\text{H}_2\text{C}=\text{CHC}_6\text{H}_4\text{PO})_3]^{4-}$ with either ethyl acrylate or methyl methacrylate, this being confirmed by multinuclear NMR (^1H and ^{31}P) and UV/vis spectroscopy, with the products also being studied by IR, MS and elemental analysis.

4.3. $[\text{XW}_9\text{O}_{34}(\text{R}^1\text{SiO})_3(\text{R}^2\text{Si})]^{4-}$

Clusters prepared from reaction with organosilane derivatives which contain a C=C bond have the potential for polymerisation.

4.3.1. $\text{R}^1, \text{R}^2 = \text{Vinyl or Allyl}$

When all the R groups are the same ($\text{R}^1, \text{R}^2 = \text{H}_2\text{C}=\text{CH}$ or $\text{H}_2\text{C}=\text{CHCH}_2$) they all have the potential to be polymerised, however steric factors are likely to prevent this from happening as the polymeric products produced would be highly cross-linked.

^1H NMR. When $\text{R} = \text{H}_2\text{C}=\text{CH}$ no major changes are seen in the spectra, the cations signals remain unchanged and the intensity of the vinyl hydrogen peaks only reduces slightly ($\sim 3.6\text{--}4.7\%$), this reduction being within the errors. It is concluded that no polymerisation was achieved due to the double bonds being close to the cluster and sterically hindered.

When $\text{R} = \text{H}_2\text{C}=\text{CHCH}_2$ the vinylic hydrogen peaks reduce in intensity by approximately 25 %; this is more significant illustrating that some polymerisation has occurred.

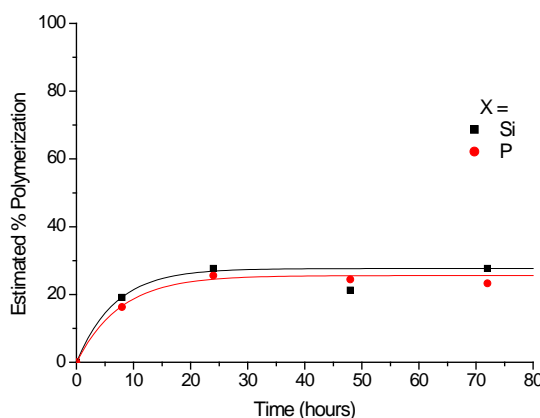


Figure 4.31. A Comparison of the polymerisation estimated from the ^1H NMR spectra for $(\text{NBu}_4)_3\text{H}_{1/0}[\text{XW}_9\text{O}_{34}(\text{H}_2\text{C}=\text{CHCH}_2\text{SiO})_3(\text{H}_2\text{C}=\text{CHCH}_2\text{Si})]$ ($\text{X} = \text{Si}$, $n = 1$ or $\text{X} = \text{P}$, $n = 0$).

The amount of polymerisation is approximately the same for both central atoms ($X = \text{Si}$ or P), showing that they have little effect on the reaction in this example (Figure 4.31).

Polymerisation for these clusters is lower than for the phosphonate derivatives, indicating that the silicon atom deactivates the double bonds more.

^{31}P NMR. When $X = \text{P}$ the ^{31}P NMR spectra exhibits one peak. The position of this peak has not moved from that for the monomer species indicating that the cluster is a complete, capped structure with four organic groups on, thus showing that it has not broken up during the reaction.

UV/vis Spectroscopy. The UV/vis spectra also show no significant changes, indicating that the polyoxotungstate unit remains intact.

4.3.2. $\text{R}^1 = t\text{Bu}$

When $\text{R}^1 = t\text{BuSiOH}$ the product can be further reacted with an organosilane group containing a double bond giving the overall product potential for polymerisation. These compounds only contain one double bond so any polymeric products created will be organic chains with the polyoxotungstate as a pendent (Figure 4.32).^{11,18}

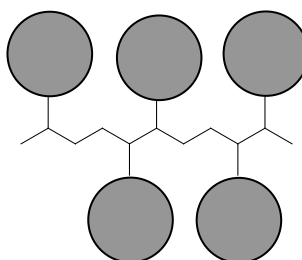


Figure 4.32. Representation of the polymer formed from a cluster with one $\text{C}=\text{C}$ group grafted onto it.

^1H NMR. When $\text{R} = \text{H}_2\text{C}=\text{CH}$ the vinylic hydrogen signals have not reduced in intensity, so there is no evidence that a reaction has occurred, however when $X = \text{Si}$ the peaks have broadened.

When $R = H_2C=CHCH_2$ the allyl peaks have reduced in intensity when compared to the cation peaks, this reduction indicates that a reaction has taken place with around a third of the double bonds reacting. This is a greater degree of polymerisation than was seen for the clusters with four double bonds on, perhaps due to each cluster only being able to react with two other clusters and the products not being cross-linked so less sterically hindered.

^{31}P NMR. The spectrum (when $X = P$) confirms that the polyoxotungstate cluster still has four organic groups grafted onto it capping the cluster and giving it a fully saturated structure.

4.4. Conclusion

In conclusion it has been demonstrated that the derivatised polyoxotungstates $[SiW_{10}O_{36}(RPO)_2]^{4-}$, $[SiW_9O_{34}(RPO)_3]^{4-}$ ($R = H_2C=CH$, $H_2C=CHCH_2$ or $H_2C=CHC_6H_4$), $[XW_9O_{34}(R^1SiO)_3(R^2Si)]^{4-}$ ($R^1 = tBu$ or R^2 , $R^2 = H_2C=CHCH_2$) all have the ability to be polymerised under free radical conditions. The extent of the reaction depends on the R group present and increases in the order vinyl < allyl < styryl, due to the distance of the double bond from the cluster and the greater conjugation of the styryl group. Generally increasing the number of polymerisable groups on a cluster decreased the overall reaction, by both increasing the steric factors, with the product becoming more cross-linked and increasing the number of bonds needing to react, with the polymerisability decreasing in the order $[SiW_{10}O_{36}(RPO)_2]^{4-} > [SiW_9O_{34}(RPO)_3]^{4-}$ and $[XW_9O_{34}(tBuSiO)_3(RSi)]^{4-} > [XW_9O_{34}(RSiO)_3(RSi)]^{4-}$. The exception to this rule being $[SiW_9O_{34}(H_2C=CHC_6H_4PO)_3]^{4-}$ which appears to react further than $[SiW_{10}O_{36}(H_2C=CHC_6H_4PO)_2]^{4-}$, an explanation for this being that the clusters react to form smaller aggregates such as dimers and trimers, this is indicated by the solubility of the product, although it is unclear why this might be the case for this example.

Comparison of the reaction of phosphonate and silyl groups shows the phosphonate groups to have a greater reactivity, although the comparison is difficult as the clusters are not equivalent.

All the polymers tested retain the electrochemical properties of the monomer unit and so retain the potential for use as a catalyst. The properties of the gels are greatly enhanced when acetonitrile is present, the reduction and oxidation being easier when the polyoxotungstate units have a degree of mobility.

4.5. References

1. M. T. Pope, *Heteropoly and Isopoly Oxometalates*, Springer-Verlag, Berlin, **1983**.
2. F. Cavani, *Catalysis Today*, **1998**, 41, 73.
3. N. Mizuno and M. Misono, *Chem. Rev.*, **1998**, 98, 199.
4. T. Okuhara, *Chem. Rev.* **2002**, 102, 3641.
5. M. Cohen, R. Neumann, *J. Mol. Catal. A: Chem.* **1999**, 146, 291.
6. T. Sakamoto, C. Pac, *Tetrahedron Lett.* **2000**, 41, 10009.
7. A. M. Khenkin, R. Neumann, A. B. Sorokin, A. Tuel, *Catal. Lett.* **1999**, 63, 189.
8. N. M. Okun, T. M. Anderson, C. L. Hill, *J. Am. Chem. Soc.* **2003**, 125, 3194.
9. K. Nomiya, H. Murasaki, M. Miwa, *Polyhedra* **1986**, 5, 1031.
10. P. Judeinstein, *Chem. Mater.* **1992**, 4, 4.
11. G. Kickelbick, *Prog. Polym. Sci.* **2003**, 83.
12. G. S. Kim, K. S. Hagen and C.L. Hill, *Inorg. Chem.*, **1992**, 31, 5316.
13. Aldrich, Applications: Free Radical Initiators.
14. D. Colombani, *Prog. Polym. Sci.*, **1997**, 22, 1649.

15. C. R. Mayer, R. Thouvenot, *Chem. Mater.* **2000**, 12, 257.
16. C. R. Mayer, V. Cabuil, T. Lalot and R. Thouvenot, *Angew. Chem. Int. Ed.* **1999**, 38, 24, 3672.
17. T. Hasegawa, H. Murakami, K. Shimizu, Y. Kasahara, S. Yoshida, T. Kurashina, H. Seki, K. Nomiya, *Inorg. Chim. Acta*, **2008**, 361, 1385.
18. A. R. Moore, H. Kwen, A. M. Beatty and E. A. Maatta, *Chem. Commun.* **2000**, 1793.

5. REACTION WITH AMINES

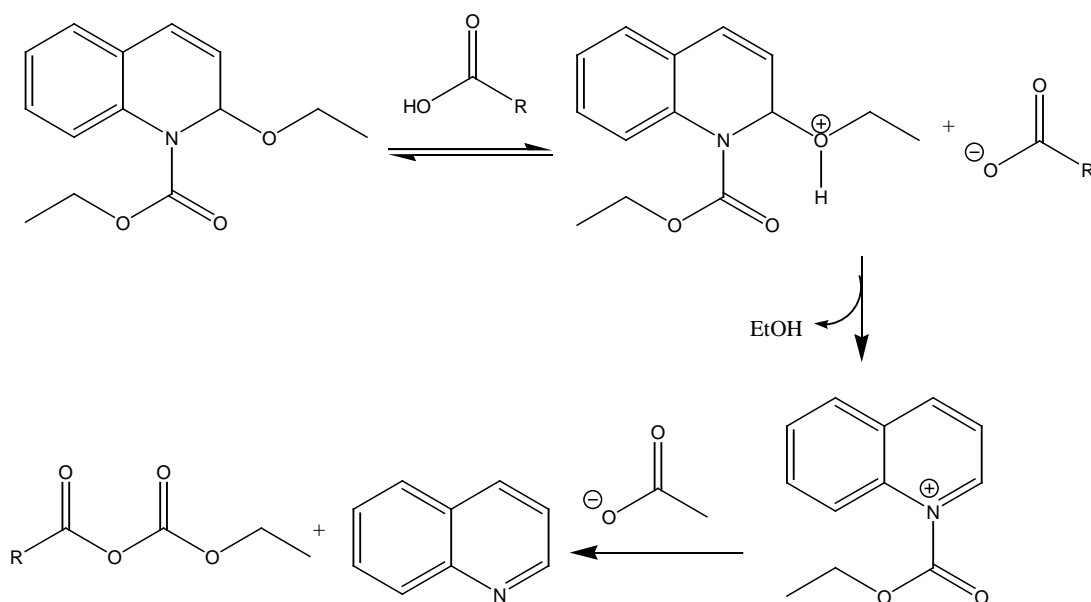
The grafting of organic groups onto a cluster provides a method to expand the functionality and properties of the cluster, as further reaction of these groups increases the number of functionalities available, therefore providing a larger range of possible materials.

5.1 $[\text{SiW}_{10}\text{O}_{36}(\text{RPO})_2]^{4-}$

5.1.1 Condensation Reactions, $\text{R} = \text{HOOC}(\text{CH}_2)_n$

Amide bonds are important in nature, their formation being catalysed by enzymes. Synthetically the reaction of an acid and amine is known as a condensation reaction, direct condensation only being achieved at high temperatures (160-180 °C)¹ which are incompatible with other functionalities. At low temperatures, acids protonate the amine making it unreactive, but a number of methods to create amide bonds via intermediates are possible, including the creation of acyl chlorides, acyl azides or anhydrides, as the attachment of a good leaving group activates the acid allowing reaction with the amine.¹

Polyoxotungstates functionalised with a carboxylic acid group have been reacted with amines in the literature,^{2,3,4} the most effective activating system being using 2-ethoxy-1-ethoxycarbonyl-1,2-dihydroquinoline (EEDQ). Under acidic conditions ethanol is eliminated from EEDQ and an ethyl formate quinolinium salt is generated, this intermediate readily reacts with the carboxylate forming an ethoxycarbonyl anhydride (Scheme 5.1).⁵



Scheme 5.1. The reaction of EEDQ with a carboxylic acid (RCOOH).

In this mixed anhydride the carboxylate site next to the ester is stabilised by resonance with the lone pairs on the oxygen to a greater extent than the carboxylate next to the R group, making the carboxylate next to the R group more electrophilic, so it reacts with the amine giving the desired amide.¹

Wells-Dawson polyoxotungstates functionalised with a carboxylic acid [$P_2W_{17}O_{61}(SnCH_2CH_2COOH)$] have been reacted with a variety of amines, the extent of the reaction being determined by the structure of the amine, with primary and secondary amines giving the corresponding amides in high yields and sterically hindered amines being more difficult to react so requiring longer reaction times and giving lower yields.²

The reactivity of the $[SiW_{10}O_{36}(HOOC(CH_2)_nPO)_2]^{4-}$ ($n = 1$ or 2) cluster towards amines will be investigated here (Compounds 38 and 39), EEDQ being used as the activating agent under similar conditions to the literature (Refluxing Acetonitrile).^{2,3}

^1H NMR. The cation (NBu_4^+) signals are present along with those for the R group; the R group signals have shifted slightly and reduced in intensity, perhaps due to reaction of the COOH group. Peaks due to benzylamine are present, these peaks being larger than expected for one group per R group, an explanation for this being that some benzylamine forms cations with H^+ ions remaining from the previous step. Quinoline peaks are present in the crude mixture, quinoline being a side product of the EEDQ reaction, however this is easily removed.

^{31}P NMR. Although the position of the main peak in the ^{31}P NMR spectrum has not changed there are a number of small peaks meaning that the product is not pure.

Mass Spectrometry. Maldi-TOF mass spectra for the products have changed from before the reaction. When $\text{R} = \text{HOOC}(\text{CH}_2)_2$ the masses correspond to a cluster with only one R group attached and varying numbers of NBu_4^+ cations and benzylamine molecules associated with these clusters. When $\text{R} = \text{HOOCCH}_2$ the mass spectra has smaller changes, the mass of the benzylamine molecule (108) being approximately the same as the RPO group (106) so making the number of R groups and benzylamine molecules present hard to distinguish.

Overall it appears that benzylamine reacts with $(\text{NBu}_4)_3\text{H}[\text{SiW}_{10}\text{O}_{36}(\text{HOOC}(\text{CH}_2)_n\text{PO})_2]$ ($n = 1$ or 2), however the evidence shows that the amide $[\text{SiW}_{10}\text{O}_{36}(\text{H}_5\text{C}_6\text{CH}_2\text{NHOC}(\text{CH}_2)_n\text{PO})_2]^{4-}$ is not obtained as a pure product, with an excess of benzylamine being present.

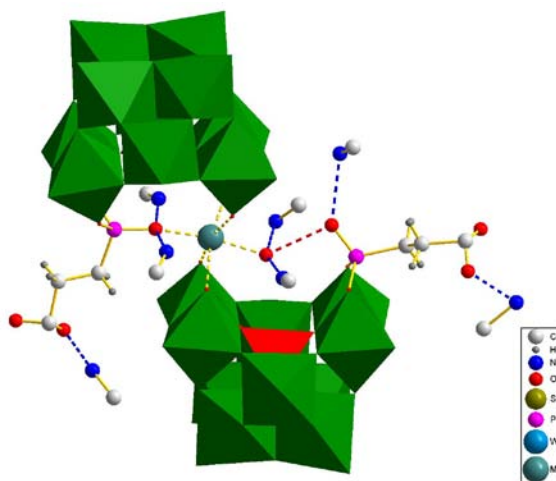
Single Crystal X-Ray Diffraction. As water is produced during the reaction, attempts to remove this water by addition of a drying agent (e.g. MgSO_4) to the reaction mixture and so force the equilibrium to the side of the product were made. This made little difference to the product formed, however crystals were obtained from this product by diffusion of diethyl ether into an acetonitrile solution. XRD data was obtained at Station 16.2smx of the SRS facility at the CCLRC Daresbury Laboratory (Table 5.1).

Table 5.1. Crystallographic Data for $(\text{NBu}_4)_4(\text{C}_6\text{H}_5\text{CH}_2\text{NH}_3)_5\text{MgH}[\text{SiW}_{10}\text{O}_{36}(\text{HOOC}(\text{CH}_2)_2\text{PO})]_2(\text{C}_6\text{H}_5\text{CH}_2\text{NH}_2)_2\cdot\text{H}_3\text{CCN}$.

Monoclinic		Spacegroup	C 2/c
Cell axes (Å)	$a = 45.6832(5)$	$b = 28.5204(3)$	$c = 31.4479(3)$
Cell angles (deg)	$\alpha = 90.00$	$\beta = 108.900(1)$	$\gamma = 90.00$
Cell Volume (Å ³)	38764.49(7)		
[Full details in appendix (Structure 21)]			

The asymmetric unit contains two $[\text{SiW}_{10}\text{O}_{36}]^{8-}$ clusters with different structures to that expected, both having one RPO group and one vacant site. The vacant sites from the two clusters coordinate to a metal ion (which models well as Mg^{2+} derived from the MgSO_4 drying agent), this cation also coordinating to two other oxygen atoms (one from a $\text{P}=\text{O}$ group) giving it an octahedral coordination.

The R groups are unreacted carboxylic acid rather than amide groups, these hydrogen-bond to benzylamine molecules ($d_{\text{ON}} = 2.01$ or 2.46 Å). The asymmetric unit contains five other benzylamine molecules, all of which have their amino group pointing towards the polyoxotungstate clusters (Figure 5.1).

**Figure 5.1.** $[\text{SiW}_{10}\text{O}_{36}(\text{HOOC}(\text{CH}_2)_2\text{PO})]^{6-}$ clusters, showing the coordination to the Mg^{2+} ion (turquoise) and the nitrogen atoms on the benzylamines (blue), including a water molecule which also hydrogen-bonds to a $\text{P}=\text{O}$ group.

The expected charge of the two clusters is 12- (both have a charge of 6- when singly derivatised), however only four NBu_4^+ cations are present. These along with the metal ion (Mg^{2+}) have a charge of 6+, therefore it is suggested that the benzylamine molecules must be RNH_3^+ cations and some H^+ ions must be present. It has not been possible to determine H positions from the quality of data so it is not possible to solve this issue.

There are eight sets of two clusters per unit cell, the asymmetric unit repeating along a *c*-glide plane (Figure 5.2).

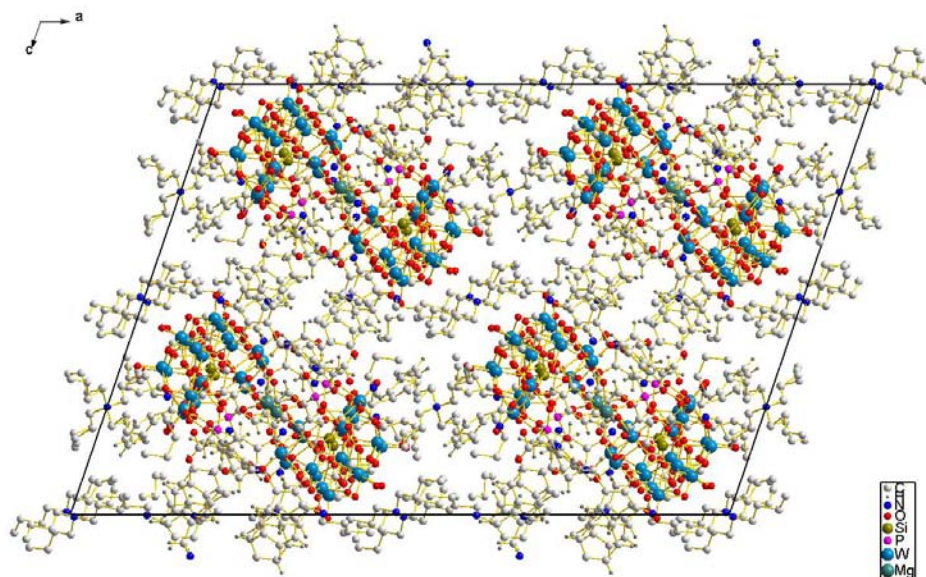
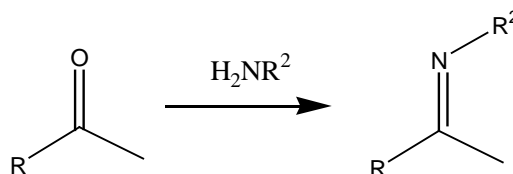


Figure 5.2. The structure of $(\text{NBu}_4)_4(\text{C}_6\text{H}_5\text{CH}_2\text{NH}_3)_5\text{MgH}[\text{SiW}_{10}\text{O}_{36}(\text{HOOC}(\text{CH}_2)_2\text{PO})_2(\text{C}_6\text{H}_5\text{CH}_2\text{NH}_2)_2\cdot\text{H}_3\text{CCN}]$ viewed along the *b*-axis.

5.1.2 Imine Formation, $\text{R} = \text{H}_3\text{CCCOC}_6\text{H}_4$



Scheme 5.2

Ketone groups can react with amines by nucleophilic attack at the electrophilic carbonyl centre to form imines (Scheme 5.2). A ketone group attached to a polyoxotungstate introduces

the potential for this type of reaction, thus introducing further functionality to the cluster. These reactions can also produce polymeric species, an example being the reaction of an amine functionalised polyoxotungstate $[\text{SiW}_{10}\text{O}_{36}(\text{H}_2\text{N}(\text{CH}_2)_3\text{Si})_2\text{O}]^{4-}$ with pyromellitic dianhydride and 4, 4'-oxydianiline to form polyimides (Figure 5.3).⁶

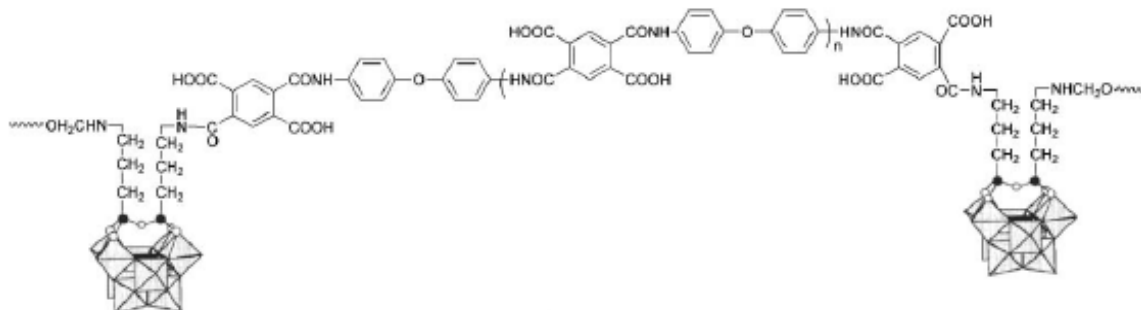
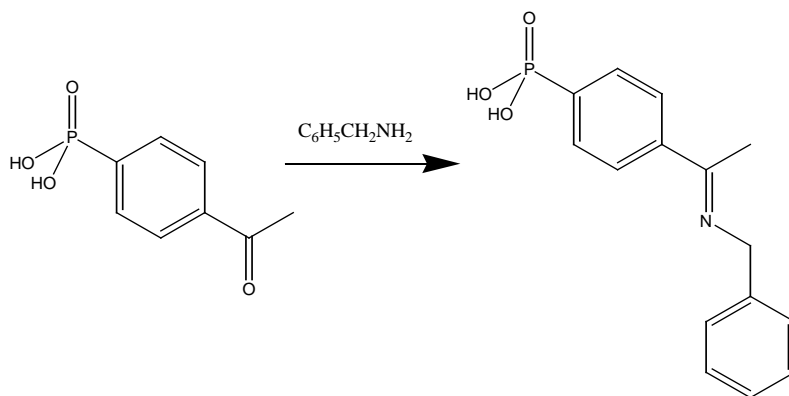


Figure 5.3. Representation of the polyimide species produced by Yang et al.⁶

The reactivity of the ketone groups towards amines was investigated. Firstly the reactivity of 4-acetylphenylphosphonic acid to benzylamine was tested, and in an acetonitrile solution this gave a white precipitate, analysis of which proved it to be the desired imide (Scheme 5.3).



Scheme 5.3. The Reaction of acetophenone phosphonic acid with benzylamine.

A similar reaction was attempted using an acetonitrile solution of $(\text{NR}^1_4)_3\text{H}[\text{SiW}_{10}\text{O}_{36}(\text{H}_3\text{CCOC}_6\text{H}_4\text{PO})_2]$. A small quantity of white precipitate was obtained after stirring the resulting solution overnight; however this precipitate contained no polyoxotungstate. The major product

was obtained as a green solid by evaporation of the remaining solution, and these products (Compound 40 and 41) were analysed by multinuclear NMR (^1H and ^{31}P), IR, MS, EA and Single Crystal XRD.

Crystals of the product had the formula $(\text{NEt}_4)_3(\text{C}_6\text{H}_5\text{CH}_2\text{NH}_3)_3[\text{SiW}_{10}\text{O}_{36}(\text{H}_3\text{CCOC}_6\text{H}_4\text{PO})]$, and the other data agreeing with this result.

^1H NMR. The spectra show peaks due to the appropriate cations (NBu_4^+ or NEt_4^+), the $\text{H}_3\text{CCOC}_6\text{H}_4$ group and the benzylamine molecules. In comparison with the cation peaks the intensities of the $\text{H}_3\text{CCOC}_6\text{H}_4$ group peaks have reduced to approximately half of that for the doubly derivatised product. The peaks have not moved, however a second CH_3 peak is seen at 2.38 ppm showing that two different types of methyl are present; this is explained by some of the $\text{C}=\text{O}$ groups having either reacted or coordinating to benzylamine molecules. The intensity of the benzylamine signals shows that three molecules are present, and if these were all protonated their charges (3+) combined with those for the cations (3+) would balance the charge of the cluster when only one RPO^{2+} group is attached (6-).

^{31}P NMR. The spectra for both salts (NBu_4^+ or NEt_4^+) have one peak at 17.7 ppm, this having shifted from that for $[\text{SiW}_{10}\text{O}_{36}(\text{H}_3\text{CCOC}_6\text{H}_4\text{PO})_2]^{4-}$ (14.0 ppm) as there is no longer a hydrogen-bonding interaction between two $\text{P}=\text{O}$ groups. The hydrogen-coupled spectra shows the peak to have the same coupling as for $[\text{SiW}_{10}\text{O}_{36}(\text{H}_3\text{CCOC}_6\text{H}_4\text{PO})_2]^{4-}$ indicating that the organic group has not changed during the reaction.

IR Spectroscopy. Fewer peaks are observed in the fingerprint region of the IR spectra in comparison to that for the doubly derivatised products. The peak positions are similar to those for the product of the reaction of $[\text{SiW}_{10}\text{O}_{36}(\text{HOOC}(\text{CH}_2)_n\text{PO})_2]^{4-}$ with benzylamine, showing the central cluster to be similar. A greater number of peaks would be expected if the cluster is less

symmetrical than the doubly derivatised structure, however this is not observed perhaps because the signals overlap, with the peaks that are seen being broad. The presence of the R group is confirmed by the C=O stretch at around 1680 cm^{-1} , this has shifted a small amount from that for the starting material (1684 cm^{-1}), but is still indicative of the same organic group.

Mass Spectrometry. The spectra shows peaks due to the cluster with only one RPO group attached to it, but with varying numbers of cations and benzylamine groups.

Elemental Analysis. The percentages of carbon, nitrogen and hydrogen present indicate that the formula is most likely $(\text{NR}_4)_3(\text{C}_6\text{H}_5\text{CH}_2\text{NH}_3)_3[\text{SiW}_{10}\text{O}_{36}(\text{H}_3\text{CCOC}_6\text{H}_4\text{PO})]$ (R=Bu or Et).

Single Crystal X-ray Diffraction. Crystals of the product were obtained by diffusion of diethyl ether into an acetonitrile solution (Table 5.2).

Table 5.2. Crystallographic Data for $(\text{NEt}_4)_3(\text{C}_6\text{H}_5\text{CH}_2\text{NH}_3)_3[\text{SiW}_{10}\text{O}_{36}(\text{H}_3\text{CCOC}_6\text{H}_4\text{PO})]\cdot\text{H}_3\text{CCN}$.

Monoclinic	Spacegroup		C 2/c
Cell axes (\AA)	$a = 60.3009(2)$	$b = 14.6405(5)$	$c = 25.8460(92)$
Cell angles (deg)	$\alpha = 90.00$	$\beta = 108.051(16)$	$\gamma = 90.00$
Cell Volume (\AA^3)	$21694.70(13)$		

[Full details in appendix (Structure 22)]

The $[\text{SiW}_{10}\text{O}_{36}]^{8-}$ cluster has only one $\text{H}_3\text{CCOC}_6\text{H}_4\text{PO}$ group, the two oxygen atoms in the vacant site each hydrogen-bonding to a benzylammonium molecule ($d_{\text{ON}} = 2.80\text{ \AA}$), these amines also hydrogen-bond to the oxygen which are bound to the phosphonate group ($d_{\text{ON}} \sim 2.80\text{ \AA}$) (Figure 5.4).

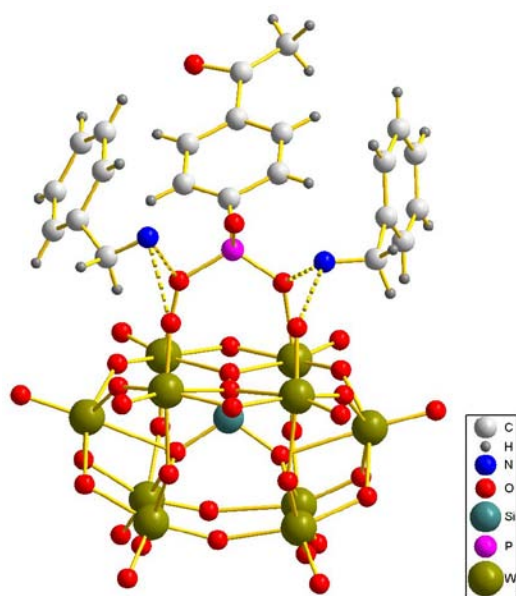


Figure 5.4. The structure of $[\text{SiW}_{10}\text{O}_{36}(\text{H}_3\text{CCOC}_6\text{H}_4\text{PO})]^{6-} \cdot (\text{C}_6\text{H}_5\text{CH}_2\text{NH}_3^+)_2$ showing the hydrogen-bonding between the cluster and the benzylammonium.

The $\text{H}_3\text{CCOC}_6\text{H}_4$ group is parallel to another group on a second cluster, these groups being out of line so not π -bonding (Figure 5.5). Pairs of clusters arranged like this form layers, alternating layers being a mirror image of the first (Figure 5.6).

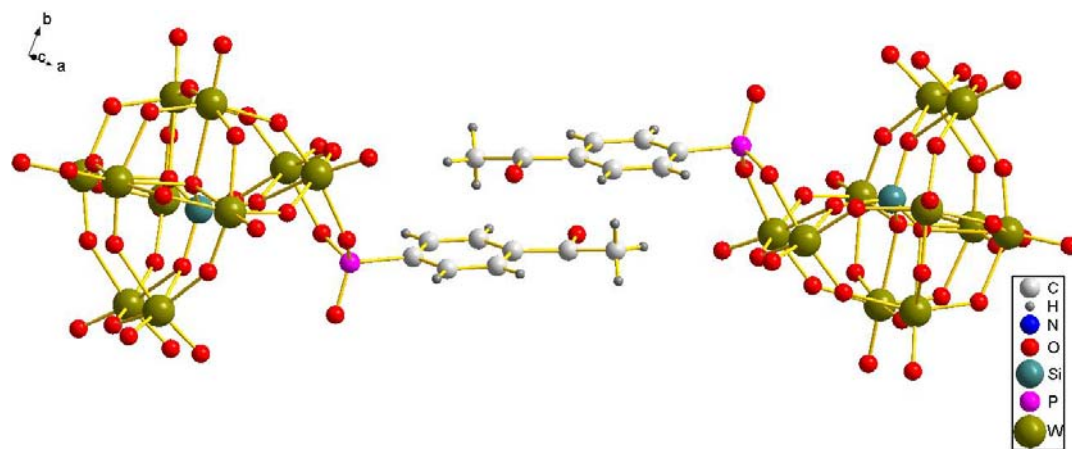


Figure 5.5. The arrangement of clusters in the crystal structure.

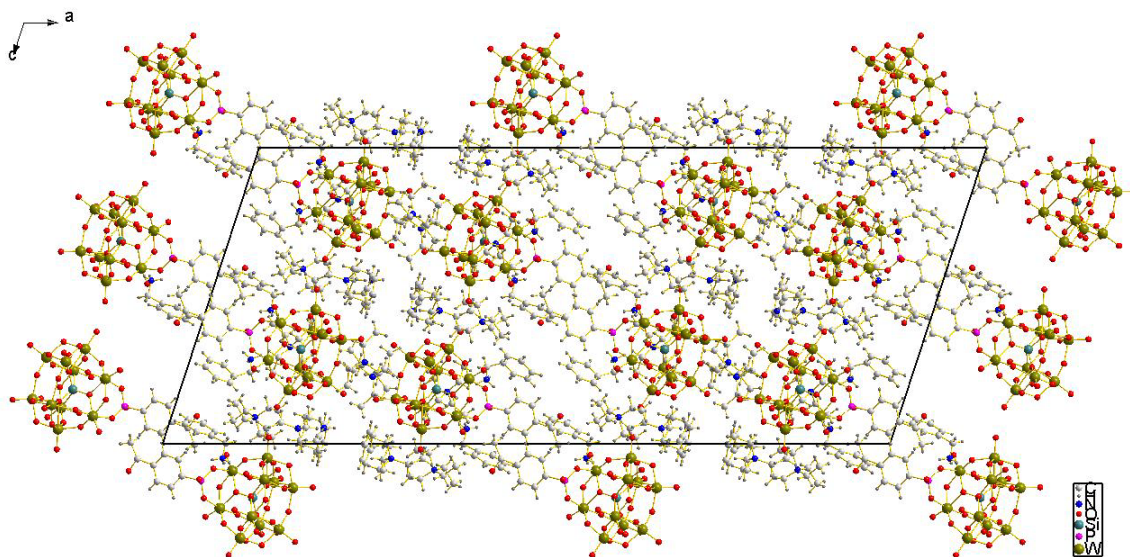


Figure 5.6. The crystal structure viewed along the b-axis.

5.1.3 Loss of R group

In all examples ($R = \text{HOOC}(\text{CH}_2)_n$ ($n=1$ or 2) or $\text{H}_3\text{CCOC}_6\text{H}_4$) the addition of benzylamine has the effect of removing one of the ‘ RPO^{2+} ’ groups from the polyoxotungstate framework and producing a singly derivatised unit. The effect of benzylamine was tested on various other derivatives which would not react with the amine ($\text{CH}_2=\text{CHCH}_2$, $\text{CH}_2=\text{CH}$ or Et) (Compounds 42-44).

^1H NMR. The ^1H NMR spectra shows the intensities of the ‘R group’ peaks to have reduced by approximately half in comparison with the cation peaks, this observation indicates that the benzylamine has had the effect of removing a RPO^{2+} group even though the R groups are not reactive towards amines. The position of the R group peaks has shifted to a slightly lower ppm value, due to a change in the environment around the phosphorus, the position of the peaks being slightly less positive than for the phosphonic acids. Peaks due to benzylamine are present, their intensity indicating that approximately three molecules are present per cluster.

^{31}P NMR. The spectra show one peak, indicating that a single product is formed, the position of the peak has shifted compared to the doubly derivatised cluster being at a slightly higher ppm value than for the phosphonic acids, this implies that the $\text{P}=\text{O}$ group no longer takes part in hydrogen-bonding, the position determined by the organic group and interactions with the solvent and amine.

IR Spectroscopy. The fingerprint region of the IR spectrum is simpler than for the doubly derivatized clusters being similar to the other products after reaction with benzylamine.

Mass Spectrometry. The mass spectra for the vinyl and allyl derivatives only show peaks for the $[\text{SiW}_{10}\text{O}_{36}]^{8-}$ cluster with no RPO groups, this shows the instability of the product under ionization conditions. When $\text{R} = \text{Et}$ the peaks are all due to $[\text{SiW}_{10}\text{O}_{36}(\text{EtPO})]^{6-}$ with varying numbers of NBu_4^+ and benzylammonium cations, confirming the production of a singly derivatised cluster.

Elemental Analysis. The percentages of carbon, nitrogen and hydrogen observed in the products are greater than that calculated for salts of the formula $(\text{NR}_4)_3(\text{C}_6\text{H}_5\text{CH}_2\text{NH}_3)_3[\text{SiW}_{10}\text{O}_{36}(\text{RPO})]$, probably due to extra benzylamine as in some cases the intensity of the benzylamine peaks is approximate.

Electrochemistry. Cyclic voltammetry of $(\text{NBu}_4)_3(\text{C}_6\text{H}_5\text{CH}_2\text{NH}_3)_3[\text{SiW}_{10}\text{O}_{36}(\text{H}_2\text{C}=\text{CHC}_6\text{H}_4\text{PO})]$ shows that the electrochemical properties of the cluster has changed; four peaks are seen between -0.9 and -1.7 V (Figure 5.7), their positions being more negative than for the fully saturated structure, meaning that reduction is more difficult. This is due to the increased charge of the cluster making the addition of extra electrons more difficult, and is a similar effect to when octahedra are lost from a fully saturated cluster.^{7,8,9}

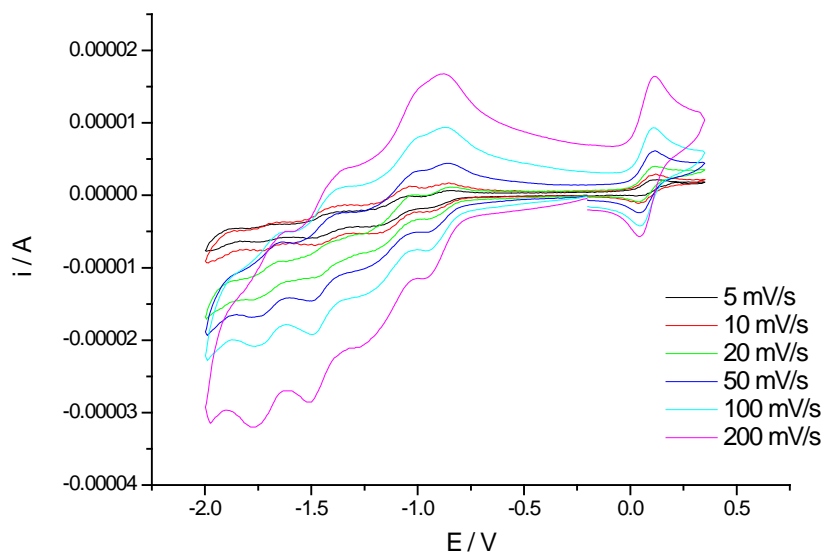


Figure 5.7. The cyclic voltammogram for $(\text{NBu}_4)_3(\text{C}_6\text{H}_5\text{CH}_2\text{NH}_3)_3[\text{SiW}_{10}\text{O}_{36}(\text{H}_2\text{C}=\text{CHC}_6\text{H}_4\text{PO})]$.

Single Crystal X-ray Diffraction. Attempts to obtain crystals for all of the mono-substituted species were unsuccessful, the solids obtained being unstable.

For all R groups the loss of an ‘RPO’ group was observed after reaction with benzylamine, showing that the group is not lost due to a reaction producing a large organic group which then ‘falls off’. The benzylamine alters the pH of the solution making it very basic (pH = 11-12) and this pH change results in the loss of the RPO group in a similar way to how the pH affects the formation of polyoxotungstates (Table 5.3). The singly derivatised product is stable at pH 11-12, so the second RPO group is not lost and a pure product is formed.

Table 5.3. The initial and final pH of the acetonitrile solution of $(\text{NR}_4)_3\text{H}[\text{SiW}_{10}\text{O}_{36}(\text{R}^1\text{PO})_2]$ upon addition of benzylamine.

	Original pH	+ benzylamine
$(\text{NEt}_4)_3\text{H}[\text{SiW}_{10}\text{O}_{36}(\text{H}_3\text{CCOC}_6\text{H}_4\text{PO})_2]$	3.0	11.0
$(\text{NBu}_4)_3\text{H}[\text{SiW}_{10}\text{O}_{36}(\text{H}_3\text{CCOC}_6\text{H}_4\text{PO})_2]$	3.7	11.9
$(\text{NEt}_4)_3\text{H}[\text{SiW}_{10}\text{O}_{36}(\text{H}_2\text{C}=\text{CHPO})_2]$	3.9	11.5
$(\text{NEt}_4)_3\text{H}[\text{SiW}_{10}\text{O}_{36}(\text{H}_2\text{C}=\text{CHCH}_2\text{PO})_2]$	2.7	11.4

pH. The effect of pH was investigated to see if other bases have the same effect on the polyoxotungstate (Table 5.4).

Table 5.4. The initial and final pH of the acetonitrile solution of $(\text{NR}_4)_3\text{H}[\text{SiW}_{10}\text{O}_{36}(\text{R}^1\text{PO})_2]$ upon addition of different reactants.

$(\text{NEt}_4)_3\text{H}[\text{SiW}_{10}\text{O}_{36}(\text{H}_2\text{C}=\text{CHCH}_2\text{PO})_2]$	Original pH	Final pH
+ benzylamine	2.7	11.4
+ butylamine	2.7	12.0
+ KOH (H_2O solution)	2.6	12.3

Butylamine has the same effect as benzylamine, the intensities of the ^1H NMR peaks indicating that one RPO group is present per three NBu_4^+ cations and that three butylamine molecules are also present (Compound 45). The IR spectrum is similar to that for the product obtained from the reaction with benzylamine, showing that the cluster has the same structure.

When using KOH to give the desired pH the product obtained was soluble in water. The ^1H NMR spectrum showed the NEt_4 and $\text{C}_3\text{H}_5\text{PO}$ peaks to be in the same ratio as before the reaction, however this does not prove that the product is still doubly derivatised, as ion exchange could have occurred with K^+ ions replacing some NEt_4^+ cations and altering the expected ratio of intensities. ^{31}P NMR shows one peak at 19.3 ppm, showing one type of $\text{H}_2\text{C}=\text{CHCH}_2\text{PO}$ group to be present, the position is different to positions observed previously (Table 5.5) most probably due to OH^- ions which are still present interacting with the oxygen atoms on the phosphorus.

Table 5.5. The positions of the phosphorus peak in the ^{31}P NMR spectrum.

	^{31}P NMR peak position/ppm (solvent)
$\text{H}_2\text{C}=\text{CHCH}_2\text{PO}(\text{OH})_2$	27.70 (D_2O)
$(\text{NEt}_4)_3\text{H}[\text{SiW}_{10}\text{O}_{36}(\text{C}_3\text{H}_5\text{PO})_2]$	24.64 (CD_3CN)
$(\text{NEt}_4)_3(\text{C}_6\text{H}_5\text{CH}_2\text{NH}_3)_3[\text{SiW}_{10}\text{O}_{36}(\text{C}_3\text{H}_5\text{PO})]$	28.34 (CD_3CN)
Product from reaction with KOH	19.31 (D_2O)

It was not possible to separate the product from the KOH reaction from any side products, all being soluble in the same solvents. The ^{31}P NMR spectrum has one peak, meaning that there is one phosphorus environment, which indicates that either no reaction has occurred or that none of the RPO groups are attached to the polyoxotungstate, because if a mono-substituted product had been obtained this would be present along with the RPO group that had been removed and two peaks would be seen.

5.1.3.1 Reaction of product

Once a singly derivatised cluster $[\text{SiW}_{10}\text{O}_{36}(\text{RPO})]^{6-}$ containing a vacant site is formed, this cluster can react further introducing the possibility of producing a cluster which is derivatised with two different groups. Hence we used our $(\text{NR}_4)_3(\text{C}_6\text{H}_5\text{CH}_2\text{NH}_3)_3[\text{SiW}_{10}\text{O}_{36}(\text{R}^1\text{PO})]$ products and reacted them with a different organo-phosphonic acid using a similar reaction to that for forming the doubly derivatized $[\text{SiW}_{10}\text{O}_{36}(\text{RPO})_2]^{4-}$. A large range of different structures were obtained of general formula $(\text{NR}_4)_3\text{H}[\text{SiW}_{10}\text{O}_{36}(\text{R}^1\text{PO})(\text{R}^2\text{PO})]$ ($\text{R} = \text{Et}$ or Bu ; R^1 and $\text{R}^2 = \text{Et}$, $\text{H}_2\text{C}=\text{CH}$, $\text{H}_2\text{C}=\text{CHCH}_2$, $\text{HOOC}(\text{CH}_2)_n$ ($n = 1$ or 2), $\text{H}_3\text{CCOC}_6\text{H}_4$ or $\text{H}_2\text{C}=\text{CHC}_6\text{H}_4$) (Compounds 46-49).

^1H NMR. In most cases the cations used were NEt_4^+ , these products being more likely to form crystals (Section 2.4.1). The two peaks due to these cations are observed in the spectra along with ones due to the appropriate R groups and a small quantity of benzylamine. The R group peaks are in approximately the correct ratio to indicate a 1:1 ratio of the two groups, although in a couple of examples the peaks for the second R group are slightly small, showing that the addition of the second group is more difficult than the first, especially when a bulky group such as $\text{H}_3\text{CCOC}_6\text{H}_4$ is involved. The reaction also appears to be more difficult when $\text{R}^2 =$

HOOCCH₂, which we attribute to the low solubility of the phosphonic acid HOOCCH₂PO(OH)₂, although the correct product is obtained when using a large excess of the acid.

Most examples show a small quantity of benzylamine (up to ~3/4 of a molecule per three NEt₄⁺ cations). As the benzylamine had been protonated in the previous step and formed benzylammonium we might expect for some to still be present, even when a great excess of NEt₄⁺ cations are present.

Taking (NEt₄)₃H[SiW₁₀O₃₆(H₃CCOC₆H₄PO)(H₂C=CHCH₂PO)] as an example, the spectrum shows the R groups with intensities in a 1:1 ratio (Figure 5.8).

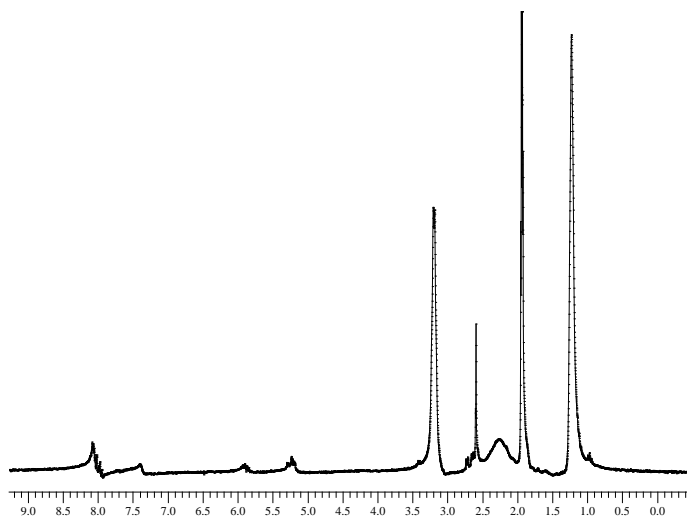


Figure 5.8. The ¹H NMR Spectrum for (NEt₄)₃H[SiW₁₀O₃₆(H₃CCOC₆H₄PO)(H₂C=CHCH₂PO)], assignments CH₃ (2.60), C₆H₄ (7.35-8.30), CH₂ (2.65), H₂C=CH (5.15-5.35) and H₂C=CH (5.80-6.03 ppm).

³¹P NMR. All the spectra show two phosphorus environments, one from each RPO group. They are in an approximately equal ratio (the R²PO peak sometimes slightly smaller). Some spectra also show a peak from the [SiW₁₀O₃₆(R¹PO)]⁴⁻ cluster showing that the reaction has not gone to completion, however these are small. The position of the phosphorus peaks vary for the RPO group from that observed in the symmetric structures; the reason for this is unclear, but is perhaps due to the inductive effects of the different R groups altering the interaction between the

two P=O groups. Taking the example $(\text{NEt}_4)_3\text{H}[\text{SiW}_{10}\text{O}_{36}(\text{H}_3\text{CCOC}_6\text{H}_4\text{PO})(\text{H}_2\text{C}=\text{CHCH}_2\text{PO})]$, the $\text{H}_3\text{CCOC}_6\text{H}_4\text{PO}$ peak is at 12.5 ppm (intensity 1) having shifted to a less positive ppm compared to previous examples and the $\text{H}_2\text{C}=\text{CHCH}_2\text{PO}$ peak is at 26.5 ppm (intensity 0.8) having shifted to a more positive value compared to $[\text{SiW}_{10}\text{O}_{36}(\text{H}_2\text{C}=\text{CHCH}_2\text{PO})_2]^{4-}$ (24.6 ppm). These shifts show that the $\text{H}_3\text{CCOC}_6\text{H}_4\text{PO}$ phosphorus is less shielded by electrons than previously and the $\text{H}_2\text{C}=\text{CHCH}_2\text{PO}$ phosphorus is more shielded, perhaps showing that a H^+ between the P=O groups is associated more closely with the $\text{H}_3\text{CCOC}_6\text{H}_4\text{PO}$ group.

IR Spectroscopy. The spectra are similar to those for $(\text{NR}_4)_3\text{H}[\text{SiW}_{10}\text{O}_{36}(\text{R}^1\text{PO})_2]$, the peaks in the fingerprint region being in the same positions as when both the R groups are the same, showing that the pseudosymmetry of the polyoxotungstate cluster is similar and unaffected by which RPO groups are present. Peaks are present due to the R groups, for example a C=O peak when $\text{R} = \text{HOOC}(\text{CH}_2)_n$ or $\text{H}_3\text{CCOC}_6\text{H}_4$.

Mass Spectrometry. The spectra show peaks due to the complete $[\text{SiW}_{10}\text{O}_{36}(\text{R}^1\text{PO})(\text{R}^2\text{PO})]^{4-}$ unit with varying numbers of cations (Figure 5.9), this confirms that two different R groups are attached to the cluster.

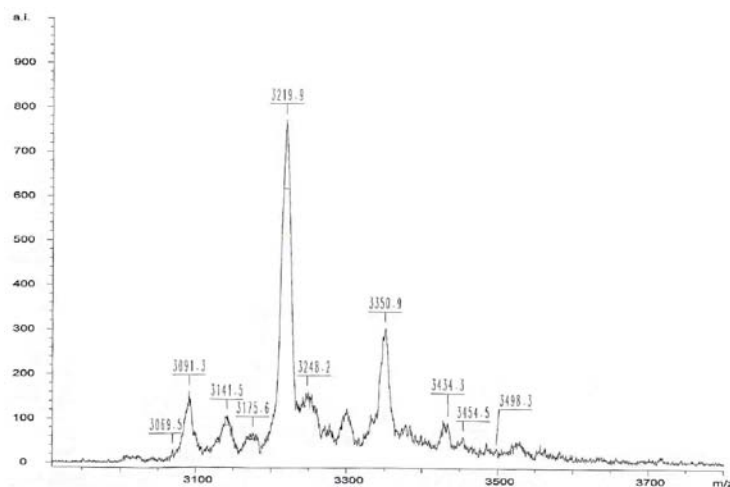


Figure 5.9. The Mass spectrum of $(\text{NEt}_4)_3\text{H}[\text{SiW}_{10}\text{O}_{36}(\text{H}_3\text{CCOC}_6\text{H}_4\text{PO})(\text{H}_2\text{C}=\text{CHCH}_2\text{PO})]$.

Some spectra are noisier than others with parts or whole RPO groups being lost, the most common groups to fragment being $\text{H}_3\text{CCOC}_6\text{H}_4$, (the H_3C or H_3CCO being easily lost) and $\text{HOOCCH}_2\text{CH}_2$ (where the HOOC with none, one or two CH_2 groups can be lost).

Elemental Analysis. The percentages of carbon, nitrogen and hydrogen in the products are higher than predicted for the formula $(\text{NR}_4)_3\text{H}[\text{SiW}_{10}\text{O}_{36}(\text{R}^1\text{PO})(\text{R}^2\text{PO})]$, which can be explained by the small quantity of benzylammonium indicated in the ^1H NMR spectra. The results indicate that three NR_4^+ cations are present per cluster, this being the same as for the doubly derivatised clusters with the formula $(\text{NR}_4)_3\text{H}[\text{SiW}_{10}\text{O}_{36}(\text{R}^1\text{PO})_2]$.

Electrochemistry. Cyclic Voltammetry was carried out for $(\text{NBu}_4)_3\text{H}[\text{SiW}_{10}\text{O}_{36}(\text{H}_2\text{C}=\text{CHC}_6\text{H}_4\text{PO})(\text{EtPO})]$ using the same conditions as previously (Ag/AgCl reference electrode) (Figure 5.10). Using Ferrocene as an internal reference the results are compared, the electrochemical properties being similar to the doubly derivatised clusters so showing that the structure is similar. The position of the peak potentials for the mixed group cluster are between those for the clusters where $\text{R}^1=\text{R}^2$ (Table 5.6), the electron withdrawing/donating properties of the two groups being an average for the groups individually.

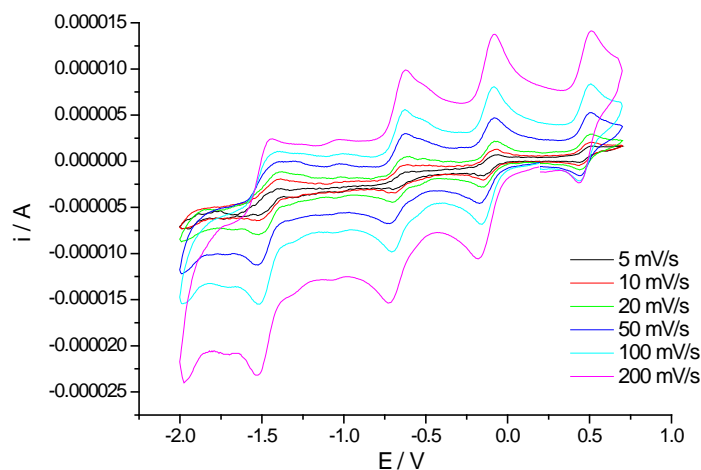


Figure 5.10. The cyclic voltammogram for $(\text{NBu}_4)_3\text{H}[\text{SiW}_{10}\text{O}_{36}(\text{H}_2\text{C}=\text{CHC}_6\text{H}_4\text{PO})(\text{EtPO})]$.

Table 5.6. The peak potentials for (NBu₄)₃H[SiW₁₀O₃₆(R¹PO)(R²PO)].

R ¹	R ²	E(3) / (mV)	E(2) / (mV)	E(1) / (mV)	E(ferrocene)
Et	Et	-2144	-1186	-623	0
H ₂ C=CHC ₆ H ₄	H ₂ C=CHC ₆ H ₄	-1869	-1118	-560	0
H ₂ C=CHC ₆ H ₄	Et	-1945	-1136	-589	0

Single Crystal X-ray Diffraction. Attempts were made to obtain crystals from all the products produced, but only (NEt₄)₃H[SiW₁₀O₃₆(H₂C=CHCH₂PO)(HOOCCH₂CH₂PO)] (Table 5.8) and (NEt₄)₃H[SiW₁₀O₃₆(H₂C=CHPO)(H₂C=CHCH₂PO)] (Table 5.9) gave crystals suitable for XRD. For (NEt₄)₃H[SiW₁₀O₃₆(H₂C=CHPO)(HOOCCH₂CH₂PO)] crystals were obtained, but these were unstable so only the unit cell could be determined (Table 5.7).

Table 5.7. Crystallographic Data for (NEt₄)₃H[SiW₁₀O₃₆(H₂C=CHPO)(HOOC(CH₂)₂PO)]₂.

Hexagonal			
Cell axes (Å)	<i>a</i> = 13.22(5)	<i>b</i> = 13.22(5)	<i>c</i> = 22.03(5)
Cell angles (deg)	<i>α</i> = 90.0	<i>β</i> = 90.0	<i>γ</i> = 120.0

Table 5.8. Crystallographic Data for (NEt₄)₃H[SiW₁₀O₃₆(H₂C=CHCH₂PO)(HOOC(CH₂)₂PO)]₂.O(CH₂CH₃)₂.

Triclinic	Spacegroup		P 1
Cell axes (Å)	<i>a</i> = 24.7346(5)	<i>b</i> = 10.8297(19)	<i>c</i> = 14.7072(3)
Cell angles (deg)	<i>α</i> = 90.00	<i>β</i> = 107.419(3)	<i>γ</i> = 90.00
Cell Volume (Å ³)	3758.93(39)		

[Full details in appendix (Structure 23)]

The structure for (NEt₄)₅H₃[SiW₁₀O₃₆(H₂C=CHCH₂PO)(HOOC(CH₂)₂PO)]₂.O(CH₂CH₃)₂ shows the cluster to have similar structural features to the other doubly derivatised structures although the two R groups are different (Figure 5.11). The difference in the R groups can be seen

in the crystal structure with extra oxygen atoms from the carboxylic acid group on only one side of each cluster, these oxygen atoms have full occupancy so showing that the atoms are real.

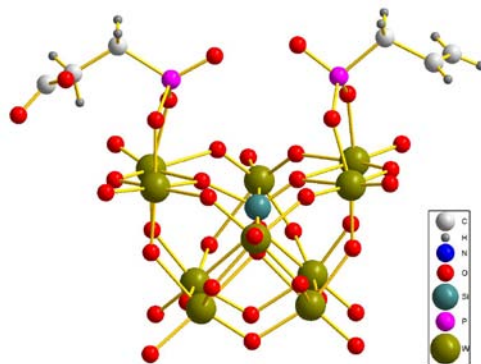


Figure 5.11. The anion structure of $[\text{SiW}_{10}\text{O}_{36}(\text{H}_2\text{C}=\text{CHCH}_2\text{PO})(\text{HOOC}(\text{CH}_2)_2\text{PO})]^{4-}$.

The asymmetric unit contains two clusters. Although the $[\text{SiW}_{10}\text{O}_{36}]^{8-}$ clusters are related by symmetry the R groups reduce this symmetry, the structure was solved using the P-1 space group so as to see all the detail of the clusters. The unit cell parameters are similar to those for $(\text{NEt}_4)_3\text{H}[\text{SiW}_{10}\text{O}_{36}(\text{RPO})_2]$ (R = $\text{H}_2\text{C}=\text{CHCH}_2$ or $\text{HOOC}(\text{CH}_2)_n$ (n = 1 or 2) the clusters forming layers made up of columns with the R groups pointing towards one another (Figure 5.12) (Section 2.4.1).

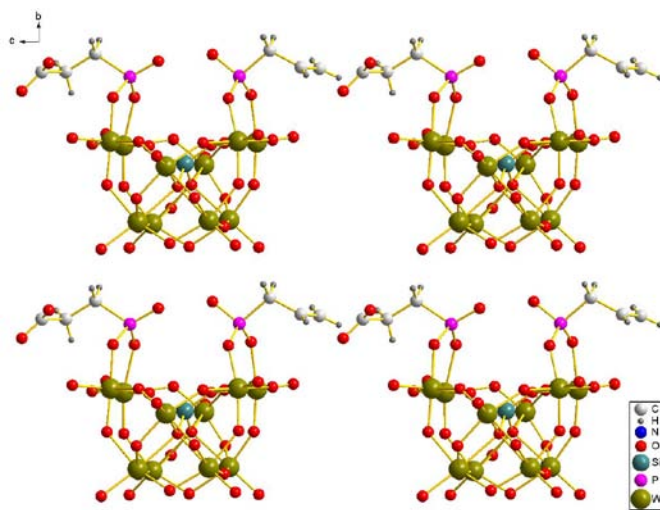


Figure 5.12. The crystal structure of $(\text{NEt}_4)_3\text{H}[\text{SiW}_{10}\text{O}_{36}(\text{H}_2\text{C}=\text{CHCH}_2\text{PO})(\text{HOOC}(\text{CH}_2)_2\text{PO})]_2 \cdot \text{O}(\text{CH}_2\text{CH}_3)_2$ viewed along the a -axis.

All the clusters within a layer are related by translation with an allyl and carboxylic acid group pointing towards one another (4.0 Å between the groups). The alternating layers are made up of clusters which are arranged with the R groups on the opposite sides to the first layer, the asymmetric unit containing one cluster from each of these two layers.

Crystals were also obtained for $(\text{NEt}_4)_3\text{H}[\text{SiW}_{10}\text{O}_{36}(\text{H}_2\text{C}=\text{CHPO})(\text{H}_2\text{C}=\text{CHCH}_2\text{PO})]$.

Table 5.9. Crystallographic Data for $(\text{NEt}_4)_3\text{H}[\text{SiW}_{10}\text{O}_{36}(\text{H}_2\text{C}=\text{CHPO})(\text{H}_2\text{C}=\text{CHCH}_2\text{PO})]$.

Orthorhombic	Spacegroup		
	P 2 n n		
Cell axes (Å)	$a = 10.6890(15)$	$b = 16.0329(19)$	$c = 19.3747(2)$
Cell angles (deg)	$\alpha = 90.00$	$\beta = 90.00$	$\gamma = 90.00$
Cell Volume (Å ³)	3320.35(6)		

[Full details in appendix (Structure 24)]

The structure shows the polyoxotungstate cluster to have retained its α -symmetry, having a spacegroup of P 2 n n and the asymmetric unit containing only half a cluster. The R groups are disordered between the two sites on top of the cluster, the third carbon on the allyl having a occupancy of a half, with the first two carbons for the allyl and those for the vinyl group appearing in the same position, although the bond lengths for these two groups will be different, this is seen by the elongated shape of second carbon in the chain (Figure 5.13).

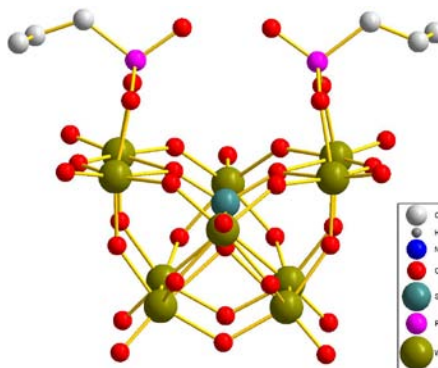


Figure 5.13. The structure of $[\text{SiW}_{10}\text{O}_{36}(\text{H}_2\text{C}=\text{CHPO})(\text{H}_2\text{C}=\text{CHCH}_2\text{PO})]^{4-}$ without hydrogen atoms.

The long range order within the crystal structure is different to those for the other doubly derivatised compounds, the clusters are in columns all pointing in the same direction, the unit cell having a cluster at each corner and one in the centre, the space between the clusters being filled by NEt_4^+ cations and solvent molecules (Figure 5.14).

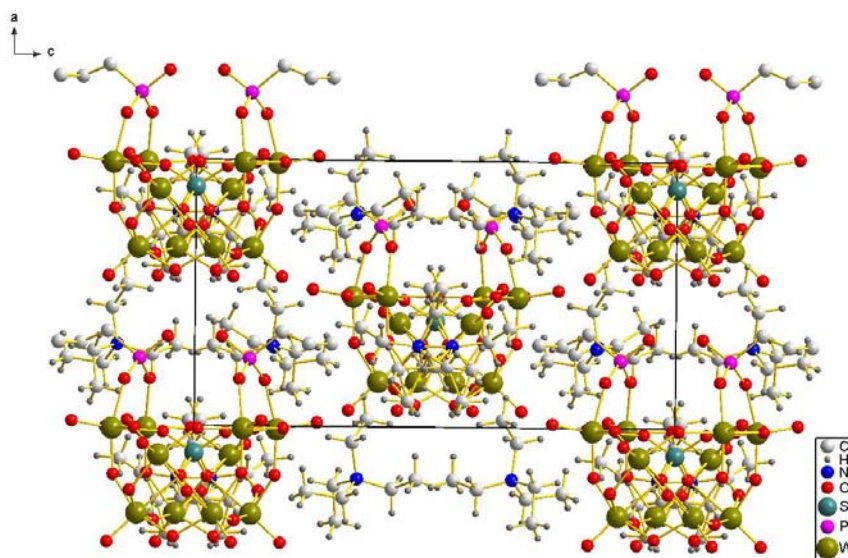


Figure 5.14. The crystal structure of $(\text{NEt}_4)_3\text{H}[\text{SiW}_{10}\text{O}_{36}(\text{H}_2\text{C}=\text{CHPO})(\text{H}_2\text{C}=\text{CHCH}_2\text{PO})]$ viewed along the b -axis.

5.1.3.2 Polymerisation

When the organic groups on the polyoxotungstate clusters contain double bonds they have the potential to be polymerised. It has been demonstrated (Chapter 4) that the styryl group could be polymerised to the greatest extent, therefore this group will be studied again. If the other group on the cluster is not reactive under the conditions used then a single chain polymer with the polyoxotungstates as pendants will be formed; ethyl was chosen as the second group, although changing this group could provide a further way to tailor the properties of the polymer produced.

The polyoxotungstate $[\text{SiW}_{10}\text{O}_{36}(\text{H}_2\text{C}=\text{CHC}_6\text{H}_4\text{PO})(\text{EtPO})]^{4-}$ has NBu_4^+ cations associated with it, these giving the best solubility so making the product easier to analyse.

^1H NMR. The spectrum for $(\text{NBu}_4)_3\text{H}[\text{SiW}_{10}\text{O}_{36}(\text{H}_2\text{C}=\text{CHC}_6\text{H}_4\text{PO})(\text{EtPO})]$ shows four environments due to the NBu_4^+ cations, the peaks due to the ethyl group which are partially hidden by these larger signals and the styryl group signals which are easily seen (between 5.30-7.95 ppm).

The effect of heating the cluster under polymerisation conditions (degassed, AIBN) was studied, comparing the intensities of the vinylic hydrogen to those for the ring (Figure 5.15). It is seen that the vinylic peaks reduce in size over time indicating that polymerisation occurs.

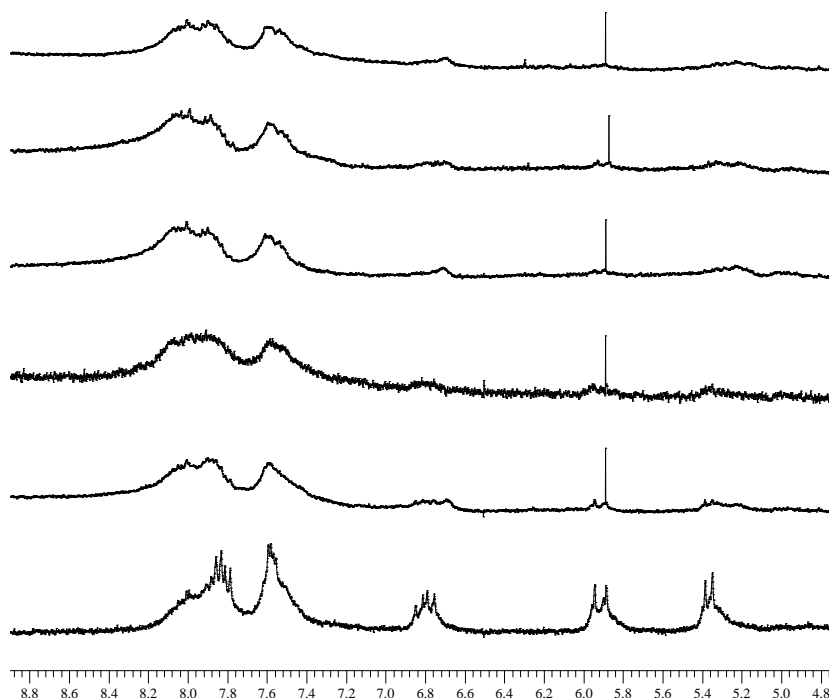


Figure 5.15. The styryl region of the ^1H NMR after 0 (bottom), 4, 8, 18, 24 and 48 hours.

Polymerisation increases until a maximum of 75 % is reached after 6 hours (Figure 5.16). This polymerisation is comparable to that for the doubly derivatised styryl alternative $(\text{NBu}_4)_3\text{H}[\text{SiW}_{10}\text{O}_{36}(\text{H}_2\text{C}=\text{CHC}_6\text{H}_4\text{PO})_2]$ (80 %), although it is reached in a shorter time (6 vs. 18

hours). As a less cross-linked product is produced a greater degree of polymerisation might have been expected, however this was not seen perhaps because when two groups are present the double bonds are held quite far apart and the reactions are independent.

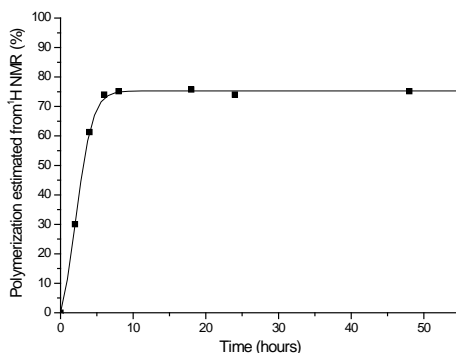


Figure 5.16. A graph showing the polymerisation for $(\text{NBu}_4)_3\text{H}[\text{SiW}_{10}\text{O}_{36}(\text{H}_2\text{C}=\text{CHC}_6\text{H}_4\text{PO})(\text{EtPO})]$ estimated from ^1H NMR spectroscopy.

^{31}P NMR. The monomer $(\text{NBu}_4)_3\text{H}[\text{SiW}_{10}\text{O}_{36}(\text{H}_2\text{C}=\text{CHC}_6\text{H}_4\text{PO})(\text{EtPO})]$ shows two main peaks in the ^{31}P NMR spectrum at 32.0 (EtPO (intensity 1) and 12.2 ppm ($\text{H}_2\text{C}=\text{CHC}_6\text{H}_4\text{PO}$ (intensity 1)), there are also some small peaks from impurities which could not be removed. After polymerisation for 2 hours, extra peaks are seen around the original positions; after 18 hours no sharp peaks are present and instead broad signals centred around the positions of the original peaks are seen. These broad signals show that the product has a reduced mobility compared with the monomer.

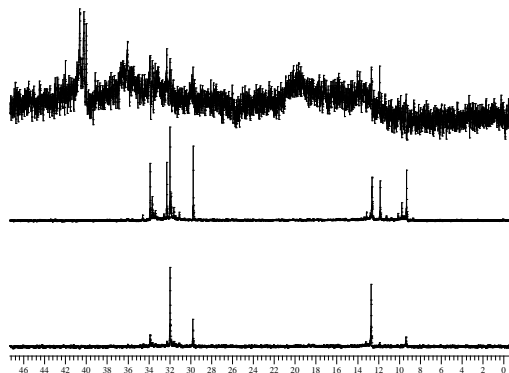


Figure 5.17. The ^{31}P NMR spectra after 0, 2 and 18 hours.

IR Spectroscopy. The spectra do not change significantly upon polymerisation, showing the doubly derivatised cluster to still be present. The only expected change is the reduction of the C=C bond signal, the signal is weak so this is not very clear.

Mass Spectrometry. The spectra for polymers obtained after 6 and 18 hours were taken, with the main set of signals between 3600-4500 m/z similar to those for the monomer. However a few extra peaks are observed, which may be assigned to $[M^+ + H_2C=CHC_6H_4(PO)]$, therefore showing that a connection has been formed between the styryl groups, the ionisation conditions for mass spectrometry causing R-PO-W bonds to break. For the polymer formed after 6 hours there are weak signals between 6500-7500 m/z , which show that a small number of dimers remaining after ionisation.

Elemental Analysis. An increase in the quantity of carbon and hydrogen present in the polymer is seen compared with the monomer species; this is most likely due to solvent as any initiator (AIBN) remaining in the product would also increase the percentage of nitrogen present. The product was dried for three days which should have removed any solvent, however the large polymeric product may have caused some solvent to become trapped.

UV/vis Spectroscopy. The styryl group can be seen on the UV/vis spectra with $\lambda_{\max} = 252.5 \text{ nm}$ ($\epsilon = 45000 \text{ Lmol}^{-1}\text{cm}^{-1}$), polymerisation should cause this peak to reduce in intensity as the styryl group is replaced with a non-conjugated phenyl group (for which λ_{\max} is shorter). However as the polymerisation time increases the peak shifts to a longer wavelength ($\lambda_{\max} = 272.5 \text{ nm}$ ($\epsilon = 48500 \text{ Lmol}^{-1}\text{cm}^{-1}$)) and a second more intense peak is seen ($\lambda_{\max} = 222.5 \text{ nm}$ ($\epsilon = 190000 \text{ Lmol}^{-1}\text{cm}^{-1}$)) (Figure 5.18).

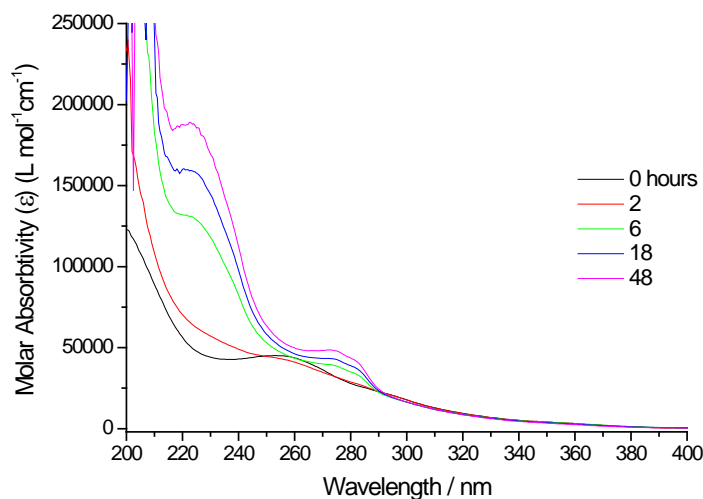


Figure 5.18. The UV/vis spectra for $(\text{NBu}_4)_3\text{H}[\text{SiW}_{10}\text{O}_{36}(\text{H}_2\text{C}=\text{CHC}_6\text{H}_4\text{PO})(\text{EtPO})]$ after polymerisation for 0, 2, 6, 18 and 48 hours.

Electrochemistry. Cyclic voltammetry shows the polymer formed from $(\text{NBu}_4)_3\text{H}[\text{SiW}_{10}\text{O}_{36}(\text{H}_2\text{C}=\text{CHC}_6\text{H}_4\text{PO})(\text{EtPO})]$ to have the same electrochemical properties as the monomer unit (Figure 5.19, Figure 5.20, Table 5.10), showing that the central polyoxotungstate unit is unaffected by the polymerisation reaction and gives a polymeric product with the potential for use as a catalyst. The peaks are broader and not as well defined as for the monomer as the clusters are less mobile.

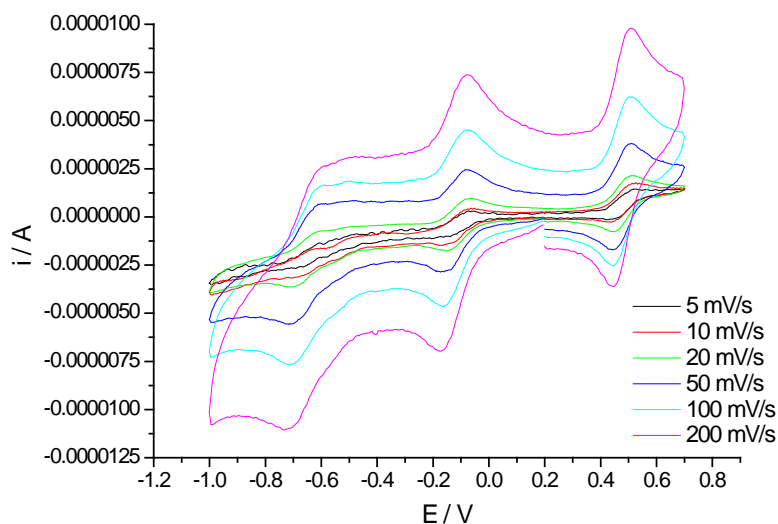


Figure 5.19. The cyclic voltammogram of $(\text{NBu}_4)_3\text{H}[\text{SiW}_{10}\text{O}_{36}(\text{H}_2\text{C}=\text{CHC}_6\text{H}_4\text{PO})(\text{EtPO})]$ between -1.0 and 0.7 V.

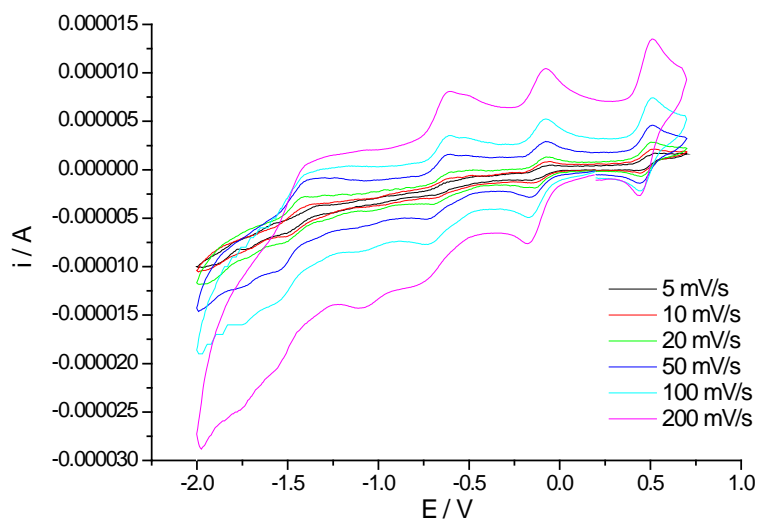


Figure 5.20. The cyclic voltammogram of $(\text{NBu}_4)_3\text{H}[\text{SiW}_{10}\text{O}_{36}(\text{H}_2\text{C}=\text{CHC}_6\text{H}_4\text{PO})(\text{EtPO})]$ between -2.0 and 0.7 V.

Table 5.10. The potential positions for the monomer and polymer of $(\text{NBu}_4)_3\text{H}[\text{SiW}_{10}\text{O}_{36}(\text{H}_2\text{C}=\text{CHC}_6\text{H}_4\text{PO})(\text{EtPO})]$.

	E(3) / (mV)	E(2) / (mV)	E(1) / (mV)	E (ferrocene)
Monomer	-1945	-1136	-589	0
Polymer	-1934	-1131	-594	0

In conclusion the evidence suggests that a polymerisation reaction has occurred, with the polyoxotungstate cluster remaining intact, and its basic structure and electrochemical properties are unchanged.

5.1.3.3 Co-polymerization

Attempts to produce co-polymers containing $(\text{NBu}_4)_3\text{H}[\text{SiW}_{10}\text{O}_{36}(\text{H}_2\text{C}=\text{CHC}_6\text{H}_4\text{PO})(\text{EtPO})]$ and either ethyl acrylate or methyl methacrylate were made. This will produce a polymer chain with polyoxotungstate pendants, the space between the clusters increasing and the properties of the co-monomer being introduced.

^1H NMR. The styryl region of the ^1H NMR spectra (Figure 5.21) shows the vinylic hydrogen peaks to have reduced in intensity compared to those for the

(NBu₄)₃H[SiW₁₀O₃₆(H₂C=CHC₆H₄PO)(EtPO)] monomer, and these peaks and those due to the ring have broadened.

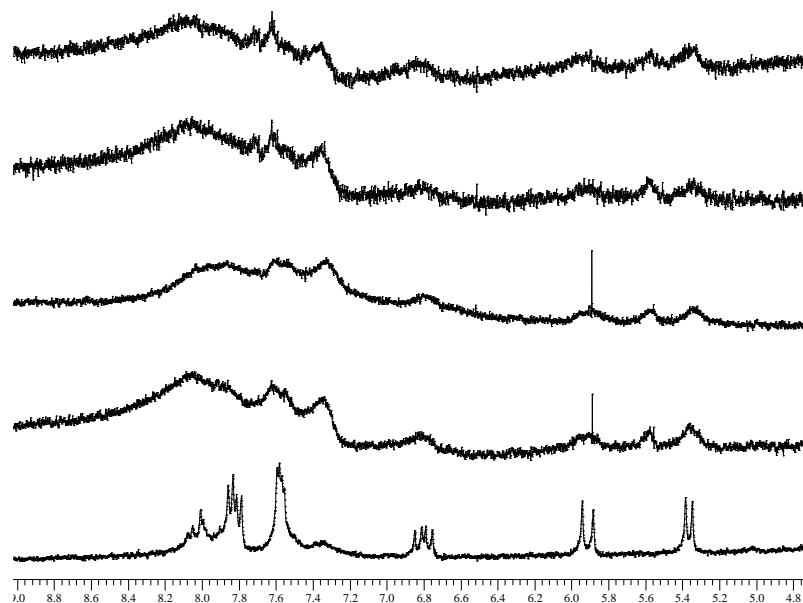


Figure 5.21. ¹H NMR Spectra (5.0 – 9.0 ppm) for the co-polymer made from (NBu₄)₃H[SiW₁₀O₃₆(H₂C=CHC₆H₄PO)(EtPO)] and methyl methacrylate showing the monomer and polymer with ratio's (1:2, 1:5, 1:10 and 1:20).

Comparing the intensities of the vinylic hydrogen peaks to the ring peaks indicates polymerisation for the co-polymers of ~60 % for methyl methacrylate and ~75 % for ethyl acrylate. The ratio of polyoxotungstate:monomer does not change these values perhaps because single polymer chains are produced in all cases.

³¹P NMR. The spectra contain broad signals at approximately the same positions as for the monomer (Figure 5.22); both signals have broadened due to the decreased mobility of the clusters caused by the styrylPO becoming part of a polymeric chain.

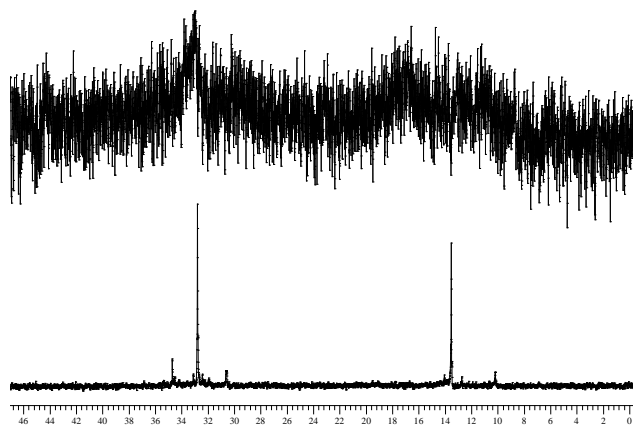


Figure 5.22. ^{31}P NMR spectra for the monomer $(\text{NBu}_4)_3\text{H}[\text{SiW}_{10}\text{O}_{36}(\text{H}_2\text{C}=\text{CHC}_6\text{H}_4\text{PO})(\text{EtPO})]$ and methyl methacrylate co-polymer (1:2) after reaction for 18 hours.

IR Spectroscopy. The fingerprint region is unchanged by the reaction showing that the polyoxotungstate clusters are intact. The presence of the co-monomer is confirmed by the carbonyl stretch ($\text{C}=\text{O}$).

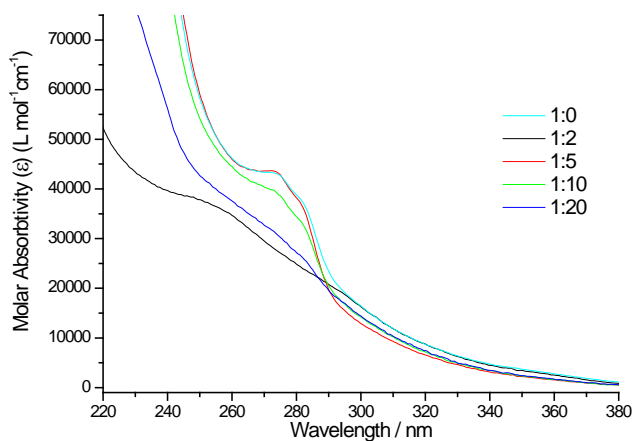
Mass Spectrometry. The spectra are similar to those for the $(\text{NBu}_4)_3\text{H}[\text{SiW}_{10}\text{O}_{36}(\text{H}_2\text{C}=\text{CHC}_6\text{H}_4\text{PO})(\text{EtPO})]$ polymer, the peaks generally being broader and the two main peaks (3842 and 4084 due to $[\text{SiW}_{10}\text{O}_{36}(\text{H}_2\text{C}=\text{CHC}_6\text{H}_4\text{PO})]^{6-}$ with five or six NBu_4^+ cations) being less intense. There are also indications of weak peaks with an extra styryl group and an ethyl acrylate or methyl methacrylate group, which indicates that the polymer has been produced, but is either in a small quantity or easily breaks up upon ionisation.

Elemental Analysis. The percentages of carbon, nitrogen and hydrogen observed for the co-polymerisation with ethyl acrylate show the values to be close to those predicted (Table 5.11), higher ratio's having a greater deviance from the original ratio than the lower ones. All co-polymers show the amount of nitrogen to be greater than predicted, indicating that either initiator (AIBN) or solvent is present, which will also affect the other values.

Table 5.11. The predicted and observed C, H, N analysis for the co-polymers.

Ratio in reaction mixture (POM:Co-Monomer)	Predicted (%)			Observed (%)			Ratio from C, N, H Analysis (POM:Co-monomer)
	N	C	H	N	C	H	
1:2	1.2	22.7	3.8	1.3	22.9	3.8	1:2
1:5	1.1	25.6	4.1	1.7	26.6	4.6	1:6
1:10	1.0	29.5	4.6	1.5	30.5	4.4	1:12
1:20	0.8	35.1	5.2	1.4	32.6	4.9	1:15

UV/vis Spectroscopy. The UV/vis spectra for the co-polymers (Figure 5.23) shows similar results to the single polymer formed from $(\text{NBu}_4)_3\text{H}[\text{SiW}_{10}\text{O}_{36}(\text{H}_2\text{C}=\text{CHC}_6\text{H}_4\text{PO})(\text{EtPO})]$, the peak at 272 nm is observed with the same molar absorptivity for the 1:5 polymer, the intensity then reducing as the amount of co-monomer increases and therefore the quantity of polyoxotungstate in a given mass of product decreasing. The polymer formed from a 1:2 ratio does not show this peak instead showing a small peak at the intensity for the monomer species.

**Figure 5.23.** The UV/vis spectra for the co-polymers formed from $(\text{NBu}_4)_3\text{H}[\text{SiW}_{10}\text{O}_{36}(\text{H}_2\text{C}=\text{CHC}_6\text{H}_4\text{PO})(\text{EtPO})]$ and ethyl acrylate.

In summary, co-polymerisation with either ethyl acrylate or methyl methacrylate gives similar results to polymerisation of $(\text{NBu}_4)_3\text{H}[\text{SiW}_{10}\text{O}_{36}(\text{H}_2\text{C}=\text{CHC}_6\text{H}_4\text{PO})(\text{EtPO})]$ alone,

however the mass spectra, elemental analysis and UV/vis show differences due to the presence of the co-monomer which will affect the properties of the product.

5.2 $[\text{SiW}_9\text{O}_{34}(\text{RPO})_3]^{4-}$

As reaction of the doubly derivatised $[\text{SiW}_{10}\text{O}_{36}(\text{RPO})_2]^{4-}$ with benzylamine results in the loss of one RPO group we decided to investigate the effect of benzylamine on the triply substituted $[\text{SiW}_9\text{O}_{34}(\text{RPO})_3]^{4-}$ anion.

$(\text{NBu}_4)_3\text{Na}[\text{SiW}_9\text{O}_{34}(\text{H}_2\text{C}=\text{CHCH}_2\text{PO})_3]$ was chosen for our investigation, the allyl group not being reactive towards the amine and being easily observed in the ^1H NMR spectra (Compound 50).

^1H NMR. After stirring overnight in a solution containing benzylamine the product was isolated and purified. ^1H NMR shows benzylamine to be present in addition to the cations and the allyl group. The position of the peak for the CH_2 attached to the phosphorus has shifted to a lower ppm, due to the interaction of the $\text{P}=\text{O}$ group changing. The intensities of the allyl peaks has reduced compared to the NBu_4^+ peaks indicating that one RPO group is present; although the peaks are often weaker than expected so there may be two groups present. The intensity of the benzylamine peaks show that approximately three molecules are present, these would be expected to coordinate to the vacant sites on the polyoxotungstate in a similar way to those in $(\text{NBu}_4)_3(\text{C}_6\text{H}_5\text{CH}_2\text{NH}_3)_3[\text{SiW}_{10}\text{O}_{36}(\text{H}_3\text{CCOC}_6\text{H}_4\text{PO})]$.

^{31}P NMR. The spectrum exhibits a single phosphorus peak, the position of which has not been changed by the reaction. Under hydrogen-coupled conditions the coupling is similar to for the fully saturated allyl derivatives showing the same interactions within the RPO group.

^{29}Si NMR. ^{29}Si NMR can be used to determine the saturation of the polyoxotungstate cluster.¹⁰ The product has one peak so is pure and single phase, the peak position (-84.6 ppm) is at a lower value compared to the triply derivatised $[\text{SiW}_9\text{O}_{34}(\text{H}_2\text{C}=\text{CHCH}_2\text{PO})_3]^{4-}$ (-88.1 ppm), and while this position is lower than that for $[\text{SiW}_9\text{O}_{34}(\text{EtPO})_2]^{6-}$ (-85.5 ppm) it is close, so indicates that two RPO groups remain on the cluster.

IR Spectroscopy. The spectrum shows some of the polyoxotungstate bands in the fingerprint region to have shifted to lower wavelengths; this is due to the saturation of the polyoxotungstate reducing and shows that it is no longer triply derivatised. The bands are at lower wavelengths than for $[\text{SiW}_9\text{O}_{34}(\text{RPO})_2]^{6-}$ (Table 5.12) showing that either the cluster has one RPO attached to it or has two groups and the previous product was not pure, containing some triply substituted clusters which shift the bands for that product.

Table 5.12. The IR bands below 1050 cm^{-1} for the $[\text{SiW}_9\text{O}_{34}]^{10-}$ cluster derivatised with none, two or three RPO groups where $\text{R} = \text{H}_2\text{C}=\text{CHCH}_2$.

$[\alpha\text{-SiW}_9\text{O}_{34}]^{10-} / \text{cm}^{-1}$	$[\text{SiW}_9\text{O}_{34}(\text{RPO})_2]^{6-} / \text{cm}^{-1}$	$[\text{SiW}_9\text{O}_{34}(\text{RPO})_3]^{4-} / \text{cm}^{-1}$	Product/ cm^{-1}
	1011.6	1002.3	~1010
983.0		980 (sh)	979.5
	950.7	956.4	945.1
930.2		924.1	
861.9	897.5	903.8	891.6 (b)
848.0	841.8	838.7	837.9
807.4	746.6	733.4	729.6

Mass Spectrometry. The mass spectrum has changed from that for the triply derivatised cluster. It has two main peaks, the peak at $3250\text{ }m/z$ being assigned to either $(\text{NBu}_4)_3\text{Na}[\text{SiW}_9\text{O}_{34}(\text{H}_2\text{C}=\text{CHCH}_2\text{PO})_3]$ (3241), $(\text{NBu}_4)_3(\text{C}_6\text{H}_5\text{CH}_2\text{NH}_3)\text{Na}[\text{SiW}_9\text{O}_{34}(\text{H}_2\text{C}=\text{CHCH}_2\text{PO})_2]$

(3261) or $(\text{NBu}_4)_3(\text{C}_6\text{H}_5\text{CH}_2\text{NH}_3)_2[\text{SiW}_9\text{O}_{34}(\text{H}_2\text{C}=\text{CHCH}_2\text{PO})]$ (3258) and the one at 3492 m/z due to the addition of a extra NBu_4^+ . The other peaks correspond to these masses having lost benzylamine and part of the allyl-phosphonate group, these losses indicating that the main peaks are not due to $(\text{NBu}_4)_3\text{Na}[\text{SiW}_9\text{O}_{34}(\text{H}_2\text{C}=\text{CHCH}_2\text{PO})_3]$.

Elemental Analysis. The results of the CHN analysis indicate that three NBu_4^+ cations and three benzylamine molecules are present per cluster. The difference in predicted values between the clusters with different numbers of RPO groups is small so can not confirm how many are present.

Electrochemistry. The cluster has different electrochemical properties to those seen for the fully saturated triply derivatised cluster, but is related to that seen for $[\text{SiW}_{10}\text{O}_{36}(\text{H}_2\text{C}=\text{CHC}_6\text{H}_4\text{PO})]^{6-}$ both structures having one vacant site and being comparable to the $[\text{SiW}_{11}\text{O}_{39}]^{8-}$ cluster (Figure 5.24).^{7,8}

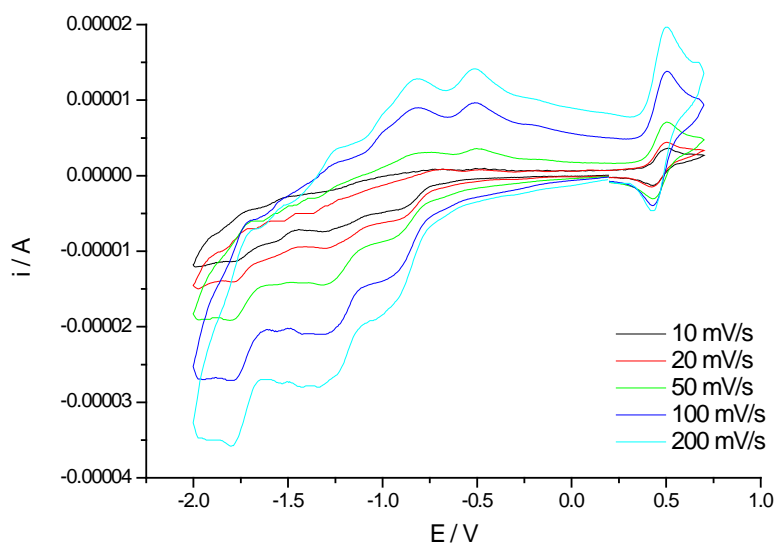


Figure 5.24. The cyclic voltammogram for $(\text{NBu}_4)_3(\text{C}_6\text{H}_5\text{CH}_2\text{NH}_3)_3[\text{SiW}_9\text{O}_{34}(\text{H}_2\text{C}=\text{CHCH}_2\text{PO})_2]$ and ferrocene using an Ag/Ag^+ reference electrode.

UV/vis Spectroscopy. λ_{max} has shifted to a lower wavelength compared to $[\text{SiW}_9\text{O}_{34}(\text{H}_2\text{C}=\text{CHCH}_2\text{PO})_3]^{4-}$, now looking similar to for $[\text{SiW}_9\text{O}_{34}(\text{H}_2\text{C}=\text{CHCH}_2\text{PO})_2]^{6-}$ so indicating that the cluster has two RPO groups attached to it (Figure 5.25).

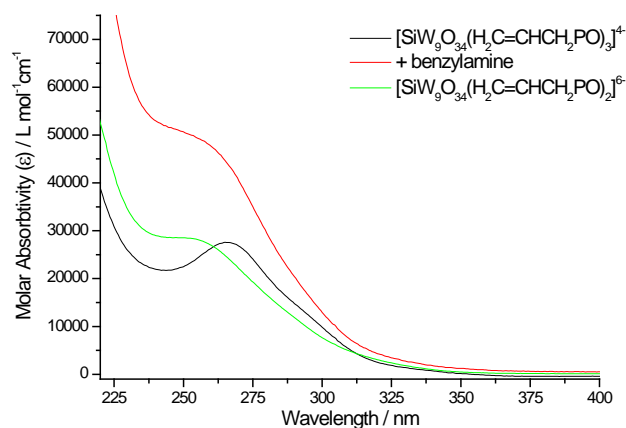


Figure 5.25. The UV/vis spectra for $[\text{SiW}_9\text{O}_{34}(\text{H}_2\text{C}=\text{CHCH}_2\text{PO})_3]^{4-}$ before and after the addition of benzylamine, compared with the spectrum for $[\text{SiW}_9\text{O}_{34}(\text{H}_2\text{C}=\text{CHCH}_2\text{PO})_2]^{6-}$

Single Crystal X-ray Diffraction. Attempts to obtain crystals suitable for single crystal XRD gave a crystalline product, however the crystals were unstable and only a very poor dataset was collected from which a structure could not be obtained.

5.2.1 Reaction of product

The addition of benzylamine to $[\text{SiW}_9\text{O}_{34}(\text{H}_2\text{C}=\text{CHCH}_2\text{PO})_3]^{4-}$ gives a pure product, ^{29}Si NMR, IR and UV/vis all point towards the product being doubly derivatised with one vacant site. The vacant site provides the potential for it to react with another phosphonic acid and give a product with mixed functional groups. This was tested using phenylphosphonic acid ($\text{C}_6\text{H}_5\text{PO}(\text{OH})_2$) (Compound 51) and ($\text{HOOCCH}_2\text{PO}(\text{OH})_2$) (Compound 52), these being selected because their peaks in the ^1H NMR spectra will be in different positions to both the allyl and cation peaks.

^1H NMR. After reaction, peaks due to the second phosphonic acid group (R^2) are present, the intensity of these peaks indicating that approximately an equal quantity of this group and the allyl group are in the product. The benzylamine peaks have almost disappeared (intensity of 0.4 compared to 13.7), this being more easily seen when $\text{R}^2 = \text{HOOCCH}_2$ as the phenyl group is at a similar position.

^{31}P NMR. The spectra (Figure 5.26) show two main signals in an equal ratio (the allyl peak being very slightly larger) at the expected positions for the RPO groups. There are indications of an impurity, but the intensity of this peak is very small (0.1).

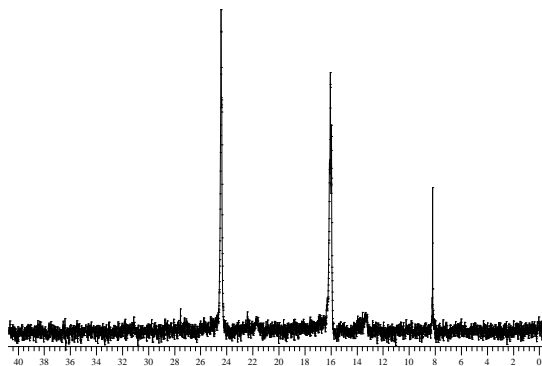


Figure 5.26. ^{31}P NMR Spectrum for $(\text{NBu}_4)_3\text{H}[\text{SiW}_{10}\text{O}_{36}(\text{H}_2\text{C}=\text{CHCH}_2\text{PO})_2(\text{C}_6\text{H}_5\text{PO})]$, assignments $\text{H}_2\text{C}=\text{CHCH}_2\text{PO}$ (24.5 ppm), $\text{C}_6\text{H}_5\text{PO}$ (16.1 ppm) and impurity (8.1 ppm).

IR Spectroscopy. The fingerprint region of the IR spectra have signals in the same position as those for the $[\text{SiW}_9\text{O}_{34}(\text{H}_2\text{C}=\text{CHCH}_2\text{PO})_3]^{4-}$ cluster showing a similar fully saturated structure is present. When $\text{R}^2 = \text{HOOCCH}_2$ an additional $\text{C}=\text{O}$ peak is seen at 1734 cm^{-1} , but when $\text{R}^2 = \text{C}_6\text{H}_5$ the additional aromatic $\text{C}=\text{C}$ signals are weak and hard to see.

Mass Spectrometry. The mass spectra both have more signals than after reaction with benzylamine, these mainly corresponding to the cluster having lost all or part of one or both RPO groups. When $\text{R}^2 = \text{C}_6\text{H}_5$ there are signals with masses for $(\text{NBu}_4)_3(\text{C}_6\text{H}_5\text{CH}_2\text{NH}_3)[\text{M}]^+$ (3498)

and $(\text{NBu}_4)_4(\text{C}_6\text{H}_5\text{CH}_2\text{NH}_3)\text{Na}[M]^+$ (3535) showing that clusters with two allyl groups and one phenyl group are present along with some remaining benzylamine.

Elemental Analysis. The percentage of carbon and nitrogen in the product when $\text{R}^2 = \text{HOOCCH}_2$ are larger than those calculated for the formula $(\text{NBu}_4)_3\text{H}[\text{SiW}_9\text{O}_{34}(\text{H}_2\text{C}=\text{CHCH}_2\text{PO})_2(\text{HOOCCH}_2\text{PO})]$, due to the small quantity of benzylamine remaining in the product. The percentages are close enough to show that three cations are present per cluster, but do not show how many RPO groups are present.

UV/vis Spectroscopy. The spectra (Figure 5.27) show λ_{max} to have shifted back to the position of a fully saturated $[\text{SiW}_9\text{O}_{34}(\text{RPO})_3]^{4-}$ cluster ($\lambda_{\text{max}} = 263.5 \text{ nm}$) although when $\text{R}^2 = \text{C}_6\text{H}_5$ this group will also absorb in this region so this may affect the position of λ_{max} .

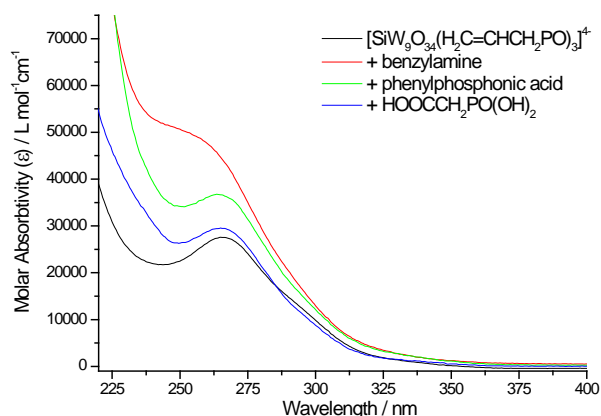


Figure 5.27. The UV/vis spectra for $[\text{SiW}_9\text{O}_{34}(\text{H}_2\text{C}=\text{CHCH}_2\text{PO})_3]^{4-}$ reacted with benzylamine and then either phenylphosphonic acid or $\text{HOOCCH}_2\text{PO}(\text{OH})_2$.

Single Crystal X-ray Diffraction. Crystals suitable for single crystal X-ray Diffraction were obtained from a DMF solution of $(\text{NBu}_4)_3\text{H}[\text{SiW}_9\text{O}_{34}(\text{H}_2\text{C}=\text{CHCH}_2\text{PO})_2(\text{H}_5\text{C}_6\text{PO})]$.

Table 5.13. Crystallographic Data for $(\text{NBu}_4)_3\text{H}[\text{SiW}_9\text{O}_{34}(\text{H}_2\text{C}=\text{CHCH}_2\text{PO})_2(\text{H}_5\text{C}_6\text{PO})]$.

Trigonal		Spacegroup		R 3 m
Cell axes (Å)	a = 22.1385(23)	b = 22.1385(23)	c = 18.8893(29)	
Cell angles (deg)	α = 90.00	β = 90.00	γ = 120.00	
Cell Volume (Å ³)	8017.57(17)			
[Full details in appendix (Structure 25)]				

The structure of the $[\text{SiW}_9\text{O}_{34}(\text{RPO})_3]^{4-}$ cluster has three-fold rotational symmetry and three mirror planes along the planes containing the P-O bonds, so having a high overall symmetry (spacegroup R 3 m). The allyl ($\text{H}_2\text{C}=\text{CHCH}_2$) and phenyl (C_6H_5) groups are disordered over the available sites as well as having disorder between two different rotations of the R groups. The occupancy of the atoms in the two groups are refined against one another, this showing the allyl group to be present in just over half the sites (occupancies of 0.261 and 0.239 (where full occupancy is 0.5 due to the symmetry)).

No metal ion is seen coordinating to the P=O groups; although some electron density is observed in this central position it is small and disordered over two sites, this could be due to a mixture of H^+ and Na^+ being present or some disordered solvent as further electron density is observed above the cluster. Three NBu_4^+ cations are seen per cluster, so an H^+ or Na^+ is needed to balance the charge although this could be disordered and hard to see.

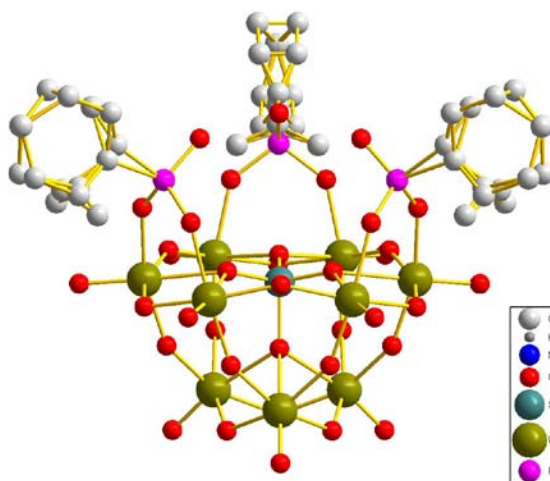


Figure 5.28. The $[\text{SiW}_9\text{O}_{34}(\text{H}_2\text{C}=\text{CHCH}_2\text{PO})_2(\text{C}_6\text{H}_5\text{PO})]^{4-}$ cluster in the crystal structure, showing the R groups to be disordered, with two possible positions for each group on the phosphorus atoms.

The arrangement of the clusters in the crystal structure is the same as for $(\text{NBu}_4)_3\text{Co}[\text{SiW}_9\text{O}_{34}(\text{H}_2\text{C}=\text{CHC}_6\text{H}_4\text{PO})_3]$ (spacegroup $R\ 3\ m$) (Section 3.2.8), and this is comparable to other structures obtained from the $[\text{XW}_9\text{O}_{34}]^{n-}$ anion $((\text{NBu}_4)_3\text{M}[\text{XW}_9\text{O}_{34}(\text{R})_3])$ ($\text{X} = \text{P}$ or Si ; $\text{M} = \text{H}^+$ or Na^+ ; $\text{R} = \text{H}_2\text{C}=\text{CHCH}_2\text{PO}$ or $t\text{BuSiOH}$), but with the c -axis around half the length.

Reaction of $[\text{SiW}_9\text{O}_{34}(\text{H}_2\text{C}=\text{CHCH}_2\text{PO})_2]^{6-}$ with phosphonic acid gives a triply derivatised structure containing two different RPO groups, mass spectrometry shows there to be two allylPO and one RPO group, agreeing with the suspected structure after reaction with benzylamine.

5.3 $[\text{XW}_9\text{O}_{34}(t\text{-BuSiO})_3(\text{Si}(\text{CH}_2)_3\text{Br})]^{4-}$

The polyoxotungstate clusters $[\text{XW}_9\text{O}_{34}]^{n-}$ ($\text{X} = \text{Si}$, $n = 10$; $\text{X} = \text{P}$, $n = 9$) can be derivatised with organosilane groups containing a Br, which can be further reacted, for example with amine molecules, via an $\text{S}_{\text{N}}2$ mechanism where the amine attacks the electrophilic carbon next to the Br atom.

Here the reaction of the clusters with glycine and sarcosine (Compounds 53-56) will be investigated, with the aim of introducing carboxylic acid functionality. Although we have introduced carboxylic acid groups via the reaction of phosphonic acids it is much more difficult to introduce this functionality using other bridging ligands. Also the reactivity of the clusters towards amino acid type molecules could introduce the possibility of attachment to proteins etc.

^1H NMR. After reaction the spectra shows four signals due to the organic component on the cluster along with those due to the NBu_4^+ cations. There is a multiplet at 3.50-3.62 ppm, and a signal in this position in $[\text{XW}_9\text{O}_{34}(\text{tBuSiO})_3(\text{Si}(\text{CH}_2)_3\text{Br})]^{4-}$ was assigned to the $\text{CH}_2\text{-Br}$ group. However a CH_2 group between a nitrogen and a carboxylic acid group would also appear in this position. The additional peak at (~2.3 ppm) is in a position to indicate a $\text{CH}_x\text{-N}$ group, which can be assigned to the CH_2 group which was originally attached to the Br before reaction with glycine, and this indicates that the desired reaction has occurred. When sarcosine is used, an N- CH_3 group is also introduced in this region of the spectrum, the peak now being broader and slightly more intense.

^{31}P NMR. ^{31}P NMR was carried out when $\text{X} = \text{P}$, showing one main peak meaning that the cluster still has a saturated capped structure. However other peaks were observed around this main peak when using sarcosine showing that the product was not pure.

IR Spectroscopy. The peak at 886 cm^{-1} due to the C-Br bond is no longer observed, while a C=O stretch is now present (1670 cm^{-1} (glycine) or 1629 cm^{-1} (sarcosine)); the rest of the spectra showing little change, indicating that the inorganic cluster remains broadly unchanged.

Mass Spectrometry. None of the spectra show conclusive evidence for the reaction. Masses corresponding to $[M^+]$ with various numbers of cations are seen, however the mass of the group replacing the Br (glycine (74) or sarcosine (88)) is similar to that for Br (79/81), being

within the errors often seen in the broad signals of the mass spectra of polyoxometalates, so the presence of the desired group can not be confirmed. Some spectra show peaks due to the anion having lost most or all of the $(\text{CH}_2)_3$ group, again meaning the product of the reaction can not be determined.

Elemental Analysis. CHN analysis shows the values to be in the same region as those predicted if the reaction with the amine has occurred, all except $[\text{SiW}_9\text{O}_{34}(\text{tBuSiO})_3(\text{Si}(\text{CH}_2)_3\text{N}(\text{CH}_3)\text{CH}_2\text{COOH})]^{4-}$ indicate that three NBu_4^+ cations (and one H^+ ion when $\text{X} = \text{Si}$) balance the charge ($[\text{SiW}_9\text{O}_{34}(\text{tBuSiO})_3(\text{Si}(\text{CH}_2)_3\text{N}(\text{CH}_3)\text{CH}_2\text{COOH})]^{4-}$ having four NBu_4^+ cations).

Due to the difficulties in determining whether the reaction had been successful it was repeated with benzylamine and *p*-xylylenediamine (Compounds 57-60) these amines having well defined peaks in the ^1H NMR and significantly larger masses than Br.

^1H NMR. The spectra show the addition of the benzylamine or xylylenediamine peaks in a ratio which indicates that one amine is present per cluster (by comparison to the cation and $\text{Si}(\text{CH}_2)_3$ group peak intensities).

Mass Spectrometry. When benzylamine is used the product has masses for $[\text{XW}_9\text{O}_{34}(\text{tBuSiO})_3(\text{Si}(\text{CH}_2)_3\text{NHCH}_2\text{C}_6\text{H}_5)]^{n-}$ ($\text{X} = \text{Si}$, $n = 4$; $\text{X} = \text{P}$, $n = 3$) and $[\text{XW}_9\text{O}_{34}(\text{tBuSiO})_3(\text{Si}(\text{CH}_2)_3)]^{n-}$, the mass of the group replacing the Br (106) is now not within the errors seen in other spectra so the peaks for the reacted species confirming that a reaction has taken place. When *p*-xylylenediamine is used peaks due to $[\text{XW}_9\text{O}_{34}(\text{tBuSiO})_3(\text{Si}(\text{CH}_2)_3\text{NHCH}_2\text{C}_6\text{H}_4\text{CH}_2\text{NH}_2)]^{n-}$ ($\text{X} = \text{Si}$, $n = 4$; $\text{X} = \text{P}$, $n = 3$) are present along with various peaks with parts of the $\text{Si}(\text{CH}_2)_3\text{NHCH}_2\text{C}_6\text{H}_4\text{CH}_2\text{NH}_2$ group removed, these confirm that the desired product is formed, and no peaks are seen for the cluster with the Br group attached to it. As *p*-xylylenediamine has two NH_2 groups it would be possible for it to react at both ends and produce dimers, however the

mass spectra do not show any evidence of this, agreeing with that seen when diamines were reacted with other polyoxometalates.² Thus producing a cluster with an amide functionality, this has also been done recently by reaction of a Dawson-type with a diol.¹¹

Conclusion. It has been demonstrated that reactions of $[\text{XW}_9\text{O}_{34}(\text{tBuSiO})_3(\text{Si}(\text{CH}_2)_3\text{Br})]^{4-}$ with amines gives $[\text{XW}_9\text{O}_{34}(\text{tBuSiO})_3(\text{Si}(\text{CH}_2)_3\text{NHR})]^{4-}$ the amine replacing the Br. This is demonstrated by the appearance of the appropriate amine peaks and shift of the CH_2 group adjacent to the Br in the ^1H NMR spectra, mass spectrometry shows peaks due to the $[\text{M}^+]$ anions, although they can only be identified as definitely being from the product when the amine is benzylamine or *p*-xylylenediamine these having masses significantly different from those for the original cluster.

5.4 Conclusion

It has been demonstrated that $[\text{SiW}_{10}\text{O}_{36}(\text{HOOC}(\text{CH}_2)_n\text{PO})_2]^{4-}$ ($n = 1$ or 2) and $[\text{SiW}_{10}\text{O}_{36}(\text{H}_3\text{CCOC}_6\text{H}_4\text{PO})_2]^{4-}$ both react with amines. However the products obtained are not the expected amides or imines, instead the amine has the effect of removing one of the RPO groups and this effect can also be demonstrated when the R group is unreactive towards the amine group (e.g. $\text{R} = \text{Et}$). These reactions give a mono-substituted product $[\text{SiW}_{10}\text{O}_{36}(\text{RPO})]^{6-}$ which is able to react with a second phosphonic acid and produce a doubly derivatised product where the two RPO groups are different. A similar effect was seen when reacting $[\text{SiW}_9\text{O}_{34}(\text{RPO})_3]^{4-}$ with benzylamine.

When reacting the capped $[\text{XW}_9\text{O}_{34}(\text{tBuSiO})_3(\text{Si}(\text{CH}_2)_3\text{Br})]^{4-}$ anion with amine molecules, the expected reaction occurs with the polyoxotungstate unit remaining intact, although the reaction is difficult to confirm in some cases.

5.5 References

1. C. A. G. N. Montalbetti and V. Falque, *Tetrahedron*, **2005**, 61, 10827.
2. S. Bareyt, S. Piligkos, B. Hasenknopf, P. Gouzerh, E. Lacôte, S. Thorimbert and M. Malacria, *Angew. Chem. Int. Ed.*, **2003**, 42, 3404.
3. S. Bareyt, S. Piligkos, B. Hasenknopf, P. Gouzerh, E. Lacôte, S. Thorimbert and M. Malacria, *J. Am. Chem. Soc.*, **2005**, 127, 6788.
4. G. Sazani and M. T. Pope, *Dalton Trans.*, **2004**, 1989.
5. B. Belleau and G. Malek, *J. Am. Chem. Soc.*, **1968**, 1651.
6. H. Chen, L. Xie, H. Lu and Y. Yang, *J. Mater. Chem.*, **2007**, 1258.
7. J. E. Toth and F. C. Anson, *J. Electroanal. Chem.*, **1988**, 256, 361.
8. M. S. Balula, J. A. Gamelas, H. M. Carapuça, A. M. V. Cavaleiro and W. Schlindwein, *Eur. J. Inorg. Chem.*, **2004**, 619.
9. A. Tézé and G. Hervé, *Inorg. Synth.*, **1990**, 27, 85.
10. N. Ammari, G. Hervé and R. Thouvenot, *New. J. Chem.*, **1991**, 15, 607.
11. J. Li, I. Huth, L-M. Chamoreau, B. Hasenknopf, E. Lacôte, S. Thorimbert and M. Malacria, *Angew. Chem. Int. Ed.*, **2009**, 48, 2035.

6. Conclusion

The aim of this research was to synthesize new organic-inorganic polyoxotungstate derivatives and use them to create polymeric materials. This was possible by firstly synthesizing organophosphonic acids and lacunary polyoxotungstate units then reacting them together.

Organophosphonic acids are synthesized via diethyl organophosphonates; diethyl allylphosphonate was obtained using the Michaelis-Arbuzov reaction, but less severe conditions were needed to obtain the styryl and 4-acetylphenyl alternatives so these were obtained using a Palladium catalysed reaction. The diethyl organophosphonate was then reacted with trimethylchlorosilane and water to give the corresponding phosphonic acid. Although the diethyl 4-acetylphenylphosphonate has been synthesized previously the diethyl styrylphosphonate and both phosphonic acid species are new, the styryl species being the first example of a styrene group attached to this type of functionality.

The polyoxotungstate anion $[\text{SiW}_{10}\text{O}_{36}]^{8-}$ is derivatised with phosphonic acids to give the functionalised cluster $[\text{SiW}_{10}\text{O}_{36}(\text{RPO})_2]^{4-}$ ($\text{R} = \text{Et}, \text{H}_2\text{C}=\text{CH}, \text{H}_2\text{C}=\text{CHCH}_2, \text{HOOCCH}_2, \text{HOOCCH}_2\text{CH}_2, \text{H}_2\text{C}=\text{CHC}_6\text{H}_4$ or $\text{H}_3\text{CCOC}_6\text{H}_4$). Crystals have been obtained for various combinations of R groups and cations, the structures being studied by single crystal XRD, all the crystal structures being new and showing the structure and interactions of the polyoxotungstates. The hybrid anions consist of a $[\gamma\text{-SiW}_{10}\text{O}_{36}]^{8-}$ unit with two phosphonate groups attached to it via W-O-P bonds in the vacancies created when forming the lacunary anion. A H^+ forms a strong hydrogen-bond between the two P=O groups at the top of the anion. The structures obtained from single crystal XRD are different depending on the cations and R groups, when $\text{R} = \text{Et}, \text{H}_2\text{C}=\text{CHCH}_2, \text{HOOCCH}_2$ or $\text{HOOCCH}_2\text{CH}_2$ the structures are all related, the anions all being

arranged in columns, all the anions within a column pointing in the same direction. The organic 'R' groups in one column point towards equivalent groups on anions in neighbouring columns creating layers. When the cations are a mixture of NBu_4^+ , NEt_4^+ and H^+ the anions in a layer all point in the same direction, but when only NEt_4^+ and H^+ are present the columns point in alternating directions within a layer. When $\text{R} = \text{HOOCCH}_2$ hydrogen-bonding is observed between the carboxylic acid groups, thus strengthening the interactions between these anions. When $\text{R} = \text{H}_2\text{C}=\text{CHC}_6\text{H}_4$ or $\text{H}_3\text{CCOC}_6\text{H}_4$ the structures are not related to the others, the arrangement of anions when $\text{R} = \text{H}_3\text{CCOC}_6\text{H}_4$ being controlled by π - π interactions of the aromatic rings.

The electrochemistry of the anions was studied by cyclic voltammetry; three reductions are seen for all anions, the first two being one electron waves and the third a two electron wave. The different electron withdrawing properties of the R groups cause minor variations in the position of the waves but these are not significant. The electrochemistry shows that the polyoxotungstate anions have retained their ability to be easily reduced, the grafting of organic groups causing them to adopt properties similar to the fully condensed $[\text{SiW}_{12}\text{O}_{40}]^{4-}$ cluster.

Derivatisation of the decatungstophosphonate $[\text{PW}_{10}\text{O}_{36}]^{7-}$ with phosphonic acids was also investigated, this was found to be successful, however ^{31}P NMR indicated that the product was not very pure and this was confirmed by IR and mass spectrometry. The impurities are thought to be due to isomerisation of the $[\text{PW}_{10}\text{O}_{36}]^{7-}$ cluster.

Derivatisation of the trivacant $[\text{XW}_9\text{O}_{34}]^{n-}$ ($\text{X} = \text{Si}$ or P) was tested to try and obtain a triply substituted product. Highly electrophilic organotrichlorosilanes easily react with the polyoxotungstate clusters to give $[\text{XW}_9\text{O}_{34}(\text{RSiO})_3(\text{RSi})]^{n-}$, $[\text{XW}_9\text{O}_{34}(t\text{-BuSiOH})_3]^{n-}$ or $[\text{XW}_9\text{O}_{34}(t\text{-BuSiO})_3(\text{RSi})]^{n-}$ ($\text{R} = \text{H}_2\text{C}=\text{CH}$ or $\text{H}_2\text{C}=\text{CHCH}_2$). The less electrophilic

organotriethoxysilane reacts under similar conditions with the addition of HCl to promote the reaction. However, reaction with organophosphonic acids is more difficult, the reaction requiring promotion by the addition of a catalytic amount of HCl and heating in refluxing acetonitrile for three days. However, this reaction still only goes to completion when $X = \text{Si}$, and when $X = \text{P}$ only a doubly functionalised product is obtained. Using a more reactive ‘ EtPO^{2+} ’ moiety, which is generated by reaction of EtPCl_2 with AgNO_3 , the reaction proceeds further to give a triply derivatised product; however this product is not pure. Single Crystal XRD has been performed on crystals obtained from some of the $(\text{NBu}_4)_3\text{H}[\text{SiW}_9\text{O}_{34}(\text{R})_3]$ products. The structures show the $[\text{SiW}_9\text{O}_{34}]^{10-}$ unit to have three RPO groups grafted on to it through W-O-P bonds in the vacancies created when making the lacunary anion, with the three P=O groups pointing towards a coordination site above the cluster containing either a H^+ or Na^+ cation. The crystal structures when $\text{R} = t\text{-BuSiOH}$ or $\text{H}_2\text{C}=\text{CHCH}_2\text{PO}$ have the same long range order (spacegroup R 3 c) and unit cell parameters, with the clusters arranged in columns. When $\text{R} = \text{EtPO}$ or $\text{H}_2\text{C}=\text{CHC}_6\text{H}_4\text{PO}$ the clusters are still arranged in a similar way, however the c -axis is shorter (spacegroup R 3 m). The other structures are not related, the order being controlled by carboxylic acid interactions or coordination to a metal ion. Interesting structures were obtained from $(\text{NBu}_4)_3\text{H}[\text{SiW}_9\text{O}_{34}(\text{H}_3\text{CCOC}_6\text{H}_4\text{PO})_3]$ with a metal atom coordinating to the P=O groups from two clusters and holding the clusters together, a similar structure also being obtained when cobalt (II) nitrate was added before the crystallisation process. Addition of cobalt (II) nitrate to $(\text{NBu}_4)_3\text{H}[\text{SiW}_9\text{O}_{34}(\text{H}_2\text{C}=\text{CHC}_6\text{H}_4\text{PO})_3]$ gave a structure with a cobalt ion coordinated to the P=O groups and a water molecule. The addition of a metal ion to the system adds any properties it possesses to the structure, for example, colour, magnetic and catalytic properties; this could be investigated further by the addition of different metal ions to the structure such as zinc, nickel or

copper. Also, the coordination properties of the metal ion could potentially be used to control the arrangement of polyoxotungstates in the crystal structure. Control of the metal ion and the organic 'R' groups attached to the polyoxotungstate could create analogue receptor sites which could be used to model protein binding.

The electrochemistry of the fully saturated $[\text{SiW}_9\text{O}_{34}(\text{RPO})_3]^{4-}$ clusters was investigated and found to give similar results to that for the $[\text{SiW}_{10}\text{O}_{36}(\text{RPO})_2]^{4-}$ clusters, the reductions being similar to those for the fully condensed $[\text{SiW}_{12}\text{O}_{40}]^{4-}$ anion. This shows that the addition of RPO groups counteracts the loss of WO_6 octahedra making the addition of an electron relatively easy as it enters a non-bonding orbital. Also the charge of the cluster is the same (4-) meaning that the addition of an electron will be similarly easy.

When $\text{X} = \text{Si}$ the anion is more reactive due to its higher charge compared to $\text{X} = \text{P}$, phosphonic acids reacting more readily to give fully saturated $[\text{XW}_9\text{O}_{34}(\text{RPO})_3]^{4-}$ clusters. The reaction of the triply vacant $[\text{SiW}_9\text{O}_{34}]^{10-}$ cluster is harder than the equivalent reaction with the doubly vacant $[\text{SiW}_{10}\text{O}_{36}]^{8-}$ and requires refluxing for three days instead of one day.

It has been demonstrated that $[\text{SiW}_{10}\text{O}_{36}(\text{RPO})_2]^{4-}$ and $[\text{SiW}_9\text{O}_{34}(\text{RPO})_3]^{4-}$ ($\text{R} = \text{H}_2\text{C}=\text{CH}$, $\text{H}_2\text{C}=\text{CHCH}_2$ and $\text{H}_2\text{C}=\text{CHC}_6\text{H}_4$) can be polymerised under free radical conditions, the best results being when using AIBN as the initiator at 80°C . The extent of the reaction depends on the R group, increasing in the order vinyl < allyl < styryl as the distance of the double bond from the polyoxotungstate increases so steric factors become less of an issue. Generally, increasing the number of polymerisable groups on a cluster decreases the number of double bonds that react due to steric factors and a greater potential for cross-linking. The extent of polymerisation decreases in the order $[\text{SiW}_{10}\text{O}_{36}(\text{RPO})_2]^{4-} > [\text{SiW}_9\text{O}_{34}(\text{RPO})_3]^{4-}$ and $[\text{XW}_9\text{O}_{34}(t\text{BuSiO})_3(\text{RSi})]^{4-} > [\text{XW}_9\text{O}_{34}(\text{RSiO})_3(\text{RSi})]^{4-}$ with the exception of $[\text{SiW}_9\text{O}_{34}(\text{H}_2\text{C}=\text{CHC}_6\text{H}_4\text{PO})_3]^{4-}$ which reacts

further possibly due to the clusters forming small aggregates. The polymers show swelling properties absorbing solvent to produce gels, the extent of the swelling depending on the composition of the polymer and the solvent. The electrochemical properties of some of the polymeric materials and gels were investigated and show that the electrochemical properties of the monomer unit are retained. The electrochemical properties of the gels are greatly enhanced when acetonitrile is present, the swelling of the gels giving the polyoxotungstate units a degree of mobility. As the materials are electrochemically active and relatively easily reduced they have potential for use as catalysts; however the swelling and electrochemical properties need to be investigated further using a larger range of solvents with the potential for tailoring the gels to absorb particular solvents by varying the co-monomer present, the catalytic properties of the materials could then be investigated.

$[\text{SiW}_{10}\text{O}_{36}(\text{HOOC}(\text{CH}_2)_n\text{PO})_2]^{4-}$ ($n = 1$ or 2) and $[\text{SiW}_{10}\text{O}_{36}(\text{H}_3\text{CCOC}_6\text{H}_4\text{PO})_2]^{4-}$ were reacted with amines with the aim of producing amide or imine species. If this reaction proved successful then reaction with a diamine would be investigated to produce a condensation polymer, however the desired reaction did not occur. Instead a RPO group was lost from the structure, this being attributed to the pH change upon addition of the amine and was observed for all RPO groups, a mono-substituted product $[\text{SiW}_{10}\text{O}_{36}(\text{RPO})]^{6-}$ being obtained. The product can react with a second phosphonic acid to produce a doubly derivatised product with two different RPO groups. A similar effect was observed when reacting $[\text{SiW}_9\text{O}_{34}(\text{H}_2\text{C}=\text{CHCH}_2\text{PO})_3]^{4-}$ with benzylamine, one $\text{H}_2\text{C}=\text{CHCH}_2\text{PO}$ group being lost to give $[\text{SiW}_9\text{O}_{34}(\text{H}_2\text{C}=\text{CHCH}_2\text{PO})_2]^{6-}$, this product was then able to react with another phosphonic acid. The products containing two types of RPO groups $[\text{SiW}_{10}\text{O}_{36}(\text{R}^1\text{PO})(\text{R}^2\text{PO})]^{4-}$ and $[\text{SiW}_9\text{O}_{34}(\text{R}^1\text{PO})_2(\text{R}^2\text{PO})]^{4-}$ are the first examples of polyoxotungstates derivatised in this way, thus opening up the possibility of creating materials

with double functionality. Further work in this area is needed to investigate the large range of possible products, their stability and potential applications.

When reacting $[\text{XW}_9\text{O}_{34}(\text{tBuSiO})_3(\text{Si}(\text{CH}_2)_3\text{Br})]^{4-}$ with amines the Br atom is replaced with an amide with the rest of the polyoxotungstate unit remaining intact. This reaction was carried out using both simple amines and amino acids, so showing the potential to bond the polyoxotungstate units to organic molecules and incorporate them into organic systems. The reaction of these anions needs investigation with larger and more complex organic molecules.

Many new and interesting polyoxotungstate species have been produced during the course of this work; the number of examples could be further increased by making more new phosphonic acids using the same methods described. Different functionalities could introduce different properties to the clusters and open up the possibilities for further reactions of the RPO groups. Also cation exchange could be investigated, the replacement of NBu_4^+ or NEt_4^+ with Na^+ , K^+ or H^+ would enable the polyoxotungstates to become soluble in different solvents such as water and H^+ cations would produce an acidic species which could be used as an acid catalyst.

Overall it has been shown that polyoxotungstates can be derivatised with one, two or three RPO groups, adding organic functionality to the clusters and introducing the possibility of further reactions. The polyoxotungstates retain their electrochemical properties, their easy of reduction giving them potential as catalysts.

7. EXPERIMENTAL

All reagents and solvents were purchased from either Aldrich or Lancaster and are used as received, apart from KBr and dry acetonitrile which are dried before use. Nitrogen gas was supplied by BOC-gases

The Infrared spectra were recorded on a Perkin Elmer Paragon 1000 FT-IR spectrometer as KBr discs.

NMR was carried out at room temperature in 5mm outside diameter tubes, ^1H NMR was recorded on a Brüker AC300 spectrometer at 300 Hz, ^{13}C and ^{31}P NMR on a Brüker AV300 at 75.5 and 121 Hz, ^{29}Si NMR on a Brüker AV400 at 79 Hz.

Elemental Analysis was performed on a Carlo Erba EA1110 Simultaneous CHNS elemental analyser.

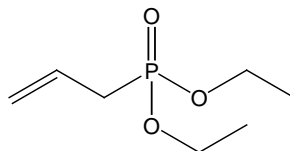
Maldi-TOF mass spectrometry was performed using a Brüker Biflex IV mass spectrometer.

UV/vis spectroscopy was recorded using a Shimadzu UV-3101PC UV-vis-NIR machine.

Single Crystal X-ray Diffraction data were collected on a Brüker Smart 6000 diffractometer equipped with a CCD detector and a copper tube source in Birmingham ($\lambda = 1.54$). On either Station 9.8 ($\lambda = 0.67$) or 16.2 ($\lambda = 0.80$) at the SRS facility at the CCLRC Daresbury Laboratory using synchrotron radiation or by the EPSRC crystallography service at Southampton ($\lambda = 0.71 \text{ \AA}$). The structures were solved and refined using SHELXL97 present in the WinGx suite of programmes and presented using Diamond.

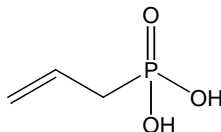
7.1. Phosphonic acids

7.1.1. Synthesis of Diethyl allylphosphonate (Compound A)¹



Triethylphosphite (14.9 g, 0.09 mol) was mixed with allylbromide (18.2 g, 0.15 mol) and refluxed for 4 hours. After cooling, the solution was distilled under reduced pressure (4 mbar at 70 °C) to avail diethyl allylphosphonate (14.1 g, 88 %) as a clear colourless liquid. δ_H (300 MHz; $CDCl_3$; Me_4Si) 1.20 (6H, t, CH_2-CH_3 , $^3J_{HH}=7$), 2.50 (2H, dd, CH_2-P , $^3J_{HH}=7$, $^2J_{PH}=22$ Hz), 4.00 (4H, m, $O-CH_2-CH_3$), 5.05-5.16 (2H, m, $CH_2=CH$), 5.58-5.78 (1H, m, $CH_2=CH$); δ_P (121 MHz, $CDCl_3$, H_3PO_4) 27.6 ppm.

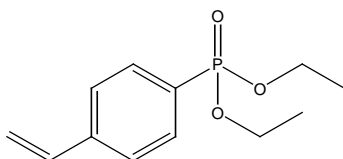
7.1.2. Synthesis of Allylphosphonic acid (Compound B)¹



A solution of diethyl allylphosphonate (8.9 g, 50 mmol), trimethylchlorosilane (44.8 g, 400 mmol) and dry potassium bromide (35.7 g, 300 mmol) in acetonitrile (250 mL) was refluxed for 3-4 days. The resultant solution was filtered over celite to remove the undissolved potassium bromide and the filtrate evaporated to yield the corresponding trimethylsilyl derivative, ($H_2C=CHCH_2PO(SiO(CH_3)_2)$). Deionized water (100 mL) was added and the solution stirred for 3 hours. The aqueous phase was washed with dichloromethane and evaporated to obtain allylphosphonic acid as a pale yellow oil (5.54 g, 91 %). $\nu_{max}(\text{film})$ 3385.8 (O-H), 1640.3

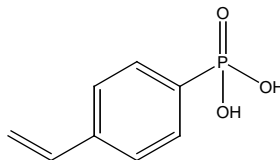
(C=C), 1143.4 (P=O), 994.3, 947.0, 827.4, 774.4, 665.6, 617.9 cm^{-1} ; δ_{H} (300 MHz; D_2O ; Me_4Si) 2.50 (2H, dd, $\text{CH}_2\text{-P}$, $^3J_{\text{HH}}=7.4$, $^2J_{\text{PH}}=21.8$), 4.50-4.85 (OH, m), 5.00-5.20 (2H, m, $\text{CH}_2=\text{CH}$), 5.60-5.85 (1H, m, $\text{CH}_2=\text{CH}$); δ_{C} (79 MHz; D_2O ; Me_4Si) 32.8 (d, $^1J_{\text{PC}}=133.6$, $\text{CH}_2\text{-P}$), 120.8 (d, $^2J_{\text{PC}}=14.3$, $\text{CH}_2=\text{CH}$), 128.4 (d, $^3J_{\text{PC}}=11.6$, $\text{CH}_2=\text{CH}$); δ_{P} (121 MHz, CD_3CN , H_3PO_4) 27.7 ppm (m, $^2J_{\text{PH}}=21.3$, $^3J_{\text{PH}}=5.6$ Hz).

7.1.3. Synthesis of Diethyl styrenephosphonate (Compound 1)



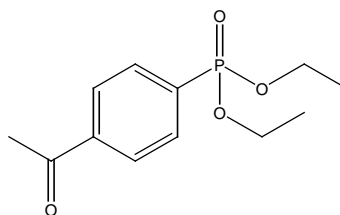
A round bottom flask equipped with a reflux condenser was charged with Palladium acetate ($\text{Pd}(\text{OAc})_2$) (0.14 g, 0.6 mmol) and triphenylphosphine (0.47 g, 1.8 mmol), the reaction vessel was evacuated and purged with nitrogen. Ethanol (120 mL), 4-bromostyrene (3.7 mL, 30 mmol), dicyclohexylmethylamine (9.6 mL, 45 mmol) and diethyl phosphite (4.7 mL, 36 mmol) were added via a syringe. The mixture was stirred at reflux for 16 hours and the solvent removed from the resulting yellow solution in *vacuo*. The solution was dissolved in ethyl acetate (~300 mL), before being washed with 2 M HCl (2 x 50 mL), sat. aq. NaHCO_3 and brine. The organic layer was dried over MgSO_4 , filtered and the volatiles were removed in *vacuo*. Yield (4.43 g, 61.5 %); $\nu_{\text{max}}(\text{film})$ 3465 (O-H), ~3000, 2983, 2906 (C-H), 1630 (C=C), 1601 (C=C ring), 1487.3, 1243 (P=O), 1132, 1023 (P-O), 967, 841 cm^{-1} ; δ_{H} (300 MHz; CDCl_3 ; Me_4Si) 1.31 (6H, t, $J_{\text{HH}}=7.0$, $\text{CH}_3\text{-CH}_2$), 3.99-4.18 (4H, m, $\text{CH}_3\text{-CH}_2$), 5.37 (1H, d, $J_{\text{HH,cis}}=11.1$, $\text{H}_2\text{C}=\text{CH}$), 5.85 (1H, d, $J_{\text{HH,trans}}=17.7$, $\text{H}_2\text{C}=\text{CH}$), 6.73 (1H, dd, $J_{\text{HH,cis}}=11.1$, $J_{\text{HH,trans}}=17.7$, $\text{H}_2\text{C}=\text{CH}$), 7.45-7.50 (2H, m, C_6H_4), 7.73-7.80 (2H, m, C_6H_4); δ_{C} (79 MHz; CDCl_3 ; Me_4Si) 15.3 ($\text{CH}_3\text{-CH}_2$), 61.0 ($\text{CH}_3\text{-CH}_2$), 113.6 (P-C), 115.5 ($\text{CH}=\text{CH}_2$), 125.1 ($J_{\text{PC}}=15.6$, C_6H_4), 131.0 ($J_{\text{PC}}=10.2$ Hz, C_6H_4), 134.7 ($\text{CH}=\text{CH}_2$), 140.4 ($\text{C-CH}=\text{CH}_2$); δ_{P} (121 MHz, CDCl_3 , H_3PO_4) 19.95 ppm; m/z (ES^+) 263 (100, $[M^+ + \text{Na}]$), 295 (40, $[M^+ + \text{Na} + \text{MeOH}]$), where $M^+ = [\text{H}_2\text{C}=\text{CHC}_6\text{H}_4\text{PO}(\text{OEt})_2]^+$.

7.1.4. Styrenephosphonic acid (Compound 2)



Diethyl styrenephosphonate (6.80 g, 28 mmol), trimethylchlorosilane (26.8 g, mmol) and dry potassium bromide (21.43 g, 300 mmol) in an acetonitrile (150 mL) solution were refluxed for 3-4 days. The resultant solution was filtered over celite and the filtrate evaporated to yield the trimethylsilyl derivative. Deionized water (100 mL) was added and the solution stirred for 3 hours. The aqueous phase was washed with dichloromethane and evaporated to obtain the acid as an off-white solid (4.42 g, 85 %); (found: C, 46.1; H, 3.7. Calc for $C_8H_9O_3P$: C, 52.2; H, 4.9 %); $\lambda_{\max}(\text{H}_2\text{O})$ (ϵ) 255 (17000), 283 (1800), 293.5 nm ($1200 \text{ mol}^{-1}\text{dm}^3\text{cm}^{-1}$); $\nu_{\max}(\text{KBr disc})$ 3446.6 (O-H), ~3000 (C-H), 2932 (C-H), 1628.8 (C=C), 1600.5 (C=C ring), 1458.2, 1208.2 (P=O), 1143.0 (P-O), 1112.7, 1006.5, 990.6, 930.7, 840.7, 645.9 cm^{-1} ; δ_{H} (300 MHz; D_2O ; Me_4Si) 5.35 (1H, d, $J_{\text{HH}}=11.1$, $\text{H}_2\text{C}=\text{CH}_2$), 5.88 (1H, d, $J_{\text{HH}}=17.7$, $\text{H}_2\text{C}=\text{CH}$), 6.75 (1H, dd, $J_{\text{HH}}=17.7$, 11.0, $\text{H}_2\text{C}=\text{CH}$), 7.48-7.55 (2H, m, C_6H_4), 7.64-7.72 (2H, m, C_6H_4); δ_{C} (79 MHz; D_2O ; Me_4Si) 116.6 ($\text{CH}=\text{CH}_2$), 127.1 ($J_{\text{PC}}=15.6$, C_6H_4), 132.2 ($J_{\text{PC}}=10.2$ Hz, C_6H_4), 137.3 ($\text{CH}=\text{CH}_2$), 142.4 ($\text{C}-\text{CH}=\text{CH}_2$); δ_{P} (121 MHz, D_2O , H_3PO_4) 17.4 ppm; m/z (ES^+) 185 [M^+], 217 [$M^+ + \text{MeOH}$], where $M^+ = [\text{H}_2\text{C}=\text{CHC}_6\text{H}_4\text{PO}(\text{OH})_2]^+$.

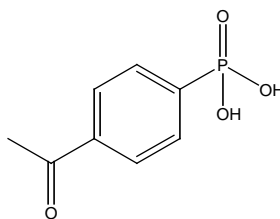
7.1.5. Diethyl 4-acetylphenylphosphonate (Compound C)²



Using the same procedure as in section 7.1.3, but with 4-bromoacetophenone (7.96 g, 40 mmol). The product was obtained as an orange oil (8.17 g, 79.8 %); $\nu_{\max}(\text{film})$ 2982.7, 2929.4 (C-H), 1690.6 (C=O), 1601.7, 1560.5 (C=C), 1440.2, 1360 (C-CH₃), 1253.1 (P=O), 1163.8, 1132.7 (P-

O), 1097.8, 1050.9, 1022.4, 967.1, 833.8, 790.0, 628.4 cm^{-1} ; δ_{H} (300 MHz; CDCl_3 ; Me_4Si) 1.31 (6H, t, $J_{\text{HH}}=7.0$, $\text{CH}_3\text{-CH}_2$), 2.60 (3H, s, $\text{CH}_3\text{C=O}$), 3.99-4.18 (4H, m, $\text{CH}_3\text{-CH}_2$), 7.90 (2H, dd, $\text{C}_6\text{H}_4\text{PO}$ 2Cs nearest P), 8.00 (2H, dd, $\text{C}_6\text{H}_4\text{PO}$ 2Cs nearest ketone); δ_{C} (79 MHz; CDCl_3 ; Me_4Si) 18.1 ($\text{CH}_3\text{-CH}_2$), 28.6 ($\text{CH}_3\text{C=O}$), 64.2 ($\text{CH}_3\text{-CH}_2$), 129.8 (d, $J_{\text{PC}}=15.3$, ring), 131.0 (d, $J_{\text{PC}}=9.8$ Hz, ring), 141.6 (C-C=O), 199.0 (C=O); δ_{P} (121 MHz, CDCl_3 , H_3PO_4) 17.75 ppm; m/z (ES^+) 279 (100, $[M^+ + \text{Na}]$), 311 (6, $[M^+ + \text{Na} + \text{MeOH}]$), where $M^+ = [\text{H}_3\text{CCOC}_6\text{H}_4\text{PO}(\text{OEt})_2]^+$.

7.1.6. 4-Acetylphenylphosphonic acid (Compound 3)



Using the same procedure as in section 7.1.4, but with diethyl 4-acetylphenylphosphonate (6.80 g, 28 mmol). Yield (4.54 g, 81.0 %); (found: C, 47.8; H, 4.4. Calc for $\text{C}_8\text{H}_9\text{O}_4\text{P}$: C, 48.0; H, 4.5 %); $\lambda_{\text{max}}(\text{H}_2\text{O})$ (ϵ) 250 nm ($25000 \text{ mol}^{-1} \text{ dm}^3 \text{ cm}^{-1}$); $\nu_{\text{max}}(\text{KBr disc})/\text{cm}^{-1}$ ~3400 (OH), ~2980, 2848 (C-H), 1654.5 (C=O), 1602.0 (C=C), 1559.7 (C=C), 1397.9, 1235.1 (P=O), 1187.6, 1125.7, 1007.6 (P-O), 970.5, 914.2, 830.5, 770.6, 630.4; δ_{H} (300 MHz; D_2O ; Me_4Si) 2.60 (3H, s, $\text{CH}_3\text{C=O}$), 7.90 (2H, m, C_6H_4), 8.00 (2H, m, C_6H_4); δ_{C} (79 MHz; D_2O ; Me_4Si) 27.7 ($\text{CH}_3\text{C=O}$), 129.5 (d, $J_{\text{PC}}=14.5$, C_6H_4), 131.9 (d, $J_{\text{PC}}=10.7$, C_6H_4), 139 (d, $J_{\text{PC}}=3.1$ Hz, P-C), 140.5 (C-C=O), 204 (C=O); δ_{P} (121 MHz, D_2O , H_3PO_4) 14.5 ppm ($^3J_{\text{PH}}=12.5$, $^4J_{\text{PH}}=3.2$ Hz); m/z (ES^+) 201 (44, $[M^+]$), 223 (100, $[M^+ + \text{Na}]$), 233 (98, $[M^+ + \text{MeOH}]$), 255 (70, $[M^+ + \text{Na} + \text{MeOH}]$), 279 (51, $[M^+ + 2\text{Na} + \text{MeOH}]$), where $M^+ = [\text{H}_3\text{CCOC}_6\text{H}_4\text{PO}(\text{OH})_2]^+$.

7.2. Synthesis of $K_8[\beta_2\text{-SiW}_{11}\text{O}_{39}]\cdot 14\text{H}_2\text{O}$ (Compound D)³

Sodium meta-silicate solution (2.75 g, 12.5 mmol) is dissolved in water (25 mL) (Solution A). Sodium tungstate (45.5 g, 0.14 mmol) is dissolved in water (75 mL) in a separate beaker, to this solution 4M HCl (41 mL) is added in 1 mL portions over 10 minutes, with vigorous stirring (there is local formation of hydrated tungstic acid that slowly disappears). Solution A is poured into the tungstate solution and the pH adjusted to 5-6 by addition of 4M HCl. This pH is maintained by addition of small amounts of 4M HCl for 100 minutes. Solid Potassium Chloride (22.5 g) is then added to the solution with gentle stirring, after 15 minutes the precipitate is collected by filtration. Purification is achieved by dissolving the product in water (215 mL) and insoluble material being removed by filtration on a fine frit. The salt is precipitated again by addition of solid potassium chloride (20 g) before being collected by filtration, washed with 2M potassium chloride and air dried to give $K_8[\beta_2\text{-SiW}_{11}\text{O}_{39}]\cdot 14\text{H}_2\text{O}$ as a white powder (13.86 g, 33.6 %). ν_{max} (KBr disc) 3448.0 (OH), 990.4, 948.4, 878.1, 855, 804.2, 731.5, 610, 537.9 cm^{-1} .

7.3. Synthesis of $K_8[\gamma\text{-SiW}_{10}\text{O}_{36}]\cdot 12\text{H}_2\text{O}$ (Compound E)³

This synthesis requires accurate pH readings on a calibrated pH meter. $K_8[\beta_2\text{-SiW}_{11}\text{O}_{39}]\cdot 14\text{H}_2\text{O}$ (5.0 g, 1 mmol) synthesised as described in section 7.2, is dissolved in water (50 mL) maintained at 25°C. Impurities in the $[\beta_2\text{-SiW}_{11}\text{O}_{39}]^{8-}$ salt give insoluble materials which have to be removed by filtration on a fine frit. The pH of the solution is quickly adjusted to 9.1 by addition of a 2M aqueous solution of K_2CO_3 . The pH is kept at this value by addition of the K_2CO_3 solution for 16 minutes. The potassium salt is then precipitated by addition of solid potassium chloride (13.3 g) during which the pH must be maintained at 9.1 by addition of small quantities of the K_2CO_3 solution. The solid is removed by filtering, washed with 1M KCl solution and air dried to give

$\text{K}_8[\gamma\text{-SiW}_{10}\text{O}_{36}]\cdot 12\text{H}_2\text{O}$ as a white powder (3.36 g, 73.3 %). $\nu_{\text{max}}(\text{KBr disc})$ 3439.8 (OH), 987.7, 942.6, 905, 865.9, 819.8, 745.8, 655, 553, 526.1 cm^{-1} .

7.4. Derivatization of $[\text{SiW}_{10}\text{O}_{36}]^{8-}$

7.4.1. Synthesis of $(\text{NBu}_4)_3\text{H}[\gamma\text{-SiW}_{10}\text{O}_{36}(\text{EtPO})_2]$ (Compound F)⁴

Powdered $\text{K}_8[\gamma\text{-SiW}_{10}\text{O}_{36}]\cdot 12\text{H}_2\text{O}$ (2.5 g, 0.8 mmol) was suspended in a mixture of NBu_4Br (0.81 g, 2.5 mmol) and $\text{EtPO}(\text{OH})_2$ (0.18 g, 1.7 mmol) in acetonitrile (42 mL). A 12M HCl solution (0.27 mL) was added dropwise under stirring, and the resulting mixture was stirred overnight at reflux. The white residue (KBr and unreacted $\text{SiW}_{10}\text{O}_{36}$) was separated by filtration and the resulting solution evaporated *in vacuo* to give crude compound. The crude compound was washed with water and recrystallized from acetonitrile by slow evaporation of the solvent at room temperature to give $(\text{NBu}_4)_3\text{H}[\gamma\text{-SiW}_{10}\text{O}_{36}(\text{EtPO})_2]$ as a white powder (2.18 g, 77.1 %). (found: N, 1.6; C, 20.1; H, 3.6. Calc. for $\text{C}_{52}\text{H}_{119}\text{N}_3\text{O}_{38}\text{P}_2\text{SiW}_{10}$: N, 1.3; C, 18.8; H, 3.6 %); $\nu_{\text{max}}(\text{KBr disc})$ 2963.9 (C-H), 1484, 1173 (P=O), 1070 (P-O), 1005.9 (P-O), 964.8, 940.0, 911.1, 882.6, 832.8, 752.0, 555.8 cm^{-1} ; δ_{H} (300 MHz; CD_3CN ; Me_4Si) 0.98 (36H, t, $J_{\text{HH}}=7.35$, $\text{CH}_3\text{-CH}_2\text{-CH}_2\text{-CH}_2\text{-N}$), 1.16-1.28 (6H, m, $\text{CH}_3\text{-CH}_2\text{-PO}$), 1.36 (24H, st, $J_{\text{HH}}=7.35$, $\text{CH}_3\text{-CH}_2\text{-CH}_2\text{-CH}_2\text{-N}$), 1.61 (28H, m, $\text{CH}_2\text{-CH}_2\text{-N}$, $\text{CH}_2\text{-PO}$), 3.06-3.13 (24H, m, $\text{CH}_2\text{-N}$); δ_{P} (121 MHz, CD_3CN , H_3PO_4) 29.4 ppm (m, $^2J_{\text{PH}}=19.9$, $^3J_{\text{PH}}=9.9$, $^2J_{\text{PW}}=10.1$ Hz); m/z (Maldi-TOF) 3524 [$M^+\text{-EtO+NBu}_4$], 3564 [$M^+\text{+NBu}_4$], 3643 [$M^+\text{-2EtPO+2NBu}_4$], 3757 [$M^+\text{-EtO+2NBu}_4$], 3869 [$M^+\text{-2EtPO}_2\text{+3NBu}_4$], 4022 [$M^+\text{-EtO+3NBu}_4\text{+Na}$], 4243 [$M^+\text{-EtO+4NBu}_4$], where $M^+ = (\text{NBu}_4)_3\text{H}[\text{SiW}_{10}\text{O}_{36}(\text{EtPO})_2]^+$.

7.4.2. Synthesis of $(\text{NEt}_4)_3\text{H}[\gamma\text{-SiW}_{10}\text{O}_{36}(\text{EtPO})_2]$ (Compound G)⁴

Was prepared and purified following a similar procedure to in section 7.4.1, but using NEt_4Br (0.52 g, 2.5 mmol) in place of NBu_4Br . Yield (1.93 g, 80.8 %). (found: N, 1.5; C, 13.5; H, 2.2. Calc for $\text{C}_{28}\text{H}_{70}\text{N}_3\text{O}_{38}\text{P}_2\text{SiW}_{10}$: N, 1.4; C, 11.2; H, 2.3 %); $\nu_{\text{max}}(\text{KBr disc})$ 2979.3 (C-H), 1484.1, 1172.9 (P=O), 1061.9, 1004.0 (P-O), 971.8, 943.0, 911.4, 882.8, 834.0, 750.0, 547.3 cm^{-1} ; δ_{H}

(300 MHz; CD₃CN; Me₄Si) 1.15-1.27 (36H, m, **CH₃-CH₂-N**), 1.27-1.40 (6H, m, **CH₃-CH₂-PO**), 1.55-1.70 (4H, m, **CH₂-PO**), 3.04-3.12 (24H, m, **CH₂-N**); δ_P (121 MHz, CD₃CN, H₃PO₄) 29.5 ppm (m, ²J_{PH}=20.0, ³J_{PH}=9.9, ²J_{PW}=10.1 Hz); *m/z* (Maldi-TOF): 2988 [*M*⁺], 3116 [*M*⁺+NBu₄], 3228 [*M*⁺-CH₃+2NBu₄], 3247 [*M*⁺+2NBu₄], 3357 [*M*⁺-CH₃+2NBu₄], where *M*⁺ = [(NBu₄)₃[SiW₁₀O₃₆(C₂H₅PO)₂]]⁺.

7.4.2.1. Crystallisation of (NBu₄)₂(NEt₄)H[SiW₁₀O₃₆(EtPO)₂] (Structure 1)

Crystals suitable for Single Crystal XRD were obtained by dissolving a mixture of (NBu₄)₃H[SiW₁₀O₃₆(EtPO)₂] (1.0 g) and (NEt₄)₃H[γ -SiW₁₀O₃₆(EtPO)₂] (0.5 g) in acetonitrile and allowing the solvent to evaporate slowly over several days. Data were collected on a Bruker SMART 6000 diffractometer ($\lambda_{\text{Cu-K}\alpha}$ = 1.54178 Å). Crystal Data. C₄₄H₁₀₃N₃O₃₈P₂SiW₁₀, M = 3210.82, Orthorhombic, a = 21.9890(9), b = 25.4008(9), c = 13.8974(6) Å, U = 7762.2(5) Å³, T = 298 K, space group P n 21 a (no. 33), Z = 4, 46156 reflections measured, 13465 unique (R_{int} = 0.063). The final values were R1(obs. data) = 0.040, R1(all data) = 0.058, wR2 = 0.094. Final refinements were carried out with anisotropic thermal parameters for all non-hydrogen atoms.

7.4.3. Synthesis of (NBu₄)₃H[γ -SiW₁₀O₃₆(H₂C=CHPO)₂] (Compound H)¹

Was prepared and purified following a similar procedure to in section 7.4.1, but using vinylphosphonic acid (H₂C=CHPO(OH)₂) (0.18g, 1.7mmol). Yield (2.27 g, 85.5 %). (found: C, 20.7; H, 3.6; N, 1.0. Calc for C₅₂H₁₁₅N₃O₃₈P₂SiW₁₀: C, 18.8; H, 3.5; N, 1.3 %); ν_{max} (KBr disc) 2964.4, 2937.4 (C-H), 1575.0 (C=C), 1486.2, 1049.2, 1006.8 (P-O), 962.4, 941.2, 906.5, 875.6, 833.2 cm⁻¹; δ_H (300 MHz; CD₃CN; Me₄Si) 0.95 (36H, t, J_{HH}=7.35 Hz, **CH₃**), 1.35 (24H, st, J_{HH}=7.35 Hz, **CH₃-CH₂**), 1.60 (24H, qn, J_{HH}=7.55 Hz, **CH₂-CH₂-N**), 3.06-3.13 (24H, m, **CH₂-N**),

5.78-6.35 (6H, m, **CH₂=CH-PO**); δ_P (121 MHz, CD₃CN, H₃PO₄) 14.8 ppm (dt, $^2J_{PH}=51.7$, $^3J_{PH}=24.9$, $^2J_{PW}=11.0$ Hz); MS (ES⁺)(%): m/z : 3074.9 (100) [M^+ -NBu₄], 2907.6 (41), 2872.7 (50), 1322.8 (61), 1296.5 (48).

7.4.4. Synthesis of (NEt₄)₃H[γ -SiW₁₀O₃₆(H₂C=CHPO)₂] (Compound I) ¹

Was prepared and purified following a similar procedure to in section 7.4.3, but using NEt₄Br (0.52 g, 2.5 mmol). Yield (1.82 g, 76.3 %); ν_{max} (KBr disc) 2982.5, 2935 (C-H), 1600 (C=C), 1484.1, 1458.0, 1173.0 (P=O), 1054.2, 1002.6 (P-O), 974.4, 942.3, 912.2, 883.9, 834.7, 754.1 cm⁻¹; δ_H (300 MHz; CD₃CN; Me₄Si) 1.12-1.32 (36H, m, **CH₃-CH₂-N**), 3.18 (24H, m, **CH₂-N**), 5.95-6.34 (6H, m, **C₂H₃PO**); δ_P (121 MHz, CD₃CN, H₃PO₄) 14.8 ppm.

7.4.5. Synthesis of (NBu₄)₃H[γ -SiW₁₀O₃₆(H₂C=CHCH₂PO)₂] (Compound J) ¹

Was prepared and purified following a similar procedure to in section 7.4.1, but using allylphosphonic acid (0.21 g, 1.7 mmol). Yield (2.26 g, 84.4 %). (found: C, 20.8; H, 3.9; N, 1.55. Calcd for C₅₄H₁₁₉N₃O₃₈P₂SiW₁₀: C, 19.4; H, 3.6; N, 1.3 %); ν_{max} (KBr disc) 2962.3, 2874.2 (C-H), 1600 (C=C), 1483.9, 1463.9, 1170, 1056.9, 1006.8 (P-O), 965.3, 943.9, 909.9, 885.5, 837.2, 752.3, 731.0 cm⁻¹; δ_H (300 MHz; CD₃CN; Me₄Si) 0.98 (36H, t, $J_{HH}=7.35$, **CH₃**), 1.38 (24H, st, $J_{HH}=7.35$, **CH₃-CH₂**), 1.62 (24H, qn, $J_{HH}=7.52$, **CH₂-CH₂-N**), 2.60 (4H, dd, $J_{PH}=7.24$, $J_{PH}=23.17$, **CH₂-P**), 3.08-3.15 (24H, m, **CH₂-N**), 5.14-5.27 (4H, m, **CH₂=CH**), 5.79-5.96 (2H, m, **CH₂=CH**); δ_P (121 MHz, CD₃CN, H₃PO₄) 24.45 (m, $^2J_{PH}=23.4$, $^3J_{PH}=^4J_{PH}=5.6$, $^2J_{PW}=11.3$ Hz); δ_C (79 Hz, DMF: DMSO-d₆ (9:1), Me₄Si) 15.6 (**CH₃-CH₂-CH₂-CH₂-N**), 21.4 (**CH₃-CH₂-CH₂-CH₂-N**), 25.2 (**CH₂-CH₂-N**), 33.7 (**CH₂-P**), 59.7 (**CH₂-N**), 120.8 (**CH₂=CH**), 128.4 ppm (**CH₂=CH**); m/z (ES⁺) (%): 3104.2 (100) [M^+ -NBu₄], 1431.0 (32), 1338.3 (47), 1309.5 (29).

7.4.6. Synthesis of $(\text{NEt}_4)_3\text{H}[\gamma\text{-SiW}_{10}\text{O}_{36}(\text{H}_2\text{C}=\text{CHCH}_2\text{PO})_2]$ (Compound K) ¹

Was prepared and purified following a similar procedure to in section 7.4.5, but using NEt_4Br (0.52 g, 2.5 mmol). Yield (1.86 g, 76.3 %). (found C, 11.9; H, 2.1; N, 1.6. Calc for $\text{C}_{30}\text{H}_{70}\text{N}_3\text{O}_{38}\text{P}_2\text{SiW}_{10}$: C, 11.9; H, 2.4; N, 1.4 %); $\nu_{\text{max}}(\text{KBr disc})$ 2985.8 (C-H), 1600 (C=C), 1485, 1459.8, 1175 (P=O), 1060, 1005.0 (P-O), 971.9, 943.9, 911.6, 883.3, 832.2, 749.2 cm^{-1} ; δ_{H} (300 MHz; CD_3CN ; Me_4Si) 1.13-1.32 (36H, m, $\text{CH}_3\text{-CH}_2\text{-N}$), 2.60 (4H, dd, $J_{\text{HH}}=7.4$, $J_{\text{PH}}=21.9$, $\text{CH}_2\text{-PO}$), 3.18 (24H, q, $J_{\text{HH}}=7.3$ Hz, $\text{CH}_2\text{-N}$), 5.05-5.27 (4H, m, $\text{CH}_2=\text{CH}$), 5.74-5.94 (2H, m, $\text{CH}_2=\text{CH}$); δ_{P} (121 MHz, CD_3CN , H_3PO_4) 24.6 ppm; m/z (Maldi-TOF) 3009 [M^+], 3138 [$M^+ + \text{NEt}_4$], 3268 [$M^+ + 2\text{NEt}_4$], 3369 [$M^+ - \text{C}_2\text{H}_3 + 3\text{NEt}_4$], 3402 [$M^+ + 3\text{NEt}_4$], 3499 [$M^+ - \text{C}_2\text{H}_3 + 4\text{NEt}_4$], where $M^+ = [(\text{NEt}_4)_3[\text{SiW}_{10}\text{O}_{36}(\text{C}_3\text{H}_5\text{PO})_2]]^+$. Crystals suitable for Single Crystal XRD were obtained by slow diffusion of diethyl ether into an acetonitrile solution containing the crude product. Data were collected on a Bruker SMART 6000 diffractometer ($\lambda_{\text{Cu-K}\alpha} = 1.54178$ Å). Structure 3. $\text{C}_{34}\text{H}_{77}\text{N}_5\text{O}_{38}\text{P}_2\text{SiW}_{10}$, $M = 3092.5$, Monoclinic, $a = 24.479(5)$, $b = 10.829(2)$, $c = 27.308(5)$ Å, $\beta = 94.51(2)^\circ$, $U = 7216.0(2)$ Å³, $T = 293$ K, space group C 2/c (no. 15), $Z = 4$, 18331 reflections measured, 6479 unique ($R_{\text{int}}=0.078$). The Final $R1(\text{obs. data}) = 0.074$, $R1(\text{all data}) = 0.097$. Final refinements were carried out with anisotropic thermal parameters for all non-hydrogen atoms except those in the solvent.

7.4.6.1. Crystallisation of $(\text{NBu}_4)_2(\text{NEt}_4)\text{H}[\text{SiW}_{10}\text{O}_{36}(\text{H}_2\text{C}=\text{CHCH}_2\text{PO})_2]$ (Structure 2)

Crystals suitable for Single Crystal XRD were obtained by dissolving a mixture of $(\text{NBu}_4)_3\text{H}[\gamma\text{-SiW}_{10}\text{O}_{36}(\text{C}_3\text{H}_5\text{PO})_2]$ (1.0 g) and $(\text{NEt}_4)_3\text{H}[\gamma\text{-SiW}_{10}\text{O}_{36}(\text{C}_3\text{H}_5\text{PO})_2]$ (0.5 g) in acetonitrile and allowing diethyl ether to diffuse into the solution over several days. Data were collected on Station 9.8 at the SRS Synchrotron source, Daresbury ($\lambda = 0.67030$ Å). Crystal Data.

$\text{C}_{46}\text{H}_{103}\text{N}_3\text{O}_{38}\text{P}_2\text{SiW}_{10}$, $M = 3234.84$, Monoclinic, $a = 18.7759(16)$, $b = 24.639(2)$, $c = 17.1317(15)$ Å, $\beta = 106.406(10)^\circ$, $U = 7602.9(11)$ Å³, $T = 200$ K, space group Cc (no. 33), $Z = 4$, 47924 reflections measured, 24702 unique ($R_{\text{int}}=0.036$). The Final $R1(\text{obs. data}) = 0.038$, $R1(\text{all data}) = 0.050$. Final refinements were carried out with anisotropic thermal parameters for all non-hydrogen atoms.

7.4.7. Synthesis of $(\text{NBu}_4)_3\text{H}[\gamma\text{-SiW}_{10}\text{O}_{36}(\text{H}_2\text{C}=\text{CHC}_6\text{H}_4\text{PO})_2]$ (Compound 4)

Was prepared and purified following a similar procedure to in section 7.4.1, but with styrylphosphonic acid (0.31 g, 1.7 mmol). Yield (2.46 g, 88.6 %). (found: C, 21.9; H, 3.7; N, 1.5. Calc for $\text{C}_{64}\text{H}_{123}\text{N}_3\text{O}_{38}\text{P}_2\text{SiW}_{10}$: C, 22.1; H, 3.55; N, 1.2 %); $\lambda_{\text{max}}(\text{CH}_3\text{CN})$ (ϵ) 258 (60000 mol⁻¹dm³cm⁻¹), 282, 291 nm; $\nu_{\text{max}}(\text{KBr disc})$ 2960.7, 2873.5 (C-H), 1600.6 (C=C), 1482.3, 1136.3 (P=O), 1058.4 (P-O), 1004.0, 972.2, 941.0, 913.2, 886.8, 837.7, 748.8 cm⁻¹; δ_{H} (300 MHz; CD₃CN; Me₄Si) 0.98 (36H, t, $J_{\text{HH}}=7.35$, **CH**₃), 1.38 (24H, st, $J_{\text{HH}}=7.35$, **CH**₃-**CH**₂), 1.62 (24H, qn, $J_{\text{HH}}=7.52$, **CH**₂-CH₂-N), 3.08-3.15 (24H, m, **CH**₂-N), 5.35 (2H, dd, $J_{\text{PH}}=15.6$, $J_{\text{HH}}=11.0$, **H**₂C=CH), 5.95 (2H, dd, $J_{\text{PH}}=15.6$, $J_{\text{HH}}=9.55$, **H**₂C=CH), 6.74-6.88 (1H, m, H₂C=CH), 7.55-7.96 ppm (8H, m, **C**₆**H**₄); δ_{P} (121 MHz, CD₃CN, H₃PO₄) 15.4 ppm ($^2J_{\text{PW}}=11.14$, $J_{\text{PH}}=14.8$, $J_{\text{PH}}=4.1$ Hz); m/z (Maldi-TOF) 3445 [$M^+-\text{C}_2\text{H}_3$], 3537 [$M^++\text{NBu}_4-\text{C}_8\text{H}_7\text{PO}-\text{C}_2\text{H}_3$], 3687 [$M^++\text{NBu}_4-\text{C}_2\text{H}_3$], 3929 [$M^++2\text{NBu}_4-\text{C}_8\text{H}_7$], where $M^+= (\text{NBu}_4)_3[\text{SiW}_{10}\text{O}_{36}(\text{H}_2\text{C}=\text{CHC}_6\text{H}_4\text{PO})_2]^+$. Data were collected on Station 16.2smx at the SRS Synchrotron source, Daresbury ($\lambda = 0.79720$ Å). Structure 4. $\text{C}_{320}\text{H}_{610}\text{N}_{15}\text{O}_{190}\text{P}_{10}\text{Si}_5\text{W}_{50}$, $M = 17350.88$, Monoclinic, $a = 14.3007(16)$, $b = 63.244(7)$, $c = 28.028(3)$ Å, $\beta = 91.1(1)^\circ$, $U = 25345(5)$ Å³, $T = 200$ K, space group $P2_1$ (no. 4), $Z = 11$, 118435 reflections measured, 53169 unique ($R_{\text{int}}=0.124$). The Final $R1(\text{obs. data}) = 0.193$, $R1(\text{all data}) = 0.193$.

data) = 0.338. Final refinements were carried out with anisotropic thermal parameters for all the tungsten atoms.

7.4.8. Synthesis of $(\text{NEt}_4)_3\text{H}[\gamma\text{-SiW}_{10}\text{O}_{36}(\text{H}_2\text{C}=\text{CHC}_6\text{H}_4\text{PO})_2]$ (Compound 5)

Was prepared and purified following a similar procedure to that in section 7.4.7, but using NEt_4Br (0.52 g, 2.5 mmol). Yield (1.93 g, 77.0 %), (found: C, 12.1; H, 2.3; N, 1.3. Calc for $\text{C}_{40}\text{H}_{74}\text{N}_3\text{O}_{38}\text{P}_2\text{SiW}_{10}$: C, 15.3; H, 2.4; N, 1.3 %); $\nu_{\text{max}}(\text{KBr disc})$ 2980.7 (C-H), 2875 (C-H), 1600 (C=C), 1483.6, 1173.0, 1137.0 (P=O), 1050 (P-O), 1002.7, 971.8, 942.7, 911.8, 884.9, 835.6, 752.6 cm^{-1} ; δ_{H} (300 MHz; CD_3CN ; Me_4Si) 1.10-1.33 (36H, m, $\text{CH}_3\text{-CH}_2\text{-N}$), 3.20 (24H, q, $\text{CH}_2\text{-N}$), 5.40 (2H, dd, $J = 15.6, 11.0$ Hz, $\text{H}_2\text{C}=\text{CH}$), 5.93 (2H, dd, $J = 15.6, 9.55$, $\text{H}_2\text{C}=\text{CH}$), 6.76-6.90 (2H, m, $\text{H}_2\text{C}=\text{CH}$), 7.55-7.95 (8H, m, C_6H_4); δ_{P} (121 MHz, CD_3CN , H_3PO_4) 15.5 ppm ($^2J_{\text{PW}} = 9.2$ Hz); m/z (Maldi-TOF) 3137 [M^+], 3162 [$M^+ + \text{Na}$], 3266 [$M^+ + \text{NEt}_4$], 3293 [$M^+ + \text{NEt}_4 + \text{Na}$], 3425 [$M^+ + 2\text{NEt}_4 + \text{Na}$], 3556 [$M^+ + 3\text{NEt}_4 + \text{Na}$], where $M^+ = (\text{NEt}_4)_3[\text{SiW}_{10}\text{O}_{36}(\text{H}_2\text{C}=\text{CHC}_6\text{H}_4\text{PO})_2]^+$.

7.4.9. Synthesis of $(\text{NBu}_4)_3\text{H}[\gamma\text{-SiW}_{10}\text{O}_{36}(\text{HOOCCH}_2\text{PO})_2]$ (Compound 6)

Was prepared and purified following a similar procedure to in section 7.4.1, but using $\text{HOOCCH}_2\text{PO}(\text{OH})_2$ (0.24 g, 1.7 mmol). Yield (1.92 g, 70.9 %). (found: C, 18.3; H, 3.5; N, 1.3. Calc for $\text{C}_{52}\text{H}_{115}\text{N}_3\text{O}_{42}\text{P}_2\text{SiW}_{10}$: C, 18.5; H, 3.4; N, 1.2 %); $\nu_{\text{max}}(\text{KBr disc})$ 3414 (O-H), 2962.4 (C-H), 2874.3 (C-H), 1718.5 (C=O), 1483.8, 1153.2, 1108.8 (P=O), 1050 (P-O), 1007.7, 968.9, 940, 911.7, 885, 839.9, 758.1 cm^{-1} ; δ_{H} (300 MHz; CD_3CN ; Me_4Si) 0.98 (36H, t, $J_{\text{HH}} = 7.35$, $\text{CH}_3\text{-CH}_2\text{-CH}_2\text{-CH}_2\text{-N}$), 1.38 (24H, st, $J_{\text{HH}} = 7.35$, $\text{CH}_3\text{-CH}_2\text{-CH}_2\text{-CH}_2\text{-N}$), 1.62 (24H, qn, $J_{\text{HH}} = 7.52$, $\text{CH}_2\text{-CH}_2\text{-N}$), 2.90 (4H, d, $J_{\text{PH}} = 23.1$, $\text{CH}_2\text{-COOH}$), 3.08-3.15 (24H, m, $\text{CH}_2\text{-N}$); δ_{P} (121 MHz, CD_3CN , H_3PO_4) 18.4 ppm ($^2J_{\text{PW}} = 11.1$ Hz); m/z (Maldi-TOF): 3492 [$M^+ - \text{HOOCCH}_2\text{PO}_3 + \text{NBu}_4$], 3638 [$M^+ + \text{NBu}_4$], 3732 [$M^+ - \text{HOOCCH}_2\text{PO}_3 + 2\text{NBu}_4$], 3874 [$M^+ + 2\text{NBu}_4$], where $M^+ = (\text{NBu}_4)_3[\text{SiW}_{10}\text{O}_{36}(\text{HOOCCH}_2\text{PO})_2]^+$.

7.4.10. Synthesis of $(\text{NEt}_4)_3\text{H}[\gamma\text{-SiW}_{10}\text{O}_{36}(\text{HOOCCH}_2\text{PO})_2]$ (Compound 7)

Was prepared and purified following a similar procedure to in section 7.4.9, but using NEt_4Br (0.52 g, 2.5 mmol). Yield (1.18 g, 48.4 %). (found: C, 11.55; H, 2.3; N, 1.05. Calc for $\text{C}_{28}\text{H}_{66}\text{N}_3\text{O}_{42}\text{P}_2\text{SiW}_{10}$: C, 11.0; H, 2.2; N, 1.4 %); $\nu_{\text{max}}(\text{KBr disc})$ 3447.9 (O-H), 2962.0, 2875 (C-H), 1718.2 (C=O), 1484.1, 1173.5 (P=O), 1050 (P-O), 1003.0, 970.1, 940, 911.0, 886.2, 837.0, 749.6 cm^{-1} ; δ_{H} (300 MHz; CD_3CN ; Me_4Si) 1.10-1.33 (36H, m, $\text{CH}_3\text{-CH}_2\text{-N}$), 2.90 (4H, d, $J_{\text{PH}}=23.1$, $\text{CH}_2\text{-COOH}$), 3.20 (24H, q, $J_{\text{HH}}=7.0$, $\text{CH}_2\text{-N}$); δ_{P} (121 MHz, CD_3CN , H_3PO_4) 18.5 ppm ($^2J_{\text{PW}}=11.2$ Hz); m/z (Maldi-TOF) 3041 [M^+], 3174 [$M^+ + \text{NEt}_4$], 3305 [$M^+ + 2\text{NEt}_4$], 3361 [$M^+ - \text{HOOCCH}_2\text{-OH} + 3\text{NEt}_4$], 3416 [$M^+ - \text{OH} + 3\text{NEt}_4$], 3436 [$M^+ + 3\text{NEt}_4$], where $M^+ = (\text{NEt}_4)_3[\text{SiW}_{10}\text{O}_{36}(\text{HOOCCH}_2\text{PO})_2]^+$. Crystals suitable for Single Crystal XRD were obtained by dissolving $(\text{NEt}_4)_3\text{H}[\gamma\text{-SiW}_{10}\text{O}_{36}(\text{HOOCCH}_2\text{PO})_2]$ (0.5 g) in DMF and allowing diethyl ether to slowly diffuse into the solution over several days. Data were collected on Station 9.8 at the SRS Synchrotron source, Daresbury ($\lambda = 0.67030$ Å). Structure 5. $\text{C}_{31}\text{H}_{74}\text{N}_4\text{O}_{43}\text{P}_2\text{SiW}_{10}$, $M = 3119.5$, Monoclinic, $a = 24.1700(2)$, $b = 10.7640(1)$, $c = 27.0430(5)$ Å, $\beta = 98.11(1)^\circ$, $U = 6965.3(0)$ Å³, $T = 200$ K, space group Cc (no. 33), $Z = 4$, 31458 reflections measured, 15511 unique ($R_{\text{int}}=0.044$). The Final $R1(\text{obs. data}) = 0.038$, $R1(\text{all data}) = 0.052$. Final refinements were carried out with anisotropic thermal parameters for the polyoxometalate cluster and the central atoms in the cations.

7.4.11. Synthesis of $(\text{NBu}_4)_3\text{H}[\gamma\text{-SiW}_{10}\text{O}_{36}(\text{HOOC}(\text{CH}_2)_2\text{PO})_2]$ (Compound L)⁴

Was prepared and purified following a similar procedure to in section 7.4.1, but using $\text{HOOC}(\text{CH}_2)_2\text{PO}(\text{OH})_2$ (0.27 g, 1.7 mmol). Yield (2.40 g, 87.95 %). (found: C, 21.3; H, 3.65; N, 1.5. Calc for $\text{C}_{54}\text{H}_{119}\text{N}_3\text{O}_{42}\text{P}_2\text{SiW}_{10}$: C, 18.9; H, 3.4; N, 1.2 %); $\nu_{\text{max}}(\text{KBr disc})$ 3420.8 (O-H),

2962.2, 2874.4 (C-H), 1734.2 (C=O), 1483.5, 1050 (P-O), 1009.2 (P-O), 975.2, 943.1, 912.1, 886.7, 839.3, 758.5 cm^{-1} ; δ_{H} (300 MHz; CD_3CN ; Me_4Si) 0.97 (36H, t, $J_{\text{HH}}=7.35$, $\text{CH}_3\text{-CH}_2\text{-CH}_2\text{-CH}_2\text{-N}$), 1.37 (24H, st, $J_{\text{HH}}=7.35$, $\text{CH}_3\text{-CH}_2\text{-CH}_2\text{-CH}_2\text{-N}$), 1.62 (24H, qn, $J_{\text{HH}}=7.55$, $\text{CH}_2\text{-CH}_2\text{-N}$), 1.98-2.12 (4H, m, $\text{CH}_2\text{-PO}$), 2.57-2.68 (4H, m, HOOC-CH_2), 3.06-3.16 (24H, m, $\text{CH}_2\text{-N}$); δ_{P} (121 MHz, CD_3CN , H_3PO_4) 26.9 ppm ($^2J_{\text{PW}}=11.1$, $^2J_{\text{PH}}=18.4$, $^3J_{\text{PH}}=10.1$ Hz); m/z (Maldi-TOF) 3498 [$M^+\text{-HOOC(CH}_2)_2\text{PO}_3\text{+NBu}_4$], 3647 [$M^+\text{+NBu}_4$], 3734 [$M^+\text{-HOOC(CH}_2)_2\text{PO}_3\text{+2NBu}_4$], 3889 [$M^+\text{+2NBu}_4$] where $M^+ = (\text{NBu}_4)_3[\text{SiW}_{10}\text{O}_{36}(\text{HOOC(CH}_2)_2\text{PO})_2]^+$.

7.4.12. Synthesis of $(\text{NEt}_4)_3\text{H}[\gamma\text{-SiW}_{10}\text{O}_{36}(\text{HOOC(CH}_2)_2\text{PO})_2]$ (Compound M) ⁴

Was prepared and purified following a similar procedure to in section 7.4.11, but using NEt_4Br (0.52 g, 2.5 mmol). Yield (1.20 g, 48.8 %). (found: C, 12.5; H, 2.4; N, 0.9. Calc for $\text{C}_{30}\text{H}_{71}\text{N}_3\text{O}_{42}\text{P}_2\text{SiW}_{10}$: C, 11.7; H, 2.3; N, 1.4 %); ν_{max} (KBr disc) 3439.1 (O-H), 2985.1, 2960 (C-H), 1734.2 (C=O), 1483.7, 1172.8 (P=O), 1050 (P-O), 1002.6 (P-O), 973.7, 943.3, 911.8, 884.1, 835.0, 754.7 cm^{-1} ; δ_{H} (300 MHz; CD_3CN ; Me_4Si) 1.10-1.33 (36H, m, $\text{CH}_3\text{-CH}_2\text{-N}$), 1.98-2.12 (4H, m, $\text{CH}_2\text{-PO}$), 2.58-2.69 (4H, m, HOOC-CH_2), 3.20 (24H, q, $J_{\text{HH}}=7.0$, $\text{CH}_2\text{-N}$); δ_{P} (121 MHz, CD_3CN , H_3PO_4) 26.9 ppm ($^2J_{\text{PW}}=11.1$ Hz); m/z (Maldi-TOF) 3050 [$M^+\text{-OH}$], 3070 [M^+], 3130 [$M^+\text{-HOOC(CH}_2)_2$], 3200 [$M^+\text{+NBu}_4$], 3258 [$M^+\text{-HOOC(CH}_2)_2\text{+2NBu}_4$], 3330 [$M^+\text{+2NBu}_4$], 3386 [$M^+\text{-HOOC(CH}_2)_2\text{+3NBu}_4$], 3520 [$M^+\text{-HOOC(CH}_2)_2\text{+4NBu}_4$], where $M^+ = (\text{NEt}_4)_3[\text{SiW}_{10}\text{O}_{36}(\text{HOOC(CH}_2)_2\text{PO})_2]^+$. Crystals suitable for Single Crystal XRD were obtained by dissolving $(\text{NEt}_4)_3\text{H}[\gamma\text{-SiW}_{10}\text{O}_{36}(\text{HOOCCH}_2\text{CH}_2\text{PO})_2]$ (0.5 g) in acetonitrile and allowing diethyl ether to diffuse into the solution over several days. Data were collected on a Bruker SMART 6000 diffractometer ($\lambda_{\text{Cu-K}\alpha} = 1.54178 \text{ \AA}$). Structure 6. $\text{C}_{42}\text{H}_{88}\text{N}_9\text{O}_{42}\text{P}_2\text{SiW}_{10}$, $M = 3319.74$, Monoclinic, $a = 24.616(11)$, $b = 10.758(5)$, $c = 32.647(15) \text{ \AA}$, $\beta = 108.42(2)^\circ$, $U =$

8202.9(6) Å³, T = 200 K, space group P 2/c (no. 33), Z = 4, 29125 reflections measured, 7917 unique ($R_{\text{int}} = 0.090$). The Final $R1(\text{obs. data}) = 0.082$, $R1(\text{all data}) = 0.138$. Final refinements were carried out with anisotropic thermal parameters for the tungsten and phosphorus atoms.

7.4.13. Synthesis of (NBu₄)₃H[γ-SiW₁₀O₃₆(H₃CCOC₆H₄PO)₂] (Compound 8)

Was prepared and purified following a similar procedure to in section 7.4.1, but using H₃CCOC₆H₄PO(OH)₂ (0.34 g, 1.7 mmol). Yield (2.27 g, 81.0 %). (found: C, 24.0; H, 3.85; N, 1.6. Calc for C₆₄H₁₂₃N₃O₄₀P₂SiW₁₀: C, 21.9; H, 3.5; N, 1.2 %); $\lambda_{\text{max}}(\text{CH}_3\text{CN})$ (ϵ) 247 nm (47000 mol⁻¹dm³cm⁻¹); $\nu_{\text{max}}(\text{KBr disc})$ 2962.0 (C-H), 2873.4 (C-H), 1684.9 (C=O), 1482.7, 1264.3, 1138.4 (P=O), 1062.4 (P-O), 1007.4, 975.6, 942.3, 912.2, 886.5, 836.6, 753.5 cm⁻¹; δ_{H} (300 MHz; CD₃CN; Me₄Si) 0.98 (36H, t, $J_{\text{HH}}=7.35$, **CH**₃-CH₂-CH₂-CH₂-N), 1.36 (24H, st, $J_{\text{HH}}=7.35$, CH₃-**CH**₂-CH₂-CH₂-N), 1.64 (24H, qn, $J_{\text{HH}}=7.52$, **CH**₂-CH₂-N), 2.60 (6H, s), 3.03-3.18 (24H, m, **CH**₂-N), 7.96-8.14 (8H, m, **C**₆**H**₄); δ_{P} (121 MHz, CD₃CN, H₃PO₄) 14.0 ppm ($^2J_{\text{PW}}=11.2$ Hz, $J_{\text{PH}}=12.8$, $J_{\text{PH}}=4.78$ Hz); m/z (Maldi-TOF) 3744 [M^+ +NBu₄], 3781 [M^+ -H₃CCOC₆H₄PO-H₃CCO+2NBu₄], 3987 [M^+ +2NBu₄], 4085 [M^+ -H₃CCOC₆H₄-H₃C+3NBu₄], 4230 [M^+ +3NBu₄], where $M^+ = (\text{NBu}_4)_3[\text{SiW}_{10}\text{O}_{36}(\text{H}_3\text{CCOC}_6\text{H}_4\text{PO})_2]^+$.

7.4.14. Synthesis of (NEt₄)₃H[γ-SiW₁₀O₃₆(H₃CCOC₆H₄PO)₂] (Compound 9)

Was prepared and purified following a similar procedure to in section 7.4.13, but using NEt₄Br (0.52 g, 2.5 mmol). Yield (2.30 g, 90.8 %). (found: C, 15.3; H, 2.2; N, 0.9. Calc for C₄₀H₇₅N₃O₄₀P₂SiW₁₀: C, 15.2; H, 2.3; N, 1.3 %); $\nu_{\text{max}}(\text{KBr disc})$ 2982.5 (C-H), 2875 (C-H), 1684.6 (C=O), 1483.6, 1264.6, 1138.1 (P=O), 1059.3 (P-O), 1002.7, 974.9, 943.0, 912.4, 885.5, 835.1, 746.1 cm⁻¹; δ_{H} (300 MHz; CD₃CN; Me₄Si) 1.10-1.30 (36H, m, **CH**₃-CH₂-N), 2.60 (6H, s),

3.18 (24H, q, $\text{CH}_2\text{-N}$), 8.00-8.21 ppm (8H, m, C_6H_4); δ_{P} (121 MHz, CD_3CN , H_3PO_4) 14.1 ppm ($^2J_{\text{PW}}=11.3$ Hz); m/z (Maldi-TOF) 3172 [M^+], 3212 [$M^+-2\text{H}_3\text{CCO}+\text{NBu}_4$], 3297 [$M^++\text{NBu}_4$], 3427 [$M^++2\text{NBu}_4$], where $M^+= (\text{NEt}_4)_3[\text{SiW}_{10}\text{O}_{36}(\text{H}_3\text{CCOC}_6\text{H}_4\text{PO})_2]^+$. Crystals suitable for Single Crystal XRD were obtained by dissolving $(\text{NEt}_4)_3\text{H}[\gamma\text{-SiW}_{10}\text{O}_{36}(\text{H}_3\text{CCOC}_6\text{H}_4\text{PO})_2]$ (0.5 g) in acetonitrile and allowing diethyl ether to slowly diffuse into the solution. Data were collected on Station 9.8 at the SRS Synchrotron source, Daresbury ($\lambda = 0.67030$ Å). Structure 7. $\text{C}_{48}\text{H}_{91}\text{N}_5\text{O}_{41}\text{P}_2\text{SiW}_{10}$, $M = 3322.8$, Triclinic, $a = 13.9167(11)$, $b = 15.4099(12)$, $c = 19.5468(15)$ Å, $\alpha = 98.55(2)^\circ$, $\beta = 110.27(1)^\circ$, $\gamma = 91.90(1)^\circ$, $U = 3872.4(5)$ Å³, $T = 200$ K, space group $P\bar{1}$ (no. 2), $Z = 2$, 34889 reflections measured, 25461 unique ($R_{\text{int}}=0.034$). The Final $R1(\text{obs. data}) = 0.049$, $R1(\text{all data}) = 0.066$. Final refinements were carried out with anisotropic thermal parameters for all non-hydrogen atoms except those in the solvent.

7.5. Synthesis of $\text{Cs}_6[\text{P}_2\text{W}_5\text{O}_{23}]$ (Compound N)⁵

Tungstic acid (H_2WO_4) (30 g, 0.12 mol) is slurred with water (200 mL) to give a bright yellow solution. To this solution 50 % aqueous cesium hydroxide (55 ml) is added dropwise with vigorous stirring, this slowly turns the solution white. The turbid solution is passed through a cake of Celite[®] to produce a clear colourless solution. Phosphonic acid (85 % H_3PO_4) is added dropwise while stirring to adjust the pH to 7.0 and the solution is stirred for an additional hour. The solution is filtered and the filtrate cooled in a refrigerator for 24 hours before being filtered again to give hexacesium pentatungstodiphosphate ($\text{Cs}_6[\text{P}_2\text{W}_5\text{O}_{23}]\cdot x\text{H}_2\text{O}$) as a white crystalline solid (48.10 g, yield not calculated as ratio of water molecules unknown). ν_{max} (KBr disc) 3401.8, 1147.0, 1050.8, 991.6, 898.7, 800, 691.0 cm^{-1} .

7.6. Synthesis of $\text{Cs}_7[\text{PW}_{10}\text{O}_{36}]$ (Compound O) ⁵

$\text{Cs}_6[\text{P}_2\text{W}_5\text{O}_{23}]\cdot x\text{H}_2\text{O}$ (37.5 g) and water (75 mL) are stirred and heated to reflux for 24 hours, the solution is hot filtered through a medium frit to yield $\text{Cs}_7[\text{PW}_{10}\text{O}_{36}]\cdot\text{H}_2\text{O}$ (7.52 g, 23.7 % from tungstic acid) The filtrate is cooled in the fridge for 48 hours and filtered to remove unconverted $\text{Cs}_6[\text{P}_2\text{W}_5\text{O}_{23}]\cdot x\text{H}_2\text{O}$ (20 g) which is used in later preparations. ν_{max} (KBr disc) 3535.4, 1086.1, 1053.4, 1024.5, 950, 937.2, 892.6, 850, 824.3, 750 cm^{-1} .

7.6.1. Synthesis of $(\text{NBu}_4)_3[\gamma\text{-PW}_{10}\text{O}_{36}(\text{EtPO})_2]$ (Compound 10)

Was prepared and purified following a similar procedure to in section 7.4.1, but using powdered $\text{Cs}_7[\text{PW}_{10}\text{O}_{36}]\cdot\text{H}_2\text{O}$ (2.0 g, 0.64 mmol), NBu_4Br (0.65 g, 2 mmol) and $\text{EtPO}(\text{OH})_2$ (0.15 g, 1.4 mmol). Yield (1.51 g, 71.0 %). (Found: C, 20.6; H, 3.9; N, 1.4. Calc. for $\text{C}_{52}\text{H}_{118}\text{N}_3\text{O}_{38}\text{P}_3\text{W}_{10}$: C, 18.8; H, 3.6; N, 1.3 %); ν_{max} (KBr disc) 2962.8 (C-H), 2874.8 (C-H), 1483.5, 1110.9 (P-O), 1049.8 (P-O), 965.2, 850, 817.9 cm^{-1} ; δ_{H} (300 MHz; CD_3CN ; Me_4Si) 0.95 (42H, t, $J_{\text{HH}}=7.35$, $\text{CH}_3\text{-CH}_2\text{-CH}_2\text{-CH}_2\text{-N}$, $\text{CH}_3\text{-CH}_2\text{-PO}$), 1.35 (24H, st, $J_{\text{HH}}=7.35$, $\text{CH}_3\text{-CH}_2\text{-CH}_2\text{-CH}_2\text{-N}$), 1.60 (28H, qn, $J_{\text{HH}}=7.55$ Hz, $\text{CH}_2\text{-CH}_2\text{-N}$, $\text{CH}_2\text{-PO}$), 3.06-3.13 (24H, m, $\text{CH}_2\text{-N}$); δ_{P} (121 MHz, CD_3CN , H_3PO_4) -12.5 ($\text{PW}_{10}\text{O}_{36}$), 28.2 ppm ($\text{PO-CH}_2\text{-CH}_3$); m/z (Maldi-TOF) 3231 (M^+ - NBu_4+Cs), 3472 ($M^++\text{NBu}_4\text{-EtPO}_2$), 3566 ($M^++\text{NBu}_4$), 3610, 3694 ($M^++2\text{NBu}_4\text{-EtPO-Et}$), 3844, 3920 ($M^++3\text{NBu}_4+\text{Na-2EtPO}$), 4074 ($M^++3\text{NBu}_4+\text{Na}$), 4207 ($M^++4\text{NBu}_4+\text{Na-EtPO-Et}$), 4314 ($M^++4\text{NBu}_4+\text{Na}$), where $M^+ = (\text{NBu}_4)_3[\text{PW}_{10}\text{O}_{36}(\text{EtPO})_2]^+$.

7.6.2. Synthesis of $(\text{NBu}_4)_3[\gamma\text{-PW}_{10}\text{O}_{36}(\text{H}_2\text{C=CHPO})_2]$ (Compound 11)

Was prepared and purified following a similar procedure to in section 7.6.1, but using $\text{C}_2\text{H}_3\text{PO}(\text{OH})_2$ (0.15 g, 1.4 mmol). Yield (1.60 g, 75.2 %). (Found: C, 20.7; H, 3.65; N, 1.4. Calc.

for $C_{52}H_{114}N_3O_{38}P_3W_{10}$: C, 18.1; H, 3.5; N, 1.3 %); ν_{\max} (KBr disc) 2962.0 (C-H), 2873.7 (C-H), 1483.6, 1114.0 (P-O), 1049.8 (P-O), 963.2, 850, 818.9 cm^{-1} ; δ_H (300 MHz; CD_3CN ; Me_4Si) 0.95 (36H, t, $J_{HH}=7.35$, $\text{CH}_3\text{-CH}_2\text{-CH}_2\text{-CH}_2\text{-N}$), 1.35 (24H, st, $J_{HH}=7.35$, $\text{CH}_3\text{-CH}_2\text{-CH}_2\text{-CH}_2\text{-N}$), 1.60 (24H, qn, $J_{HH}=7.55$ Hz, $\text{CH}_2\text{-CH}_2\text{-N}$), 3.06-3.13 (24H, m, $\text{CH}_2\text{-N}$), 5.87-6.30 (6H, m, $\text{CH}_2=\text{CH}$); δ_P (121 MHz, CD_3CN , H_3PO_4) -12.0 ($PW_{10}O_{36}$), 15.8 ppm (C_2H_3PO); m/z (Maldi-TOF) 3221 ($M^+ \text{-NBu}_4 \text{+Cs}$), 3463 ($M^+ \text{+NBu}_4\text{-C}_2\text{H}_3\text{PO-C}_2\text{H}_3$), 3557 ($M^+ \text{+NBu}_4$), 3604, 3683 ($M^+ \text{+2NBu}_4\text{-C}_2\text{H}_3\text{PO-C}_2\text{H}_3\text{O}$), 3839, 3915 ($M^+ \text{+3NBu}_4 \text{+Na-2C}_2\text{H}_3\text{PO}$), 4066 ($M^+ \text{+3NBu}_4 \text{+Na}$), 4201 ($M^+ \text{+4NBu}_4 \text{+Na-C}_2\text{H}_3\text{PO-C}_2\text{H}_3$), 4314 ($M^+ \text{+4NBu}_4 \text{+Na}$), where $M^+ = (\text{NBu}_4)_3[\text{PW}_{10}\text{O}_{36}(\text{C}_2\text{H}_3\text{PO})_2]^+$.

7.6.3. Synthesis of $(\text{NBu}_4)_3[\gamma\text{-PW}_{10}\text{O}_{36}(\text{H}_2\text{C=CHCH}_2\text{PO})_2]$ (Compound 12)

Was prepared and purified following a similar procedure to in section 7.6.1, but using $C_3H_5PO(OH)_2$ (0.21 g, 1.7 mmol). Yield (1.92 g, 71.7 %). ν_{\max} (KBr disc) 2962.1 (C-H), 2873.8 (C-H), 1483.1, 1113.1 (P-O), 1048.1 (P-O), 964.6, 850, 818.2 cm^{-1} ; δ_H (300 MHz; CD_3CN ; Me_4Si) 0.95 (36H, t, $J_{HH}=7.35$, $\text{CH}_3\text{-CH}_2\text{-CH}_2\text{-CH}_2\text{-N}$), 1.35 (24H, st, $J_{HH}=7.35$, $\text{CH}_3\text{-CH}_2\text{-CH}_2\text{-CH}_2\text{-N}$), 1.60 (24H, qn, $J_{HH}=7.55$ Hz, $\text{CH}_2\text{-CH}_2\text{-N}$), 2.50-2.68 (4H, m, $\text{CH}_2=\text{CH-CH}_2\text{-PO}$), 3.06-3.13 (24H, m, $\text{CH}_2\text{-N}$), 5.13-5.25 (4H, m, $\text{CH}_2=\text{CH}$), 5.78-5.93 (2H, m, $\text{CH}_2=\text{CH}$); δ_P (121 MHz, CD_3CN , H_3PO_4) -12.3 ($PW_{10}O_{36}$), 24.5 ppm (C_3H_5PO); m/z (Maldi-TOF) 3490 ($M^+ \text{+NBu}_4\text{-C}_3\text{H}_5\text{O-C}_3\text{H}_5$), 3590 ($M^+ \text{+NBu}_4$), 3624 ($M^+ \text{+2NBu}_4\text{-C}_3\text{H}_5\text{PO}_2$), 3807 ($M^+ \text{+2NBu}_4\text{-C}_2\text{H}_3$), 3832 ($M^+ \text{+2NBu}_4$), 3935 ($M^+ \text{+3NBu}_4\text{-C}_3\text{H}_5\text{PO-C}_3\text{H}_5\text{O}$), 4087 ($M^+ \text{+3NBu}_4$), 4304 ($M^+ \text{+4NBu}_4\text{-C}_2\text{H}_3$), 4329 ($M^+ \text{+4NBu}_4$), where $M^+ = (\text{NBu}_4)_3[\text{PW}_{10}\text{O}_{36}(\text{C}_3\text{H}_5\text{PO})_2]^+$.

7.6.4. Synthesis of (NBu₄)₃[γ-PW₁₀O₃₆(HOOCCH₂PO)₂] (Compound 13)

Was prepared and purified following a similar procedure to that in section 7.6.1, but using HOOCCH₂PO(OH)₂ (0.24 g, 1.7 mmol). Yield (1.92 g, 71.7 %). ν_{\max} (KBr disc) 3431.0 (OH), 2962.5 (C-H), 2874.4 (C-H), 1718 (C=O), 1483.5, 1115.8 (P-O), 1074.6 (P-O), 1048.5 (P-O), 975.0, 884.6, 819.6 cm⁻¹; δ_{H} (300 MHz; CD₃CN; Me₄Si) 0.95 (36H, t, $J_{\text{HH}}=7.35$, **CH**₃-CH₂-CH₂-CH₂-N), 1.35 (24H, st, $J_{\text{HH}}=7.35$, CH₃-**CH**₂-CH₂-CH₂-N), 1.60 (24H, qn, $J_{\text{HH}}=7.55$, **CH**₂-CH₂-N), 2.90 (4H, d, $J_{\text{PH}}=25.4$ Hz, **CH**₂-PO), 3.06-3.13 (24H, m, **CH**₂-N); δ_{P} (121 MHz, CD₃CN, H₃PO₄) -12.1 (PW₁₀O₃₆), 18.1 ppm (HOOCCH₂PO); m/z (Maldi-TOF) 3706 ($M^+ + 2\text{NBu}_4\text{-HOOCCH}_2\text{PO-HOOCCH}_2$), 3833 ($M^+ - 2\text{OH}$), 3852 ($M^+ - \text{OH}$), 3899 ($M^+ + 3\text{NBu}_4\text{-2HOOCCH}_2\text{PO}$), 3944 ($M^+ + 3\text{NBu}_4\text{-HOOCCH}_2\text{PO-HOOCCH}_2$), 4075 ($M^+ + 3\text{NBu}_4\text{-2OH}$), 4141 ($M^+ + 4\text{NBu}_4\text{-2HOOCCH}_2\text{PO}$), 4224 ($M^+ + 4\text{NBu}_4\text{-HOOCCH}_2\text{PO-HO}$), 4293 ($M^+ + 4\text{NBu}_4\text{-HOOCCH}_2\text{PO}$), 4335 ($M^+ + 4\text{NBu}_4\text{-OH}$), where $M^+ = (\text{NBu}_4)_3[\text{PW}_{10}\text{O}_{36}(\text{HOOCCH}_2\text{PO})_2]^+$.

7.6.5. Synthesis of (NBu₄)₃[γ-PW₁₀O₃₆(HOOC(CH₂)₂PO)₂] (Compound 14)

Was prepared and purified following a similar procedure to that in section 7.6.1, but using HOOC(CH₂)₂PO(OH)₂ (0.21 g, 1.7 mmol). Yield (1.97 g, 70.4 %). ν_{\max} (KBr disc) 3426.7 (O-H), 2962.6 (C-H), 2874.3 (C-H), 1734 (C=O), 1483.4, 1112.2 (P-O), 1048.7 (P-O), 964.9, 850, 816.2 cm⁻¹; δ_{H} (300 MHz; CD₃CN; Me₄Si) 0.95 (36H, t, $J_{\text{HH}}=7.35$, **CH**₃-CH₂-CH₂-CH₂-N), 1.35 (24H, st, $J_{\text{HH}}=7.35$, CH₃-**CH**₂-CH₂-CH₂-N), 1.60 (24H, qn, $J_{\text{HH}}=7.55$ Hz, **CH**₂-CH₂-N), 2.02-2.19 (4H, m, **CH**₂-PO), 2.52-2.67 (4H, m, HOOC-**CH**₂), 3.06-3.13 (24H, m, **CH**₂-N); δ_{P} (CD₃CN) -12.0 (PW₁₀O₃₆), 26.5 ppm (CH₂PO).

7.6.6. Synthesis of $(\text{NBu}_4)_3[\gamma\text{-PW}_{10}\text{O}_{36}(\text{H}_2\text{C}=\text{CHC}_6\text{H}_4\text{PO})_2]$ (Compound 15)

Was prepared and purified following a similar procedure to that in section 7.6.1, but using $\text{C}_3\text{H}_5\text{PO}(\text{OH})_2$ (0.21 g, 1.7 mmol). Yield (1.92 g, 69.1 %). $\nu_{\text{max}}(\text{KBr disc})$ 2962.5 (C-H), 2874.0 (C-H), 1483.3, 1111.6 (P-O), 1052.4 (P-O), 965.5 (P-O), 850, 818.0, 750, 652.1 cm^{-1} ; δ_{H} (300 MHz; CD_3CN ; Me_4Si) 0.95 (36H, t, $J_{\text{HH}}=7.35$, $\text{CH}_3\text{-CH}_2\text{-CH}_2\text{-CH}_2\text{-N}$), 1.35 (24H, st, $J_{\text{HH}}=7.35$, $\text{CH}_3\text{-CH}_2\text{-CH}_2\text{-CH}_2\text{-N}$), 1.60 (24H, qn, $J_{\text{HH}}=7.55$, $\text{CH}_2\text{-CH}_2\text{-N}$), 3.06-3.13 (24H, m, $\text{CH}_2\text{-N}$), 5.45 (2H, dd, $J_{\text{PH}}=15.6$, $J_{\text{HH}}=11.0$ Hz, $\text{H}_2\text{C}=\text{CH}$), 5.90 (2H, dd, $J_{\text{PH}}=15.6$, $J_{\text{HH}}=9.55$ Hz, $\text{H}_2\text{C}=\text{CH}$), 6.70-6.85 (2H, m, $\text{H}_2\text{C}=\text{CH}$), 7.45-7.90 (8H, m, C_6H_4); δ_{P} (121 MHz, CD_3CN , H_3PO_4) -11.9 ($\text{PW}_{10}\text{O}_{36}$), 17.3 ppm (PO); m/z (Maldi-TOF) 3439 ($M^+ \text{-C}_2\text{H}_3$), 3624, 3682 ($M^+ \text{+NBu}_4\text{-C}_2\text{H}_3$), 3714 ($M^+ \text{+NBu}_4$), 3757 ($M^+ \text{+2NBu}_4\text{-2C}_8\text{H}_7$), 3866 ($M^+ \text{+3NBu}_4\text{-2C}_8\text{H}_7\text{PO}$), 3914, 3993 ($M^+ \text{+3NBu}_4\text{-2C}_8\text{H}_7$), 4144 ($M^+ \text{+4NBu}_4\text{-2C}_8\text{H}_7\text{PO}$), 4385 ($M^+ \text{+5NBu}_4\text{-2C}_8\text{H}_7\text{PO}$), where $M^+ = (\text{NBu}_4)_3[\text{PW}_{10}\text{O}_{36}(\text{H}_2\text{C}=\text{CHC}_6\text{H}_4\text{PO})_2]^+$.

7.7. Synthesis of $\alpha\text{-A-K}_{7-x}\text{Na}_x[\text{PW}_{11}\text{O}_{39}]\cdot 14\text{H}_2\text{O}$ (Compound P)⁶

Sodium tungstate (45.38 g, 0.14 mmol) is dissolved in water (75 mL) and H_3PO_4 (12.5 mL) is added with vigorous stirring. Acetic acid (22 mL) is added and the mixture stirred at reflux for 1 hour, before adding KCl (15 g) and cooling. The precipitate is collected by filtration and air dried. (41.1g, yield not calculated as counter ion ratio unknown). $\nu_{\text{max}}(\text{KBr disc})$ 1085.9, 1046.3, 951.9, 865, 812.7, 741.4 cm^{-1} .

7.8. Synthesis of $\alpha\text{-A-K}_9[\text{PW}_9\text{O}_{34}]\cdot 16\text{H}_2\text{O}$ (Compound Q)⁶

2M Potassium Carbonate (30 mL) was added to a solution of $\alpha\text{-A-K}_{7-x}\text{Na}_x[\text{PW}_{11}\text{O}_{39}]\cdot 14\text{H}_2\text{O}$ (32 g) in water (100 mL). The precipitate appears instantly, is collected by filtration and washed with

ethanol before being air dried to give white crystals. (24.36 g, 78.5 % from sodium tungstate).

$\nu_{\max}(\text{KBr disc})$ 1056.8, 1000.9, 931.9, 908.6, 819.7, 738.0 cm^{-1} .

7.9. Synthesis of $\text{Na}_{10}[\alpha\text{-SiW}_9\text{O}_{34}]\cdot\text{solvent}$ (Compound R)³

Sodium tungstate (45.5 g, 0.14 mol) and Sodium silicate solution (2.75 g, 12.5 mmol) are dissolved in hot water (80-100°C) (50 mL). To this solution is added 6M HCl (32.5 mL) dropwise over 30 minutes. The solution is boiled until the volume is ~75 mL and unreacted silica is removed by filtration over Celite[®]. Anhydrous sodium carbonate (12.5 g) is dissolved in water (37.5 mL) in a separate beaker; this solution is slowly added to the first solution with gentle stirring. The solution is stirred for 1 hour and a precipitate slowly forms, this is removed by filtration using a sintered glass filter. The solid is stirred with a 4M NaCl solution (250 mL) and filtered again. It is then washed successively with two 25 mL portions of ethanol and 25 mL of diethyl ether and dried under vacuum to give $\text{Na}_{10}[\alpha\text{-SiW}_9\text{O}_{34}]\cdot\text{H}_2\text{O}$ (19.8 g, 57.8 %) as a white solid. $\nu_{\max}(\text{KBr disc})$ 3405.7, 983.0, 930.2, 861.9, 848 (sh), 807.4, 692.1, 555.7, 526.8 cm^{-1} .

7.9.1. Reaction with trichlorosilane

7.9.1.1. Synthesis of $(\text{NBu}_4)_3[\text{PW}_9\text{O}_{34}(\text{C}_2\text{H}_3\text{SiO})_3(\text{C}_2\text{H}_3\text{Si})]$ (Compound S)⁷

To a well-stirred solution of $\text{K}_9[\text{PW}_9\text{O}_{34}]\cdot 16\text{H}_2\text{O}$ (2.50 g, 0.87 mmol) in dry acetonitrile (50 mL) under nitrogen, solid NBu_4Br (1.5 g, 4.7 mmol) and $\text{C}_2\text{H}_3\text{SiCl}_3$ (0.75 mL, 4.6 mmol) were added; the resulting mixture was stirred overnight at 0°C. The white solid formed ($\text{NaCl} + \text{NaBr}$) was separated by filtration and the solution slowly evaporated at room temperature to yield yellow crystals. The crude compound was recrystallized from acetonitrile. Yield (2.07 g, 73.7 %).

$\lambda_{\max}(\text{CD}_3\text{CN})$ (ϵ) 265.5 (27,000 $\text{dm}^3\text{mol}^{-1}\text{cm}^{-1}$); $\nu_{\max}(\text{KBr disc})$ 2961.9, 2873.3 (C-H), 1663.1

(C=C), 1481.4, 1405.6 (Si-C), 1126.0, 1000 (P-O), 954.8, 868.8, 817.1, 730.9 cm^{-1} ; δ_{H} (300 MHz; CD_3CN ; Me_4Si) 0.97 (36H, t, $J_{\text{HH}}=7.35$, $\text{CH}_3\text{-CH}_2\text{-CH}_2\text{-CH}_2\text{-N}$), 1.37 (24H, st, $J_{\text{HH}}=7.35$, $\text{CH}_3\text{-CH}_2\text{-CH}_2\text{-CH}_2\text{-N}$), 1.61 (24H, $J_{\text{HH}}=7.54$, qn, $\text{CH}_2\text{-CH}_2\text{-N}$), 3.07-3.13 (24H, m, $\text{CH}_2\text{-N}$), 5.85-6.10 (12H, m, C_2H_3); δ_{P} (121 MHz; CD_3CN ; H_3PO_4) -16.43 ppm; m/z (EI) 1275 (40), 1323 (43), 1369 (100), 2932 (37), 2983 (89), 3142 (40); Crystals suitable for Single Crystal XRD were obtained by slow diffusion of diethyl ether into an acetonitrile solution containing the crude product. Data were collected on a Bruker SMART 6000 diffractometer ($\lambda_{\text{Cu-K}\alpha} = 1.54178 \text{ \AA}$). Structure 8. $\text{C}_{56}\text{H}_{120}\text{N}_3\text{O}_{37}\text{PSi}_4\text{W}_9$, $M = 3225.5$, Orthorhombic, $a = 26.508(7)$, $b = 14.434(4)$, $c = 24.426(7) \text{ \AA}$, $U = 9346(4) \text{ \AA}^3$, $T = 293 \text{ K}$, space group $P c a 2_1$ (no. 29), $Z = 4$, 57182 reflections measured, 16454 unique ($R_{\text{int}} = 0.060$). The Final $R_1(\text{obs. data}) = 0.044$, $R_1(\text{all data}) = 0.068$. Final refinements were carried out with anisotropic thermal parameters for all non-hydrogen atoms

7.9.1.2. Synthesis of $(\text{NBu}_4)_3[\text{PW}_9\text{O}_{34}(\text{C}_3\text{H}_5\text{SiO})_3(\text{C}_3\text{H}_5\text{Si})]$ (Compound T)¹

Was prepared following a similar procedure to section 7.9.1.1, but using $\text{C}_3\text{H}_5\text{SiCl}_3$ (0.77 g, 4.38 mmol). Yield (1.31g, 46.6 %). (Found C 25.1; H 4.4; N 2.3. Calc. C 21.9; H 3.9; N 1.3); $\lambda_{\text{max}}(\text{CD}_3\text{CN})$ (ϵ) 264 nm ($23,500 \text{ dm}^3\text{mol}^{-1}\text{cm}^{-1}$); $\nu_{\text{max}}(\text{KBr disc})$ 2963.7, 2875.1 (C-H), 1600 (C=C), 1484.8, 1382.0 (Si-C), 1125 (P-O), 1110.2 (P-O), 961.5, 870.0, 817, 738.2 cm^{-1} ; δ_{H} (300 MHz; CD_3CN ; Me_4Si) 0.97 (36H, t, $J_{\text{HH}}=7.35$, $\text{CH}_3\text{-CH}_2\text{-CH}_2\text{-CH}_2\text{-N}$), 1.37 (24H, st, $J_{\text{HH}}=7.35$, $\text{CH}_2\text{-CH}_2\text{-CH}_2\text{-N}$), 1.61 (24H, qn, $J_{\text{HH}}=7.54$, $\text{CH}_2\text{-CH}_2\text{-N}$), 1.80-1.89 (8H, m, $\text{CH}_2\text{-Si}$), 3.07-3.13 (24H, m, $\text{CH}_2\text{-N}$), 4.40-5.10 (12H, m, $\text{CH}_2=\text{CH}$); δ_{P} (121 MHz; CD_3CN ; H_3PO_4) -16.52 ppm; m/z (Maldi-TOF) 3499 ($M^+ + \text{NBu}_4\text{-H}_2\text{C}=\text{CH}$), 3541 ($M^+ + \text{NBu}_4 + \text{Na}$), 3583 ($M^+ + 2\text{NBu}_4\text{-O}_2(\text{SiCH}_2\text{CH}$

=CH₂)₂), 3625 (M^+ +2NBu₄-OSi(CH₂CH=CH₂)₂), 3667 (M^+ +2NBu₄-O₂SiCH₂CH=CH₂), 3715 (M^+ +2NBu₄-CH₂CH=CH₂), where M^+ = (NBu₄)₃[PW₉O₃₄(C₃H₅SiO)₃(C₃H₅Si)].

7.9.1.3. Synthesis of (NBu₄)₃H[SiW₉O₃₄(C₂H₃SiO)₃(C₂H₃Si)] (Compound 16)

Was prepared following a similar procedure to in section 7.9.1.1, but using Na₁₀[SiW₉O₃₄].H₂O (2.20 g, 0.87 mmol). Yield (2.26 g, 74.9 %). (Found C 25.25; H 4.8; N 2.7. Calc. C 24.9; H 4.5; N 1.6.); λ_{\max} (CD₃CN) (ϵ) 263.5 nm (29,000 dm³mol⁻¹cm⁻¹); ν_{\max} (KBr disc) 2961.8 (C-H), 2874.2 (C-H), 1559.8 (C=C), 1485.7, 1382.3 (Si-C), 1051.1, 966.0, 921.2, 803.6, 526.6 cm⁻¹; δ_{H} (300 MHz; CD₃CN; Me₄Si) 0.97 (48H, t, J_{HH} =7.35, **CH**₃-CH₂-CH₂-CH₂-N), 1.38 (32H, st, J_{HH} =7.35, CH₃-**CH**₂-CH₂-CH₂-N), 1.61 (32H, qn, J_{HH} =7.54, **CH**₂-CH₂-N), 3.07-3.13 (32H, m, **CH**₂-N), 5.84-6.25 (12H, m, **C**₂**H**₃Si); m/z (Maldi-TOF) 3457 (M^+ +NBu₄), 3696 (M^+ +2NBu₄), 3764 (M^+ +4NBu₄-(H₃C₂)₄O₃Si), 3836 (M^+ +4NBu₄-H₃C₂O₃Si), 3931 (M^+ +3NBu₄), 4005 (M^+ +4NBu₄-(H₃C₂)₄O₃Si), 4079 (M^+ +4NBu₄-H₃C₂O₃Si), 4216 (M^+ +4NBu₄), where M^+ = (NBu₄)₃[SiW₉O₃₄(H₃C₂SiO)₃(H₃C₂Si)].

7.9.1.4. Synthesis of (NBu₄)₃H[SiW₉O₃₄(C₃H₅SiO)₃(C₃H₅Si)] (Compound 17)

Was prepared following a similar procedure to in section 7.9.1.3, but using C₃H₅SiCl₃ (0.93 mL, 4.38 mmol). Yield (1.65 g, 54 %). (Found C 28.6; H 5.5; N 2.3. Calc. C 25.9; H 4.7; N 1.6); λ_{\max} (CD₃CN) (ϵ) 263.5 nm (28,000 dm³mol⁻¹cm⁻¹); ν_{\max} (KBr disc) 2962.9, 2874.7 (C-H), 1485.3, 1381.9 (Si-C), 1110.6, 964.6, 898.4, 750.4, 532.9 cm⁻¹; δ_{H} (300 MHz; CD₃CN; Me₄Si) 0.97 (48H, t, J_{HH} =7.35, **CH**₃-CH₂-CH₂-CH₂-N), 1.37 (32H, st, J_{HH} =7.35, CH₃-**CH**₂-CH₂-CH₂-N), 1.61 (32H, qn, J_{HH} =7.54, **CH**₂-CH₂-N), 1.76-1.89 (8H, m, **CH**₂-Si) 3.07-3.13 (32H, m, **CH**₂-N), 4.91-5.12 (8H, m, **CH**₂=CH), 5.70-5.95 ppm (4H, m, CH₂=**CH**); m/z (Maldi-TOF) 3448 (M^+ +NBu₄-

H₅C₃Si), 3511 (M^+ +NBu₄), 3567 (M^+ +2NBu₄-H₅C₃SiO₂), 3896 (M^+ +3NBu₄-H₅C₃SiO₃), 4042 (M^+ +4NBu₄-(H₅C₃)₃SiO₃), 4087 (M^+ +4NBu₄-(H₅C₃)₂SiO₃), 4139 (M^+ +4NBu₄-H₅C₃SiO₃), where $M^+ = (\text{NBu}_4)_3[\text{SiW}_9\text{O}_{34}(\text{H}_5\text{C}_3\text{SiO})_3(\text{H}_5\text{C}_3\text{Si})]^+$.

7.9.1.5. Synthesis of (NBu₄)₃[PW₉O₃₄(*t*-BuSiOH)₃] (Compound U)⁷

To a well-stirred solution of K₉[PW₉O₃₄].16H₂O (10 g, 3.48 mmol) in dry acetonitrile (200 mL) under nitrogen were added solid NBu₄Br (6.0 g, 18.6 mmol) and *t*-BuSiCl₃ (2.10 g, 10 mmol); the resulting mixture was stirred overnight at 0 °C. The white solid formed (NaCl + NaBr) was separated by filtration and the resulting solution slowly evaporated at room temperature to yield clear crystals (6.98g, 61%). (Found C 22.1; H 3.7; N 1.3. Calc. C 22.1; H 3.4; N 1.3) $\lambda_{\text{max}}(\text{CD}_3\text{CN})$ (ϵ) 265 nm (25,500 dm³mol⁻¹cm⁻¹); $\nu_{\text{max}}(\text{KBr disc})$ 3469.5 (O-H), 2963.2 (C-H), 2876.2 (C-H), 1100.7 (P-O), 1002.6 (P-O), 974.7, 930, 864.8, 726.0 cm⁻¹; $\delta_{\text{H}}(300 \text{ MHz; CD}_3\text{CN; Me}_4\text{Si})$ 0.97 (36H, t, $J_{\text{HH}}=7.35$, **CH**₃-CH₂-CH₂-CH₂-N), 1.00 (27H, s, *t*-Bu), 1.37 (24H, st, $J_{\text{HH}}=7.35$, CH₃-**CH**₂-CH₂-CH₂-N), 1.61 (24H, qn, $J_{\text{HH}}=7.54$, **CH**₂-CH₂-N), 3.07-3.13 (24H, m, **CH**₂-N), 4.94 (1H, s, OH); $\delta_{\text{P}}(121 \text{ MHz; CD}_3\text{CN; H}_3\text{PO}_4)$ -15.69 ppm; m/z (EI) 3206 (M^+ -*t*-Bu), 3265 (M^+), 3286 (M^+ +NBu₄-2*t*BuSiOH), 3449 (M^+ +NBu₄-*t*Bu), 3506 (M^+ +NBu₄), where $M^+ = (\text{NBu}_4)_3[\text{PW}_9\text{O}_{34}(\textit{t}\text{BuSiOH})_3]$. Crystals suitable for Single Crystal XRD were obtained by slow diffusion of diethyl ether into an acetonitrile solution containing the crude product. Data were collected on a Bruker SMART 6000 diffractometer ($\lambda_{\text{Cu-K}\alpha} = 1.54178 \text{ \AA}$). Structure 9. C₆₂H₁₃₈N₃O₄₇PSi₃W₉, M = 3445.7, Trigonal, a = 22.3113(5), b = 22.3113(5), c = 37.8917(12) Å, U = 16335(1) Å³, T = 200 K, space group R 3 c (no. 161), Z = 6. The Final R1(obs. data) = 0.055, R1(all data) = 0.086. The crystal structure was solved with all non-hydrogen atoms anisotropic except the solvent molecule and with no hydrogen atoms on the solvent.

7.9.1.6. Synthesis of $(\text{NBu}_4)_3\text{H}[\text{SiW}_9\text{O}_{34}(\text{t-BuSiOH})_3]$ (Compound 18)

Was prepared following a similar procedure to in section 7.9.1.5, but using $\text{Na}_{10}[\text{SiW}_9\text{O}_{34}]\cdot\text{H}_2\text{O}$ (4.30 g, 1.74 mmol) and half quantities of the other reagents. The crude compound was recrystallized from acetonitrile to give white crystals of $(\text{NBu}_4)_3[\text{SiW}_9\text{O}_{34}(\text{t-BuSiOH})_3]$ (4.88 g, 80 %). (Found C 23.3; H. 4.4; N 1.5. Calculated C 22.1; H 4.2; N 1.3.) $\lambda_{\text{max}}(\text{CD}_3\text{CN})$ (ϵ) 261 nm ($25,000 \text{ dm}^3\text{mol}^{-1}\text{cm}^{-1}$); $\nu_{\text{max}}(\text{KBr disc})$ 2962.5 (C-H), 2875.6 (C-H), 1486.6, 1382.2 (Si-C), 1027.6, 983, 923.6, 860, 823.7, 807, 723.4, 517.0 cm^{-1} ; $\delta_{\text{H}}(300 \text{ MHz; CD}_3\text{CN; Me}_4\text{Si})$ 0.97 (36H, t, $J_{\text{HH}}=7.35$, $\text{CH}_3\text{-CH}_2\text{-CH}_2\text{-CH}_2\text{-N}$), 1.00 (27H, s, *t*-Bu), 1.37 (24H, st, $J_{\text{HH}}=7.35$, $\text{CH}_3\text{-CH}_2\text{-CH}_2\text{-CH}_2\text{-N}$), 1.61 (24H, qn, $J_{\text{HH}}=7.54$, $\text{CH}_2\text{-CH}_2\text{-N}$), 3.07-3.13 (24H, m, $\text{CH}_2\text{-N}$); m/z (Maldi-TOF) 3366 ($M^+ + \text{NBu}_4\text{-tBuSiOH-tBu}$), 3462 ($M^+ + \text{NBu}_4\text{-tBu}$), 3517 ($M^+ + \text{NBu}_4$), 3536 ($M^+ + \text{NBu}_4 + \text{Na}$), 3758 ($M^+ + 2\text{NBu}_4$), where $M^+ = (\text{NBu}_4)_3[\text{SiW}_9\text{O}_{34}(\text{tBuSiOH})_3]$. Crystals suitable for Single Crystal XRD were obtained by diffusion of diethyl ether into an acetonitrile solution of the crude product. Data were collected on a Bruker SMART 6000 diffractometer ($\lambda_{\text{Cu-K}\alpha} = 1.54178 \text{ \AA}$). Structure 10. $\text{C}_{62.33}\text{H}_{138}\text{N}_4\text{O}_{37}\text{Si}_4\text{W}_9$, $M = 3299.8$, Trigonal, $a = 22.5166(12)$, $b = 22.5166(12)$, $c = 35.9924(14) \text{ \AA}$, $U = 15803.3(13) \text{ \AA}^3$, $T = 293 \text{ K}$, space group $R \bar{3} c$ (no. 161), $Z = 6$, 31938 reflections measured, 5048 unique ($R_{\text{int}}=0.193$). The Final $R1(\text{obs. data}) = 0.068$, $R1(\text{all data}) = 0.154$.

7.9.1.7. Synthesis of $(\text{NBu}_4)_3[\text{PW}_9\text{O}_{34}(\text{t-BuSiO})_3(\text{H}_2\text{C=CHSi})]$ (Compound V)⁷

To a stirred solution of $(\text{NBu}_4)_3[\text{PW}_9\text{O}_{34}(\text{t-BuSiOH})_3]$ (3.0 g, 0.46 mmol) in dry DMF (10 mL) under nitrogen, $\text{C}_2\text{H}_5\text{SiCl}_3$ (0.32 mL, 2 mmol) was added. The solution was stirred overnight at room temperature. Yield (2.46 g, 80.7 %). $\lambda_{\text{max}}(\text{CD}_3\text{CN})$ (ϵ) 265.5 nm ($26,000 \text{ dm}^3\text{mol}^{-1}\text{cm}^{-1}$); $\nu_{\text{max}}(\text{KBr disc})$ 2974.0 (C-H), 2925.8 (C-H), 1602.7 (C=C), 1465.8, 1407.9 (Si-C), 1116.7,

1035.7, 1002.9, 931.6, 860.2, 804.3, 727.1, 707.8 cm^{-1} ; δ_{H} (300 MHz; CD_3CN ; Me_4Si) 0.95 (36H, t, $J_{\text{HH}}=7.35$, $\text{CH}_3\text{-CH}_2\text{-CH}_2\text{-CH}_2\text{-N}$), 1.00 (27H, s, *t*Bu), 1.37 (24H, st, $J_{\text{HH}}=7.35$, $\text{CH}_3\text{-CH}_2\text{-CH}_2\text{-CH}_2\text{-N}$), 1.62 (24H, qn, $J_{\text{HH}}=7.54$, $\text{CH}_2\text{-CH}_2\text{-N}$), 3.07-3.17 (24H, m, $\text{CH}_2\text{-N}$), 6.02-6.08 (m, 3H, $\text{C}_2\text{H}_3\text{Si}$); δ_{P} (121 MHz; CD_3CN ; H_3PO_4) -16.72 ppm; m/z (ESI) 2832 (38) ($M^+ - 2\text{NBu}_4$), 3073 (100) ($M^+ - \text{NBu}_4$), 3347 (20) ($M^+ + \text{Na}$), where $M^+ = (\text{NBu}_4)_3[\text{PW}_9\text{O}_{34}(\text{t-BuSiO})_3(\text{C}_2\text{H}_3\text{Si})]$.

7.9.1.8. Synthesis of $(\text{NBu}_4)_3[\text{PW}_9\text{O}_{34}(\text{t-BuSiO})_3(\text{H}_2\text{C}=\text{CHCH}_2\text{Si})]$ (Compound W)⁷

Was prepared using a similar method to in Section 7.9.1.7, but using $\text{C}_3\text{H}_5\text{SiCl}_3$ (0.35 mL, 2 mmol). Yield (2.13 g, 69.4 %). (Found C 21.5; H 3.4; N 1.3. Calc. C 22.7; H 4.2; N 1.3). $\lambda_{\text{max}}(\text{CD}_3\text{CN})$ (ϵ) 265.5 nm ($25,000 \text{ dm}^3\text{mol}^{-1}\text{cm}^{-1}$); $\nu_{\text{max}}(\text{KBr disc})$ 2960.5 (C-H), 2875.7 (C-H), 1633.6 (C=C), 1485.1, 1380.9 (Si-C), 1110.9, 1037.6, 1001.0, 972.1, 929.6, 858.3, 802.3, 719.4 cm^{-1} ; δ_{H} (300 MHz; CD_3CN ; Me_4Si) 0.95 (36H, t, $J_{\text{HH}}=7.35$, $\text{CH}_3\text{-CH}_2\text{-CH}_2\text{-CH}_2\text{-N}$), 1.00 (27H, s, *t*Bu), 1.37 (24H, st, $J_{\text{HH}}=7.35$, $\text{CH}_3\text{-CH}_2\text{-CH}_2\text{-CH}_2\text{-N}$), 1.62 (26H, m, $\text{CH}_2\text{-CH}_2\text{-N}$, $\text{H}_2\text{C-Si}$), 3.07-3.18 (24H, m, $\text{CH}_2\text{-N}$), 4.92-5.06 (2H, m, $\text{H}_2\text{C}=\text{CHCH}_2$), 5.86-6.02 (1H, m, $\text{H}_2\text{C}=\text{CHCH}_2$); δ_{P} (121 MHz; CD_3CN ; H_3PO_4) -16.65 ppm. m/z (ESI) 3018 (45) ($M^+ - \text{NBu}_4 - \text{H}_2\text{C}=\text{CHCH}_2\text{Si}$), 3086 (100) ($M^+ - \text{NBu}_4$), where $M^+ = (\text{NBu}_4)_3[\text{PW}_9\text{O}_{34}(\text{tBuSiO})_3(\text{H}_2\text{C}=\text{CHCH}_2\text{Si})]$. Crystals suitable for Single Crystal XRD were obtained by slow diffusion of diethyl ether into a DMF solution containing the crude product. Data were collected on a Bruker SMART 6000 diffractometer ($\lambda_{\text{Cu-K}\alpha} = 1.54178 \text{ \AA}$). Structure 11. $\text{C}_{62}\text{H}_{138}\text{N}_3\text{O}_{37}\text{PSi}_4\text{W}_9$, $M = 3315.7$, Trigonal, $a = 22.4981(4)$, $b = 22.4981(4)$, $c = 36.7371(11) \text{ \AA}$, $U = 16103.7(6) \text{ \AA}^3$, $T = 293 \text{ K}$, space group $R\bar{3}c$ (no. 161), $Z = 6$, 31955 reflections measured, 6308 unique ($R_{\text{int}}=0.074$). The Final $R1(\text{obs. data}) = 0.047$, $R1(\text{all data}) = 0.081$.

7.9.1.9. Synthesis of (NBu₄)₃[PW₉O₃₄(*t*-BuSiO)₃(Br(CH₂)₃Si)] (Compound 19)

Was prepared following a similar procedure to that in section 7.9.1.7, but using Br(CH₂)₃SiCl₃ (0.51 g, 2 mmol). Yield (2.25 g, 73.5 %). (Found C 23.8; H 4.6; N 1.8. Calc. C 21.4; H 4.2; N 1.3.); $\lambda_{\max}(\text{CD}_3\text{CN})$ (ϵ) 264.5 nm (26,500 dm³mol⁻¹cm⁻¹); $\nu_{\max}(\text{KBr disc})$ 2962.2 (C-H), 2875.9 (C-H), 1474.8, 1117.2 (P-O), 1038.0, 956.1, 865.6, 812.3, 726.7 cm⁻¹; $\delta_{\text{H}}(300 \text{ MHz; CD}_3\text{CN; Me}_4\text{Si})$ 0.73-0.82 (2H, m, Si-CH₂), 0.97 (36H, t, $J_{\text{HH}}=7.35$, CH₃-CH₂-CH₂-CH₂-N), 1.00 (27H, s, *t*-Bu), 1.37 (24H, st, $J_{\text{HH}}=7.35$, CH₃-CH₂-CH₂-CH₂-N), 1.61 (24H, qn, $J_{\text{HH}}=7.54$, CH₂-CH₂-N), 1.80-1.93 (2H, m, Si-CH₂-CH₂), 3.07-3.13 (24H, m, CH₂-N), 3.53-3.63 (2H, m, CH₂-Br); $\delta_{\text{P}}(121 \text{ MHz; DMF:DMSO-}d_6; \text{H}_3\text{PO}_4)$ -15.7, -16.5; m/z (Maldi-TOF) 3695 ($M^+ + 2\text{NBu}_4\text{-O}_3\text{Si(CH}_2)_3\text{Br}$), 3716 ($M^+ + 2\text{NBu}_4\text{-O}_2\text{Si(CH}_2)_3\text{Br}$), 3929 ($M^+ + 3\text{NBu}_4\text{-O}_3\text{Si(CH}_2)_3\text{Br}$), 4066 ($M^+ + 3\text{NBu}_4\text{-Br}$), 4172 ($M^+ + 4\text{NBu}_4\text{-O}_3\text{Si(CH}_2)_3\text{Br}$), 4325 ($M^+ + 4\text{NBu}_4\text{-Br} + \text{Na}$), where $M^+ = (\text{NBu}_4)_3[\text{PW}_9\text{O}_{34}(\text{tBuSiO})_3(\text{Br(CH}_2)_3\text{Si})]$. Crystals suitable for Single Crystal XRD were obtained by diffusion of diethyl ether into an acetonitrile solution containing the product. Data were collected on a Bruker SMART 6000 diffractometer ($\lambda_{\text{Cu-K}\alpha} = 1.54178 \text{ \AA}$). Structure 12. C₆₃H₁₄₁N₃O₃₇PSi₄W₉Br, $M = 3410.7$, Trigonal, $a = 22.408(2)$, $b = 22.408(2)$, $c = 36.571(6) \text{ \AA}$, $U = 15902(3) \text{ \AA}^3$, $T = 298 \text{ K}$, space group R 3 c (no. 161), $Z = 6$, 33067 reflections measured, 6223 unique ($R_{\text{int}}=0.057$). The Final $R1(\text{obs. data}) = 0.032$, $R1(\text{all data}) = 0.047$.

7.9.1.10. Synthesis of (NBu₄)₃H[SiW₉O₃₄(*t*-BuSiO)₃(H₂C=CHSi)] (Compound 20)

Was prepared using a similar procedure to in section 7.9.1.7, but using (NBu₄)₃[SiW₉O₃₄(*t*-BuSiOH)₃] (1.5 g, 0.46 mmol) and half quantities of the other reagents. The product was obtained by diffusion of diethyl ether into the solution through the gas phase. Yield (1.05 g, 57.2 %). (Found C 25.0; H 4.7; N 1.8. Calc. C 22.5; H 4.2; N 1.3.); $\lambda_{\max}(\text{CD}_3\text{CN})$ (ϵ) 263 nm (26,000

$\text{dm}^3\text{mol}^{-1}\text{cm}^{-1}$); $\nu_{\text{max}}(\text{KBr disc})$ 2961.5 (C-H), 2875.1 (C-H), 1485.6, 1384.1 (Si-C), 1115.5, 1024.0, 983, 921.9, 860, 816.1, 721.4, 519.4 cm^{-1} ; $\delta_{\text{H}}(300 \text{ MHz}; \text{CD}_3\text{CN}; \text{Me}_4\text{Si})$ 0.97 (36H, t, $J_{\text{HH}}=7.35$, $\text{CH}_3\text{-CH}_2\text{-CH}_2\text{-CH}_2\text{-N}$), 1.00 (27H, s, *t*-Bu), 1.37 (24H, st, $J_{\text{HH}}=7.35$, $\text{CH}_3\text{-CH}_2\text{-CH}_2\text{-CH}_2\text{-N}$), 1.61 (24H, qn, $J_{\text{HH}}=7.54$, $\text{CH}_2\text{-CH}_2\text{-N}$), 3.07-3.13 (24H, m, $\text{CH}_2\text{-N}$), 5.86-6.02 (3H, m, C_2H_3); m/z (Maldi-TOF) 3465 ($M^+ + \text{NBu-O}_2\text{SiC}_2\text{H}_3$), 3496 ($M^+ + \text{NBu}_4\text{-SiC}_2\text{H}_3$), 3521 ($M^+ + \text{NBu}_4\text{-C}_2\text{H}_3$), 3539 ($M^+ + \text{NBu}_4\text{-CH}_2$), 3711 ($M^+ + 2\text{NBu}_4\text{-O}_2\text{SiC}_2\text{H}_3$), 3737 ($M^+ + 2\text{NBu}_4\text{-SiC}_2\text{H}_3$), 3762 ($M^+ + 2\text{NBu}_4\text{-C}_2\text{H}_3$), 3800 ($M^+ + 2\text{NBu}_4$), where $M^+ = (\text{NBu}_4)_3\text{H}[\text{SiW}_9\text{O}_{34}(t\text{-BuSiO})_3(\text{C}_2\text{H}_3\text{Si})]^+$.

7.9.1.11. Synthesis of $(\text{NBu}_4)_3\text{H}[\text{SiW}_9\text{O}_{34}(t\text{-BuSiO})_3(\text{H}_2\text{C}=\text{CHCH}_2\text{Si})]$ (Compound 21)

Was prepared via a similar method to in section 7.9.1.10, but using $\text{C}_3\text{H}_5\text{SiCl}_3$ (0.18 mL, 1 mmol). Yield (0.95 g, 62.1 %); (Found C 27.3; H 5.4; N 3.2. Calc. C 22.8; H 4.2; N 1.3). $\lambda_{\text{max}}(\text{CD}_3\text{CN})$ (ϵ) 262.5 nm ($24,000 \text{ dm}^3\text{mol}^{-1}\text{cm}^{-1}$); $\nu_{\text{max}}(\text{KBr disc})$ 2961.5 (C-H), 2875 (C-H), 1657, 1600, 1485.6, 1384 (Si-C), 1115, 1024.0, 983, 922, 816, 721.4 cm^{-1} ; $\delta_{\text{H}}(300 \text{ MHz}; \text{CD}_3\text{CN}; \text{Me}_4\text{Si})$ 0.97 (36H, t, $J_{\text{HH}}=7.35$, $\text{CH}_3\text{-CH}_2\text{-CH}_2\text{-CH}_2\text{-N}$), 1.00 (27H, s, *t*-Bu), 1.37 (24H, st, $J_{\text{HH}}=7.35$, $\text{CH}_3\text{-CH}_2\text{-CH}_2\text{-CH}_2\text{-N}$), 1.61 (24H, qn, $J_{\text{HH}}=7.54$, $\text{CH}_2\text{-CH}_2\text{-N}$), 3.07-3.13 (24H, m, $\text{CH}_2\text{-N}$), 4.42-4.60 (m, 5H, C_3H_5); m/z (Maldi-TOF) 3447 ($M^+ + \text{NBu}_4\text{-O}_3\text{SiC}_3\text{H}_5$), 3464 ($M^+ + \text{NBu}_4\text{-O}_2\text{SiC}_3\text{H}_5$), 3386 ($M^+ + \text{NBu}_4\text{-OSiC}_3\text{H}_5$), 3502 ($M^+ + \text{NBu}_4\text{-SiC}_3\text{H}_5$), 3520, 3540 ($M^+ + \text{NBu}_4\text{-C}_3\text{H}_5$), 3581 ($M^+ + \text{NBu}_4$), 3705 ($M^+ + 2\text{NBu}_4\text{-O}_2\text{SiC}_3\text{H}_5$), 3744 ($M^+ + 2\text{NBu}_4\text{-SiC}_3\text{H}_5$), 3782 ($M^+ + 2\text{NBu}_4\text{-C}_3\text{H}_5$), where $M^+ = (\text{NBu}_4)_3\text{H}[\text{SiW}_9\text{O}_{34}(t\text{-BuSiO})_3(\text{C}_3\text{H}_5\text{Si})]^+$.

7.9.1.12. Synthesis of $(\text{NBu}_4)_3\text{H}[\text{SiW}_9\text{O}_{34}(t\text{-BuSiO})_3(\text{Br}(\text{CH}_2)_3\text{Si})]$ (Compound 22)

Was prepared following a similar procedure to that in section 7.9.1.10, but using $\text{BrC}_3\text{H}_6\text{SiCl}_3$ (0.26 mL, 1 mmol). Yield (1.44 g, 87.7 %). (Found C 26.8; H 5.6; N 3.2. Calc. C 22.5; H 4.2; N

1.3). $\lambda_{\max}(\text{CD}_3\text{CN})$ (ϵ) 262 nm ($23,000 \text{ dm}^3 \text{ mol}^{-1} \text{ cm}^{-1}$); $\nu_{\max}(\text{KBr disc})$ 2964.3 (C-H), 2780.9 (C-H), 1472.0, 1024.6, 983, 920, 885.7, 805.5, 736.3 cm^{-1} ; $\delta_{\text{H}}(300 \text{ MHz; CD}_3\text{CN; Me}_4\text{Si})$ 0.72-0.87 (m, 2H, **CH**₂-Si), 0.97 (t, 36H, **CH**₃-CH₂-CH₂-CH₂-N, $J_{\text{HH}}=7.35$), 1.37 (st, 24H, CH₃-**CH**₂-CH₂-CH₂-N, $J_{\text{HH}}=7.35$), 1.61 (qn, 24H, **CH**₂-CH₂-N, $J_{\text{HH}}=7.54$), 1.80-1.93 (m, 2H, Si-CH₂-**CH**₂), 3.07-3.13 (m, 24H, **CH**₂-N), 3.50-3.62 (m, 2H, **CH**₂-Br); m/z (Maldi-TOF) 3653 ($M^+ + \text{NBu}_4$), 3791 ($M^+ + \text{NBu}_4\text{-CH}_2\text{Br}$), 3811 ($M^+ + \text{NBu}_4\text{-Br}$), 3892 ($M^+ + \text{NBu}_4$), 4039 ($M^+ + 2\text{NBu}_4\text{-CH}_2\text{Br}$), 4142 ($M^+ + 2\text{NBu}_4$), where $M^+ = (\text{NBu}_4)_3[\text{SiW}_9\text{O}_{34}(t\text{-BuSiO})_3(\text{BrC}_3\text{H}_6\text{Si})]^+$.

7.9.2. Reaction with triethoxysilane

7.9.2.1. Synthesis of $(\text{NBu}_4)_3\text{H}[\text{SiW}_9\text{O}_{34}(t\text{-BuSiO})_3(\text{Si}(\text{CH}_2)_3\text{SH})]$ (Compound 23)

To a stirred solution of $(\text{NBu}_4)_3[\text{SiW}_9\text{O}_{34}(t\text{-BuSiOH})_3]$ (1.0 g, 0.30 mmol) in dry DMF (3 mL) under nitrogen, $\text{HS}(\text{CH}_2)_3\text{Si}(\text{OEt})_3$ (0.13 mL, 0.62 mmol) and conc. HCl (0.5 mL) were added. The solution was stirred overnight at room temperature and then filtered. The product was purified by diffusion of diethyl ether into the remaining solution. Yield (0.67 g, 66.5 %) (Found C 23.6; H 4.6; N 1.9. Calc. C 22.5; H 4.3; N 1.25). $\lambda_{\max}(\text{CD}_3\text{CN})$ (ϵ) 263 nm ($27,000 \text{ dm}^3 \text{ mol}^{-1} \text{ cm}^{-1}$); $\nu_{\max}(\text{KBr disc})$ 2961.3 (C-H), 2874.6 (C-H), 1484.0, 1382.0, 1120, 1023.5, 980, 919.7, 889.6, 815.7, 723.6, 521.8 cm^{-1} ; $\delta_{\text{H}}(300 \text{ MHz; CD}_3\text{CN; Me}_4\text{Si})$ 0.58-0.80 (2H, m, SiCH₂), 0.97 (36H, t, $J_{\text{HH}}=7.35$, **CH**₃-CH₂-CH₂-CH₂-N), 1.00 (27H, s, *t*-Bu), 1.37 (24H, st, $J_{\text{HH}}=7.35$, CH₃-**CH**₂-CH₂-CH₂-N), 1.55-1.80 (26H, m, **CH**₂-CH₂-N, CH₂), 2.48-2.60 (2H, m, CH₂SH), 3.07-3.13 (24H, m, **CH**₂-N); m/z (Maldi-TOF) 3506 ($M^+ + \text{NBu}_4\text{-Si}(\text{CH}_2)_3\text{SH}$), 3526 ($M^+ + \text{NBu}_4\text{-Si}(\text{CH}_2)_3\text{SH} + \text{Na}$), 3546 ($M^+ + \text{NBu}_4\text{-CH}_2)_3\text{SH}$), 3623 ($M^+ + \text{NBu}_4$), 3644 ($M^+ + \text{NBu}_4 + \text{Na}$), 3757

($M^+ + 2\text{NBu}_4\text{-Si(CH}_2)_3\text{SH}$), 3790 ($M^+ + 2\text{NBu}_4\text{-(CH}_2)_3\text{SH}$), 3818 ($M^+ + 2\text{NBu}_4\text{-CH}_2\text{SH}$), 3866 ($M^+ + 2\text{NBu}_4$), 3882 ($M^+ + 2\text{NBu}_4 + \text{Na}$), where $M^+ = (\text{NBu}_4)_3[\text{SiW}_9\text{O}_{34}(t\text{-BuSiO})_3(\text{Si(CH}_2)_3\text{SH})]^+$.

7.9.2.2. Synthesis of $(\text{NBu}_4)_3[\text{PW}_9\text{O}_{34}(t\text{-BuSiO})_3(\text{Si(CH}_2)_3\text{SH})]$ (Compound 24)

Following a similar procedure to section 7.9.2.1, but using $(\text{NBu}_4)_3[\text{PW}_9\text{O}_{34}(t\text{-BuSiOH})_3]$ (1.0 g, 0.30 mmol). Yield (0.71 g, 70.4 %). (Found C 22.7; H 4.2; N 1.25. Calc. C 22.5; H 4.25; N 1.25). $\lambda_{\text{max}}(\text{CD}_3\text{CN})$ (ϵ) 259 nm ($26,000 \text{ dm}^3\text{mol}^{-1}\text{cm}^{-1}$); $\nu_{\text{max}}(\text{KBr disc})$ 2961.7, 2875.7 (C-H), 1486.3, 1386.0, 1100.7, 1036.1, 973.6, 930, 866.1, 811.7, 727.4, 517.8 cm^{-1} ; $\delta_{\text{H}}(300 \text{ MHz; CD}_3\text{CN; Me}_4\text{Si})$ 0.68-0.84 (2H, m, SiCH_2), 1.00 (36H, t, $J_{\text{HH}}=7.35$, $\text{CH}_3\text{-CH}_2\text{-CH}_2\text{-CH}_2\text{-N}$), 1.05 (27H, s, $t\text{Bu}$), 1.37 (24H, st, $J_{\text{HH}}=7.35$, $\text{CH}_3\text{-CH}_2\text{-CH}_2\text{-CH}_2\text{-N}$), 1.55-1.78 (26H, m, $\text{CH}_2\text{-CH}_2\text{-N}$, CH_2), 2.52-2.66 (2H, m, CH_2SH), 3.07-3.13 (24H, m, $\text{CH}_2\text{-N}$); $\delta_{\text{P}}(121 \text{ MHz; DMF:DMSO-}d_6; \text{H}_3\text{PO}_4)$ -15.7 ppm; m/z (Maldi-TOF) 3210 ($M^+ - \text{O}_3\text{Si(CH}_2)_3\text{SH}$), 3228 ($M^+ - \text{O}_2\text{Si(CH}_2)_3\text{SH}$), 3379 (M^+), 3397 ($M^+ + \text{Na}$), 3438 ($M^+ + \text{NBu}_4\text{-OSi(CH}_2)_3\text{SH-}t\text{Bu}$), 3457 ($M^+ + \text{NBu}_4\text{-O}_3\text{Si(CH}_2)_3\text{SH}$), 3474 ($M^+ + \text{NBu}_4\text{-O}_2\text{Si(CH}_2)_3\text{SH}$), where $M^+ = (\text{NBu}_4)_3[\text{PW}_9\text{O}_{34}(t\text{-BuSiO})_3(\text{Si(CH}_2)_3\text{SH})]^+$.

7.9.3. Reaction with phosphonic acid

7.9.3.1. Synthesis of $(\text{NBu}_4)_3\text{Na/H}_2[\text{PW}_9\text{O}_{34}(\text{EtPO})_2]$ (Compound X)⁸

Powdered $\text{K}_9[\text{PW}_9\text{O}_{34}]\cdot 16\text{H}_2\text{O}$ (2.30 g, 0.8 mmol), was suspended in a mixture of NBu_4Br (0.81 g, 2.5 mmol) and EtPO(OH)_2 (0.27 g, 2.5 mmol) in acetonitrile (45 mL). A 12M HCl solution (0.27 mL) was added dropwise and the resulting mixture was stirred at reflux overnight. The white residue (NaBr and unreacted $\text{SiW}_9\text{O}_{34}$) was separated by filtration and the resulting solution evaporated *in vacuo*. The crude compound was washed with water. Yield (2.04 g, 70.9 %). (Found: C, 21.9; H, 4.3; N, 1.4. Calc. for $\text{C}_{52}\text{H}_{118}\text{N}_3\text{O}_{36}\text{P}_3\text{W}_9$: C, 20.1; H, 3.9; N, 1.35);

$\lambda_{\max}(\text{H}_3\text{CCN})$ (ϵ) 246 nm ($23000 \text{ dm}^3 \text{ mol}^{-1} \text{ cm}^{-1}$); $\nu_{\max}(\text{KBr disc})$ 2962.7 (C-H), 2874.2 (C-H), 1482.4, 1094.3 (P-O), 1020.5 (P-O), 960.5, 876.7, 750.8 cm^{-1} ; δ_{H} (300 MHz; CD_3CN ; Me_4Si) 0.97 (42H, t, $J_{\text{HH}}=7.35$, $\text{CH}_3\text{-CH}_2\text{-CH}_2\text{-CH}_2\text{-N}$, $\text{CH}_3\text{-CH}_2\text{-PO}$), 1.37 (24H, st, $J_{\text{HH}}=7.35$, $\text{CH}_3\text{-CH}_2\text{-CH}_2\text{-CH}_2\text{-N}$), 1.61 (28H, qn, $J_{\text{HH}}=7.54$ Hz, $\text{CH}_2\text{-CH}_2\text{-N}$, $\text{CH}_2\text{-PO}$), 3.07-3.13 (24H, m, $\text{CH}_2\text{-N}$); δ_{P} (121 MHz, DMF:DMSO-d_6 (9:1), H_3PO_4) -12.55 (PW_9O_{34}), 30.05 ppm (EtPO); m/z (Maldi-TOF) 2520 ($M^+ - 3\text{NBu}_4 + 4\text{Na}$), 2678 ($M^+ - 2\text{NBu}_4$), 2818 ($M^+ - \text{NBu}_4 - \text{EtPO} - \text{Na}$), where $M^+ = (\text{NBu}_4)_3\text{Na}_2[\text{PW}_9\text{O}_{34}(\text{EtPO})_2]^+$.

7.9.3.2. Synthesis of $(\text{NBu}_4)_3\text{H}_2[\text{PW}_9\text{O}_{34}(\text{C}_2\text{H}_3\text{PO})_2]$ (Compound 25)

Was prepared and purified following a similar procedure to in section 7.9.3.1, but using $\text{C}_2\text{H}_3\text{PO}(\text{OH})_2$ (0.27 g, 2.5 mmol). Yield (1.66 g, 57.8 %). (Found: C, 22.8; H, 4.3; N, 1.8. Calc. for $\text{C}_{52}\text{H}_{114}\text{N}_3\text{O}_{36}\text{P}_3\text{W}_9$: C, 20.1; H, 3.7; N, 1.35); $\lambda_{\max}(\text{H}_3\text{CCN})$ (ϵ) 248.5 nm ($24500 \text{ dm}^3 \text{ mol}^{-1} \text{ cm}^{-1}$); $\nu_{\max}(\text{KBr disc})$ 2962.2 (C-H), 2873.5 (C-H), 1481.8, 1094.7 (P-O), 1026.0 (P-O), 962.4, 877.4, 752.8 cm^{-1} ; δ_{H} (300 MHz; CD_3CN ; Me_4Si) 0.97 (36H, t, $J_{\text{HH}}=7.35$, $\text{CH}_3\text{-CH}_2\text{-CH}_2\text{-CH}_2\text{-N}$), 1.37 (24H, st, $J_{\text{HH}}=7.35$, $\text{CH}_3\text{-CH}_2\text{-CH}_2\text{-CH}_2\text{-N}$), 1.61 (24H, qn, $J_{\text{HH}}=7.54$ Hz, $\text{CH}_2\text{-CH}_2\text{-N}$), 3.07-3.13 (24H, m, $\text{CH}_2\text{-N}$), 5.72-6.30 (6H, m, C_2H_3); δ_{P} (121 MHz, DMF:DMSO-d_6 (9:1), H_3PO_4) -12.44 (PW_9O_{34}), 13.41 ppm ($\text{C}_2\text{H}_3\text{PO}$); m/z (Maldi-TOF) 2514 ($M^+ - 3\text{NBu}_4 + 4\text{Na}$), 2672 ($M^+ - 2\text{NBu}_4$), 2814 ($M^+ - \text{NBu}_4 - \text{C}_2\text{H}_3\text{PO} - \text{Na}$), where $M^+ = (\text{NBu}_4)_3\text{Na}_2[\text{PW}_9\text{O}_{34}(\text{H}_3\text{C}_2\text{PO})_2]^+$.

7.9.3.3. Synthesis of $(\text{NBu}_4)_3\text{H}_2[\text{PW}_9\text{O}_{34}(\text{C}_3\text{H}_5\text{PO})_2]$ (Compound Y)⁸

Was prepared and purified following a similar procedure to in section 7.9.3.1, but using $\text{C}_3\text{H}_5\text{PO}(\text{OH})_2$ (0.32 g, 2.6 mmol). Yield (2.24 g, 77.4 %). $\lambda_{\max}(\text{H}_3\text{CCN})$ (ϵ) 248 nm (25000

$\text{dm}^3\text{mol}^{-1}\text{cm}^{-1}$); ν_{max} (KBr disc) 2962.0 (C-H), 2873.6 (C-H), 1482.1, 1092.8 (P-O), 1010 (P-O), 961.3, 877.0, 752.4 cm^{-1} ; δ_{H} (300 MHz; CD_3CN ; Me_4Si) 0.98 (36H, t, $J_{\text{HH}}=7.35$, $\text{CH}_3\text{-CH}_2\text{-CH}_2\text{-CH}_2\text{-N}$), 1.38 (24H, st, $J_{\text{HH}}=7.35$, $\text{CH}_3\text{-CH}_2\text{-CH}_2\text{-CH}_2\text{-N}$), 1.62 (24H, qn, $J_{\text{HH}}=7.52$, $\text{CH}_2\text{-CH}_2\text{-N}$), 2.56 (4H, dd, $J_{\text{HH}}=7.24$, $J_{\text{HP}}=23.17$, $\text{CH}_2\text{-PO}$), 3.08-3.15 (24H, m, $\text{CH}_2\text{-N}$), 5.13-5.25 (4H, m, $\text{CH}_2=\text{CH}$), 5.78-5.93 (2H, m, $\text{CH}_2=\text{CH}$); δ_{P} (121 MHz, DMF:DMSO-d_6 (9:1), H_3PO_4) -12.5 (PW_9O_{34}), 23.1 ppm ($\text{C}_3\text{H}_5\text{PO}$); m/z (Maldi-TOF) 3495 ($M^+ + 2\text{NBu}_4\text{-Na-C}_3\text{H}_5\text{PO-C}_3\text{H}_5\text{O}$), 3532 ($M^+ + 2\text{NBu}_4\text{-2Na-C}_3\text{H}_5\text{PO}$), 3548 ($M^+ + 2\text{NBu}_4\text{-Na-C}_3\text{H}_5\text{PO}$), where $M^+ = (\text{NBu}_4)_3\text{Na}_2[\text{PW}_9\text{O}_{34}(\text{C}_3\text{H}_5\text{PO})_2]^+$.

7.9.3.4. $(\text{NBu}_4)_3\text{H}_3[\text{SiW}_9\text{O}_{34}(\text{EtPO})_2]$ (Compound 26)

Was prepared using a similar procedure to in section 7.9.3.1, with $\text{Na}_{10}[\text{SiW}_9\text{O}_{34}]\cdot\text{H}_2\text{O}$ (2.0 g, 0.8 mmol). Yield (1.60 g, 64.3 %) λ_{max} (CD_3CN) (ϵ) 246.5 nm ($25,000\text{ dm}^3\text{mol}^{-1}\text{cm}^{-1}$), ν_{max} (KBr disc) 2962.5 (C-H), 2875 (C-H), 1485, 1458.3, 1185 (P-C), 1015 (P-O), 957.9, 899.5, 736.4 cm^{-1} ; δ_{H} (300 MHz; CD_3CN ; Me_4Si) 0.98 (36H, t, $J_{\text{HH}}=7.2$, $\text{CH}_3\text{-CH}_2\text{-CH}_2\text{-CH}_2\text{-N}$), 1.05-1.23 (6H, m, $\text{CH}_3\text{-CH}_2\text{-PO}$), 1.39 (24H, st, $J_{\text{HH}}=7.2$, $\text{CH}_3\text{-CH}_2\text{-CH}_2\text{-CH}_2\text{-N}$), 1.55-1.83 (30H, m, $\text{CH}_2\text{-CH}_2\text{-N}$, $\text{CH}_3\text{-CH}_2\text{-PO}$), 3.07-3.20 (24H, m, $\text{CH}_2\text{-N}$); δ_{P} (121 MHz; CD_3CN ; H_3PO_4) 29.4; δ_{Si} (79 MHz; DMF:DMSO-d_6 9:1; Me_4Si) -85.5, -87.8; m/z (Maldi-TOF) 2528 ($M^+ - 3\text{NBu}_4 + 3\text{Na}$), 2646 ($M^+ - 2\text{NBu}_4 - 2\text{Na}$), 2814 ($M^+ - \text{NBu}_4 - 2\text{Na} - \text{EtPO}$), where $M^+ = (\text{NBu}_4)_3\text{Na}_3[\text{SiW}_9\text{O}_{34}(\text{C}_2\text{H}_5\text{PO})_2]^+$.

7.9.3.5. $(\text{NBu}_4)_3\text{H}_3[\text{SiW}_9\text{O}_{34}(\text{H}_2\text{C}=\text{CHPO})_2]$ (Compound 27)

Was obtained using the same procedure as in section 7.9.3.4, but replacing $\text{EtPO}(\text{OH})_2$ by $\text{C}_2\text{H}_3\text{PO}(\text{OH})_2$ (0.27 g, 2.5 mmol). Yield (1.50 g, 60.4 %) λ_{max} (CD_3CN) (ϵ) 248.5 nm ($25,000\text{ dm}^3\text{mol}^{-1}\text{cm}^{-1}$); ν_{max} (KBr disc) 2962.6 (C-H), 2874.1 (C-H), 1600 (C=C), 1484.9, 1172.7 (P-O),

1015 (P-O), 956.8, 899.4, 844.5, 748.5 cm^{-1} ; δ_{H} (300 MHz; CD_3CN ; Me_4Si) 0.98 (36H, t, $J_{\text{HH}}=7.2$, $\text{CH}_3\text{-CH}_2\text{-CH}_2\text{-CH}_2\text{-N}$), 1.37 (24H, st, $J_{\text{HH}}=7.2$ Hz, $\text{CH}_3\text{-CH}_2\text{-CH}_2\text{-CH}_2\text{-N}$), 1.55-1.73 (24H, m, $\text{CH}_2\text{-CH}_2\text{-N}$), 3.07-3.20 (24H, m, $\text{CH}_2\text{-N}$), 5.82-6.18 (m, 6H, C_2H_3); δ_{P} (121 MHz; CD_3CN ; H_3PO_4) 16.3, 15.5, 13.3 ppm; m/z (Maldi-TOF) 3232 ($M^+ + \text{NBu}_4\text{-C}_2\text{H}_3\text{PO-C}_2\text{H}_3$), 3418 ($M^+ + \text{NBu}_4 + \text{C}_2\text{H}_3\text{PO}$), 3470 ($M^+ + \text{NBu}_4 + \text{C}_2\text{H}_3\text{PO} + 2\text{Na}$), 3842 ($M^+ + 3\text{NBu}_4\text{-Na}$), 4083 ($M^+ + 4\text{NBu}_4\text{-Na}$), where $M^+ = (\text{NBu}_4)_3\text{Na}_2[\text{SiW}_9\text{O}_{34}(\text{C}_2\text{H}_3\text{PO})_2]^+$.

7.9.3.6. $(\text{NBu}_4)_3\text{H}_3[\text{SiW}_9\text{O}_{34}(\text{H}_2\text{C}=\text{CHCH}_2\text{PO})_2]$ (Compound 28)

Was obtained using the procedure in section 7.9.3.4, but with $\text{C}_3\text{H}_5\text{PO}(\text{OH})_2$ (0.31 g, 2.5 mmol). Yield (1.55 g, 61.8 %); $\lambda_{\text{max}}(\text{CD}_3\text{CN})$ (ϵ) 250 nm ($28,500 \text{ dm}^3\text{mol}^{-1}\text{cm}^{-1}$); $\nu_{\text{max}}(\text{KBr disc})$ 2961.6 (C-H), 2873.8 (C-H), 1600 (C=C), 1484.5, 1153.1 (P-O), 1011.6 (P-O), 950.7, 897.5, 841.8, 746.6 cm^{-1} ; δ_{H} (300 MHz; CD_3CN ; Me_4Si) 0.98 (36H, t, $J_{\text{HH}}=7.2$, $\text{CH}_3\text{-CH}_2\text{-CH}_2\text{-CH}_2\text{-N}$), 1.39 (24H, st, $J_{\text{HH}}=7.2$, $\text{CH}_3\text{-CH}_2\text{-CH}_2\text{-CH}_2\text{-N}$), 1.63 (24H, qn, $J_{\text{HH}}=7.7$, $\text{CH}_2\text{-CH}_2\text{-N}$), 2.53 (4H, dd, $J_{\text{HH}}=7.0$, $J_{\text{HP}}=22.8$ Hz, $\text{CH}_2=\text{CH-CH}_2\text{-PO}$), 3.07-3.20 (24H, m, $\text{CH}_2\text{-N}$), 5.11-5.25 (4H, m, $\text{CH}_2=\text{CH-CH}_2\text{-PO}$), 5.75-5.94 (2H, m, $\text{CH}_2=\text{CH-CH}_2\text{-PO}$); δ_{P} (121 MHz; DMF:DMSO-d_6 9:1; H_3PO_4) 23.5 ppm; m/z 3281 ($M^+ + \text{C}_3\text{H}_5\text{PO} + \text{Na}$), 3479 ($M^+ + \text{NBu}_4 + \text{C}_3\text{H}_5\text{PO}$), 3506 ($M^+ + \text{NBu}_4 + \text{C}_3\text{H}_5\text{PO} + \text{Na}$), 3693 ($M^+ + 2\text{NBu}_4 + \text{C}_3\text{H}_5\text{PO}$), 3720 ($M^+ + 2\text{NBu}_4 + \text{C}_3\text{H}_5\text{PO}$), 4078 ($M^+ + 4\text{NBu}_4\text{-C}_2\text{H}_3$), where $M^+ = (\text{NBu}_4)_3\text{Na}_2[\text{SiW}_9\text{O}_{34}(\text{C}_3\text{H}_5\text{PO})_2]^+$.

7.9.3.7. $(\text{NBu}_4)_3\text{Na}[\text{SiW}_9\text{O}_{34}(\text{EtPO})_3]$ (Compound 29)

Powdered $\text{Na}_{10}[\text{SiW}_9\text{O}_{34}]\cdot\text{H}_2\text{O}$ (2.0 g, 0.8 mmol) was suspended in a mixture of NBu_4Br (0.81 g, 2.5 mmol) and $\text{EtPO}(\text{OH})_2$ (0.35 g, 3.2 mmol) in acetonitrile (45 mL). A 12M HCl solution (0.54 mL) was added dropwise and the resulting mixture was stirred at reflux for 72 hours. The white

residue (NaBr and unreacted $\text{SiW}_9\text{O}_{34}$) was separated by filtration and the resulting solution evaporated *in vacuo*. The crude compound was washed with water and crystals were grown by diffusion of Diether ether into an acetonitrile solution at room temperature. $(\text{NBu}_4)_3\text{Na}[\text{SiW}_9\text{O}_{34}(\text{C}_2\text{H}_5\text{PO})_3]$ (1.60 g, 61.4 %) (Found C, 21.6; H, 4.0; N, 1.4. Calc. for $\text{C}_{54}\text{H}_{123}\text{NaN}_3\text{O}_{37}\text{P}_3\text{SiW}_9$: C, 20.2; H, 3.85; N, 1.3 %); $\lambda_{\text{max}}(\text{CD}_3\text{CN})$ (ϵ) 265 nm($29,000 \text{ dm}^3\text{mol}^{-1}\text{cm}^{-1}$); $\nu_{\text{max}}(\text{KBr disc})$ 2963.3 (C-H), 2875.4 (C-H), 1485.6, 1459.2, 1186.4 (P=O), 1128.2 (P-O), 1015.5 (P-O), 954.1, 923.8, 903.5, 836.8, 737.3 cm^{-1} ; $\delta_{\text{H}}(300 \text{ MHz; CD}_3\text{CN; Me}_4\text{Si})$ 0.98 (36H, t, $J_{\text{HH}}=7.2$ $\text{CH}_3\text{-CH}_2\text{-CH}_2\text{-CH}_2\text{-N}$), 1.10-1.23 (6H, m, $\text{CH}_2\text{-PO}$), 1.39 (24H, st, $J_{\text{HH}}=7.2$ $\text{CH}_3\text{-CH}_2\text{-CH}_2\text{-CH}_2\text{-N}$), 1.55-1.83 (33H, m, $\text{CH}_2\text{-CH}_2\text{-N}$, $\text{CH}_3\text{-CH}_2\text{-PO}$), 3.07-3.20 (24H, m, $\text{CH}_2\text{-N}$); $\delta_{\text{P}}(121 \text{ MHz; CD}_3\text{CN; H}_3\text{PO}_4)$ 29.5; $\delta_{\text{Si}}(79 \text{ MHz; DMF:DMSO-d}_6 \text{ 9:1; Me}_4\text{Si})$ -88.37 ppm; m/z (Maldi-TOF) 3433 ($M^+ + \text{NBu}_4\text{-Na}$), 3454 ($M^+ + \text{NBu}_4$), 3476 ($M^+ + \text{NBu}_4 + \text{Na}$), 3676 ($M^+ + 2\text{NBu}_4$), 3699 ($M^+ + 2\text{NBu}_4$), 3718 ($M^+ + 2\text{NBu}_4 + \text{Na}$), where $M^+ = (\text{NBu}_4)_3\text{Na}[\text{SiW}_9\text{O}_{34}(\text{C}_2\text{H}_5\text{PO})_3]$. Data were collected at the EPSRC crystallography service at Southampton ($\lambda = 0.71073 \text{ \AA}$). Crystal Data. $\text{C}_{54}\text{H}_{124}\text{N}_3\text{O}_{37}\text{P}_3\text{SiW}_9$, $M = 3183.21$, Trigonal, $a = 20.725(24)$, $b = 20.725(22)$, $c = 22.471(3) \text{ \AA}$, $U = 8359(11) \text{ \AA}^3$, $T = 120 \text{ K}$, space group $R \bar{3} m$ (no. 160), $Z = 3$, 19865 reflections measured, 3518 unique ($R_{\text{int}} = 0.099$). The Final $R1(\text{obs. data}) = 0.072$, $R1(\text{all data}) = 0.098$. Final refinements were carried out with anisotropic thermal parameters for tungsten, phosphorus and silicon atoms.

7.9.3.8. $(\text{NBu}_4)_3\text{Na}[\text{SiW}_9\text{O}_{34}(\text{H}_2\text{C=CHPO})_3]$ (Compound 30)

Was obtained using the procedure in section 7.9.3.7, but replacing $\text{EtPO}(\text{OH})_2$ by $\text{C}_2\text{H}_3\text{PO}(\text{OH})_2$ (0.35 g). Crystals were grown by diffusion of Et_2O into a DMF solution at room temperature. $(\text{NBu}_4)_3[\text{SiW}_9\text{O}_{34}(\text{H}_2\text{C=CHPO})_3].((\text{CH}_3)_2\text{NCOH})_{1.5}$ Yield (1.73 g, 67.6 %) (Found C, 22.3; H,

3.8; N, 1.9. Calc. for $C_{58.5}H_{127.5}NaN_{4.5}O_{38.5}P_3SiW_9$: C, 21.2; H, 3.85; N, 1.9 %) $\lambda_{max}(CD_3CN)$ (ϵ) 266 nm ($27,000 \text{ dm}^3\text{mol}^{-1}\text{cm}^{-1}$); $\nu_{max}(\text{KBr disc})$ 2962.7 (C-H), 2875.2 (C-H), 1600 (C=C), 1484.2, 1194.5 (P-C), 1129.0 (P-O), 1002.5 (P-O), 956.9, 924.3, 904.0, 839.9, 730.5 cm^{-1} ; $\delta_H(300 \text{ MHz; } CD_3CN; \text{Me}_4\text{Si})$ 0.98 (36H, t, $J_{HH}=7.2$, $\text{CH}_3\text{-CH}_2\text{-CH}_2\text{-CH}_2\text{-N}$), 1.37 (24H, st, $J_{HH}=7.2$, $\text{CH}_3\text{-CH}_2\text{-CH}_2\text{-CH}_2\text{-N}$), 1.55-1.72 (24H, m, $\text{CH}_2\text{-CH}_2\text{-N}$), 3.07-3.20 (24H, m, $\text{CH}_2\text{-N}$), 5.82-6.18 (9H, m, C_2H_3); $\delta_P(121 \text{ MHz; } CD_3CN; \text{H}_3\text{PO}_4)$ 14.9; $\delta_{Si}(79 \text{ MHz; } \text{DMF:DMSO-d}_6 \text{ 9:1; Me}_4\text{Si})$ -87.85 ppm; m/z (Maldi-TOF) 3161 (M^+), 3404 ($M^+ + \text{NBu}_4$), 3426 ($M^+ + \text{NBu}_4 + \text{Na}$), 3461 ($M^+ + \text{NBu}_4 + 2\text{Na}$), 3646 ($M^+ + 2\text{NBu}_4$), 3669 ($M^+ + 2\text{NBu}_4 + \text{Na}$), 3889 ($M^+ + 3\text{NBu}_4$) where $M^+ = (\text{NBu}_4)_3[\text{SiW}_9\text{O}_{34}(\text{C}_2\text{H}_3\text{PO})_3]^+$. Data were collected on a Bruker SMART 6000 diffractometer ($\lambda_{\text{Cu-K}\alpha} = 1.54178 \text{ \AA}$). Structure 14. $C_{117}H_{257}N_9O_{78}P_6Si_2W_{18}Na_2$, $M = 6635.6$, Monoclinic, $a = 18.7349(7)$, $b = 41.2914(18)$, $c = 28.3336(12) \text{ \AA}$, $U = 19787.8(14) \text{ \AA}^3$, $T = 200 \text{ K}$, space group $P 2_1/n$ (no. 14), $Z = 4$, 87060 reflections measured, 22669 unique ($R_{\text{int}} = 0.145$). The Final $R1(\text{obs. data}) = 0.084$, $R1(\text{all data}) = 0.136$. Final refinements were carried out with anisotropic thermal parameters for tungsten, phosphorus, silicon and nitrogen atoms.

7.9.3.9. $(\text{NBu}_4)_3\text{Na}[\text{SiW}_9\text{O}_{34}(\text{H}_2\text{C}=\text{CHCH}_2\text{PO})_3]$ (Compound 31)

Was obtained using the procedure in section 7.9.3.7, but replacing $\text{EtPO}(\text{OH})_2$ with $\text{C}_3\text{H}_5\text{PO}(\text{OH})_2$ (0.39 g, 3.2 mmol). Crystals suitable were grown by diffusion of Et_2O into an acetonitrile solution at room temperature. Yield (1.68 g, 64.8 %) (Found C, 21.2; H, 3.7; N, 1.3. Calc. for $C_{57}H_{123}NaN_3O_{37}P_3SiW_9$: C, 21.1; H, 3.8; N, 1.3 %); $\lambda_{max}(CD_3CN)$ (ϵ) 265 nm ($25,000 \text{ dm}^3\text{mol}^{-1}\text{cm}^{-1}$); $\nu_{max}(\text{KBr disc})$ 2962.5 (C-H), 2874.8 (C-H), 1600 (C=C), 1484.3, 1190, 1130 (P-O), 1002.3 (P-O), 956.4, 924.1, 903.8, 838.7, 733.4 cm^{-1} ; $\delta_H(300 \text{ MHz; } CD_3CN; \text{Me}_4\text{Si})$ 0.98 (36H, t, $J_{HH}=7.2$, $\text{CH}_3\text{-CH}_2\text{-CH}_2\text{-CH}_2\text{-N}$), 1.39 (24H, st, $J_{HH}=7.2$, $\text{CH}_3\text{-CH}_2\text{-CH}_2\text{-CH}_2\text{-N}$), 1.63

(24H, qn, $J_{\text{HH}}=7.7$, **CH₂**-CH₂-N), 2.53 (4H, dd, $J_{\text{HH}}=7.0$, $J_{\text{HP}}=22.8$, **CH₂**-PO), 3.07-3.20 (24H, m, **CH₂**-N), 5.11-5.25 (4H, m, **CH₂**=CH), 5.75-5.94 (2H, m, CH₂=**CH**); δ_{P} (121 MHz; CD₃CN; H₃PO₄) 23.3; δ_{Si} (79 MHz; DMF:DMSO-d₆ 9:1; Me₄Si) -88.1; m/z (Maldi-TOF) 3395 (M^+ +NBu₄+Na-C₃H₅PO), 3422 (M^+ +NBu₄-C₃H₅), 3454 (M^+ +NBu₄), 3621 (M^+ +2NBu₄-C₃H₅PO), 3643 (M^+ +2NBu₄-2(C₃H₅)), 3672 (M^+ +2NBu₄-C₂H₃), 3702 (M^+ +2NBu₄) where M^+ = (NBu₄)₃[SiW₉O₃₄(C₃H₅PO)₃]⁺. Data were collected on Station 9.8 at the SRS Synchrotron source, Daresbury (λ = 0.67030 Å). Structure 15. C₅₉H₁₂₇N₄O_{37.5}P₃SiW₉Na, M = 3291.29, Trigonal, a = 22.2078(16), b = 22.2078(16), c = 34.914(5) Å, U = 14912(3) Å³, T = 30 K, space group R 3 c (no. 161), Z = 6, 41885 reflections measured, 9245 unique (R_{int} = 0.066). The Final R1(obs. data) = 0.043, R1(all data) = 0.065. Final refinements were carried out with anisotropic thermal parameters for all non-hydrogen atoms except those in the solvent molecules.

7.9.3.10. (NBu₄)₃Na[SiW₉O₃₄(HOOCCH₂PO)₃] (Compound 32)

Was obtained using the same procedure as in section 7.9.3.7, but replacing EtPO(OH)₂ by HOOCCH₂PO(OH)₂ (0.45 g, 3.2 mmol). Yield (1.45 g, 43.7 %) (Found C, 21.8; H, 3.8; N, 1.8. Calc. for C₅₄H₁₁₇NaN₃O₄₃P₃SiW₉: C, 19.8; H, 3.6; N, 1.3 %) λ_{max} (CD₃CN) (ϵ) 260.5 nm (24,500 dm³mol⁻¹cm⁻¹); ν_{max} (KBr disc) 2962.5 (C-H), 2874.9 (C-H), 1600 (C=C), 1484.2, 1177.7, 1130 (P-O), 1014.7 (P-O), 958.5, 900.5, 843.3, 746.1 cm⁻¹; δ_{H} (300 MHz; CD₃CN; Me₄Si) 0.98 (36H, t, $J_{\text{HH}}=7.4$, **CH₃**-CH₂-CH₂-CH₂-N), 1.37 (24H, st, $J_{\text{HH}}=7.2$, CH₃-**CH₂**-CH₂-CH₂-N), 1.55-1.72 (24H, m, **CH₂**-CH₂-N), 2.82 (6H, d, $J_{\text{HH}}=22.4$ Hz, CH₂PO), 3.07-3.20 (24H, m, **CH₂**-N); δ_{P} (121 MHz; CD₃CN; H₃PO₄) 16.0; m/z (Maldi-TOF) 3530 (M^+ +NBu₄+Na), 3719 (M^+ +2NBu₄-OH), 3759 (M^+ +2NBu₄), 3997 (M^+ +3NBu₄), 4085 (M^+ +4NBu₄-HOOCCH₂PO-HOOC), where M^+ = (NBu₄)₃[SiW₉O₃₄(HOOCCH₂PO)₂]⁺.

7.9.3.11. (NBu₄)₃Na[SiW₉O₃₄(HOOCCH₂CH₂PO)₃] (Compound 33)

Was obtained using the same procedure as in section 7.9.3.7, but replacing EtPO(OH)₂ by HOOCCH₂CH₂PO(OH)₂ (0.49 g, 3.2 mmol). Crystals were grown by diffusion of diether ether into a DMF solution at room temperature. Yield (2.10 g, 79.2 %) (Found C, 22.9; H, 4.5; N, 1.4. Calc. for C₅₇H₁₂₃NaN₃O₄₃P₃SiW₉: C, 20.5; H, 3.7; N, 1.3 %) $\lambda_{\max}(\text{CD}_3\text{CN})$ (ϵ) 265.5 nm (23,500 dm³mol⁻¹cm⁻¹); $\nu_{\max}(\text{KBr disc})$ 2963.5 (C-H), 2875.8 (C-H), 1600 (C=C), 1484.8, 1161.6, 1004.8 (P-O), 958.8, 958.8, 925, 904.4, 840.5, 733.5 cm⁻¹; $\delta_{\text{H}}(300 \text{ MHz; CD}_3\text{CN; Me}_4\text{Si})$ 1.00 (36H, t, $J_{\text{HH}}=7.2$, **CH**₃-CH₂-CH₂-CH₂-N), 1.40 (24H, st, $J_{\text{HH}}=7.2$, **CH**₃-**CH**₂-CH₂-CH₂-N), 1.55-1.72 (24H, m, **CH**₂-CH₂-N), 1.86-2.02 (6H, m, CH₂-PO), 2.52-2.70 (6H, m, CH₂-COOH), 3.08-3.22 (24H, m, **CH**₂-N); $\delta_{\text{P}}(121 \text{ MHz; CD}_3\text{CN; H}_3\text{PO}_4)$ 27.6; m/z (Maldi-TOF) 3318 (M^+), 3430 (M^+ +NBu₄-HOOCCH₂CH₂), 3560 (M^+ +NBu₄), 3672 (M^+ +NBu₄+2Na-HOOCCH₂CH₂PO), 3801 (M^+ +NBu₄+Na), where $M^+ = (\text{NBu}_4)_3[\text{SiW}_9\text{O}_{34}(\text{HOOCCH}_2\text{CH}_2\text{PO})_3]^+$. Data were collected on a Bruker SMART 6000 diffractometer ($\lambda_{\text{Cu-K}\alpha} = 1.54178 \text{ \AA}$). Structure 17. C₅₇H₁₂₃N₃O₄₃P₃SiW₉, $M = 3337.22$, Tetragonal, $a = 38.9645(14)$, $b = 38.9645(14)$, $c = 14.1781(7) \text{ \AA}$, $U = 21525.7(15) \text{ \AA}^3$, $T = 200 \text{ K}$, space group P 4/n (no. 85), $Z = 8$, 134814 reflections measured, 13975 unique ($R_{\text{int}}=0.102$). The Final $R_1(\text{obs. data}) = 0.090$, $R_1(\text{all data}) = 0.150$. Final refinements were carried out with anisotropic thermal parameters for all non-hydrogen and non-carbon atoms.

7.9.3.12. (NBu₄)₃Na[SiW₉O₃₄(H₃CCOC₆H₄PO)₃] (Compound 34)

Was obtained using the procedure in section 7.9.3.7, but replacing EtPO(OH)₂ by H₃CCOC₆H₄PO(OH)₂ (0.64 g, 3.2 mmol). Crystals were grown by diffusion of diether ether into a DMF solution at room temperature. Yield (2.22 g, 63.9 %). (Found C, 24.9; H, 3.9; N, 1.4 Calc. for C₇₂H₁₂₉NaN₃O₄₀P₃SiW₉: C, 24.8; H, 3.7; N, 1.2 %) $\lambda_{\max}(\text{CD}_3\text{CN})$ (ϵ) 249.5 nm (98,000

$\text{dm}^3\text{mol}^{-1}\text{cm}^{-1}$); ν_{max} (KBr disc) 2962.2 (C-H), 2874.0 (C-H), 1684.4 (C=O), 1483.5, 1200.3, 1137.4 (P-O), 1024.2 (P-O), 1002.5 (P-O), 958.1, 924.8, 905.2, 840.8, 735.5 cm^{-1} ; δ_{H} (300 MHz; CD_3CN ; Me_4Si) 0.98 (36H, t, $J_{\text{HH}}=7.2$, $\text{CH}_3\text{-CH}_2\text{-CH}_2\text{-CH}_2\text{-N}$), 1.36 (24H, st, $J_{\text{HH}}=7.2$, $\text{CH}_3\text{-CH}_2\text{-CH}_2\text{-CH}_2\text{-N}$), 1.50-1.69 (24H, m, $\text{CH}_2\text{-CH}_2\text{-N}$), 2.60 (9H, s, H_3CCO), 3.00-3.16 (24H, m, $\text{CH}_2\text{-N}$), 7.88-8.08 (12H, m, C_6H_4); δ_{P} (121 MHz; CD_3CN ; H_3PO_4) 14.3; m/z (Maldi-TOF) 3736 ($M^+ + \text{NBu}_4$), 3971 ($M^+ + 2\text{NBu}_4$), where $M^+ = (\text{NBu}_4)_3\text{Na}[\text{SiW}_9\text{O}_{34}(\text{H}_3\text{CCOC}_6\text{H}_4\text{PO})_3]^+$. Data were collected on a Bruker SMART 6000 diffractometer ($\lambda_{\text{Cu-K}\alpha} = 1.54178 \text{ \AA}$). Structure 18. $\text{C}_{162}\text{H}_{290}\text{N}_{12}\text{O}_{86}\text{P}_6\text{Si}_2\text{W}_{18}\text{Na}$, $M = 7357.7$, Triclinic, $a = 18.5991(18)$, $b = 19.2421(16)$, $c = 20.8677(19) \text{ \AA}$, $\alpha = 94.186(6)^\circ$, $\beta = 116.047(5)^\circ$, $\gamma = 114.979(5)^\circ$, $U = 5767.8(9) \text{ \AA}^3$, $T = 200 \text{ K}$, space group P -1 (no. 2), $Z = 1$, 37161 reflections measured, 17620 unique ($R_{\text{int}}=0.056$). The Final $R_1(\text{obs. data}) = 0.044$, $R_1(\text{all data}) = 0.059$. Final refinements were carried out with anisotropic thermal parameters for all non-hydrogen atoms except those in the solvent and the metal ion.

Crystals suitable for Single Crystal XRD were also obtained by slow diffusion of diethyl ether into a DMF solution containing the crude product and Cobalt (II) nitrate. Data were collected on a Bruker SMART 6000 diffractometer ($\lambda_{\text{Cu-K}\alpha} = 1.54178 \text{ \AA}$). Structure 19. $\text{C}_{157}\text{H}_{280}\text{N}_{15}\text{O}_{90}\text{P}_6\text{Si}_2\text{W}_{18}\text{Co}_2$, $M = 7487.12$, Monoclinic, $a = 22.0375(13)$, $b = 31.3129(19)$, $c = 33.7086(19) \text{ \AA}$, $\beta = 91.085(3)^\circ$, $U = 23257(2) \text{ \AA}^3$, $T = 293 \text{ K}$, space group C 2/c (no. 15), $Z = 4$, 71703 reflections measured, 14651 unique ($R_{\text{int}}=0.069$). The Final $R_1(\text{obs. data}) = 0.049$, $R_1(\text{all data}) = 0.075$. Final refinements were carried out with anisotropic thermal parameters for tungsten, phosphorus and silicon atoms and the atoms at the centres of the cations.

7.9.3.13. (NBu₄)₃Na[SiW₉O₃₄(H₂C=CHC₆H₄PO)₃] (Compound 35)

Was obtained using the same procedure as in section 7.9.3.7, but replacing EtPO(OH)₂ by H₃C=CHC₆H₄PO(OH)₂ (0.59 g, 3.2 mmol). Yield (2.10 g, 77.1 %) (Found C, 23.5; H, 3.9; N, 1.3. Calc. for C₇₂H₁₃₂NaN₃O₃₇P₃SiW₉ C, 25.2; H, 3.8; N, 1.2 %); λ_{max} (CD₃CN) (ϵ) 260.5 nm (75000 dm³mol⁻¹cm⁻¹); ν_{max} (KBr disc) 2963.0 (C-H), 2874.7 (C-H), 1600 (C=C), 1483.2, 1200 (P-C), 1133.7 (P-O), 1025 (P-O), 1000.6 (P-O), 957.6, 924.0, 905.5, 836.8, 733.0 cm⁻¹; δ_{H} (300 MHz; CD₃CN; Me₄Si) 0.98 (36H, t, $J_{\text{HH}}=7.2$, **CH**₃-CH₂-CH₂-CH₂-N), 1.37 (24H, st, $J_{\text{HH}}=7.2$, CH₃-**CH**₂-CH₂-CH₂-N), 1.54-1.72 (24H, m, **CH**₂-CH₂-N), 3.04-3.20 (24H, m, **CH**₂-N), 5.35 (3H, d, **H**₂C=CH), 5.88 (3H, d, **H**₂C=CH), 6.80 (3H, dd, H₂C=**CH**), 7.42-7.88 (12H, m, C₆H₄); δ_{P} (121 MHz; CD₃CN; H₃PO₄) 13.5; m/z (Maldi-TOF) 3428 (M^+), 3646 (M^+ +NBu₄-H₂C=CH), 3665 (M^+ +NBu₄), where M^+ = (NBu₄)₃Na[SiW₉O₃₄(H₂C=CHC₆H₄PO)₃]. Crystals suitable for Single Crystal XRD were obtained by slow diffusion of diethyl ether into a DMF solution containing the crude product and Cobalt(II) nitrate. Data were collected on a Bruker SMART 6000 diffractometer ($\lambda_{\text{Cu-K}\alpha}$ = 1.54178 Å). Structure 16. C₇₅H₁₃₈N₄O₃₉P₃SiW₉Co, M = 3554.47, Trigonal, a = 21.405(5), b = 21.405(5), c = 21.217(9) Å, U = 8418(4) Å³, T = 293 K, space group R 3 m (no. 160), Z = 3, 14261 reflections measured, 3383 unique (R_{int} =0.049). The Final R1(obs. data) = 0.041, R1(all data) = 0.051.

7.9.4. Cation exchange**7.9.4.1. [PW₉O₃₄]⁹⁻**

A solution of K₉[PW₉O₃₄].16H₂O (1.0 g, 0.35 mmol) in water (15 mL) was treated with a saturated solution of NBu₄Br (1.94 g, 7.0 mmol) in water (15 mL). A white precipitate formed

instantly, after a few minutes the solution was filtered, washed with water and air dried. Yield (0.46 g, Yield not calculated as cation ratio is unknown). ν_{\max} (KBr disc) 2961.5 (C-H), 2935.0 (C-H), 2873.3 (C-H), 1483.7, 1152.4 (P-O), 1106.4 (P-O), 1053.4 (P-O), 957.2 (P-O), 886.6, 753.8 cm^{-1} ; δ_{P} (121 MHz; CD_3CN ; H_3PO_4) -11.9 ppm.

7.9.4.1.1. $(\text{NBu}_4)_3[\text{PW}_{11}\text{O}_{39}(\text{EtPO})_2]$ (Compound Z)⁹

The product obtained in section 7.9.4.1 (1.0 g, 0.32 mmol) was dissolved in acetonitrile (12.5 mL) (Solution A). ‘ EtPO^{2+} ’ was prepared by addition of AgNO_3 (0.43 g) to a solution of EtPCl_2 (0.16 g) in acetonitrile (5 mL), the solution filtered and added to solution A. The resulting solution was stirred for 48 hours, the solvent was removed *in vacuo* and the precipitate washed with water and ether to give a yellow product.

7.9.4.2. $[\text{SiW}_9\text{O}_{34}]^{10-}$

Using the method in section 7.9.4.1, but with $\text{Na}_{10}[\text{SiW}_9\text{O}_{34}]$ (2.5 g, 1 mmol) and NBu_4Br (5.55 g, 0.02 mol), a small quantity of an oily deposit was obtained which could not be isolated.

7.9.4.3. $[\text{SiW}_9\text{O}_{34}]^{10-}$

The procedure was followed as in section 7.9. except that sodium carbonate was replaced with NBu_4Br during the precipitation of the product, to give a white solid. ν_{\max} (KBr disc) 2961.2 (C-H), 2873.7 (C-H), 1483.3, 1010.1 (Si-O), 967.7 (Si-O), 919.2, 883.0, 800.0 cm^{-1} .

7.9.5. Reaction with EtPCl₂

7.9.5.1. (NBu₄)₃H₂[PW₉O₃₄(EtPO)₂] ‘all in one’ method (Compound 36)

AgNO₃ (0.24 g, 1.4 mmol) was added to EtPCl₂ (0.072 mL, 0.5 mmol) in acetonitrile (5 mL), the yellow solution was quickly filtered from the white precipitate. This solution was added to an acetonitrile solution (20 mL) containing NBu₄Br (0.19 g, 0.7 mmol) and a suspension of K₉[PW₉O₃₄].16H₂O (0.5 g, 0.18 mmol). The resulting solution was stirred at room temperature for 1, 3 or 5 days, extra ‘EtPO²⁺’ solution being made and added after 36 hours for the longer reaction times. The resulting solution was filtered to remove any unreacted PW₉O₃₄ and evaporated *in vacuo* to give a yellow solid which was washed with water. Yield (0.55 g, 98.2 % (assuming formula above)) (Found C, 19.9; H, 3.8; N, 0.7. Calc. for C₅₄H₁₂₃NaN₃O₃₇P₄W₉: C, 20.4; H, 3.7; N, 1.35%) $\lambda_{\max}(\text{CD}_3\text{CN})$ (ϵ) 259.5 nm (26,500 dm³mol⁻¹cm⁻¹); $\nu_{\max}(\text{KBr disc})$ 2963.3 (C-H), 2874.8 (C-H), 1458.9, 1200, 1098.5 (P-O), 1027.9 (P-O), 969.9, 939.0, 877.7, 750.1 cm⁻¹; $\delta_{\text{H}}(300 \text{ MHz; CD}_3\text{CN; Me}_4\text{Si})$ 0.98 (36H, t, $J_{\text{HH}}=7.2$, **CH**₃-CH₂-CH₂-CH₂-N), 1.05-1.23 (6H, m, **CH**₃-CH₂-PO), 1.39 (24H, st, $J_{\text{HH}}=7.2$, CH₃-**CH**₂-CH₂-CH₂-N), 1.55-1.83 (24H, m, **CH**₂-CH₂-N), 1.70-1.90 (6H, m, **CH**₃-CH₂-PO), 3.07-3.20 (24H, m, **CH**₂-N); $\delta_{\text{P}}(121 \text{ MHz; CD}_3\text{CN; H}_3\text{PO}_4)$ -12.5 (PW₉O₃₄), 32.0 ppm ($J_{\text{PW}}=19.4 \text{ Hz}$, EtPO); m/z (Maldi-TOF) 3180 (M^+), 3226 ($M^++2\text{Na}$), 3422 ($M^++\text{NBu}_4$), 3466 ($M^++\text{NBu}_4+2\text{Na}$), where $M^+ = (\text{NBu}_4)_3[\text{PW}_9\text{O}_{34}(\text{C}_2\text{H}_5\text{PO})_3]^+$. Data were collected on station 16.2smx at the SRS Synchrotron source, Daresbury ($\lambda = 0.79720 \text{ \AA}$). Structure 20. C₅₄H₁₂₃N₃O₃₇P₄W₉, M = 3368.9, Monoclinic, a = 19.131(9), b = 20.933(10), c = 23.461(11) Å, $\beta = 100.853(4)$, U = 9227(8) Å³, T = 150 K, space group P a (no. 7), Z = 2, 42452 reflections measured, 19764 unique ($R_{\text{int}}=0.205$). The Final $R1(\text{obs. data}) = 0.138$, $R1(\text{all data}) = 0.363$.

7.9.5.2. (NBu₄)₃Na[SiW₉O₃₄(EtPO)₃] ‘all in one’ method (Compound 37)

Was prepared using a similar method to in section 7.9.5.1, but using Na₁₀[SiW₉O₃₄].H₂O (0.5 g, 0.2 mmol) and NBu₄Br (0.22 g, 0.8 mmol). Yield (0.47 g, 73.3 %). (Found C, 21.6; H, 4.75; N, 2.4. Calc. for C₅₄H₁₂₃NaN₃O₃₇P₃SiW₉: C, 20.2; H, 3.85; N, 1.3 %) $\lambda_{\max}(\text{CD}_3\text{CN})$ (ϵ) 263 nm (25,000 dm³mol⁻¹cm⁻¹); $\nu_{\max}(\text{KBr disc})$ 2967.4 (C-H), 2875 (C-H), 1466.1, 1124.7 (P-O), 1030.8 (P-O), 950, 912.1, 900, 830, 717.9 cm⁻¹; $\delta_{\text{H}}(300 \text{ MHz; CD}_3\text{CN; Me}_4\text{Si})$ 0.98 (36H, t, $J_{\text{HH}}=7.2$ CH₃-CH₂-CH₂-CH₂-N), 1.05-1.28 (6H, m, CH₂-PO), 1.45 (24H, st, $J_{\text{HH}}=7.2$ CH₃-CH₂-CH₂-CH₂-N), 1.56-1.83 (30H, m, CH₂-CH₂-N, CH₃-CH₂-PO), 3.04-3.20 (24H, m, CH₂-N); $\delta_{\text{P}}(121 \text{ MHz; CD}_3\text{CN; H}_3\text{PO}_4)$ 29.9, 34.4 ppm; m/z (Maldi-TOF) 3184 (M^+ -Na), 3320 (M^+ +NBu₄-O₃PEt), 3426 (M^+ +NBu₄-Na), 3475 (M^+ +NBu₄+2Na), 3550 (M^+ +2NBu₄-O₃PEt), 3668 (M^+ +2NBu₄), where M^+ = (NBu₄)₃Na[SiW₉O₃₄(C₂H₅PO)₃]⁺.

7.10. Polymerization of (NBu₄)₃H[SiW₁₀O₃₆(RPO)₂]

(NBu₄)₃H[SiW₁₀O₃₆(RPO)₂] (R = H₂C=CH, H₂C=CHCH₂ or H₂C=CHC₆H₄) (0.15 g, 0.04 mmol) was dissolved in 1,2-dichloroethane (2 mL) and filtered, initiator AIBN (4 mg) was added, the solution degassed using N₂, placed in a sealed tube and heated at 80°C for time, t . The solution was then evaporated in *vacuo* and dried to give the product as a yellow solid.

Example of polymer for (NBu₄)₃H[SiW₁₀O₃₆(H₂CCHC₆H₄PO)₂]. Yield (0.09 g, 60.0 %) $\lambda_{\max}(\text{CH}_3\text{CN})$ (ϵ) 258 nm (28500 mol⁻¹dm³cm⁻¹); $\nu_{\max}(\text{KBr disc})$ 2960, 2873 (C-H), 1482, 1135, 1059 (P-O), 1006, 974, 942, 910, 888, 836, 753 cm⁻¹; δ_{H} (300 MHz; CD₃CN; Me₄Si) 0.98 (36H, t, $J_{\text{HH}}=7.35$, CH₃-CH₂-CH₂-CH₂-N), 1.38 (24H, st, $J_{\text{HH}}=7.35$ Hz, CH₃-CH₂-CH₂-CH₂-N), 1.62 (24H, qn, $J_{\text{HH}}=7.52$ Hz, 24H, CH₂-CH₂-N), 3.08-3.15 (24H, m, CH₂-N), 5.35 (0.40H, dd, $J_{\text{PH}}=15.6$, $J_{\text{HH}}=11.0$, H₂C=CH), 5.95 (0.36H, dd, $J_{\text{PH}}=15.6$, $J_{\text{HH}}=9.55$ Hz, H₂C=CH), 6.74-6.88

(0.35H, m, $\text{H}_2\text{C}=\text{CH}$), 7.55-7.96 (8H, m, C_6H_4); δ_{P} (121 MHz, CD_3CN , H_3PO_4) 15.41 ppm; m/z (Maldi-TOF) 4476 [$M^+ + 4\text{NBu}_4 + \text{H}_2\text{CCH}$], 4230 [$M^+ + 3\text{NBu}_4 + \text{H}_2\text{CCH}$], 4078 [$M^+ + 3\text{NBu}_4 - \text{C}_8\text{H}_7\text{O}$], 3844 [$M^+ + 2\text{NBu}_4 - \text{C}_8\text{H}_7$], 3794 [$M^+ + 2\text{NBu}_4 - \text{C}_8\text{H}_7\text{PO}$], 3552 [$M^+ + \text{NBu}_4 - \text{C}_8\text{H}_7\text{PO}$], where $M^+ = (\text{NBu}_4)_3\text{H}[\gamma\text{-SiW}_{10}\text{O}_{36}(\text{H}_2\text{CCHC}_6\text{H}_4\text{PO})_2]^+$.

7.11. Co-polymerization of $(\text{NBu}_4)_3\text{H}[\text{SiW}_{10}\text{O}_{36}(\text{H}_2\text{C}=\text{CHC}_6\text{H}_4\text{PO})_2]$

$(\text{NBu}_4)_3\text{H}[\text{SiW}_{10}\text{O}_{36}(\text{CH}_2\text{CHC}_6\text{H}_4\text{PO})_2]$ (0.15 g, 0.04 mmol) was dissolved in 1,2-dichloroethane (2 mL) and filtered, initiator AIBN (4 mg) was added followed by the co-monomer (styrene, acrylic acid, ethyl acrylate, acrylamide or methyl methacrylate). The solution was degassed with N_2 , placed in a sealed tube and heated at 80°C for 24 hours. The co-polymer was obtained as a solid which was removed and dried.

Example of co-polymer $(\text{NBu}_4)_3\text{H}[\gamma\text{-SiW}_{10}\text{O}_{36}(\text{H}_2\text{C}=\text{CHC}_6\text{H}_4\text{PO})_2]:\text{H}_2\text{C}=\text{CHCONH}_2$ (1:10). Yield (0.105 g, 58.42 %). (found: C, 24.6; H, 3.8; N, 3.0. Calc for $\text{C}_{94}\text{H}_{173}\text{N}_{13}\text{O}_{48}\text{P}_2\text{SiW}_{10}$ (1:10): C, 26.9; H, 4.1; N, 4.3; Calc. for $\text{C}_{79}\text{H}_{148}\text{N}_8\text{O}_{43}\text{P}_2\text{SiW}_{10}$ (1:5): C, 24.8; H, 3.8; N, 2.9 %); $\lambda_{\text{max}}(\text{CH}_3\text{CN})$ (ϵ) 258 nm ($10500 \text{ mol}^{-1}\text{dm}^3\text{cm}^{-1}$); $\nu_{\text{max}}(\text{KBr disc})$ 2962, 2873 (C-H), 1670 (C=O), 1482, 1135, 1055 (P-O), 1006, 973, 942, 911, 886, 837, 754 cm^{-1} ; δ_{H} (300 MHz; CD_3CN ; Me_4Si) 0.98 (36H, t, $J_{\text{HH}}=7.35$, $\text{CH}_3\text{-CH}_2\text{-CH}_2\text{-CH}_2\text{-N}$), 1.38 (24H, st, $J_{\text{HH}}=7.35$, $\text{CH}_3\text{-CH}_2\text{-CH}_2\text{-CH}_2\text{-N}$), 1.62 (24H, qn, $J_{\text{HH}}=7.52$, $\text{CH}_2\text{-CH}_2\text{-N}$), 3.08-3.15 (24H, m, $\text{CH}_2\text{-N}$), 5.35 (0.37H, dd, $J_{\text{PH}}=15.6$, $J_{\text{HH}}=11.0$, $\text{H}_2\text{C}=\text{CH}$), 5.95 (0.19H, dd, $J_{\text{PH}}=15.6$, $J_{\text{HH}}=9.55$ Hz, $\text{H}_2\text{C}=\text{CH}$), 6.74-6.88 (0.15H, m, $\text{H}_2\text{C}=\text{CH}$), 7.55-7.96 ppm (8H, m, C_6H_4); m/z (Maldi-TOF) 4177 [$M^+ + 2\text{NBu}_4 - \text{C}_8\text{H}_7 + aa$], 4119 [$M^+ + 9aa$], 4082 [$M^+ + 2\text{NBu}_4 - \text{C}_8\text{H}_7\text{O}$] or [$M^+ + 8aa + 2\text{Na}$], 3968 [$M^+ + \text{NBu}_4 - \text{C}_8\text{H}_7 + 5aa$] or [$M^+ + 7aa$], 3744 [$M^+ + \text{NBu}_4 + \text{Na}$] or [$M^+ + 4aa$], 3535 [$M^+ + aa$], where $M^+ = (\text{NBu}_4)_3\text{H}[\gamma\text{-SiW}_{10}\text{O}_{36}(\text{H}_2\text{CCHC}_6\text{H}_4\text{PO})_2]^+$ and $aa = \text{H}_2\text{CCHCONH}_2$.

7.12. Polymerization of $(\text{NBu}_4)_3\text{Na}[\text{SiW}_9\text{O}_{34}(\text{RPO})_3]$

Following a similar procedure to in section 7.10, but using $(\text{NBu}_4)_3\text{Na}[\text{SiW}_9\text{O}_{34}(\text{RPO})_3]$ ($\text{R} = \text{H}_2\text{C}=\text{CH}$, $\text{H}_2\text{C}=\text{CHCH}_2$ or $\text{H}_2\text{C}=\text{CHC}_6\text{H}_4$) (0.15 g, 0.04 mmol).

Example of polymer for $(\text{NBu}_4)_3\text{Na}[\text{SiW}_9\text{O}_{34}(\text{H}_2\text{CCHC}_6\text{H}_4\text{PO})_3]$ (16 hours). Yield (0.12 g, 80.0 %). $\lambda_{\text{max}}(\text{CH}_3\text{CN})$ (ϵ) 261 nm ($27000 \text{ mol}^{-1}\text{dm}^3\text{cm}^{-1}$); $\nu_{\text{max}}(\text{KBr disc})$ 2963.4, 2874.9 (C-H), 1483.6, 1206.0, 1132.7, 1025.5 (P-O), 1000.4, 957.3, 924.1, 905.6, 835.9, 733.6 cm^{-1} ; δ_{H} (300 MHz; CD_3CN ; Me_4Si) 0.94 (36H, t, $J_{\text{HH}}=7.35$, $\text{CH}_3\text{-CH}_2\text{-CH}_2\text{-CH}_2\text{-N}$), 1.45 (24H, st, $J_{\text{HH}}=7.35$, $\text{CH}_3\text{-CH}_2\text{-CH}_2\text{-CH}_2\text{-N}$), 1.58 (24H, qn, $J_{\text{HH}}=7.52$, 24H, $\text{CH}_2\text{-CH}_2\text{-N}$), 2.97-3.18 (24H, m, $\text{CH}_2\text{-N}$), 5.35 (0.5H, d, $\text{H}_2\text{C}=\text{CH}$), 5.88 (0.5H, d, $\text{H}_2\text{C}=\text{CH}$), 6.80 (0.6H, dd, $\text{H}_2\text{C}=\text{CH}$), 7.42-7.88 (12H, m, C_6H_4); δ_{P} (121 MHz; CD_3CN ; H_3PO_4) 13.5 ppm; m/z (Maldi-TOF) 3792 ($M^+ + 2\text{NBu}_4\text{-H}_2\text{CCHC}_6\text{H}_4$), 7242 [$M^+ + 4\text{NBu}_4\text{-H}_2\text{CCH}$], where $M^+ = (\text{NBu}_4)_3[\text{SiW}_9\text{O}_{34}(\text{H}_2\text{CCHC}_6\text{H}_4\text{PO})_3]^+$.

7.13. Co-polymerisation of $(\text{NBu}_4)_3\text{Na}[\text{SiW}_9\text{O}_{34}(\text{H}_2\text{C}=\text{CHC}_6\text{H}_4\text{PO})_3]$

Was prepared following a similar procedure to in section 7.11, but using $(\text{NBu}_4)_3\text{Na}[\text{SiW}_9\text{O}_{34}(\text{H}_2\text{C}=\text{CHC}_6\text{H}_4\text{PO})_3]$ (0.15 g, 0.04 mmol).

7.14. Reaction with amines

7.14.1. Reaction of $(\text{NBu}_4)_3\text{H}[\text{SiW}_{10}\text{O}_{36}(\text{HOOCCH}_2\text{PO})_2]$ with benzylamine

(Compound 38)

$(\text{NBu}_4)_3\text{H}[\text{SiW}_{10}\text{O}_{36}(\text{HOOCCH}_2\text{PO})_2]$ (0.342 g, 0.1 mmol) was dissolved in dry acetonitrile (10 mL), benzylamine (0.022 mL, 0.2 mmol) was added (along with a drying agent (MgSO_4) in some cases) and the resulting solution stirred overnight at room temperature. The solution was filtered

and evaporated *in vacuo*, the solid was washed with water (20 mL), diethyl ether (10 mL) and dried, the crude product ((NBu₄)₃(C₆H₅CH₂NH₃)₃[SiW₁₀O₃₆(HOOCCH₂PO)]) was recrystallised by diffusion of diethyl ether into an acetonitrile solution of product. Yield (0.24 g, 64.7 %). ν_{\max} (KBr disc) 3446.2 (O-H), 2960.8 (C-H), 2873.0 (C-H), 1718 (C=O), 1484.1, 1150.8, 962.8, 900, 871.9, 830.2, 750.0 cm⁻¹; δ_{H} (300 MHz; DMSO-d₆; Me₄Si) 0.95 (36H, t, J_{HH}=7.35, **CH**₃-CH₂-CH₂-CH₂-N), 1.34 (24H, st, J_{HH}=7.35, CH₃-**CH**₂-CH₂-CH₂-N), 1.58 (24H, qn, J_{HH}=7.52 Hz, **CH**₂-CH₂-N), 2.58 (2H, d, J_{PH}=21.7, **CH**₂-COOH), 3.06-3.25 (24H, m, **CH**₂-N), 4.01 (6H, s, **CH**₂-NH₃⁺), 7.27-7.52 (15H, m, C₆H₅); δ_{P} (121 MHz, DMSO-d₆, H₃PO₄) 20.0 ppm; *m/z* (Maldi-TOF): 3486 [*M*⁺-C₆H₅CH₂NH₃], 3638 [*M*⁺+C₆H₅CH₂NH₃-HOOCCH₂O], 3716 [*M*⁺+C₆H₅CH₂NH₃], 3843 [*M*⁺+NBu₄], 4084 [*M*⁺+2NBu₄], where *M*⁺ = (NBu₄)₃(C₆H₅CH₂NH₃)₃[SiW₁₀O₃₆(HOOCCH₂PO)]⁺.

7.14.2. Reaction of (NBu₄)₃H[SiW₁₀O₃₆(HOOC(CH₂)₂PO)₂] with benzylamine

(Compound 39)

Was prepared following a similar procedure to in section 7.14.1, but using (NBu₄)₃H[SiW₁₀O₃₆(HOOC(CH₂)₂PO)₂] (0.345 g, 0.1 mmol) to give (NBu₄)₃(C₆H₅CH₂NH₃)₃[SiW₁₀O₃₆(HOOC(CH₂)₂PO)]. Yield (0.18 g, 48.2 %). ν_{\max} (KBr disc) 3446.8 (O-H), 2960 (C-H), 2875 (C-H), 1735 (C=O), 1482.8, 1150, 949.7, 900, 869.8, 831.8, 749.2 cm⁻¹; δ_{H} (300 MHz; DMSO-d₆; Me₄Si) 0.92 (36H, t, J_{HH}=7.35, **CH**₃-CH₂-CH₂-CH₂-N), 1.32 (24H, st, J_{HH}=7.35, CH₃-**CH**₂-CH₂-CH₂-N), 1.58 (26H, m, **CH**₂-CH₂-N, **CH**₂-PO), 2.28-2.42 (2H, m, **CH**₂-COOH), 3.08-3.25 (24H, m, **CH**₂-N), 4.06 (6H, s, CH₂-NH₃⁺), 7.22-7.52 (15H, m, C₆H₅); δ_{P} (121 MHz, CD₃CN, H₃PO₄) 28.6 ppm; *m/z* (Maldi-TOF): 3407 [*M*⁺-2C₆H₅CH₂NH₃], 3498 [*M*⁺-

$3\text{C}_6\text{H}_5\text{CH}_2\text{NH}_3\text{-HOOC}^+ \text{NBu}_4]$, 3648 $[M^+ - 2\text{C}_6\text{H}_5\text{CH}_2\text{NH}_3 + \text{NBu}_4]$, where $M^+ = (\text{NBu}_4)_3(\text{C}_6\text{H}_5\text{CH}_2\text{NH}_3)_3[\text{SiW}_{10}\text{O}_{36}(\text{HOOCCH}_2\text{CH}_2\text{PO})]^+$.

7.14.2.1. Crystals of $(\text{NBu}_4)_4(\text{C}_6\text{H}_5\text{CH}_2\text{NH}_3)_7\text{Mg}[\text{SiW}_{10}\text{O}_{36}(\text{HOOC}(\text{CH}_2)_2\text{PO})]_2$

(Structure 21)

Crystals suitable for Single Crystal XRD were obtained by slow diffusion of diethyl ether into an acetonitrile solution containing the crude product obtained when MgSO_4 was added as a drying agent. Data were collected on station 16.2smx at the SRS Synchrotron source, Daresbury ($\lambda = 0.79720 \text{ \AA}$). The structure was solved with all atoms anisotropic except the carbons and the four oxygen atoms on the carboxylic acid groups. Crystal Data. $\text{C}_{119}\text{H}_{217}\text{N}_{11}\text{O}_{78}\text{P}_2\text{Si}_2\text{W}_{20}$, $M = 6869.5$, Monoclinic, $a = 45.683(50)$, $b = 28.520(31)$, $c = 31.448(34) \text{ \AA}$, $\beta = 108.9(1)^\circ$, $U = 38764(7) \text{ \AA}^3$, $T = 150 \text{ K}$, space group $C 2/c$ (no. 15), $Z = 8$, 94591 reflections measured, 22413 unique ($R_{\text{int}} = 0.065$). The Final $R1(\text{obs. data}) = 0.056$, $R1(\text{all data}) = 0.093$.

7.14.3. Reaction of $(\text{NBu}_4)_3\text{H}[\text{SiW}_{10}\text{O}_{36}(\text{H}_3\text{CCOC}_6\text{H}_4\text{PO})_2]$ with amines (Compound 40)

$(\text{NBu}_4)_3\text{H}[\text{SiW}_{10}\text{O}_{36}(\text{H}_3\text{CCOC}_6\text{H}_4\text{PO})_2]$ (0.90 g, 0.26 mmol), was dissolved in acetonitrile (50 mL) and RNH_2 ($R = \text{C}_6\text{H}_5\text{CH}_2$ or C_4H_9) (10 equiv) added, and the resulting solution was stirred overnight. Diethyl ether was added to the solution to give the product as an off-white precipitate which was removed by filtration. When $R = \text{C}_6\text{H}_5\text{CH}_2$, the product is $(\text{NBu}_4)_3(\text{C}_6\text{H}_5\text{CH}_2\text{NH}_3)_3[\text{SiW}_{10}\text{O}_{36}(\text{H}_3\text{CCOC}_6\text{H}_4\text{PO})]$ Yield (0.94 g, 98.8 %). (found: C, 31.5; H, 4.2; N, 3.3. Calc for $\text{C}_{77}\text{H}_{145}\text{N}_6\text{O}_{48}\text{PSiW}_{10}$: C, 29.2; H, 4.0; N, 2.3); $\nu_{\text{max}}(\text{KBr disc})$ 2961.0 (C-H), 2873.2 (C-H), 1676.8 (C=O), 1484.1 (P-C), 1130.3, 950.0, 900, 872.2, 830.8, 749.2, 699.4 cm^{-1} ; δ_{H} (300 MHz;

CD₃CN; Me₄Si) 0.97 (36H, t, $J_{\text{HH}}=7.35$, **CH₃-CH₂-CH₂-CH₂-N**), 1.38 (24H, st, $J_{\text{HH}}=7.35$, **CH₃-CH₂-CH₂-CH₂-N**), 1.62 (24H, qn, $J_{\text{HH}}=7.52$, **CH₂-CH₂-N**), 2.47 (0.75H, s, **CH₃-C=O**), 2.60 (2.25H, s, **CH₃-C=O**), 3.02-3.18 (24H, m, **CH₂-N**), 4.05 (6H, s, CH₂-NH₃⁺), 7.20-7.54 (15H, m, C₆H₅), 7.58-8.00 (4H, m, C₆H₄); δ_{P} (121 MHz, DMSO-d₆, H₃PO₄) 17.8 ppm ($J_{\text{PH}}=12.8$, $J_{\text{PH}}=4.78$ Hz); m/z (Maldi-TOF): 3308 [$M^+ - \text{NBu}_4 - \text{C}_6\text{H}_5\text{CH}_2\text{NH}_3$], 3547 [$M^+ - \text{C}_6\text{H}_5\text{CH}_2\text{NH}_3$], 3771 [$M^+ + \text{C}_6\text{H}_5\text{CH}_2\text{NH}_3$], 3791 [$M^+ + \text{C}_6\text{H}_5\text{CH}_2\text{NH}_3 + \text{Na}$], 3840 [$M^+ + \text{NBu}_4 + \text{C}_6\text{H}_5\text{CH}_2\text{NH}_3$], where $M^+ = (\text{NBu}_4)_3(\text{C}_6\text{H}_5\text{CH}_2\text{NH}_3)_3[\text{SiW}_{10}\text{O}_{36}(\text{H}_3\text{CCOC}_6\text{H}_4\text{PO})]^+$.

7.14.4. Reaction of (NEt₄)₃H[SiW₁₀O₃₆(H₃CCOC₆H₄PO)₂] with benzylamine

(Compound 41)

Was prepared following a similar procedure to in section 7.14.1, but using (NEt₄)₃H[SiW₁₀O₃₆(H₃CCOC₆H₄PO)₂] (0.90 g, 0.28 mmol) and C₆H₅CH₂NH₃ (0.45 mL) to give (NEt₄)₃(C₆H₅CH₂NH₃)₃[SiW₁₀O₃₆(H₃CCOC₆H₄PO)], Yield (0.77 g, 82.7 %). (found: C, 21.9; H, 3.15; N, 2.8. Calc for C₅₃H₉₇N₆O₄₈PSiW₁₀: C, 19.1; H, 2.9; N, 2.5); ν_{max} (KBr disc) 2961.0 (C-H), 2873.2 (C-H), 1676.8 (C=O), 1484.1 (P-C), 1130.3, 950.0, 900, 872.2, 830.8, 749.2, 699.4 cm⁻¹; δ_{H} (300 MHz; CD₃CN; Me₄Si) 0.97 (36H, t, $J_{\text{HH}}=7.35$, **CH₃-CH₂-CH₂-CH₂-N**), 1.38 (24H, st, $J_{\text{HH}}=7.35$, **CH₃-CH₂-CH₂-CH₂-N**), 1.62 (24H, qn, $J_{\text{HH}}=7.52$, **CH₂-CH₂-N**), 2.47 (0.75H, s, **CH₃-C=O**), 2.60 (2.25H, s, **CH₃-C=O**), 3.02-3.18 (24H, m, **CH₂-N**), 4.05 (6H, s, CH₂-NH₃⁺), 7.20-7.54 (15H, m, C₆H₅), 7.58-8.00 (4H, m, C₆H₄); δ_{P} (121 MHz, DMSO-d₆, H₃PO₄) 17.8 ppm ($J_{\text{PH}}=12.8$, $J_{\text{PH}}=4.78$ Hz); m/z (Maldi-TOF): 3308 [$M^+ - \text{NBu}_4 - \text{C}_6\text{H}_5\text{CH}_2\text{NH}_3$], 3547 [$M^+ - \text{C}_6\text{H}_5\text{CH}_2\text{NH}_3$], 3771 [$M^+ + \text{C}_6\text{H}_5\text{CH}_2\text{NH}_3$], 3791 [$M^+ + \text{C}_6\text{H}_5\text{CH}_2\text{NH}_3 + \text{Na}$], 3840 [$M^+ + \text{NBu}_4 + \text{C}_6\text{H}_5\text{CH}_2\text{NH}_3$], where $M^+ = (\text{NBu}_4)_3(\text{C}_6\text{H}_5\text{CH}_2\text{NH}_3)_3[\text{SiW}_{10}\text{O}_{36}(\text{H}_3\text{CCOC}_6\text{H}_4\text{PO})]^+$. Crystals suitable for Single Crystal XRD were obtained by slow diffusion of diethyl ether into an

acetonitrile solution containing the crude product. Data were collected on a Bruker SMART 6000 diffractometer ($\lambda_{\text{Cu-K}\alpha} = 1.54178 \text{ \AA}$). Structure 22. $\text{C}_{54}\text{H}_{107}\text{N}_6\text{O}_{38}\text{PSiW}_{10}$, $M = 3504.2$, Monoclinic, $a = 60.300(2)$, $b = 14.641(5)$, $c = 25.846(9) \text{ \AA}$, $\beta = 108.051(16)$, $U = 21695(13) \text{ \AA}^3$, $T = 200 \text{ K}$, space group $C 2/c$ (no. 15), $Z = 8$, 51017 reflections measured, 11175 unique ($R_{\text{int}}=0.129$). The Final $R1(\text{obs. data}) = 0.076$, $R1(\text{all data}) = 0.155$. The structure was solved with the oxygen and tungsten atoms anisotropic.

7.14.5. Reaction of $(\text{NBu}_4)_3\text{H}[\text{SiW}_{10}\text{O}_{36}(\text{EtPO})_2]$ with benzylamine (Compound 42)

Was prepared following a similar procedure to in section 7.14.1, but using $(\text{NBu}_4)_3\text{H}[\text{SiW}_{10}\text{O}_{36}(\text{EtPO})_2]$ (0.90 g, 0.3 mmol) to give $(\text{NEt}_4)_3(\text{C}_6\text{H}_5\text{CH}_2\text{NH}_3)_3[\text{SiW}_{10}\text{O}_{36}(\text{EtPO})]$, Yield (0.92 g, 97.6 %). $\nu_{\text{max}}(\text{KBr disc})/\text{cm}^{-1}$ 2961.3 (C-H), 2873.6 (C-H), 1484.4, 1109.6, 1064.3, 948.5, 900, 870.8, 829.1, 749.5, 698.8; δ_{H} (300 MHz; CD_3CN ; Me_4Si) 0.97 (36H, t, $J_{\text{HH}}=7.35$, $\text{CH}_3\text{-CH}_2\text{-CH}_2\text{-CH}_2\text{-N}$), 1.06-1.20 (3H, m, $\text{CH}_3\text{-CH}_2\text{-PO}$), 1.36 (24H, st, $J_{\text{HH}}=7.35$, $\text{CH}_3\text{-CH}_2\text{-CH}_2\text{-CH}_2\text{-N}$), 1.62 (26H, m, $\text{CH}_2\text{-CH}_2\text{-N}$, $\text{CH}_2\text{-PO}$), 3.00-3.20 (24H, m, $\text{CH}_2\text{-N}$), 4.08 (6H, s, $\text{CH}_2\text{-NH}_3^+$), 7.16-7.58 (15H, m, C_6H_5); δ_{P} (121 MHz, CD_3CN , H_3PO_4) 34.5 ppm; m/z (Maldi-TOF): 3369 [$M^+ - 2\text{C}_6\text{H}_5\text{CH}_2\text{NH}_3 + \text{Na}$], 3480 [$M^+ - 3\text{C}_6\text{H}_5\text{CH}_2\text{NH}_3 + \text{NBu}_4$], 3609 [$M^+ - 2\text{C}_6\text{H}_5\text{CH}_2\text{NH}_3 + \text{NBu}_4 + \text{Na}$], 3685 [$M^+ - \text{C}_6\text{H}_5\text{CH}_2\text{NH}_3 + \text{NBu}_4$], 3843 [$M^+ - \text{C}_6\text{H}_5\text{CH}_2\text{NH}_3 + 2\text{NBu}_4$] where $M^+ = (\text{NBu}_4)_3(\text{C}_6\text{H}_5\text{CH}_2\text{NH}_3)_3[\text{SiW}_{10}\text{O}_{36}(\text{EtPO})]^+$.

7.14.6. Reaction of $(\text{NEt}_4)_3\text{H}[\text{SiW}_{10}\text{O}_{36}(\text{H}_2\text{C=CHPO})_2]$ with benzylamine (Compound 43)

Was prepared following a similar procedure to in section 7.14.1, but using $(\text{NEt}_4)_3\text{H}[\text{SiW}_{10}\text{O}_{36}(\text{H}_2\text{C=CHPO})_2]$ (0.60 g, 0.2 mmol) to give $((\text{NEt}_4)_3(\text{C}_6\text{H}_5\text{CH}_2\text{NH}_3)_3$

[SiW₁₀O₃₆(H₂C=CHPO)], Yield (0.64 g, 99.0 %). ν_{\max} (KBr disc)/cm⁻¹ 2982.5 (C-H), 1617 (C=C), 1483.0, 1173.3, 1130.7, 947.8, 870.4, 830, 753.6, 699.0; δ_{H} (300 MHz; CD₃CN; Me₄Si) 1.16-1.30 (36H, m, **CH**₃-CH₂-N), 3.15-3.30 (24H, m, **CH**₂-N), 3.98 (6H, s, **CH**₂-NH₃⁺), 5.65-6.08 (**C**₂**H**₃), 7.20-7.70 (15H, m, **C**₆**H**₅); δ_{P} (121 MHz, CD₃CN, H₃PO₄) 18.5 ppm; m/z (Maldi-TOF): 3027 [M^+ -NEt₄-H₂C=CHPO], 3157 [M^+ -H₂C=CHPO], 3288 [M^+ +NEt₄-H₂C=CHPO], where M^+ = (NEt₄)₃(C₆H₅CH₂NH₃)₃[SiW₁₀O₃₆(H₂C=CHPO)]⁺.

7.14.7. Reaction of (NEt₄)₃H[SiW₁₀O₃₆(H₂C=CHCH₂PO)₂] with benzylamine (Compound 44)

Was prepared following a similar procedure to in section 7.14.1, but using (NEt₄)₃H[SiW₁₀O₃₆(H₂C=CHCH₂PO)₂] (0.60 g, 0.18 mmol) to give (NEt₄)₃(C₆H₅CH₂NH₃)₃[SiW₁₀O₃₆(H₂C=CHCH₂PO)]. Yield (0.50 g, 85.6 %) (Found C 20.95; N 2.25; H 3.2. Calc. C 17.75; N 2.6; H 2.7). ν_{\max} (KBr disc) 2982.9 (C-H), 1636.2, 1600 (C=C), 1483.7, 1457.7, 1173.1 (P=O), 1133.0, 1002.3, 947.2, 870.6, 753.5 700.2 cm⁻¹; δ_{H} (300 MHz; CD₃CN; Me₄Si) 1.10-1.34 (36H, m, **CH**₃-CH₂-N), 2.35 (2H, dd, **CH**₂-P, J_{HH}=7.24, J_{HP}=23.17), 3.08-3.30 (m, 24H, **CH**₂-N), 4.00-4.22 (6H, m, C₆H₅**CH**₂NH₃), 4.98-5.17 (2H, m, **CH**₂=CH), 5.68-5.88 (1H, m, CH₂=**CH**), 7.20-7.60 (15H, m, **C**₆**H**₅CH₂NH₃); δ_{P} (121 MHz, CD₃CN, H₃PO₄) 28.3 ppm; m/z (Maldi-TOF) 2895.9 (M^+ -NEt₄-2C₆H₅CH₂NH₃), 3044 (M^+ -C₆H₅CH₂NH₃-C₃H₅PO), 3121 (M^+ -C₃H₅PO₃), 3173 (M^+ -C₃H₅PO+Na), 3304 (M^+ -C₃H₅PO+NEt₄+Na), where M^+ = ((NEt₄)₃(C₆H₅CH₂NH₃)₃[SiW₁₀O₃₆(H₂C=CHCH₂PO)]⁺.

7.14.8. Reaction of (NEt₄)₃H[SiW₁₀O₃₆(H₂C=CHCH₂PO)₂] with butylamine**(Compound 45)**

Was prepared following a similar procedure to in section 7.14.7, but using (NEt₄)₃H[SiW₁₀O₃₆(H₂C=CHCH₂PO)₂] (0.30 g, 0.1 mmol) and C₄H₉PO(OH)₂ (0.14 mL, 1.4 mmol) to give (NEt₄)₃(C₄H₉NH₃)₃[SiW₁₀O₃₆(H₂C=CHCH₂PO)]. Yield (0.25 g, 79.5 %). ν_{\max} (KBr disc) 2960.4 (C-H), 1600 (C=C), 1483.8, 1173.7, 1003.0, 950.4, 900, 873.2, 830, 754.1, 668.2 cm⁻¹; δ_{H} (300 MHz; DMSO-d₆; Me₄Si) 0.86-1.00 (6H, m, **CH**₃-CH₂-CH₂-CH₂-NH₃⁺), 1.06-1.28 (36H, m, **CH**₃-CH₂-N), 1.30-1.42 (4H, m, CH₃-**CH**₂-CH₂-CH₂-NH₃⁺), 1.48-1.68 (4H, m, **CH**₂-CH₂-NH₃⁺), 2.70-2.90 (2H, m, **CH**₂-PO), 3.08-3.40 (24H, m, **CH**₂-N), 4.98-5.12 (2H, m, **H**₂C=CH), 5.70-5.82 (1H, m, H₂C=**CH**); δ_{P} (121 MHz, DMF:DMSO-d₆, H₃PO₄) 26.1 ppm; m/z (Maldi-TOF) 3228 [M^+ -NBu₄], 3372 [M^+ -C₃H₅-C₄H₉NH₃], 3499 [M^+ +Na], 3579 [M^+ -C₄H₉NH₃+Na], 3608 [M^+ +C₄H₉NH₃+2Na], 3713 (M^+ +NBu₄), where M^+ = (NBu₄)₃(C₄H₉NH₃)₃[SiW₁₀O₃₆(H₂C=CHCH₂PO)]⁺.

7.14.9. Examples of reactions to give (NEt₄)₃H[SiW₁₀O₃₆(R¹PO)(R²PO)]**7.14.9.1. (NEt₄)₃H[SiW₁₀O₃₆(H₃CCOC₆H₄PO)(EtPO)] (Compound 46)**

(NEt₄)₃(C₆H₅CH₂NH₃)₃[SiW₁₀O₃₆(H₃CCOC₆H₄PO)] (0.20 g, 0.06 mmol), NEt₄Br (0.036 g, 0.17 mmol) and EtPO(OH)₂ (0.009 g, 0.08 mmol) were dissolved in acetonitrile (10 mL) and 12M HCl (0.02 mL) added dropwise. The resulting solution was refluxed overnight, before being filtered to remove a small amount of white solid and the solution evaporated in vacuo to give a pale greeny solid which was washed with water and air dried. Yield (0.105 g, 56.7 %). (found: C, 15.3; H, 2.5; N, 1.7. Calc. for C₃₄H₇₂N₃O₃₉P₂SiW₁₀: C, 13.3; H, 2.3; N, 1.4 %. Calc. for four cations C. 15.7; N 1.75; H 2.9); λ_{\max} (CH₃CN) (ϵ) 248.5 nm (53000 mol⁻¹dm³cm⁻¹); ν_{\max} (KBr disc)

2983.8 (C-H), 1685.1 (C=O), 1483.1 (P-C), 1172.8, 1136.1, 1002.2, 970.2, 910.2, 885.4, 836.5, 750.9, 631.5 cm^{-1} ; δ_{H} (300 MHz; DMSO- d_6 ; Me $_4$ Si) 0.90-1.06 (2H, m, **CH** $_3$ -CH $_2$ -PO), 1.06-1.22 (36H, m, **CH** $_3$ -CH $_2$ -N), 1.70-1.84 (3H, m, **CH** $_2$ -PO), 2.65 (3H, s, **CH** $_3$ -C=O), 3.06-3.30 (24H, m, **CH** $_2$ -N), 4.05 (0.5H, s, CH $_2$ -NH $_3^+$), 7.42-7.50 (1.5H, m, C $_6$ H $_5$), 7.65-8.20 (4H, m, C $_6$ H $_4$); δ_{P} (121 MHz, DMSO- d_6 , H $_3$ PO $_4$) 10.3 (H $_3$ CCOC $_6$ H $_4$ PO), 34.4 (EtPO) Hz; m/z (Maldi-TOF): 3075 [M^+], 3112 [M^+ +NBu $_4$ -EtPO-CH $_3$], 3204 [M^+ +2NBu $_4$], 3242 [M^+ +2NBu $_4$ -EtPO-CH $_3$], 3294 [M^+ +2NBu $_4$ -H $_3$ CCO], 3333 [M^+ +2NBu $_4$], 3423 [M^+ +3NBu $_4$ -H $_3$ CCO], where M^+ = (NBu $_4$) $_3$ H[SiW $_{10}$ O $_{36}$ (H $_3$ CCOC $_6$ H $_4$ PO)(EtPO)] $^+$.

7.14.9.2. (NBu $_4$) $_3$ H[SiW $_{10}$ O $_{36}$ (EtPO)(H $_2$ C=CHC $_6$ H $_4$ PO)] (Compound 47)

Following the same procedure as section 7.14.9.1, but using (NBu $_4$) $_3$ (C $_6$ H $_5$ CH $_2$ NH $_3$) $_3$ [SiW $_{10}$ O $_{36}$ (EtPO)] (0.65 g, 0.18 mmol), NBu $_4$ Br (0.16 g, 0.05 mmol) and H $_2$ C=CHC $_6$ H $_4$ PO(OH) $_2$ (0.05 g, 0.27 mmol). Yield (0.46 g, 75.2 %). λ_{max} (CH $_3$ CN) (ϵ) 253 nm (45000 mol $^{-1}$ dm 3 cm $^{-1}$); ν_{max} (KBr disc) 2962.3 (C-H), 2874.0 (C-H), 1636.2 (C=C), 1483.1, 1136.2, 1066.8, 1007.4, 973.1, 942.1, 911.9, 885.7, 837.6, 800.1, 757.7, 652.0 cm^{-1} ; δ_{H} (300 MHz; CD $_3$ CN; Me $_4$ Si) 0.75-0.90 (2H, m, CH $_3$ -CH $_2$ -PO), 0.95-1.15 (36H, m, **CH** $_3$ -CH $_2$ -CH $_2$ -CH $_2$ -N), 1.28-1.50 (24H, m, CH $_3$ -**CH** $_2$ -CH $_2$ -CH $_2$ -N), 1.50-1.84 (27H, m, **CH** $_2$ -CH $_2$ -N, CH $_2$ -PO), 2.97-3.22 (24H, m, **CH** $_2$ -N), 5.35 (1H, d, **H** $_2$ C=CH), 5.90 (1H, m, **H** $_2$ C=CH), 6.74-6.88 (1H, m, H $_2$ C=**CH**), 7.45-8.03 (4H, m, C $_6$ H $_4$); δ_{P} (121 MHz, CD $_3$ CN, H $_3$ PO $_4$) 13.5 (H $_2$ C=CHC $_6$ H $_4$ PO), 30.6 (EtPO) Hz; m/z (Maldi-TOF): 3565 [M^+ +NBu $_4$ -EtPO], 3641 [M^+ +NBu $_4$], 3883 [M^+ +2NBu $_4$], 4087, where M^+ = (NBu $_4$) $_3$ H[SiW $_{10}$ O $_{36}$ (EtPO)(H $_2$ C=CHC $_6$ H $_4$ PO)] $^+$.

7.14.9.3. (NEt₄)₃H[SiW₁₀O₃₆(H₂C=CHPO)(H₂C=CHCH₂PO)] (Compound 48)

Following the same procedure as in section 7.14.9.1, but using (NEt₄)₃(C₆H₅CH₂NH₃)₃[SiW₁₀O₃₆(H₂C=CHPO)] (0.20 g, 0.06 mmol), NEt₄Br (0.036 g, 0.2 mmol) and CH₂=CHCH₂PO(OH)₂ (0.0098 g, 0.08 mmol) to give a pale greeny solid. Yield (0.15 g, 80.2 %). ν_{\max} (KBr disc) 2985.7 (C-H), 1600 (C=C), 1483.1, 1458.2, 1172.5 (P=O), 1068, 1002.4 (P-O), 973.5, 942.9, 911.9, 884.5, 834.7, 753.8 cm⁻¹; δ_{H} (300 MHz; CD₃CN; Me₄Si) 1.12-1.35 (36H, m, **CH**₃-CH₂-N), 2.62 (2H, dd, **CH**₂-PO), 3.08-3.28 (24H, m, **CH**₂-N), 5.13-5.30 (2H, m, **H**₂C=CHCH₂), 5.82-6.02 (1H, m, H₂C=**CH**CH₂), 6.16-6.32 (3H, m, **CH**₂=CHPO), 7.32-7.50 (m, **C**₆**H**₅); δ_{P} (121 MHz, CD₃CN, H₃PO₄) 16.8 (H₂C=CHPO), 24.3 ppm (H₂C=CHCH₂PO); m/z (Maldi-TOF) 2998 [M^+], 3126 [M^+ +NEt₄], 3255 [M^+ +2NEt₄], 3393.9 [M^+ +3NEt₄], 3524.1 [M^+ +4NEt₄], where M^+ = (NEt₄)₃H[SiW₁₀O₃₆(H₂C=CHPO)(H₂C=CHCH₂PO)]. Crystals suitable for Single Crystal XRD were obtained by slow diffusion of diethyl ether into an acetonitrile solution containing the crude product. Data were collected on a Bruker SMART 6000 diffractometer ($\lambda_{\text{Cu-K}\alpha}$ = 1.54178 Å). The structure was solved with all atoms in the cluster anisotropic. Structure 24. C₃₁H₇₁N₅O₃₈P₂SiW₁₀, M = 3050.46, Orthorhombic, a = 10.689(15), b = 16.033(19), c = 19.375(2) Å, U = 3320.4(6) Å³, T = 200 K, space group P 2₁ n n (no. 34), Z = 2, 19169 reflections measured, 4997 unique (R_{int} =0.090). The Final R_1 (obs. data) = 0.062, R_1 (all data) = 0.075.

7.14.9.4. (NEt₄)₃H[SiW₁₀O₃₆(H₂C=CHCH₂PO)(HOOCCH₂CH₂PO)] (Compound 49)

Following the same procedure as in section 7.14.9.1, but using (NEt₄)₃(C₆H₅CH₂NH₃)₃[SiW₁₀O₃₆(H₂C=CHCH₂PO)] (0.30 g, 0.1 mmol), NEt₄Br (0.065 g, 0.4 mmol) and HOOCCH₂CH₂PO(OH)₂ (0.034 g, 0.22 mmol) to give a pale green solid. Yield (0.160 g, 52.6 %) (Found C 12.95; N 0.8; H 2.2. Calc C 11.85; N 1.4; H 2.3). ν_{\max} (KBr disc) 2984.8 (C-H), 1734.2

(C=O), 1600 (C=C), 1483.3, 1458.0, 1172.7 (P=O), 1068 (P-O), 1002.3 (P-O), 970.6, 944.4, 911.5, 885.6, 835.5, 750.2 cm^{-1} ; δ_{H} (300 MHz; CD_3CN ; Me_4Si) 1.10-1.35 (36H, m, $\text{CH}_3\text{-CH}_2\text{-N}$), 2.01-2.20 (2H, m, $\text{CH}_2\text{-CH}_2\text{-PO}$), 2.48-2.70 (4H, m, HOOCCH_2 , $\text{H}_2\text{C=CHCH}_2\text{PO}$), 3.10-3.28 (24H, m, $\text{CH}_2\text{-N}$), 5.12-5.28 (2H, m, $\text{H}_2\text{C=CH}$), 5.78-6.00 (1H, m, $\text{H}_2\text{C=CH}$), 7.32-7.50 (m, C_6H_5); δ_{P} (121 MHz, CD_3CN , H_3PO_4) 24.55 ($\text{H}_2\text{C=CHCH}_2\text{PO}$), 29.04 ppm ($\text{HOOCCH}_2\text{CH}_2\text{PO}$); m/z (Maldi-TOF) 3039.5 [M^+], 3137.0, 3168.9 [$M^+ + \text{NEt}_4$], 3205.6 [$M^+ - \text{H}_2\text{C=CHCH}_2\text{PO} + 2\text{NEt}_4$], 3225.6 [$M^+ - \text{HOOCCH}_2\text{CH}_2 + 2\text{NEt}_4$], 3247.0 [$M^+ - \text{HOOCCH}_2 + 2\text{NEt}_4$], 3300.4 [$M^+ + 2\text{NEt}_4$], where $M^+ = (\text{NEt}_4)_3\text{H}[\text{SiW}_{10}\text{O}_{36}(\text{H}_2\text{C=CHCH}_2\text{PO})(\text{HOOCCH}_2\text{CH}_2\text{PO})]^+$. Crystals suitable for Single Crystal XRD were obtained by diffusion of diethyl ether into an acetonitrile solution containing the product. Data were collected on station 9.8 at the SRS Synchrotron source, Daresbury ($\lambda = 0.67030 \text{ \AA}$). Structure 23. $\text{C}_{56}\text{H}_{123}\text{N}_5\text{O}_{81}\text{P}_4\text{Si}_2\text{W}_{20}$, $M = 5995.63$, Triclinic, $a = 24.735(5)$, $b = 10.8297(19)$, $c = 14.707(3) \text{ \AA}$, $\beta = 107.419(3)^\circ$, $U = 3758.9(12) \text{ \AA}^3$, $T = 150 \text{ K}$, space group $P -1$ (no. 2), $Z = 1$, 15983 reflections measured, 14663 unique ($R_{\text{int}} = 0.050$). The Final $R1(\text{obs. data}) = 0.058$, $R1(\text{all data}) = 0.070$. The structure was solved with all atoms isotopic except most of the tungsten atoms (W3 and W8 were isotopic).

7.14.10. Polymerisation of $(\text{NBu}_4)_3\text{H}[\text{SiW}_{10}\text{O}_{36}(\text{EtPO})(\text{H}_2\text{C=CHC}_6\text{H}_4\text{PO})]$

Was prepared following a similar procedure to in section 7.10, but using $(\text{NBu}_4)_3\text{H}[\text{SiW}_{10}\text{O}_{36}(\text{EtPO})(\text{H}_2\text{C=CHC}_6\text{H}_4\text{PO})]$ (0.07 g, 0.02 mmol), 1,2-dichloroethane (1.5 mL) and AIBN (2 mg).

7.14.11. Co-polymerisation of $(\text{NBu}_4)_3\text{H}[\text{SiW}_{10}\text{O}_{36}(\text{EtPO})(\text{H}_2\text{C}=\text{CHC}_6\text{H}_4\text{PO})]$

Following a similar procedure to in section 7.11, but using $(\text{NBu}_4)_3\text{H}[\text{SiW}_{10}\text{O}_{36}(\text{EtPO})(\text{H}_2\text{C}=\text{CHC}_6\text{H}_4\text{PO})]$ (0.07 g, 0.02 mmol) and $\text{H}_2\text{C}=\text{CHCOOC}_2\text{H}_5$ in varying ratios.

7.14.12. Reaction of $(\text{NBu}_4)_3\text{H}[\text{SiW}_9\text{O}_{34}(\text{H}_2\text{C}=\text{CHCH}_2\text{PO})_3]$ with benzylamine (Compound 50)

Was prepared following a similar procedure to in section 7.14.1, but using $(\text{NBu}_4)_3\text{H}[\text{SiW}_9\text{O}_{34}(\text{H}_2\text{C}=\text{CHCH}_2\text{PO})_2]$ (0.90 g, 0.3 mmol), Yield (0.88 g, 84.9 %) to give $(\text{NBu}_4)_3(\text{C}_6\text{H}_5\text{CH}_2\text{NH}_3)_3[\text{SiW}_9\text{O}_{34}(\text{H}_2\text{C}=\text{CHCH}_2\text{PO})_2]$. $\nu_{\text{max}}(\text{KBr disc})$ 2960.8 (C-H), 2873.4 (C-H), 1600 (C=C), 1484.2, 1147.8, 979.5, 945.1, 891.6, 837.9, 729.6 cm^{-1} ; δ_{H} (300 MHz; CD_3CN ; Me_4Si) 0.97 (36H, t, $\text{J}_{\text{HH}}=7.35$, $\text{CH}_3\text{-CH}_2\text{-CH}_2\text{-CH}_2\text{-N}$), 1.37 (24H, st, $\text{J}_{\text{HH}}=7.35$, $\text{CH}_3\text{-CH}_2\text{-CH}_2\text{-CH}_2\text{-N}$), 1.62 (24H, m, $\text{CH}_3\text{-CH}_2\text{-CH}_2\text{-CH}_2\text{-N}$), 2.18 (4H, dd, $\text{CH}_2\text{-PO}$), 3.00-3.24 (24H, m, $\text{CH}_2\text{-N}$), 4.01 (6H, s, $\text{CH}_2\text{-NH}_3^+$), 4.96-5.10 (4H, m, $\text{H}_2\text{C}=\text{CH}$), 5.65-5.86 (2H, m, $\text{H}_2\text{C}=\text{CH}$), 7.20-7.62 (15H, m, C_6H_5); δ_{P} (121 MHz, CD_3CN , H_3PO_4) 24.2; δ_{Si} (79 MHz; DMF:DMSO-d_6 9:1; Me_4Si) -84.6 Hz; m/z (Maldi-TOF): 3250 $[M^+-2\text{C}_6\text{H}_5\text{CH}_2\text{NH}_3]$, 3340 $[M^+-\text{C}_6\text{H}_5\text{CH}_2\text{NH}_3]$, 3492 $[M^+-2\text{C}_6\text{H}_5\text{CH}_2\text{NH}_3+\text{NBu}_4]$, 3515 $[M^+-2\text{C}_6\text{H}_5\text{CH}_2\text{NH}_3+\text{NBu}_4+\text{Na}]$, 3550 $[M^++\text{C}_6\text{H}_5\text{CH}_2\text{NH}_3]$, where $M^+ = (\text{NBu}_4)_3(\text{C}_6\text{H}_5\text{CH}_2\text{NH}_3)_3[\text{SiW}_9\text{O}_{34}(\text{H}_2\text{C}=\text{CHCH}_2\text{PO})_2]^+$.

7.14.13. $(\text{NBu}_4)_3\text{H}[\text{SiW}_9\text{O}_{34}(\text{H}_2\text{C}=\text{CHCH}_2\text{PO})_2(\text{C}_6\text{H}_5\text{PO})]$ (Compound 51)

Was prepared following a similar procedure to in section 7.14.9.1, but using $(\text{NBu}_4)_3(\text{C}_6\text{H}_5\text{CH}_2\text{NH}_3)_3[\text{SiW}_9\text{O}_{34}(\text{H}_2\text{C}=\text{CHCH}_2\text{PO})_2]$ (0.20 g, 0.06 mmol) and $\text{C}_6\text{H}_5\text{PO}(\text{OH})_2$ (0.04 g, 0.2 mmol). Yield (0.26 g, 37.5 %). $\lambda_{\text{max}}(\text{CD}_3\text{CN})$ (ϵ) 263.5 nm ($37000 \text{ dm}^3 \text{ mol}^{-1} \text{ cm}^{-1}$); $\nu_{\text{max}}(\text{KBr disc})$ 2962.6 (C-H), 2873.9 (C-H), 1600 (C=C), 1483.4, 1138.3 (P-O), 1009.6 (P-O),

957.1, 923.8, 903.4, 839.6, 731.7 cm^{-1} ; δ_{H} (300 MHz; CD_3CN ; Me_4Si) 0.98 (36H, t, $J_{\text{HH}}=7.35$, $\text{CH}_3\text{-CH}_2\text{-CH}_2\text{-CH}_2\text{-N}$), 1.38 (24H, st, $J_{\text{HH}}=7.35$, $\text{CH}_3\text{-CH}_2\text{-CH}_2\text{-CH}_2\text{-N}$), 1.62 (24H, m, $\text{CH}_2\text{-CH}_2\text{-N}$), 2.58 (4H, dd, $\text{CH}_2\text{-PO}$), 3.02-3.18 (24H, m, $\text{CH}_2\text{-N}$), 5.12-5.25 (4H, m, $\text{H}_2\text{C=CH}$), 5.78-5.94 (2H, m, $\text{H}_2\text{C=CH}$), 7.44-7.58 (C_6H_5), 7.78-7.93 (4H, m, C_6H_4); δ_{P} (121 MHz, CD_3CN , H_3PO_4) 16.1, (Ph-P=O), 24.5 ($\text{CH}_2\text{-PO}$); m/z (Maldi-TOF): 3256 [M^+], 3291 [$M^+\text{-C}_6\text{H}_5\text{PO-H}_5\text{C}_3\text{PO}$], 3329 [$M^+\text{-C}_6\text{H}_5\text{PO-H}_5\text{C}_3$], 3351 [$M^+\text{-C}_6\text{H}_5\text{PO-H}_5\text{C}_2$], 3518 [$M^+\text{+NBu}_4$], 3533 [$M^+\text{+2NBu}_4\text{-C}_6\text{H}_5\text{PO-H}_5\text{C}_3\text{PO}$], 3570 [$M^+\text{+2NBu}_4\text{-C}_6\text{H}_5\text{PO-H}_5\text{C}_3$], 3590 [$M^+\text{+2NBu}_4\text{-C}_6\text{H}_5\text{PO-H}_5\text{C}_2$], 3606 [$M^+\text{+2NBu}_4\text{-C}_6\text{H}_5\text{PO}$], 3630 [$M^+\text{+2NBu}_4\text{-C}_6\text{H}_5\text{O}$], where $M^+ = (\text{NBu}_4)_3[\text{SiW}_9\text{O}_{34}(\text{H}_2\text{C=CHCH}_2\text{PO})_2(\text{H}_5\text{C}_6\text{PO})]^+$. Crystals suitable for Single Crystal XRD were obtained by slow diffusion of diethyl ether into a DMF solution containing the crude product. Data were collected on a Bruker SMART 6000 diffractometer ($\lambda_{\text{Cu-K}\alpha} = 1.54178 \text{ \AA}$). Structure 25. $\text{C}_{63}\text{H}_{123}\text{N}_3\text{O}_{37}\text{P}_3\text{SiW}_9$, $M = 3290.29$, Trigonal, $a = 22.139(2)$, $b = 22.139(2)$, $c = 18.889(3) \text{ \AA}$, $U = 8017.6(17) \text{ \AA}^3$, $T = 293 \text{ K}$, space group $R\bar{3}m$ (no. 160), $Z = 3$, 13853 reflections measured, 2390 unique ($R_{\text{int}}=0.079$). The Final $R_1(\text{obs. data}) = 0.048$, $R_1(\text{all data}) = 0.075$. The structure was solved with the main polyoxotungstate structure anisotropic.

7.14.14. $(\text{NBu}_4)_3\text{H}[\text{SiW}_9\text{O}_{34}(\text{H}_2\text{C=CHCH}_2\text{PO})_2(\text{HOOCCH}_2\text{PO})]$ (Compound 52)

Was prepared following a similar procedure to in section 7.14.13, but using $\text{HOOCCH}_2\text{PO}(\text{OH})_2$ (0.026 g, 0.17 mmol), Yield (0.23 g, 41.8 %). $\lambda_{\text{max}}(\text{CD}_3\text{CN})$ (ϵ) 265 nm ($29500 \text{ dm}^3 \text{ mol}^{-1} \text{ cm}^{-1}$); $\nu_{\text{max}}(\text{KBr disc})$ 2962.6 (C-H), 2874.7 (C-H), 1734.3 (C=O), 1600 (C=C), 1483.7, 1149.8 (P-O), 1106.1 (P-O), 1012.4 (P-O), 961.1, 927.4, 893.3, 842.3, 734.6 cm^{-1} ; δ_{H} (300 MHz; CD_3CN ; Me_4Si) 0.98 (36H, t, $J_{\text{HH}}=7.35$, $\text{CH}_3\text{-CH}_2\text{-CH}_2\text{-CH}_2\text{-N}$), 1.37 (24H, st, $J_{\text{HH}}=7.35$, $\text{CH}_3\text{-CH}_2\text{-CH}_2\text{-CH}_2\text{-N}$), 1.64 (24H, m, $\text{CH}_2\text{-CH}_2\text{-N}$), 2.53 (4H, dd, $\text{CH}_2\text{-PO}$), 2.80 (2H, d, $\text{CH}_2\text{-COOH}$), 3.00-

3.22 (24H, m, **CH**₂-N), 4.00 (CH₂-NH₂), 5.08-5.28 (4H, m, **H**₂C=CH), 5.75-6.00 (2H, m, H₂C=CH), 7.34-7.58 (C₆H₅); δ_P (121 MHz, CD₃CN, H₃PO₄) 17.8, (HOOC-CH₂-P=O), 23.5 (CH₂-PO); m/z (Maldi-TOF): 3338 [M^+ +NBu₄-C₃H₅PO-C₃H₅O], 3355 [M^+ +NBu₄-C₃H₅PO-C₃H₅], 3580 [M^+ +2NBu₄-C₃H₅PO-C₃H₅O], 3599 [M^+ +2NBu₄-C₃H₅PO-C₃H₅], 3793 [M^+ +3NBu₄-2C₃H₅PO], 3811 [M^+ +2NBu₄-C₃H₅PO-C₃H₅O], where M^+ = (NBu₄)₃[SiW₉O₃₄(H₂C=CHCH₂PO)₂(HOOCCH₂PO)]⁺.

7.15. Reaction of (NBu₄)₃[XW₉O₃₄(*t*-BuSiO)₃(Si(CH₂)₃Br)] with amines

7.15.1. Reaction of (NBu₄)₃[PW₉O₃₄(*t*-BuSiO)₃(Si(CH₂)₃Br)] with glycine (Compound 53)

(NBu₄)₃[PW₉O₃₄(*t*-BuSiO)₃(Si(CH₂)₃Br)] (0.50 g, 0.15 mmol) was dissolved in DMF (1.5 mL) and glycine (NH₂CH₂COOH) (0.011 g, 0.15 mmol) added. The solution was stirred overnight at room temperature to give a cloudy solution, this was filtered and the solvent left to evaporate. The crude product was dissolved in acetonitrile and diethyl ether diffused into the solution over several days to give (NBu₄)₃[PW₉O₃₄(*tt*-BuSiO)₃(Si(CH₂)₃NHCH₂COOH)]. Yield (0.18 g, 35.2 %) (Found C 24.25; N 1.65; H 4.2. Calc. C 22.9; N 1.65; H 4.3). ν_{\max} (KBr disc) 3447.4 (O-H), 2962.0, 2875.7 (C-H), 1654.1 (C=O), 1474.1, 1116.0 (P=O), 1037.3 (P-O), 1000, 955.9, 866.1, 815.9, 728.7 cm⁻¹; δ_H (300 MHz; CD₃CN; Me₄Si) 0.70-0.85 (2H, m, Si-CH₂), 0.97 (36H, t, J_{HH}=7.35, CH₃-CH₂-CH₂-CH₂-N), 1.00 (27H, s, *t*-Bu), 1.38 (24H, st, J_{HH}=7.35, CH₃-CH₂-CH₂-CH₂-N), 1.61 (24H, qn, J_{HH}=7.54, CH₂-CH₂-N), 1.79-1.90 (2H, m, Si-CH₂-CH₂), 2.20-2.34 (2H, m, CH₂-NH), 3.07-3.18 (24H, m, CH₂-N), 3.50-3.62 (2H, m, N-CH₂-COOH); δ_P (121 MHz; DMF:DMSO-d₆; H₃PO₄) -16.7 ppm; m/z (Maldi-TOF) 3521 (M^+ +NBu₄-(CH₂)₂NHCH₂COOH),

3711 ($M^+ + 2\text{NBu}_4\text{-OSi}(\text{CH}_2)_3\text{NHCH}_2\text{COOH}$), 3939 ($M^+ + 3\text{NBu}_4\text{-O}_3\text{Si}(\text{CH}_2)_3\text{NHCH}_2\text{COOH}$), where $M^+ = (\text{NBu}_4)_3[\text{PW}_9\text{O}_{34}(t\text{-BuSiO})_3(\text{Si}(\text{CH}_2)_3\text{NHCH}_2\text{COOH})]^+$.

7.15.2. Reaction of $(\text{NBu}_4)_3[\text{PW}_9\text{O}_{34}(t\text{-BuSiO})_3(\text{Si}(\text{CH}_2)_3\text{Br})]$ with sarocine (Compound 54)

Was prepared following a similar procedure to in section 7.15.1, but using sarocine (0.013 g, 0.15 mmol). Yield (0.23 g, 44.9 %) (Found C 25.3; N 1.8; H 4.4. Calc. C 23.2; N 1.6; H 4.3). $\nu_{\text{max}}(\text{KBr disc})$ 3422.1 (O-H), 2961.8, 2934.8, 2875.7 (C-H), 1670.2 (C=O), 1484.4, 1111.6, 1027.1 (P-O), 955.0, 866.0, 820.3, 737.6 cm^{-1} ; $\delta_{\text{H}}(300 \text{ MHz; CD}_3\text{CN; Me}_4\text{Si})$ 0.67-0.85 (2H, m, Si-**CH**₂), 0.95 (36H, t, $J_{\text{HH}}=7.35$, **CH**₃-CH₂-CH₂-CH₂-N), 1.00 (27H, s, *t*-Bu), 1.43 (24H, st, $J_{\text{HH}}=7.35$, CH₃-**CH**₂-CH₂-CH₂-N), 1.60 (24H, qn, $J_{\text{HH}}=7.54$, **CH**₂-CH₂-N), 1.77-1.90 (2H, m, Si-CH₂-**CH**₂), 2.18-2.30 (2H, m, **CH**₂-NH), 3.00-3.18 (24H, m, **CH**₂-N), 3.48-3.62 (5H, m, N-(**CH**₃)-**CH**₂-COOH); $\delta_{\text{P}}(121 \text{ MHz; DMF:DMSO-}d_6; \text{H}_3\text{PO}_4)$ -16.6 ppm; m/z (Maldi-TOF) 3432 ($M^+ + \text{Na}$), 3472 ($M^+ + \text{Na}$), 3667 ($M^+ + \text{NBu}_4$), 3764 ($M^+ + 2\text{NBu}_4\text{-Si}(\text{CH}_2)_3\text{N}(\text{CH}_3)\text{CH}_2\text{COOH} + \text{Na}$), 3823 ($M^+ + 2\text{NBu}_4\text{-N}(\text{CH}_3)\text{CH}_2\text{COOH}$), 3904 ($M^+ + 2\text{NBu}_4$), where $M^+ = (\text{NBu}_4)_3[\text{PW}_9\text{O}_{34}(t\text{-BuSiO})_3(\text{Si}(\text{CH}_2)_3\text{N}(\text{CH}_3)\text{CH}_2\text{COOH})]^+$.

7.15.3. Reaction of $(\text{NBu}_4)_3\text{H}[\text{SiW}_9\text{O}_{34}(t\text{-BuSiO})_3(\text{Si}(\text{CH}_2)_3\text{Br})]$ with glycine (Compound 55)

Was prepared following a similar procedure to in section 7.15.1, but using $(\text{NBu}_4)_3\text{H}[\text{SiW}_9\text{O}_{34}(t\text{-BuSiO})_3(\text{Si}(\text{CH}_2)_3\text{Br})]$ (0.5 g, 0.15 mmol) to give $(\text{NBu}_4)_3\text{H}[\text{SiW}_9\text{O}_{34}(t\text{-BuSiO})_3(\text{Si}(\text{CH}_2)_3\text{NHCH}_2\text{COOH})]$. Yield (0.18 g, 52.9 %) (Found C 23.0; N 1.6; H 4.45. Calc. C 22.9; N 1.65; H 4.3). $\nu_{\text{max}}(\text{KBr disc})$ 3405.7 (O-H), 2961.1, 2874.5 (C-

H), 1669.9 (C=O), 1484.7, 1109.6 (P=O), 1040.0 (P-O), 964.0, 920.8, 865, 803.9 cm^{-1} ; δ_{H} (300 MHz; CD_3CN ; Me_4Si) 0.67-0.83 (2H, m, Si-**CH₂**), 0.97 (36H, t, $J_{\text{HH}}=7.35$, **CH₃-CH₂-CH₂-CH₂-N**), 1.00 (27H, s, *t*-Bu), 1.46 (24H, st, $J_{\text{HH}}=7.35$, **CH₃-CH₂-CH₂-CH₂-N**), 1.60 (24H, qn, $J_{\text{HH}}=7.54$, **CH₂-CH₂-N**), 1.76-1.90 (2H, m, Si-CH₂-**CH₂**), 2.12-2.38 (2H, m, **CH₂-NH**), 3.02-3.16 (24H, m, **CH₂-N**), 3.48-3.62 ppm (2H, m, N-**CH₂-COOH**); m/z (Maldi-TOF) 3664 ($M^+ + \text{NBu}_4 + \text{Na}$), 3740 ($M^+ + 2\text{NBu}_4 - \text{Si}(\text{CH}_2)_3\text{NHCH}_2\text{COOH}$), 3796 ($M^+ + 3\text{NBu}_4 - \text{CH}_2\text{NHCH}_2\text{COOH}$), 3906 ($M^+ + 2\text{NBu}_4 + \text{Na}$), 3991 ($M^+ + 3\text{NBu}_4 - \text{OSi}(\text{CH}_2)_3\text{NHCH}_2\text{COOH} + \text{Na}$), 4048 ($M^+ + 3\text{NBu}_4 - \text{CH}_2\text{NHCH}_2\text{COOH}$), 4150 ($M^+ + 3\text{NBu}_4 + \text{Na}$), where $M^+ = (\text{NBu}_4)_3[\text{SiW}_9\text{O}_{34}(\text{t-BuSiO})_3(\text{Si}(\text{CH}_2)_3\text{NHCH}_2\text{COOH})]^+$.

7.15.4. Reaction of $(\text{NBu}_4)_3\text{H}[\text{SiW}_9\text{O}_{34}(\text{t-BuSiO})_3(\text{Si}(\text{CH}_2)_3\text{Br})]$ with sarocine

(Compound 56)

Was prepared following a similar procedure to in section 7.15.3, but using sarocine (0.013 g, 0.15 mmol). $(\text{NBu}_4)_3\text{H}[\text{SiW}_9\text{O}_{34}(\text{t-BuSiO})_3(\text{Si}(\text{CH}_2)_3\text{N}(\text{CH}_3)\text{CH}_2\text{COOH})]$, Yield (0.20 g, 39.1 %) (Found C 27.35; N 1.9; H 5.0. Calc. C 23.2; N 1.6; H 4.3). ν_{max} (KBr disc) 3433.4 (O-H), 2963.9, 2875.6 (C-H), 1629.6 (C=O), 1466.9, 1021.5 (P-O), 965.0, 922.7, 904.5, 838.0, 740.1 cm^{-1} ; δ_{H} (300 MHz; CD_3CN ; Me_4Si) 0.72-0.87 (2H, m, Si-**CH₂**), 0.96 (36H, t, $J_{\text{HH}}=7.35$, **CH₃-CH₂-CH₂-CH₂-N**), 0.99 (27H, s, *t*-Bu), 1.38 (24H, st, $J_{\text{HH}}=7.35$, **CH₃-CH₂-CH₂-CH₂-N**), 1.62 (24H, qn, $J_{\text{HH}}=7.54$, **CH₂-CH₂-N**), 1.79-1.89 (2H, m, Si-CH₂-**CH₂**), 2.23-2.40 (2H, m, **CH₂-NH**), 3.00-3.16 (24H, m, **CH₂-N**), 3.50-3.62 ppm (5H, m, N-(**CH₃**)-**CH₂-COOH**); m/z (Maldi-TOF) 3705 ($M^+ + 2\text{NBu}_4 - \text{O}_3\text{Si}(\text{CH}_2)_3\text{N}(\text{CH}_3)\text{CH}_2\text{COOH}$), 3783 ($M^+ + 2\text{NBu}_4(\text{CH}_2)_2\text{NHCH}_2\text{COOH}$), 3836 ($M^+ + 2\text{NBu}_4 - \text{CH}_2\text{COOH}$), 3944 ($M^+ + 3\text{NBu}_4 - \text{O}_3\text{Si}(\text{CH}_2)_3\text{NHCH}_2\text{COOH}$), 4023 ($M^+ + 2\text{NBu}_4 -$

$(\text{CH}_2)_2\text{N}(\text{CH}_3)\text{CH}_2\text{COOH}$), 4076 ($M^+ + 2\text{NBu}_4\text{-CH}_2\text{COOH}$), where $M^+ = (\text{NBu}_4)_3[\text{PW}_9\text{O}_{34}(\text{t-BuSiO})_3(\text{Si}(\text{CH}_2)_3\text{NHCH}_2\text{COOH})]^+$.

7.15.5. Reaction of $(\text{NBu}_4)_3[\text{PW}_9\text{O}_{34}(\text{t-BuSiO})_3(\text{Si}(\text{CH}_2)_3\text{Br})]$ with benzylamine (Compound 57)

Was prepared following a similar procedure to in section 7.15.1, but using benzylamine (0.016 g, 0.15 mmol) to give $(\text{NBu}_4)_3\text{H}[\text{SiW}_9\text{O}_{34}(\text{t-BuSiO})_3(\text{Si}(\text{CH}_2)_3\text{NHCH}_2\text{C}_6\text{H}_5)]$. Yield (0.16 g, 31.1 %) (Found C 27.5; N 2.05; H 4.2. Calc. C 24.5; N 1.6; H 3.5). $\nu_{\text{max}}(\text{KBr disc})$ 3447.8 (O-H), 2961.5, 2875.5 (C-H), 1654.1, 1474.3, 1116.9 (P=O), 1039.4 (P-O), 974.0, 955.7, 865.0, 812.6, 728.0 cm^{-1} ; $\delta_{\text{H}}(300 \text{ MHz; CD}_3\text{CN; Me}_4\text{Si})$ 0.74-0.90 (2H, m, Si-**CH**₂), 0.97 (36H, t, $J_{\text{HH}}=7.35$, **CH**₃-CH₂-CH₂-CH₂-N), 1.00 (27H, s, *t*-Bu), 1.40 (24H, st, $J_{\text{HH}}=7.35$, **CH**₃-CH₂-CH₂-CH₂-N), 1.61 (24H, qn, $J_{\text{HH}}=7.54$, **CH**₂-CH₂-N), 1.77-1.87 (2H, m, Si-CH₂-**CH**₂), 3.05-3.20 (24H, m, **CH**₂-N), 3.50-3.62 (2H, m, N-**CH**₂), 4.10-4.20 (2H, m, **CH**₂-C₆H₅), 7.22-7.60 (5H, m, **C**₆**H**₅); $\delta_{\text{P}}(121 \text{ MHz; DMF:DMSO-d}_6; \text{H}_3\text{PO}_4)$ -16.7 ppm; m/z (Maldi-TOF) 3463 ($M^+ + \text{Na}$), 3509 ($M^+ + \text{NBu}_4\text{-Si}(\text{CH}_2)_3\text{NHCH}_2\text{C}_6\text{H}_5$), 3551 ($M^+ + \text{NBu}_4\text{-(CH}_2)_3\text{NHCH}_2\text{C}_6\text{H}_5 + \text{Na}$), 3593 ($M^+ + \text{NBu}_4\text{-NHCH}_2\text{C}_6\text{H}_5$), 3692 ($M^+ + \text{NBu}_4 + \text{Na}$), 3727 ($M^+ + \text{NBu}_4 + 2\text{Na}$), 3930 ($M^+ + 2\text{NBu}_4 + \text{Na}$), where $M^+ = (\text{NBu}_4)_3[\text{PW}_9\text{O}_{34}(\text{t-BuSiO})_3(\text{Si}(\text{CH}_2)_3\text{NHCH}_2\text{C}_6\text{H}_5)]^+$.

7.15.6. Reaction of $(\text{NBu}_4)_3\text{H}[\text{SiW}_9\text{O}_{34}(\text{t-BuSiO})_3(\text{Si}(\text{CH}_2)_3\text{Br})]$ with benzylamine (Compound 58)

Was prepared following a similar procedure to in section 7.15.5, but using $(\text{NBu}_4)_3\text{H}[\text{SiW}_9\text{O}_{34}(\text{t-BuSiO})_3(\text{Si}(\text{CH}_2)_3\text{Br})]$ (0.5 g, 0.15 mmol) to give $(\text{NBu}_4)_3\text{H}[\text{SiW}_9\text{O}_{34}(\text{t-BuSiO})_3(\text{Si}(\text{CH}_2)_3\text{NHCH}_2\text{C}_6\text{H}_5)]$. Yield (0.22 g, 42.6 %) (Found C 22.9; N 3.0; H 3.7. Calc. C

24.5; N 1.6; H 4.3). ν_{\max} (KBr disc) 3461.7 (O-H), 2962.0, 2874.8 (C-H), 1654.1, 1483.5, 1042.6 (P=O), 966.1, 921.3, 803.9 cm^{-1} ; δ_{H} (300 MHz; CD_3CN ; Me_4Si) 0.68-0.85 (2H, m, Si-**CH₂**), 0.95 (36H, t, $J_{\text{HH}}=7.35$, **CH₃**-CH₂-CH₂-CH₂-N), 1.00 (27H, s, *t*-Bu), 1.35 (24H, st, $J_{\text{HH}}=7.35$, CH₃-**CH₂**-CH₂-CH₂-N), 1.58 (24H, qn, $J_{\text{HH}}=7.54$, **CH₂**-CH₂-N), 1.78-1.88 (2H, m, Si-CH₂-**CH₂**), 2.96-3.12 (24H, m, **CH₂**-N), 3.50-3.60 (2H, m, N-**CH₂**-COOH), 4.08-4.12 (3H, m, **CH₂**-C₆H₅), 7.28-7.60 ppm (5H, m, **C₆H₅**); m/z (Maldi-TOF) 3671 (M^+ +NBu₄), 3809 (M^+ +2NBu₄-NHCH₂C₆H₅), 3917 (M^+ +2NBu₄), 4052 (M^+ +3NBu₄-NHCH₂C₆H₅), 4155 (M^+ +3NBu₄), where $M^+ = (\text{NBu}_4)_3[\text{SiW}_9\text{O}_{34}(t\text{-BuSiO})_3(\text{Si}(\text{CH}_2)_3\text{NHCH}_2\text{C}_6\text{H}_5)]^+$.

7.15.7. Reaction of (NBu₄)₃[PW₉O₃₄(*t*-BuSiO)₃(Si(CH₂)₃Br)] with *p*-xylylenediamine (Compound 59)

Was prepared following a similar procedure to in section 7.15.1, but using *p*-xylylenediamine (0.02 g, 0.15 mmol) to give (NBu₄)₃[PW₉O₃₄(*t*-BuSiO)₃(Si(CH₂)₃NHCH₂C₆H₄CH₂NH₂)]. Yield (0.20 g, 38.5 %) (Found C 23.7; N 1.95; H 4.0. Calc. C 25.1; N 2.0; H 4.5). ν_{\max} (KBr disc) 3421.6 (O-H), 2961.3, 2875.0 (C-H), 1654.1, 1482.1, 1116.2 (P=O), 1023.8 (P-O), 953.9, 862.6, 734.6 cm^{-1} ; δ_{H} (300 MHz; CD_3CN ; Me_4Si) 0.64-0.80 (2H, m, Si-**CH₂**), 0.95 (36H, t, $J_{\text{HH}}=7.35$, **CH₃**-CH₂-CH₂-CH₂-N), 0.97 (27H, s, *t*-Bu), 1.40 (24H, st, $J_{\text{HH}}=7.35$, CH₃-**CH₂**-CH₂-CH₂-N), 1.56 (24H, qn, $J_{\text{HH}}=7.54$, **CH₂**-CH₂-N), 1.70-1.90 (2H, m, Si-CH₂-**CH₂**), 2.50-2.63 (2H, m, CH₂-**CH₂**-NH), 3.05-3.20 (24H, m, CH₃-**CH₂**-N), 3.50-3.68 (2H, m, NH-**CH₂**), 3.95-4.08 (2H, m, CH₂-**NH₂**), 7.26-7.58 (4H, m, **C₆H₄**); δ_{P} (121 MHz; DMF:DMSO-*d*₆; H₃PO₄) -16.7 ppm; m/z (Maldi-TOF) 3571 (M^+ +NBu₄-NHCH₂C₆H₄CH₂NH₂), 3711 (M^+ +NBu₄), 3922 (M^+ +2NBu₄-CH₂NH₂), 4061 (M^+ +3NBu₄-NHCH₂C₆H₄CH₂NH₂), 4321 (M^+ +4NBu₄-C₆H₄CH₂NH₂), where $M^+ = (\text{NBu}_4)_3[\text{PW}_9\text{O}_{34}(t\text{-BuSiO})_3(\text{Si}(\text{CH}_2)_3\text{NHCH}_2\text{C}_6\text{H}_4\text{CH}_2\text{NH}_2)]^+$.

7.15.8. Reaction of $(\text{NBu}_4)_3\text{H}[\text{SiW}_9\text{O}_{34}(\text{t-BuSiO})_3(\text{Si}(\text{CH}_2)_3\text{Br})]$ with *p*-xylylenediamine (Compound 60)

Was prepared following a similar procedure to in section 7.15.7, but using $(\text{NBu}_4)_3\text{H}[\text{SiW}_9\text{O}_{34}(\text{t-BuSiO})_3(\text{Si}(\text{CH}_2)_3\text{Br})]$ (0.5 g, 0.15 mmol) to give $(\text{NBu}_4)_3\text{H}[\text{SiW}_9\text{O}_{34}(\text{t-BuSiO})_3(\text{Si}(\text{CH}_2)_3\text{NHCH}_2\text{C}_6\text{H}_4\text{CH}_2\text{NH}_2)]$. Yield (0.21 g, 40.4 %). $\nu_{\text{max}}(\text{KBr disc})$ 3422.1 (O-H), 2962.1, 1654.1, 1474.3, 1110, 1036.2 (P-O), 922.9, 807.3, 730 cm^{-1} ; $\delta_{\text{H}}(300 \text{ MHz; CD}_3\text{CN; Me}_4\text{Si})$ 0.70-0.82 (2H, m, Si-**CH**₂), 0.95 (36H, t, $J_{\text{HH}}=7.35$, **CH**₃-CH₂-CH₂-CH₂-N), 0.95 (27H, s, *t*-Bu), 1.32 (24H, st, $J_{\text{HH}}=7.35$, CH₃-**CH**₂-CH₂-CH₂-N), 1.56 (24H, qn, $J_{\text{HH}}=7.54$, **CH**₂-CH₂-N), 1.70-1.84 (2H, m, Si-CH₂-**CH**₂), 2.54-2.60 (2H, m, **CH**₂-NH), 3.03-3.20 (24H, m, **CH**₂-N), 3.48-3.62 (2H, m, N-**CH**₂-COOH), 3.99-4.08 (2H, m, **CH**₂-NH₂), 7.20-7.55 ppm (4H, m, **C**₆**H**₄); *m/z* (Maldi-TOF) 3685 ($M^+ + 2\text{NBu}_4 - \text{O}_3\text{Si}(\text{CH}_2)_3\text{NHCH}_2\text{C}_6\text{H}_4\text{CH}_2\text{NH}_2$), 3818 ($M^+ + 2\text{NBu}_4 - \text{NH}_2\text{CH}_2(\text{CH}_2)_3\text{NHCH}_2\text{C}_6\text{H}_4\text{CH}_2\text{NH}_2$), 3948 ($M^+ + 2\text{NBu}_4$), 4062 ($M^+ + 3\text{NBu}_4 - \text{CH}_2\text{C}_6\text{H}_4\text{CH}_2\text{NH}_2$), where $M^+ = (\text{NBu}_4)_3[\text{SiW}_9\text{O}_{34}(\text{t-BuSiO})_3(\text{Si}(\text{CH}_2)_3\text{NHCH}_2\text{C}_6\text{H}_4\text{CH}_2\text{NH}_2)]^+$.

7.16. Electrochemistry

Cyclic Voltammetry measurements were carried out using a 273 A potentiostat (Princeton Applied Research) controlled by a PC. A three electrode cell was employed comprising a glassy carbon working electrode, platinum wire counter electrode and a reference electrode (SCE, Ag/AgCl or Ag/Ag⁺). The working electrode was polished with successively finer (1.0 μm , 0.3 μm and 0.05 μm) grades of alumina, washed with ultra pure water and dried. The cell and glassware were cleaned with a hot mixture of nitric and sulphuric acids, rinsed with copious quantities of ultrapure water and dried. Water was purified with a tandem thx-gradient A10

system (Millipore). Formal potentials were estimated as the average of the anodic and cathodic peak and quoted relative to ferrocene which was used as an internal reference.

7.17. References

1. L. Churchill, *From Polyoxometalates to Functional Polymers, Masters Project*, University of Birmingham, **2005**.
2. L. J. Gooßen and M. K. Dezfuli, *Synlett*, **2005**, 3, 445.
3. A. Tézé and G. Hervé, *Inorg. Synth.*, **1990**, 27, 85.
4. C. R. Mayer, P. Herson and R. Thouvenot, *Inorg. Chem.*, **1999**, 38, 6152.
5. W.H. Knoth and R.L. Harlow, *J. Am. Chem. Soc.*, **1981**, 103, 1865.
6. R. Contant, *Can. J. Chem.*, **1987**, 65, 568.
7. A. Mazeaud, N. Ammari, F. Robert and R. Thouvenot, *Angew. Chem. Int. Ed. Engl.*, **1996**, 35, 1961.
8. C. R. Mayer and R. Thouvenot, *J. Chem. Soc., Dalton Trans.*, **1998**, 7.
9. G. S. Kim, K. Hagen and C. Hill, *Inorg. Chem.*, **1992**, 31, 5316.

8. APPENDIX

The cif's for the crystal structures are included on a CD as both cif (wordpad files) and pdfs, all the structural information including the bond lengths and angles are included in these files.

- Structure 1 – $(\text{NBu}_4)_2(\text{NEt}_4)\text{H}[\text{SiW}_{10}\text{O}_{36}(\text{EtPO})_2]$
- Structure 2 – $(\text{NBu}_4)_2(\text{NEt}_4)\text{H}[\text{SiW}_{10}\text{O}_{36}(\text{H}_2\text{C}=\text{CHCH}_2\text{PO})_2]$
- Structure 3 – $(\text{NEt}_4)_3\text{H}[\text{SiW}_{10}\text{O}_{36}(\text{H}_2\text{C}=\text{CHCH}_2\text{PO})_2]$
- Structure 4 – $(\text{NBu}_4)_3\text{H}[\text{SiW}_{10}\text{O}_{36}(\text{H}_2\text{C}=\text{CHC}_6\text{H}_4\text{PO})_2]$
- Structure 5 – $(\text{NEt}_4)_3\text{H}[\text{SiW}_{10}\text{O}_{36}(\text{HOOCCH}_2\text{PO})_2]$
- Structure 6 – $(\text{NEt}_4)_3\text{H}[\text{SiW}_{10}\text{O}_{36}(\text{HOOCCH}_2\text{CH}_2\text{PO})_2]$
- Structure 7 – $(\text{NEt}_4)_3\text{H}[\text{SiW}_{10}\text{O}_{36}(\text{H}_3\text{CCOC}_6\text{H}_4\text{PO})_2]$
- Structure 8 – $(\text{NBu}_4)_3[\text{PW}_9\text{O}_{34}(\text{H}_2\text{C}=\text{CHSiO})_3(\text{H}_2\text{C}=\text{CHSi})]$
- Structure 9 – $(\text{NBu}_4)_3[\text{PW}_9\text{O}_{34}(t\text{BuSiOH})_3]$
- Structure 10 – $(\text{NBu}_4)_3\text{H}[\text{SiW}_9\text{O}_{34}(t\text{BuSiOH})_3]$
- Structure 11 – $(\text{NBu}_4)_3[\text{PW}_9\text{O}_{34}(t\text{BuSiO})_3(\text{H}_2\text{C}=\text{CHCH}_2\text{Si})]$
- Structure 12 – $(\text{NBu}_4)_3[\text{PW}_9\text{O}_{34}(t\text{BuSiOH})_3(\text{Br}(\text{CH}_2)_3\text{Si})]$
- Structure 13 – $(\text{NBu}_4)_3\text{H}[\text{SiW}_9\text{O}_{34}(\text{EtPO})_3]$
- Structure 14 – $(\text{NBu}_4)_3\text{Na}[\text{SiW}_9\text{O}_{34}(\text{H}_2\text{C}=\text{CHPO})_3]$
- Structure 15 – $(\text{NBu}_4)_3\text{Na}[\text{SiW}_9\text{O}_{34}(\text{H}_2\text{C}=\text{CHCH}_2\text{PO})_3]$
- Structure 16 – $(\text{NBu}_4)_3\text{Co}[\text{SiW}_9\text{O}_{34}(\text{H}_2\text{C}=\text{CHC}_6\text{H}_4\text{PO})_3]$
- Structure 17 – $(\text{NBu}_4)_3\text{Na}[\text{SiW}_9\text{O}_{34}(\text{HOOCCH}_2\text{CH}_2\text{PO})_3]$
- Structure 18 – $(\text{NBu}_4)_6\text{M}[\text{SiW}_9\text{O}_{34}(\text{H}_3\text{CCOC}_6\text{H}_4\text{PO})_3]_2$
- Structure 19 – $(\text{NBu}_4)_5\text{Co}[\text{SiW}_9\text{O}_{34}(\text{H}_3\text{CCOC}_6\text{H}_4\text{PO})_3]_2$
- Structure 20 – $(\text{NBu}_4)_3[\text{PW}_9\text{O}_{34}(\text{EtPO})_3]$
- Structure 21 – $(\text{NBu}_4)_4(\text{C}_6\text{H}_5\text{CH}_2\text{NH}_3)_5\text{MgH}[\text{SiW}_{10}\text{O}_{36}(\text{HOOCCH}_2\text{CH}_2\text{COOH})]_2$
- Structure 22 – $(\text{NEt}_4)_3(\text{C}_6\text{H}_5\text{CH}_2\text{NH}_3)_3[\text{SiW}_{10}\text{O}_{36}(\text{H}_3\text{CCOC}_6\text{H}_4\text{PO})]$
- Structure 23 – $(\text{NEt}_4)_3\text{H}[\text{SiW}_{10}\text{O}_{36}(\text{H}_2\text{C}=\text{CHCH}_2\text{PO})(\text{HOOC}(\text{CH}_2)_2\text{PO})]$
- Structure 24 – $(\text{NEt}_4)_3\text{H}[\text{SiW}_{10}\text{O}_{36}(\text{H}_2\text{C}=\text{CHPO})(\text{H}_2\text{C}=\text{CHCH}_2\text{PO})]$
- Structure 25 – $(\text{NBu}_4)_3\text{H}[\text{SiW}_9\text{O}_{34}(\text{H}_2\text{C}=\text{CHCH}_2\text{PO})(\text{C}_6\text{H}_5\text{PO})]$